

AD-A263 266



DTIC
ELECTF
APR 21 1993
S C D



Scientific and
Engineering
Studies

Compiled 1985

Signal
Processing
Studies

A. H. Nuttall

NAVAL UNDERWATER SYSTEMS CENTER

DISTRIBUTION STATEMENT A
Approved for public release

Reproduced From
Best Available Copy



Scientific and Engineering Studies

Compiled 1985

Signal Processing Studies

A. H. Nuttall

Accession For	
NTIS CRA&I	<input checked="" type="checkbox"/>
DTIC TAB	<input type="checkbox"/>
Unannounced	<input type="checkbox"/>
Justification	
By _____	
Distribution /	
Availability Codes	
Dist	Avail and/or Special
A-1	

DTIC QUALITY INSPECTED 1

PUBLISHED BY

NAVAL UNDERWATER SYSTEMS CENTER

NEWPORT LABORATORY, NEWPORT, RHODE ISLAND

NEW LONDON LABORATORY, NEW LONDON, CONNECTICUT

93 4 20 023

1985 4/27

93-08383



Foreword

This collection of technical reports and technical memoranda deals with the following topics: accurate efficient evaluation of cumulative or exceedance probability distributions directly from characteristic functions; determination of the performance of general second-order processors with nonstationary Gaussian inputs; the exact operating characteristics of a sum of an envelope-detected narrowband Gaussian process and sine wave; the resolution of the right-left ambiguity of a randomly moving line array; the operating characteristics of a cross-correlator with sample mean removal; statistical characterization of the under-ice profile; and the evaluation of densities and distributions from knowledge of high-order moments.

Some of the material presented here is based heavily on earlier work by the author, which can be found in the following volumes in addition to the referenced technical reports:

Performance of Detection and Communication Systems, NUSC Scientific and Engineering Studies, 1974;

Spectral Estimation, NUSC Scientific and Engineering Studies, 1977;

Coherence Estimation, NUSC Scientific and Engineering Studies, 1979;

Receiver Performance Evaluation and Spectral Analysis, NUSC Scientific and Engineering Studies, 1981; and

Signal Processing Studies, NUSC Scientific and Engineering Studies, 1983.

Dr. William A. Von Winkle
Associate Technical Director
for Technology
NAVAL UNDERWATER SYSTEMS CENTER

Compiled 1985

Table of Contents

Foreword

- TR 7023** **Accurate Efficient Evaluation of Cumulative or Exceedance Probability Distributions Directly From Characteristic Functions**
A. H. Nuttall
- TR 7035** **Exact Performance of General Second-Order Processors for Gaussian Inputs**
A. H. Nuttall
- TR 7117** **Exact Operating Characteristics for Linear Sum of Envelopes of Narrowband Gaussian Process and Sinewave**
A. H. Nuttall and B. Dedreux
- TM 831150** **Resolution of Ambiguity for Randomly Moving Line Array**
A. H. Nuttall
- TR 7045** **Operating Characteristics of Crosscorrelator With or Without Sample Mean Removal**
A. H. Nuttall
- TM 841208** **Under-Ice Roughness: Shot Noise Model**
A. H. Nuttall
- TR 7377** **Evaluation of Densities and Distributions via Hermite and Generalized Laguerre Series Employing High-Order Expansion Coefficients Determined Recursively via Moments or Cumulants**
A. H. Nuttall
- TM 831078** **Error of Zero-Crossing Location for Straight-Line Interpolation of Sampled Sinewave in Noise**
A. H. Nuttall
- TM 841013** **Mean and Variance of Product Array Response; Application to a Cross-Line Array**
A. H. Nuttall

Subject Matter Index

Accurate Efficient Evaluation Of Cumulative or Exceedance Probability Distributions Directly From Characteristic Functions

A. H. Nuttall

ABSTRACT

An accurate and efficient method of evaluating the entire cumulative or exceedance probability distribution, via one fast Fourier transform of the sampled characteristic function, is presented. The sampling rate applied to the characteristic function results in aliasing of the probability density function, while the limited extent of the sampling gives rise to a systematic disturbance in the calculated probability distribution. Both types of errors are easily recognizable and can be controlled by a trial and error procedure whereby the calculated distributions are plotted for observation and modification.

The size of the fast Fourier transform determines the number of distribution values available, but has no effect on the accuracy of the result. Regardless of the number of characteristic function evaluations required for accurate results, the storage required is just that corresponding to the size of the fast Fourier transform.

A program for the procedure is presented and the inputs required of the user are indicated. Several representative examples and plots illustrate the utility of the approach.

TABLE OF CONTENTS

	<u>Page</u>
List of Illustrations	iii
List of Symbols	iv
Introduction	1
Derivation of Procedure	2
Shifted Random Variable	2
Approximation to Cumulative Distribution Function	3
Relationship of Approximation	4
Calculation of $C(v)$	7
Relation to Requicha's Method, ref. 5	10
Summary of Procedure	11
Examples	12
1. Chi-Square	12
2. Gaussian	14
3. Smirnov	16
4. Noncentral Chi-Square	24
5. Product of Correlated Gaussian Variates	25
Applications	30
Summary	33
Appendices	
A. Sampling for a Fourier Transform	A-1
B. Listings of Programs for Five Examples	B-1
References	R-1

LIST OF ILLUSTRATIONS

<u>Figure</u>	<u>Page</u>
1. Probability Density Function of Secondary Random Variable y ..	3
2. Infinitely Aliased Probability Density Function $\tilde{p}_y(v)$	6
3. Chi-Square; $L=200$, $\Delta=.075$, $b=0$, $M=256$	13
4. Gaussian; $L=7$, $\Delta=.3$, $b=2.5\pi$, $M=256$	15
5. Gaussian; $L=6$, $\Delta=.3$, $b=2.5\pi$, $M=256$	17
6. Gaussian; $L=7$, $\Delta=.5$, $b=2.5\pi$, $M=256$	18
7. Gaussian; $L=7$, $\Delta=.3$, $b=5\pi/3$, $M=256$	19
8. Gaussian; $L=7$, $\Delta=.4$, $b=2.5\pi$, $M=256$	20
9. Smirnov; $L=3000$, $\Delta=1$, $b=0$, $M=256$	22
10. Comparison with Requicha's Method; $\Delta=1$, $b=0$, $M=1024$	23
11. Noncentral Chi-Square; $\Delta=.05$, $b=0$, $M=256$	26
12. Gaussian Product; $L=5$, $\Delta=.06$, $b=5\pi/3$, $M=256$	29

LIST OF SYMBOLS

x	random variable of primary interest
$f_x(\xi)$	characteristic function of random variable x
$p_x(v)$	probability density function of random variable x
b	bias or shift added to x
y	random variable $y=x+b$
$f_y(\xi)$	characteristic function of random variable y
μ_x	mean of random variable x
$p_y(v)$	probability density function of random variable y
$P_x(v)$	cumulative distribution function of random variable x
$P_y(v)$	cumulative distribution function of random variable y
$g(\xi, v)$	auxiliary function (6)
Im	imaginary part
μ_y	mean of random variable y
$C(v)$	right-hand side of (8)
Δ	sampling increment in argument ξ of characteristic function
$\tilde{p}_y(v)$	aliased version of $p_y(v)$; (12)
$\delta_\Delta(\xi)$	impulse train (13)
M	size of FFT employed
z_n	sequence of characteristic function samples; (20)
\hat{z}_n	collapsed sequence; (21)
L	limit on integral of characteristic function; (28)
N	number of nonzero z_n ; $N=L/\Delta$
overbar	ensemble average

ACCURATE EFFICIENT EVALUATION OF CUMULATIVE OR
EXCEEDANCE PROBABILITY DISTRIBUTIONS DIRECTLY FROM
CHARACTERISTIC FUNCTIONS

INTRODUCTION

The performance of a signal processor can often be evaluated in terms of the characteristic function of the decision variable, either numerically or in closed form; see for example, refs. 1 and 2. However, a closed form for the corresponding probability density function or cumulative distribution function is seldom available, and numerical procedures must be employed. Several such procedures have been published in the literature, refs. 3-8. However they have limited accuracy or they require extensive storage or analytical manipulations and calculations.

We present a technique which is limited in accuracy only by the round-off noise of the computer or by the errors of the special functions required in the characteristic function calculation. The amount of storage depends only on the number of cumulative or exceedance distribution function values requested and does not influence the accuracy of the final probability values. The entire cumulative and exceedance distribution function values result as the output of one fast Fourier transform (FFT). The size of the FFT dictates the storage required and the spacing of the calculated probability values, but not their accuracy.

The addition and subtraction of integrand functions given in ref. 7 can be entirely circumvented and yet enable use of an FFT, through proper manipulation of the origin contribution of the characteristic function. Specific connections with past results will be noted at appropriate points in the derivations.

DERIVATION OF PROCEDURE

Shifted Random Variable

The primary random variable of interest is the real quantity x with given characteristic function $f_x(\xi)$ which is related to the probability density function p_x of random variable x via Fourier transform *

$$f_x(\xi) = \int dv \exp(i\xi v) p_x(v). \quad (1)$$

We define secondary random variable y as

$$y = x+b, \quad (2)$$

where bias (shift) b is a constant, chosen such that random variable y has insignificant probability of being less than zero. However, we also pick b as small as possible, so that the characteristic function of y ,

$$f_y(\xi) = f_x(\xi) \exp(ib\xi), \quad (3)$$

will vary slowly with ξ . In fact, b can be negative, as for example if x were limited to values larger than some positive threshold. The approach here is not limited to positive random variables x , as were some of the results in ref. 7, but is applicable to any random variable distribution.

By way of example, for an exponential probability density function for random variable x , we choose $b=0$; while for a Gaussian random variable, $b = -\mu + 8\sigma_x$ yields a probability less than $1E-15$ of y being negative. The probability density function of random variable y therefore appears as depicted in figure 1.

* Integrals and sums without limits are over $(-\infty, +\infty)$.



Figure 1. Probability Density Function of Secondary Random Variable y

The cumulative distribution functions of random variables y and x are related according to

$$\int_{-\infty}^v dt p_y(t) = P_y(v) = P_x(v-b); \quad P_x(v) = P_y(v+b). \quad (4)$$

Thus we can inspect $P_x(v)$ in the neighborhood of $v=-b$ (the lower edge of interest of x) by looking at cumulative distribution function $P_y(v)$ in the neighborhood of $v=0$. More precisely, we will investigate $P_y(v)$ for values of v greater than zero, since this is the region of significant variation of $P_y(v)$; this is called the positive neighborhood of $v=0$.

Approximation to Cumulative Distribution Function

From ref. 4, eq. 7, we have the cumulative distribution function of random variable y in terms of the characteristic function according to

$$P_y(v) = \frac{1}{2} - \int_{0^+}^{+\infty} d\xi g(\xi, v), \quad (5)$$

where we have defined auxiliary function

$$g(\xi, v) = \text{Im} \left\{ \exp(-i\xi v) \frac{f_y(\xi)}{\pi \xi} \right\}. \quad (6)$$

Observe for later use that

$$g(0^+, v) = \lim_{\xi \rightarrow 0^+} \text{Im} \left\{ (1 - i\xi v) \frac{1 + i\xi \mu_y}{\pi \xi} \right\} = \frac{\mu_y - v}{\pi}, \quad (7)$$

where μ_y is the mean of random variable y .

For v in the neighborhood of zero, $\exp(-i\xi v)$ in (6) varies slowly with ξ , and we have the approximation, via the Trapezoidal rule, to (5) as

$$P_y(v) \cong \frac{1}{2} - \frac{\Delta}{2} g(0^+, v) - \sum_{n=1}^{+\infty} \Delta g(n\Delta, v) \cong C(v), \quad (8)$$

where the right-hand side of (8) has been defined as $C(v)$. Here, Δ is the sampling interval in ξ , and is small enough to track changes in $\exp(-i\xi v) * f_y(\xi)/\xi$. We choose the Trapezoidal rule in (8) over other integration rules, such as Simpson's rule, because it results in minimum aliasing for Fourier transforms relative to all other rules; see appendix A for elaboration and proof.

Observe from (8) that

$$P_y(0) \cong C(0) \quad \text{means} \quad C(0) \cong 0, \quad (9)$$

since $P_y(0)$ is insignificant by the choice of b in (2); this relation will be used later.

Relationship of Approximation

Although we want to evaluate the exact cumulative distribution function $P_y(v)$, we have instead arrived at an approximation $C(v)$ via (8). How are these two related? To determine the relationship, we manipulate (6)-(8) as follows:

$$\begin{aligned} C(v) &= \frac{1}{2} + \frac{\Delta}{2} \frac{v - \mu_y}{\pi} - \sum_{n=1}^{+\infty} \text{Im} \left\{ \exp(-in\Delta v) \frac{f_y(n\Delta)}{\pi n} \right\} = \\ &= \frac{1}{2} + \frac{\Delta}{2} \frac{v - \mu_y}{\pi} - \text{Im} \left\{ \sum_{n=1}^{+\infty} \exp(-in\Delta v) \frac{f_y(n\Delta)}{\pi n} \right\} = \end{aligned} \quad (10)$$

$$= \frac{1}{2} + \frac{\Delta}{2} \frac{v - \mu_y}{\pi} - \frac{1}{i2\pi} \sum_{n \neq 0} \exp(-in\Delta v) \frac{f_y(n\Delta)}{n}. \quad (11)$$

The removal of the imaginary operation from within the summation in (10) is a crucial step; it does not create a problem in divergence since $n > 0$. This is in contrast with the integral of (5) and (6), where removal of the imaginary operation would create a divergent integral. This postponement of the removal of the imaginary operation, until after the approximation to the integral was developed in (8), is the major difference with the results in ref. 7.

Taking a derivative of (11), we obtain

$$\begin{aligned}
 C'(v) &= \frac{\Delta}{2\pi} + \frac{\Delta}{2\pi} \sum_{n \neq 0} \exp(in\Delta v) f_y(n\Delta) = \\
 &= \frac{\Delta}{2\pi} \sum_n \exp(-in\Delta v) f_y(n\Delta) = \\
 &= \frac{1}{2\pi} \int d\mathfrak{f} \exp(-i\mathfrak{f}v) f_y(\mathfrak{f}) \Delta \delta_{\Delta}(\mathfrak{f}) = \\
 &= p_y(v) \otimes \delta_{\frac{2\pi}{\Delta}}(v) = \sum_n p_y\left(v - n \frac{2\pi}{\Delta}\right) \equiv \tilde{p}_y(v), \tag{12}
 \end{aligned}$$

where infinite impulse train

$$\delta_{\Delta}(\mathfrak{f}) = \sum_n \delta(\mathfrak{f} - n\Delta), \tag{13}$$

where \otimes denotes convolution, and where we have used the relation

$$\frac{1}{2\pi} \int dt \exp(-i\omega t) \Delta \delta_{\Delta}(t) = \delta_{\frac{2\pi}{\Delta}}(\omega). \tag{14}$$

This last result follows from ref. 9, p. 28, rule 11, with $u(t) = \delta(t)$, $T = \Delta$, $F = 1/T$, and $\omega = 2\pi f$. Relation (12) indicates that $C'(v)$ is an infinitely aliased version of the probability density function $p_y(v)$, with resultant period $2\pi/\Delta$ in v . For small enough sampling increment Δ in (8), there will be very little overlap of the displaced versions of p_y in (12), thereby yielding the good approximation

$$\tilde{p}_y(v) = p_y(v) \quad \text{for } 0 \leq v \leq 2\pi/\Delta. \quad (15)$$

The situation for relation (12) is depicted in figure 2.

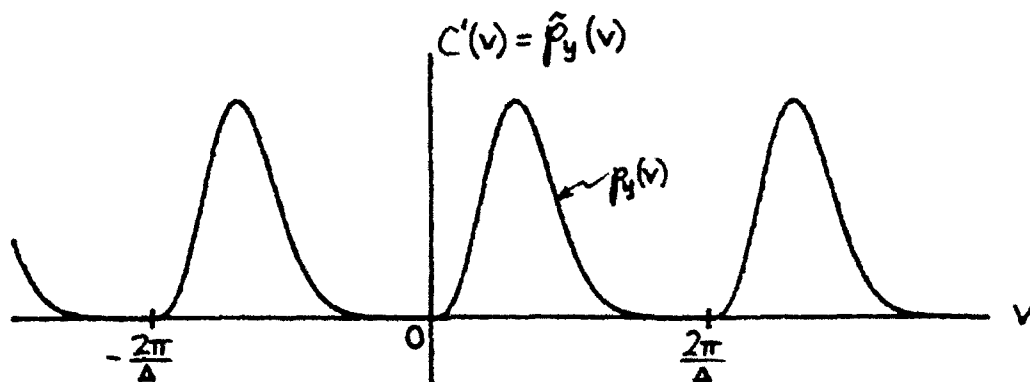


Figure 2. Infinitely Aliased Probability Density Function $\tilde{p}_y(v)$

There now follows from (12),

$$C(v) = C(0) + \int_0^v du \tilde{p}_y(u) \equiv C(0) + \tilde{P}_y(v), \quad (16)$$

where $C(0)$ is given by (10) as

$$C(0) = \frac{1}{2} - \frac{\Delta\mu_y}{2\pi} - \text{Im} \left\{ \sum_{n=1}^{+\infty} \frac{f_y(n\Delta)}{\pi n} \right\}. \quad (17)$$

Relation (16) is an exact relation, showing that $C(v)$ is the integral of the infinitely aliased version of $p_y(v)$, starting at $v=0$, plus an additive constant which is substantially zero; see (9).

So for v in the positive neighborhood of zero, (4), (8), (16), and (9) yield

$$P_x(v-b) = P_y(v) \equiv C(v) = C(0) + \tilde{P}_y(v) \equiv \tilde{P}_y(v). \quad (18)$$

Thus the quantity we want, the left-most term in (18), is well-approximated by calculated quantity $C(v)$, which itself is approximately the integral of the infinitely aliased version of $p_y(v)$.

Calculation of C(v)

Let $v = \frac{2\pi k}{M\Delta}$ in (10), where M and k are arbitrary integers. Then

$$\begin{aligned} C\left(\frac{2\pi k}{M\Delta}\right) &= \frac{1}{2} + \frac{k}{M} - \frac{\Delta\mu_y}{2\pi} - \operatorname{Im} \left\{ \sum_{n=1}^{+\infty} \exp(-i2\pi nk/M) \frac{f_y(n\Delta)}{\pi n} \right\} = \\ &= \frac{1}{2} + \frac{k}{M} - \frac{1}{\pi} \operatorname{Im} \left\{ \sum_{n=0}^{+\infty} \exp(-i2\pi nk/M) z_n \right\}, \end{aligned} \quad (19)$$

where we define complex sequence

$$z_n = \begin{cases} i \frac{1}{2} \Delta\mu_y & \text{for } n=0 \\ f_y(n\Delta)/n & \text{for } n \geq 1 \end{cases}. \quad (20)$$

Now define collapsed sequence (ref. 7, pp. 13-16) as

$$\hat{z}_n = \sum_{j=0}^{+\infty} z_{n+Mj} \quad \text{for } 0 \leq n \leq M-1. \quad (21)$$

Then since z_n receives the same weight as z_{n+Mj} in (19), regardless of the value of k, (19) can be expressed as

$$C\left(\frac{2\pi k}{M\Delta}\right) = \frac{1}{2} + \frac{k}{M} - \frac{1}{\pi} \operatorname{Im} \left\{ \sum_{n=0}^{M-1} \exp(-i2\pi nk/M) \hat{z}_n \right\}. \quad (22)$$

Relation (22) is exact and valid for all k. Since we are only interested in the positive neighborhood of $v=0$ in (18), we confine attention in (22) to $0 \leq k \leq M-1$.^{*} Relation (22) can then be accomplished by an M-point FFT if M is chosen to be a power of 2. Notice that storage only for the M complex numbers $\{\hat{z}_n\}$ in (21) is required, even though the $\{z_n\}$ sequence in (20) is of infinite length.

^{*} Values for other k are available from (22) when we observe that

$$C\left(\frac{2\pi(M+k)}{M\Delta}\right) = 1 + C\left(\frac{2\pi k}{M\Delta}\right) \text{ for all } k.$$

Observe that the size of M in no way affects the error of the calculation of $C(\frac{2\pi k}{M\Delta})$ or estimation of $P_y(v)$. Rather, M specifies the spacing at which $C(\frac{2\pi k}{M\Delta})$ is calculated, and can be coarse if desired. The accuracy of the estimate of $P_y(v)$ is governed thus far by Δ , through the aliasing depicted in figure 2.

Reference to (18) now yields

$$P_x(\frac{2\pi k}{M\Delta} - b) \cong C(\frac{2\pi k}{M\Delta}) \quad \text{for } 0 \leq k \leq M-1, \quad (23)$$

where the latter quantity is given by (22). Thus the M -point FFT sweeps out the argument range $(-b, -b+2\pi/\Delta)$ for the cumulative distribution function P_x .

If we want the exceedance distribution function of y instead of the cumulative distribution function, we use (18) and (22) to get

$$1 - C(\frac{2\pi k}{M\Delta}) = \frac{1}{2} - \frac{k}{M} + \frac{1}{\pi} \operatorname{Im} \left\{ \sum_{n=0}^{M-1} \exp(-i2\pi nk/M) \hat{z}_n \right\} \quad \text{for } 0 \leq k \leq M-1. \quad (24)$$

(By the footnote to (22), we have $1 - C(2\pi/\Delta) = -C(0)$.)

Since μ_y must be known in (20) in order to use this approach, we need the mean μ_x of random variable x , since from (2)

$$\mu_y = \mu_x + b. \quad (25)$$

The quantity μ_x can be found analytically from characteristic function $f_x(\mathcal{F})$ according to

$$f'_x(0) = i\mu_x; \quad (26)$$

see (1).

In addition to the error caused by aliasing associated with nonzero sampling increment Δ , an additional error occurs because we cannot calculate all the coefficients $\{z_n\}$ in (20) and (21) out to $n=+\infty$. Rather, we terminate the calculation at integer $n=N$, such that $|z_n|$ is sufficiently small as to be negligible for $n \geq N$. Letting

$$L = N\Delta, \quad (27)$$

this is equivalent to ignoring the contribution to (5) of the tail error

$$-\int_L^{+\infty} d\mathfrak{F} g(\mathfrak{F}, v) = -\text{Im} \int_L^{+\infty} d\mathfrak{F} \exp(-i\mathfrak{F}v) \frac{f_y(\mathfrak{F})}{\pi\mathfrak{F}}. \quad (28)$$

If the asymptotic behavior of $f_y(\mathfrak{F})$ for large \mathfrak{F} is known, this error can sometimes be evaluated in closed form and used to ascertain an adequate value of L . Instead, we have observed that tail error (28) causes a characteristic low-level sinusoidal variation in the calculated cumulative distribution function for small v near 0, and in the calculated exceedance distribution function for large v near $2\pi/\Delta$. When this sinusoidal variation is deemed excessive, L can be increased until the effect disappears or decreases to acceptable levels. This trial and error approach avoids the necessity of analytically upper-bounding the magnitude of error (28), which is often very tedious and generally pessimistic.

So there are two errors to be concerned with: aliasing due to nonzero sampling interval Δ and tail error due to non infinite limit L . Later examples will demonstrate how these errors manifest themselves in the cumulative and exceedance distribution functions and how they can be controlled by a trial and error approach.

Relation to Requicha's Method, ref. 5

From ref. 5, eqs. 7, 9, 10, the cumulative distribution function is given by an expression that can be manipulated into the form (using current notation)

$$F_k = \frac{k}{M} - \frac{1}{\pi} \operatorname{Im} \left\{ \sum_{n=1}^{M/2} \exp(-i2\pi kn/M) \frac{f_y(n\Delta)}{n} \right\} + \frac{1}{\pi} \operatorname{Im} \left\{ \sum_{n=1}^{M/2} \frac{f_y(n\Delta)}{n} \right\}. \quad (29)$$

Although this is similar to the upper line of (19) here, it differs in several important respects:

1. F_k does not use mean μ_y at all; it is therefore not using a direct approximation to the specified integral in (5) and (6).
2. From (29), there follows $F_0 = 0$, $F_M = 1$; however, these results are not strictly true for the actual cumulative distribution function at these end points, thereby leading to poor estimates in the neighborhoods of these points. This is due to the arbitrary origin established in ref. 5, eq. 6.
3. The sums in (29) utilize characteristic function samples $f_y(n\Delta)$ only for $n \leq M/2$, where M is the size of the FFT. This is a very severe and unnecessary restriction; in fact, the sum on n in (29) ought to be conducted to the point where the tail contribution, (28), is negligible, regardless of the value of M .
4. In ref. 5, if eq. 4 is substituted into eq. 1, and the summation limits are extended to $\pm\infty$, we get exactly the second line of (12) here. When the probability density function is integrated to get the cumulative distribution function in ref. 5, eq. 6, the resultant cumulative distribution function is arbitrarily set to zero at $v=0$. We instead have from (9) and (17),

$$P_y(0) \cong C(0) = \frac{1}{2} - \frac{\Delta\mu_y}{2\pi} - \frac{1}{\pi} \operatorname{Im} \left\{ \sum_{n=1}^{+\infty} \frac{f_y(n\Delta)}{n} \right\}, \quad (30)$$

which is small, but not necessarily zero. This consideration is very important on the tails of the cumulative and exceedance distribution functions.

Summary of Procedure

The cumulative distribution function of y is given by

$$P_y\left(\frac{2\pi k}{M\Delta}\right) = C\left(\frac{2\pi k}{M\Delta}\right) = \frac{1}{2} + \frac{k}{M} - \frac{1}{\pi} \operatorname{Im} \left\{ \sum_{n=0}^{M-1} \exp(-i2\pi nk/M) \hat{z}_n \right\}$$

for $0 \leq k \leq M-1$, (31)

where M is the size of the FFT and storage employed. Also

$$\hat{z}_n = \sum_{j=0}^{+\infty} z_{n+Mj} \quad \text{for } 0 \leq n \leq M-1, \quad (32)$$

where

$$z_n = \begin{cases} \frac{1}{2} i \Delta \mu_y & \text{for } n=0 \\ f_y(n\Delta)/n & \text{for } 1 \leq n \leq N \\ 0 & \text{for } n > N \end{cases}. \quad (33)$$

(The value for $n=N$ should be scaled by $1/2$ for the Trapezoidal rule).

The zero values for z_n , when $n > N$, serve to terminate the collapsed sum in (32) at a finite upper limit. The value of N is given by the integer part of L/Δ , where Δ and L must be chosen so as to minimize aliasing and tail error, respectively. The characteristic function of random variable y needed in (33) is given by

$$f_y(\mathcal{F}) = f_x(\mathcal{F}) \exp(ib\mathcal{F}), \quad (34)$$

in terms of the characteristic function of the primary random variable x , where shift b must be chosen such that $y = b+x$ is positive with probability virtually 1. The mean $\mu_y = b + \mu_x$ can be determined analytically from knowledge of characteristic function $f_x(\mathcal{F})$. Finally, the exceedance distribution function for random variable y is obtained by subtracting (31) from 1.

EXAMPLES

Programs for the following five examples are listed in appendix B.

1. Chi-Square

A chi-square variate of $2K$ degrees of freedom has probability density function (ref. 10)

$$p_x(v) = \frac{v^{K-1} \exp(-v/2)}{2^K (K-1)!} \quad \text{for } v > 0 \quad (35)$$

and characteristic function

$$f_x(\mathcal{F}) = (1 - i2\mathcal{F})^{-K}. \quad (36)$$

Since random variable x is obviously nonnegative by (35), we can choose shift $b=0$; i.e. $y=x$. A plot of the cumulative and exceedance distribution functions of random variable y obtained from characteristic function (36) with $K=4$ is given in figure 3 for $0 \leq v \leq 2\pi/\Delta$. The values of Δ and L have been chosen such that aliasing and tail error are insignificant.

The ordinate scale for figure 3 is a logarithmic one. The lower right end of the exceedance distribution function curve decreases smoothly to the region $1E-11$, where round-off noise is encountered. The exceedance distribution function values continue to decrease with v until, finally, negative values (due to round-off noise) are generated. For negative probability values, the logarithm of the absolute value is plotted, but mirrored below the $1E-12$ level. These values have no physical significance, of course; they are plotted to illustrate the level of accuracy attainable by this procedure with appropriate choices of Δ and L .

For this example, $N=L/\Delta=2666$, while $M=256$. Thus collapsing, according to (21) or (32), by over a factor of 10 has been employed and a small size FFT has been utilized. Nevertheless the error realized for the cumulative and exceedance distribution functions is in the $1E-12$ range, the limit of accuracy of the Hewlett Packard 9845B Desk Calculator used here. Finer spacing in the distribution outputs is achievable by merely increasing M .

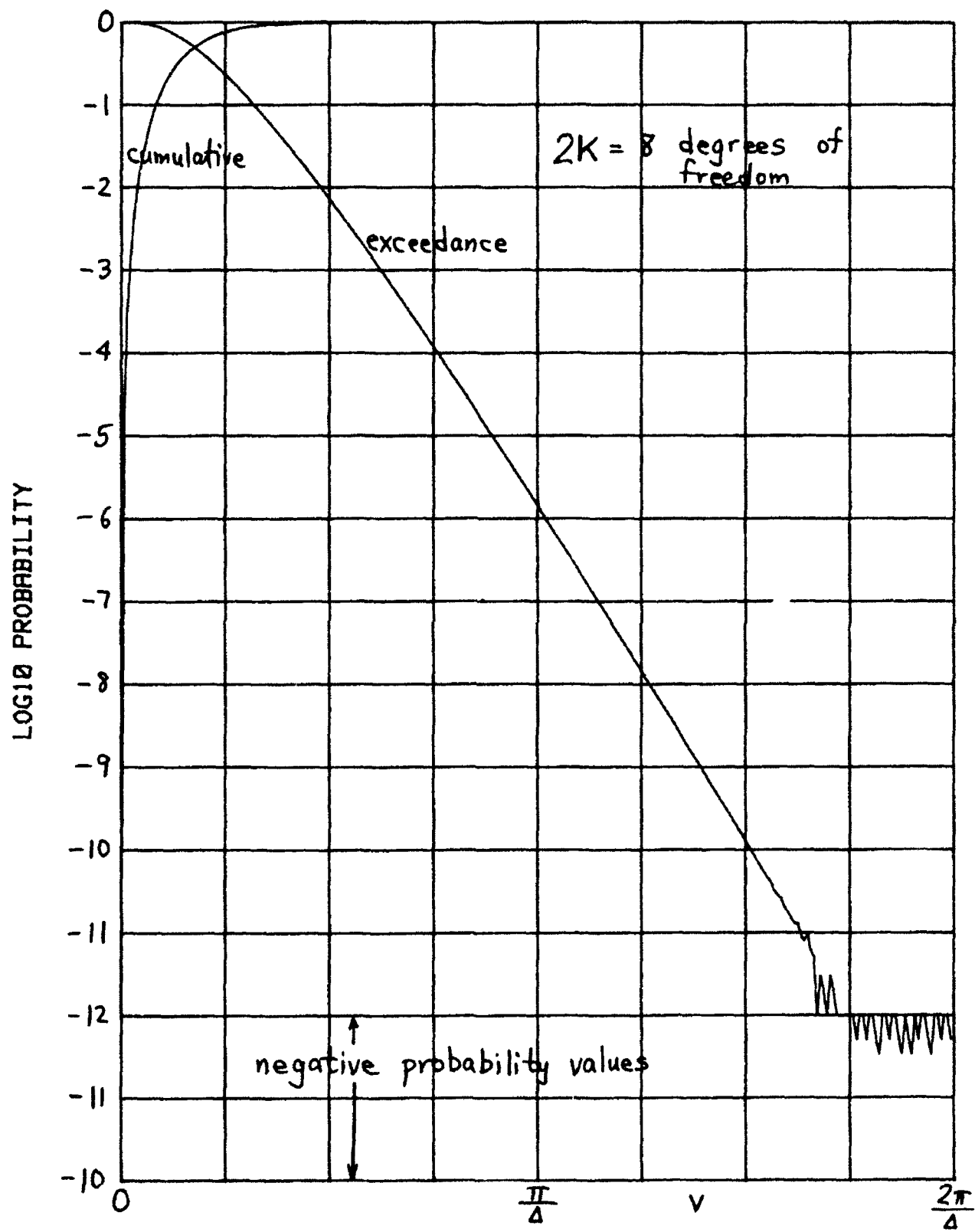


Figure 3. Chi-Square; L=200, $\Delta=.075$, b=0, M=256

2. Gaussian

The characteristic function for a zero-mean unit-variance random variable is

$$f_x(\xi) = \exp(-\xi^2/2), \quad (37)$$

and the probability density function and cumulative distribution function are (ref. 11, eq. 10.5.3)

$$p_x(v) = (2\pi)^{-1/2} \exp(-v^2/2), \quad P_x(v) = \Phi(v). \quad (38)$$

For $b = 5\pi/2$, using (4),

$$P_y(0) = P_x(-b) = \Phi(-b) = 2E-15. \quad (39)$$

which is negligible, as desired.

Plots of the cumulative and exceedance distribution functions for random variable y are given in figure 4 for $L=7$, $\Delta=.3$. The logarithmic ordinate gives rise to the characteristic parabolic shape on the tails of the distributions. Once again, the probabilities decrease to the level of the round-off noise and fluctuate around $1E-12$ near the edges of the fundamental aliased interval $(0, 2\pi/\Delta)$. The fact that the cumulative distribution function of y starts in the round-off noise at $v=0$ indicates that $b=5\pi/2$ was large enough to guarantee $y > 0$ with probability virtually 1. Also indicated on the figure is the origin for random variable x . We have, from (4),

$$P_x(u) = P_y(u+b); \quad (40)$$

thus for example

$$\text{Prob}(x < 0) = P_x(0) = P_y(b) = .5. \quad (41)$$

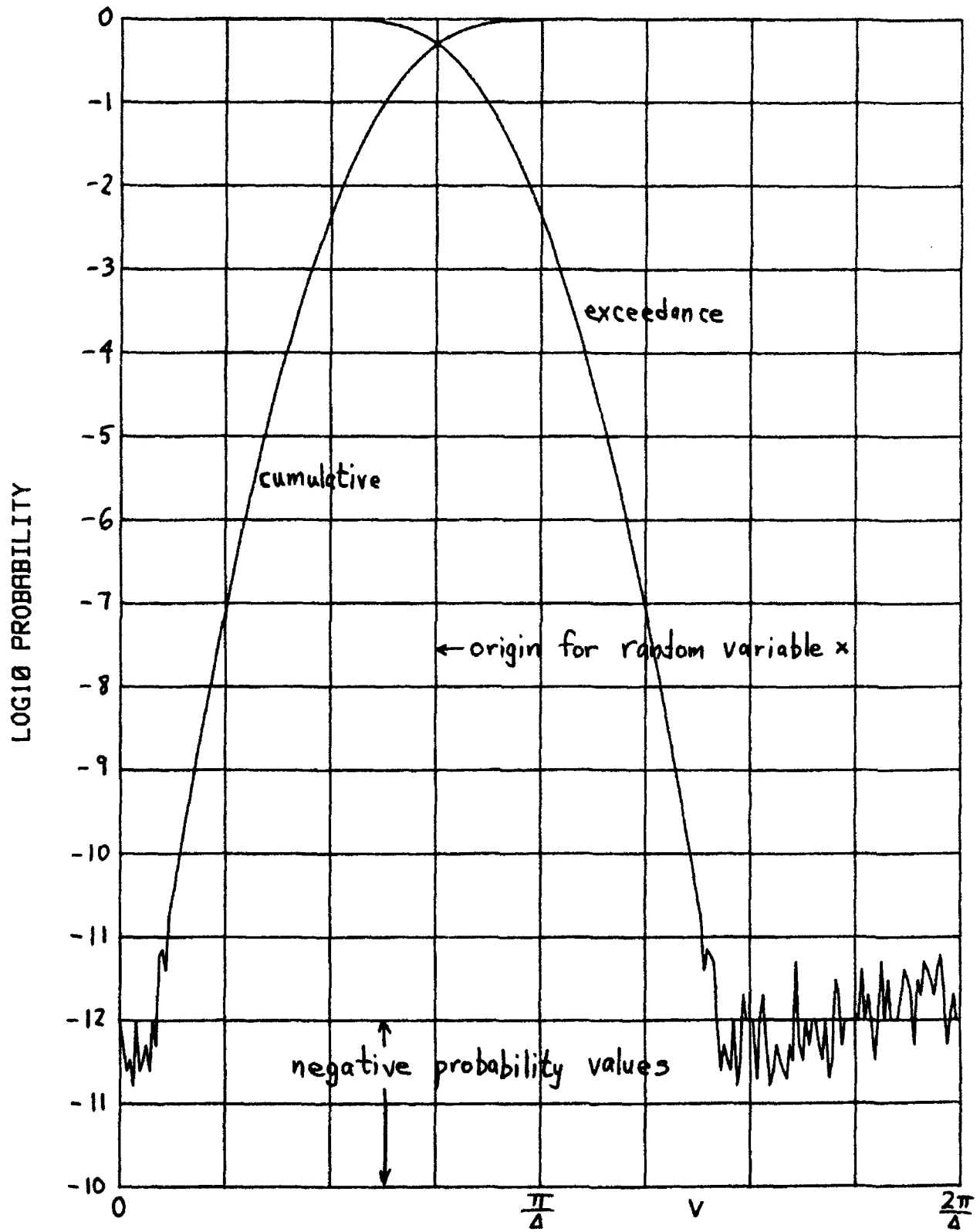


Figure 4. Gaussian; $L=7$, $\Delta=.3$, $b=2.5\pi$, $M=256$

In figure 5, the only change is to decrease limit L from 7 to 6. The tail error mentioned in (28) et seq. then dominates the round-off noise and has a sinusoidal variation. Aliasing is not a problem, as witnessed by the fact that the cumulative and exceedance distribution functions of random variable y have decayed below $1E-12$ well before the edges of the interval are reached.

When limit L is restored to 7, and sampling increment Δ is increased to .5, aliasing becomes significant, as shown in figure 6. The exceedance distribution function has not yet decayed to the round-off noise level at $v=2\pi/\Delta$, and the cumulative distribution function shows a large negative probability region near $v=0$. Shift b has been maintained at the value $5\pi/2$, corresponding to (39).

When L and Δ are restored to their values 7 and .3 as for figure 4, but b is decreased to $5\pi/3$, the probability of y becoming negative is, from (4) and (38), $\Phi(-5\pi/3) = .82E-7$. This is reflected in the cumulative distribution function for y in figure 7 at $v=0$, where the probability value is well above the round-off noise level. Also, the exceedance distribution function develops significantly negative values near $v = 2\pi/\Delta$.

Accurate evaluation of the cumulative and exceedance distribution functions can only be achieved when L , Δ , and b are properly chosen. Probably the optimum combination for the Gaussian variate is displayed in figure 8, where Δ has been increased to .4, the distributions are centered on the fundamental aliased interval $(0, 2\pi/\Delta)$ by choice of b , and L is taken at 7 to avoid tail error.

3. Smirnov

The limiting characteristic function of a measure of goodness of fit based on the sample distribution function was derived by Smirnov and is given by (ref. 12, eq. 30.104)

$$f_x(\xi) = \left(\frac{s}{\sin(s)} \right)^{1/2} \quad \text{where } s = (1+i)\sqrt{\xi} \quad \text{for } \xi \geq 0. \quad (42)$$

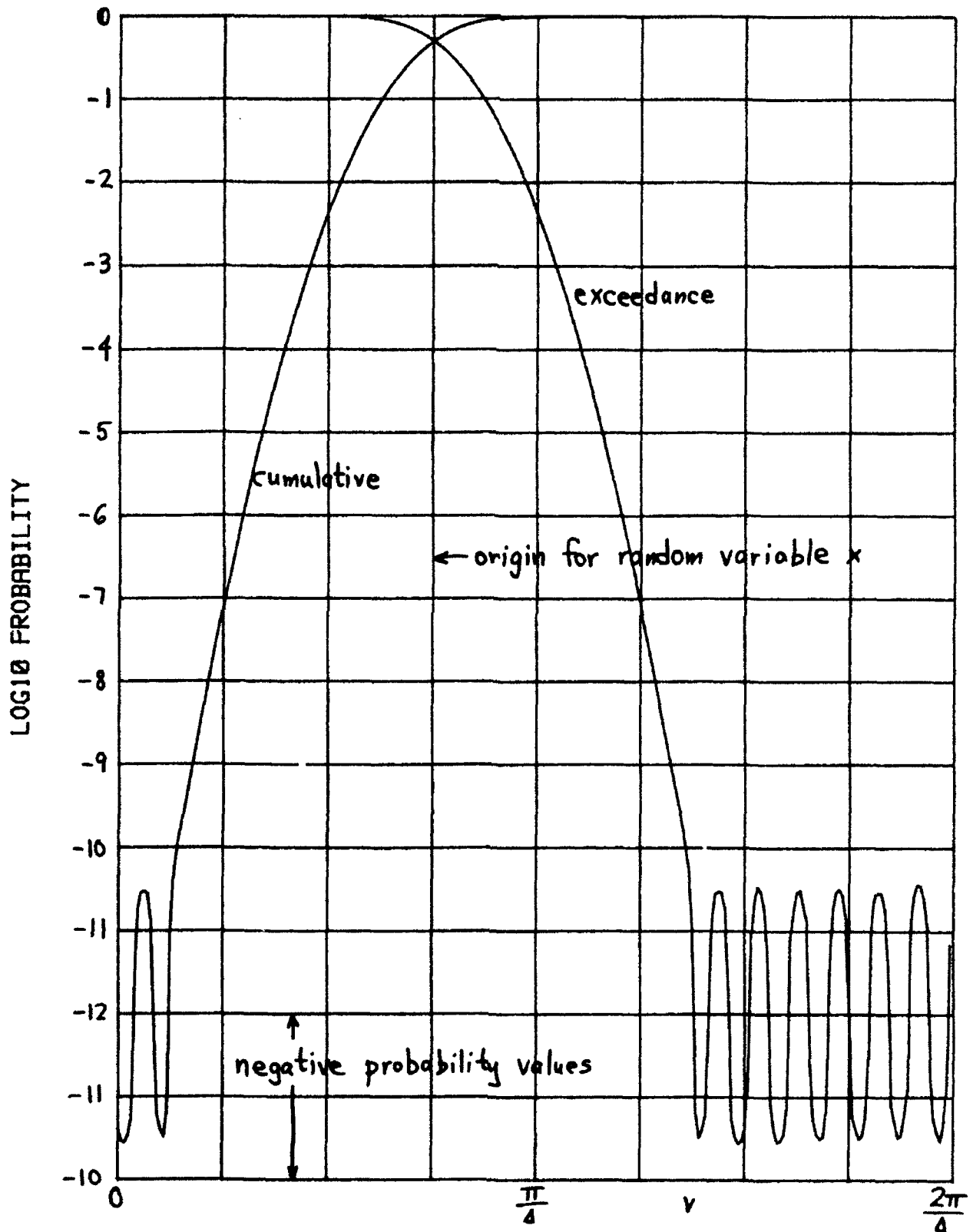


Figure 5. Gaussian; $L=6$, $\Delta=.3$, $b=2.5\pi$, $M=256$

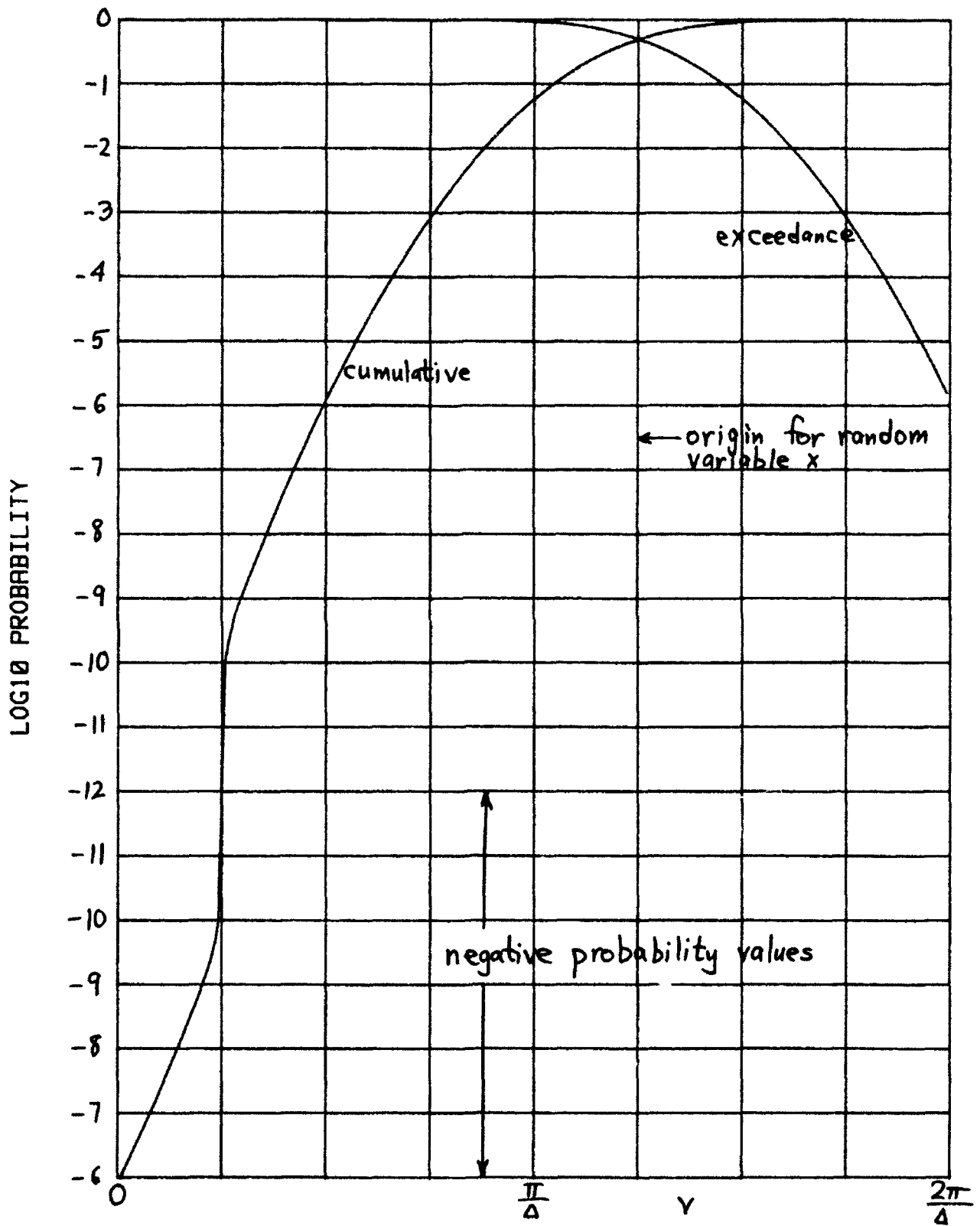


Figure 6. Gaussian; $L=7$, $\Delta=.5$, $b=2.5\pi$, $M=256$

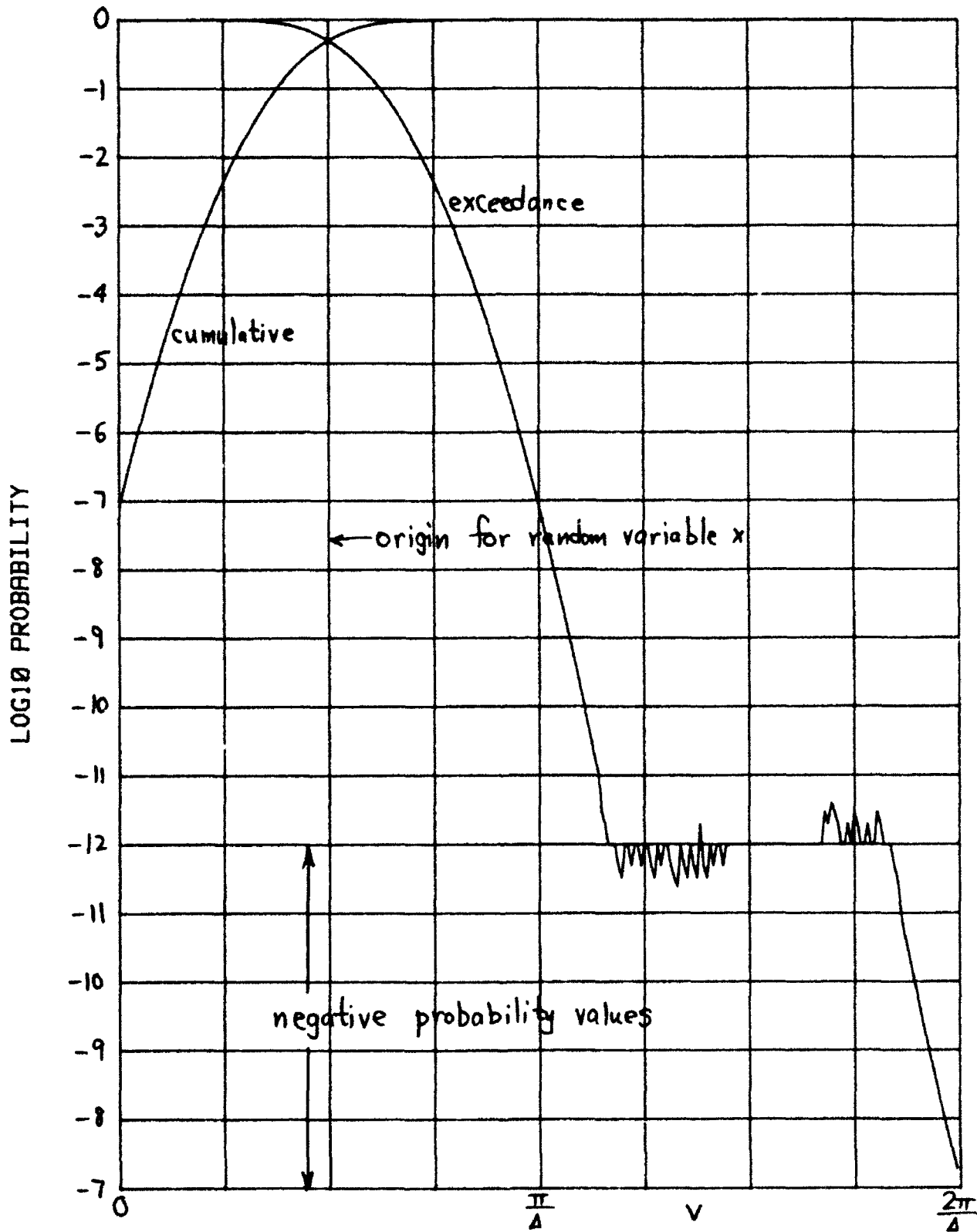


Figure 7. Gaussian; $L=7$, $\Delta=.3$, $b=5\pi/3$, $M=256$

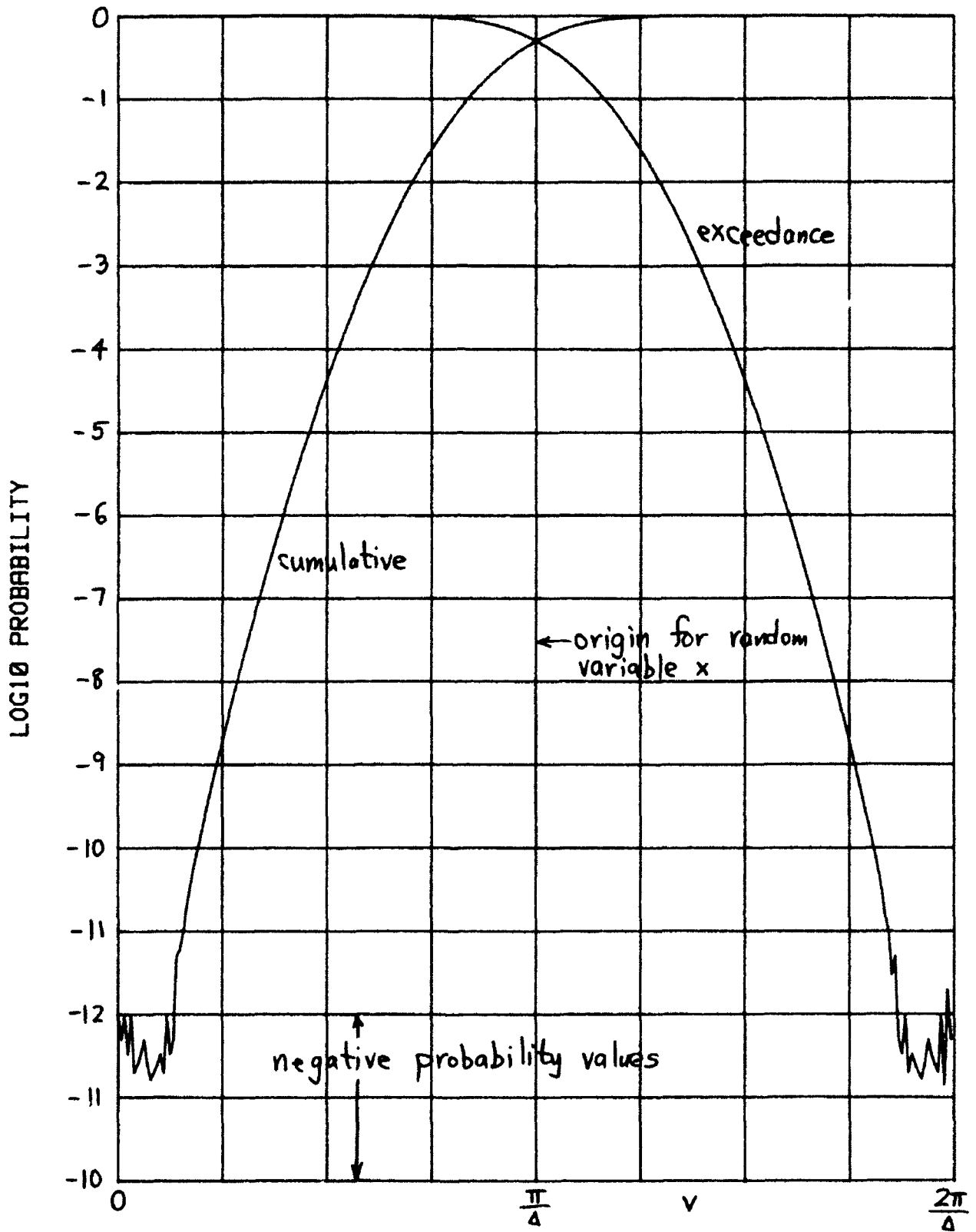


Figure 8. Gaussian; $L=7$, $\Delta=.4$, $b=2.5\pi$, $M=256$

An expansion about $\xi=0$ yields

$$f_x(\xi) = 1 + i \frac{1}{6} \xi - \frac{1}{40} \xi^2; \quad \text{i.e., } \mu_x = 1/6, \sigma_x^2 = 1/45. \quad (43)$$

And since the goodness of fit is always positive, random variable x is positive and we can choose

$$b=0. \quad (44)$$

Since

$$\sin((1+i)\sqrt{\xi}) \sim i \frac{1}{2} \exp(\sqrt{\xi}(1-i)) \quad \text{as } \xi \rightarrow +\infty, \quad (45)$$

it follows that

$$f_x(\xi) \sim 2^{3/4} \xi^{1/4} \exp(-\frac{1}{2}\sqrt{\xi} + i(\frac{1}{2}\sqrt{\xi} - \frac{\pi}{8})) \quad \text{as } \xi \rightarrow +\infty. \quad (46)$$

The phase of this term rotates according to $\sqrt{\xi}/2$; if we were to choose $b \neq 0$, $f_y(\xi)$ would rotate faster than $f_x(\xi)$ (linear with ξ rather than $\sqrt{\xi}$). This could necessitate a faster sampling rate, which is undesirable.

The cumulative and exceedance distribution functions are plotted in figure 9. L and Δ have been chosen so as to avoid tail error and aliasing. The exceedance distribution function is seen to decay exponentially until it reaches approximately $2E-11$; the bump in the curve at this point is a manifestation of the limited accuracy of the trigonometric functions built into the calculator employed. Larger values of v lead to round-off noise around the $1E-12$ level.

A comparison of results for this characteristic function, with Requicha's method described in (29) et seq., is given in figure 10 for FFT size $M=1024$. The plot labeled with $N=L=512$ is precisely Requicha's method. Aliasing is known to be insignificant for $\Delta=1$, as seen by reference to figure 9 and observing that extrapolation of the straight line section of the exceedance distribution function would result in probability values near $1E-13$ at $v=2\pi/\Delta$. The dashed portion of the $N=L=512$ curve in figure 10 in fact

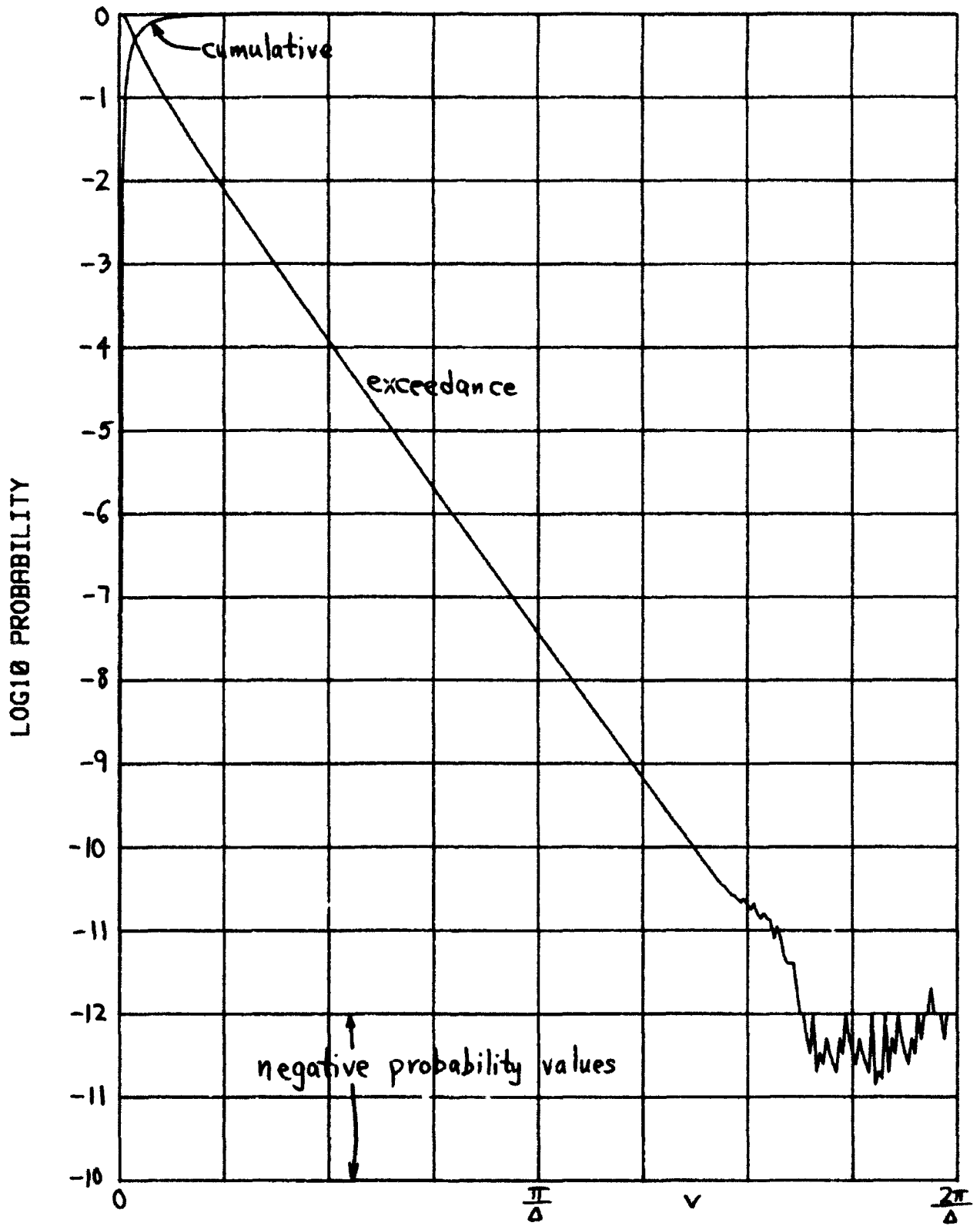


Figure 9. Smirnov; L=3000, $\Delta=1$, b=0, M=256

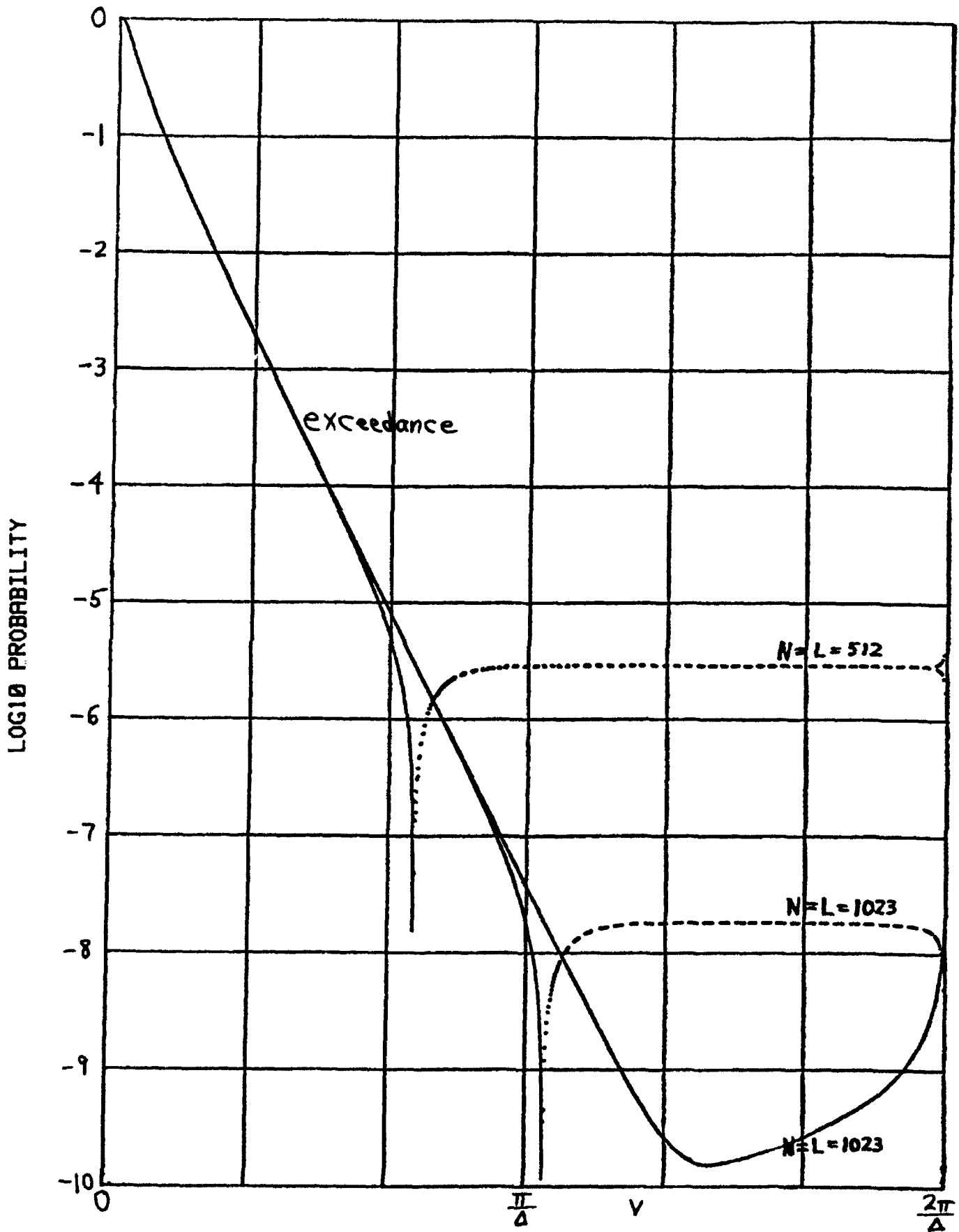


Figure 10. Comparison with Requicha's Method;
 $\Delta=1$, $b=0$, $M=1024$

corresponds to negative probability estimates; these grossly inaccurate results are due to an inadequate value of limit L , leading to large tail error.

When N is simply increased to 1023, the middle curve in figure 10 results from Requicha's method. Again, negative estimates are indicated by the dashed portion of this curve, although two orders of magnitude smaller than above. The reasons for these errors have been delineated in (29) et seq.

The bottom-most curve in figure 10 (solid curve) is that obtained by the method proposed in this report for $L = 1023$. Exceedance distribution function estimates in the $1E-10$ range are obtained, but the error returns to the $1E-8$ range at $v=2\pi/\Delta$. No negative probability values occur. Also, by simply increasing limit L , while keeping FFT size M fixed, the error can be reduced significantly further, as already witnessed by figure 9.

4. Noncentral Chi-Square

Here the random variable x is given by

$$x = \sum_{k=1}^K (g_k + d_k)^2 \quad (47)$$

where $\{d_k\}$ are constants, and $\{g_k\}$ are independent Gaussian random variables with zero-mean and unit variance. The characteristic function of x is

$$f_x(\xi) = (1-i2\xi)^{-K/2} \exp\left(\frac{id^2\xi}{1-i2\xi}\right), \quad (48)$$

where deflection d is defined according to

$$d^2 = \sum_{k=1}^K d_k^2. \quad (49)$$

We actually consider a more general characteristic function than (48), namely

$$f_x(\xi) = (1-i2\xi)^{-\nu} \exp\left(\frac{id^2\xi}{1-i2\xi}\right) = \exp\left(\frac{id^2\xi}{1-i2\xi} - \nu \ln(1-i2\xi)\right), \quad (50)$$

where ν is an arbitrary positive real constant. Suppose that we use the principal value logarithm for $\ln(z)$, where the branch cut lies along the negative real axis of the complex z plane (ref. 13, sect. 4.1.1). Then since the argument of the logarithm in (50) never crosses the branch cut, form (50) gives the correct characteristic function values automatically for all real ξ , and any ν .

The probability density function and exceedance distribution function corresponding to (50) are (ref. 14, 6.631 4)

$$p_x(v) = \frac{1}{2} \exp\left(-\frac{d^2+v}{2}\right) \left(\frac{\sqrt{v}}{d}\right)^{\nu-1} I_{\nu-1}(d\sqrt{v}) \quad \text{for } v > 0,$$

$$1 - P_x(v) = \int_{\sqrt{v}}^{+\infty} dt \, t \exp\left(-\frac{d^2+t^2}{2}\right) \left(\frac{t}{d}\right)^{\nu-1} I_{\nu-1}(dt) \equiv Q_\nu(d, \sqrt{v}) \quad \text{for } v > 0. \quad (51)$$

Since the probability density function in (51) is never negative (ref. 13, sect. 9.6.1), (50) is a legal characteristic function. Also because random variable x is always positive according to (51), we choose shift $b=0$. Plots of the exceedance distribution function, as determined from characteristic function (50) are displayed for various values of d in figure 11. The values of L were chosen for each d value so as to control the tail error below the $1E-10$ level plotted. Direct calculation of the exceedance distribution function directly from (51) would be a formidable task for arbitrary ν values.

5. Product of Correlated Gaussian Variates

Let

$$x = st \quad (52)$$

where s and t are zero-mean unit-variance Gaussian random variables with correlation coefficient ρ . The joint probability density function of s and t is

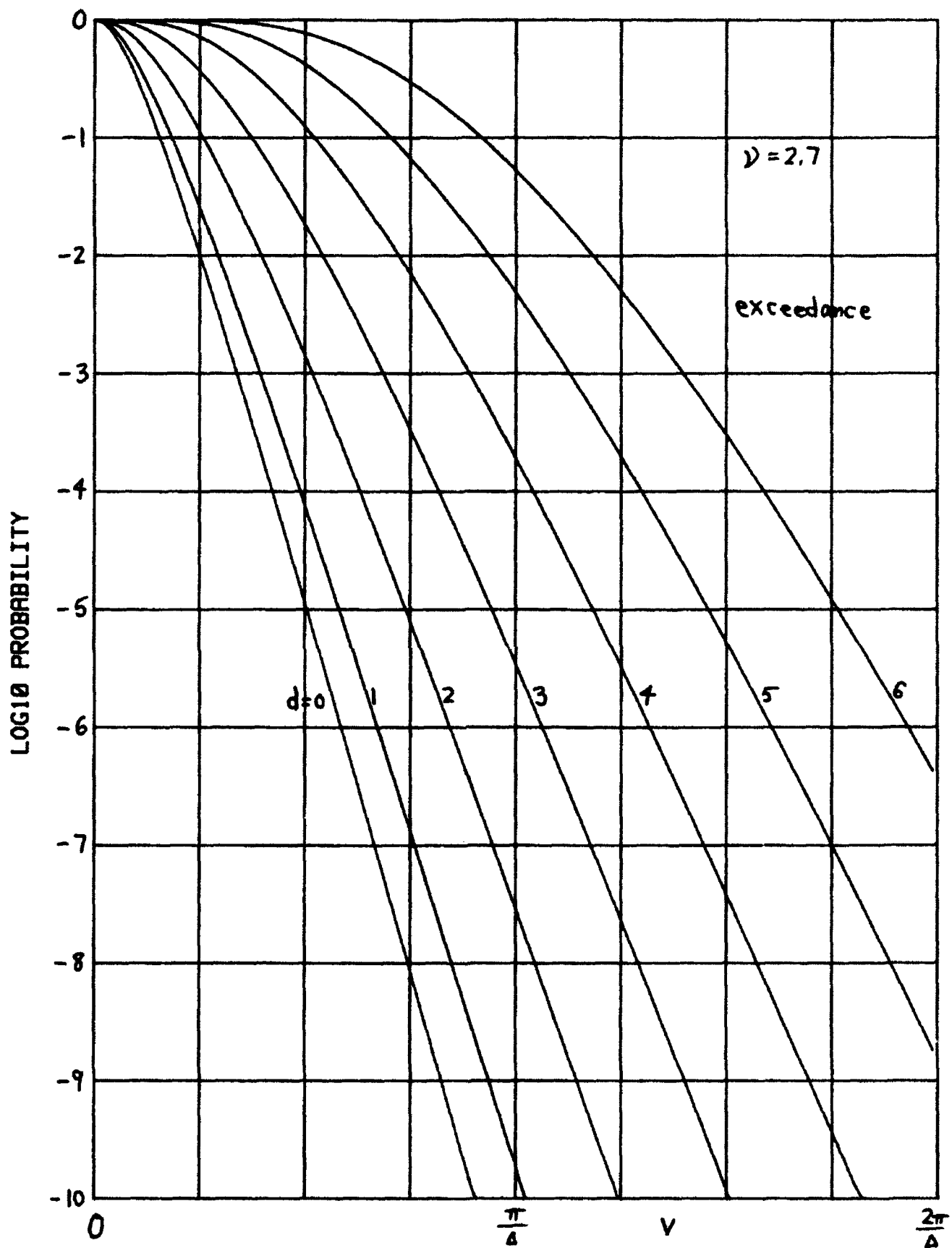


Figure 11. Non-Central Chi-Square; $\Delta = .05$, $b = 0$, $M = 256$

$$p_{st}(u,v) = \left(2\pi\sqrt{1-\rho^2}\right)^{-1} \exp\left[-\frac{u^2+v^2-2\rho uv}{2(1-\rho^2)}\right]. \quad (53)$$

The characteristic function of x is then

$$\begin{aligned} f_x(\xi) &= \overline{\exp(i\xi st)} = \iint du dv \exp(i\xi uv) p_{st}(u,v) = \\ &= \left[1-i2\rho\xi+(1-\rho^2)\xi^2\right]^{-1/2} = \left[1-i(1+\rho)\xi\right]^{-1/2} \left[1+i(1-\rho)\xi\right]^{-1/2}, \end{aligned} \quad (54)$$

via repeated use of ref. 14, eq. 3.323 2. The corresponding probability density function of x is

$$p_x(v) = \int \frac{dy}{|y|} p_{st}(y, \frac{v}{y}) = \frac{1}{\pi\sqrt{1-\rho^2}} \exp\left(\frac{\rho v}{1-\rho^2}\right) K_0\left(\frac{|v|}{1-\rho^2}\right) \text{ for all } v, \quad (55)$$

via ref. 14, eq. 3.478 4.

(If we transform this probability density function according to (1) and use ref. 14, eq. 6.611 9 and ref. 13, eq. 4.4.15, we get precisely (54). Alternatively, if we transform (54) and modify the contour to wrap around the branch line along the imaginary axis and then use ref. 14, eq. 3.388 2, we get (55). Or we can use ref. 14, eq. 3.754 2.)

We actually consider a more general characteristic function than (54), namely

$$\begin{aligned} f_x(\xi) &= \left[1-i2\rho\xi+(1-\rho^2)\xi^2\right]^{-\nu} = \exp\left(-\nu \ln\left[1-i2\rho\xi+(1-\rho^2)\xi^2\right]\right) = \\ &= \left[\frac{1}{1-\rho^2} + \left\{\sqrt{1-\rho^2}\xi - i\frac{\rho}{\sqrt{1-\rho^2}}\right\}^2\right]^{-\nu}. \end{aligned} \quad (56)$$

The mean of this random variable x is given by

$$\mu_x = 2\nu\rho. \quad (57)$$

The probability density function corresponding to (56) is

$$p_x(v) = \frac{1}{2\pi} \int d\xi \exp(-i\xi v) f_x(\xi) =$$

$$= \frac{1}{2\pi\sqrt{1-\rho^2}} \int_{-\infty - i\rho/\sqrt{1-\rho^2}}^{+\infty - i\rho/\sqrt{1-\rho^2}} dy \exp\left(\frac{\rho v}{1-\rho^2} - i \frac{yv}{\sqrt{1-\rho^2}}\right) \left(\frac{1}{1-\rho^2} + y^2\right)^{-v}, \quad (58)$$

where we let

$$y = \sqrt{1-\rho^2} \xi - i \frac{\rho}{\sqrt{1-\rho^2}}. \quad (59)$$

We can move the contour in (58) to the real y -axis, because the branch points of the integrand are at $y = \pm i/\sqrt{1-\rho^2}$ which are outside the path of integration, since $|\rho| < 1$. Then using ref. 14, eq. 3.771 2 and ref. 13, eq. 6.1.17, we obtain

$$p_x(v) = \left(\sqrt{\pi} \Gamma(v) \sqrt{1-\rho^2}\right)^{-1} \left(\frac{|v|}{2}\right)^{v-\frac{1}{2}} \exp\left(\frac{\rho v}{1-\rho^2}\right) K_{v-\frac{1}{2}}\left(\frac{|v|}{1-\rho^2}\right) \quad \text{for all } v. \quad (60)$$

Since this probability density function is never negative (ref. 13, sect. 9.6.1), (56) is a legal characteristic function. If we Fourier transform (60) via ref. 14, 6.699 12, we get (56) directly.

There is no simple relation for the cumulative distribution function of this random variable. Nevertheless, it is a simple matter to evaluate directly from characteristic function (56). The \ln in (56) causes no problems since its argument never crosses the branch cut. A plot for $v=7.7$ and $\rho=-.3$ is displayed in figure 12. The rate of decay of the distribution is different for each tail. The round-off noise is clearly visible at both ends of the range of v values.

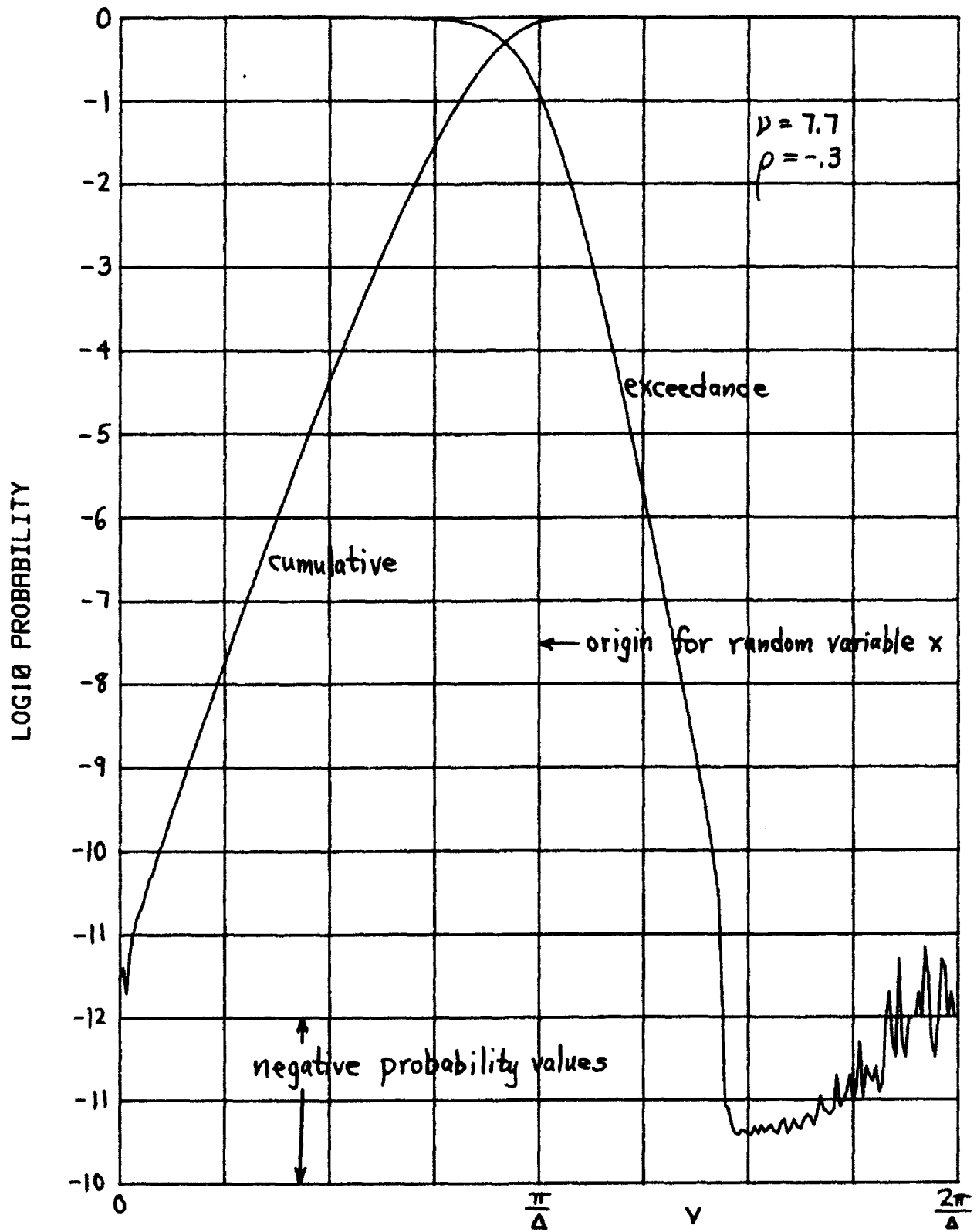


Figure 12. Gaussian Product; $L=5$, $\Delta=.06$, $b=5G\pi/3$, $M=256$

APPLICATIONS

We now have the capability to handle the following type of statistical problem in a fairly easy fashion. Consider random variable

$$x = \sum_{k=1}^K r_k^{v_k}, \quad (61)$$

where $\{r_k\}$ are arbitrary random variables, statistically independent of each other, and with different distributions. Power v_k is arbitrary (except that v_k must be a positive integer for those r_k that can become negative). Let the probability density function of random variable r_k be $p_k(v)$. Then the characteristic function of $r_k^{v_k}$ is

$$\begin{aligned} g_k(\xi) &= \overline{\exp(i\xi r_k^{v_k})} = \int dv \exp(i\xi v^{v_k}) p_k(v) = \\ &= \frac{1}{v_k} \int \frac{dt}{t} \exp(i\xi t) t^{1/v_k} p_k\left(t^{1/v_k}\right). \end{aligned} \quad (62)$$

If (62) is not integrable in closed form, it can be evaluated by means of an FFT (one for each k if the probability density functions or v_k are all different). Then the characteristic function of random variable x in (61) is given by

$$f_x(\xi) = \prod_{k=1}^K \{g_k(\xi)\}. \quad (63)$$

Now the techniques of this report are directly applicable to (63).

An additional example is afforded by

$$x = \sum_{k=1}^K \alpha_k v_k^2 + \left(\sum_{k=1}^K \beta_k v_k \right)^2 + \sum_{k=1}^K \gamma_k v_k, \quad (64)$$

where $\{\alpha_k\}$, $\{\beta_k\}$, and $\{\gamma_k\}$ are constants, and $\{v_k\}$ are independent random variables with arbitrary probability density functions. The characteristic function of x is

$$f_x(\xi) = \overline{\exp(i\xi x)} = \int dV p_V(V) \exp(i\xi [\sum_{k=1}^K \alpha_k v_k^2 + (\sum_{k=1}^K \beta_k v_k)^2 + \sum_{k=1}^K \gamma_k v_k]), \quad (65)$$

where $V = (v_1, v_2, \dots, v_K)$. Now since

$$\left(\frac{ia}{\pi}\right)^{1/2} \int dy \exp(-ia y^2 + iby) = \exp\left(\frac{ib^2}{4a}\right) \text{ for } a \neq 0, \quad (66)$$

we identify $a = \xi/4$, $b = \xi \sum \beta_k v_k$, eliminate the square in the exponent, and express (65) as

$$\begin{aligned} f_x(\xi) &= \int dV p_V(V) \exp(i\xi \sum_{k=1}^K \alpha_k v_k^2 + i\xi \sum_{k=1}^K \gamma_k v_k) * \\ &\quad * \left(\frac{i\xi}{4\pi}\right)^{1/2} \int dy \exp\left(-\frac{i\xi y^2}{4} + i\xi y \sum_{k=1}^K \beta_k v_k\right) = \\ &= \left(\frac{i\xi}{4\pi}\right)^{1/2} \int dy \exp\left(-\frac{i\xi y^2}{4}\right) \prod_{k=1}^K \left\{ \int dv_k p_k(v_k) \exp(i\xi (\alpha_k v_k^2 + \gamma_k v_k + y \beta_k v_k)) \right\}, \quad (67) \end{aligned}$$

where

$$P_V(V) = \prod_{k=1}^K \{p_k(v_k)\}. \quad (68)$$

The inner integrals in (67) can either be done analytically or numerically. Then the remaining single integral on y must be numerically evaluated to find characteristic function $f_x(\xi)$. As an example, if v_k is exponentially distributed

$$p_k(v) = a_k \exp(-a_k v) \text{ for } v > 0, \quad (69)$$

then the inner integrals in (67) are w-functions; see ref. 13, ch. 7. A simpler method of handling general quadratic expressions like (64) with Gaussian \bar{V} is presented in ref. 15.

SUMMARY

An accurate method for efficient evaluation of the cumulative and exceedance distribution functions has been derived and applied to several examples to illustrate its utility. Choice of the sampling increment Δ applied to the characteristic function controls the aliasing problem, and selection of the limit L minimizes the tail error; the effects of both of these parameters can be observed from sample plots of the distributions and can be modified if needed. Additionally, shift b must be chosen so as to yield a positive random variable with probability virtually 1. The number of distribution values yielded depends on the size of the FFT employed and can be independently selected to yield the desired spacing in distribution values.

APPENDIX A. SAMPLING FOR A FOURIER TRANSFORM

Suppose we are interested in evaluating Fourier transform

$$G(f) = \int dt \exp(-i2\pi ft) g(t). \quad (A-1)$$

If we sample at interval Δ in t in (A-1), and use integration weighting $w(t)$, we have the approximation to $G(f)$,

$$\begin{aligned} \tilde{G}(f) &\equiv \int dt \exp(-i2\pi ft) g(t) \delta_{\Delta}(t) w(t) \\ &= G(f) \otimes \frac{1}{\Delta} \delta_{\frac{1}{\Delta}}(f) \otimes W(f) \\ &= \frac{1}{\Delta} \sum_n G(f - \frac{n}{\Delta}) \otimes W(f), \end{aligned} \quad (A-2)$$

where infinite impulse train (sampling function)

$$\delta_{\Delta}(t) = \sum_n \delta(t - n\Delta), \quad (A-3)$$

and \otimes denotes convolution.

The term

$$\frac{1}{\Delta} \sum_n G(f - \frac{n}{\Delta}) \quad (A-4)$$

in (A-2) is an infinitely aliased version of desired function $G(f)$; this aliasing is an unavoidable effect due to sampling at increment Δ . However, to minimize any further aliasing in (A-2), we would like $W(f) = \delta(f)$, which requires $w(t) = 1$ for all t ; strictly, all we need is

$$w(n\Delta) = 1 \quad \text{for all } n. \quad (A-5)$$

That is, the best weighting in (A-2) is uniform.

As an example, for Simpson's rule, we have weighting

$$w(n\Delta) = \dots, \frac{2}{3}, \frac{4}{3}, \frac{2}{3}, \frac{4}{3}, \frac{2}{3}, \dots = 1 + \frac{1}{3}(-1)^n \text{ or } 1 - \frac{1}{3}(-1)^n, \quad (\text{A-6})$$

which can be represented as samples of time function

$$w(t) = 1 + \frac{1}{3} \exp(i\pi t/\Delta) \text{ or } 1 - \frac{1}{3} \exp(i\pi t/\Delta). \quad (\text{A-7})$$

The corresponding transform is

$$\begin{aligned} W(f) &= \int dt \exp(-i2\pi ft) w(t) = \\ &= \delta(f) + \frac{1}{3} \delta(f - \frac{1}{2\Delta}) \quad \text{or} \quad \delta(f) - \frac{1}{3} \delta(f - \frac{1}{2\Delta}). \end{aligned} \quad (\text{A-8})$$

But this window function substituted in (A-2) results in an extra aliasing lobe in $\tilde{G}(f)$, halfway between the unavoidable major lobes of (A-4) at multiples of $1/\Delta$, of magnitude $1/3$ as large. This effect very adversely affects the quality of $\tilde{G}(f)$ insofar as its approximation to the desired $G(f)$ is concerned. Thus the best sampling plan in (A-2) is the equal weight structure of (A-5) when one wants to approximate the Fourier transform of (A-1). For a bounded region, this is modified to the Trapezoidal rule, i.e., half-size weights at the boundaries.

APPENDIX B. LISTINGS OF PROGRAMS FOR FIVE EXAMPLES

The following listings are programs in BASIC for the Hewlett Packard 9845B Desktop Calculator. The FFT utilized is one with the capability of a zero subscript and is listed at the end of the appendix. Mathematically, the FFT programmed is

$$Z_m = \sum_{k=0}^{M-1} \exp(-i2\pi mk/M) z_k \quad \text{for } 0 \leq m \leq M-1,$$

where the arrays $\{z_k\}_0^{M-1}$ and $\{Z_m\}_0^{M-1}$ are handled directly, including the zero-subscript terms z_0 and Z_0 .

A detailed explanation of the first program below for Chi-Squared random variables is as follows: line 20 specifies the parameter K, where 2K is the number of squared-Gaussian random variables summed to yield random variable x. Lines 30-60 require inputs L, Δ, b, M respectively, on the part of the user. Line 110 is the input of mean μ_x of random variable x, as evaluated analytically from characteristic function $f_x(\mathcal{F})$. Lines 180-210 specifically evaluate the characteristic function $f_y(\mathcal{F})$ at general point \mathcal{F} . All of these lines mentioned thus far require inputs on the part of the user and are so noted in the listing by the presence of a single ! on each line; the comments after a double !! are for information purposes only and need not be modified. This convention is also adopted in the remaining listings.

Lines 220-240 accomplish the collapsing operation of (32)-(33). The cumulative and exceedance distribution functions are finally evaluated and stored in arrays X(*) and Y(*) in lines 400-410.

Some further elaboration is necessary for the listing of the Smirnov characteristic function as given by (42). Since a characteristic function is a continuous function of real \mathcal{F} , the square root in (42) is not a principal value square root, but in fact must yield a continuous function in \mathcal{F} . In

order to achieve this, the argument of the square root is traced continuously from $\xi=0$ (line 110). If an abrupt change in phase is detected, a polarity indicator takes note of this fact (line 250) and corrects the final values of characteristic function $f_y(\xi)$ (lines 260-270). No problems are encountered with complex $\sin(z)$ since it is analytic for all z .

```

10 ! CHI-SQUARE CHARACTERISTIC FUNCTION 1/(1-i 2 xi)^4
20   K=4                      ! 2K=8 degrees of freedom
30   L=200                    ! Limit on integral of char. function
40   Delta=.075              ! Sampling increment on char. function
50   Bs=0                     ! Shift b
60   M=2^8                    ! Size of FFT
70   PRINTER IS 0
80   PRINT "L =";L,"Delta =";Delta,"b =";Bs,"M =";M
90   REDIM X(0:M-1),Y(0:M-1)
100  DIM X(0:1023),Y(0:1023)
110  Mux=2*K                   ! Mean of random variable x
120  Muy=Mux+Bs
130  X(0)=0
140  Y(0)=.5*Delta*Muy
150  N=INT(L/Delta)
160  FOR Ns=1 TO N
170  Xi=Delta*Ns              !! Argument xi of char. fn.
180  C=Xi+Xi                  ! Calculation of
190  CALL Mul(1,-C,1,-C,A,B)  ! characteristic
200  CALL Mul(A,B,A,B,C,D)   ! function fy(xi)
210  CALL Div(1,0,C,D,Fyr,Fyi) ! for K=4
220  Ms=Ns MOD M              !! Collapsing
230  X(Ms)=X(Ms)+Fyr/Ns
240  Y(Ms)=Y(Ms)+Fyi/Ns
250  NEXT Ns
260  CALL Fft10z(M,X(*),Y(*)) !! 0 subscript FFT

```

```

270 PLOTTER IS "GRAPHICS"
280 GRAPHICS
290 SCALE 0,M,-14,0
300 LINE TYPE 3
310 GRID M/8,1
320 PENUP
330 LINE TYPE 1
340 B=Bs*M*Delta/(2*PI)           !! Origin for random variable x
350 MOVE B,0
360 DRAW B,-14
370 PENUP
380 FOR Ks=0 TO M-1
390 T=Y(Ks)/PI-Ks/M
400 X(Ks)=.5-T                     !! Cumulative probability in X(*)
410 Y(Ks)=Pr=.5+T                 !! Exceedance probability in Y(*)
420 IF Pr>=1E-12 THEN Y=LGT(Pr)
430 IF Pr<=-1E-12 THEN Y=-24-LGT(-Pr)
440 IF ABS(Pr)<1E-12 THEN Y=-12
450 PLOT Ks,Y
460 NEXT Ks
470 PENUP
480 PRINT Y(0);Y(1);Y(M-2);Y(M-1)
490 FOR Ks=0 TO M-1
500 Pr=X(Ks)
510 IF Pr>=1E-12 THEN Y=LGT(Pr)
520 IF Pr<=-1E-12 THEN Y=-24-LGT(-Pr)
530 IF ABS(Pr)<1E-12 THEN Y=-12
540 PLOT Ks,Y
550 NEXT Ks
560 PENUP
570 PAUSE
580 DUMP GRAPHICS
590 PRINT LIN(5)
600 PRINTER IS 16
610 END
620 |
630 SUB Mu1(X1,Y1,X2,Y2,A,B)      ! Z1*Z2
640 A=X1*X2-Y1*Y2
650 B=X1*Y2+X2*Y1
660 SUBEND
670 |
680 SUB Div(X1,Y1,X2,Y2,A,B)     ! Z1/Z2
690 T=X2*X2+Y2*Y2
700 A=(X1*X2+Y1*Y2)/T
710 B=(Y1*X2-X1*Y2)/T
720 SUBEND
730 |
740 SUB Fft10z(N,X(*),Y(*)      ! N <= 2^10 = 1024, N=2^INTEGER      0 subscript

```

```

10 ! GAUSSIAN CHARACTERISTIC FUNCTION exp(-.5 xi^2)
20 L=7 ! Limit on integral of char. function
30 Delta=.3 ! Sampling increment on char. function
40 Bs=.375*(2*PI/Delta) ! Shift b, as fraction of alias interval
50 M=2^8 ! Size of FFT
60 PRINTER IS 0
70 PRINT "L =";L,"Delta =";Delta,"b =";Bs,"M =";M
80 REDIM X(0:M-1),Y(0:M-1)
90 DIM X(0:1023),Y(0:1023)
100 Mux=0 ! Mean of random variable x
110 Muy=Mux+Bs
120 X(0)=0
130 Y(0)=.5*Delta*Muy
140 N=INT(L/Delta)
150 FOR Ns=1 TO N
160 Xi=Delta*Ns !! Argument xi of char. fn.
170 A=EXP(-.5*Xi*Xi) ! Calculation of
180 B=Bs*Xi ! characteristic
190 Fyr=A*COS(B) ! function
200 Fyi=A*SIN(B) ! fy(xi)
210 Ms=Ns MOD M !! Collapsing
220 X(Ms)=X(Ms)+Fyr/Ns
230 Y(Ms)=Y(Ms)+Fyi/Ns
240 NEXT Ns
250 CALL Fft10z(M,X(*),Y(*)) !! 0 subscript FFT
260 PLOTTER IS "GRAPHICS"
270 GRAPHICS
280 SCALE 0,M,-14,0
290 LINE TYPE 3
300 GRID M/8,1
310 PENUP
320 LINE TYPE 1
330 B=Bs*M*Delta/(2*PI) !! Origin for random variable x
340 MOVE B,0
350 DRAW B,-14
360 PENUP
370 FOR Ks=0 TO M-1
380 T=Y(Ks)/PI-Ks/M
390 X(Ks)=.5-T !! Cumulative probability in X(*)
400 Y(Ks)=Pr=.5+T !! Exceedance probability in Y(*)
410 IF Pr>=1E-12 THEN Y=LGT(Pr)
420 IF Pr<=-1E-12 THEN Y=-24-LGT(-Pr)
430 IF ABS(Pr)<1E-12 THEN Y=-12
440 PLOT Ks,Y
450 NEXT Ks
460 PENUP
470 PRINT Y(0);Y(1);Y(M-2);Y(M-1)
480 FOR Ks=0 TO M-1
490 Pr=X(Ks)
500 IF Pr>=1E-12 THEN Y=LGT(Pr)
510 IF Pr<=-1E-12 THEN Y=-24-LGT(-Pr)
520 IF ABS(Pr)<1E-12 THEN Y=-12
530 PLOT Ks,Y
540 NEXT Ks
550 PENUP
560 PAUSE
570 DUMP GRAPHICS
580 PRINT LIN(5)
590 PRINTER IS 16
600 END
610 !
620 SUB Fft10z(N,X(*),Y(*)) ! N <= 2^10 = 1024, N=2^INTEGER 0 subscri

```

```

10 ! SMIRNOV CHARACTERISTIC FUNCTION [s/sin(s)]^1/2 where s=(1+i)sqr(xi)
20 L=3000 ! Limit on integral of char. function
30 Delta=1 ! Sampling increment on char. function
40 Bs=0 ! Shift b
50 M=2^8 ! Size of FFT
60 PRINTER IS 0
70 PRINT "L =";L,"Delta =";Delta,"b =";Bs,"M =";M
80 REDIM X(0:M-1),Y(0:M-1)
90 DIM X(0:1023),Y(0:1023)
100 Mux=1/6 ! Mean of random variable x
110 R=0 ! Argument of square root
120 P=1 ! Polarity indicator
130 Muy=Mux+Bs
140 X(0)=0
150 Y(0)=.5*Delta*Muy
160 N=INT(L/Delta)
170 FOR Ns=1 TO N
180 Xi=Delta*Ns !! Argument xi of char. fn.
190 A=SQR(Xi) ! Calculation
200 CALL Sin(A,A,B,C) ! of
210 CALL Div(A,A,B,C,D,E) ! characteristic
220 CALL Sqr(D,E,A,B) ! function
230 Ro=R ! fy(xi)
240 R=ATN(B/A) !
250 IF ABS(R-Ro)>>1.6 THEN P=-P !
260 Fyr=A*P !
270 Fyi=B*P !
280 Ms=Ns MOD M !! Collapsing
290 X(Ms)=X(Ms)+Fyr/Ns
300 Y(Ms)=Y(Ms)+Fyi/Ns
310 NEXT Ns
320 CALL Fft10z(M,X(*),Y(*)) !! 0 subscript FFT
330 PLOTTER IS "GRAPHICS"
340 GRAPHICS
350 SCALE 0,M,-14,0
360 LINE TYPE 3
370 GRID M/8,1
380 PENUP
390 LINE TYPE 1
400 B=Bs*M*Delta/(2*PI) !! Origin for random variable x
410 MOVE B,0
420 DRAW B,-14
430 PENUP
440 FOR Ks=0 TO M-1
450 T=Y(Ks)/PI-Ks/M
460 X(Ks)=.5-T !! Cumulative probability in X(*)
470 Y(Ks)=Pr=.5+T !! Exceedance probability in Y(*)
480 IF Pr>=1E-12 THEN Y=LGT(Pr)
490 IF Pr<=-1E-12 THEN Y=-24-LGT(-Pr)
500 IF ABS(Pr)<1E-12 THEN Y=-12
510 PLOT Ks,Y
520 NEXT Ks

```



```

530  PENUP
540  PRINT Y<0>;Y<1>;Y<M-2>;Y<M-1>
550  FOR Ks=0 TO M-1
560  Pr=X(Ks)
570  IF Pr>=1E-12 THEN Y=LGT(Pr)
580  IF Pr<=-1E-12 THEN Y=-24-LGT(-Pr)
590  IF ABS(Pr)<1E-12 THEN Y=-12
600  PLOT Ks,Y
610  NEXT Ks
620  PENUP
630  PAUSE
640  DUMP GRAPHICS
650  PRINT LIN<5>
660  PRINTER IS 16
670  END
680  !
690  SUB Div(X1,Y1,X2,Y2,A,B)           ! Z1/Z2
700  T=X2*X2+Y2*Y2
710  A=(X1*X2+Y1*Y2)/T
720  B=(Y1*X2-X1*Y2)/T
730  SUBEND
740  !
750  SUB Sqr(X,Y,A,B)                 ! PRINCIPAL SQR(Z)
760  IF X<>0 THEN 800
770  A=B=SQR(.5*ABS(Y))
780  IF Y<0 THEN B=-B
790  GOTO 910
800  F=SQR(SQR(X*X+Y*Y))
810  T=.5*ATN(Y/X)
820  A=F*COS(T)
830  B=F*SIN(T)
840  IF X>0 THEN 910
850  T=A
860  A=-B
870  B=T
880  IF Y>=0 THEN 910
890  A=-A
900  B=-B
910  SUBEND
920  !
930  SUB Sin(X,Y,A,B)                 ! SIN(Z)
940  E=EXP(Y)
950  A=.5*SIN(X)*(E+1/E)
960  IF ABS(Y)<.1 THEN 990
970  S=.5*(E-1/E)
980  GOTO 1010
990  S=Y*Y
1000 S=Y*(120+S*(20+S))/120
1010 B=COS(X)*S
1020 SUBEND
1030 !
1040 SUB Fft10z(N,X(*),Y(*))         ! N <= 2^10 = 1024, N=2^INTEGER      @ subscrij

```

```

10 ! NON-CENTRAL CHI-SQUARE CHARACTERISTIC FUNCTION
20 !  $\exp(i d^2 xi / s) / s^{nu}$  where  $s = 1 - i 2 xi$ 
30   Nu=2.7           ! Power law nu
40   Ds=3            ! Deflection d
50   L=500           ! Limit on integral of char. function
60   Delta=.05       ! Sampling increment on char. function
70   Bs=0            ! Shift b
80   M=2^8           ! Size of FFT
90   PRINTER IS 0
100  PRINT "L =";L,"Delta =";Delta,"b =";Bs,"M =";M
110  REDIM X(0:M-1),Y(0:M-1)
120  DIM X(0:1023),Y(0:1023)
130  D2=Ds*Ds                ! Calculate parameter
140  Mux=2*Nu+D2             ! Mean of random variable x
150  Muy=Mux+Bs
160  X(0)=0
170  Y(0)=.5*Delta*Muy
180  N=INT(L/Delta)
190  FOR Ns=1 TO N
200  Xi=Delta*Ns            !! Argument xi of char. fn.
210  T=Xi+Xi                ! Calculation of
220  CALL Div(0,D2*Xi,1,-T,A,B) ! characteristic
230  CALL Log(1,-T,C,D)     ! function
240  CALL Exp(A-Nu*C,B-Nu*D+Bs*Xi,Fyr,Fyi) !  $f_y(xi)$ 
250  Ms=Ns MOD M           !! Collapsing
260  X(Ms)=X(Ms)+Fyr/Ns
270  Y(Ms)=Y(Ms)+Fyi/Ns
280  NEXT Ns
290  CALL Fft10z(M,X(*),Y(*)) !! 0 subscript FFT
300  PLOTTER IS "GRAPHICS"
310  GRAPHICS
320  SCALE 0,M,-14,0
330  LINE TYPE 3
340  GRID M/8,1
350  PENUP
360  LINE TYPE 1
370  B=Bs*M*Delta/(2*PI)   !! Origin for random variable x
380  MOVE B,0
390  DRAW B,-14
400  PENUP
410  FOR Ks=0 TO M-1
420  T=Y(Ks)/PI-Ks/M
430  X(Ks)=.5-T            !! Cumulative probability in X(*)
440  Y(Ks)=Pr=.5+T        !! Exceedance probability in Y(*)
450  IF Pr>=1E-12 THEN Y=LGT(Pr)
460  IF Pr<=-1E-12 THEN Y=-24-LGT(-Pr)
470  IF ABS(Pr)<1E-12 THEN Y=-12
480  PLOT Ks,Y
490  NEXT Ks
500  PENUP

```

```

510 PRINT Y(0);Y(1);Y(M-2);Y(M-1)
520 FOR Ks=0 TO M-1
530 Pr=X(Ks)
540 IF Pr>=1E-12 THEN Y=LGT(Pr)
550 IF Pr<=-1E-12 THEN Y=-24-LGT(-Pr)
560 IF ABS(Pr)<1E-12 THEN Y=-12
570 PLOT Ks,Y
580 NEXT Ks
590 PENUP
600 PAUSE
610 DUMP GRAPHICS
620 PRINT LIN(5)
630 PRINTER IS 16
640 END
650 !
660 SUB Div(X1,Y1,X2,Y2,A,B)           ! Z1/Z2
670 T=X2*X2+Y2*Y2
680 A=(X1*X2+Y1*Y2)/T
690 B=(Y1*X2-X1*Y2)/T
700 SUBEND
710 !
720 SUB Exp(X,Y,A,B)                 ! EXP(Z)
730 T=EXP(X)
740 A=T*COS(Y)
750 B=T*SIN(Y)
760 SUBEND
770 !
780 SUB Log(X,Y,A,B)                 ! PRINCIPAL LOG(Z)
790 A=.5*LOG(X*X+Y*Y)
800 IF X<>0 THEN 830
810 B=.5*PI*SGN(Y)
820 GOTO 850
830 B=ATN(Y/X)
840 IF X<0 THEN B=B+PI*(1-2*(Y<0))
850 SUBEND
860 !
870 SUB Fft10z(N,X(*),Y(*))          ! N <= 2^10 = 1024, N=2^INTEGER      0 subscrip

```

```

10 ! GAUSSIAN PRODUCT CHARACTERISTIC FUNCTION (56)
20  Nu=7.7                ! Power Nu
30  Rho=-.3              ! Correlation coefficient
40  L=5                  ! Limit on integral of char. function
50  Delta=.06           ! Sampling increment on char. function
60  Bs=.5*(2*PI/Delta)  ! Shift b, as fraction of alias interval
70  M=2^8                ! Size of FFT
80  PRINTER IS 0
90  PRINT "L =";L,"Delta =";Delta,"b =";Bs,"M =";M
100 REDIM X(0:M-1),Y(0:M-1)
110 DIM X(0:1023),Y(0:1023)
120 T1=1-Rho*Rho        ! Calculate
130 T2=2*Rho            ! parameters
140 Mux=2*Nu*Rho        ! Mean of random variable x
150 Muy=Mux+Bs
160 X(0)=0
170 Y(0)=.5*Delta*Muy
180 N=INT(L/Delta)
190 FOR Ns=1 TO N
200 Xi=Delta*Ns         !! Argument xi of char. fn.
210 CALL Log(1+T1*Xi*Xi,-T2*Xi,A,B) ! Calculation of
220 CALL Exp(-Nu*A,Bs*Xi-Nu*B,Fyr,Fyi) ! characteristic function fy(xi)
230 Ms=Ns MOD M        !! Collapsing
240 X(Ms)=X(Ms)+Fyr/Ns
250 Y(Ms)=Y(Ms)+Fyi/Ns
260 NEXT Ns
270 CALL Fft10z(M,X(*),Y(*))      !! 0 subscript FFT
280 PLOTTER IS "GRAPHICS"
290 GRAPHICS
300 SCALE 0,M,-14,0
310 LINE TYPE 3
320 GRID M/8,1
330 PENUP
340 LINE TYPE 1
350 B=Bs*M*Delta/(2*PI)          !! Origin for random variable x
360 MOVE B,0
370 DRAW B,-14
380 PENUP

```

```

390   FOR Ks=0 TO M-1
400   T=Y(Ks)/PI-Ks/M
410   X(Ks)=.5-T           !! Cumulative probability in X(*)
420   Y(Ks)=Pr=.5+T       !! Exceedance probability in Y(*)
430   IF Pr>=1E-12 THEN Y=LGT(Pr)
440   IF Pr<=-1E-12 THEN Y=-24-LGT(-Pr)
450   IF ABS(Pr)<1E-12 THEN Y=-12
460   PLOT Ks,Y
470   NEXT Ks
480   PENUP
490   PRINT Y(0);Y(1);Y(M-2);Y(M-1)
500   FOR Ks=0 TO M-1
510   Pr=X(Ks)
520   IF Pr>=1E-12 THEN Y=LGT(Pr)
530   IF Pr<=-1E-12 THEN Y=-24-LGT(-Pr)
540   IF ABS(Pr)<1E-12 THEN Y=-12
550   PLOT Ks,Y
560   NEXT Ks
570   PENUP
580   PAUSE
590   DUMP GRAPHICS
600   PRINT LIN(5)
610   PRINTER IS 16
620   END
630   !
640   SUB Exp(X,Y,A,B)           ! EXP(Z)
650   T=EXP(X)
660   A=T*COS(Y)
670   B=T*SIN(Y)
680   SUBEND
690   !
700   SUB Log(X,Y,A,B)           ! PRINCIPAL LOG(Z)
710   A=.5*LOG(X*X+Y*Y)
720   IF X<>0 THEN 750
730   B=.5*PI*SGN(Y)
740   GOTO 770
750   B=ATN(Y/X)
760   IF X<0 THEN B=B+PI*(1-2*(Y<0))
770   SUBEND
780   !
790   SUB Fft10z(N,X(*),Y(*))    ! N <= 2^10 = 1024, N=2^INTEGER    0 subscript

```

```

10  SUB Fft10z(N,X(*),Y(*))      ! N <= 2^10 = 1024, N=2^INTEGER      0 subscript
20  DIM C(0:256)
30  INTEGER I1,I2,I3,I4,I5,I6,I7,I8,I9,I10,J,K
40  DATA 1,.999981175283,.999924701839,.999830581796,.999698818696,.9995294175
01,.999322384588,.999077727753,.998795456205,.998475580573,.998118112900
50  DATA .997723066644,.997290456679,.996820299291,.996312612183,.995767414468
,.995184726672,.994564570734,.993906970002,.993211949235,.992479534599
60  DATA .9917089753669,.990902635428,.990058210262,.989176509965,.988257567731
,.987301418158,.986308097245,.985277642389,.984210092387,.983105487431
70  DATA .981963869110,.980785280403,.979569765685,.978317370720,.977028142658
,.975702130039,.974339382786,.972939952206,.971503890986,.970031253195
80  DATA .968522094274,.966976471045,.965394441698,.963776065795,.962121404269
,.960430519416,.958703474896,.956940335732,.955141168306,.953306040354
90  DATA .951435020969,.949528180593,.947585591018,.945607325381,.943593458162
,.941544065183,.939459223602,.937339011913,.935183509939,.932992798835
100 DATA .930766961079,.928506080473,.926210242138,.923879532511,.921514039342
,.919113851690,.916679059921,.914209755704,.911706032005,.909167983091
110 DATA .906595704515,.903989293123,.901348847046,.898674465694,.895966249756
,.893224301196,.890448723245,.887639620403,.884797098431,.881921264348
120 DATA .879012226429,.876070094195,.873094978418,.870086991109,.867046245516
,.863972856122,.860866938638,.857728610000,.854557988365,.851355193105
130 DATA .848120344803,.844853565250,.841554977437,.838224705555,.834862874986
,.831469612303,.828045045258,.824589302785,.821102514991,.817584813152
140 DATA .814036329706,.810457198253,.806847553544,.803207531481,.799537269108
,.795836904609,.792106577300,.788346427627,.784556597156,.780737228572
150 DATA .776888465673,.773010453363,.769103337646,.765167265622,.761202385484
,.757208846506,.753186799044,.749136394523,.745057785441,.740951125355
160 DATA .736816568877,.732654271672,.728464390448,.724247082951,.720002507961
,.715730825284,.711432195745,.707106781187,.702754744457,.698376249409
170 DATA .693971460890,.689540544737,.685083667773,.680600997795,.676092703575
,.671558954847,.666999922304,.662415777590,.657806693297,.653172842954
180 DATA .648514401022,.643831542890,.639124444864,.634393284164,.629638238915
,.624859488142,.620057211763,.615231590581,.610382806276,.605511041404
190 DATA .600616479384,.595699304492,.590759701859,.585797857456,.580813958096
,.575808191418,.570780745887,.565731810784,.560661576197,.555570233020
200 DATA .550457972937,.545324988422,.540171472730,.534997619887,.529803624686
,.524589682678,.519355990166,.514102744193,.508830142543,.503538383726
210 DATA .498227666973,.492898192230,.487550160148,.482183772079,.476799230063
,.471396736826,.465976495768,.460538710958,.455083587126,.449611329655
220 DATA .444122144570,.438616238539,.433093818853,.427555093430,.422000270800
,.416429560098,.410843171058,.405241314005,.399624199846,.393992040061
230 DATA .388345046699,.382683432365,.377007410216,.371317193952,.365612997805
,.359895036535,.354163525420,.348418680249,.342660717312,.336889853392
240 DATA .331106305760,.325310292162,.319502030816,.313681740399,.307849640042
,.302005949319,.296150888244,.290284677254,.284407537211,.278519689385
250 DATA .272621355450,.266712757475,.260794117915,.254865659605,.248927605746
,.242980179903,.237023605994,.231058108281,.225083911360,.219101240157
260 DATA .213110319916,.207111376192,.201104634842,.195090322016,.189068664150
,.183039887955,.177004220412,.170961888760,.164913120490,.158858143334
270 DATA .152797185258,.146730474455,.140658239333,.134580708507,.128498110794
,.122410675199,.116318630912,.110222207294,.104121633872,.980171403296E-1
280 DATA .919089564971E-1,.857973123444E-1,.796824379714E-1,.735645635997E-1,.
674439195637E-1,.613207363022E-1,.551952443497E-1,.490676743274E-1
290 DATA .429382569349E-1,.368072229414E-1,.306748031766E-1,.245412285229E-1,.
184067299058E-1,.122715382857E-1,.613588464915E-2,0
300  READ C(*)
310  K=1024/N
320  FOR J=0 TO N/4
330  C(J)=C(K*J)
340  NEXT J
350  N1=N/4
360  N2=N1+1
370  N3=N2+1

```

```

380  N4=N1+N3
390  Log2n=INT(1.4427*LOG(N)+.5)
400  FOR I1=1 TO Log2n
410  I2=2^(Log2n-I1)
420  I3=2*I2
430  I4=N/I3
440  FOR I5=1 TO I2
450  I6=(I5-1)*I4+1
460  IF I6<=N2 THEN 500
470  N6=-C(N4-I6-1)
480  N7=-C(I6-N1-1)
490  GOTO 520
500  N6=C(I6-1)
510  N7=-C(N3-I6-1)
520  FOR I7=0 TO N-I3 STEP I3
530  I8=I7+I5
540  I9=I8+I2
550  N8=X(I8-1)-X(I9-1)
560  N9=Y(I8-1)-Y(I9-1)
570  X(I8-1)=X(I8-1)+X(I9-1)
580  Y(I8-1)=Y(I8-1)+Y(I9-1)
590  X(I9-1)=N6*N8-N7*N9
600  Y(I9-1)=N6*N9+N7*N8
610  NEXT I7
620  NEXT I5
630  NEXT I1
640  I1=Log2n+1
650  FOR I2=1 TO 10
660  C(I2-1)=1
670  IF I2>Log2n THEN 690
680  C(I2-1)=2^(I1-I2)
690  NEXT I2
700  K=1
710  FOR I1=1 TO C(9)
720  FOR I2=I1 TO C(8) STEP C(9)
730  FOR I3=I2 TO C(7) STEP C(8)
740  FOR I4=I3 TO C(6) STEP C(7)
750  FOR I5=I4 TO C(5) STEP C(6)
760  FOR I6=I5 TO C(4) STEP C(5)
770  FOR I7=I6 TO C(3) STEP C(4)
780  FOR I8=I7 TO C(2) STEP C(3)
790  FOR I9=I8 TO C(1) STEP C(2)
800  FOR I10=I9 TO C(0) STEP C(1)
810  J=I10
820  IF K>J THEN 890
830  A=X(K-1)
840  X(K-1)=X(J-1)
850  X(J-1)=A
860  A=Y(K-1)
870  Y(K-1)=Y(J-1)
880  Y(J-1)=A
890  K=K+1
900  NEXT I10
910  NEXT I9
920  NEXT I8
930  NEXT I7
940  NEXT I6
950  NEXT I5
960  NEXT I4
970  NEXT I3
980  NEXT I2
990  NEXT I1
1000 SUBEND

```

! 2^10=1024

REFERENCES

1. A. H. Nuttall, "Detection Performance Characteristics for a System with Quantizers, Or-ing, and Accumulator," *Journal of Acoustical Society of America*, Vol. 73, No. 5, pp. 1631-1642, May 1983; also NUSC Technical Report 6815, 1 October 1982.
2. A. H. Nuttall, "Operating Characteristics of an Or-ing and Selection Processor with Pre- and Post-Averaging," NUSC Technical Report 6929, 4 May 1983.
3. C. W. Helstrom, "Approximate Calculation of Cumulative Probability from a Moment-Generating Function," *Proc. IEEE*, Vol. 57, No. 3, pp. 368-9, March 1969.
4. A. H. Nuttall, "Numerical Evaluation of Cumulative Probability Distribution Functions Directly from Characteristic Functions," *Proc. IEEE*, Vol. 57, No. 11, pp. 2071-2, November 1969; also NUSL Report No. 1032, 11 August 1969.
5. A. A. G. Requicha, "Direct Computation of Distribution Functions from Characteristic Functions using the Fast Fourier Transform," *Proc. IEEE*, Vol. 58, No. 7, pp. 1154-5, July 1970.
6. E. O. Brigham, "Evaluation of Cumulative Probability Distribution Functions: Improved Numerical Methods," *Proc. IEEE*, Vol 58, No. 9, pp. 1367-8, September 1970.
7. A. H. Nuttall, "Alternate Forms for Numerical Evaluation of Cumulative Probability Distributions Directly from Characteristic Functions," *Proc. IEEE*, Vol 58, No. 11, pp. 1872-3, November 1970; also NUSC Report No. NL-3012, 12 August 1970.

8. L. Wang, "Numerical Calculation of Cumulative Probability from the Moment-Generating Function," Proc. IEEE, Vol. 60, No. 11, pp. 1452-3, November 1972.
9. P. M. Woodward, Probability and Information Theory, with Applications to Radar, Pergamon Press, N.Y., 1957.
10. A. H. Nuttall, "On the Distribution of a Chi-Squared Variate Raised to a Power," NUSC Technical Memorandum 831059, 19 April 1983.
11. H. Cramer, Mathematical Methods of Statistics, Princeton University Press, 1961.
12. M. Kendall and A. Stuart, The Advanced Theory of Statistics, Vol. 2, 4th edition, Macmillan Publishing Co., Inc., N.Y., 1979.
13. Handbook of Mathematical Functions, U.S. Department of Commerce, National Bureau of Standards, Applied Mathematics Series 55, U.S. Government Printing Office, Washington, DC, June 1964.
14. I. S. Gradshteyn and I. M. Ryzhik, Table of Integrals, Series, and Products, Academic Press Inc., N.Y., 1980.
15. A. H. Nuttall, "Exact Performance of General Second-Order Processors for Gaussian Inputs," NUSC Technical Report 7035, 15 October 1983.

Exact Performance of General Second-Order Processors for Gaussian Inputs

A. H. Nuttall

ABSTRACT

The characteristic function of general second-order processors with nonstationary nonzero mean Gaussian inputs is derived in closed form. Three classes of processors are considered; in the first, the decision variable is the sum of K independent terms, each of second-order form involving two statistically dependent Gaussian random variables; the second class of processor is a narrowband crosscorrelator of arbitrary Gaussian processes, with accumulation of K independent lowpass filter output samples; in the third class, the decision variable is a general quadratic-plus-linear form of M random variables, all statistically dependent on each other. Specializations to various forms of weighted energy detectors and correlators are made. Also, the characteristic function for the first class of processor subject to fading is evaluated.

Programs for evaluating the cumulative and exceedance distribution functions of all three classes of processors are given and have been used to plot representative examples of performance. A comparison with a simulation result corroborates the analysis and program of the first class of processor.

TABLE OF CONTENTS

	<u>Page</u>
List of Illustrations	iii
List of Symbols	iv
Introduction	1
A Particular Second-Order Processor	3
Special Forms of Second-Order Processor (8)	10
Narrowband Cross-Correlator	14
Reduction of Hermitian and Linear Form	20
Quadratic and Linear Form	24
Examples	33
Summary and Discussion	42
 Appendices	
A. Second-Order Processor	A-1
B. Fading for Second-Order Processor	B-1
C. Narrowband Cross-Correlator	C-1
D. Reduced Quadratic and Linear Form	D-1
E. Simulation of Second-Order Processor	E-1
 References	 R-1

LIST OF ILLUSTRATIONS

<u>Figure</u>		<u>Page</u>
1.	Narrowband Cross-Correlator	14
2.	Distributions for Second-Order Processor	34
3.	Simulation Comparison of Second-Order Processor	36
4.	Second-Order Processor, $K=10$, Identical Statistics	37
5.	Second-Order Processor with Fading	38
6.	Distributions for Narrowband Cross-Correlator	39
7.	Distributions for Quadratic and Linear Form	41

LIST OF SYMBOLS

s, t	jointly-Gaussian random variables
a, b, c, d, e	constant weights
x	output random variable of second-order processor
$f_x(\xi)$	characteristic function of random variable x
overbar	statistical average
D_1, D_2	denominator constants in characteristic function
N_0, N_1, N_2	numerator constants in characteristic function
μ_x	mean of random variable x
σ_x^2	variance of random variable x
K	number of independent terms in random variables x and v
M_{ij}	mean parameters, (12)
r	power scale factor, (18)-(19)
$s_1(t), s_2(t)$	input signals to narrowband cross-correlator
$n_1(t), n_2(t)$	input noises to narrowband cross-correlator
$z(t)$	lowpass filter output
v	narrowband cross-correlator system output random variable
$a_j(t), b_j(t)$	in-phase and quadrature components of $s_j(t)$; $j = 1, 2$
$A_j(t), P_j(t)$	envelope and phase modulation of $s_j(t)$
$x_j(t), y_j(t)$	in-phase and quadrature components of $n_j(t)$
σ_j^2	variance of $x_j(t)$ and $y_j(t)$, (27)-(28)
γ	complex correlation coefficient of noises, (27)
ρ, λ	real and imaginary parts of γ , (27)
$w(k)$	weight in narrowband cross-correlator
$\mu_z(s+n)$	mean of random variable z with signal and noise present
R_z	signal-to-noise ratio of random variable z
M	size of Hermitian and quadratic forms
X	random complex vector, $M \times 1$
A	constant complex linear weight matrix
B	constant complex Hermitian weight matrix

LIST OF SYMBOLS (Con'd)

a_m	elements of A
b_{mn}	elements of B
q	Hermitian and quadratic form outputs
X^H	transpose and conjugate of X
E	mean of random vector X, (46)
\tilde{X}	ac component of X, (46)
K	covariance matrix of X, (46)
W	linearly transformed random variables, (54)
C	modal matrix of BK, (58)
Λ	eigenvalue matrix of BK, (58)
λ_m	elements of Λ
D	auxiliary vector, (59)
d_m	elements of D, (68)
v_m	elements of \bar{W} , (68)
$\chi_q(n)$	n^{th} cumulant of random variable q
U, V	components of X, (71)
N	number of elements in U and V; $M=2N$
B^{ij}	partitioned matrices of B
$A^{(j)}$	partitioned vectors of A
u_n, v_n	components of U, V respectively
K_{uv}	partitioned matrices of K, (73)
K_0	common covariance matrix in special case, (89)
Q	modal matrix of K_0 , (92)
Γ	eigenvalue matrix of K_0 , (92)
γ_n	elements of Γ

EXACT PERFORMANCE OF GENERAL SECOND-ORDER PROCESSORS FOR GAUSSIAN INPUTS

INTRODUCTION

The performance of weighted energy detectors and correlators for processing deterministic and/or random signals in the presence of nonstationary noise is a topic of frequent interest. Most often, a second-moment approach is adopted, whereby the means and variances of the decision variable under the various hypotheses are evaluated and employed in a central limit assumption to get approximate false alarm and/or detection probabilities. This approach is suspect for small false alarm probabilities or for cases where the decision variable is not the sum of a large number of independent random variables all of comparable variance.

A recent technical report [1] has presented an accurate and efficient method for evaluating cumulative and exceedance distribution functions directly from characteristic functions. This approach is very fruitful for determining the performance of general time-varying second-order processors with nonstationary nonzero mean Gaussian inputs, since the characteristic function of the decision variable can be evaluated in closed form in these cases.

We will consider three classes of processors and derive the characteristic functions for all three decision variables in closed form. The first two classes are special cases of the third, but are of interest in their own right, since they include and immediately reduce to many practical processors in current use. Also there is no need to solve for the eigenvalues and eigenvectors of a general symmetric matrix that is encountered in the third more-general class of processors. Rather, the characteristic functions are given directly in terms of specified processor weights and input statistics.

There has been considerable effort on this problem in the past; for example, see [2,3] and the references listed therein. Most of the lengthy analytical derivations and results have been aimed at getting workable

expressions for the probability density function and/or cumulative distribution function. Here, when we consider our three classes of processors, we encounter characteristic functions which are more general than that given in the recent paper for a filtered analog processor [3, eq. 5]; thus specialization of our results will yield those of [3] and the references listed therein. The technique employed here to proceed directly to the cumulative and exceedance distribution functions is a numerical one, as given in [1], and does not require any series expansions or analytical manipulations at all. The asymptotic behaviors of the cumulative and exceedance distribution functions on both tails are easily observed and will be found to corroborate the comment made in [3, p. 673] that these tails are generally exponential rather than Gaussian; however, there can be a considerable transition region.

The programs listed in the appendices require the user merely to input his processor weights, signal constants, and noise statistical parameters in a series of data statements at the top of the program, and to select values for

- L, limit on integral of characteristic function,
- Δ , sampling increment on characteristic function,
- b, additive constant, to guarantee a positive random variable, and
- M_f , size of FFT and storage required.

Selection of L and Δ is largely a matter of trial and error and is amply documented in the examples in [1].

A PARTICULAR SECOND-ORDER PROCESSOR

Before we embark on the analysis of the particular second-order processor of interest in this section, we solve the following simpler statistical problem. Let s and t be real jointly-Gaussian random variables with means m_s, m_t , standard deviations σ_s, σ_t , and correlation coefficient ρ ; thus s and t are statistically dependent. Consider the random variable

$$x = as^2 + bt^2 + cst + ds + et, \quad (1)$$

where weightings a, b, c, d, e are arbitrary real constants. The characteristic function of random variable x is defined by*

$$\begin{aligned} f_x(\xi) &= \overline{\exp(i\xi x)} = \overline{\exp(i\xi(as^2 + bt^2 + cst + ds + et))} = \\ &= \iint du dv \exp(i\xi(au^2 + bv^2 + cuv + du + ev)) p_{st}(u,v), \end{aligned} \quad (2)$$

where the joint probability density function of s and t is

$$p_{st}(u,v) = \left(2\pi \sigma_s \sigma_t \sqrt{1-\rho^2}\right)^{-1} \exp \left[-\frac{\left(\frac{u-m_s}{\sigma_s}\right)^2 + \left(\frac{v-m_t}{\sigma_t}\right)^2 - 2\rho \left(\frac{u-m_s}{\sigma_s}\right) \left(\frac{v-m_t}{\sigma_t}\right)}{2(1-\rho^2)} \right]. \quad (3)$$

Substitution of (3) in (2) and use of the double integral

$$\iint dx dy \exp[-\alpha x^2 - \beta y^2 + 2\gamma xy + ux + vy] = \frac{\pi}{\sqrt{\alpha\beta-\gamma^2}} \exp \left[\frac{\beta u^2 + \alpha v^2 + 2\gamma uv}{4(\alpha\beta-\gamma^2)} \right] \quad (4)$$

for $\alpha_r > 0, \beta_r > 0, \alpha_r \beta_r > \gamma_r^2$,

* Integrals without limits are over $(-\infty, +\infty)$.

(where sub r denotes the real part of complex constants $\alpha, \beta, \gamma, \nu, \nu$) yields, after an extensive amount of manipulations, the characteristic function of random variable x as the compact closed form expression

$$f_x(\mathfrak{F}) = \left(1 - i\mathfrak{F}D_1 - \mathfrak{F}^2D_2\right)^{-1/2} \exp\left[i\mathfrak{F} \frac{N_0 - i\mathfrak{F}N_1 - \mathfrak{F}^2N_2}{1 - i\mathfrak{F}D_1 - \mathfrak{F}^2D_2}\right]. \quad (5)$$

The required real constants in (5) are given directly in terms of the processor weights and statistical parameters as

$$\begin{aligned} D_1 &= 2(a\sigma_s^2 + b\sigma_t^2 + c\rho\sigma_s\sigma_t) \quad , \\ D_2 &= (4ab - c^2)(1 - \rho^2)\sigma_s^2\sigma_t^2 \quad , \\ N_0 &= am_s^2 + bm_t^2 + cm_s m_t + dm_s + em_t \quad , \\ N_1 &= (4ab - c^2)\left(\frac{1}{2}m_s^2\sigma_t^2 + \frac{1}{2}m_t^2\sigma_s^2 - \rho m_s m_t \sigma_s \sigma_t\right) + \\ &\quad + (2ae - cd)\sigma_s(m_t\sigma_s - \rho m_s\sigma_t) + \\ &\quad + (2bd - ce)\sigma_t(m_s\sigma_t - \rho m_t\sigma_s) - \\ &\quad - \left(\frac{1}{2}d^2\sigma_s^2 + \frac{1}{2}e^2\sigma_t^2 + de\rho\sigma_s\sigma_t\right) \quad , \\ N_2 &= -(ae^2 + bd^2 - cde)(1 - \rho^2)\sigma_s^2\sigma_t^2 \quad . \end{aligned} \quad (6)$$

For later reference, the mean and variance of x follow from (5), upon expansion of $\ln f_x(\mathfrak{F})$ in a power series in \mathfrak{F} , as

$$\begin{aligned} \nu_x &= N_0 + \frac{1}{2}D_1, \\ \sigma_x^2 &= \frac{1}{2}D_1^2 + 2N_0D_1 - D_2 - 2N_1. \end{aligned} \quad (7)$$

(When $D_1 = 0$ in (6), it can be shown that $D_2 < 0$; thus characteristic function (5) never possesses any singularities along the real ξ axis.)

Second-Order Processor

Now let x be the sum of K independent terms of the form of (1):

$$x = \sum_{k=1}^K (a_k s_k^2 + b_k t_k^2 + c_k s_k t_k + d_k s_k + e_k t_k) \quad , \quad (8)$$

where real constants a_k, b_k, c_k, d_k, e_k can depend arbitrarily on k , and where means * m_{sk}, m_{tk} , standard deviations σ_{sk}, σ_{tk} , and correlation coefficients ρ_k are unrestricted (except that $\sigma_{sk} \geq 0, \sigma_{tk} \geq 0, |\rho_k| \leq 1$). The pair of random variables s_k, t_k is statistically independent of the pair s_n, t_n for all $k \neq n$. Thus random variable x is composed of a sum of K groups of random variables, where each group is statistically independent of every other group, but each group itself contains two statistically dependent random variables.

This processor in (8) is the general form of interest in this section. It can be time-varying when the weights $\{a_k, b_k, c_k, d_k, e_k\}$ vary with k , and nonstationary when the statistical parameters $\{m_{sk}, m_{tk}, \sigma_{sk}, \sigma_{tk}, \rho_k\}$ vary with k .

The characteristic function of (8) follows from (5) as

$$f_x(\xi) = \left[\prod_{k=1}^K \left\{ 1 - i\xi D_1(k) - \xi^2 D_2(k) \right\} \right]^{-1/2} * \exp \left[i\xi \sum_{k=1}^K \frac{N_0(k) - i\xi N_1(k) - \xi^2 N_2(k)}{1 - i\xi D_1(k) - \xi^2 D_2(k)} \right] \quad , \quad (9)$$

* These means can be interpreted as the deterministic signal components of the channels s and t , if desired.

where the identification of $D_1(k)$, etc., is obvious from (6). Only one (continuous) square root and one exponential per \mathfrak{F} value is required in (9), regardless of the number of terms added, K . The mean and variance of random variable x in (8) follows from (9) as

$$\begin{aligned} \nu_x &= \sum_{k=1}^K \left[N_0(k) + \frac{1}{2} D_1(k) \right], \\ \sigma_x^2 &= \sum_{k=1}^K \left[\frac{1}{2} D_1^2(k) + 2N_0(k) D_1(k) - D_2(k) - 2N_1(k) \right]. \end{aligned} \quad (10)$$

Any analytical attempt at determining the probability density function or cumulative distribution function corresponding to characteristic function (9) would be a formidable task indeed. However, it is a very simple task via the method of [1] to get accurate numerical values for the cumulative and exceedance distribution functions. The program listing in appendix A accomplishes this task, based upon characteristic function (9) and the constants listed in (6). All the weights $\{a_k, b_k, c_k, d_k, e_k\}_1^K$ and statistical parameters $\{m_{sk}, m_{tk}, \sigma_{sk}, \sigma_{tk}, \rho_k\}_1^K$ are arbitrary. Observe that (9) is far more general than the characteristic function considered in [3, eq. 5], which itself required a very lengthy analytic treatment to get the probability density function and cumulative distribution function. In fact, there is little hope of getting any tractable analytic results for (9) when K is greater than 2.

Special Case 1

Suppose weightings a, b, c, d, e in (8) are independent of k and that statistics σ_s, σ_t, ρ are also independent of k . The decision variable x in (8) then simplifies to

$$x = \sum_{k=1}^K (as_k^2 + bt_k^2 + cs_k t_k + ds_k + et_k) \quad . \quad (11)$$

Then D_1, D_2, N_2 are independent of k . If we define mean parameters

$$\begin{aligned} M_{20} &= \sum_{k=1}^K m_{sk}^2, & M_{02} &= \sum_{k=1}^K m_{tk}^2, & M_{11} &= \sum_{k=1}^K m_{sk} m_{tk}, \\ M_{10} &= \sum_{k=1}^K m_{sk}, & M_{01} &= \sum_{k=1}^K m_{tk}, \end{aligned} \quad (12)$$

the characteristic function of x in (9) then takes the simpler form

$$f_x(\xi) = \left(1 - i\xi D_1 - \xi^2 D_2\right)^{-K/2} \exp \left[i\xi \frac{N_0' - i\xi N_1' - \xi^2 N_2'}{1 - i\xi D_1 - \xi^2 D_2} \right], \quad (13)$$

where D_1 and D_2 are still given by (6), and

$$\begin{aligned} N_0' &= aM_{20} + bM_{02} + cM_{11} + dM_{10} + eM_{01}, \\ N_1' &= (4ab - c^2) \left(\frac{1}{2} \sigma_t^2 M_{20} + \frac{1}{2} \sigma_s^2 M_{02} - \rho \sigma_s \sigma_t M_{11} \right) + \\ &\quad + (2ae - cd) \sigma_s (\sigma_s M_{01} - \rho \sigma_t M_{10}) + \\ &\quad + (2bd - ce) \sigma_t (\sigma_t M_{10} - \rho \sigma_s M_{01}) - \\ &\quad - K \left(\frac{1}{2} d^2 \sigma_s^2 + \frac{1}{2} e^2 \sigma_t^2 + de \rho \sigma_s \sigma_t \right), \\ N_2' &= -K (ae^2 + bd^2 - cde) (1 - \rho^2) \sigma_s^2 \sigma_t^2. \end{aligned} \quad (14)$$

(The choice of $K = 2$ and $N_2' = 0$ in (13) corresponds to the form given in [3, eq. 5].) Observe that the characteristic function in (13) (and therefore the performance) of the processor in (11) depends on the means $\{m_{sk}\}$ and $\{m_{tk}\}$ only through the parameters $\{M_{ij}\}$ defined in (12). The mean and variance

of random variable x in (11) follow from characteristic function (13) as

$$\begin{aligned} u_x &= N_0' + \frac{1}{2} KD_1, \\ \sigma_x^2 &= \frac{1}{2} KD_1^2 + 2N_0'D_1 - KD_2 - 2N_1'. \end{aligned} \quad (15)$$

Special Case 2

Let us also assume $d = 0$, $e = 0$ in (11) above; then the pertinent decision variable is given by

$$x = \sum_{k=1}^K (as_k^2 + bt_k^2 + cs_k t_k) \quad . \quad (16)$$

D_1 and D_2 are still given by (6), and there follows from (14),

$$\begin{aligned} N_0' &= aM_{20} + bM_{02} + cM_{11} \quad , \\ N_1' &= (4ab - c^2) \left(\frac{1}{2} \sigma_t^2 M_{20} + \frac{1}{2} \sigma_s^2 M_{02} - \rho \sigma_s \sigma_t M_{11} \right) \quad , \\ N_2' &= 0 \quad . \end{aligned} \quad (17)$$

The characteristic function of x is given by (13), with $N_2' = 0$. The mean and variance of x in (16) are given by (15).

Fading for Special Case 2

Let the mean parameters $\{M_{ij}\}$ in (12) be subject to slow fading; i.e., replace

$$M_{20} \text{ by } rM_{20}, M_{02} \text{ by } rM_{02}, M_{11} \text{ by } rM_{11}, \quad (18)$$

where power scale factor r has probability density function

$$p_r(u) = \frac{v^v}{\Gamma(v)} u^{v-1} e^{-vu} \quad \text{for } u > 0, v > 0;$$

$$\bar{r} = 1, \sigma_r^2 = \frac{1}{v}, \chi_r(n) = \frac{(n-1)!}{v^{n-1}} \quad \text{for } n \geq 1. \quad (19)$$

This form of fading is encountered in diversity combination receivers; see, for example, [4, eq. 9 et seq.] and [5, eq. 24 et seq.]. Then (13), (17), and (18) yield the conditional characteristic function, for a specified r , as

$$f_x(\mathcal{F}|r) = \left(1 - i\mathcal{F}D_1 - \mathcal{F}^2D_2\right)^{-K/2} \exp\left[i\mathcal{F}r \frac{N_0' - i\mathcal{F}N_1'}{1 - i\mathcal{F}D_1 - \mathcal{F}^2D_2}\right]. \quad (20)$$

Weighting (20) according to the probability density function in (19), and performing the integral, there follows, for the characteristic function of the decision variable x in (16), the result

$$f_x(\mathcal{F}) = \frac{\left(1 - i\mathcal{F}D_1 - \mathcal{F}^2D_2\right)^{v - \frac{K}{2}}}{\left(1 - i\mathcal{F}(D_1 + N_0'/v) - \mathcal{F}^2(D_2 + N_1'/v)\right)^v}. \quad (21)$$

(The limit of (21) as $v \rightarrow +\infty$ is again (13) with $N_2' = 0$, as in (17); this agrees with the fact that the corresponding limit of the probability density function in (19) is $p_r(u) = \delta(u-1)$.) The mean and variance of x in (16) follow from characteristic function (21) as

$$\mu_x = N_0' + \frac{1}{2} KD_1,$$

$$\sigma_x^2 = \frac{1}{2} KD_1^2 + 2N_0'D_1 - KD_2 - 2N_1' + N_0'^2/v. \quad (22)$$

Observe that mean μ_x is independent of v , the power law in fading (19). A program for the cumulative and exceedance distribution functions corresponding to characteristic function (21) is given in appendix B.

SPECIAL FORMS OF SECOND-ORDER PROCESSOR (8)

Before embarking on the analysis of the other two classes of processors, we will explicitly detail some of the special forms that processor (8) reduces to, under particular selections of the weightings and statistical parameters. A rather broad collection of typical processors will be seen to be included. In the following, any unspecified weights $\{a_k, b_k, c_k, d_k, e_k\}$ are zero, and any unspecified statistical parameters that do not appear in the final characteristic function are irrelevant.

I. Gaussian

$$d_k = 1$$

$$x = \sum_{k=1}^K s_k$$

$$f_x(\mathfrak{F}) = \exp \left[i \mathfrak{F} \sum_{k=1}^K m_{sk} - \frac{1}{2} \mathfrak{F}^2 \sum_{k=1}^K \sigma_{sk}^2 \right]$$

II. Chi-square of K Degrees of Freedom

$$a_k = 1, \quad m_{sk} = 0, \quad \sigma_{sk} = 1$$

$$x = \sum_{k=1}^K s_k^2$$

$$f_x(\mathfrak{F}) = (1 - i\mathfrak{F}^2)^{-K/2}$$

III. Non-Central Chi-Square (Q_M Distribution if $K = 2M$)

$$a_k = 1, \quad \sigma_{sk} = \sigma_s$$

$$x = \sum_{k=1}^K s_k^2$$

$$f_x(\mathcal{F}) = \left(1 - i\mathcal{F}2\sigma_s^2\right)^{-K/2} \exp\left[\frac{i\mathcal{F} \sum_{k=1}^K m_{sk}^2}{1 - i\mathcal{F}2\sigma_s^2}\right]$$

IV. Weighted Energy Detector

$$a_k \neq 0, \quad d_k \neq 0$$

$$x = \sum_{k=1}^K (a_k s_k^2 + d_k s_k)$$

$$f_x(\mathcal{F}) = \left[\prod_{k=1}^K \left\{1 - i\mathcal{F}2a_k\sigma_{sk}^2\right\}\right]^{-\frac{1}{2}} \exp\left[i\mathcal{F} \sum_{k=1}^K \frac{a_k m_{sk}^2 + d_k m_{sk} + i\mathcal{F} \frac{1}{2} d_k^2 \sigma_{sk}^2}{1 - i\mathcal{F}2a_k\sigma_{sk}^2}\right]$$

V. Weighted Cross-Correlator

$$c_k \neq 0$$

$$x = \sum_{k=1}^K c_k s_k t_k$$

$$D_1(k) = 2c_k \rho_k \sigma_{sk} \sigma_{tk},$$

$$D_2(k) = -c_k^2 (1 - \rho_k^2) \sigma_{sk}^2 \sigma_{tk}^2,$$

$$N_0(k) = c_k m_{sk} m_{tk},$$

$$N_1(k) = -c_k^2 \left(\frac{1}{2} m_{sk}^2 \sigma_{tk}^2 + \frac{1}{2} m_{tk}^2 \sigma_{sk}^2 - \rho_k m_{sk} m_{tk} \sigma_{sk} \sigma_{tk} \right),$$

$$N_2(k) = 0.$$

Characteristic function $f_x(\mathbf{F})$ is given by (9).

VI. Two-Channel Energy Detector

$$a_k \neq 0, \quad b_k \neq 0$$

$$x = \sum_{k=1}^K (a_k s_k^2 + b_k t_k^2)$$

$$D_1(k) = 2(a_k \sigma_{sk}^2 + b_k \sigma_{tk}^2),$$

$$D_2(k) = 4a_k b_k (1 - \rho_k^2) \sigma_{sk}^2 \sigma_{tk}^2,$$

$$N_0(k) = a_k m_{sk}^2 + b_k m_{tk}^2,$$

$$N_1(k) = 4a_k b_k \left(\frac{1}{2} m_{sk}^2 \sigma_{tk}^2 + \frac{1}{2} m_{tk}^2 \sigma_{sk}^2 - \rho_k m_{sk} m_{tk} \sigma_{sk} \sigma_{tk} \right),$$

$$N_2(k) = 0.$$

Characteristic function $f_x(\mathbf{F})$ is given by (9). A simple application of this particular processor was encountered in [6, eqs. 25-26].

VII. Two-Channel Energy Detector and Cross-Correlator

$$a_k \neq 0, \quad b_k \neq 0, \quad c_k \neq 0$$

$$x = \sum_{k=1}^K (a_k s_k^2 + b_k t_k^2 + c_k s_k t_k)$$

$$D_1(k) = 2(a_k \sigma_{sk}^2 + b_k \sigma_{tk}^2 + c_k \rho_k \sigma_{sk} \sigma_{tk}) ,$$

$$D_2(k) = (4a_k b_k - c_k^2)(1 - \rho_k^2) \sigma_{sk}^2 \sigma_{tk}^2 ,$$

$$N_0(k) = a_k m_{sk}^2 + b_k m_{tk}^2 + c_k m_{sk} m_{tk} ,$$

$$N_1(k) = (4a_k b_k - c_k^2) \left(\frac{1}{2} m_{sk}^2 \sigma_{tk}^2 + \frac{1}{2} m_{tk}^2 \sigma_{sk}^2 - \rho_k m_{sk} m_{tk} \sigma_{sk} \sigma_{tk} \right) ,$$

$$N_2(k) = 0 .$$

Characteristic function $f_x(\underline{s})$ is given by (9).

NARROWBAND CROSS-CORRELATOR

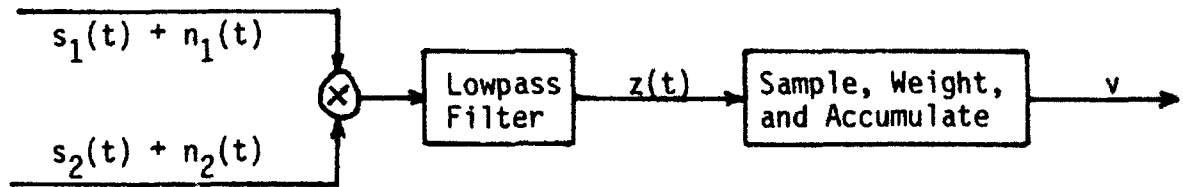


Figure 1. Narrowband Cross-Correlator

The processor of interest in this section is depicted in figure 1. Input signals $s_1(t)$ and $s_2(t)$ are arbitrary deterministic narrowband real waveforms:

$$\begin{aligned} s_j(t) &= \text{Re}\{\underline{s}_j(t) \exp(i2\pi f_0 t)\} = A_j(t) \cos(2\pi f_0 t + P_j(t)) = \\ &= a_j(t) \cos(2\pi f_0 t) - b_j(t) \sin(2\pi f_0 t) \quad \text{for } j = 1, 2, \end{aligned} \quad (23)$$

where input signal complex envelope

$$\underline{s}_j(t) = A_j(t) \exp(iP_j(t)) = a_j(t) + ib_j(t) \quad (24)$$

in terms of polar or rectangular low-frequency components, respectively.

Input noises $n_1(t)$ and $n_2(t)$ are zero-mean correlated narrowband jointly-Gaussian processes which may be nonstationary:

$$n_j(t) = \text{Re}\{\underline{n}_j(t) \exp(i2\pi f_0 t)\} = x_j(t) \cos(2\pi f_0 t) - y_j(t) \sin(2\pi f_0 t), \quad (25)$$

where noise complex envelope

$$\underline{n}_j(t) = x_j(t) + iy_j(t) \quad \text{for } j = 1, 2. \quad (26)$$

The statistics of the input noise complex envelopes are arbitrary:

$$\overline{|n_1(t)|^2} = 2\sigma_1^2,$$

$$\overline{|n_2(t)|^2} = 2\sigma_2^2,$$

$$\overline{n_1(t) n_2^*(t)} = 2\sigma_1\sigma_2\gamma, \quad \text{where } \gamma = \rho + i\lambda = |\gamma|\exp(i\phi),$$

$$\overline{n_j(t) n_m(t)} = 0 \text{ for all } j, m. \quad (27)$$

The quantities σ_1 , σ_2 , γ can all vary with time t , for nonstationary noise processes. There follows, for the statistics of the in-phase and quadrature components defined in (25),

$$\overline{x_1^2} = \overline{y_1^2} = \sigma_1^2, \quad \overline{x_1 y_1} = 0,$$

$$\overline{x_2^2} = \overline{y_2^2} = \sigma_2^2, \quad \overline{x_2 y_2} = 0,$$

$$\overline{x_1 x_2} = \overline{y_1 y_2} = \sigma_1\sigma_2\rho,$$

$$\overline{x_2 y_1} = -\overline{x_1 y_2} = \sigma_1\sigma_2\lambda. \quad (28)$$

The reason for breaking out this narrowband cross-correlator as a separate problem is now apparent from (28). Namely, at each time instant, a group of four random variables are statistically dependent on each other. This case does not fall into the framework of (8) above, since only two random variables were dependent there.

Using the narrowband character of all the waveforms in (24) and (26), the lowpass filter output in figure 1 may be expressed as

$$z(t) = \frac{1}{2}[x_1(t) + a_1(t)][x_2(t) + a_2(t)] + \frac{1}{2}[y_1(t) + b_1(t)][y_2(t) + b_2(t)]. \quad (29)$$

The final system output in figure 1 is the weighted sum of K terms,

$$v = \sum_{k=1}^K w(k) z(t_k), \quad (30)$$

where it is assumed that the time separations between samples at instants $\{t_k\}$ lead to statistically independent random variables $\{z(t_k)\}$. The weights and statistics can change with sample time t_k , in an arbitrary fashion.

Based upon the method in [7], we find the characteristic function of $z(t)$ in (29) to be given by

$$f_z(\mathfrak{F}, t) = \frac{1}{1 - i\mathfrak{F}D_1 + \mathfrak{F}^2 D_2} \exp \left[i\mathfrak{F} \frac{N_0 + i\mathfrak{F}N_1}{1 - i\mathfrak{F}D_1 + \mathfrak{F}^2 D_2} \right], \quad (31)$$

where the constants (in their most compact form) are given by

$$D_1 = \sigma_1 \sigma_2 \rho,$$

$$D_2 = \frac{1}{4} \sigma_1^2 \sigma_2^2 (1 - \rho^2 - \lambda^2),$$

$$N_0 = \frac{1}{2} (a_1 a_2 + b_1 b_2),$$

$$N_1 = \frac{1}{8} \left[\sigma_2^2 (a_1^2 + b_1^2) + \sigma_1^2 (a_2^2 + b_2^2) - 2\sigma_1 \sigma_2 \rho (a_1 a_2 + b_1 b_2) - 2\sigma_1 \sigma_2 \lambda (a_2 b_1 - a_1 b_2) \right]. \quad (32)$$

(The characteristic function and constants in (31) and (32) are not to be interchanged or confused with any earlier results in previous sections. In fact, observe there is no square root involved in (31).) All of the parameters in (32) can vary with time t .

In terms of the signal polar definitions in (24) and the complex noise correlation coefficient γ in (27), alternative expressions to (32) (where we have emphasized the t -dependence) are

$$D_1 = \sigma_1(t) \sigma_2(t) \operatorname{Re}\{\gamma(t)\} = \sigma_1(t) \sigma_2(t) |\gamma(t)| \cos \phi(t),$$

$$D_2 = \frac{1}{4} \sigma_1^2(t) \sigma_2^2(t) (1 - |\gamma(t)|^2),$$

$$N_0 = \frac{1}{2} \operatorname{Re}\{\underline{s}_1^*(t) \underline{s}_2(t)\} = \frac{1}{2} A_1(t) A_2(t) \cos[P_1(t) - P_2(t)],$$

$$N_1 = \frac{1}{8} \left[\sigma_2^2(t) |\underline{s}_1(t)|^2 + \sigma_1^2(t) |\underline{s}_2(t)|^2 - 2 \sigma_1(t) \sigma_2(t) \operatorname{Re}\{\underline{s}_1^*(t) \underline{s}_2(t) \gamma(t)\} \right] =$$

$$= \frac{1}{8} \left[\sigma_2^2(t) A_1^2(t) + \sigma_1^2(t) A_2^2(t) - 2 \sigma_1(t) \sigma_2(t) A_1(t) A_2(t) |\gamma(t)| \cos[P_1(t) - P_2(t) - \phi(t)] \right]. \quad (33)$$

The mean and variance of $z(t)$ in (29) follow from (31) as

$$\mu_z = D_1 + N_0,$$

$$\sigma_z^2 = D_1^2 + 2D_2 + 2D_1N_0 + 2N_1. \quad (34)$$

Finally, the characteristic function of the narrowband cross-correlator output v in (30) follows from (31) as

$$f_v(\mathcal{F}) = \prod_{k=1}^K f_z(\mathcal{F}w(k), t_k) =$$

$$= \left[\prod_{k=1}^K \left\{ 1 - i\mathcal{F}w(k) D_1(k) + \mathcal{F}^2 w^2(k) D_2(k) \right\} \right]^{-1} \exp \left[i\mathcal{F} \sum_{k=1}^K \frac{w(k) N_0(k) + i\mathcal{F}w^2(k) N_1(k)}{1 - i\mathcal{F}w(k) D_1(k) + \mathcal{F}^2 w^2(k) D_2(k)} \right], \quad (35)$$

where we have allowed all the parameters in (32) and (33) to vary with time t_k . The mean and variance of output v follow from (35) as

$$\mu_v = \sum_{k=1}^K w(k) [D_1(k) + N_0(k)],$$

$$\sigma_v^2 = \sum_{k=1}^K w^2(k) \left[D_1^2(k) + 2D_2(k) + 2D_1(k)N_0(k) + 2N_1(k) \right]. \quad (36)$$

A program for the evaluation of the cumulative and exceedance distribution functions via (35) is given in appendix C.

In comparison with earlier results in [3] and [7], we have obtained the following extensions here:

1. The input signals are arbitrary narrowband waveforms; they are not limited to two sine waves at the same frequency;
2. The Gaussian input noises can be nonstationary;
3. The number of terms summed to yield the narrowband cross-correlator output can be greater than 1;
4. The characteristic function is in its most compact form, and the constants are expressed directly in terms of given quantities, having eliminated all auxiliary variables.

Output Signal-to-Noise Ratio

It is sometimes desirable to have simple expressions for the output signal-to-noise ratio of the narrowband cross-correlator in figure 1. In terms of the lowpass filter output $z(t)$, we observe first from (32)-(34) that

$$v_z(s) = v_z(s+n) - v_z(n) = N_0 = \frac{1}{2} A_1 A_2 \cos(P_1 - P_2) . \quad (37)$$

We then have two alternative definitions of the signal-to-noise ratio at the lowpass filter output:

$$R_z(n) = \frac{v_z^2(s)}{\sigma_z^2(n)} = \frac{A_1^2 A_2^2 \cos^2(P_1 - P_2)}{2 \sigma_1^2 \sigma_2^2 (1 + \rho^2 - \lambda^2)} ,$$

$$R_z(s+n) = \frac{v_z^2(s)}{\sigma_z^2(s+n)} = \frac{A_1^2 A_2^2 \cos^2(P_1 - P_2)}{4(D_1^2 + 2D_2 + 2D_1 N_0 + 2N_1)} . \quad (38)$$

These closed form expressions allow for arbitrary noise correlations and are considerably simpler than [7, eqs. 41-43]. The signal-to-noise ratios of system output v in figure 1 are K times greater than either form in (38).

Specialization to Narrowband Energy Detector

If the signal and noise parameters in (24) and (27) are chosen as

$$\begin{aligned} a_1(t) &= a_2(t) = a(t) , \\ b_1(t) &= b_2(t) = b(t) , \\ \sigma_1(t) &= \sigma_2(t) = \sigma(t) , \\ \rho(t) &= 1, \lambda(t) = 0 , \end{aligned} \tag{39}$$

then figure 1 reduces to identical input channels, that is, a narrowband energy detector. There follows from (32),

$$\begin{aligned} D_1 &= \sigma^2(t), \quad D_2 = 0 , \\ N_0 &= \frac{1}{2}(a^2(t) + b^2(t)) = \frac{1}{2} A^2(t), \quad N_1 = 0 , \end{aligned} \tag{40}$$

and (31) becomes

$$f_z(\xi, t) = \frac{1}{1 - i\xi\sigma^2(t)} \exp\left[i\xi \frac{A^2(t)/2}{1 - i\xi\sigma^2(t)} \right]. \tag{41}$$

Corresponding results for the system output v are easily obtained from this.

$$P_z(u, t) = \left[1 - Q\left(\frac{A(t)}{\sigma(t)}, \frac{\sqrt{2u}}{\sigma(t)} \right) \right] U(u).$$

REDUCTION OF HERMITIAN AND LINEAR FORM

The most general case of interest in this section is as follows:
random complex matrix

$$X = [x_1 \ x_2 \ \dots \ x_M]^T \quad (42)$$

is $M \times 1$; constant complex matrix

$$A = [a_1 \ a_2 \ \dots \ a_M]^T \quad (43)$$

is $M \times 1$; and constant complex matrix

$$B = \begin{bmatrix} b_{11} & \dots & b_{1M} \\ b_{M1} & \dots & b_{MM} \end{bmatrix} \quad (44)$$

is $M \times M$ and Hermitian. The Hermitian and linear form we consider is

$$\begin{aligned} q &= X^H B X + \frac{1}{2}(X^H A + A^H X) = \\ &= \sum_{m,n=1}^M x_m^* b_{mn} x_n + \frac{1}{2} \sum_{m=1}^M (x_m^* a_m + a_m^* x_m), \end{aligned} \quad (45)$$

which is real. Random variable q is a weighted sum of all possible products of $\{x_m^*\}$ and $\{x_n\}$, plus linear combinations.* A and B are called the weighting matrices.

* For $M=2$ or 4 , and real variables and weights, (45) reduces to the earlier forms given in (1) and (29).

We will concentrate in this section on reducing form (45) to a weighted sum of squares of uncorrelated random variables. This stepping stone does not require any Gaussian assumptions on X and is therefore useful as a separate item.

The relevant statistics pertaining to random vector X are

$$\bar{X} = E \quad (\text{mean matrix}),$$

$$\tilde{X} = X - \bar{X} = X - E,$$

$$\text{Cov}\{X\} = \overline{\tilde{X}\tilde{X}^H} = K \quad (\text{covariance matrix}), \quad (46)$$

where statistics matrices E and K are given. $M \times M$ matrix K is always Hermitian and non-negative definite. We assume K is positive definite; otherwise eliminate the linearly dependent components of \tilde{X} . We allow x_m and x_n to be correlated with each other for any m and n ; this situation is much more general than the investigations above.

Let C be a constant $M \times M$ matrix and form the linearly transformed variables

$$W = C^H X = [w_1 \ w_2 \ \dots \ w_M]^T. \quad (47)$$

Then the statistics of W are given by

$$\bar{W} = C^H E,$$

$$\tilde{W} = W - \bar{W} = C^H \tilde{X},$$

$$\text{Cov}\{W\} = \overline{\tilde{W}\tilde{W}^H} = C^H \overline{\tilde{X}\tilde{X}^H} C = C^H K C. \quad (48)$$

Also, from (47), since

$$X = C^{-H} W, \quad (49)$$

then we can express (45) as

$$q = W^H C^{-1} B C^{-H} W + \frac{1}{2}(W^H D + D^H W), \quad (50)$$

where we define constant $M \times 1$ matrix

$$D = C^{-1} A = [d_1 \ d_2 \ \dots \ d_M]^T. \quad (51)$$

We want to have, from (48) and (50),

$$C^H K C = I \quad (52)$$

and

$$C^{-1} B C^{-H} = \Lambda = \text{diag}(\lambda_1 \ \lambda_2 \ \dots \ \lambda_M); \quad \text{i.e. } C^H B^{-1} C = \Lambda^{-1}, \quad (53)$$

for then, in addition to the relation between the means,

$$\bar{W} = C^H \bar{E}, \quad (54)$$

we have the desirable properties

$$\text{Cov}\{W\} = I, \quad (55)$$

and

$$q = W^H \Lambda W + \frac{1}{2}(W^H D + D^H W) = \sum_{m=1}^M \lambda_m |w_m|^2 + \text{Re} \sum_{m=1}^M d_m^* w_m. \quad (56)$$

That is, the random vector W given by (47) is composed of uncorrelated unit-variance components, and q is a weighted sum of magnitude-squares of these components, in addition to a linear sum.

We now have to address the problem of determining the $M \times M$ matrices C and Λ in (52) and (53). From [8, p. 106, Theorem 2], we identify

$$M \rightarrow K, \quad K \rightarrow B^{-1}, \quad \mathcal{L} \rightarrow \mathcal{L}^{-1}; \quad (57)$$

then according to [8, p. 107, eq. 29], we must solve for C and \mathcal{L} in the equation

$$B^{-1}C = KC\mathcal{L}^{-1}, \quad \text{i.e.} \quad BKC = C\mathcal{L}. \quad (58)$$

So the only matrix that need be considered is the $M \times M$ product BK . C is the modal matrix, and \mathcal{L} the eigenvalue matrix, of BK . Also, from (51),

$$D = C^H A, \quad \text{since } C^{-1} = C^H. \quad (59)$$

Letting $C = [C^{(1)} \dots C^{(M)}]$, where eigenvector $C^{(m)}$ is a $M \times 1$ matrix, (58) can be expressed as

$$BKC^{(m)} = \lambda_m C^{(m)} \quad \text{for } 1 \leq m \leq M. \quad (60)$$

Several important properties hold for \mathcal{L} and C :

The $\{\lambda_m\}_1^M$ are all real, but can be positive, zero, or negative.

If K and B are real, then C is real. (61)

If B is positive definite, then $\lambda_m > 0$ for $1 \leq m \leq M$.

If $A = 0$ and $E = 0$, there is no need to solve (58) for C , because $D = 0$ and $\bar{W} = 0$.

QUADRATIC AND LINEAR FORM

If random vector X is real Gaussian, if A is real, and if B is real symmetric, then mean E and covariance K are real, and it follows that modal matrix C is also real. Also from (47) and (59), W and D are real. Equation (45) reduces to

$$q = X^T B X + X^T A = \sum_{m,n=1}^M x_m b_{mn} x_n + \sum_{m=1}^M a_m x_m, \quad (62)$$

which is a quadratic form and linear form.

Letting mean \bar{W} in (54) be expressed as

$$\bar{W} = [v_1 \ v_2 \ \dots \ v_M]^T, \quad (63)$$

the Gaussian character of X and the linear transformation (47) allow us to write the probability density function of W as a product:

$$p(W) = \prod_{m=1}^M \left\{ (2\pi)^{-1/2} \exp\left(-\frac{1}{2} (w_m - v_m)^2\right) \right\}. \quad (64)$$

Here we used property (55). Since we now have, from (56),

$$q = \sum_{m=1}^M (\lambda_m w_m^2 + d_m w_m), \quad (65)$$

the characteristic function of q is

$$\begin{aligned} f_q(\xi) &= \overline{\exp(i\xi q)} = \overline{\exp\left(i\xi \sum_{m=1}^M (\lambda_m w_m^2 + d_m w_m)\right)} = \\ &= \left[\prod_{m=1}^M \left\{ 1 - i2\lambda_m \xi \right\} \right]^{-1/2} \exp\left[i\xi \sum_{m=1}^M \frac{\lambda_m v_m^2 + d_m v_m + i\xi d_m^2/2}{1 - i2\lambda_m \xi} \right], \quad (66) \end{aligned}$$

where the square root must be a continuous function of ξ , not a principal value square root.* Notice that only one square root and one exponential is required per ξ value. Observe that the characteristic function depends on the separate values $\{v_m\}_1^M$ and $\{d_m\}_1^M$, not merely on their sums. If $A = E = 0$, the exponential is unity, by virtue of (54) and (59). And if $M=2$, (66) reduces to (5), while $M=4$ leads to form (31).

To summarize, the characteristic function $f_q(\xi)$ in (66) for random variable q in (62) requires the constants $\{\lambda_m\}$, $\{d_m\}$, and $\{v_m\}$ for $1 \leq m \leq M$. The initially given quantities are weighting matrices A , B and statistics matrices E , K . We first solve the equation (58),

$$BKC = C\Lambda, \quad (67)$$

for eigenvalue matrix Λ and modal matrix C corresponding to BK . Then

$$\begin{aligned} \Lambda &= \text{diag}(\lambda_1 \ \lambda_2 \ \dots \ \lambda_M) ; \\ D &= C^T A = [d_1 \ d_2 \ \dots \ d_M]^T , \\ \bar{W} &= C^T E = [v_1 \ v_2 \ \dots \ v_M]^T . \end{aligned} \quad (68)$$

If the mean of input X is zero, $E = 0$, and if the linear weighting form is zero, $A = 0$, then there is no need to solve for modal matrix C of BK in (67). Then $D = \bar{W} = 0$ and the exponential term in (66) is unity. One only need compute eigenvalue matrix Λ of BK in this case.

A program for the evaluation of the cumulative and exceedance distribution functions corresponding to characteristic function (66) is listed in appendix D. The inputs to the program are considered to be M , $\{\lambda_m\}$,

* That is, the square root is the analytic continuation of the function defined as 1 at $\xi=0$.

$\{d_m\}$, $\{v_m\}$; that is, it is presumed that (67) and (68) have already been solved prior to use of the program.

The cumulants of q are obtained from (66) as

$$\chi_q(n) = \left. \begin{cases} \sum_{m=1}^M (\lambda_m + \lambda_m v_m^2 + d_m v_m) = \nu_q & \text{for } n = 1 \\ 2^{n-1} (n-1)! \sum_{m=1}^M \lambda_m^{n-2} \left[\lambda_m^2 + n \left(\lambda_m v_m + \frac{1}{2} d_m \right)^2 \right] & \text{for } n \geq 2 \end{cases} \right\}. \quad (69)$$

In particular, the variance of q is

$$\chi_q(2) = 2 \sum_{m=1}^M \left[\lambda_m^2 + 2 \left(\lambda_m v_m + \frac{1}{2} d_m \right)^2 \right] = \sigma_q^2. \quad (70)$$

If another random variable is formed by the sum of several independent random variables q_j with the form (62), but with different sizes M_j , the new characteristic function is the product of terms like (66).

Breakdown of X into Two Components

It is useful to investigate a particular version of the general results above, because the resultant forms correspond to some often-realized practical energy detectors and correlators. We let $M = 2N$, and

$$X = \begin{bmatrix} U \\ V \end{bmatrix}, \quad B = \begin{bmatrix} B^{11} & B^{12} \\ B^{21} & B^{22} \end{bmatrix}, \quad A = \begin{bmatrix} A^{(1)} \\ A^{(2)} \end{bmatrix}, \quad (71)$$

where U , V , $A^{(1)}$, $A^{(2)}$ are $N \times 1$ real matrices, and $\{B^{ij}\}$ are $N \times N$ real matrices. Also B^{11} and B^{22} are symmetric, while $B^{21} = B^{12T}$. Then (62) can be expressed as

$$\begin{aligned}
q &= X^T B X + X^T A = \begin{bmatrix} U^T & V^T \end{bmatrix} \begin{bmatrix} B^{11} & B^{12} \\ B^{21} & B^{22} \end{bmatrix} \begin{bmatrix} U \\ V \end{bmatrix} + \begin{bmatrix} U^T & V^T \end{bmatrix} \begin{bmatrix} A^{(1)} \\ A^{(2)} \end{bmatrix} = \\
&= U^T B^{11} U + U^T B^{12} V + V^T B^{21} U + V^T B^{22} V + U^T A^{(1)} + V^T A^{(2)} = \\
&= U^T B^{11} U + 2U^T B^{12} V + V^T B^{22} V + U^T A^{(1)} + V^T A^{(2)} = \\
&= \sum_{m,n=1}^N \left(u_m b_{mn}^{11} u_n + 2u_m b_{mn}^{12} v_n + v_m b_{mn}^{22} v_n \right) + \sum_{n=1}^N \left(u_n a_n^{(1)} + v_n a_n^{(2)} \right) = \\
&= \text{all possible auto and cross combinations of random} \\
&\quad \text{variables } \{u_n\}_1^N \text{ and } \{v_n\}_1^N, \text{ plus linear combinations.} \quad (72)
\end{aligned}$$

We also have, from (47) and (68),

$$\begin{aligned}
W &= C^T X = C^T \begin{bmatrix} U \\ V \end{bmatrix}, \quad \bar{W} = C^T \begin{bmatrix} \bar{U} \\ \bar{V} \end{bmatrix} = C^T \begin{bmatrix} E_u \\ E_v \end{bmatrix}, \quad D = C^T \begin{bmatrix} A^{(1)} \\ A^{(2)} \end{bmatrix}, \\
K &= \text{Cov}\{X\} = \overline{X X^T} = \overline{\begin{bmatrix} \bar{U} \\ \bar{V} \end{bmatrix} \begin{bmatrix} \bar{U}^T & \bar{V}^T \end{bmatrix}} = \begin{bmatrix} K_{uu} & K_{uv} \\ K_{vu} & K_{vv} \end{bmatrix}. \quad (73)
\end{aligned}$$

Then the fundamental matrix required in (67) is expressible as

$$BK = \begin{bmatrix} B^{11} & B^{12} \\ B^{21} & B^{22} \end{bmatrix} \begin{bmatrix} K_{uu} & K_{uv} \\ K_{vu} & K_{vv} \end{bmatrix}, \quad (74)$$

which is a $2N \times 2N$ matrix. Also random variable (65) is now

$$q = \sum_{m=1}^{2N} \left(\lambda_m w_m^2 + d_m w_m \right), \quad (75)$$

which has $2N$ terms. The characteristic function of q , in general, follows from (66) and (68) as

$$f_q(\xi) = \left[\prod_{m=1}^{2N} \{1 - i2\lambda_m \xi\} \right]^{-1/2} \exp \left[i \xi \sum_{m=1}^{2N} \frac{\lambda_m v_m^2 + d_m v_m + i \xi d_m^2 / 2}{1 - i2\lambda_m \xi} \right], \quad (76)$$

where

$$\bar{W} = [v_1 \dots v_{2N}]^T = C^T \begin{bmatrix} E_u \\ E_v \end{bmatrix}, \quad D = [d_1 \ d_2 \ \dots \ d_{2N}]^T = C^T \begin{bmatrix} A^{(1)} \\ A^{(2)} \end{bmatrix}. \quad (77)$$

(If $A^{(1)} = A^{(2)} = E_u = E_v = 0$, then $D = 0$ and $\bar{W} = 0$, and there is no need to solve for modal matrix C ; the exponential in $f_q(\xi)$ in (76) is then unity.)

As a special case, if $A = 0$, $B^{11} = 0$, $B^{22} = 0$, then (71) and (73) yield

$$B = \begin{bmatrix} 0 & B^{12} \\ B^{21} & 0 \end{bmatrix}, \quad D = 0, \quad (78)$$

and (72) gives

$$q = 2U^T B^{12} v = 2 \sum_{m,n=1}^N u_m b_{mn}^{12} v_n =$$

= all possible cross combinations of $\{u_n\}_1^N$ and $\{v_n\}_1^N$. (79)

Then (74) specializes to

$$BK = \begin{bmatrix} 0 & B^{12} \\ B^{21} & 0 \end{bmatrix} \begin{bmatrix} K_{uu} & K_{uv} \\ K_{vu} & K_{vv} \end{bmatrix} = \begin{bmatrix} B^{12} K_{vu} & B^{12} K_{vv} \\ B^{21} K_{uu} & B^{21} K_{uv} \end{bmatrix} \quad (80)$$

and (75) reduces to

$$q = \sum_{m=1}^{2N} \lambda_m w_m^2, \quad (81)$$

with characteristic function

$$f_q(\xi) = \left[\prod_{m=1}^{2N} \{1 - i2\lambda_m \xi\} \right]^{-1/2} \exp \left[i \xi \sum_{m=1}^{2N} \frac{\lambda_m w_m^2}{1 - i2\lambda_m \xi} \right] \quad (82)$$

following directly from (76) and (78).

For the particular example of

$$B^{12} = \frac{1}{2} \text{diag}(l_1 \ l_2 \ \dots \ l_N) + \frac{1}{2} [g_1 \ g_2 \ \dots \ g_N]^T [h_1 \ h_2 \ \dots \ h_N], \quad (83)$$

then

$$q = \sum_{n=1}^N l_n u_n v_n + \left(\sum_{n=1}^N g_n u_n \right) \left(\sum_{n=1}^N h_n v_n \right), \quad (84)$$

with the same characteristic function (82).

As a still more-special case, let $B^{12} = \frac{1}{2} I$; then (79) and (81) give the simple cross-correlator (but with correlated inputs for all time separations)

$$q = \sum_{n=1}^N u_n v_n = \sum_{m=1}^{2N} \lambda_m w_m^2, \quad (85)$$

and (80) and (77) become

$$BK = \frac{1}{2} \begin{bmatrix} K_{vu} & K_{vv} \\ K_{uu} & K_{uv} \end{bmatrix}, \quad \bar{w} = C^T \begin{bmatrix} E_u \\ E_v \end{bmatrix} = [v_1 \ \dots \ v_{2N}]^T. \quad (86)$$

The important equations that must be solved are always

$$BKC = C\Lambda \quad (87)$$

or

$$BKC^{(m)} = \lambda_m C^{(m)} \quad \text{for } 1 \leq m \leq M = 2N, \quad (88)$$

where all matrices B, K, C, Λ are $2N \times 2N$. The characteristic function of (85) is again (82).

Special Case of Correlator (85)

Here we let components U and V have the same covariance and a scaled cross-correlation; that is, let

$$K_{uu} = K_0, \quad K_{vv} = K_0, \quad K_{uv} = \rho K_0, \quad (89)$$

where ρ is a scale factor. This case corresponds, for example, to a common signal in two independent components:

$$\begin{aligned} u(t) &= s(t) + n_1(t), \\ v(t) &= s(t) + n_2(t), \end{aligned} \quad (90)$$

where $s(t)$, $n_1(t)$, $n_2(t)$ are all independent and have a common covariance. Then (85) becomes

$$BK = \frac{1}{2} \begin{bmatrix} \rho K_0 & K_0 \\ K_0 & \rho K_0 \end{bmatrix}. \quad (91)$$

Now suppose that we can determine the $N \times N$ eigenvalue matrix Γ and modal matrix Q of K_0 , that is

$$K_0 Q = Q \Gamma; \quad \Gamma = \text{diag}(\gamma_1, \gamma_2 \dots \gamma_N). \quad (92)$$

Then we have the standard relations [8]

$$K_0 = Q \Gamma Q^T \quad \text{where} \quad Q Q^T = I. \quad (93)$$

We can now express the $2N \times 2N$ matrix in (91) as

$$\begin{aligned} BK &= \frac{1}{2} \begin{bmatrix} Q \rho \Gamma Q^T & Q \Gamma Q^T \\ Q \Gamma Q^T & Q \rho \Gamma Q^T \end{bmatrix} = \\ &= \begin{bmatrix} Q & 0 \\ 0 & Q \end{bmatrix} \begin{bmatrix} \frac{1}{2} \rho \Gamma & \frac{1}{2} \Gamma \\ \frac{1}{2} \Gamma & \frac{1}{2} \rho \Gamma \end{bmatrix} \begin{bmatrix} Q^T & 0 \\ 0 & Q^T \end{bmatrix}, \end{aligned} \quad (94)$$

and $2N \times 2N$ identity matrix

$$I_{2N} = \begin{bmatrix} Q & 0 \\ 0 & Q \end{bmatrix} \begin{bmatrix} I & 0 \\ 0 & I \end{bmatrix} \begin{bmatrix} Q^T & 0 \\ 0 & Q^T \end{bmatrix}. \quad (95)$$

There follows

$$BK - \lambda I_{2N} = \begin{bmatrix} Q & 0 \\ 0 & Q \end{bmatrix} \begin{bmatrix} \frac{1}{2} \rho \Gamma - \lambda I & \frac{1}{2} \Gamma \\ \frac{1}{2} \Gamma & \frac{1}{2} \rho \Gamma - \lambda I \end{bmatrix} \begin{bmatrix} Q^T & 0 \\ 0 & Q^T \end{bmatrix}. \quad (96)$$

But the middle matrix in (96) can be developed in detail in the partitioned form

$$\begin{bmatrix} \frac{1}{2}\rho\gamma_1 - \lambda & & & & \frac{1}{2}\gamma_1 & & & \\ & \ddots & & & & \ddots & & \\ & & \frac{1}{2}\rho\gamma_N - \lambda & & & & \frac{1}{2}\gamma_N & \\ \hline \frac{1}{2}\gamma_1 & & & & \frac{1}{2}\rho\gamma_1 - \lambda & & & \\ & \ddots & & & & \ddots & & \\ & & \frac{1}{2}\gamma_N & & & & \frac{1}{2}\rho\gamma_N - \lambda & \end{bmatrix} \cdot \quad (97)$$

This matrix is singular when the kth row is equal to, or the negative of, the k+Nth row. This leads to the eigenvalues $\{\lambda_n\}_1^{2N}$ of matrix BK:

$$\begin{aligned} \lambda_1 &= \frac{1}{2}(\rho+1)\gamma_1, \dots, \lambda_N = \frac{1}{2}(\rho+1)\gamma_N, \\ \lambda_{N+1} &= \frac{1}{2}(\rho-1)\gamma_1, \dots, \lambda_{2N} = \frac{1}{2}(\rho-1)\gamma_N. \end{aligned} \quad (98)$$

Thus we need only solve for the N eigenvalues $\{\gamma_n\}_1^N$ of matrix K_0 , and then use them as above to determine all 2N eigenvalues of BK; this is a significant shortcut.

If also $E_u = E_v = 0$, then $\bar{W} = 0$ from (86), and the characteristic function of q in (85) follows from (82) and (98) as

$$\begin{aligned} f_q(\xi) &= \left[\prod_{m=1}^N \left\{ (1-i(\rho+1)\gamma_m \xi)(1-i(\rho-1)\gamma_m \xi) \right\} \right]^{-1/2} = \\ &= \left[\prod_{m=1}^N \left\{ 1 - i2\rho\gamma_m \xi + (1-\rho^2)\gamma_m^2 \xi^2 \right\} \right]^{-1/2}. \end{aligned} \quad (99)$$

This is a generalization of [1, eq. 54], which held for a single pair of Gaussian random variables.

EXAMPLES

The program listed in appendix A for the second-order processor (8) and attendant characteristic function (9) has been employed to yield the result in figure 2. The particular values for the number of terms K , the weights, and the input statistics are listed in lines 20-120. There is no physical significance attached to this particular example; rather it has been run simply to illustrate the extreme generality that the technique is capable of. Some negative values for the weights, means, and correlation coefficients have been employed to emphasize this generality. This simple example (and others to follow) can be used as a check case on any user-written program to evaluate cumulative and exceedance distribution functions.

The selection of parameters L , Δ , b in lines 130-150 is discussed in detail in [1]; the reader is referred there for the deleterious effects that can occur for improper choices of L , Δ , b . The selection of M_f , the FFT size in line 160, is rather arbitrary; it controls the spacing at which the probability distributions are computed, but has no effect upon the accuracy of the results (except for round-off noise). Additional computational details on the particular program for characteristic function (9) are given in appendix A.

The ordinate scale for figure 2 is a logarithmic one. The lower right end of the exceedance distribution function curve decreases smoothly to the region $1E-11$, where roundoff noise is encountered. The exceedance distribution function values continue to decrease with x until, finally, negative values (due to roundoff noise) are generated. For negative probability values, the logarithm of the absolute value is plotted, but mirrored below the $1E-12$ level. These values have no physical significance, of course; they are plotted to illustrate the level of accuracy attainable by this procedure with appropriate choices of L and Δ .

The rates of decay of the cumulative and exceedance distribution functions in figure 2 are markedly different for this particular example. Additionally, since the decays are both linear on this logarithmic ordinate, it means that both tail distributions are exponential, not Gaussian. These attributes of the cumulative and exceedance distribution functions are easily

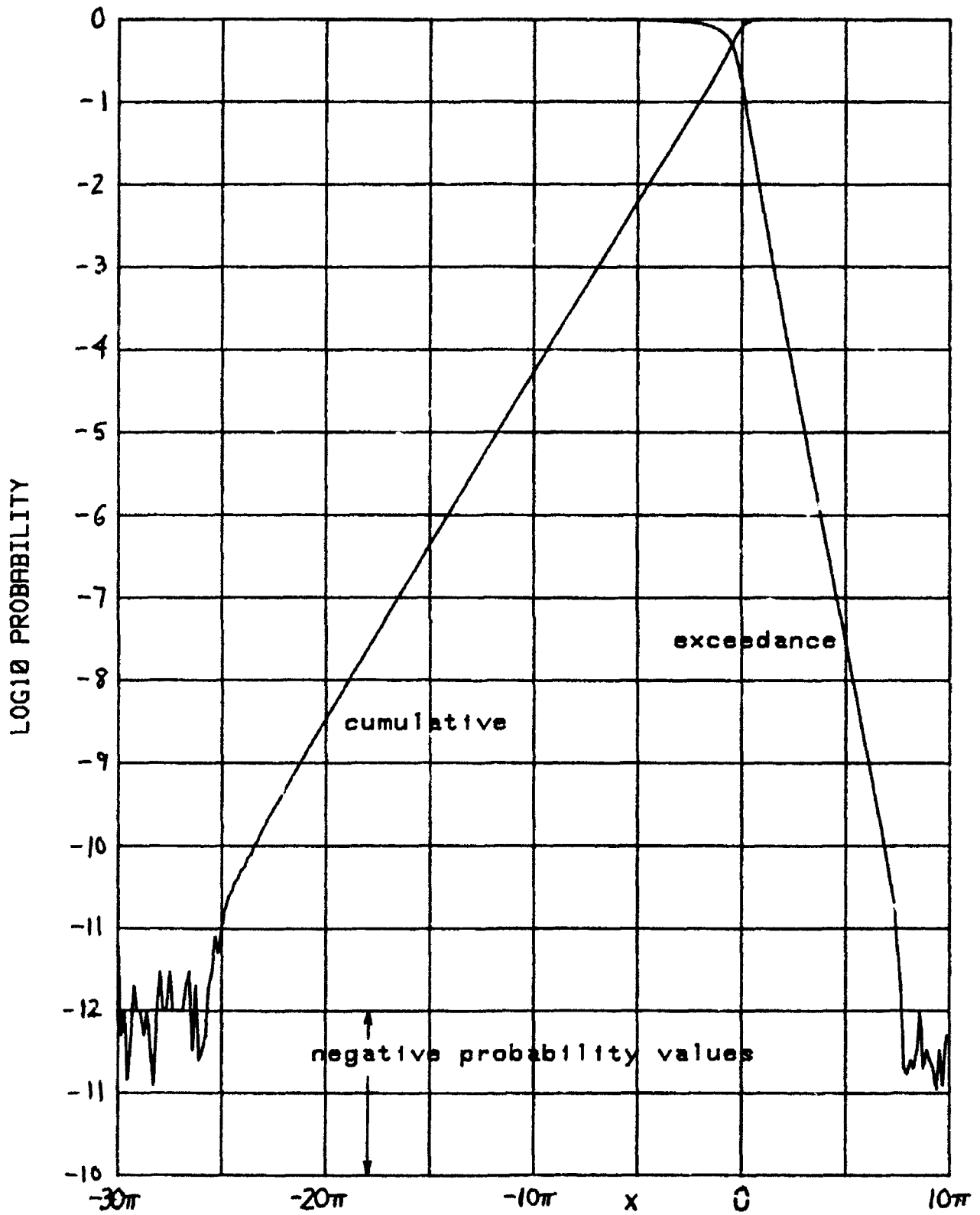


Figure 2. Distributions for Second-Order Processor

and quickly discernible by use of the numerical technique in [1], for a limitless variety of weights and input statistics, with a minimum of effort on the part of the user.

As a check on the program in appendix A, the second-order processor in (8) was simulated, and 10,000 independent trials were used to determine its performance for the exact same parameters as used for figure 2 above. The program is listed in appendix E and the results are given in figure 3. The corroboration is excellent, even near the $1E-4$ probability level.

As the number of terms, K , in the second-order processor (8) is increased, and if the statistics are identical, the random variable x should approach Gaussian, at least near its mean. The example in figure 4 was run for $K = 10$, and all weights and statistics independent of k ; the particular choices were

$$\begin{aligned} a &= .6, b = -.6, c = .3, d = -.2, e = .2, \\ m_s &= .5, m_t = -.5, \sigma_s = 1, \sigma_t = 1, \rho = .4, \\ L &= 4, \Delta = .05, b = 20\pi, M_f = 256. \end{aligned} \tag{100}$$

The cumulative and exceedance distribution functions in figure 4 both display a parabolic shape near the mean of x , which signifies Gaussian behavior of the random variable, as expected. However, on the tails, the distributions are tending to linear, which means an exponential decay there. This observation for this example confirms the comments of [7, p. 673].

The cumulative and exceedance distribution functions for an example of the second-order processor with fading are displayed in figure 5, as determined from characteristic function (21) and the corresponding program in appendix B. The power law, ν , for the fading probability density function (19) is 2.7 for this example, but can be easily changed. The particular constants employed are listed in lines 20-110 in appendix B.

An example of the distributions for the narrowband cross-correlator of figure 1 is presented in figure 6, as evaluated from characteristic function

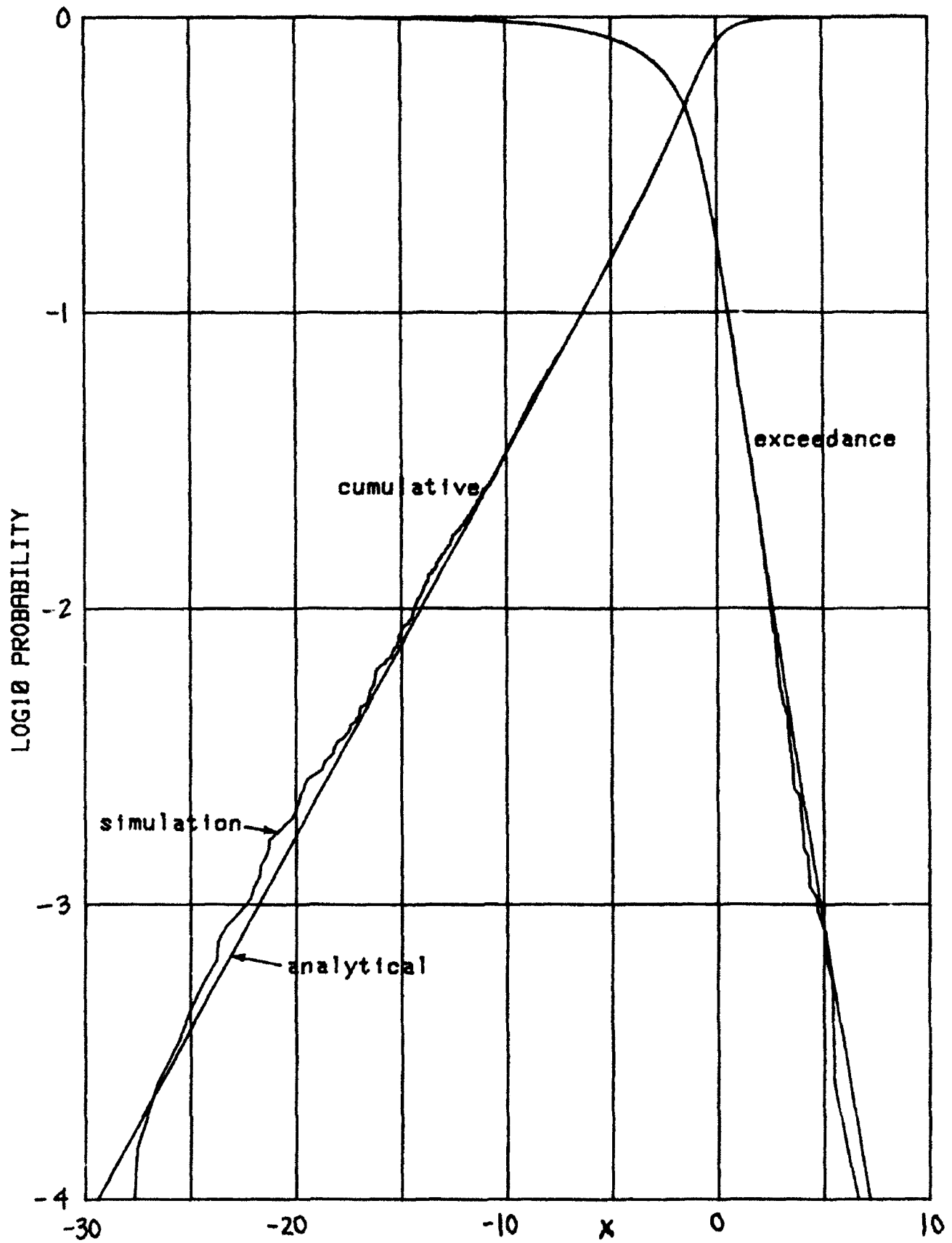


Figure 3. Simulation Comparison of Second-Order Processor

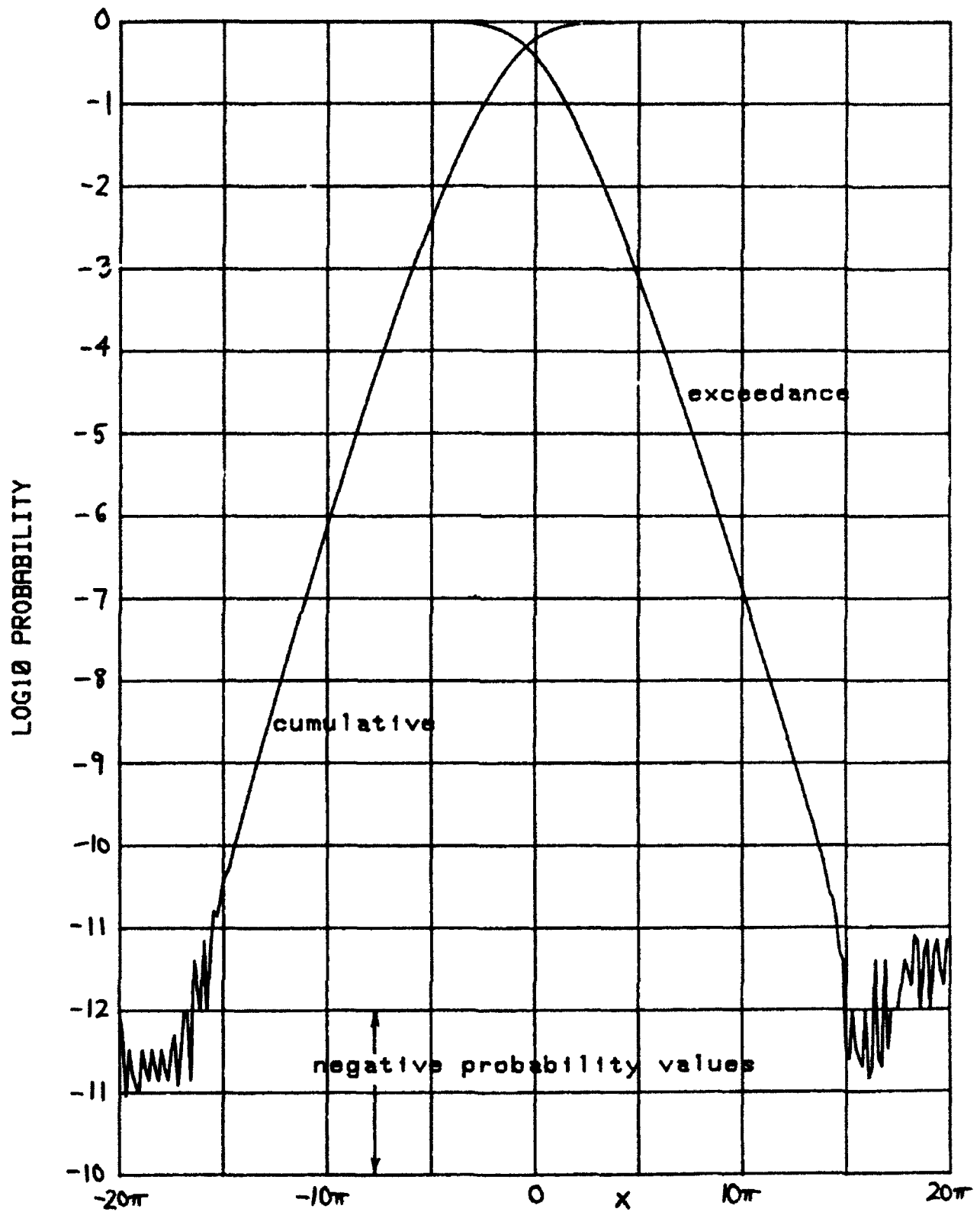


Figure 4. Second-Order Processor, $K=10$, Identical Statistics

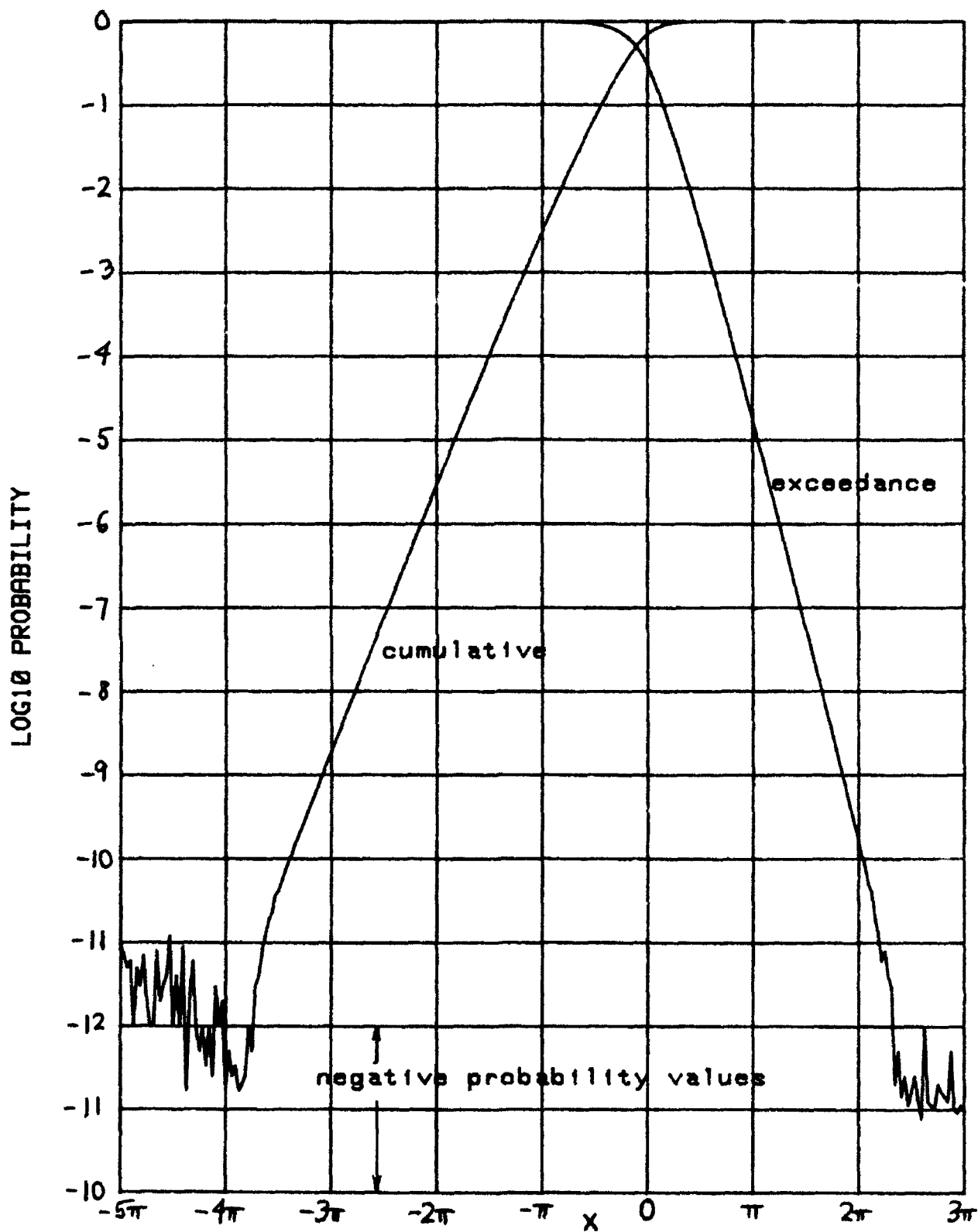


Figure 5. Second-Order Processor with Fading

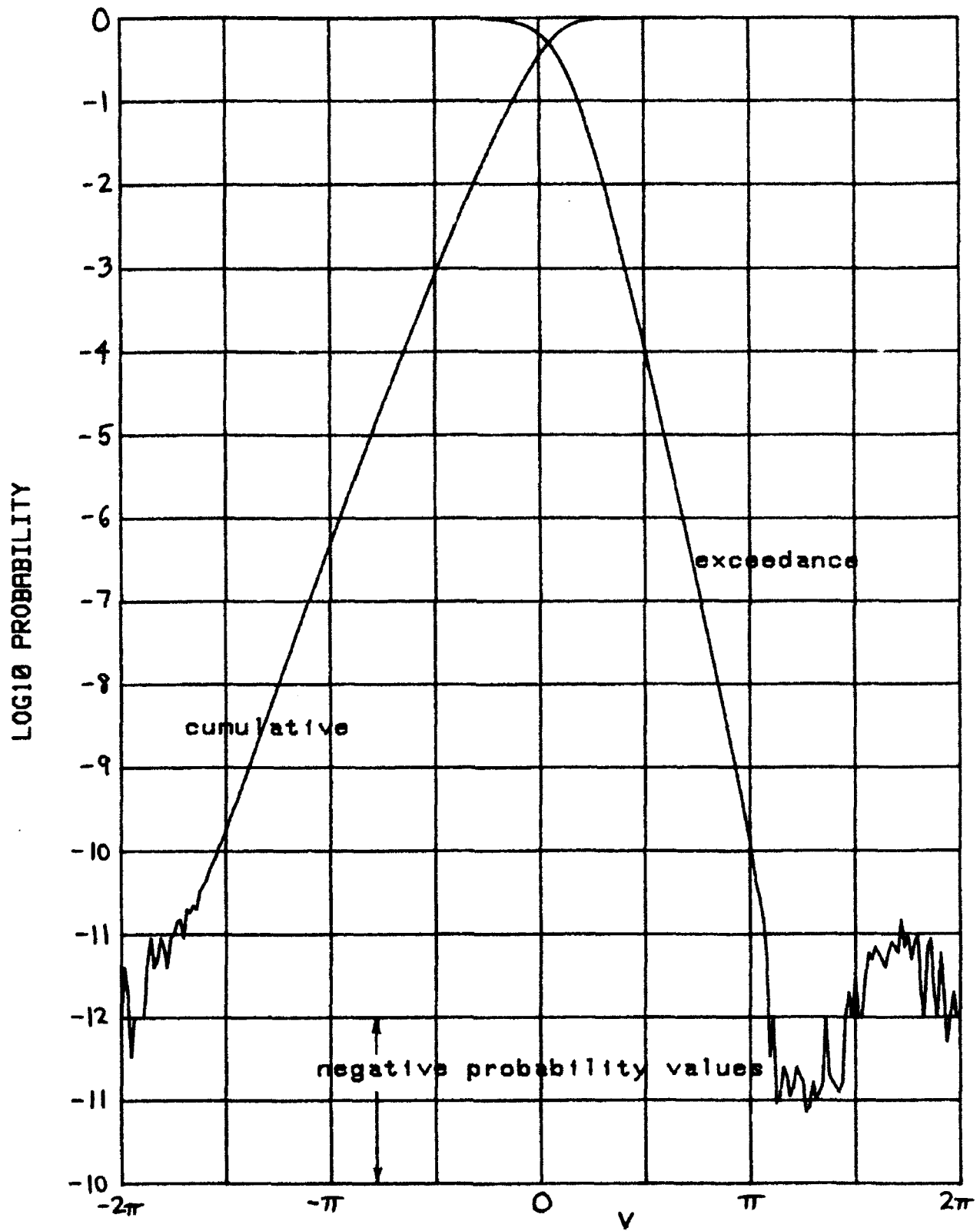


Figure 6. Distributions for Narrowband Cross-Correlator

(35) and the program in appendix C. The weightings, signal components, and noise statistics have no special values or interrelationships; the particular values used here are listed in lines 20-110.

The distributions for the reduced quadratic and linear form (65) and accompanying characteristic function (66) are presented in figure 7 for the numerical example employed in the program listing in appendix D. If the given form is instead that of (62), then (67)-(68) must first be solved before the program in appendix D can be employed; that is, one must augment these results with the capability for extracting the eigenvalues (and eigenvectors in some cases) of the $M \times M$ matrix BK . The size of the FFT, M_f , has been increased to 1024 in figure 7; this results in finer spacing of the distribution values and additional spikes in the round-off noise region centered about $1E-12$.

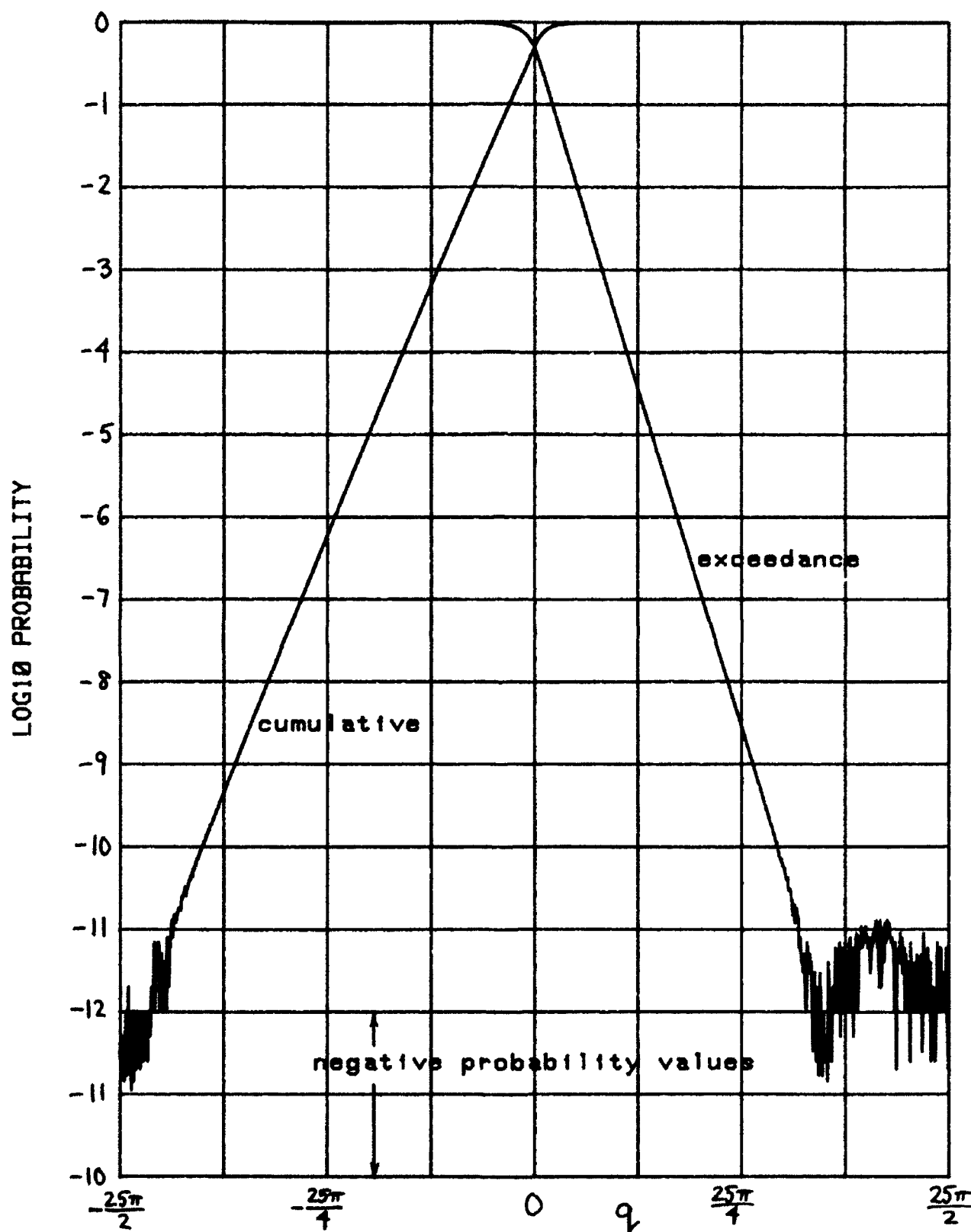


Figure 7. Distributions for Quadratic and Linear Form

SUMMARY AND DISCUSSION

Closed form expressions for the characteristic functions of the decision variables of three classes of second-order processors have been derived. The input noise to the processors must be Gaussian, but it can be nonstationary with arbitrary statistics. Programs for the direct evaluation of the exact cumulative and exceedance distribution functions have been generated and then exercised for completely general values of the weights, signal parameters, and noise statistics. There is no assumption needed about a large number of statistically independent contributors, nor need any signal-to-noise ratio be either small or large. The first two classes of processors are restricted in form, but include many of the practical devices often encountered in detection and estimation problems. The third class covers the most general second-order processor; it requires the solution for the eigenvalue and modal matrices of an $M \times M$ matrix (where M is the size of the general quadratic form) in addition to the program furnished here. The approach utilized here allows a user to quickly and easily obtain accurate quantitative information about the performance of a particular processor, and to investigate the effects of making changes in any of the input constants or parameters.

Approximations to the performance of continuous quadratic processors are possible by use of the above procedures. For example,

$$\iint dt_1 dt_2 x(t_1) \beta(t_1, t_2) x(t_2) \cong \Delta_1 \Delta_2 \sum_{m,n} x(m\Delta_1) \beta(m\Delta_1, n\Delta_2) x(n\Delta_2), \quad (10')$$

which is of the form $X^T B X$ encountered in (62). Also

$$\iint dt_1 dt_2 u(t_1) \beta(t_1, t_2) v(t_2) \cong \Delta_1 \Delta_2 \sum_{m,n} u(m\Delta_1) \beta(m\Delta_1, n\Delta_2) v(n\Delta_2), \quad (102)$$

which is of the form $U^T B^{12} V$ encountered in (79).

Receiver operating characteristics, that is, detection probability vs false alarm probability, can be easily determined from the above results. First store the exceedance distribution for zero signal strength in an array. Then plot the exceedance distributions for nonzero signal strengths vs this stored array of numbers, each point for a common threshold. The common thresholds are most easily realized by keeping sampling increment Δ and FFT size M_f the same throughout all the computations.

APPENDIX A. SECOND-ORDER PROCESSOR

This program computes the cumulative and exceedance distribution functions of random variable (8) via characteristic function (9). The required inputs are listed in lines 20-120 and are annotated consistently with (8). The parameters D_1 , D_2 , N_0 , N_1 , N_2 required in characteristic function (9) are pre-computed once in loop 290-510 for the sake of execution time. The mean of x is entered in line 520. When we enter loop 590-830 for the actual calculation of the characteristic function (9), the number of computations are minimized. For example, only one complex exponential and square root are required per ξ value, in lines 740-750. The square root in (9) is not a principal value square root, but in fact must yield a continuous function in ξ . In order to achieve this, the argument of the square root is traced continuously from $\xi = 0$ (line 530). If an abrupt change in phase is detected, a polarity indicator takes note of this fact (line 780) and corrects the final values of characteristic function $f_y(\xi)$ (line 790). More detail on the selection of L , Δ , b in lines 130-150 is available in [1].

```

10 ! SECOND-ORDER PROCESSOR
20   K=5                ! Number of terms summed
30   DATA .6,-.5,.4,-.3,.2 ! a(k) weightings
40   DATA .9,.8,.7,-.6,-.5 ! b(k) weightings
50   DATA -.6,-.8,1,1.2,1.4 ! c(k) weightings
60   DATA .1,-.2,-.3,.4,.5 ! d(k) weightings
70   DATA -.7,.6,.5,.4,-.3 ! e(k) weightings
80   DATA .2,.3,.4,-.5,-.6 ! Means of random variables s(k)
90   DATA .8,-.7,-.6,.5,.4 ! Means of random variables t(k)
100  DATA .1,.3,.5,.7,.9    ! Standard deviations of s(k)
110  DATA .2,.4,.6,.8,1     ! Standard deviations of t(k)
120  DATA .4,-.5,.6,.7,-.8 ! Correlation coeffs. of s(k) and t(k)
130  L=25                    ! Limit on integral of char. function
140  Delta=.05               ! Sampling increment on char. function
150  Bs=.75*(2*PI/Delta)    ! Shift b, as fraction of alias interval
160  Mf=2^8                  ! Size of FFT
170  PRINTER IS 0
180  PRINT "L =";L,"Delta =";Delta,"b =";Bs,"Mf =";Mf
190  REDIM A(1:K),B(1:K),C(1:K),D(1:K),E(1:K)
200  REDIM Ms(1:K),Mt(1:K),Ss(1:K),St(1:K),Rho(1:K)
210  REDIM D1(1:K),D2(1:K),N0(1:K),N1(1:K),N2(1:K)
220  REDIM X(0:Mf-1),Y(0:Mf-1)
230  DIM A(1:10),B(1:10),C(1:10),D(1:10),E(1:10)
240  DIM Ms(1:10),Mt(1:10),Ss(1:10),St(1:10),Rho(1:10)
250  DIM D1(1:10),D2(1:10),N0(1:10),N1(1:10),N2(1:10)
260  DIM X(0:1023),Y(0:1023)
270  READ A(*),B(*),C(*),D(*),E(*) ! Enter
280  READ Ms(*),Mt(*),Ss(*),St(*),Rho(*) ! constants

```

```

290   FOR J=1 TO K           ! Calculation
300   T1=Ms(J)^2           ! of
310   T2=Mt(J)^2           ! parameters
320   T3=Ss(J)^2
330   T4=St(J)^2
340   T5=Ms(J)*Mt(J)
350   T6=Rho(J)*Ss(J)*St(J)
360   T7=4*A(J)*B(J)-C(J)^2
370   T8=(1-Rho(J)^2)*T3*T4
380   T9=Mt(J)*Ss(J)
390   T10=Ms(J)*St(J)
400   T11=D(J)^2
410   T12=E(J)^2
420   T13=D(J)*E(J)
430   D1(J)=2*(A(J)*T3+B(J)*T4+C(J)*T6)
440   D2(J)=T7*T8
450   N0(J)=A(J)*T1+B(J)*T2+C(J)*T5+D(J)*Ms(J)+E(J)*Mt(J)
460   T=T7*(.5*(T1*T4+T2*T3)-T5*T6)
470   T=T+(2*A(J)*E(J)-C(J)*D(J))*Ss(J)*(T9-Rho(J)*T10)
480   T=T+(2*B(J)*D(J)-C(J)*E(J))*St(J)*(T10-Rho(J)*T9)
490   N1(J)=T-.5*(T11*T3+T12*T4)-T13*T6
500   N2(J)=- (A(J)*T12+B(J)*T11-C(J)*T13)*T8
510   NEXT J
520   Mux=SUM(N0)+.5*SUM(D1) ! Mean of random variable x
530   R=0                  ! Argument of square root
540   P=1                  ! Polarity indicator
550   Muy=Mux+Bs
560   X(0)=0
570   Y(0)=.5*Delta*Muy
580   N=INT(L/Delta)
590   FOR Ns=1 TO N
600   Xi=Delta*Ns         ! Argument xi of char. fn.
610   X2=Xi*Xi           ! Calculation
620   Pr=1               ! of
630   Pi=Sr=Si=0        ! characteristic
640   FOR J=1 TO K      ! function
650   Dr=1-X2*D2(J)     ! fy(xi)
660   Di=-Xi*D1(J)
670   CALL Mul(Pr,Pi,Dr,Di,A,B)
680   Pr=A
690   Pi=B
700   CALL Div(N0(J)-X2*N2(J),-Xi*N1(J),Dr,Di,A,B)
710   Sr=Sr+A
720   Si=Si+B
730   NEXT J
740   CALL Exp(-Xi*Si,Xi*(Sr+Bs),A,B)
750   CALL Sqr(Pr,Pi,C,D)
760   Ro=R
770   R=ATN(D/C)
780   IF ABS(R-Ro)>1.6 THEN P=-P
790   CALL Div(A,B,C*P,D*P,Fyr,Fyi)
800   Ms=Ns MOD Mf       ! Collapsing
810   X(Ms)=X(Ms)+Fyr/Ns
820   Y(Ms)=Y(Ms)+Fyi/Ns
830   NEXT Ns
840   CALL Fft10z(Mf,X(*),Y(*)) ! 0 subscript FFT

```

```

850 PLOTTER IS "GRAPHICS"
860 GRAPHICS
870 SCALE 0,Mf,-14,0
880 LINE TYPE 3
890 GRID Mf/0,1
900 PENUP
910 LINE TYPE 1
920 B=Bs*Mf*Delta/(2*PI) ! Origin for random variable x
930 MOVE B,0
940 DRAW B,-14
950 PENUP
960 FOR Ks=0 TO Mf-1
970 T=Y(Ks)/PI-Ks/Mf
980 X(Ks)=.5-T ! Cumulative probability in X(*)
990 Y(Ks)=Pr=.5+T ! Exceedance probability in Y(*)
1000 IF Pr>=1E-12 THEN Y=LGT(Pr)
1010 IF Pr<=-1E-12 THEN Y=-24-LGT(-Pr)
1020 IF ABS(Pr)<1E-12 THEN Y=-12
1030 PLOT Ks,Y
1040 NEXT Ks
1050 PENUP
1060 PRINT Y(0);Y(1);Y(Mf-2);Y(Mf-1)
1070 FOR Ks=0 TO Mf-1
1080 Pr=X(Ks)
1090 IF Pr>=1E-12 THEN Y=LGT(Pr)
1100 IF Pr<=-1E-12 THEN Y=-24-LGT(-Pr)
1110 IF ABS(Pr)<1E-12 THEN Y=-12
1120 PLOT Ks,Y
1130 NEXT Ks
1140 PENUP
1150 PAUSE
1160 DUMP GRAPHICS
1170 PRINT LIN(5)
1180 PRINTER IS 16
1190 END
1200 !
1210 SUB Mu1(X1,Y1,X2,Y2,A,B) ! Z1*Z2
1220 A=X1*X2-Y1*Y2
1230 B=X1*Y2+X2*Y1
1240 SUBEND
1250 !
1260 SUB Div(X1,Y1,X2,Y2,A,B) ! Z1/Z2
1270 T=X2*X2+Y2*Y2
1280 A=(X1*X2+Y1*Y2)/T
1290 B=(Y1*X2-X1*Y2)/T
1300 SUBEND
1310 !
1320 SUB Exp(X,Y,A,B) ! EXP(Z)
1330 T=EXP(X)
1340 A=T*COS(Y)
1350 B=T*SIN(Y)
1360 SUBEND
1370 !

```

```

1380 SUB Sqr(X,Y,A,B)                                ! PRINCIPAL SQR(Z)
1390 IF X<>0 THEN 1430
1400 A=B=SQR(.5*ABS(Y))
1410 IF Y<0 THEN B=-B
1420 GOTO 1540
1430 F=SQR(SQR(X*X+Y*Y))
1440 T=.5*ATN(Y/X)
1450 A=F*COS(T)
1460 B=F*SIN(T)
1470 IF X>0 THEN 1540
1480 T=A
1490 A=-B
1500 B=T
1510 IF Y>=0 THEN 1540
1520 A=-A
1530 B=-B
1540 SUBEND
1550 !
1560 SUB Fft10z(N,X(*),Y(*)) ! N <= 2^10 = 1024, N=2^INTEGER 0 subscript
1570 DIM C(0:256)
1580 INTEGER I1,I2,I3,I4,I5,I6,I7,I8,I9,I10,J,K
1590 DATA 1,.999981175283,.999924701839,.999830581796,.999698818696,.9995294175
01,.999322304588,.999077727753,.998795456205,.998475580573,.998118112900
1600 DATA .997723066644,.997290456679,.996820299291,.996312612183,.995767414468
,.995184726672,.994564570734,.993906970002,.993211949235,.992479534599
1610 DATA .991709753669,.990902635428,.990058210262,.989176509965,.988257567731
,.987301418158,.986308097245,.985277642389,.984210092387,.983105487431
1620 DATA .981963869110,.980785280403,.979569765685,.978317370720,.977028142658
,.975702130039,.974309382786,.972939952206,.971503890986,.970031253195
1630 DATA .968522094274,.966976471045,.965394441698,.963776065795,.962121404269
,.960430519416,.958703474896,.956940335732,.955141168306,.953306040354
1640 DATA .951435020969,.949528180593,.947585591018,.945607325381,.943593458162
,.941544065183,.939459223602,.937339011913,.935183509939,.932992798835
1650 DATA .930766961079,.928506080473,.926210242138,.923879532511,.921514039342
,.919113851690,.916679059921,.914209755704,.911706032005,.909167983091
1660 DATA .906595704515,.903989293123,.901348847046,.898674465694,.895966249756
,.893224301196,.890448723215,.887639620403,.884797098431,.881921264348
1670 DATA .879012226429,.876070094195,.873094978418,.870086991109,.867046245516
,.863972056122,.860866938638,.857728610000,.854557988365,.851355193105
1680 DATA .848120344803,.844853565250,.841554977437,.838224705555,.834862874986
,.831469612303,.828045045258,.824589302785,.821102514991,.817584813152
1690 DATA .814036329706,.810457198253,.806847553544,.803207531481,.799537269108
,.795836904609,.792106577300,.788346427627,.784556597156,.780737228572
1700 DATA .776888465673,.773010453363,.769103337646,.765167265622,.761202385484
,.757208846506,.753186799044,.749136394523,.745057785441,.740951125355
1710 DATA .736816568877,.732654271672,.728464390448,.724247082951,.720002507961
,.715730825284,.711432195745,.707106781187,.702754744457,.698376249409
1720 DATA .693971460890,.689540544737,.685083667773,.680600997795,.676092703575
,.671558954847,.666999922304,.662415777590,.657806693297,.653172842954
1730 DATA .648514401022,.643831542890,.639124444864,.634393284164,.629638238915
,.624859488142,.620057211763,.615231590581,.610382806276,.605511041404
1740 DATA .600616479384,.595699304492,.590759701859,.585797857456,.580813958096
,.575808191418,.570780745887,.565731810784,.560661576197,.555570233020
1750 DATA .550457972937,.545324988422,.540171472730,.534997619887,.529803624686
,.524589682678,.519355990166,.514102744193,.508830142543,.503538383726

```

```

1760 DATA .498227666973,.492898192230,.487550160148,.482183772079,.476799230063
,.471396736826,.465976495768,.460538710958,.455083587126,.449611329655
1770 DATA .444122144570,.438616238539,.433093818853,.427555093430,.422000270800
,.416429560098,.410843171058,.405241314005,.399624199846,.393992040061
1780 DATA .388345046699,.382683432365,.377007410216,.371317193952,.365612997805
,.359895036535,.354163525420,.348418680249,.342660717312,.336889853392
1790 DATA .331106305760,.325310292162,.319502030816,.313681740399,.307849640042
,.302005949319,.296150888244,.290284677254,.284407537211,.278519689385
1800 DATA .272621355450,.266712757475,.260794117915,.254865659605,.248927605746
,.242980179903,.237023605994,.231058108281,.225083911360,.219101240157
1810 DATA .213110319916,.207111376192,.201104634842,.195090322016,.189068664150
,.183039887955,.177004220412,.170961888760,.164913120490,.158858143334
1820 DATA .152797185258,.146730474455,.140658239333,.134580708507,.128498110794
,.122410675199,.116318630912,.110222207294,.104121633872,.980171403296E-1
1830 DATA .919089564971E-1,.857973123444E-1,.796824379714E-1,.735645635997E-1,.
674439195637E-1,.613207363022E-1,.551952443497E-1,.490676743274E-1
1840 DATA .429382569349E-1,.368072229414E-1,.306748031766E-1,.245412285229E-1,.
184067299058E-1,.122715382857E-1,.613588464915E-2,0
1850 READ C(*)
1860 K=1024/N
1870 FOR J=0 TO N/4
1880 C(J)=C(K*J)
1890 NEXT J
1900 N1=N/4
1910 N2=N1+1
1920 N3=N2+1
1930 N4=N1+N3
1940 Log2n=INT(1.4427*LOG(N)+.5)
1950 FOR I1=1 TO Log2n
1960 I2=2^(Log2n-I1)
1970 I3=2*I2
1980 I4=N/I3
1990 FOR I5=1 TO I2
2000 I6=(I5-1)*I4+1
2010 IF I6<=N2 THEN 2050
2020 N6=-C(N4-I6-1)
2030 N7=-C(I6-N1-1)
2040 GOTO 2070
2050 N6=C(I6-1)
2060 N7=-C(N3-I6-1)
2070 FOR I7=0 TO N-I3 STEP I3
2080 I8=I7+I5
2090 I9=I8+I2
2100 N8=X(I8-1)-X(I9-1)
2110 N9=Y(I8-1)-Y(I9-1)
2120 X(I8-1)=X(I8-1)+X(I9-1)
2130 Y(I8-1)=Y(I8-1)+Y(I9-1)
2140 X(I9-1)=N6*N8-N7*N9
2150 Y(I9-1)=N6*N9+N7*N8
2160 NEXT I7
2170 NEXT I5
2180 NEXT I1
2190 I1=Log2n+1
2200 FOR I2=1 TO 10          ! 2^10=1024
2210 C(I2-1)=1
2220 IF I2>Log2n THEN 2240
2230 C(I2-1)=2^(I1-I2)
2240 NEXT I2

```

```
2250 K=1
2260 FOR I1=1 TO C(9)
2270 FOR I2=I1 TO C(8) STEP C(9)
2280 FOR I3=I2 TO C(7) STEP C(8)
2290 FOR I4=I3 TO C(6) STEP C(7)
2300 FOR I5=I4 TO C(5) STEP C(6)
2310 FOR I6=I5 TO C(4) STEP C(5)
2320 FOR I7=I6 TO C(3) STEP C(4)
2330 FOR I8=I7 TO C(2) STEP C(3)
2340 FOR I9=I8 TO C(1) STEP C(2)
2350 FOR I10=I9 TO C(0) STEP C(1)
2360 J=I10
2370 IF K>J THEN 2440
2380 A=X(K-1)
2390 X(K-1)=X(J-1)
2400 X(J-1)=A
2410 A=Y(K-1)
2420 Y(K-1)=Y(J-1)
2430 Y(J-1)=A
2440 K=K+1
2450 NEXT I10
2460 NEXT I9
2470 NEXT I8
2480 NEXT I7
2490 NEXT I6
2500 NEXT I5
2510 NEXT I4
2520 NEXT I3
2530 NEXT I2
2540 NEXT I1
2550 SUBEND
```

APPENDIX B. FADING FOR SECOND-ORDER PROCESSOR

This program computes the cumulative and exceedance distribution functions for characteristic function (21), when the power fading factor r in (18) has probability density function (19). The parameters D_1 , D_2 , N_0 , N_1 are pre-computed once in lines 210-310. The logarithms in lines 430 and 440 have arguments that never cross the branch line along the negative real axis for the principal value logarithm; hence the calculated characteristic function is automatically continuous for all x .

```

10 ! FADING FOR SECOND-ORDER PROCESSOR
20   Nu=2.7           ! Power law for fading
30   K=5             ! Number of terms summed
40   Ak=.7          ! a(k) weighting
50   Bk=-.9         ! b(k) weighting
60   Ck=-.6         ! c(k) weighting
70   DATA .2,.3,.4,-.5,-.6 ! Means of random variables s(k)
80   DATA .8,-.7,-.6,.5,.4 ! Means of random variables t(k)
90   Ss=.3           ! Standard deviation of s(k)
100  St=.2           ! Standard deviation of t(k)
110  Rho=-.4         ! Correlation coeff. of s(k) and t(k)
120  L=150           ! Limit on integral of char. function
130  Delta=.25       ! Sampling increment on char. function
140  Bs=.625*(2*PI/Delta) ! Shift b, as fraction of alias interval
150  Mf=2^8          ! Size of FFT
160  PRINTER IS 0
170  PRINT "L =";L,"Delta =";Delta,"b =";Bs,"Mf =";Mf
180  REDIM Ms(1:K),Mt(1:K),X(0:Mf-1),Y(0:Mf-1)
190  DIM Ms(1:10),Mt(1:10),X(0:1023),Y(0: 123)
200  READ Ms(*),Mt(*)           ! Enter constants
210  M20=DOT(Ms,Ms)             ! Calculation
220  M02=DOT(Mt,Mt)             ! of
230  M11=DOT(Ms,Mt)             ! parameters
240  T1=Ss*Ss
250  T2=St*St
260  T3=Rho*Ss*St
270  T4=4*Ak*Bk-Ck*Ck
280  N0p=Ak*M20+Bk*M02+Ck*M11
290  N1p=T4*(.5*(T2*M20+T1*M02)-T3*M11)
300  D1=2*(Ak*T1+Bk*T2+Ck*T3)
310  D2=T4*(1-Rho*Rho)*T1*T2
320  D1p=D1+N0p/Nu
330  D2p=D2+N1p/Nu
340  Mux=N0p+.5*K*D1           ! Mean of random variable x
350  Muy=Mux+Bs
360  T=Nu-.5*K

```



```

370 X(0)=0
380 Y(0)=.5*Delta*Muy
390 N=INT(L/Delta)
400 FOR Ns=1 TO N
410 Xi=Delta*Ns ! Argument xi of char. fn.
420 X2=Xi*Xi ! Calculation
430 CALL Log(1-X2*D2,-Xi*D1,A,B) ! of
440 CALL Log(1-X2*D2p,-Xi*D1p,C,D) ! characteristic
450 T1=T*A-Nu*C ! function
460 T2=T*B-Nu*D+Bs*Xi ! fy(xi)
470 CALL Exp(T1,T2,Fyr,Fyi)
480 Ms=Ns MOD Mf ! Collapsing
490 X(Ms)=X(Ms)+Fyr/Ns
500 Y(Ms)=Y(Ms)+Fyi/Ns
510 NEXT Ns
520 CALL Fft10z(Mf,X(*),Y(*)) ! 0 subscript FFT
530 PLOTTER IS "GRAPHICS"
540 GRAPHICS
550 SCALE 0,Mf,-14,0
560 LINE TYPE 3
570 GRID Mf/8,1
580 PENUP
590 LINE TYPE 1
600 B=Bs*Mf*Delta/(2*PI) ! Origin for random variable x
610 MOVE B,0
620 DRAW B,-14
630 PENUP
640 FOR Ks=0 TO Mf-1
650 T=Y(Ks)/PI-Ks/Mf
660 X(Ks)=.5-T ! Cumulative probability in X(*)
670 Y(Ks)=Pr=.5+T ! Exceedance probability in Y(*)
680 IF Pr>=1E-12 THEN Y=LGT(Pr)
690 IF Pr<=-1E-12 THEN Y=-24-LGT(-Pr)
700 IF ABS(Pr)<1E-12 THEN Y=-12
710 PLOT Ks,Y
720 NEXT Ks
730 PENUP
740 PRINT Y(0);Y(1);Y(Mf-2);Y(Mf-1)
750 FOR Ks=0 TO Mf-1
760 Pr=X(Ks)
770 IF Pr>=1E-12 THEN Y=LGT(Pr)
780 IF Pr<=-1E-12 THEN Y=-24-LGT(-Pr)
790 IF ABS(Pr)<1E-12 THEN Y=-12
800 PLOT Ks,Y
810 NEXT Ks
820 PENUP
830 PAUSE
840 DUMP GRAPHICS
850 PRINT LIN(5)
860 PRINTER IS 16
870 END
880 !

```

```
890 SUB Exp(X,Y,A,B)           ! EXP(Z)
900 T=EXP(X)
910 A=T*COS(Y)
920 B=T*SIN(Y)
930 SUBEND
940 !
950 SUB Log(X,Y,A,B)           ! PRINCIPAL LOG(Z)
960 A=.5*LOG(X*X+Y*Y)
970 IF X<>0 THEN 1000
980 B=.5*PI*SGN(Y)
990 GOTO 1020
1000 B=ATN(Y/X)
1010 IF X<0 THEN B=B+PI*(1-2*(Y<0))
1020 SUBEND
1030 !
1040 SUB Fft10z(N,X(*),Y(*))   ! N <= 2^10 = 1024, N=2^INTEGER      0 subscript
```

APPENDIX C. NARROWBAND CROSS-CORRELATOR

This program computes the cumulative and exceedance distribution functions of random variable (30) via characteristic function (35). The parameters D_1 , D_2 , N_0 , N_1 are pre-computed in lines 280-390 and weighted according to (35)-(36) in lines 400-440. All the functions employed are analytic.

```

10 ! NARROWBAND CROSS-CORRELATOR
20   K=5                               ! Number of terms summed
30   DATA .6,-.5,.4,-.3,.2           ! w(k)      weightings
40   DATA .9,.8,.7,-.6,-.5           ! a1(k)     signal 1 in-phase components
50   DATA -.6,-.8,1,1.2,1.4           ! b1(k)     signal 1 quadrature components
60   DATA .1,-.2,-.3,.4,.5           ! a2(k)     signal 2 in-phase components
70   DATA -.7,.6,.5,.4,-.3           ! b2(k)     signal 2 quadrature components
80   DATA .1,.3,.5,.7,.9             ! sigma1(k) noise 1 standard deviations
90   DATA .2,.4,.6,.8,1              ! sigma2(k) noise 2 standard deviations
100  DATA .4,-.5,.6,.7,-.8           ! rho(k)    noise in-phase corr. coeffs.
110  DATA .9,-.7,-.5,.3,-.1           ! lambda    noise quadrature corr. coeffs.
120  L=50                               ! Limit on integral of char. function
130  Delta=.5                           ! Sampling increment on char. function
140  Bs=.5*(2*PI/Delta)                 ! Shift b, as fraction of alias interval
150  Mf=2^8                             ! Size of FFT
160  PRINTER IS 0
170  PRINT "L =",L,"Delta =",Delta,"b =",Bs,"Mf =",Mf
180  REDIM W(1:K),A1(1:K),B1(1:K),A2(1:K),B2(1:K)
190  REDIM S1(1:K),S2(1:K),Rho(1:K),Lambda(1:K)
200  REDIM D1(1:K),D2(1:K),N0(1:K),N1(1:K)
210  REDIM X(0:Mf-1),Y(0:Mf-1),W2(1:K)
220  DIM W(1:10),A1(1:10),B1(1:10),A2(1:10),B2(1:10)
230  DIM S1(1:10),S2(1:10),Rho(1:10),Lambda(1:10)
240  DIM D1(1:10),D2(1:10),N0(1:10),N1(1:10)
250  DIM X(0:1023),Y(0:1023),W2(1:10)
260  READ W(*),A1(*),B1(*),A2(*),B2(*) ! Enter
270  READ S1(*),S2(*),Rho(*),Lambda(*) ! constants
280  FOR J=1 TO K                       ! Calculation
290    S1s=S1(J)^2                       ! of
300    S2s=S2(J)^2                       ! parameters
310    T1=S1(J)*S2(J)
320    D1(J)=T2=T1*Rho(J)
330    D2(J)=.25*S1s*S2s*(1-Rho(J)^2-Lambda(J)^2)
340    T3=A1(J)*A2(J)+B1(J)*B2(J)
350    N0(J)=.5*T3
360    T4=A2(J)*B1(J)-A1(J)*B2(J)
370    T5=S2s*(A1(J)^2+B1(J)^2)+S1s*(A2(J)^2+B2(J)^2)
380    N1(J)=.125*(T5-2*T2*T3-2*T1*Lambda(J)*T4)
390  NEXT J
400  MAT W2=W.W
410  MAT D1=W.D1
420  MAT D2=W2.D2
430  MAT N0=W.N0
440  MAT N1=W2.N1
450  Mux=SUM(N0)+SUM(D1)                ! Mean of random variable u
460  Muy=Mux+Bs

```

TR 7035

```
470 X(0)=0
480 Y(0)=.5*Delta*Muy
490 N=INT(L/Delta)
500 FOR Ns=1 TO N
510 Xi=Delta*Ns ! Argument xi of char. fn.
520 X2=Xi*Xi ! Calculation
530 Pr=1 ! of
540 Pi=Sr=Si=0 ! characteristic
550 FOR J=1 TO K ! function
560 Dr=1+X2*D2(J) ! fy(xi)
570 Di=-Xi*D1(J)
580 CALL Mul(Pr,Pi,Dr,Di,A,B)
590 Pr=A
600 Pi=B
610 CALL Div(N0(J),Xi*N1(J),Dr,Di,A,B)
620 Sr=Sr+A
630 Si=Si+B
640 NEXT J
650 CALL Exp(-Xi*Si,Xi*(Sr+Bs),A,B)
660 CALL Div(A,B,Pr,Pi,Fyr,Fyi)
670 Ms=Ns MOD Mf ! Collapsing
680 X(Ms)=X(Ms)+Fyr/Ns
690 Y(Ms)=Y(Ms)+Fyi/Ns
700 NEXT Ns
710 CALL Fft10z(Mf,X(*),Y(*)) ! 0 subscript FFT
720 PLOTTER IS "GRAPHICS"
730 GRAPHICS
740 SCALE 0,Mf,-14,0
750 LINE TYPE 3
760 GRID Mf/8,1
770 PENUP
780 LINE TYPE 1
790 B=Bs*Mf*Delta/(2*PI) ! Origin for random variable v
800 MOVE B,0
810 DRAW B,-14
820 PENUP
830 FOR Ks=0 TO Mf-1
840 T=Y(Ks)/PI-Ks/Mf
850 X(Ks)=.5-T ! Cumulative probability in X(*)
860 Y(Ks)=Pr=.5+T ! Exceedance probability in Y(*)
870 IF Pr>=1E-12 THEN Y=LGT(Pr)
880 IF Pr<=-1E-12 THEN Y=-24-LGT(-Pr)
890 IF ABS(Pr)<1E-12 THEN Y=-12
900 PLOT Ks,Y
910 NEXT Ks
920 PENUP
930 PRINT Y(0);Y(1);Y(Mf-2);Y(Mf-1)
940 FOR Ks=0 TO Mf-1
950 Pr=X(Ks)
960 IF Pr>=1E-12 THEN Y=LGT(Pr)
970 IF Pr<=-1E-12 THEN Y=-24-LGT(-Pr)
980 IF ABS(Pr)<1E-12 THEN Y=-12
990 PLOT Ks,Y
1000 NEXT Ks
1010 PENUP
1020 PAUSE
```

```
1030 DUMP GRAPHICS
1040 PRINT LIN(5)
1050 PRINTER IS 16
1060 END
1070 !
1080 SUB Mul(X1,Y1,X2,Y2,A,B)           ! Z1*Z2
1090 A=X1*X2-Y1*Y2
1100 B=X1*Y2+X2*Y1
1110 SUBEND
1120 !
1130 SUB Div(X1,Y1,X2,Y2,A,B)         ! Z1/Z2
1140 T=X2*X2+Y2*Y2
1150 A=(X1*X2+Y1*Y2)/T
1160 B=(Y1*X2-X1*Y2)/T
1170 SUBEND
1180 !
1190 SUB Exp(X,Y,A,B)                 ! EXP(Z)
1200 T=EXP(X)
1210 A=T*COS(Y)
1220 B=T*SIN(Y)
1230 SUBEND
1240 !
1250 SUB Fft10z(N,X(*),Y(*))          ! N = 2^10 = 1024, N=2^INTEGER 0 subscript
```

APPENDIX D. REDUCED QUADRATIC AND LINEAR FORM

This program computes the cumulative and exceedance distribution functions of random variable (65) via characteristic function (66). The required inputs to the program are M and the $\{\lambda_m\}$, $\{d_m\}$, $\{v_m\}$ of (68). The square root in (66) must again be continuous and is handled exactly as in appendix A. The parameters required in the exponential of (66) are pre-computed in lines 170-210, and the mean of q is entered in line 220.

```

10 ! REDUCED QUADRATIC AND LINEAR FORM
20   M=5                ! Number of terms summed
30   DATA .2,-.3,.4,.5,-.6 ! Lambda values
40   DATA -.1,.3,.5,.7,-.9 ! d values
50   DATA .6,.5,-.4,-.3,.2 ! Nu values
60   L=800              ! Limit on integral of char. function
70   Delta=.08         ! Sampling increment on char. function
80   Bs=.5*(2*PI/Delta) ! Shift b, as fraction of alias interval
90   Mf=2^10           ! Size of FFT
100  PRINTER IS 0
110  PRINT "L =";L,"Delta =";Delta,"b =";Bs,"Mf =";Mf
120  REDIM Lambda(1:M),D(1:M),Nu(1:M),A(1:M),B(1:M),C(1:M)
130  REDIM X(0:Mf-1),Y(0:Mf-1)
140  DIM Lambda(1:10),D(1:10),Nu(1:10),A(1:10),B(1:10),C(1:10)
150  DIM X(0:1023),Y(0:1023)
160  READ Lambda(*),D(*),Nu(*) ! Enter constants
170  FOR Ms=1 TO M             ! Calculation
180  A(Ms)=2*Lambda(Ms)       ! of parameters
190  B(Ms)=(Lambda(Ms)*Nu(Ms)+D(Ms))*Nu(Ms)
200  C(Ms)=.5*D(Ms)^2
210  NEXT Ms
220  Muq=SUM(Lambda)+SUM(B)   ! Mean of random variable q
230  R=0                      ! Argument of square root
240  P=1                      ! Polarity indicator
250  Muy=Muq+Bs
260  X(0)=0
270  Y(0)=.5*Delta*Muy
280  N=INT(L/Delta)
290  FOR Ns=1 TO N
300  Xi=Delta*Ns             ! Argument xi of char. fn.
310  Pr=1                    ! Calculation
320  Pi=Sr=Si=0             ! of
330  FOR Ms=1 TO M          ! characteristic
340  T=-A(Ms)*Xi            ! function
350  CALL Mul(Pr,Pi,1,T,A,B) ! fy(xi)
360  Pr=A
370  Pi=B
380  CALL Div(B(Ms),C(Ms)*Xi,1,T,A,B)
390  Sr=Sr+A
400  Si=Si+B
410  NEXT Ms

```

```

420 CALL Exp(-Si*Xi,(Sr+Bs)*Xi,A,B)
430 CALL Sqr(Pr,Pi,C,D)
440 Ro=R
450 R=ATN(D/C)
460 IF ABS(R-Ro)>1.6 THEN P=-P
470 CALL Div(A,B,C*P,D*P,Fyr,Fyi)
480 Ms=Ns MOD Mf ! Collapsing
490 X(Ms)=X(Ms)+Fyr/Ns
500 Y(Ms)=Y(Ms)+Fyi/Ns
510 NEXT Ns
520 CALL Fft10z(Mf,X(*),Y(*)) ! 0 subscript FFT
530 PLOTTER IS "GRAPHICS"
540 GRAPHICS
550 SCALE 0,Mf,-14,0
560 LINE TYPE 3
570 GRID Mf/8,1
580 PENUP
590 LINE TYPE 1
600 B=Bs*Mf*Delta/(2*PI) ! Origin for random variable q
610 MOVE B,0
620 DRAW B,-14
630 PENUP
640 FOR Ks=0 TO Mf-1
650 T=Y(Ks)/PI-Ks/Mf
660 X(Ks)=.5-T ! Cumulative probability in X(*)
670 Y(Ks)=Pr=.5+T ! Exceedance probability in Y(*)
680 IF Pr>=1E-12 THEN Y=LGT(Pr)
690 IF Pr<=-1E-12 THEN Y=-24-LGT(-Pr)
700 IF ABS(Pr)<1E-12 THEN Y=-12
710 PLOT Ks,Y
720 NEXT Ks
730 PENUP
740 PRINT Y(0);Y(1);Y(Mf-2);Y(Mf-1)
750 FOR Ks=0 TO Mf-1
760 Pr=X(Ks)
770 IF Pr>=1E-12 THEN Y=LGT(Pr)
780 IF Pr<=-1E-12 THEN Y=-24-LGT(-Pr)
790 IF ABS(Pr)<1E-12 THEN Y=-12
800 PLOT Ks,Y
810 NEXT Ks
820 PENUP
830 PAUSE
840 DUMP GRAPHICS
850 PRINT LIN(5)
860 PRINTER IS 16
870 END
880 !

```

```

890  SUB Mu1(X1,Y1,X2,Y2,A,B)          !  Z1*Z2
900  A=X1*X2-Y1*Y2
910  B=X1*Y2+X2*Y1
920  SUBEND
930  !
940  SUB Div(X1,Y1,X2,Y2,A,B)          !  Z1/Z2
950  T=X2*X2+Y2*Y2
960  A=(X1*X2+Y1*Y2)/T
970  B=(Y1*X2-X1*Y2)/T
980  SUBEND
990  !
1000 SUB Exp(X,Y,A,B)                  !  EXP(Z)
1010 T=EXP(X)
1020 A=T*COS(Y)
1030 B=T*SIN(Y)
1040 SUBEND
1050 !
1060 SUB Sqr(X,Y,A,B)                  !  PRINCIPAL SQR(Z)
1070 IF X<>0 THEN 1110
1080 A=B=SQR(.5*ABS(Y))
1090 IF Y<0 THEN B=-B
1100 GOTO 1220
1110 F=SQR(SQR(X*X+Y*Y))
1120 T=.5*ATN(Y/X)
1130 A=F*COS(T)
1140 B=F*SIN(T)
1150 IF X>0 THEN 1220
1160 T=A
1170 A=-B
1180 B=T
1190 IF Y>=0 THEN 1220
1200 A=-A
1210 B=-B
1220 SUBEND
1230 !
1240 SUB Fft10z(N,X(*),Y(*))          ! N <= 2^10 = 1024, N=2^INTEGER      0 subscript

```


APPENDIX E. SIMULATION OF SECOND-ORDER PROCESSOR

This program simulates random variable x in second-order processor (8) directly. The weights and statistics are entered in lines 30-130. A pair of independent zero-mean unit-variance Gaussian random variables are generated in lines 310-380. The sample cumulative and exceedance distribution functions are computed in lines 510-590.

```

10 ! SIMULATION OF SECOND-ORDER PROCESSOR
20   Tt=10000           ! Number of trials
30   K=5               ! Number of terms summed
40   DATA .6,-.5,.4,-.3,.2 ! a(k) weightings
50   DATA .9,.8,.7,-.6,-.5 ! b(k) weightings
60   DATA -.6,-.8,1,1.2,1.4 ! c(k) weightings
70   DATA .1,-.2,-.3,.4,.5 ! d(k) weightings
80   DATA -.7,.6,.5,.4,-.3 ! e(k) weightings
90   DATA .2,.3,.4,-.5,-.6 ! Means of random variables s(k)
100  DATA .8,-.7,-.6,.5,.4 ! Means of random variables t(k)
110  DATA .1,.3,.5,.7,.9    ! Standard deviations of s(k)
120  DATA .2,.4,.6,.8,1    ! Standard deviations of t(k)
130  DATA .4,-.5,.6,.7,-.8 ! Correlation coeffs. of s(k) and t(k)
140  REDIM A(1:K),B(1:K),C(1:K),D(1:K),E(1:K)
150  REDIM Ms(1:K),Mt(1:K),Ss(1:K),St(1:K),Rho(1:K)
160  REDIM A1(1:K),Be(1:K),X(1:Tt)
170  DIM A(1:10),B(1:10),C(1:10),D(1:10),E(1:10)
180  DIM Ms(1:10),Mt(1:10),Ss(1:10),St(1:10),Rho(1:10)
190  DIM A1(1:10),Be(1:10),X(1:10000)
200  READ A(*),B(*),C(*),D(*),E(*)
210  READ Ms(*),Mt(*),Ss(*),St(*),Rho(*)
220  FOR J=1 TO K
230  A1(J)=Ss(J)*Rho(J)
240  Be(J)=Ss(J)*SQR(1-Rho(J)^2)
250  NEXT J
260  RANDOMIZE SQR(.6)
270  L=LOG(.25)

```

TR 7035

```
280  FOR I=1 TO Tt
290  X=0
300  FOR J=1 TO K
310  V1=RND-.5           ! GENERATE TWO
320  V2=RND-.5           ! INDEPENDENT
330  S=V1*V1+V2*V2       ! GAUSSIAN
340  IF S>.25 THEN 310   ! RANDOM
350  Q=(L-LOG(S))/S      ! VARIABLES VIA
360  Q=SQR(Q+Q)          ! ACCEPTANCE
370  G1=V1*Q             ! AND
380  G2=V2*Q             ! REJECTION
390  S=Ms(J)+A1(J)*G1+Be(J)*G2
400  T=Mt(J)+St(J)*G1
410  X=X+A(J)*S+S+B(J)*T+T+C(J)*S*T+D(J)*S+E(J)*T
420  NEXT J
430  X(I)=X
440  NEXT I
450  MAT SORT X
460  PLOTTER IS "GRAPHICS"
470  GRAPHICS
480  SCALE -30,10,-4,0
490  GRID 5,1
500  PENUP
510  FOR I=1 TO Tt
520  Y=LGT((I-.5)/Tt)
530  PLOT X(I),Y
540  NEXT I
550  PENUP
560  FOR I=1 TO Tt
570  Y=LGT(1-(I-.5)/Tt)
580  PLOT X(I),Y
590  NEXT I
600  PENUP
610  END
```

REFERENCES

1. A. H. Nuttall, "Accurate Efficient Evaluation of Cumulative or Exceedance Probability Distributions Directly from Characteristic Functions", NUSC Technical Report 7023, 1 October 1983.
2. M. M. Siddiqui, "Approximations to the Distribution of Quadratic Forms", The Annals of Mathematical Statistics, Vol. 36, pp. 677-682, 1965.
3. C. S. Brice and L. C. Andrews, "New Expressions for the pdf and cdf of the Filtered Output of an Analog Cross Correlator", IEEE Trans. on Information Theory, Vol. IT-28, No. 4, pp. 668-677, July 1982.
4. A. H. Nuttall, "Error Probability Characteristics for Multiple Alternative Communication with Diversity, But Without Fading", NUSC Technical Report 6473, 4 May 1981.
5. A. H. Nuttall and P. G. Cable, "Operating Characteristics for Maximum Likelihood Detection of Signals in Gaussian Noise of Unknown Level; Part III, Random Signals of Unknown Level", NUSC Technical Report 4783, 31 July 1974.
6. A. H. Nuttall, "Probability Distribution of Array Response for Randomly-Perturbed Element Gains", NUSC Technical Report 5687A, 20 May 1981.
7. L. C. Andrews, "The Probability Density Function for the Output of a Cross-Correlator with Bandpass Inputs", IEEE Trans. on Information Theory, Vol. IT-19, No. 1, pp. 13-19, January 1973.
8. J. N. Franklin, Matrix Theory, Prentice-Hall Inc., NY, 1968.

Exact Operating Characteristics for Linear Sum of Envelopes of Narrowband Gaussian Process and Sinewave

A. H. Nuttall

B. Dedreux

ABSTRACT

The characteristic function of a linear sum of M independent Rice variates is derived and evaluated exactly and then used in a numerical procedure to determine the exceedance distribution function, as a function of the threshold, the input signal-to-noise ratio (SNR), and M . Plots of the detection probability and false alarm probability for a wide range of SNR's are given, for values of M up to 8192. In addition, the required threshold values and input SNR's are tabulated and plotted for specific values of M , false alarm probability, and detection probability. A program and explanation are included for those users interested in extending results to their particular application.

TABLE OF CONTENTS

	Page
LIST OF ILLUSTRATIONS	ii
LIST OF TABLES	iii
LIST OF SYMBOLS	iv
INTRODUCTION	1
METHOD OF EVALUATION	3
Characteristic Function Details	3
Special Cases	7
Asymptotic Performance for Large M	8
RESULTS	11
SUMMARY	33
APPENDICES	
A. DERIVATION OF RICE CHARACTERISTIC FUNCTION	A-1
B. DESCRIPTION OF PROGRAMS AND LISTINGS	B-1
REFERENCES	R-1

LIST OF ILLUSTRATIONS

FIGURE	PAGE
1 Required Input S/N for $P_D=.5$	13
2 Required Input S/N for $P_D=.9$	14
3 Required Input S/N for $P_D=.95$	15
4 Required Input S/N for $P_D=.99$	16
5 Required Input S/N for $P_D=.999$	17
6 Receiver Operating Characteristics for $M=1$	19
7 Receiver Operating Characteristics for $M=2$	20
8 Receiver Operating Characteristics for $M=4$	21
9 Receiver Operating Characteristics for $M=8$	22
10 Receiver Operating Characteristics for $M=16$	23
11 Receiver Operating Characteristics for $M=32$	24
12 Receiver Operating Characteristics for $M=64$	25
13 Receiver Operating Characteristics for $M=128$	26
14 Receiver Operating Characteristics for $M=256$	27
15 Receiver Operating Characteristics for $M=512$	28
16 Receiver Operating Characteretistics for $M=1024$	29
17 Receiver Operating Characteristics for $M=2048$	30
18 Receiver Operating Characteristics for $M=4096$	31
19 Receiver Operating Characteristics for $M=8192$	32

LIST OF TABLES

TABLE	PAGE
1. Normalized Thresholds Required for Specified M and P_{FA}	12
2. Parameter Cards	B-5
3. Table Cards	B-5
4. File Cards	B-5
5. Command Cards	B-5
6. Plot Device Cards	B-6
7. Sample Input Deck for P_D vs. P_{FA}	B-6
8. Sample Input Deck for SNR vs. M	B-7
9. Sample Input Deck for Printing SNR	B-7
10. Print Out of SNR vs. M	B-8
11. Description of Subroutines	B-10

LIST OF SYMBOLS

M	Number of independent envelope samples summed
e_m	m -th envelope sample
x	Decision variable; sum of M envelope samples
P_D	Detection probability
P_{FA}	False alarm probability
A	Sinewave amplitude
σ	Noise standard deviation
α	A/σ , voltage measure of input signal-to-noise ratio
S/N	$\alpha^2/2$, power measure of input signal-to-noise ratio
$p_e(u)$	Probability density function of envelope random variable e_m
$f_e(\xi)$	Characteristic function of envelope random variable e_m
I_0	Modified Bessel function of order zero
${}_1F_1$	Confluent hypergeometric function
μ_x	Mean of random variable x
$f_x(\xi)$	Characteristic function of decision variable x
$Q_x(u)$	Exceedance distribution function of random variable x ; (8)
Im, Re	Imaginary part, Real part
Δ	Sampling increment in ξ ; (12)
N	Size of FFT; (13)-(14)
L	Limit employed on integral on ξ in (9)
b	Bias employed to shift random variable x
Φ	Cumulative distribution function of normalized Gaussian random variable; (19)
Φ^{-1}	Inverse function to Φ defined in (19)
σ_x	Standard deviation of random variable x
dB	Required input signal-to-noise ratio per-sample in decibels
β	Parameter incorporating specified P_D and P_{FA} ; (28)

EXACT OPERATING CHARACTERISTICS FOR LINEAR SUM OF ENVELOPES OF NARROWBAND GAUSSIAN PROCESS AND SINEWAVE

INTRODUCTION

The operating characteristics for a linear envelope-detector of a sinewave in narrowband Gaussian noise, followed by summation of M independent envelope samples, were presented in [1] and [2, sect. 8.3]. That approach was based upon evaluation of the first 31 moments of the envelope variate and their use in a type A Gram-Charlier series approximation, or in modified approximations involving averages over different numbers of terms in the series [1, pp. 758-9]. However, there are possible pitfalls to the above approach. First, evaluation of very low exceedance probabilities, like 10^{-10} , may be inaccurate; see [1, Fig. 1]. Second, the effect of a systematic error would be hard to detect, if present, since the method yields only an approximation to the exceedance distribution function, and not its exact value.

We will use an exact approach here, based upon evaluation of the characteristic function of the envelope detector output, from which the exceedance distribution function can be precisely evaluated numerically [3,4]. In this fashion, we avoid moment evaluations altogether; we can evaluate false alarm probabilities in the 10^{-10} range easily (with double precision computer arithmetic); and we can control truncation and aliasing errors to any desired degree; see [3] for details. The results of [4] can not be applied here because each independent envelope sample is the result of a nonlinear operation, namely a square root, applied to a sum of two squares of Gaussian random variables with non-zero means.

In the plots of detection probability vs. false alarm probability to be presented herein, both abscissa and ordinate use the same normal probability scales, regardless of the number of envelope samples M considered. This allows for easier interpolation, and is in distinction to [1], where a different false alarm probability abscissa was used for each M [1, pp. 759-62]. Also, the parameter employed here for indexing the curves is α , a voltage signal-to-noise ratio which is equal to the ratio of the sinewave amplitude to the

rms noise level, rather than the dB parameter employed in [1]. This leads to curves that are more nearly equally spaced, and therefore to easier and finer interpolation capability.

Finally, we present five figures for the required input signal-to-noise ratio per sample required to realize specified false alarm and detection probabilities, as a function of M , the number of envelope samples added. The five figures correspond to detection probability $P_D = .5, .9, .95, .99, \text{ and } .999$ respectively, and each figure contains false alarm probabilities $P_{FA} = 10^{-n}$ for $n=1(1)8$. This total of 40 curves greatly augments the 2 cases presented in [1, Fig. 16] and [2, Fig. 8.18].

A program for the evaluation of the input signal-to-noise ratio required for a specified set of values of M , P_{FA} , and P_D is furnished, along with an explanation of its use. In this fashion, values of M , P_{FA} , and P_D intermediate to those considered here can be easily investigated.

METHOD OF EVALUATION

Characteristic Function Details

In [3,4], a method of calculating the cumulative and exceedance distribution functions directly from a given characteristic function was presented. To utilize those results here, we need the characteristic function of summation random variable

$$x = \sum_{m=1}^M e_m \quad , \quad (1)$$

where e_m is the envelope of a narrowband filter output with a sinewave signal of amplitude A and Gaussian noise of power σ^2 . Through proper normalization, the probability density function of envelope e_m takes the familiar Rice form

$$p_e(u) = u \exp\left(-\frac{u^2 + \alpha^2}{2}\right) I_0(\alpha u) \quad \text{for } u \geq 0 \quad , \quad (2)$$

where the single parameter

$$\alpha = \frac{A}{\sigma} \quad (3)$$

is a voltage measure of signal-to-noise ratio per envelope sample. The power measure of signal-to-noise ratio per sample is

$$\frac{S}{N} = \frac{A^2/2}{\sigma^2} = \frac{\alpha^2}{2} \quad . \quad (4)$$

The quantities in (3) and (4) will be referred to as input signal-to-noise ratios, since they are per-sample measures, prior to the summation in (1) which yields the output or decision variable x .

The characteristic function corresponding to random variable e in (2) is given by Fourier transform

$$f_e(\xi) = \int_{-\infty}^{+\infty} du \exp(i\xi u) p_e(u) = \int_0^{+\infty} du u \exp\left(i\xi u - \frac{u^2 + \alpha^2}{2}\right) I_0(\alpha u) \quad , \quad (5)$$

and will be called the Rice characteristic function. A series expansion for (5) is developed in appendix A, and has been programmed in double precision for numerical use here. As a particular special case, for $\alpha=0$, no signal, we have the Rayleigh probability density function and characteristic function:

$$p_e^{(0)}(u) = u \exp(-u^2/2) \quad \text{for } u \geq 0 \quad ,$$

$$f_e^{(0)}(\xi) = \exp(-\xi^2/2) \left[{}_1F_1\left(-\frac{1}{2}; \frac{1}{2}; \frac{\xi^2}{2}\right) + i\left(\frac{\pi}{2}\right)^{1/2} \xi \right] \quad . \quad (6)$$

The latter follows by use of [5, 3.896 3.4] and via manipulation of the hypergeometric function series along with Kummer's transformation [5, 9.212 1]. Formula (6) is particularly attractive numerically, since the series expansion of ${}_1F_1$ contains all **neg**ative terms except for one. It should be observed that the imaginary part of Rayleigh characteristic function $f_e^{(0)}(\xi)$ in (6) decays very rapidly with ξ ; this useful feature will also be shared by the Rice characteristic function, $f_e(\xi)$, and is due to the fact that the odd part of the Rice probability density function in (2) is smooth for all u , and is in fact entire in u , for any α . By contrast, the even part of the Rice probability density function in (2) has a discontinuous derivative for real u , thereby leading to slow decay of the real part of $f_e(\xi)$.

The characteristic function of output variable x in (1), for statistically independent envelope samples $\{e_m\}$, is given by

$$f_x(\xi) = [f_e(\xi)]^M \quad , \quad (7)$$

in terms of the Rice characteristic function (5). This relation could be used directly to find the exceedance distribution function of x according to [3, (5)-(6)]

$$Q_x(u) = \int_u^{+\infty} dt p_x(t) = \frac{1}{2} + \int_{0^+}^{+\infty} d\xi \operatorname{Im} \left\{ \exp(-iu\xi) \frac{f_x(\xi)}{\pi\xi} \right\} \quad . \quad (8)$$

However, the slow decay of $\text{Re}\{f_x(\xi)\}$ prompts us to use a modified version given in [6, (15)]:

$$Q_x(u) = \frac{2}{\pi} \int_{0^+}^{+\infty} \frac{d\xi}{\xi} \cos(u\xi) \text{Im}\{f_x(\xi)\} \quad \text{for } u > 0 \quad (9)$$

This form is applicable to positive random variables, of which x , as given by (1) and (2), is certainly a member.

To see why form (9) is preferred over (8), we develop (7) as

$$f_x(\xi) = [f_r(\xi) + if_i(\xi)]^M = \sum_{m=0}^M \binom{M}{m} i^m [f_i(\xi)]^m [f_r(\xi)]^{M-m} \quad (10)$$

where $f_r(\xi)$ and $f_i(\xi)$ are the real and imaginary parts of Rice characteristic function $f_e(\xi)$. Then

$$\text{Im}\{f_x(\xi)\} = \sum_{\substack{m=1 \\ m \text{ odd}}}^M (-1)^{\frac{m-1}{2}} \binom{M}{m} [f_i(\xi)]^m [f_r(\xi)]^{M-m} \quad (11)$$

contains $f_i(\xi)$ to at least the first power in all terms, thereby yielding a rapid decay with ξ .

Development (11) has been used to show why $\text{Im}\{f_x(\xi)\}$ decays rapidly with ξ . However, when we employ (9) in a numerical evaluation, we simply take the imaginary part of the power in (7), and do not use (11) at all; (11) is an alternating series of large terms for large M .

Actual numerical evaluation of (9) proceeds as follows [3]: for the Trapezoidal rule with sampling increment Δ in ξ ,

$$Q_x(u) = \frac{2}{\pi} \left[\frac{1}{2} u_x \Delta + \sum_{n=1}^{\infty} \frac{1}{n} \cos(un\Delta) \text{Im}\{f_x(n\Delta)\} \right] \quad (12)$$

where we used $f_x(\xi) \sim 1 + i\mu_x \xi$ as $\xi \rightarrow 0$. Then, restricting the u values to a particular selection,

$$Q_x\left(\frac{2\pi m}{N\Delta}\right) = \frac{2}{\pi} \left[\frac{1}{2} \mu_x \Delta + \sum_{n=1}^{\infty} \frac{1}{n} \cos(2\pi mn/N) \operatorname{Im}\{f_x(n\Delta)\} \right] =$$

$$= \frac{2}{\pi} \operatorname{Re} \sum_{n=0}^{N-1} z_n \exp(-i2\pi mn/N) \quad , \quad (13)$$

where collapsed sequence $\{z_n\}_0^{N-1}$ is defined as

$$z_0 = \frac{1}{2} \mu_x \Delta + \sum_{j=1}^{\infty} \frac{1}{jN} \operatorname{Im}\{f_x(jN\Delta)\} \quad ,$$

$$z_n = \sum_{j=0}^{\infty} \frac{1}{n+jN} \operatorname{Im}\{f_x((n+jN)\Delta)\} \quad \text{for } 1 \leq n \leq N-1 \quad . \quad (14)$$

Form (13) is particularly attractive since it can be accomplished via an N -point FFT. It can be shown that only the values for $0 \leq m \leq N/2$ are useful in (13); the remainder are heavily aliased and must be discarded. Thus there is a trade-off: use of only the imaginary part of $f_x(\xi)$ results in aliasing twice as coarse. However, the rapid decay of the imaginary part far outweighs the aliasing.

The summations in (12) and (14) cannot be conducted to infinity. Rather the integral on ξ in (9) is terminated at limit L , where the truncation error is guaranteed to be sufficiently small. A trial and error procedure [3] yielded the following rules which control the truncation and aliasing errors:

$$L = \min(9, 17/\sqrt{M}),$$

$$\Delta = .12/\sqrt{M},$$

$$b = \min(0, -M\sqrt{\pi/2} + \sqrt{M}6). \quad (15)$$

The inverse \sqrt{M} dependence of L and Δ for large M can be anticipated by observing that the characteristic function of random variable x in (1) then

approaches a Gaussian function with argument proportional to M^2 . The bias (or shift) b is added to random variable x in order to yield a new random variable that remains just positive, even for large M ; this allows us to take maximum advantage of the fundamental aliasing interval $(0, \pi/\Delta)$ in u in (12) and (13). The linear term (in M) of b in (15) is due to the mean of the Rayleigh variate (for $\alpha=0$) which is $\sqrt{\pi/2}$; the algebraic term in \sqrt{M} is due to the fact that the standard deviation of random variable x in (1) increases according to \sqrt{M} .

In order to use this characteristic function approach, we also need the mean of random variable x in (1). Using (2), this is given by [5, 6.631 1]

$$\begin{aligned} \mu_x = M\mu_e &= M \int_0^{\infty} du u^2 \exp\left(-\frac{u^2 + \alpha^2}{2}\right) I_0(\alpha u) = \\ &= M \left(\frac{\pi}{2}\right)^{1/2} \exp\left(-\frac{\alpha^2}{2}\right) {}_1F_1\left(\frac{3}{2}; 1; \frac{\alpha^2}{2}\right) \end{aligned} \quad (16)$$

This non-alternating series yields accurate values for the mean.

Special Cases

For general M , the characteristic function approach described above must be used. However, for $M = 1$ and 2 , closed form expressions for the false alarm and detection probabilities are possible. Specifically, from (1) and (2), for $u \geq 0$,

$$\left. \begin{aligned} P_{FA} &= \int_u^{\infty} dt p_e(t) = \int_u^{\infty} dt t \exp(-t^2/2) = \exp(-u^2/2) \\ P_D &= \int_u^{\infty} dt t \exp\left(-\frac{t^2 + \alpha^2}{2}\right) I_0(\alpha t) = Q(\alpha, u) \end{aligned} \right\} \text{for } M = 1. \quad (17)$$

And for $M = 2$, the false alarm probability can be determined by convolving two Rayleigh probability density functions of the form of (6), to give, for $u \geq 0$,

$$P_{FA} = \exp(-u^2/2) + \sqrt{\pi} u \exp(-u^2/4) \left[\Phi\left(\frac{u}{\sqrt{2}}\right) - \frac{1}{2} \right] \quad \text{for } M = 2. \quad (18)$$

Here, Φ is the cumulative distribution function of a normalized Gaussian random variable:

$$\Phi(u) = \int_{-\infty}^u dt (2\pi)^{-1/2} \exp(-t^2/2) \quad . \quad (19)$$

The detection probability of random variable x in (1) is not available in closed form for $M > 1$.

Asymptotic Performance for Large M

For large M , decision variable x in (1) is approximately Gaussian. The mean of x was given in (16); a similar approach for the mean square of x yields the variance as

$$\sigma_x^2 = M\sigma_e^2 = M(2 + \alpha^2 - \mu_e^2) \quad . \quad (20)$$

The probability density function of x is then approximately

$$p_x(u) \approx \frac{1}{\sqrt{2\pi} \sigma_x} \exp\left[-\frac{(u - \mu_x)^2}{2\sigma_x^2}\right], \quad (21)$$

with exceedance distribution function

$$Q_x(u) \approx \Phi\left(\frac{\mu_x - u}{\sigma_x}\right) = \Phi\left(\frac{M\mu_e - u}{\sqrt{M}\sigma_e}\right) \quad . \quad (22)$$

For input signal-to-noise ratio $S/N=0$, we have $\alpha=0$ from (4), and (22), (16), and (20) specialize to

$$P_{FA} \approx \Phi\left(\frac{M\sqrt{\pi/2} - u}{\sqrt{M}\sqrt{2 - \frac{\pi}{2}}}\right) \quad . \quad (23)$$

On the other hand, for $S/N > 0$, (22) yields the detection probability P_D . We now use the inverse function $\tilde{\Phi}$ to definition (19) and solve (23) and (22) according to

$$\frac{M\sqrt{\pi/2} - u}{\sqrt{M}\sqrt{2 - \frac{\pi}{2}}} = \tilde{\Phi}(P_{FA}) \quad , \quad \frac{M\mu_e - u}{\sqrt{M}\sigma_e} = \tilde{\Phi}(P_D) \quad . \quad (24)$$

Eliminating threshold u in (24), we have

$$\sigma_e \tilde{\Phi}(P_D) = \sqrt{M}\left(\mu_e - \sqrt{\frac{\pi}{2}}\right) + \sqrt{2 - \frac{\pi}{2}} \tilde{\Phi}(P_{FA}) \quad . \quad (25)$$

But also, for large M , the required per-sample input signal-to-noise ratio α will be small, giving

$$\begin{aligned} \mu_e &= \sqrt{\frac{\pi}{2}} {}_1F_1\left(-\frac{1}{2}; 1; -\frac{\alpha^2}{2}\right) \approx \sqrt{\frac{\pi}{2}} \left(1 + \frac{\alpha^2}{4}\right) \quad , \\ \sigma_e^2 &= 2 + \alpha^2 - \mu_e^2 \approx 2 - \frac{\pi}{2} \quad . \end{aligned} \quad (26)$$

Substituting these results in (25) and solving for α , we have the required per-sample input signal-to-noise ratio measures for large M in the alternative forms

$$\begin{aligned} \alpha &\approx 2\left(\frac{4-\pi}{\pi}\right)^{1/4} \frac{\beta^{1/2}}{M^{1/4}} = 1.446 \frac{\beta^{1/2}}{M^{1/4}} \quad , \\ \frac{S}{N} &= \frac{\alpha^2}{2} \approx 2\left(\frac{4-\pi}{\pi}\right)^{1/2} \frac{\beta}{M^{1/2}} = 1.045 \frac{\beta}{M^{1/2}} \quad , \end{aligned}$$

$$\text{dB} = 10 \log \frac{S}{N} \approx 10 \log\left(2\sqrt{\frac{4-\pi}{\pi}}\right) + 10 \log(\beta) - 5 \log(M) = .193 + 10 \log(\beta) - 5 \log(M), \quad (27)$$

where the single parameter

$$\beta = \tilde{\Phi}(P_D) - \tilde{\Phi}(P_{FA}) \quad (28)$$

TR 7117

incorporates the specified false alarm and detection probabilities. (27) displays the familiar $5 \log M$ decibel decay for large M associated with the incoherent addition in (1); see also [2, p. 279, Ex. 8.8].

RESULTS

For a given value of M , the output variable in (1),

$$x = \sum_{m=1}^M e_m \quad , \quad (29)$$

will exceed threshold u with false alarm probability P_{FA} when signal-to-noise ratio α is zero. That is

$$P_{FA} = \text{Prob}(x > u \mid \alpha = 0; M). \quad (30)$$

For specified values of M and P_{FA} , this relation can be solved numerically for u ; the values of normalized threshold u/M are listed in table 1 for $M=2^n$, $n=0(1)13$ and for $P_{FA}=10^{-n}$, $n=1(1)8$.

The detection probability depends on threshold u , M , and signal-to-noise ratio $\alpha(>0)$:

$$P_D = \text{Prob}(x > u \mid \alpha; M). \quad (31)$$

For specified values of M , P_D , and u , this relation can be solved numerically for the required input signal-to-noise ratio α . When the threshold results in Table 1 are employed, the results yield the required input signal-to-noise ratio for specified false alarm probability and detection probability at a particular M . These are plotted in figures 1-5 for

$$P_D = .5, .9, .95, .99, .999, \quad (32)$$

respectively. The abscissa is $\log_2 M$, and the ordinate is in decibels, as defined in (27). The fit of (27) is very good for large M , especially for the larger P_{FA} values. These results in figures 1-5 greatly extend the one in [1, Fig. 16] and [2, Fig. 8.18].

Table 1. Normalized Thresholds Required for Specified M and P_{FA}

$M \backslash P_{FA}$	1E-1	1E-2	1E-3	1E-4
1	2.14596603	3.03485426	3.71692219	4.29193205
2	1.87154046	2.46578168	2.92459903	3.31372579
4	1.68491649	2.08494224	2.39281962	2.65432267
8	1.55592564	1.82779134	2.03544098	2.21134522
16	1.46605729	1.65246898	1.79362769	1.91266565
32	1.40314416	1.53192213	1.62866385	1.70984877
64	1.35896377	1.44846093	1.51524477	1.57104117
128	1.32787317	1.39035933	1.43673968	1.47534630
256	1.30596258	1.34974198	1.38210498	1.40896493
512	1.29050601	1.32125803	1.34392160	1.36268942
1024	1.27959472	1.30123656	1.31715039	1.33030674
2048	1.27188832	1.28713956	1.29833595	1.30758095
4096	1.26644357	1.27720181	1.28509047	1.29159844
8192	1.26259580	1.27018998	1.27575385	1.28034098

$M \backslash P_{FA}$	1E-5	1E-6	1E-7	1E-8
1	4.79852591	5.25652177	5.67769243	6.06970852
2	3.65817649	3.97074674	4.25904998	4.52806135
4	2.88639585	3.09755766	3.29282208	3.47544423
8	2.36734857	2.50933650	2.64073862	2.76376208
16	2.01795589	2.11363367	2.20209577	2.28487698
32	1.78141625	1.84629005	1.90615996	1.96210527
64	1.62006566	1.66438962	1.70520835	1.74328423
128	1.50917003	1.53967893	1.567 1937	1.59383081
256	1.43244246	1.45357776	1.47297026	1.49100181
512	1.37906412	1.39378248	1.40726893	1.41979378
1024	1.34176981	1.35206123	1.36148146	1.37022180
2048	1.31562790	1.32284604	1.32944798	1.33556910
4096	1.29725887	1.30233301	1.30697131	1.31126956
8192	1.28432858	1.28790149	1.29116614	1.29419029

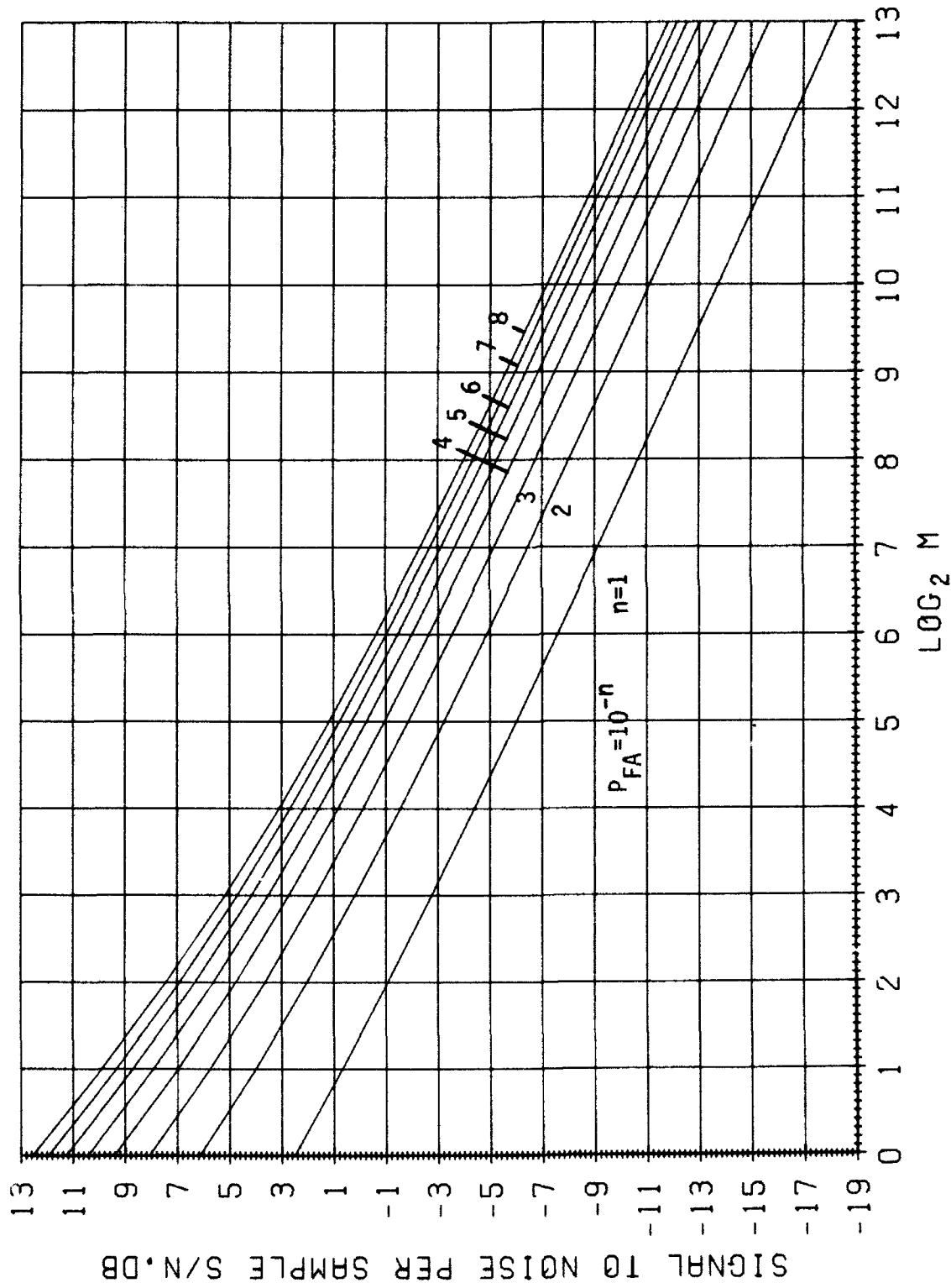


Figure 1. Required Input S/N for $P_n = .5$

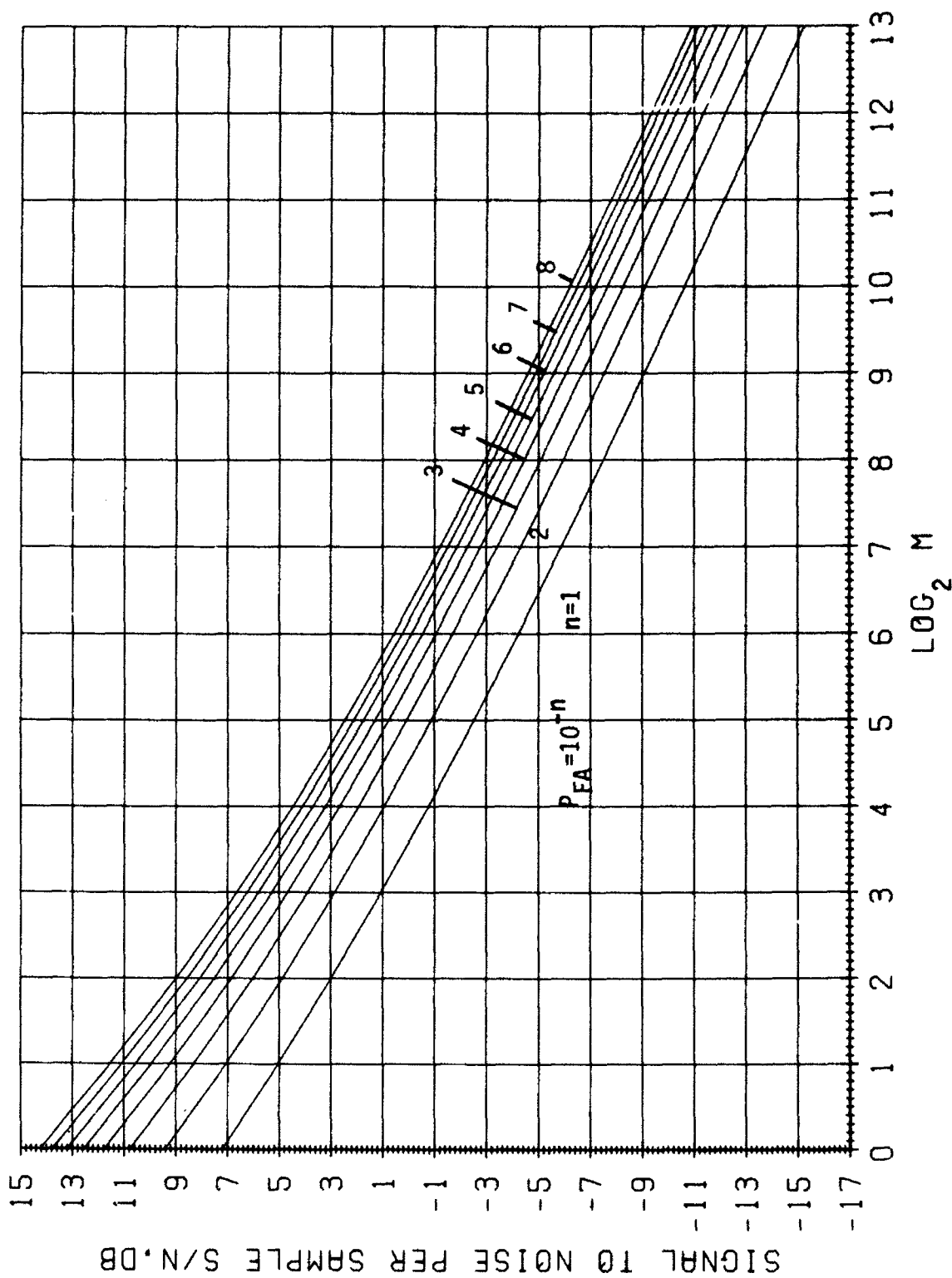


Figure 2. Required Input S/N for $P_D=0.9$

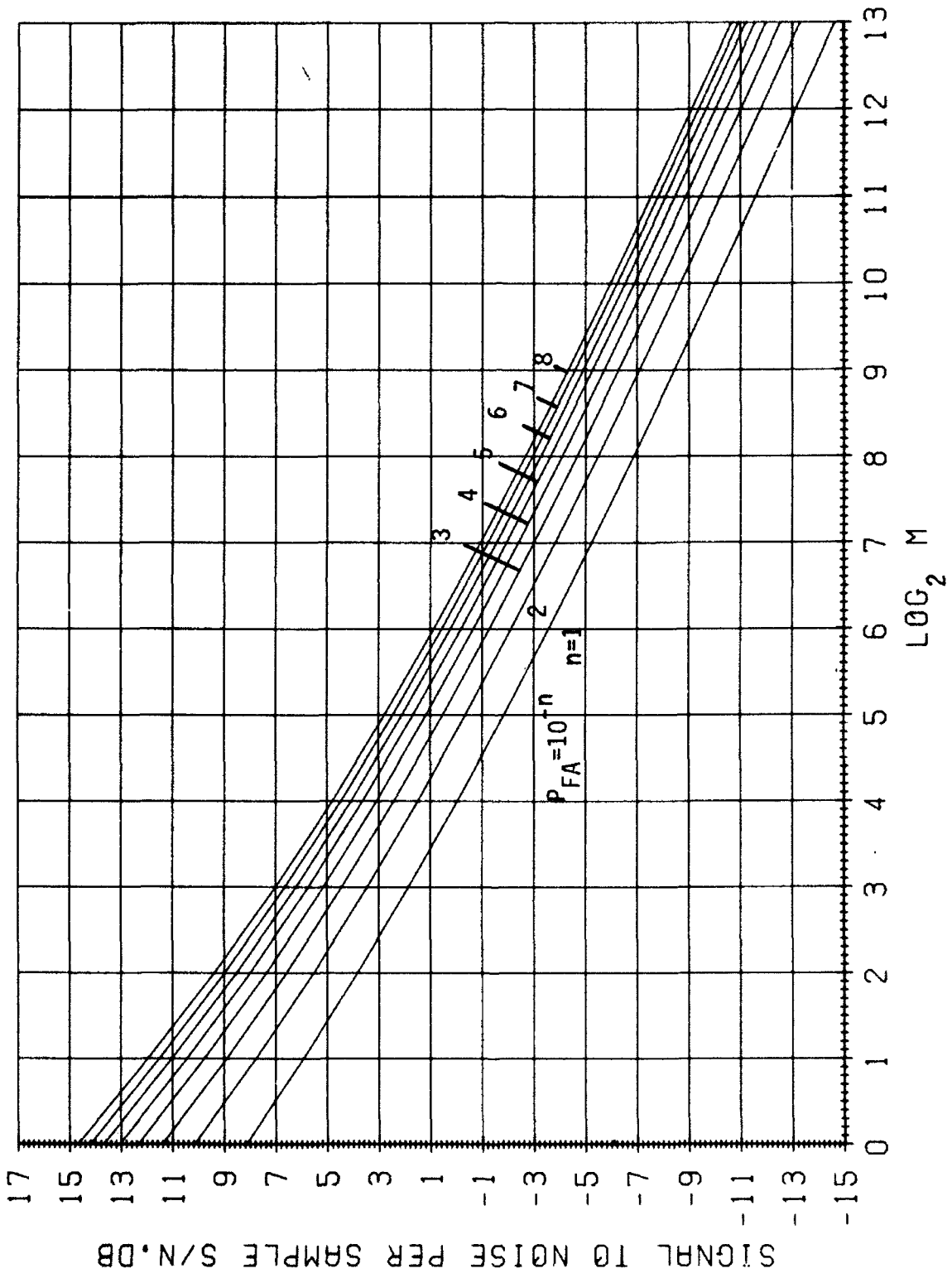


Figure 3. Required Input S/N for $P_D = .95$

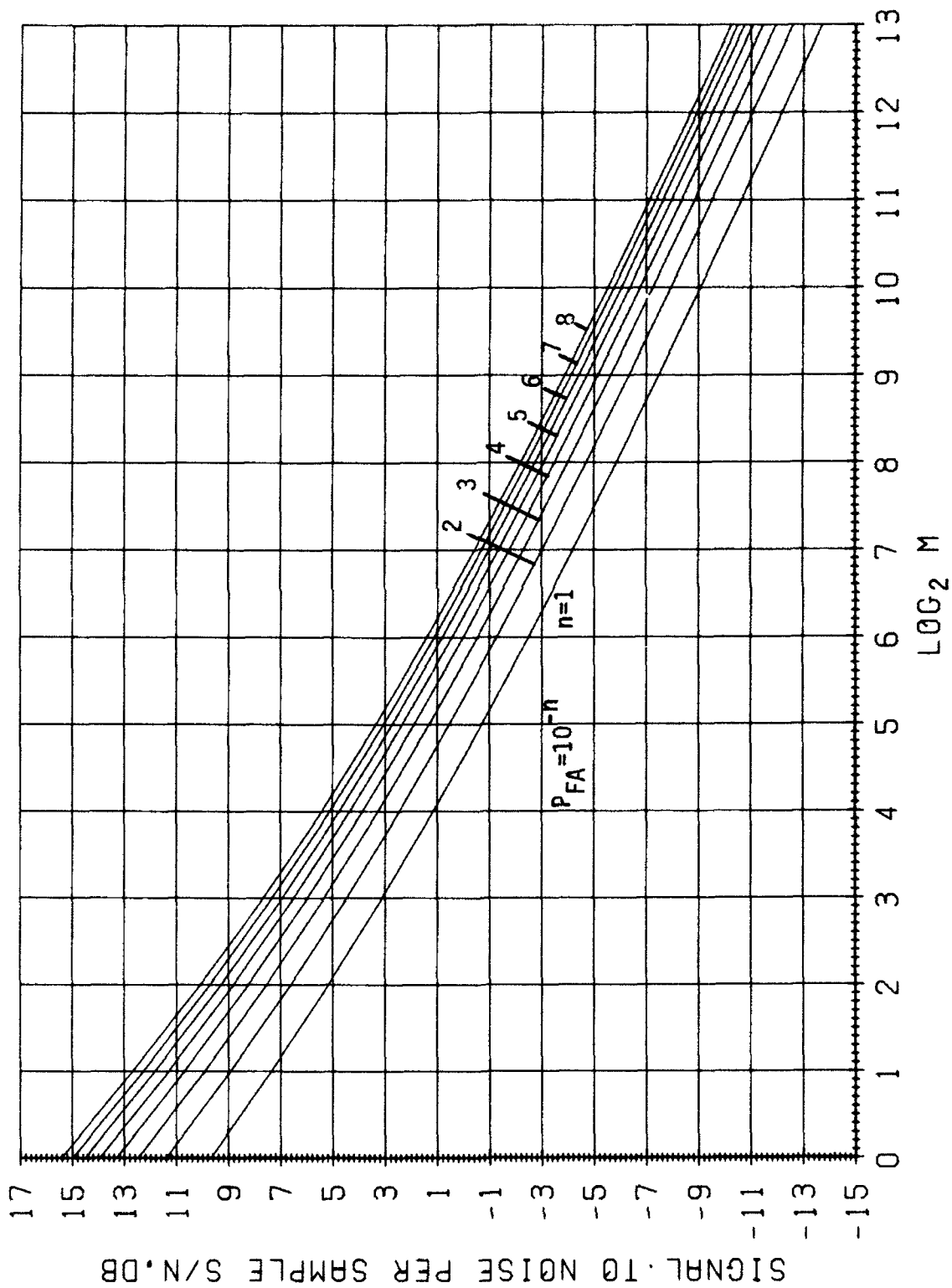


Figure 4. Required Input S/N for $P_D = .99$

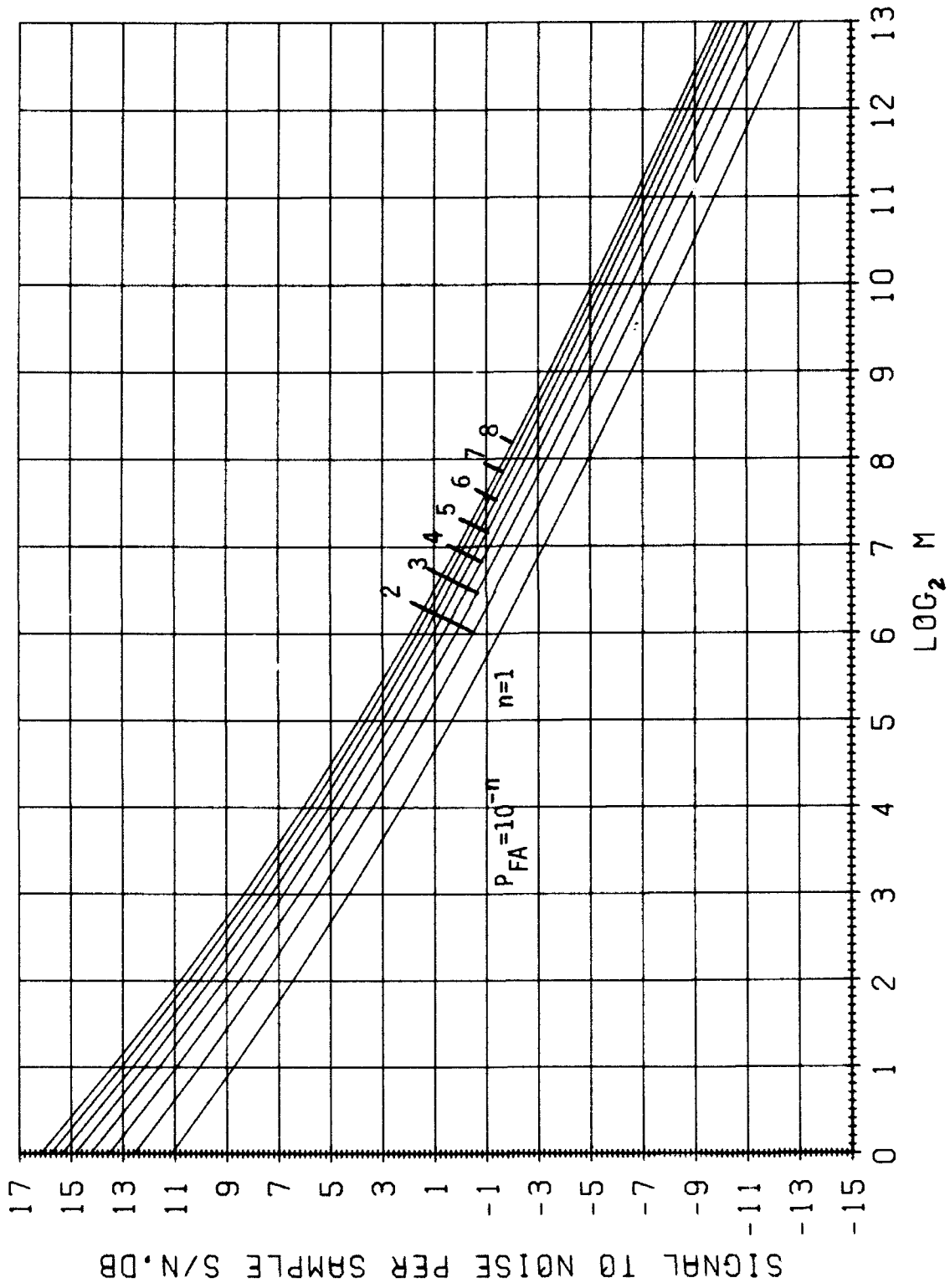


Figure 5. Required Input S/N for $P_D = .999$

The results in figures 1 through 5 only cover a selected set of detection and false alarm probability values. A more complete description is afforded by the receiver operating characteristics, namely detection probability vs. false alarm probability, with signal-to-noise ratio as a parameter. In figures 6 through 19 are given these operating characteristics for

$$M = 1, 2, 4, 8, 16, 32, 64, 128, 256, 512, 1024, 2048, 4096, 8192, \quad (33)$$

respectively. The false alarm probability covers the range 10^{-10} to .5, while the detection probability covers 10^{-10} to .999. Both abscissa and ordinate in these figures employ the inverse function to the Gaussian cumulative distribution function Φ defined in (19); thus, a truly Gaussian random variable would plot as a series of equally spaced parallel straight lines (with parameter α). Observe that the curves are nearly equally spaced with parameter α , except for very small α , where the nonlinear envelope operation causes small signal suppression and a crowding together of the curves.

If the decision variable x is presumed Gaussian, and the operating characteristics overlayed on the exact results in figures 6-19, it is found that the two sets of curves for $M=8192$ are virtually identical in the range of P_{FA} and P_D plotted. However, for $M=16$, the Gaussian approximation is somewhat optimistic; for example, the exact curve for $\alpha=2.75$ is well-approximated by the Gaussian approach for $\alpha=2.62$. For small M , the Gaussian approximation is overly optimistic for small P_{FA} ; however, the two sets cross near $P_{FA}=.5$, which is not a practical range of interest anyway.

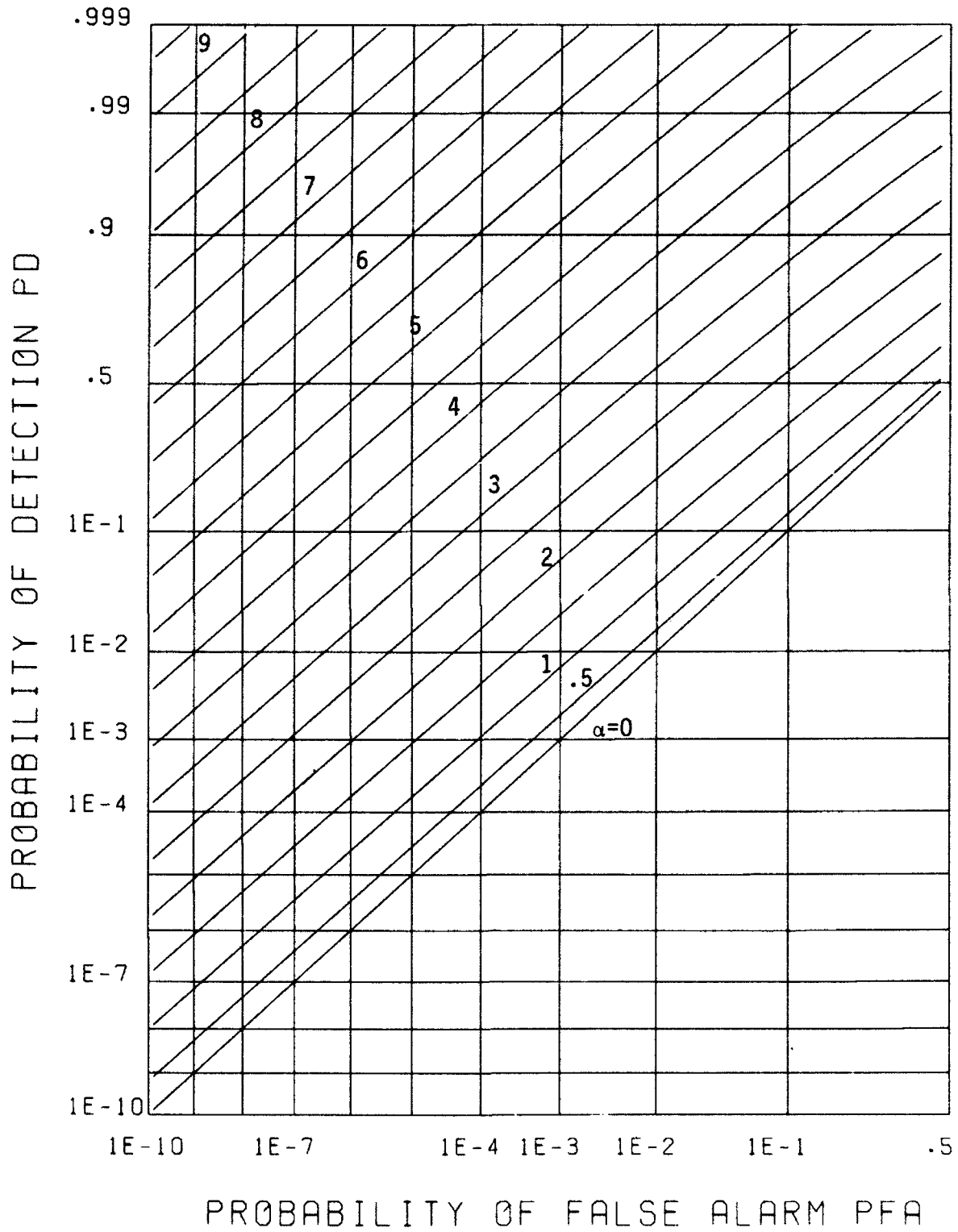


Figure 6. Receiver Operating Characteristics for M=1

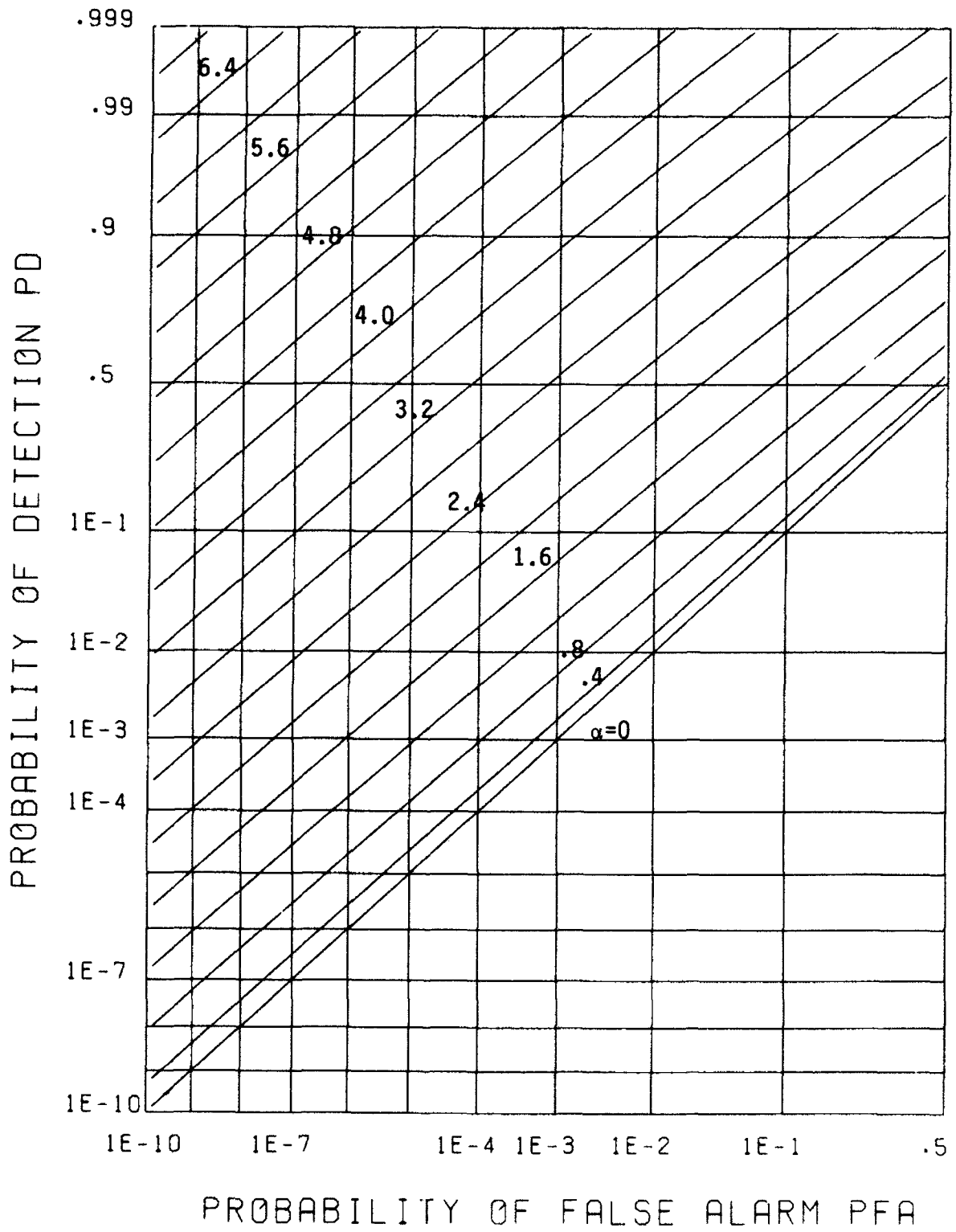


Figure 7. Receiver Operating Characteristics for M=2

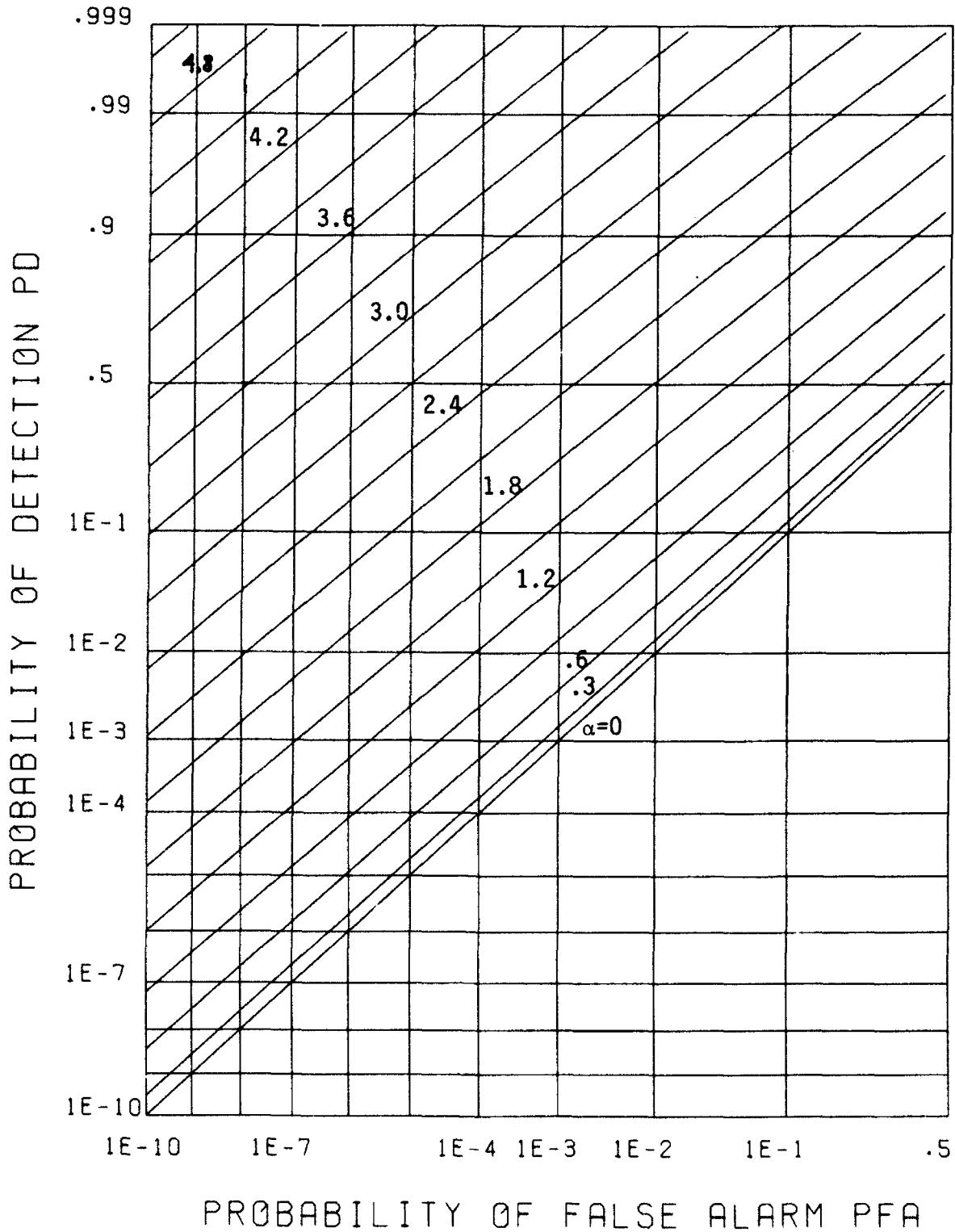


Figure 8. Receiver Operating Characteristics for M=4

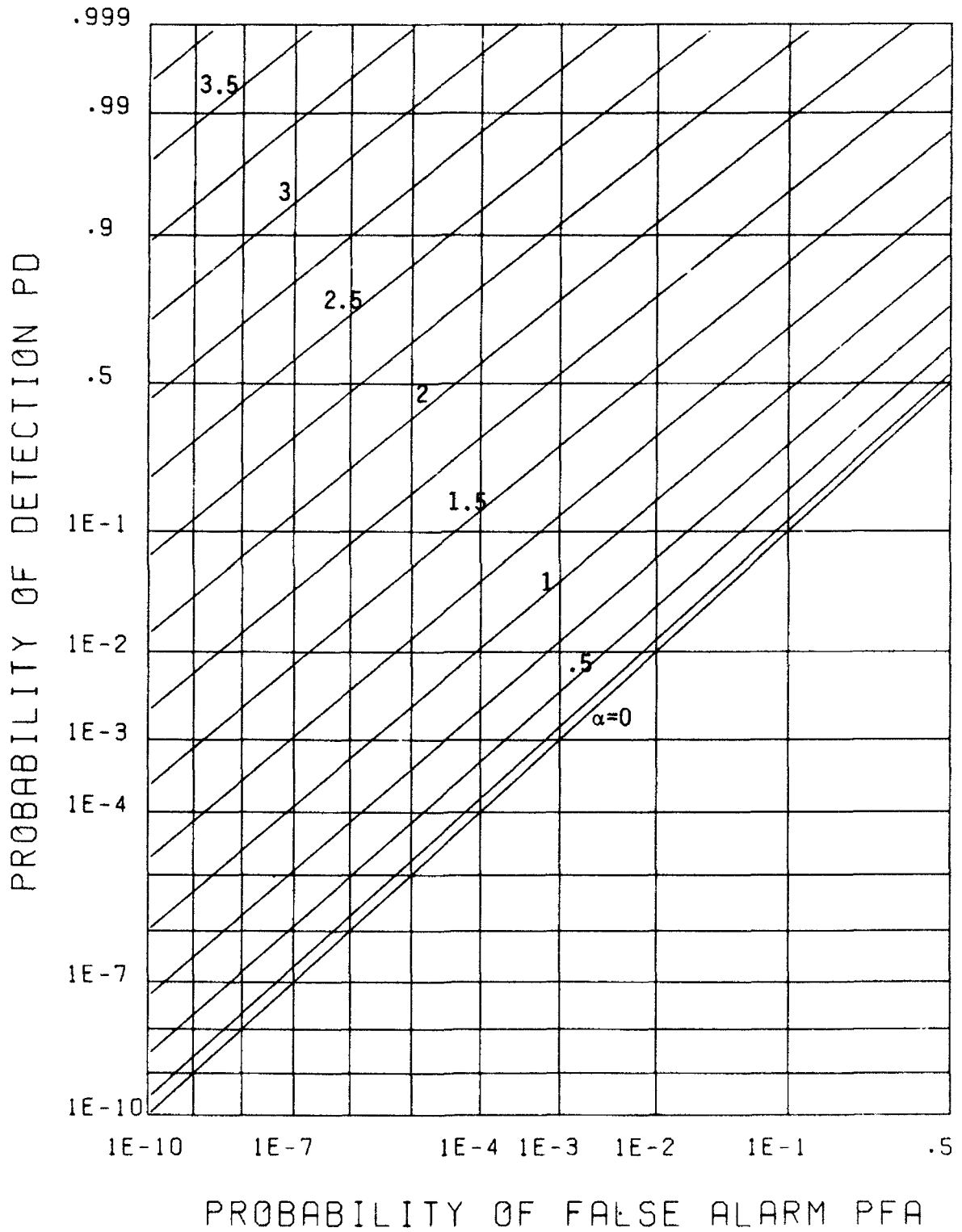


Figure 9. Receiver Operating Characteristics for $M=8$

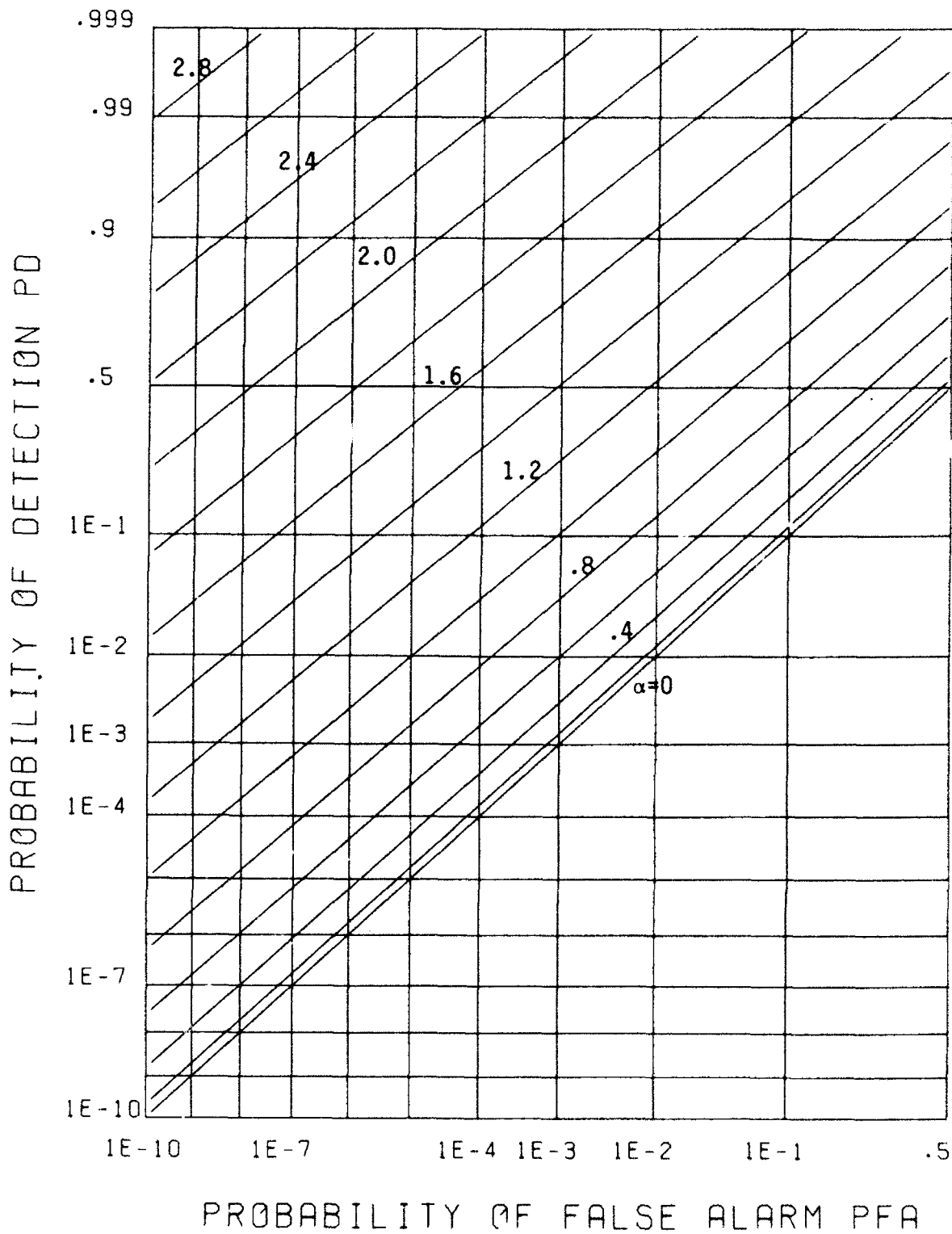


Figure 10. Receiver Operating Characteristics for $M=16$

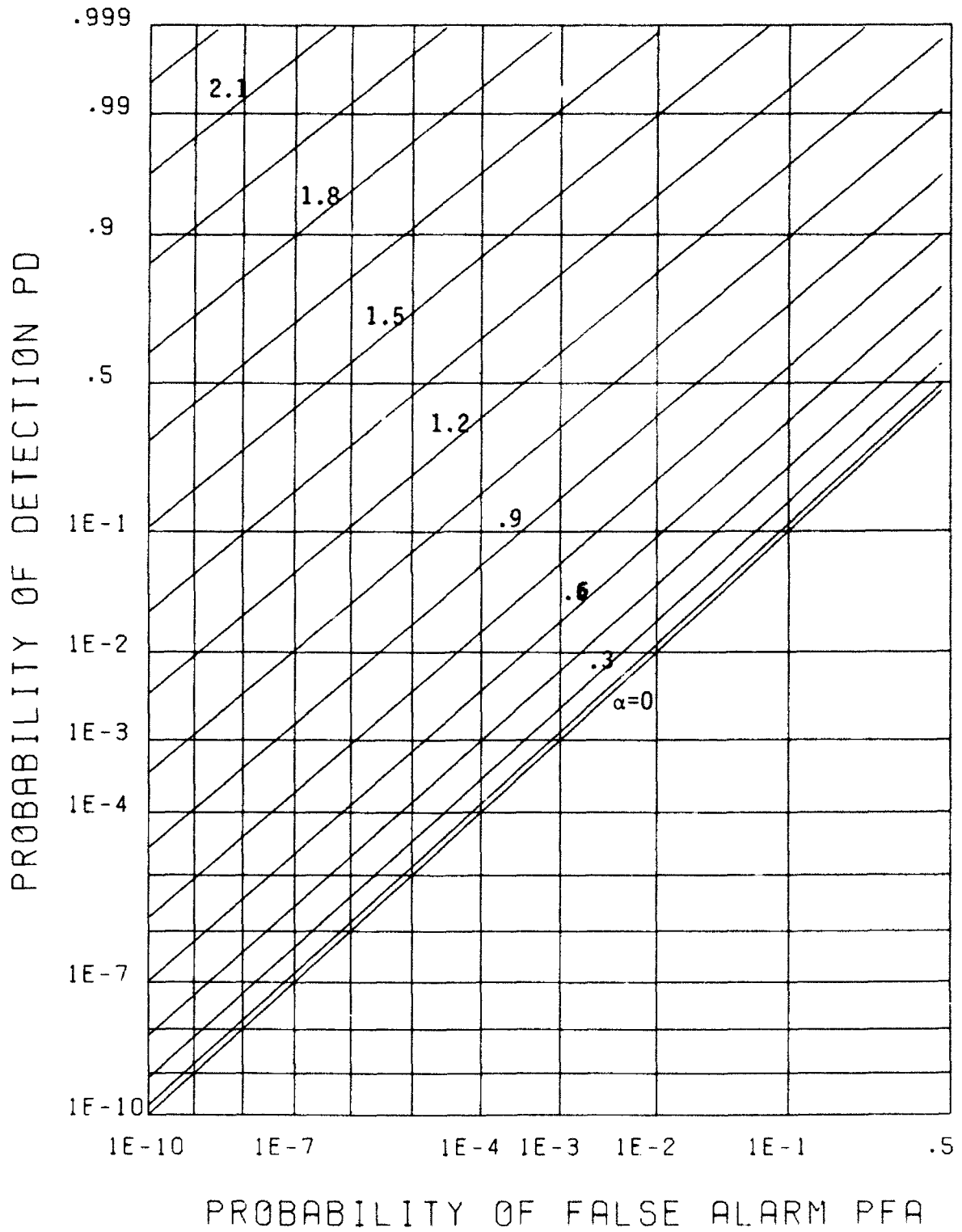


Figure 11. Receiver Operating Characteristics for $M=32$

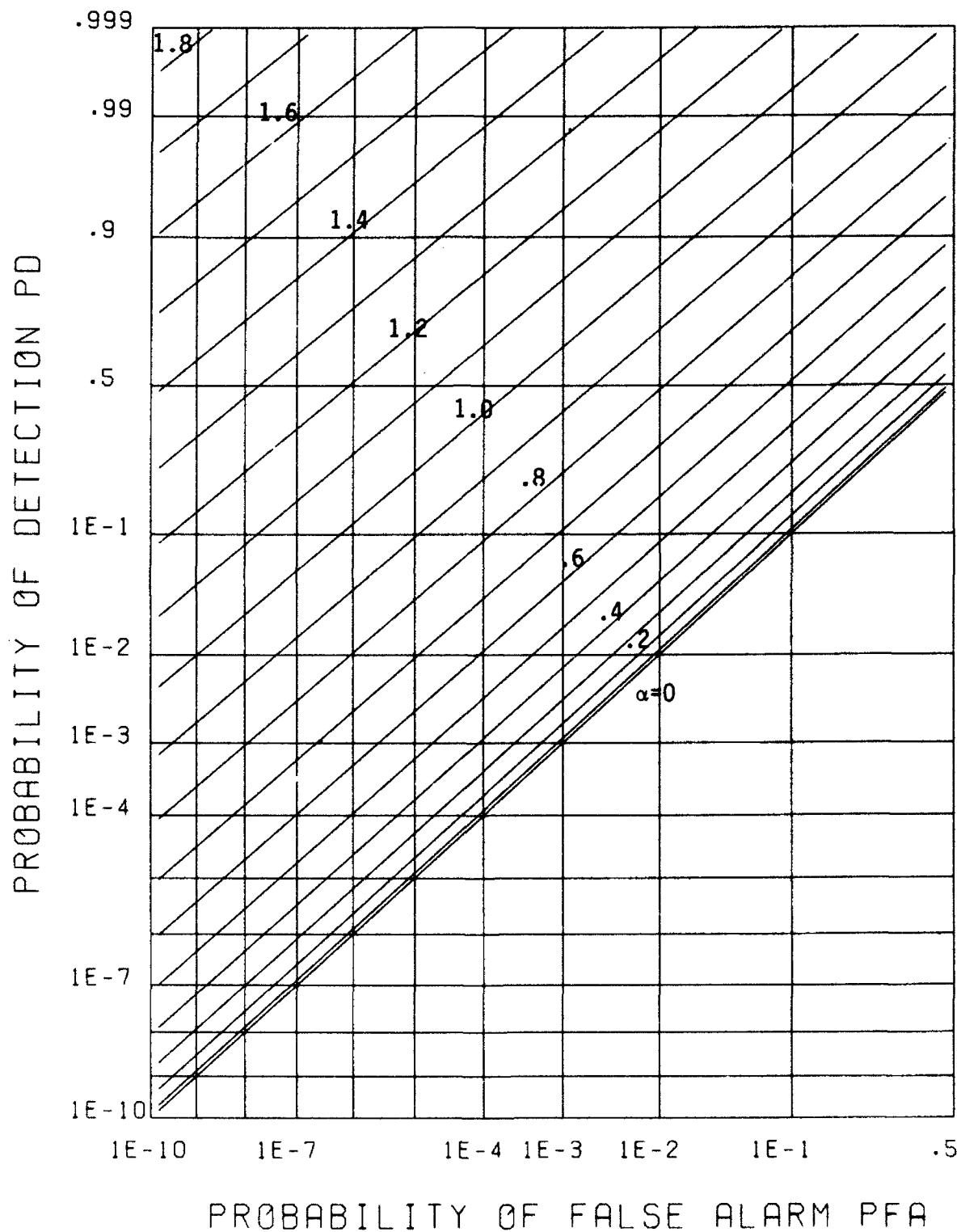


Figure 12. Receiver Operating Characteristics for $M=64$

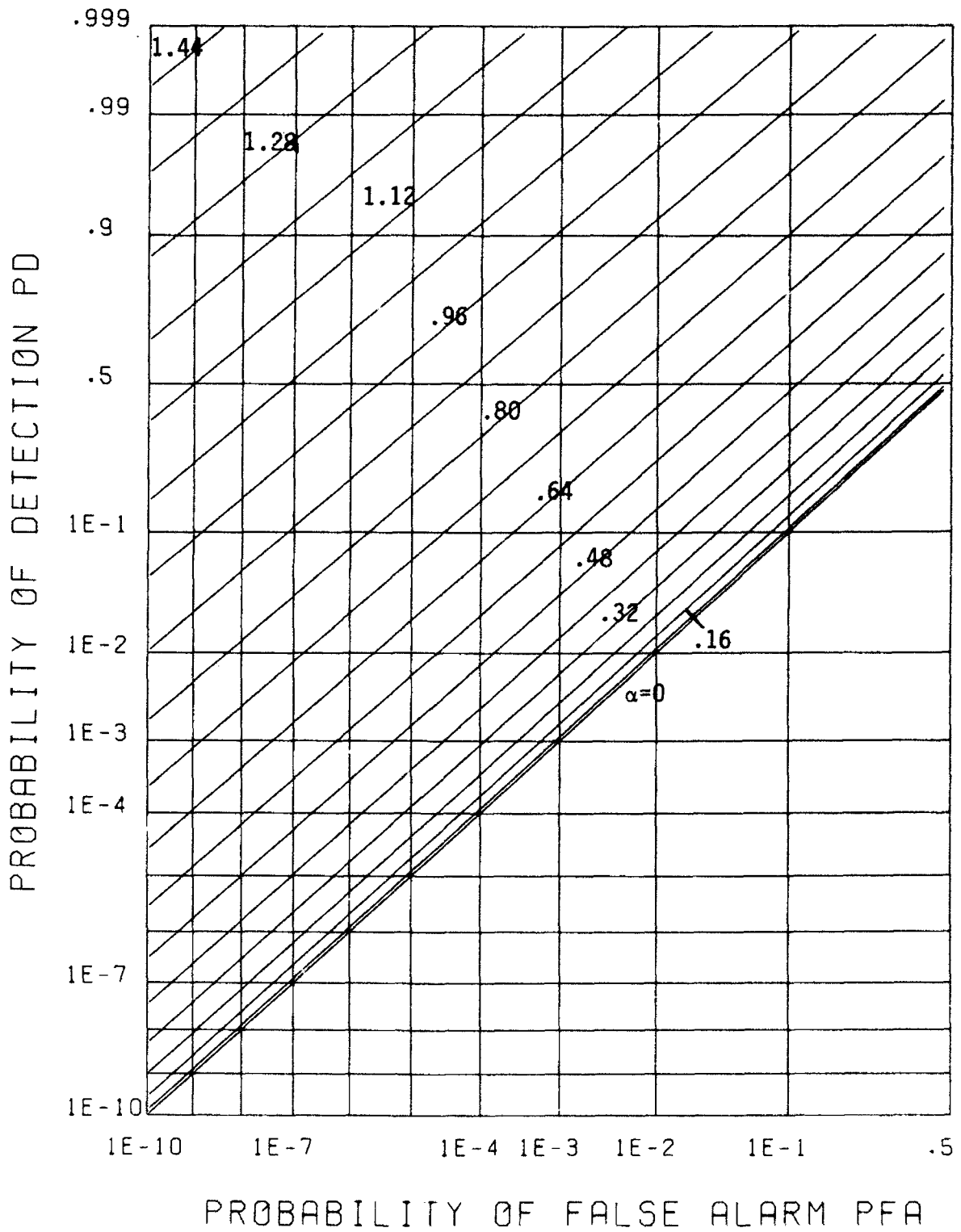


Figure 13. Receiver Operating Characteristics for $M=128$

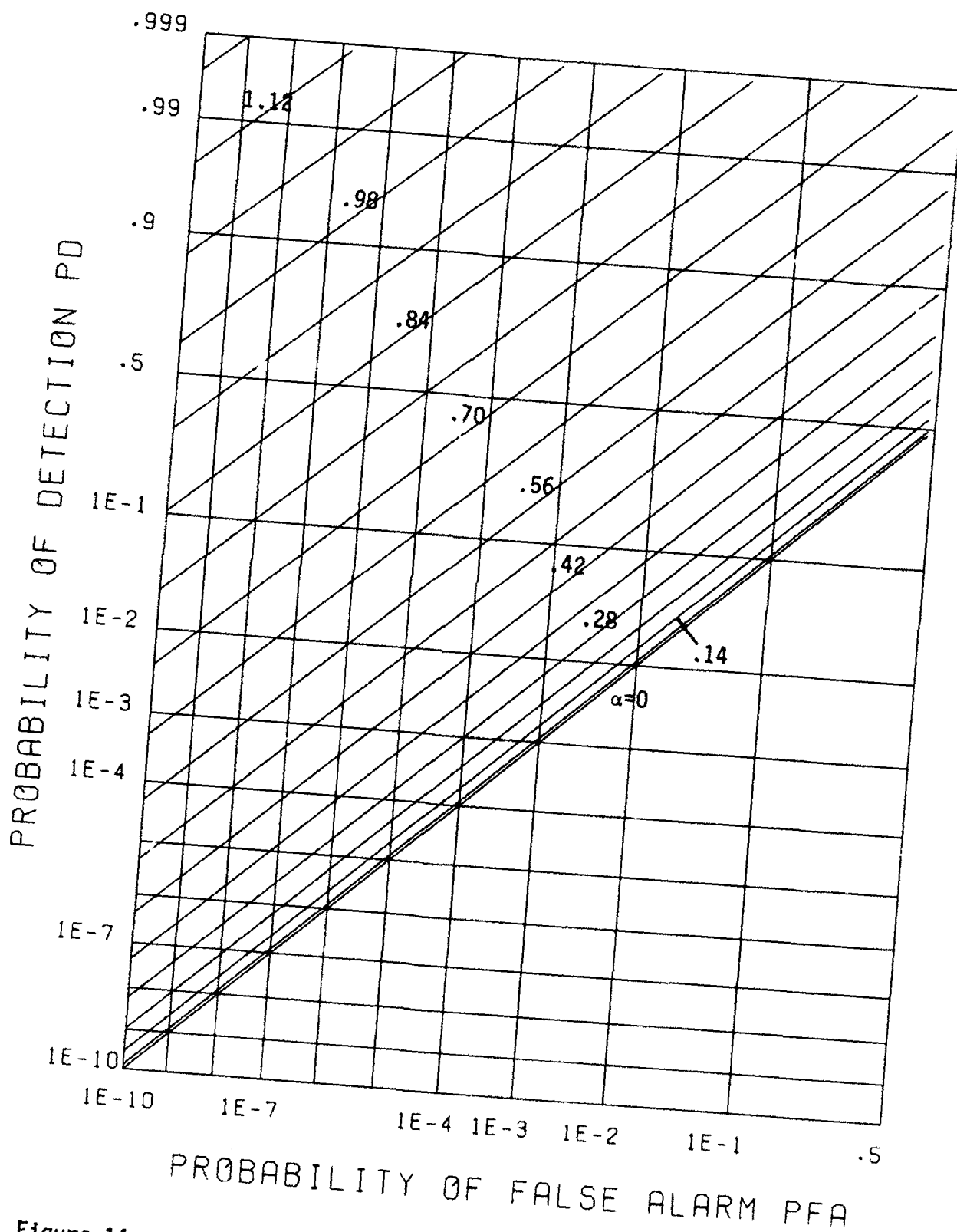


Figure 14. Receiver Operating Characteristics for $M=256$

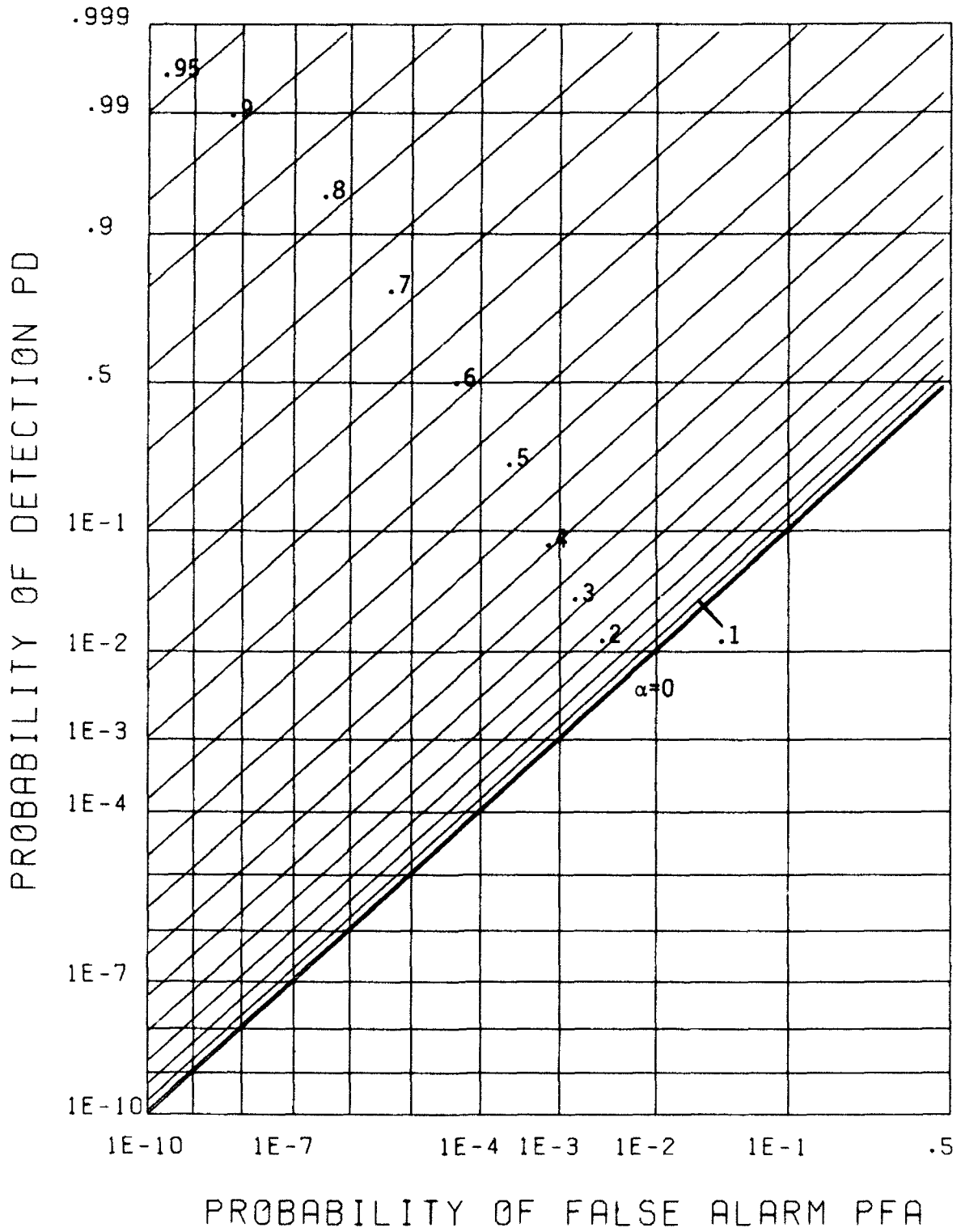


Figure 15. Receiver Operating Characteristics for $M=512$

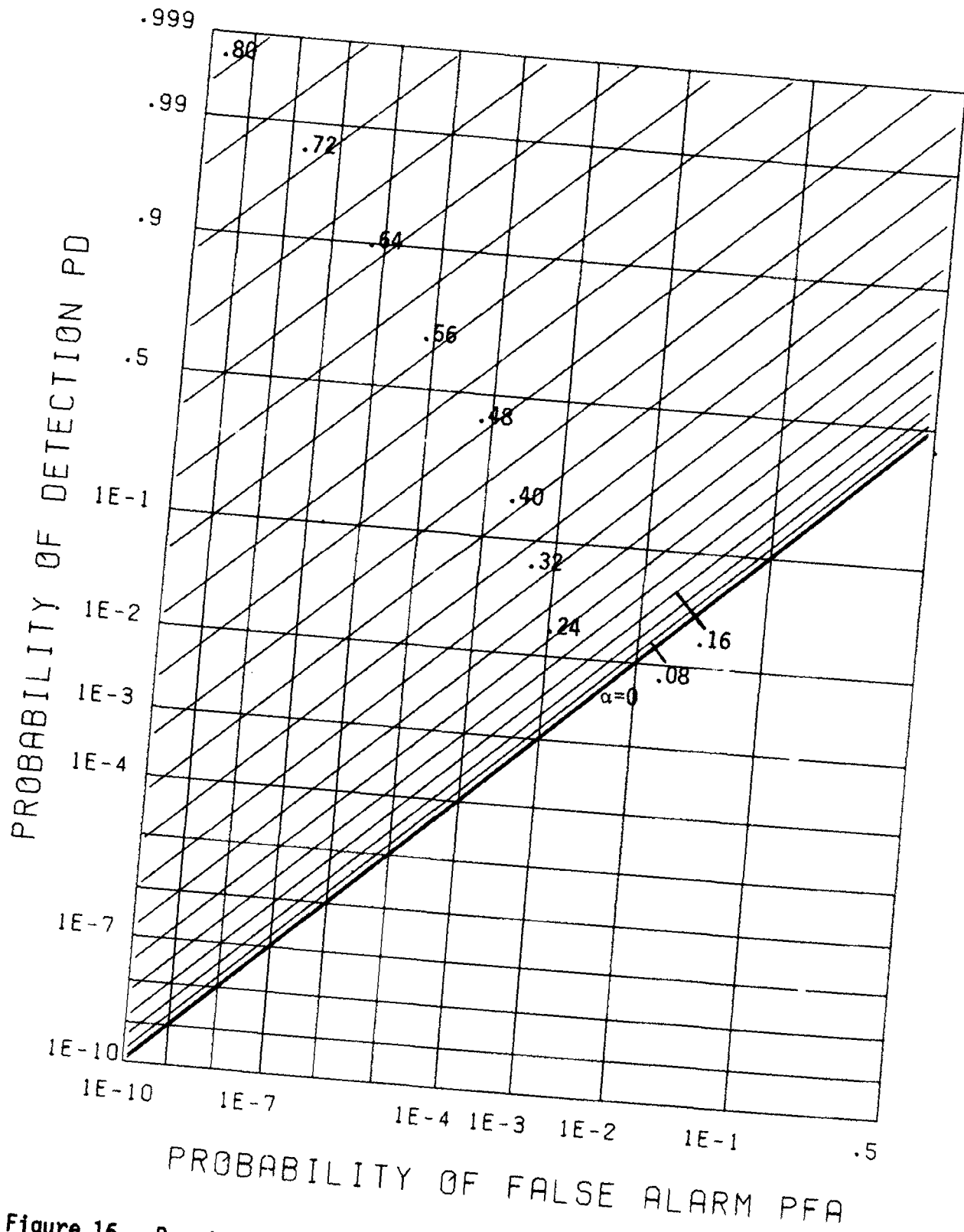


Figure 16. Receiver Operating Characteristics for M=1024

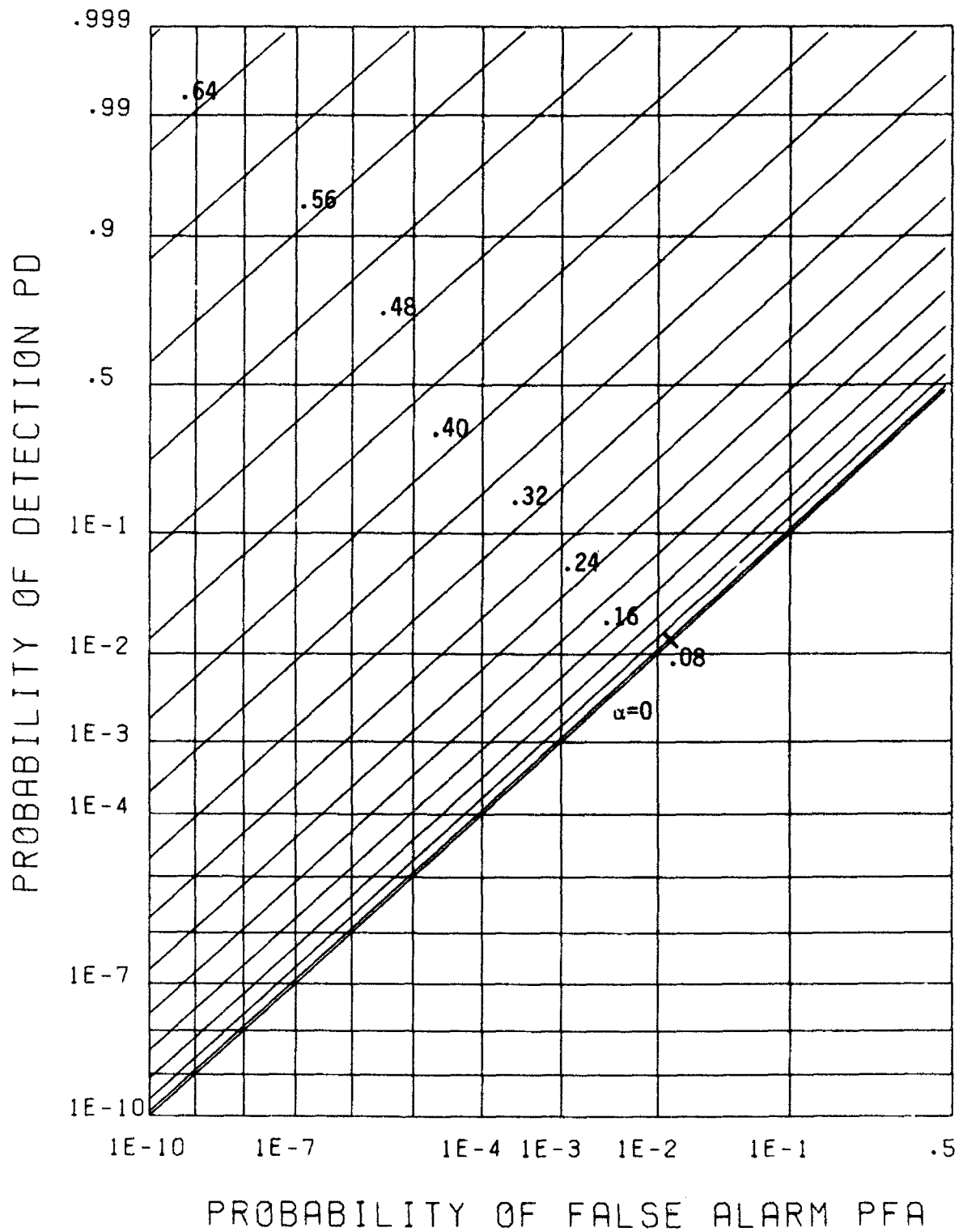


Figure 17. Receiver Operating Characteristics for M=2048

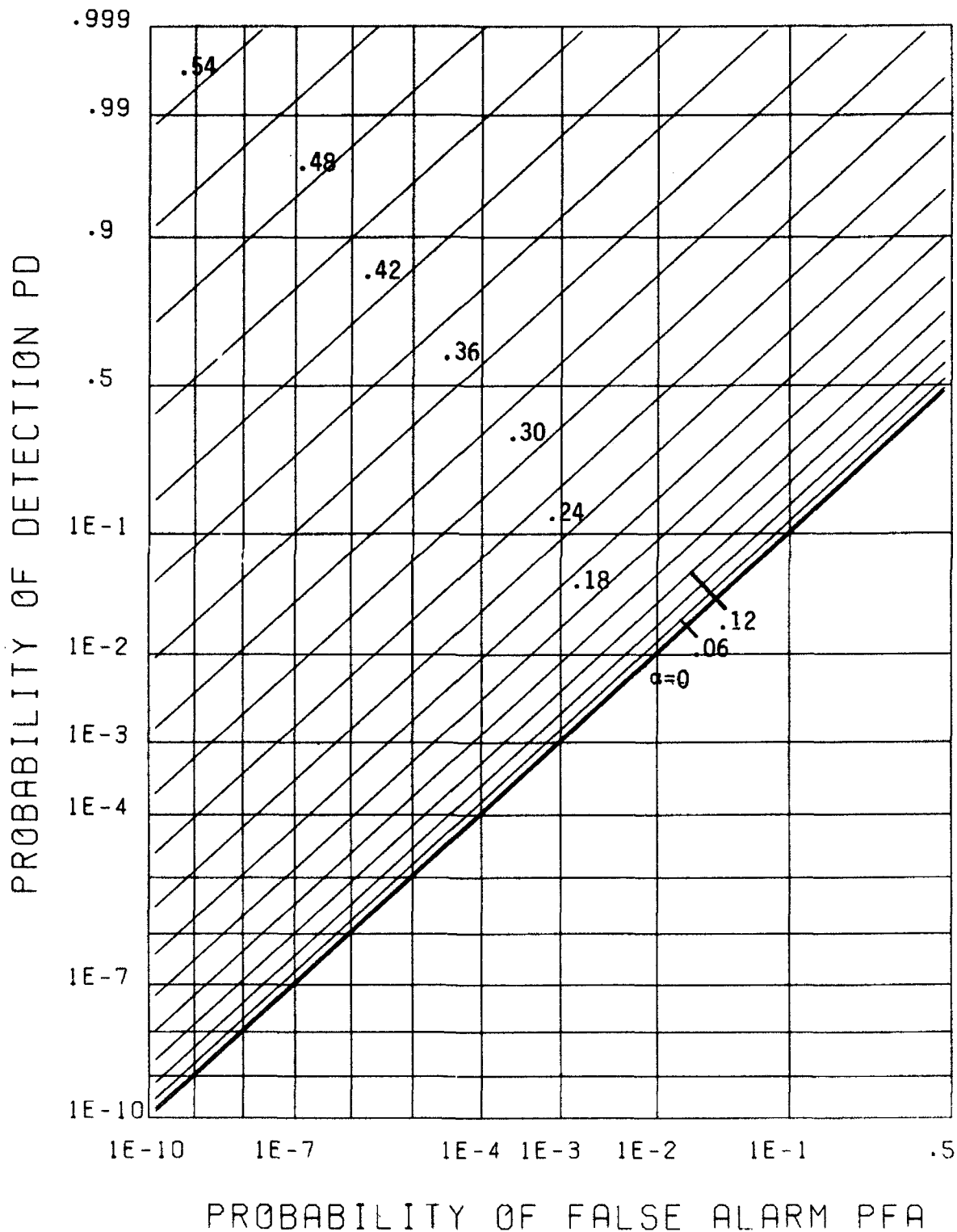


Figure 18. Receiver Operating Characteristics for M=4096

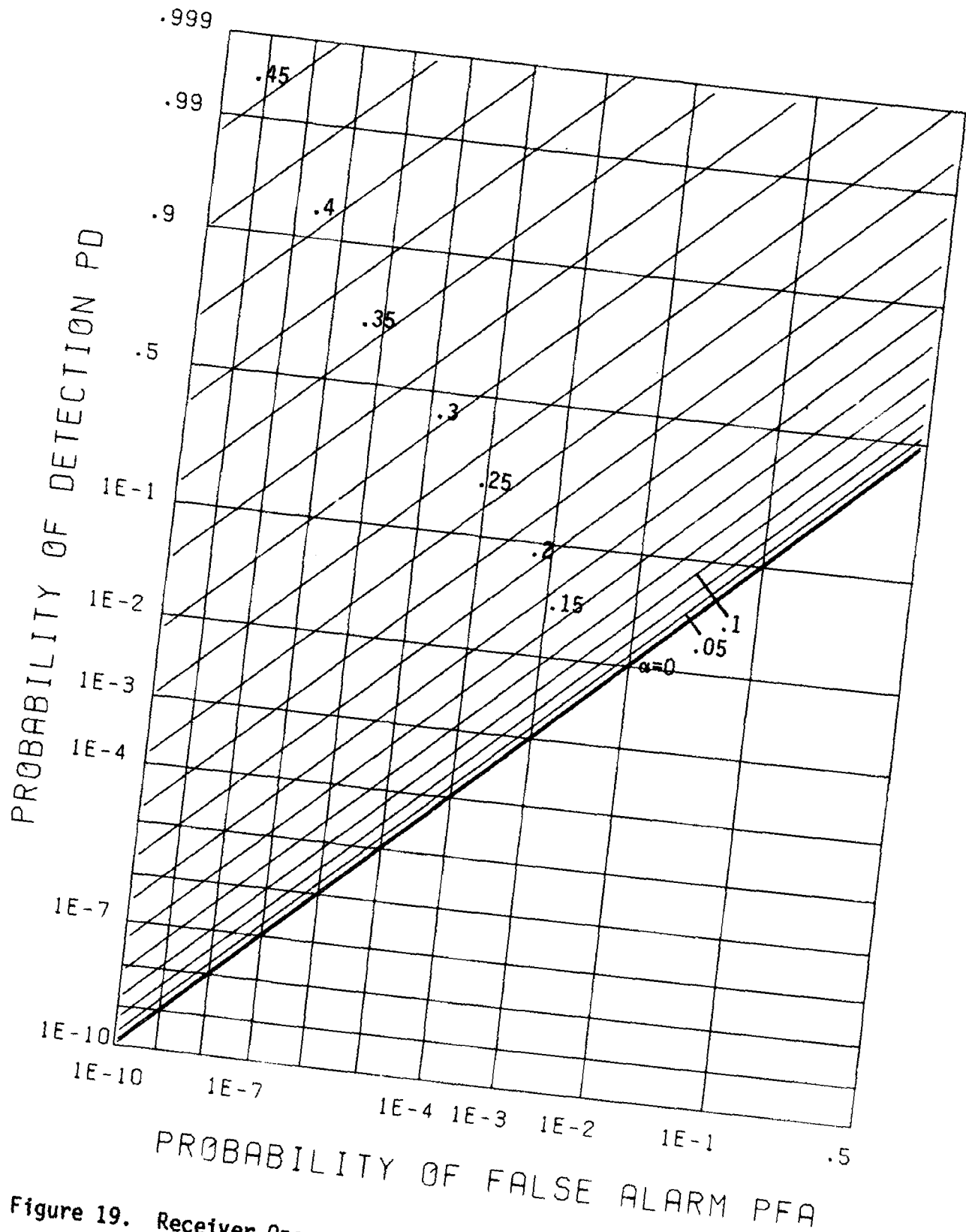


Figure 19. Receiver Operating Characteristics for $M=8192$

SUMMARY

A method for exact evaluation of the exceedance distribution function, of a linear sum of M envelopes of a narrowband Gaussian process and sinewave, has been utilized to determine the receiver operating characteristics for a wide range of values of M and signal-to-noise ratio. Also, the required input signal-to-noise ratio vs. M has been determined for a selected set of false alarm and detection probabilities. Programs are also supplied by which other values of the various parameters can be investigated by the user.

Agreement between the current results and those in [1,2] is very good over the range of common values plotted. For M larger than 8192, the approximation given in (27) and (28) is recommended, since the summation variable is then well represented by a Gaussian random variable.

APPENDIX A. DERIVATION OF RICE CHARACTERISTIC FUNCTION

The normalized probability density function of a Rice random variable was given in (2) as

$$p_e(u) = u \exp\left(-\frac{u^2 + \alpha^2}{2}\right) I_0(\alpha u) \quad \text{for } u \geq 0 \quad . \quad (\text{A-1})$$

The corresponding characteristic function is

$$\begin{aligned} f_e(\xi) &= \int_{-\infty}^{+\infty} du \exp(i\xi u) p_e(u) = \int_0^{+\infty} du u \exp\left(i\xi u - \frac{u^2 + \alpha^2}{2}\right) I_0(\alpha u) = \\ &= \exp(-r) \sum_{n=0}^{\infty} \frac{(r/2)^n}{(n!)^2} \int_0^{\infty} du u^{2n+1} \exp(i\xi u - u^2/2) \quad , \end{aligned} \quad (\text{A-2})$$

where we have expanded I_0 in a power series [5, 8.447 1] and defined power signal-to-noise ratio

$$r = \alpha^2/2 \quad . \quad (\text{A-3})$$

(If desired, a power series in ξ could be developed by expanding $\exp(i\xi u)$ in a power series instead of I_0 .)

We define

$$C_n(\xi) = \frac{1}{2^n (n!)^2} \int_0^{\infty} du u^{2n+1} \exp(i\xi u - u^2/2) \quad \text{for } n \geq 0 \quad , \quad (\text{A-4})$$

and get the characteristic function series

$$f_e(\xi) = \exp(-r) \sum_{n=0}^{\infty} r^n C_n(\xi) \quad . \quad (\text{A-5})$$

In order to get a recurrence on $C_n(\xi)$, we also define

$$B_k(\xi) = \int_0^{\infty} dw w^k \exp(i\xi w - w^2/2) \quad \text{for } k \geq 0 \quad , \quad (\text{A-6})$$

for then

$$C_n(\xi) = \frac{B_{2n+1}(\xi)}{2^n (n!)^2} \quad . \quad (A-7)$$

By integrating by parts on (A-6), there follows

$$B_k = i\xi B_{k-1} + (k-1)B_{k-2} \quad \text{for } k \geq 1 \quad . \quad (A-8)$$

This recurrence can be started with [5, 3.896 3&4]

$$B_0 = \exp(-\xi^2/2) \left[\sqrt{\frac{\pi}{2}} + i\xi {}_1F_1\left(\frac{1}{2}; \frac{3}{2}; \frac{\xi^2}{2}\right) \right] \quad . \quad (A-9)$$

By looking at three adjacent terms of recurrence (A-8), we can generate the alternative recurrence

$$B_k = (2k-3-\xi^2)B_{k-2} - (k-2)(k-3)B_{k-4} \quad . \quad (A-10)$$

By means of (A-7), this translates into

$$C_n = \frac{1}{n^2} \left[\left(2n - \frac{1+\xi^2}{2}\right) C_{n-1} - \frac{n - \frac{1}{2}}{n-1} C_{n-2} \right] \quad \text{for } n \geq 2 \quad . \quad (A-11)$$

Starting values are (via manipulation of hypergeometric series and Kummer's transformation) expressible as

$$C_0 = \exp(-\xi^2/2) \left[{}_1F_1\left(-\frac{1}{2}; \frac{1}{2}; \frac{\xi^2}{2}\right) + i\sqrt{\frac{\pi}{2}} \xi \right],$$

$$C_1 = \exp(-\xi^2/2) \left[{}_1F_1\left(-\frac{3}{2}; \frac{1}{2}; \frac{\xi^2}{2}\right) + i\sqrt{\frac{\pi}{2}} (3-\xi^2)\frac{\xi}{2} \right]. \quad (A-12)$$

Each of the series for ${}_1F_1$ consists of terms of the same polarity, except for one term, and are therefore useful for obtaining very accurate initial values. C_0 is the characteristic function of the Rayleigh probability

density function. Relations (A-11)-(A-12) constitute recurrences on both the real and imaginary parts of C_n .

It was found that the terms $\exp(-r) r^n$ in (A-5) became very large for large n , while the C_n terms became very small. In order to avoid overflow and underflow, we defined the total term

$$A_n = \exp(-r) r^n C_n \quad . \quad (A-13)$$

Reference to (A-11) readily yields the recurrence on A_n , and (A-12) furnishes corresponding obvious starting values for A_0 and A_1 .

APPENDIX B. DESCRIPTION OF PROGRAMS AND LISTINGS

Overview

Information obtained via evaluation of the Rice characteristic function may be displayed in three formats.

FORMAT 1: Display PD vs. PFA

The user defines the number of samples M and the range of values for α , a voltage signal-to-noise ratio measure. An algorithm then utilizes the Rice characteristic function for $\alpha=0$ and for the alphas specified by the user. This results in the production of a threshold vs. PFA and M ($\alpha=0$) and threshold vs. PD and M ($\alpha>0$) tables. These two tables are stored on an output file. For each user-defined M , a plot routine displays PD vs. PFA for the set of user-defined alphas.

FORMAT 2: Display SNR vs M

The user supplies the input which specifies a PD. The algorithm then solves for the threshold values corresponding to $PFA=10^{*-IPFA}$, ($IPFA=1, \dots, 8$) and $M=2^{*IM}$, ($IM=0, \dots, 13$) and $\alpha=0$. A root finding technique is then employed to solve for the SNR defined by a threshold value and user-defined PD. An SNR is found for each threshold value. The results are stored in an output file. A plot routine displays the required SNR vs. M for $PFA=10^{*-IPFA}$, ($IPFA=1, 2, \dots, 8$).

FORMAT 3: Print SNR

The user specifies a value for PD, PFA, M . The program solves for the threshold corresponding to PFA and M . A root finding technique is then employed to determine the SNR corresponding to this threshold and user-defined PD and M . The results are printed.

Description of Input

Inputs to the program consist of cards which either specify values (PARAMETER CARDS), activate the reading of tabularized values (TABLES), assign files (FILE NAME CARDS), process data (COMMAND CARDS), or specify a plot device (PLOT DEVICE CARDS). The basic format of a card is

$$\text{CARD NAME} = \text{value units}$$

where CARD NAME is an alphanumeric expression from Tables 2-6. The alphanumeric must begin in column 1, value is a floating point or integer number, and units is an alphanumeric.

Parameter cards, file names, and tables constitute the data upon which commands operate. If two cards with the same name specify different data, then the last entry overrides the other.

For the programmers convenience, FORTRAN variable names associated with file names or parameters may be located in the Tables 2 through 6. Since input and values stored represent the same physical quantity, it is convenient to refer to both in this paper by the same variable name. The convention adopted is to express the variable by the lower case letters and reserve upper case letters for constants.

Parameter Cards

Parameter cards are used to specify an axis length or assign a range of values to a parameter. These cards are shown in Table 2. For example,

NUMBER OF SAMPLES MINIMUM = 1.
NUMBER OF SAMPLES MAXIMUM = 8192.
NUMBER OF SAMPLES FACTOR = 2.

implies that the program will process data for $M=1,2,4,8,16,\dots,4096,8192$.

Table Cards

A table card contains the values that are to be assigned to a variable. The last card that must appear in a table is an EOF card. This card terminates the reading of the table. Table cards exist for PD and PFA only. A list of the table cards appears in Table 4. For example,

```
PROBABILITY OF DETECTION TABLE
.5
.7
.99
EOF
```

This table assigns values of .5, .7, .99 to PD.

Files Cards

A file card allows for dynamic assignment of all mass storage files. This is accomplished by linking internal FORTRAN unit numbers to files during execution. The file card is shown in Table 4. Two of the three algorithms use files. They are

```
Display PD vs PFA : A file is used to store output.
Display SNR vs M  : A file is used to store output.
```

For example,

```
OUTPUT FILE = PDFILE
```

directs the output of a program to a file called PDFILE.

Command Cards

Command cards are used to compute, plot, or terminate a run stream. Command cards are given in Table 5.

Plot Device Cards

Plot device cards direct the plot output to either a TEKTRONIX, FR80, or a CALCOMP plotter. The cards necessary for that operation are shown in Table 6.

Examples of Output

Example 1: Display PD vs PFA

The input deck for the first example appears in Table 7. This deck designates that PD vs. PFA data will be computed for $M=1$ and $\alpha=.5, 1.0, 1.5, \dots, 9.5$. The output is stored on a file called FILE1. The plot corresponding to the data is shown in figure 6. The second half of the run stream computes PD vs. PFA data for $M=2$ and $\alpha=0., .4, .8, \dots, 7.2$. The output is stored in FILE2. The plot of the data appears in figure 7.

Example 2: Display SNR vs. M

The input deck for the second example appears in Table 8. The first half of the input deck designates that the SNR vs. M plots will be computed for a value $PD=.5$. The output is displayed in figure 1. The parameter cards specify that the axis will be scaled as follows: -19 DB (minimum), 13 DB (maximum), 2 DB (increment), and 5 inches long for the SNR axis and 6.86 inches long for the number of samples axis. It should be noted that the limits for the number of samples axis are predefined by the program to be 1 (minimum), 8192 (maximum), 2 (factor). The output is stored in a file called PDFIL1. The second half of the run stream computes SNR vs. M for a value $PD=.9$. The axis limits for SNR were changed to -17 DB (minimum), 15 DB (maximum), 2 DB (increment). Alpha curves were computed for $\alpha=0., .4, .8, \dots, 7.2$. This output is stored in file PDFIL2. A plot of this data appears in figure 2.

Example 3: Print SNR

The input deck for the third example appears in Table 9. The output appears in Table 10.

TABLE 2. PARAMETER CARDS

INPUT CARDS	UNITS
SNR AXIS LENGTH = <i>snraxs</i>	IN
SAMPLE AXIS LENGTH = <i>smpaxs</i>	IN
PD AXIS LENGTH = <i>pdaxs</i>	IN
PFA AXIS LENGTH = <i>pfaaxs</i>	IN
SNR MINIMUM = <i>snrmin</i>	DB
SNR MAXIMUM = <i>snrmax</i>	DB
SNR INCREMENT = <i>snrinc</i>	DB
ALPHA MINIMUM = <i>alpmin</i>	
ALPHA MAXIMUM = <i>alpmax</i>	
ALPHA INCREMENT = <i>alpinc</i>	
NUMBER OF SAMPLES MINIMUM = <i>smpmin</i>	
NUMBER OF SAMPLES MAXIMUM = <i>smpmax</i>	
NUMBER OF SAMPLES FACTOR = <i>smpfct</i>	

TABLE 3. TABLE CARDS

INPUT CARDS	VARIABLE
PROBABILITY OF DETECTION TABLE	PD
PROBABILITY OF FALSE ALARM TABLE	PFA

TABLE 4. FILE CARDS

```

-----
INPUT CARDS
-----
OUTPUT FILE = name

```

TABLE 5. COMMAND CARDS

```

-----
INPUT CARDS
-----
RUN MAIN
COMPUTE PD VS PFA
COMPUTE SNR VS M
PLOT PD VS PFA
PLOT SNR VS M
END

```

TABLE 6. PLOT DEVICE CARDS

INPUT CARDS	OPTIONS
BAUD RATE = 960. PLOT DEVICE = device RESET PLOT DEVICE	FR80, TEKTR0, CALCOMP

TABLE 7. SAMPLE INPUT DECK FOR PD VS PFA

```

RUN MAIN
BAUD RATE = 960.
PLOT DEVICE = TEKTR0
RESET PLOT DEVICE
PD AXIS LENGTH = 6.86 IN
PFA AXIS LENGTH = 5. IN
OUTPUT FILE = FILE1
NUMBER OF SAMPLES MINIMUM = 1
ALPHA MINIMUM = .5
ALPHA MAXIMUM = 9.5
ALPHA INCREMENT = .5
COMPUTE PD VS PFA
PLOT PD VS PFA
OUTPUT FILE = FILE2
NUMBER OF SAMPLES MINIMUM = 2
ALPHA MINIMUM = 0.
ALPHA MAXIMUM = 7.2
ALPHA INCREMENT = .4
COMPUTE PD VS PFA
PLOT PD VS PFA
END

```

TABLE 8. SAMPLE INPUT DECK FOR SNR vs M

```

RUN MAIN
BAUD RATE = 960.
TEMPORARY FILE = FALSE
PLOT DEVICE = TEKTR0
RESET PLOT DEVICE
OUTPUT FILE = PDFIL1
SNR MINIMUM = -19. DB
SNR MAXIMUM = 13. DB
SNR INCREMENT = 2. DB
SNR AXIS LENGTH = 5. IN
SAMPLE AXIS LENGTH = 6.86 IN
PROBABILITY OF DETECTION TABLE
.5
EOF
COMPUTE SNR VS M
PLOT SNR VS M
OUTPUT FILE = PDFIL2
SNR MINIMUM = -17. DB
SNR MAXIMUM = 15. DB
SNR INCREMENT = 2. DB
PROBABILITY OF DETECTION TABLE
.9
EOF
COMPUTE SNR VS M
PLOT SNR VS M
END

```

TABLE 9. SAMPLE INPUT DECK FOR PRINTING SNR

```

RUN MAIN
PROBABILITY OF DETECTION TABLE
.5
.9
EOF
PROBABILITY OF FALSE ALARM TABLE
.1
.001
EOF
NUMBER OF SAMPLES MINIMUM = 1.
NUMBER OF SAMPLES MAXIMUM = 2048.
NUMBER OF SAMPLES FACTOR = 2.
PRINT SNR
END

```

TABLE 10. PRINT OUT OF SNR VS M

PD =	0.500	PFA = 0.100D+00	PD =	0.900	PFA = 0.100D+00
M =	1	SNR = 2.50	M =	1	SNR = 7.18
M =	2	SNR = 0.68	M =	2	SNR = 5.03
M =	4	SNR = -1.08	M =	4	SNR = 2.99
M =	8	SNR = -2.77	M =	8	SNR = 1.05
M =	16	SNR = -4.41	M =	16	SNR = -0.79
M =	32	SNR = -6.02	M =	32	SNR = -2.55
M =	64	SNR = -7.59	M =	64	SNR = -4.24
M =	128	SNR = -9.15	M =	128	SNR = -5.89
M =	256	SNR = -10.69	M =	256	SNR = -7.50
M =	512	SNR = -12.22	M =	512	SNR = -9.08
M =	1024	SNR = -13.74	M =	1024	SNR = -10.64
M =	2048	SNR = -15.26	M =	2048	SNR = -12.18

PD =	0.500	PFA = 0.100D-02	PD =	0.900	PFA = 0.100D-02
M =	1	SNR = 8.06	M =	1	SNR = 10.76
M =	2	SNR = 5.74	M =	2	SNR = 8.29
M =	4	SNR = 3.63	M =	4	SNR = 6.01
M =	8	SNR = 1.69	M =	8	SNR = 3.89
M =	16	SNR = -0.14	M =	16	SNR = 1.92
M =	32	SNR = -1.87	M =	32	SNR = 0.06
M =	64	SNR = -3.54	M =	64	SNR = -1.72
M =	128	SNR = -5.16	M =	128	SNR = -3.42
M =	256	SNR = -6.75	M =	256	SNR = -5.07
M =	512	SNR = -8.31	M =	512	SNR = -6.68
M =	1024	SNR = -9.86	M =	1024	SNR = -8.26
M =	2048	SNR = -11.39	M =	2048	SNR = -9.82

Listing of Program

This section contains a listing of three master programs and associated subroutines. Subroutines which read input and plot the output have been omitted. Table 11 contains a list of the subroutine names and a brief description of the pertinent subroutines.

TABLE 11. DESCRIPTION OF SUBROUTINES

NAME -----	DESCRIPTION -----
CMPDVA	MASTER PROGRAM FOR COMPUTING PD VS PFA
CMPSVS	MASTER PROGRAM FOR COMPUTING SNR VS M
PRTSNR	MASTER PROGRAM FOR COMPUTING AND PRINTING SNR
FFT	COMPUTES THE FAST FOURIER TRANSFORM OF A FUNCTION
RDC	COMPUTES AN APPROXIMATE S/N FOR A GIVEN PD, PFA, M (SEE REF 7)
FNPD	COMPUTES THE PROBABILITY OF DETECTION FOR A GIVEN M, S/N, AND THRESHOLD
FNPF	COMPUTES THE PROBABILITY OF FALSE ALARM FOR A GIVEN M AND THRESHOLD
FNF11	COMPUTES THE CONFLUENT HYPERGEOMETRIC FUNCTION
RICE	COMPUTES THE CHARACTERISTIC FUNCTION OF A RICE VARIATE
FNIPHI	COMPUTES THE INVERSE OF THE CUMULATIVE GAUSSIAN DISTRIBUTION
DIST	COMPUTES THE EXCEEDANCE DISTRIBUTION FUNCTION FOR A GIVEN M AND S/N

```

SUBROUTINE FFT(N,X,Y)
IMPLICIT DOUBLE PRECISION (A-H,O-Z)
DIMENSION C(0:256),X(0:1023),Y(0:1023),L(0:9)
DATA PI/3.14159265358979324D0/

T=2.D0*PI/N
J1=N/4
DO 100 J=0,J1
C(J)=DCOS(T*DIFLOTJ(J))
100 CONTINUE

N1=N/4
N2=N1+1
N3=N2+1
N4=N3+N1
L2=JIDINT(1.4427D0*DLOG(DIFLOTJ(N))+.5D0)
DO 600 I1=1,L2
I2=2** (L2-I1)
I3=2D0*I2
I4=N/I3

DO 500 I5=1,I2
I6=I4*(I5-1)+1
IF( I6.LE.N2 ) GO TO 350
V6=-C(N4-I6-1)
V7=-C(I6-N1-1)
GO TO 375
350 V6=C(I6-1)
V7=-C(N3-I6-1)
375 L3=N-I3

DO 400 I7=0,L3,I3
I8=I7+I5
I9=I8+I2
V8=X(I8-1)-X(I9-1)
V9=Y(I8-1)-Y(I9-1)
X(I8-1)=X(I8-1)+X(I9-1)
Y(I8-1)=Y(I8-1)+Y(I9-1)
X(I9-1)=V6*V8-V7*V9
Y(I9-1)=V6*V9+V7*V8
400 CONTINUE
500 CONTINUE
600 CONTINUE

I1=L2+1
DO 700 I2=1,10
L(I2-1)=1.D0
IF( I2.GT.L2 ) GO TO 700
L(I2-1)=2** (I1-I2)
700 CONTINUE

```

```
IC0=L(0)
IC1=L(1)
IC2=L(2)
IC3=L(3)
IC4=L(4)
IC5=L(5)
IC6=L(6)
IC7=L(7)
IC8=L(8)
IC9=L(9)
```

```
      K=1
      DO 1900 I1=1,IC9
      DO 1800 I2=I1,IC8,IC9
      DO 1700 I3=I2,IC7,IC8
      DO 1600 I4=I3,IC6,IC7
      DO 1500 I5=I4,IC5,IC6
      DO 1400 I6=I5,IC4,IC5
      DO 1300 I7=I6,IC3,IC4
      DO 1200 I8=I7,IC2,IC3
      DO 1100 I9=I8,IC1,IC2
      DO 1000 I10=I9,IC0,IC1
      J=I10
      IF( K,GT.J ) GO TO 900
      A=X(K-1)
      X(K-1)=X(J-1)
      X(J-1)=A
      A=Y(K-1)
      Y(K-1)=Y(J-1)
      Y(J-1)=A
900   K=K+1
1000  CONTINUE
1100  CONTINUE
1200  CONTINUE
1300  CONTINUE
1400  CONTINUE
1500  CONTINUE
1600  CONTINUE
1700  CONTINUE
1800  CONTINUE
1900  CONTINUE

      RETURN
      END
```



```

SUBROUTINE FNPD(ALPHA,V,AM,AL,AD,ABS,PD)
IMPLICIT DOUBLE PRECISION (A-H,O-Z)
DATA PI/3.14159265358979324D0/

```

```

SNR=.5D0*ALPHA*ALPHA
CALL FNF11(1.5D0,1.D0,SNR,F11)
FAC=DSQRT(.5D0*PI)*EXP(-SNR)*F11
AMUY=AM*FAC+ABS
AM2=AM/2.D0
VD=V*AD
EXC=.5*AD*AMUY
NS1=JIDINT(AL/AD)
DO 100 NS=1,NS1
XI=AD*NS
CALL RICE(XI,SNR,FR,FI)
A=DATAN2(FI,FR)
FYI=DSIN(AM*A+ABS*XI)*(FR*FR+FI*FI)**AM2
ADD=FYI*DCOS(VD*DFLOTJ(NS))/DFLOTJ(NS)
EXC=EXC+ADD
100 CONTINUE
PD=2.D0*EXC/PI

RETURN
END

```

```

SUBROUTINE FNPF(V,AM,AL,AD,ABS,PF)
IMPLICIT DOUBLE PRECISION (A-H,O-Z)
DATA PI/3.14159265358979324D0/

```

```

FAC=DSQRT(.5D0*PI)
AMUY=AM*FAC+ABS
AM2=AM/2.D0
VD=V*AD
EXC=.5*AD*AMUY
NS1=JIDINT(AL/AD)
DO 100 NS=1,NS1
XI=AD*NS
X2=.5D0*XI*XI
E=EXP(-X2)
CALL FNF11(-.5D0,.5D0,X2,F11)
FR=E*F11
FI=E*FAC*XI
A=DATAN2(FI,FR)
FYI=DSIN(AM*A+ABS*XI)*(FR*FR+FI*FI)**AM2
ADD=FYI*DCOS(VD*DFLOTJ(NS))/DFLOTJ(NS)
EXC=EXC+ADD
100 CONTINUE
PF=2.D0*EXC/PI

RETURN
END

```

```

SUBROUTINE RDC(AM,PF,PD,ALPHA)
IMPLICIT DOUBLE PRECISION (A-H,O-Z)

A=DLOG(.62D0/PF)
R=DLOG(PD/(1.D0-PD))
FACT=6.2D0 + 4.54D0/DSQRT(AM+.44D0)
SNRDB=-5.D0*DLOG10(AM) + DLOG10(A+.12D0*A*B+1.7D0*B)*FACT
ALPHA=DSQRT(2.D0*10.D0**(.1D0*SNRDB))
RETURN
END

```

```

SUBROUTINE FNF11(A,B,X,F11)
IMPLICIT DOUBLE PRECISION (A-H,O-Z)

F11=1.D0
T=1.D0
DO 100 K=1,300
U=K-1
T=T*(A+U)*X/((B+U)*K)
F11=F11+T
IF( DABS(T).LE.DABS(F11)*1.D-18 ) GO TO 200
100 CONTINUE
PRINT 101
101 FORMAT(2X,'300 TERMS IN FNF11')
200 CONTINUE

RETURN
END

```

```

SUBROUTINE FNIPHI(X,PHI)
IMPLICIT DOUBLE PRECISION (A-H,O-Z)

100 Y=DMAX1(X,1.D-12)
Y=DMIN1(Y,1.D0-1.D-12)
D=X-.5D0
IF( DABS(D).GT. .01D0 ) GO TO 250
PHI=2.50662827463D0*D*(1.D0+D*D*1.04719755120D0)
GO TO 300
250 PHI=Y
IF( Y.GT. .5D0 ) PHI=.5D0-(Y-.5D0)
PHI=DSQRT(-2.D0*DLOG(PHI))
T=1.B0+PHI*(1.432788D0+PHI*(.189269D0+PHI*.001308D0))
PHI=PHI-(2.515517D0+PHI*(.802853D0+PHI*.010328D0))/T
IF( Y.LT. .5D0 ) PHI=-PHI
300 RETURN
END

```

```

SUBROUTINE DIST(AM,ALPHA,MF,X,Y)
IMPLICIT DOUBLE PRECISION (A-H,O-Z)
DIMENSION X(0:1023), Y(0:1023)
COMMON /PDVFF/AL,AD,ABS
DATA PI/3.1415926535897932400/

SNR=.5D0*ALPHA*ALPHA
CALL FNF11(1.5D0,1.D0,SNR,F11)
AMU=DSQRT(.5D0*PI)*DEXP(-SNR)*F11
AMUS=AM*AMU+ABS
AM2=AM/2.D0

DO 100 I=0,1023
X(I)=0.D0
Y(I)=0.D0
100 CONTINUE

X(0)=.5D0*AMUS*AD
NS1=JIDINT(AL/AD)
DO 1000 NS=1,NS1
XI=AD*NS
CALL RICE(XI,SNR,U,V)
T=DATAN2(V,U)
FI=DSIN(AM*T+ABS*XI)*(U*U+V*V)**AM2
MS=JMOD(NS,MF)
X(MS)=X(MS)+FI/NS
1000 CONTINUE

CALL FFT(MF,X,Y)

FAC=2.D0/PI
KS1=MF/2.D0
DO 2000 KS=0,KS1
T=X(KS)*FAC
X(KS)=1.D0-T
Y(KS)=T
2000 CONTINUE

RETURN
END

```

```

SUBROUTINE RICE(X,SNR,FR,FI)
IMPLICIT DOUBLE PRECISION (A-H,O-Z)
DATA PI/3.14159265358979324D0/

X2=.5D0*X*X
E=DEXP(-X2-SNR)
CALL FNF11(-.5D0,.5D0,X2,F11)
AOR=E*F11
AOI=E*DSQRT(.5D0*PI)*X
CALL FNF11(-1.5D0,.5D0,X2,F11)
ANR=E*SNR*F11
ANI=SNR*(1.5D0-X2)*AOI
FR=AOR+ANR
FI=AOI+ANI
BR=DMAX1(DABS(AOR),DABS(FR))
BI=DMAX1(DABS(AOI),DABS(FI))
T=.5D0+X2

SNR2=SNR**2
DO 100 N=2,200
FO=N**2
F1=SNR*(N+N-T)/FO
F2=SNR2*(N-.5D0)/((N-1)*FO)
R=F1*ANR-F2*AOR
V=F1*ANI-F2*AOI
AOR=ANR
AOI=ANI
ANR=R
ANI=V
FR=FR+R
FI=FI+V
BR=DMAX1(BR,DABS(FR))
BI=DMAX1(BI,DABS(FI))
IF( DABS(V).LE.5.D-19*DABS(FI) .AND. DABS(R).LE.5.D-19*DABS(FR))
1 GO TO 200
100 CONTINUE
PRINT 101
101 FORMAT(2X,'200 TERMS IN RICE')
200 DR=18,-DLOG10(DABS(BR/FR))
DI=18,-DLOG10(DABS(BI/FI))
RETURN
END

```

```

SUBROUTINE CMPDVA
PARAMETER MF=2**10
PARAMETER PBDNUM=18
DOUBLE PRECISION AL,AD,ABS,BSA,AM,ALPHA,ALFA,X(0:1023),Y(0:1023)
PARAMETER (NUMFIL=30)
CHARACTER*6 FILES(NUMFIL)
COMMON /FILEC/FILES
CHARACTER*6 PBDNAM
EQUIVALENCE
1 (PBDNAM,FILES(18))
PARAMETER (NUMPAR=200)
COMMON /PARAMC/PARAMS(NUMPAR)
EQUIVALENCE
1 (SMPMIN,PARAMS(187)),
1 (SNMIN,PARAMS(184)), (SNMAX,PARAMS(185)), (SNDEL,PARAMS(186))
COMMON/PDVPF/AL,AD,ABS
DOUBLE PRECISION PI
DATA PI/3.14159265358979324D0/

C
C OPEN THE FILE
C CALL OPNFIL(PBDNUM,PBDNAM)
C
C COMPUTE THE NUMBER OF SNR CURVES
C
C NSN=(SNMAX-SNMIN)/SNDEL + 1
C
C STORE HEADER INFO
C WRITE(PBDNUM) SMPMIN,SNMIN,SNMAX,SNDEL,NSN
C
C AM = SMPMIN
C AL = DMIN1(9.D0,17.D0/DSQRT(AM))
C AD = .12D0/DSQRT(AM)
C BSA = -DSQRT(PI/2.D0)*AM + 6.D0*DSQRT(AM)
C ABS = DMIN1(0.D0,BSA)
C
C COMPUTE SNR VS PFA
C ALFA=0.D0
C CALL DIST(AM,ALFA,MF,X,Y)
C
C STORE THE SNR VS PD
C WRITE(PBDNUM) (Y(I),I=0,512)
C
C DO 1000 ISN=1,NSN
C SNR= SNMIN + SNDEL*(ISN-1)
C
C ALPHA = SNR
C CALL DIIST(AM,ALPHA,MF,X,Y)
C
C STORE THE SNR VS PD
C WRITE(PBDNUM) (Y(I),I=0,512)
C
1000 CONTINUE
2000 CONTINUE

RETURN
END

```

```

SUBROUTINE PRTSNR
IMPLICIT DOUBLE PRECISION (A-H,O-Z)
DIMENSION PFA(10),PD(10),V(14,8),SNR(14,8)
DATA PI/3.14159265358979324D0/
REAL SMPMIN,SMPMAX,SMPFCT,PARAMS
PARAMETER NUMPAR=200
COMMON/PARAMC/PARAMS(NUMPAR)
EQUIVALENCE
1 (SMPMIN,PARAMS(187)),(SMPMAX,PARAMS(188)),(SMPFCT,PARAMS
COMMON/PDPF/NPD,NPFA,PD,PFA

MMAX=ALOG10(SMPMAX/SMPMIN)/ALOG10(SMPFCT) + 1

F1=DSQRT(.5D0*PI)
F2=DSQRT(2.D0-.5D0*PI)
DO 1000 IM=1,MMAX
AM=SMPMIN*SMPFCT**(IM-1)
AL = DMIN1(9.D0,17.D0/DSQRT(AM))
AD = .12D0/DSQRT(AM)
BSA = -DSQRT(PI/2.D0)*AM + 6.D0*DSQRT(AM)
ABS = DMIN1(0.D0,BSA)
AMU=F1*AM
SIG=F2*DSQRT(AM)
DO 900 IPF=1,NPFA
PF=PFA(IPF)
IF( AM.GT. 1.D0 ) GO TO 250
VN=DSQRT(-2.*DLOG(PF))
GO TO 750
250 CALL FNIPHI(PF,YF)
V1=AMU-SIG*YF+ABS
IF( IPF.GT.1 ) V1=DMAX1(V1,VN)
V2=V1+.5D0
IF( V1.NE.VN ) GO TO 300
P1=PN
GO TO 325
300 CALL FNPFF(V1,AM,AL,AD,ABS,P1)
325 CALL FNPFF(V2,AM,AL,AD,ABS,P2)
IF( DABS(P1-PF).LT.DABS(P2-PF) ) GO TO 350
V0=V1
P0=P1
VN=V2
PN=P2
GO TO 400
350 V0=V2
P0=P2
VN=V1
PN=P1
400 CALL FNIPHI(P0,Y0)
GO TO 550
500 CALL FNPFF(VN,AM,AL,AD,ABS,PN)
550 CALL FNIPHI(PN,YN)
IF( DABS(PN-PF).LE.1D-9*PF ) GO TO 750
T=(V0*(YN-YF)+VN*(YF-Y0))/(YN-Y0)

```

```

      VO=VN
      YO=YN
      UN=T
      GO TO 500
750   V(IM,IPF)=VN
900   CONTINUE
1000  CONTINUE

      DD 4000 IPD=1,NPD

      CALL FNIPHI(PD(IPD),YD)
      DD 3000 IM=1,MMAX
      AM=SMPMIN*SMPFCT**(IM-1)
      AL = DMIN1(9.DO,17.DO/DSQRT(AM))
      AD = .12DO/DSQRT(AM)
      BSA = -DSQRT(PI/2.DO)*AM + 6.DO*DSQRT(AM)
      ABS = DMIN1(0.DO,BSA)
      DD 2900 IPF=1,NPFA
      PF=PFA(IPF)
      CALL RDC(AM,PF,PD(IPD),A1)
      A2=A1*1.01DO
      VV=V(IM,IPF)
      CALL FNPD(A1,VV,AM,AL,AD,ABS,P1)
      CALL FNPD(A2,VV,AM,AL,AD,ABS,P2)
      IF( DABS(P1-PD(IPD)).LT.DABS(P2-PD(IPD)) ) GO TO 2350
      A0=A1
      P0=P1
      AN=A2
      PN=P2
      GO TO 2400
2350  A0=A2
      P0=P2
      AN=A1
      PN=P1
2400  CALL FNIPHI(P0,Y0)
      GO TO 2550
2500  CALL FNPD(AN,VV,AM,AL,AD,ABS,PN)
2550  CALL FNIPHI(PN,YN)
      IF( DABS(PN-PD(IPD)).LE.1D-6*PD(IPD) ) GO TO 2750
      T=(A0*(YN-YD)+AN*(YD-Y0))/(YN-Y0)
      A0=AN
      YO=YN
      AN=T
      GO TO 2500
2750  SNR(IM,IPF)=10.*DLOG10(.5DO*AN*AN)
2900  CONTINUE
3000  CONTINUE

```

```
      DO 3200 IPF=1,NPFA
      PRINT 3001
3001  FORMAT(2(/))
      PRINT 3011, PD(IPD),PFA(IPF)
3011  FORMAT(2X,'PD =',F10.3,5X,'PFA =',D10.3)
      DO 3100 IM=1,MMAX
      M=SMPMIN*SMPFCT**(IM-1)
      PRINT 3021, M,SNR(IM,IPF)
3021  FORMAT(2X,'M =',I5,5X,'SNR =',F7.2)
3100  CONTINUE
3200  CONTINUE

4000  CONTINUE
```

```
      RETURN
      END
```

```
      SUBROUTINE CMPSVS
      IMPLICIT DOUBLE PRECISION (A-H,O-Z)
      PARAMETER MMAX=14
      PARAMETER NUMFIL=30, PBDNUM=18
      CHARACTER*6 FILES(NUMFIL)
      COMMON/FILEC/FILES
      CHARACTER*6 PBDNAM
      EQUIVALENCE (PBDNAM,FILES(18))
      DIMENSION PFA(10),PD(10),V(14,8),ALPHA(14,8)
      DIMENSION THRS(14,8)
      DATA PI/3.14159265358979324D0/
      COMMON/PDPF/NPD,NPFA,PD,PFA
```

```
      CALL OPNFIL(PBDNUM,PBDNAM)
```



```

F1=DSQRT(.5D0*PI)
F2=DSQRT(2.D0-.5D0*PI)
DO 1000 IM=1,MMAX
AM=2.** (IM-1)
AL = DMIN1(9.D0,17.D0/DSQRT(AM))
AD = .12D0/DSQRT(AM)
BSA = -DSQRT(PI/2.D0)*AM + 6.D0*DSQRT(AM)
ABS = DMIN1(0.D0,BSA)
AMU=F1*AM
SIG=F2*DSQRT(AM)
DO 900 IPF=1,8
PF=10.**(-DFLOTJ(IPF))
IF( AM.GT. 1.D0 ) GO TO 250
VN=DSQRT(-2.*DLOG(PF))
GO TO 750
250 CALL FNIPHI(PF,YF)
V1=AMU-SIG*YF+ABS
IF( IPF.GT.1 ) V1=DMAX1(V1,VN)
V2=V1+.5D0
IF( V1.NE.VN ) GO TO 300
P1=PN
GO TO 325
300 CALL FNPF(V1,AM,AL,AD,ABS,P1)
325 CALL FNPF(V2,AM,AL,AD,ABS,P2)
IF( DABS(P1-PF).LT.DABS(P2-PF) ) GO TO 350
V0=V1
P0=P1
VN=V2
PN=P2
GO TO 400
350 V0=V2
P0=P2
VN=V1
PN=P1
400 CALL FNIPHI(P0,Y0)
GO TO 550
500 CALL FNPF(VN,AM,AL,AD,ABS,PN)
550 CALL FNIPHI(PN,YN)
IF( DABS(PN-PF).LE.1D-9*PF ) GO TO 750
T=(V0*(YN-YF)+VN*(YF-Y0))/(YN-Y0)
V0=VN
Y0=YN
VN=T
GO TO 500
750 V(IM,IPF)=VN
THRS(IM,IPF)=(VN-ABS)/AM
900 CONTINUE
1000 CONTINUE

```

```

WRITE(PBDNUM)  NPD,(PD(I),I=1,10)
DO 4000 IPD=1,NPD

CALL FNIPHI(PD(IPD),YD)
DO 3000 IM=1,MMAX
AM=2.DO**(IM-1)
AL = DMIN1(9.DO,17.DO/DSQRT(AM))
AD = .12DO/DSQRT(AM)
BSA = -DSQRT(PI/2.DO)*AM + 6.DO*DSQRT(AM)
ABS = DMIN1(0.DO,BSA)
DO 2900 IPF=1,8
PF=10.DO**(-DFLOTJ(IPF))
CALL RDC(AM,PF,PD(IPD),A1)
A2=A1*1.01DO
VV=V(IM,IPF)
CALL FNPD(A1,VV,AM,AL,AD,ABS,P1)
CALL FNPD(A2,VV,AM,AL,AD,ABS,P2)
IF( DABS(P1-PD(IPD)).LT.DABS(P2-PD(IPD)) ) GO TO 2350
A0=A1
P0=P1
AN=A2
PN=P2
GO TO 2400
2350 A0=A2
P0=P2
AN=A1
PN=P1
2400 CALL FNIPHI(P0,Y0)
GO TO 2550
2500 CALL FNPD(AN,VV,AM,AL,AD,ABS,PN)
2550 CALL FNIPHI(PN,YN)
IF( DABS(PN-PD(IPD)).LE.1D-6*PD(IPD) ) GO TO 2750
T=(A0*(YN-YD)+AN*(YD-YO))/(YN-YO)
A0=AN
YO=YN
AN=T
GO TO 2500
2750 ALPHA(IM,IPF)=AN
2900 CONTINUE
3000 CONTINUE

WRITE(PBINUM) ((ALPHA(IM,IPF),IPF=1,8),IM=1,MMAX)

4000 CONTINUE

RETURN
END

```

\$

REFERENCES

1. G. H. Robertson, "Operating Characteristics for a Linear Detector of CW Signals in Narrowband Gaussian Noise," Bell System Technical Journal, pp. 755-774, April 1967.
2. A. D. Whalen, Detection of Signals in Noise, Academic Press, Inc., N.Y., 1971.
3. A. H. Nuttall, Accurate Efficient Evaluation of Cumulative or Exceedance Distributions Directly from Characteristic Functions, NUSC Technical Report 7023, 1 October 1983.
4. A. H. Nuttall, Exact Performance of General Second-Order Processors for Gaussian Inputs, NUSC Technical Report 7035, 15 October 1983.
5. I. S. Gradshteyn and I. M. Ryzhik, Table of Integrals, Series, and Products, Academic Press, Inc., 1980.
6. A. H. Nuttall, "Alternate Forms for Numerical Evaluation of Cumulative Probability Distributions Directly from Characteristic Functions," Proc. IEEE, Vol. 58, No. 11, pp. 1872-3, November 1970; also NUSC Report No. NL-3012, 12 August 1970.
7. W. Alberhseim, "A Closed-Form Approximation to Robertson's Detection Characteristics," Proc. IEEE, Vol. 69, No. 7, page 839, July 1981.

Resolution of Ambiguity For Randomly Moving Line Array

A. H. Nuttall

ABSTRACT

The generalized likelihood ratio detector, for deciding between the right-left ambiguity of a line array attempting to estimate the angle of arrival of a plane wave, is derived. Two scenarios are considered, the first with noisy measured antenna angle, the second with noiseless antenna angle measurements. The detector for both cases is a cross-correlator of the sample ac components of the measured antenna and source angle waveforms.

INTRODUCTION

A line array inherently has a cone of ambiguity in its response. When the array lies in the horizontal plane, and a source is located in that same plane, the ambiguity reduces to a right-left uncertainty, which cannot be resolved without some maneuvering on the part of the source or array. If the line array is moving randomly, unintentionally or uncontrollably, this movement can serve as a means of making a high quality decision about the source direction, if the array angle, as well as the source angle relative to the line array, are measured.

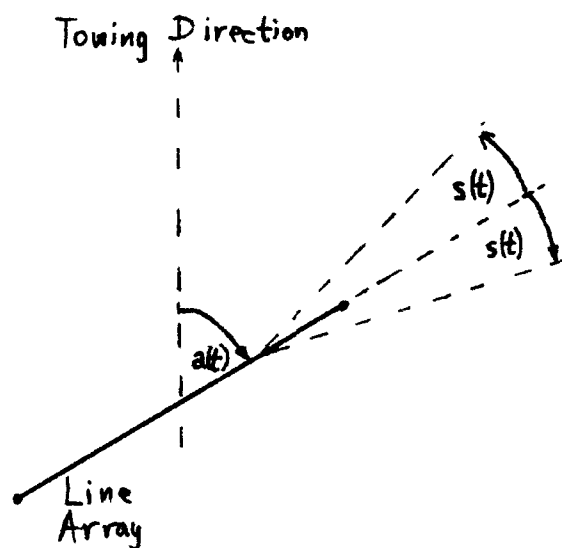


Figure 1. Geometry of Line Array and Source

The situation of interest here is described in figure 1. The line array is being towed due north; however, it is undergoing rigid bar rotation about this direction in a random manner, as described by random process $a(t)$, which is the actual antenna angle relative to the towing direction.

The actual source angle, relative to the line array end-fire direction, is $s(t)$. Furthermore, the actual source angle, relative to the towing direction, is θ , an unknown constant; it is presumed that θ is constant

throughout the observation interval. Reference to figure 1 reveals that these various quantities are interrelated according to the alternatives

$$\mathbf{e} = \left\{ \begin{array}{l} a(t) + s(t) \text{ for hypothesis 1, } H_1 \\ a(t) - s(t) \text{ for hypothesis 2, } H_2 \end{array} \right\} . \quad (1)$$

However, it is unknown which hypothesis is correct; nevertheless, it is desired to make a reliable decision, so that an accurate estimate of the source direction can be made. From (1), observe that we can express

$$s(t) = \left\{ \begin{array}{l} \mathbf{e} - a(t) \text{ for } H_1 \\ -\mathbf{e} + a(t) \text{ for } H_2 \end{array} \right\} , \quad (2)$$

which will be needed in later developments.

NOISY MEASURED ANTENNA ANGLE

In this section, the measured antenna angle is not $a(t)$ as desired, but rather is

$$x(t) = a(t) + m(t) , \quad (3)$$

where $m(t)$ is an unavoidable additive noise process. Also the measured source angle is not $s(t)$, but instead is

$$y(t) = s(t) + n(t) , \quad (4)$$

where $n(t)$ is likewise an undesirable additive perturbation, due to limited observation time, array length, ambient noise, etc. The three random processes $a(t)$, $m(t)$, $n(t)$ are presumed to be zero-mean Gaussian processes, independent of each other.

Combining (2)-(4), the situation is as follows: the available measurements upon which a decision must be reached are the two waveforms

$$\left. \begin{aligned} x(t) &= a(t) + m(t) \\ y(t) &= \theta - a(t) + n(t) \end{aligned} \right\} \text{for } H_1 , \quad (5A)$$

or

$$\left. \begin{aligned} x(t) &= a(t) + m(t) \\ y(t) &= -\theta + a(t) + n(t) \end{aligned} \right\} \text{for } H_2 . \quad (5B)$$

On the basis of waveforms $x(t)$ and $y(t)$, what is the best decision and what is the corresponding estimate of θ ?

Derivation of Generalized Likelihood Ratio

Let Δ be the time sampling increment applied to measurement waveforms $x(t)$ and $y(t)$; assume that the samples of the three processes are statistically independent at this rate. Denote

$$x_k = x(k\Delta) \text{ for } 1 \leq k \leq K, \quad (6)$$

$$y_k = y(k\Delta) \text{ for } 1 \leq k \leq K,$$

where $K\Delta$ is the total observation time, and let the collections of samples be denoted by

$$X = x_1, x_2, \dots, x_K, \quad Y = y_1, y_2, \dots, y_K, \quad A = a_1, a_2, \dots, a_K. \quad (7)$$

Then for a fixed A and a hypothesized value θ_h for the source angle, the conditional probability density function under H_1 , of the total set of measurements X, Y , is

$$p_1(X, Y | \theta_h, A) = \prod_{k=1}^K \left\{ \frac{1}{\sigma_m} \phi \left(\frac{x_k - a_k}{\sigma_m} \right) \frac{1}{\sigma_n} \phi \left(\frac{y_k - \theta_h + a_k}{\sigma_n} \right) \right\}, \quad (8)$$

where the normalized Gaussian probability density function is

$$\phi(t) = (2\pi)^{-1/2} \exp(-t^2/2). \quad (9)$$

Here we used (5A) and the Gaussian character of processes $m(t)$ and $n(t)$ with standard deviations σ_m and σ_n respectively.

We now must weight (8) by the Gaussian probability density function for process $a(t)$ and integrate over A , to determine the unconditional probability density function of X, Y , for hypothesized value θ_h . Carrying out the integrals and simplifying the result, we obtain

$$p_1(X, Y|\theta_h) = \left(2\pi\sigma_a\sigma_m\sigma_n R_3^{1/2}\right)^{-K} * \exp\left[-\frac{R_{an}}{2R_3\sigma_m^2} \sum_k x_k^2 - \frac{R_{am}}{2R_3\sigma_n^2} \sum_k (y_k - \theta_h)^2 - \frac{1}{R_3\sigma_m^2\sigma_n^2} \sum_k x_k (y_k - \theta_h)\right], \quad (10)$$

where we define

$$R_{am} = \frac{1}{\sigma_a^2} + \frac{1}{\sigma_m^2}, \quad R_{an} = \frac{1}{\sigma_a^2} + \frac{1}{\sigma_n^2}, \quad R_3 = \frac{1}{\sigma_a^2} + \frac{1}{\sigma_m^2} + \frac{1}{\sigma_n^2}, \quad (11)$$

and use the shorthand notation

$$\sum_k = \sum_{k=1}^K. \quad (12)$$

In a similar fashion, the unconditional probability density function of X, Y under H₂, for hypothesized value θ_h, is given by

$$p_2(X, Y|\theta_h) = \left(2\pi\sigma_a\sigma_m\sigma_n R_3^{1/2}\right)^{-K} * \exp\left[-\frac{R_{an}}{2R_3\sigma_m^2} \sum_k x_k^2 - \frac{R_{am}}{2R_3\sigma_n^2} \sum_k (y_k + \theta_h)^2 + \frac{1}{R_3\sigma_m^2\sigma_n^2} \sum_k x_k (y_k + \theta_h)\right]. \quad (13)$$

Now if θ_h were known, we could evaluate the likelihood ratio by taking the ratio of (10) and (13). However, we must resort instead to a generalized likelihood ratio, by computing the two values of θ_h that maximize (10) and (13) respectively, and then taking the ratio of the two maxima [1, p. 92]. This procedure is not optimum in any sense; however, it often leads to physical processors that perform well.

The values of θ_h that maximize (10) and (13) are given respectively by

$$\theta_1 = \frac{1}{K} \sum_k y_k + \frac{\sigma_a^2}{\sigma_a^2 + \sigma_m^2} \frac{1}{K} \sum_k x_k \quad \text{for } H_1, \quad (14A)$$

$$\theta_2 = -\frac{1}{K} \sum_k y_k + \frac{\sigma_a^2}{\sigma_a^2 + \sigma_m^2} \frac{1}{K} \sum_k x_k \quad \text{for } H_2, \quad (14B)$$

These results have a reasonable physical interpretation: From (5A), the sum $x(t) + y(t)$ would eliminate the random process $a(t)$, and the sample mean of the sum would give an estimate of θ under H_1 . However, $m(t)$ contaminates the $a(t)$ contribution according to (3); thus the scale factor $\sigma_a^2/(\sigma_a^2 + \sigma_m^2)$ in (14A) indicates how trustworthy the sample mean of $x(t)$ is. The noise $n(t)$ in $y(t)$ is unavoidable but is partially suppressed by the inherent averaging of the sample mean of $y(t)$. A similar argument holds for $x(t) - y(t)$ under H_2 .

The logarithm of the generalized likelihood ratio is (proportional to)

$$\begin{aligned} T &= \frac{1}{2} R_3 \sigma_m^2 \sigma_n^2 \ln \frac{p_2(x, y | \theta_2)}{p_1(x, y | \theta_1)} = \\ &= -\frac{1}{4} R_{am} \sigma_m^2 \sum_k (y_k + \theta_2)^2 + \frac{1}{2} \sum_k x_k (y_k + \theta_2) + \\ &+ \frac{1}{4} R_{am} \sigma_m^2 \sum_k (y_k - \theta_1)^2 + \frac{1}{2} \sum_k x_k (y_k - \theta_1), \end{aligned} \quad (15)$$

where we used (10) and (13) with θ_1 and θ_2 substituted for θ_h . Now let

$$S_x = \sum_k x_k, \quad S_y = \sum_k y_k, \quad P = \sum_k x_k y_k. \quad (16)$$

Then (15) becomes, upon use of (14) and simplification and cancellation of various terms,

$$\begin{aligned}
 T &= P - \frac{1}{K} S_x S_y = \\
 &= \sum_k x_k y_k - \frac{1}{K} \sum_m x_m \sum_n y_n =
 \end{aligned}
 \tag{17A}$$

$$= \sum_k \tilde{x}_k \tilde{y}_k ,
 \tag{17B}$$

where

$$\begin{aligned}
 \tilde{x}_k &= x_k - \frac{1}{K} \sum_m x_m \quad \text{for } 1 \leq k \leq K , \\
 \tilde{y}_k &= y_k - \frac{1}{K} \sum_n y_n \quad \text{for } 1 \leq k \leq K ,
 \end{aligned}
 \tag{18}$$

are defined as the sample ac components of measurements X and Y; that is, the sample means are subtracted from the measurements.

The generalized likelihood ratio test in (17) says to cross-correlate the sample ac components of both measured waveforms and to compare with zero (assuming H_1 and H_2 are equally likely a priori). That is, the test is

$$T = \sum_{k=1}^K \tilde{x}_k \tilde{y}_k \underset{H_1}{\overset{H_2}{\gtrless}} 0 .
 \tag{19}$$

Observe that this decision rule makes no use of the variances of any of the processes $a(t)$, $m(t)$, $n(t)$, although this information was presumed known in the above derivation. Of course, the source angle estimates in (14) do require knowledge of the signal-to-noise ratio σ_a^2/σ_m^2 in the $x(t)$ measurement of the antenna angle $a(t)$. Once the decision of H_1 vs H_2 is made via (19), the corresponding estimate of the actual source angle θ is taken from (14).

On the Performance of Test (19)

From (5) and (6), we find that

$$\overline{x_k y_k} = \left\{ \begin{array}{ll} -\sigma_a^2 & \text{for } H_1 \\ \sigma_a^2 & \text{for } H_2 \end{array} \right\},$$

$$\overline{x_m y_n} = 0 \text{ for } m \neq n. \quad (20)$$

Then (17A) yields the mean value of the generalized likelihood ratio test statistic as

$$T = \left\{ \begin{array}{ll} -(K-1) \sigma_a^2 & \text{for } H_1 \\ (K-1) \sigma_a^2 & \text{for } H_2 \end{array} \right\}. \quad (21)$$

Since the statistics of T are desired different under the two hypotheses, (21) indicates that large K and σ_a^2 are desired. That is, a large observation time and a widely-moving antenna give better performance of the test; both of these conclusions are physically plausible.

Although generalized likelihood ratio test (19) does not require knowledge of any variances, the performance (in terms of the error probability) does depend on all the variances. However, the performance does not depend on the actual value θ of the source angle. To see this, we employ (5) in (18) to obtain

$$\tilde{y}_k = \left\{ \begin{array}{ll} -a_k + n_k - (-S_a + S_n)/K & \text{for } H_1 \\ a_k + n_k - (S_a + S_n)/K & \text{for } H_2 \end{array} \right\}, \quad (22)$$

where

$$S_a = \sum_k a_k, \quad S_n = \sum_k n_k. \quad (23)$$

Thus θ is absent from (22), and since θ is not involved in $x(t)$ or x_k , test statistic T is independent of θ .

If we develop (19) in more detail and make use of (18) and (5), we find we can express

$$T_1 = - \left[\sum_k (a_k + m_k)(a_k - n_k) - \frac{1}{K} \sum_k (a_k + m_k) \sum_k (a_k - n_k) \right] \text{ for } H_1,$$

$$T_2 = \left[\sum_k (a_k + m_k)(a_k + n_k) - \frac{1}{K} \sum_k (a_k + m_k) \sum_k (a_k + n_k) \right] \text{ for } H_2. \quad (24)$$

Thus the statistics of T_1 are identical to those of $-T_2$.

Based upon the results in [2,3], an exact analysis of the cumulative and exceedance distribution functions of test statistic (17A) is possible and will be documented in a NUSC technical report shortly; in fact, a more general processor, where the sample means term is scaled prior to subtraction, will be analyzed.

NOISELESS MEASURED ANTENNA ANGLE

In this section, the noise $m(t)$ in the antenna angle measurement is zero; thus, from (3),

$$x(t) = a(t) \quad (25)$$

under H_1 and H_2 . We also remove the Gaussian assumption on the statistics of antenna movement $a(t)$, and allow $a(t)$ to be completely general. Furthermore, we allow any statistical dependence among the samples A of $a(t)$ in (7). However, we retain the Gaussian assumption on the additive noise process $n(t)$ in (4) and (5), and keep the statistical independence of its samples $\{n(k\Delta)\}_1^K$.

Derivation of Generalized Likelihood Ratio

Based upon these premises, the conditional probability density function under H_1 of measurements X, Y , for a fixed A and hypothesized θ_h , is

$$p_1(X, Y | \theta_h, A) = \prod_{k=1}^K \left\{ \delta(x_k - a_k) \frac{1}{\sigma_n} \phi \left(\frac{y_k - \theta_h + a_k}{\sigma_n} \right) \right\}. \quad (26)$$

(This is also the limit of (8) as $\sigma_m \rightarrow 0^+$.) Then letting joint probability density function $p_a(A)$ represent the arbitrary statistical dependence of samples A , the unconditional probability density function under H_1 of X, Y is

$$\begin{aligned} p_1(X, Y | \theta_h) &= \int dA p_a(A) p_1(X, Y | \theta_h, A) = \\ &= (\sqrt{2\pi} \sigma_n)^{-K} \exp \left[-\frac{1}{2\sigma_n^2} \sum_k (y_k - \theta_h + x_k)^2 \right] p_a(X), \end{aligned} \quad (27)$$

using (26), (9), and the sifting property of delta functions. (If measurement noise $m(t)$ in (3) were non-zero, this simplification of the probability density function in (27) would not be possible.)

The value of θ_h that maximizes probability density function (27), regardless of the form of the probability density function p_a , is

$$\theta_1 = \frac{1}{K} \sum_k (x_k + y_k) , \quad (28)$$

which is simply the sample mean of the sum waveform $x(t) + y(t)$. This result is consistent with the earlier one in (14A), for $\sigma_m = 0$, and the ensuing discussion.

In a similar fashion, the probability density function of X, Y under H_2 is

$$p_2(X, Y | \theta_h) = (\sqrt{2\pi} \sigma_n)^{-K} \exp \left[-\frac{1}{2\sigma_n^2} \sum_k (y_k + \theta_h - x_k)^2 \right] p_a(X) , \quad (29)$$

and the maximizing choice of θ_h is

$$\theta_2 = \frac{1}{K} \sum_k (x_k - y_k) , \quad (30)$$

which is the sample mean of difference waveform $x(t) - y(t)$.

There follows, from (27)-(30), the logarithm of the generalized likelihood ratio as

$$2\sigma_n^2 \ln \frac{p_2(X, Y | \theta_2)}{p_1(X, Y | \theta_1)} = -\sum_k (y_k + \theta_2 - x_k)^2 + \sum_k (y_k - \theta_1 + x_k)^2 . \quad (31)$$

The generalized likelihood ratio test for the two hypotheses in (1) is therefore

$$\sum_k (x_k + y_k - \theta_1)^2 \underset{H_1}{\overset{H_2}{>}} \sum_k (x_k - y_k - \theta_2)^2, \quad (32)$$

or upon substitution of (28) and (30), and use of (18), simply

$$\sum_k \tilde{x}_k \tilde{y}_k \underset{H_1}{\overset{H_2}{>}} 0. \quad (33)$$

As in the previous section, the cross-correlation of the sample ac components of the measurements X, Y should be compared with zero. This decision rule holds for any statistics of antenna movement $a(t)$.

The alternative form in (32) has an interesting interpretation: Reference to (27)-(28) reveals that θ_1 is the best constant fit to $\{x_k + y_k\}_1^K$ in a least squares sense. Thus the left side of (32) is the actual value of the least squares error of a constant fit to the sum waveform. Similarly, the right side of (32) is the least squares error of a constant fit to the difference waveform. Whichever error is smaller, that hypothesis is selected. This decision rule, (32), is consistent with the observation from (5) and (25) that

$$\begin{aligned} x(t) + y(t) &= \theta + n(t) \quad \text{under } H_1, \\ x(t) - y(t) &= \theta - n(t) \quad \text{under } H_2. \end{aligned} \quad (34)$$

That is, except for zero-mean measurement noise $n(t)$, the sum waveform is constant under H_1 , whereas the difference waveform is constant under H_2 .

An alternative form for (32) and (33) is

$$T = \sum_k x_k y_k - \frac{1}{K} \sum_m x_m \sum_n y_n \begin{matrix} H_2 \\ \gtrsim \\ H_1 \end{matrix} 0, \quad (35)$$

just as in (17A). All the ensuing discussion there through (24) is directly relevant for this case as well.

SUMMARY

The generalized likelihood ratio test statistic, for both the noisy as well as the noiseless antenna angle measurement, is a cross-correlator of the sample ac components of the measured antenna and source angle waveforms. Exact performance of this processor can be accomplished, since the test statistic is a quadratic form of correlated Gaussian random variables; in fact, the complete cumulative and exceedance distribution functions of the quantity

$$\sum_{k=1}^K x_k y_k - \frac{\gamma}{K} \sum_{m=1}^K x_m \sum_{n=1}^K y_n, \quad (36)$$

for any scaling γ , is capable of exact analysis and will be presented in a future NUSC technical report.

REFERENCES

1. H. L. Van Trees, Detection, Estimation, and Modulation Theory, Part I, J. Wiley and Sons, Inc., N.Y., 1968.
2. A. H. Nuttall, "Accurate Efficient Evaluation of Cumulative or Exceedance Probability Distributions Directly from Characteristic Functions", NUSC Technical Report 7023, 1 October 1983.
3. A. H. Nuttall, "Exact Performance of General Second-Order Processors for Gaussian Inputs", NUSC Technical Report 7035, 15 October 1983.

Operating Characteristics of Crosscorrelator With or Without Sample Mean Removal

A. H. Nuttall

ABSTRACT

The characteristic function of the output of a crosscorrelator, with the sample means removed from each channel, is derived in closed form. More generally, if scaled versions of the sample means are subtracted prior to multiplication of the channel inputs and summation, a closed form for the characteristic function of the correlator output is derived. These results are used to plot the exact operating characteristics of the crosscorrelator, as functions of the threshold, the general scaling factors applied to the sample means, the number of terms, N , summed to yield the output, the actual means at the inputs, and the signal-to-noise ratios of the random signal components at each of the system inputs. Programs for the various cases considered are documented and exercised. Comparisons are made with a Gaussian approximation, which can be used to extend the results to larger values of N than considered here, if needed. Asymptotic results for the exceedance distribution functions also have been derived, but they are not too useful for large N .

TABLE OF CONTENTS

	PAGE
LIST OF ILLUSTRATIONS	iii
LIST OF SYMBOLS	vii
INTRODUCTION	1
PROBLEM DEFINITION	3
Input Statistics	3
A Signal and Noise Model	3
Crosscorrelator Output	5
CHARACTERISTIC FUNCTION OF CROSSCORRELATOR OUTPUT	7
Derivation	7
Cumulants of Correlator Output	10
Special Case of $\gamma=1$, Sample Mean Removal	10
Special Case of $\gamma=0$, Sample Mean Not Removed	11
Interrelationship of Two Special Cases	12
Specialization to the Signal and Noise Model	12
ANALYTIC RESULTS FOR $\gamma=1$, SAMPLE MEAN REMOVAL	15
General Probability Results	15
Possible Normalization of q	17
Specialization to the Signal and Noise Model	18
Reduction to Identical Signal Components	19
General Distribution Integrals	22
Distributions for $N=2$	22
Distributions for $N=3$	24
Distributions for $N=4$	24
Distributions for $N=5$	25
GRAPHICAL RESULTS FOR $\gamma=1$, SAMPLE MEAN REMOVAL	27
Summary of Particular Case Considered	27
Operating Characteristics for $\gamma=1$	28
Gaussian Approximation	29
ANALYTIC RESULTS FOR $\gamma=0$, SAMPLE MEAN NOT REMOVED	33
Specialization to the Signal and Noise Model	33
Normalized Crosscorrelator Output	34
Reduction to Identical Signal Components	35

TABLE OF CONTENTS (Cont'd)

	PAGE
Asymptotic Behavior of Cumulative and Exceedance Distribution Functions	37
Distributions for $N=1$	38
Distributions for $N=2$	38
Distributions for $N=4$	40
GRAPHICAL RESULTS FOR $\gamma=0$, SAMPLE MEAN NOT REMOVED	45
Summary of Particular Case Considered	45
Operating Characteristics for $\gamma=0$	45
Gaussian Approximation	46
SUMMARY	49
APPENDICES	
A. CORRELATOR OUTPUT INDEPENDENCE OF MEANS	A-1
B. A USEFUL INTEGRAL OF EXPONENTIALS OF MATRIX FORMS	B-1
C. PROGRAM FOR CUMULATIVE AND EXCEEDANCE DISTRIBUTION FUNCTIONS VIA CHARACTERISTIC FUNCTION (23)-(24)	C-1
D. PROGRAM FOR EVALUATION OF OPERATING CHARACTERISTICS FOR $\gamma=1$	D-1
E. ASYMPTOTIC EXPANSIONS FOR DISTRIBUTIONS WHEN $r>0$	E-1
F. EXCEEDANCE DISTRIBUTION FUNCTION FOR $\gamma=0$, $N=1$, $r>0$	F-1
G. PROGRAM FOR EVALUATION OF OPERATING CHARACTERISTICS FOR $\gamma=0$	G-1
REFERENCES	R-1

LIST OF ILLUSTRATIONS

FIGURE	PAGE
1. Operating Characteristics for Crosscorrelator with Sample Mean Removal, N=2	51
2. Operating Characteristics for Crosscorrelator with Sample Mean Removal, N=3	52
3. Operating Characteristics for Crosscorrelator with Sample Mean Removal, N=4	53
4. Operating Characteristics for Crosscorrelator with Sample Mean Removal, N=6	54
5. Operating Characteristics for Crosscorrelator with Sample Mean Removal, N=8	55
6. Operating Characteristics for Crosscorrelator with Sample Mean Removal, N=12	56
7. Operating Characteristics for Crosscorrelator with Sample Mean Removal, N=16	57
8. Operating Characteristics for Crosscorrelator with Sample Mean Removal, N=24	58
9. Operating Characteristics for Crosscorrelator with Sample Mean Removal, N=32	59
10. Operating Characteristics for Crosscorrelator with Sample Mean Removal, N=48	60
11. Operating Characteristics for Crosscorrelator with Sample Mean Removal, N=64	61
12. Operating Characteristics for Crosscorrelator with Sample Mean Removal, N=96	62
13. Operating Characteristics for Crosscorrelator with Sample Mean Removal, N=128	63
14. Operating Characteristics for Crosscorrelator with Sample Mean Removal, N=256	64
15. Operating Characteristics for Crosscorrelator without Sample Mean Removal, N=1, r=1	65
16. Operating Characteristics for Crosscorrelator without Sample Mean Removal, N=1, r=2	66

LIST OF ILLUSTRATIONS (Cont'd)

FIGURE	PAGE
17. Operating Characteristics for Crosscorrelator without Sample Mean Removal, $N=2$, $r=1$	67
18. Operating Characteristics for Crosscorrelator without Sample Mean Removal, $N=2$, $r=2$	68
19. Operating Characteristics for Crosscorrelator without Sample Mean Removal, $N=2$, $r=4$	69
20. Operating Characteristics for Crosscorrelator without Sample Mean Removal, $N=3$, $r=1$	70
21. Operating Characteristics for Crosscorrelator without Sample Mean Removal, $N=3$, $r=2$	71
22. Operating Characteristics for Crosscorrelator without Sample Mean Removal, $N=4$, $r=1$	72
23. Operating Characteristics for Crosscorrelator without Sample Mean Removal, $N=4$, $r=2$	73
24. Operating Characteristics for Crosscorrelator without Sample Mean Removal, $N=8$, $r=1$	74
25. Operating Characteristics for Crosscorrelator without Sample Mean Removal, $N=8$, $r=2$	75
26. Operating Characteristics for Crosscorrelator without Sample Mean Removal, $N=16$, $r=1$	76
27. Operating Characteristics for Crosscorrelator without Sample Mean Removal, $N=16$, $r=2$	77
28. Operating Characteristics for Crosscorrelator without Sample Mean Removal, $N=32$, $r=1$	78
29. Operating Characteristics for Crosscorrelator without Sample Mean Removal, $N=32$, $r=2$	79
30. Operating Characteristics for Crosscorrelator without Sample Mean Removal, $N=64$, $r=1$	80
31. Operating Characteristics for Crosscorrelator without Sample Mean Removal, $N=64$, $r=2$	81
32. Operating Characteristics for Crosscorrelator without Sample Mean Removal, $N=128$, $r=1$	82

LIST OF ILLUSTRATIONS (Cont'd)

FIGURE	PAGE
33. Operating Characteristics for Crosscorrelator without Sample Mean Removal, $N=128$, $r=2$	83
34. Operating Characteristics for Crosscorrelator without Sample Mean Removal, $N=256$, $r=1$	84
35. Operating Characteristics for Crosscorrelator without Sample Mean Removal, $N=256$, $r=2$	85
C-1. Cumulative and Exceedance Distribution Functions	C-4
E-1. Contours of Integration for Cumulative Distribution Function	E-2
E-2. Contours of Integration for Exceedance Distribution Function	E-3
F-1. Equivalent Contours for (F-1)	F-1
F-2. Equivalent Contours for (F-9)	F-4
F-3. Regions of Integration	F-10

LIST OF SYMBOLS

N	Number of terms summed to yield crosscorrelator output
u_n, v_n	Two channel inputs at sample time n
overbar	Statistical average
μ_u, μ_v	Means in two input channels
σ_u, σ_v	Standard deviations in two input channels
ρ	Correlation coefficient between two input channels
$u_s(n), v_s(n)$	Random signal components at inputs
$u_d(n), v_d(n)$	Random noise disturbances at inputs
S_u, S_v	Powers of random signal components
ρ_s	Correlation coefficient between signal components
D_u, D_v	Powers of random noise disturbances
R_u, R_v	Signal-to-noise ratios of random components of two input channels, (8)
\tilde{u}_n, \tilde{v}_n	Sample ac components of inputs
q_n	Crosscorrelator output, (12)
α, β	Scale factors applied to sample means
γ	Scale factor utilized in crosscorrelator output, (12)
U, V	Column matrices of two channel inputs
Q	$N \times N$ matrix, (16)
1	Column matrix of ones, (17)
$p_q(u)$	Probability density function of random variable q and argument u
$f_q(\xi)$	Characteristic function of random variable q and argument ξ
det	Determinant
$E_1, E_2, F_1, F_2, G_1, G_2$	Parameters of characteristic function, (24)
$\chi_q(n)$	n -th cumulant of random variable q
μ_q, σ_q	Mean and standard deviation of q
$I_\nu(z)$	Modified Bessel function of first kind
$K_\nu(z)$	Modified Bessel function of second kind
$P_q(u)$	Cumulative distribution function of q
$1 - P_q(u)$	Exceedance distribution function of q
h	Normalized crosscorrelator output, (49), (94)
R	Signal-to-noise ratio for identical signal components, (56A), (78)

LIST OF SYMBOLS (Cont'd)

C_+, C_-	Contours for determining cumulative and exceedance distribution functions, (63), (64)
P_F, P_D	False alarm and detection probabilities
ϕ	Normalized Gaussian probability density function, (84)
Φ	Normalized Gaussian cumulative distribution function, (84)
Φ_x^{-1}	Inverse Φ function
m_k, σ_k	Mean and standard deviation under hypothesis k, (86), (128)
r_u, r_v	Normalized means in two channels, (97)
r	Common normalized mean, (99), (124)
w	Auxiliary variable equal to $1+2R$, (102)
$U(u)$	Unit step function, (109)
$Q(a,b)$	Q-function of Marcum
$Q_M(a,b)$	Q_M -function, ref. 8
$q_M(u), \tilde{q}_M(u)$	Auxiliary functions, (115)

OPERATING CHARACTERISTICS OF CROSSCORRELATOR
WITH OR WITHOUT SAMPLE MEAN REMOVAL

INTRODUCTION

The detection of weak signals in two channels is often accomplished by crosscorrelating the two waveforms and comparing with a threshold. For the case where a large number of independent products are added to yield the correlator output, the central limit theorem is often employed, with questionable validity for low false alarm probabilities, i.e. large thresholds. Also, this approximation may not be valid for intermediate numbers of terms added.

Here we wish to get exact operating characteristics for the crosscorrelator, namely detection probability vs. false alarm probability, even for probabilities as low as $1E-10$. In particular, we desire results for an arbitrary number of products summed, for any degree of correlation between corresponding individual samples of the two channel inputs, and for any input signal and noise power levels.

Furthermore, it sometimes happens that the two input channels contain dc components, which can be considered either desirable or otherwise, depending on the application. Here we will consider these dc components as nuisance terms and will subtract them out prior to crosscorrelation. More precisely, since the actual values of the dc components in each channel will generally be unknown, we will estimate them via the sample means (over the available record lengths) and subtract these estimates from the available data. This subtraction feature creates new random variables, all of which are statistically dependent on each other, and thereby significantly complicates the analysis. Nevertheless, this crosscorrelation of the sample ac components of the input channels is encountered in practical situations, and in one recent study [1], it was in fact the generalized likelihood ratio detector under two different realistic scenarios. Accordingly, it merits study and accurate quantitative evaluation of performance capability.

More generally, we consider subtraction of scaled versions of the sample means of each channel prior to multiplication and summation. Then as special cases, we can investigate the crosscorrelator with or without sample mean removal, or any intermediate case of interest.

The major analytical result here is a closed form for the characteristic function of the correlator output, in the most compact form involving only two rooting operations and one exponential. Although this processor could be analyzed by the general method given in [2], in terms of the eigenvalues and eigenvectors of a correlation matrix, it would be less accurate and considerably more time consuming, even with computer aid, especially for a large number of terms summed. The actual numerical procedure adopted here for proceeding from the characteristic function to the exceedance distribution functions (false alarm and detection probabilities) is that given in [3], and utilized to advantage in [2,3,4].

PROBLEM DEFINITION

INPUT STATISTICS

The two channel inputs to the crosscorrelator are synchronously sampled in time, yielding random variables $\{u_n\}_1^N$ and $\{v_n\}_1^N$, where N is the total number of data samples taken in each channel. These random variables are Gaussian with the following statistics:

$$\left. \begin{array}{l} \text{means} \quad \overline{u_n} = \mu_u, \quad \overline{v_n} = \mu_v, \\ \text{variances} \quad \overline{(u_n - \overline{u_n})^2} = \sigma_u^2, \quad \overline{(v_n - \overline{v_n})^2} = \sigma_v^2, \\ \text{covariances} \quad \overline{(u_n - \overline{u_n})(v_n - \overline{v_n})} = \rho \sigma_u \sigma_v, \end{array} \right\} \begin{array}{l} \text{all} \\ \text{independent} \\ \text{of } n. \end{array} \quad (1)$$

(An overbar denotes a statistical average.) That is, the means and variances in each channel, although different, do not change with time, and the degree of correlation between channels is constant. Also

$$\left. \begin{array}{l} u_m \text{ is statistically independent of } u_n \text{ if } m \neq n, \\ v_m \text{ is statistically independent of } v_n \text{ if } m \neq n, \\ u_m \text{ is statistically independent of } v_n \text{ if } m \neq n. \end{array} \right\} \quad (2)$$

However, u_n and v_n are statistically dependent on each other, for all n , to the extent ρ indicated in (1).

A SIGNAL AND NOISE MODEL

To better fix the mathematical definitions above, consider in this subsection the following possible signal and noise model:

$$\left. \begin{array}{l} u_n = \mu_u + u_s(n) + u_d(n) \\ v_n = \mu_v + v_s(n) + v_d(n) \end{array} \right\} \quad \text{for } 1 \leq n \leq N, \quad (3)$$

where random signal components $u_s(n)$, $v_s(n)$ are zero-mean and partially correlated with each other:

$$\left. \begin{aligned} \overline{u_s(n)} &= 0, \quad \overline{v_s(n)} = 0, \\ \overline{u_s^2(n)} &= S_u, \quad \overline{v_s^2(n)} = S_v, \quad \overline{u_s(n) v_s(n)} = \rho_s (S_u S_v)^{1/2} \end{aligned} \right\} \text{for all } n. \quad (4)$$

Thus S_u , S_v are the powers of the random signal components in each channel.

Also, the random noise disturbances $u_d(n)$, $v_d(n)$ in (3) are zero-mean and independent of each other:

$$\left. \begin{aligned} \overline{u_d(n)} &= 0, \quad \overline{v_d(n)} = 0, \\ \overline{u_d^2(n)} &= D_u, \quad \overline{v_d^2(n)} = D_v, \quad \overline{u_d(n) v_d(n)} = 0 \end{aligned} \right\} \text{for all } n. \quad (5)$$

Thus D_u , D_v are the powers of the random noise disturbances in each channel. Finally, except for the statistical dependencies indicated in (4) between $u_s(n)$ and $v_s(n)$, all the $4N$ random components in (3) are independent of each other.

For this particular signal and noise model in (3)-(5), the master parameters in (1) take the special form

$$\sigma_u^2 = S_u + D_u, \quad \sigma_v^2 = S_v + D_v, \quad \rho_{\sigma_u \sigma_v} = \rho_s (S_u S_v)^{1/2}, \quad (6)$$

from which there follows

$$\rho = \rho_s \left(\frac{R_u}{1+R_u} \frac{R_v}{1+R_v} \right)^{1/2}, \quad (7)$$

where the signal-to-noise ratios (per sample) of the random components in (3) have been defined as

$$R_u = \frac{S_u}{D_u} = \frac{\overline{u_s^2(n)}}{\overline{u_d^2(n)}}, \quad R_v = \frac{S_v}{D_v} = \frac{\overline{v_s^2(n)}}{\overline{v_d^2(n)}} \quad \text{for all } n. \quad (8)$$

Thus the parameters σ_u , σ_v , ρ in (1) depend only on the statistics of the random components in model (3), and not on the dc components μ_u and μ_v . Observe that even if $\rho_s=1$ and $R_u=\infty$, ρ would still be less than 1; the one noisy channel prevents full correlation between inputs.

CROSSCORRELATOR OUTPUT

We define the sample ac components of each channel of the crosscorrelator as

$$\left. \begin{aligned} \tilde{u}_n &= u_n - \frac{1}{N} \sum_{m=1}^N u_m \\ \tilde{v}_n &= v_n - \frac{1}{N} \sum_{m=1}^N v_m \end{aligned} \right\} \text{for } 1 \leq n \leq N, \quad (9)$$

where we have subtracted the corresponding sample means from each and every data sample. Thus $\{\tilde{u}_n\}_1^N$ and $\{\tilde{v}_n\}_1^N$ have zero-means and have statistics completely independent of the unknown actual values of input means μ_u , μ_v . However, in trade, we now must deal with a new set of $2N$ random variables, all of which are statistically dependent on each other; this is the feature which complicates the ensuing analysis. The test statistic (decision variable) of interest is the crosscorrelator output after sample mean removal,

$$q = \sum_{n=1}^N \tilde{u}_n \tilde{v}_n = \sum_{n=1}^N u_n v_n - \frac{1}{N} \sum_{m=1}^N u_m \sum_{n=1}^N v_n, \quad (10)$$

which is independent of the actual unknown values of input means μ_U and μ_V . If we knew the input means, we could subtract them directly and not have to resort to sample means.

More generally, we consider the modified channel components

$$\left. \begin{aligned} \tilde{u}_n &= u_n - \frac{\alpha}{N} \sum_{m=1}^N u_m \\ \tilde{v}_n &= v_n - \frac{\beta}{N} \sum_{m=1}^N v_m \end{aligned} \right\} \text{for } 1 \leq n \leq N \quad (11)$$

and the crosscorrelator output

$$q = \sum_{n=1}^N \tilde{u}_n \tilde{v}_n = \sum_{n=1}^N u_n v_n - \frac{\gamma}{N} \sum_{m=1}^N u_m \sum_{n=1}^N v_n, \quad (12)$$

instead of (9) and (10). Scale factors α and/or β in (11) may be unequal to 1; the final parameter γ in (12) is given by

$$\gamma = \alpha + \beta - \alpha\beta = 1 - (\alpha-1)(\beta-1). \quad (13)$$

The case of $\gamma=0$ in (12) obviously corresponds to the case of no sample mean removal. On the other hand, if either* $\alpha=1$ or $\beta=1$, then $\gamma=1$, and we have removal of the sample mean; i.e., (12) reduces to (10). We shall be interested here in the analysis of the general case represented by (12), for arbitrary γ .

* It is demonstrated in appendix A that if scale factor $\alpha=1$ but $\beta \neq 1$, correlator output q is completely independent of μ_U , μ_V , β .

CHARACTERISTIC FUNCTION OF CROSSCORRELATOR OUTPUT

DERIVATION

We express the collection of random variables in (1) and (2) in column matrix form according to

$$U = [u_1 \ u_2 \ \dots \ u_N]^T, \quad V = [v_1 \ v_2 \ \dots \ v_N]^T, \quad (14)$$

where superscript T denotes transpose. The crosscorrelator output q in (12) can then be written as quadratic form

$$q = U^T Q V, \quad (15)$$

where: NxN matrix

$$Q = I - \frac{\gamma}{N} \mathbf{1} \mathbf{1}^T, \quad (16)$$

I is the NxN identity matrix, and

$$\mathbf{1} = [1 \ 1 \ \dots \ 1]^T \quad (17)$$

is a Nx1 column matrix of ones.

Since U and V are Gaussian, their joint probability density function is, in terms of the parameters in (1),

$$p(U, V) = \left[2\pi\sigma_U\sigma_V(1-\rho^2) \right]^{1/2} \exp \left[-\frac{1}{2(1-\rho^2)} * \right. \\ \left. * \left\{ \frac{1}{\sigma_U^2} (U - \mu_U \mathbf{1})^T (U - \mu_U \mathbf{1}) + \frac{1}{\sigma_V^2} (V - \mu_V \mathbf{1})^T (V - \mu_V \mathbf{1}) - \frac{2\rho}{\sigma_U\sigma_V} (U - \mu_U \mathbf{1})^T (V - \mu_V \mathbf{1}) \right\} \right] \quad (18)$$

The characteristic function of correlator output q in (15) is then given by the statistical average

$$\begin{aligned}
f_q(\xi) &= \overline{\exp(i\xi q)} = \overline{\exp(i\xi U^T Q V)} = \\
&= \iint dU dV p(U, V) \exp(i\xi U^T Q V) = \\
&= \left[2\pi\sigma_u\sigma_v(1-\rho^2)^{1/2} \right]^{-N} \iint dU dV \exp \left[i\xi U^T Q V - \frac{1}{2(1-\rho^2)} * \right. \\
&\left. * \left\{ \frac{1}{\sigma_u^2} (U - \mu_u \mathbf{1})^T (U - \mu_u \mathbf{1}) + \frac{1}{\sigma_v^2} (V - \mu_v \mathbf{1})^T (V - \mu_v \mathbf{1}) - \frac{2\rho}{\sigma_u\sigma_v} (U - \mu_u \mathbf{1})^T (V - \mu_v \mathbf{1}) \right\} \right]. \quad (19)
\end{aligned}$$

At this point, in order to evaluate this 2N-fold integral, we employ the general integral result (B-2) and (B-6) in appendix B, identifying the matrices there as

$$\begin{aligned}
A &= \frac{1}{\sigma_u^2(1-\rho^2)} I, \quad B = \frac{1}{\sigma_v^2(1-\rho^2)} I, \quad C = i\xi Q + \frac{\rho}{\sigma_u\sigma_v(1-\rho^2)} I, \\
D &= \frac{\sigma_v\mu_u - \rho\sigma_u\mu_v}{\sigma_u^2\sigma_v(1-\rho^2)} \mathbf{1}, \quad E = \frac{\sigma_u\mu_v - \rho\sigma_v\mu_u}{\sigma_u\sigma_v^2(1-\rho^2)} \mathbf{1}. \quad (20)
\end{aligned}$$

We also need the following auxiliary results for special matrix forms; namely, for arbitrary scalars c_1, c_2 , the matrix determinant

$$\det(c_1 I + c_2 \mathbf{1} \mathbf{1}^T) = c_1^{N-1} (c_1 + Nc_2), \quad (21)$$

and the matrix inverse

$$(c_1 I + c_2 \mathbf{1} \mathbf{1}^T)^{-1} = \frac{1}{c_1} I - \frac{c_2}{c_1(c_1 + Nc_2)} \mathbf{1} \mathbf{1}^T. \quad (22)$$

Employment of appendix B and (20)-(22) then yields, after a very considerable amount of effort, a closed form for the characteristic function in (19) (in its most compact form)

$$f_q(\xi) = \frac{\exp \left[i\xi \frac{G_1 + i\xi G_2}{1 - i\xi F_1 + \xi^2 F_2} \right]}{\left(1 - i\xi E_1 + \xi^2 E_2 \right)^{\frac{N-1}{2}} \left(1 - i\xi F_1 + \xi^2 F_2 \right)^{\frac{1}{2}}}, \quad (23)$$

where

$$E_1 = 2\rho\sigma_u\sigma_v, \quad E_2 = \sigma_u^2\sigma_v^2(1-\rho^2),$$

$$F_1 = E_1(1-\gamma), \quad F_2 = E_2(1-\gamma)^2,$$

$$G_1 = N(1-\gamma)\mu_u\mu_v, \quad G_2 = \frac{1}{2}N(1-\gamma)^2(\sigma_u^2\sigma_v^2 + \sigma_v^2\mu_u^2 - 2\rho\sigma_u\sigma_v\mu_u\mu_v). \quad (24)$$

The square roots in (23) are principal value, being +1 at $\xi=0$. This characteristic function has four branch points and two essential singularities which overlap two of the branch points; the complexity of this characteristic function of q precludes tractable analytical results for the probability density function or exceedance distribution function of the correlator output, except in very special cases. Nevertheless, since the characteristic function in (23) is easily numerically evaluated with computer aid, it readily lends itself to the procedure presented in [2,3]. A program for the evaluation of the cumulative and exceedance distribution functions corresponding to characteristic function (23)-(24) is given in appendix C for arbitrary values of

- N, number of terms summed
- γ , scale factor in sample mean removal
- μ_u , mean in u-channel
- μ_v , mean in v-channel
- σ_u , standard deviation in u-channel
- σ_v , standard deviation in v-channel
- ρ , correlation coefficient between channels.

A sample plot of the cumulative and exceedance distribution functions for a typical selection of numerical values for the above parameters is also presented in appendix C.

CUMULANTS OF CORRELATOR OUTPUT

By taking the natural logarithm of the characteristic function in (23) and expanding in a power series in ξ , the cumulants of random variable q can be extracted:

$$\begin{aligned} \chi_q(n) = & \frac{1}{2}(n-1)! [N-1+(1-\gamma)^n] (\sigma_u \sigma_v)^n (S^n + D^n) + \\ & + \frac{1}{2} n! N(1-\gamma)^n (\sigma_u \sigma_v)^{n-1} \mu_u \mu_v (S^{n-1} + D^{n-1}) + \\ & + \frac{1}{4} n! N(1-\gamma)^n (\sigma_u \sigma_v)^{n-2} (\sigma_u^2 \mu_v^2 + \sigma_v^2 \mu_u^2) (S^{n-1} - D^{n-1}), \end{aligned} \quad (25)$$

where here

$$S = \rho + 1, \quad D = \rho - 1. \quad (26)$$

In particular, the mean and variance of q are available by using $n=1$ and 2 respectively in (25):

$$\begin{aligned} \mu_q = & (N-\gamma)\rho\sigma_u\sigma_v + N(1-\gamma)\mu_u\mu_v, \\ \sigma_q^2 = & (N-2\gamma+\gamma^2)(1+\rho^2)\sigma_u^2\sigma_v^2 + N(1-\gamma)^2(\sigma_u^2\mu_v^2 + \sigma_v^2\mu_u^2 + 2\rho\sigma_u\sigma_v\mu_u\mu_v). \end{aligned} \quad (27)$$

SPECIAL CASE OF $\gamma=1$, SAMPLE MEAN REMOVAL

For $\gamma=1$, the general characteristic function in (23) reduces to

$$f_q(\xi; \gamma=1) = \left(1 - i\xi E_1 + \xi^2 E_2 \right)^{-\frac{N-1}{2}}, \quad (28)$$

where E_1 and E_2 are still given by (24), and are independent of means μ_u and μ_v , as shown earlier. The cumulants in (25) reduce to

$$\chi_q(n) = \frac{1}{2}(n-1)!(N-1)(\sigma_u\sigma_v)^n[(\rho+1)^n + (\rho-1)^n], \quad (29)$$

and in particular, the mean and variance of q are

$$\begin{aligned} \mu_q &= (N-1)\rho\sigma_u\sigma_v, \\ \sigma_q^2 &= (N-1)(1+\rho^2)\sigma_u^2\sigma_v^2. \end{aligned} \quad (30)$$

SPECIAL CASE OF $\gamma=0$, SAMPLE MEAN NOT REMOVED

For $\gamma=0$, the characteristic function in (23) reduces to

$$f_q(\mathfrak{F}; \gamma=0) = (1 - i\mathfrak{F}E_1 + \mathfrak{F}^2E_2)^{-N/2} \exp\left[i\mathfrak{F} \frac{G_1^{(0)} + i\mathfrak{F}G_2^{(0)}}{1 - i\mathfrak{F}E_1 + \mathfrak{F}^2E_2}\right], \quad (31)$$

where

$$\begin{aligned} E_1 &= 2\rho\sigma_u\sigma_v, & E_2 &= \sigma_u^2\sigma_v^2(1-\rho^2), \\ G_1^{(0)} &= N\mu_u\mu_v, & G_2^{(0)} &= \frac{1}{2}N(\sigma_u^2\mu_v^2 + \sigma_v^2\mu_u^2 - 2\rho\sigma_u\sigma_v\mu_u\mu_v). \end{aligned} \quad (32)$$

The cumulants are obtained by setting $\gamma=0$ in (25), and in particular, the mean and variance of correlator output q are

$$\begin{aligned} \mu_q &= N(\rho\sigma_u\sigma_v + \mu_u\mu_v), \\ \sigma_q^2 &= N\left[(1+\rho^2)\sigma_u^2\sigma_v^2 + \sigma_u^2\mu_v^2 + \sigma_v^2\mu_u^2 + 2\rho\sigma_u\sigma_v\mu_u\mu_v\right]. \end{aligned} \quad (33)$$

INTERRELATIONSHIP OF TWO SPECIAL CASES

Let the general characteristic function in (23) be denoted by $f_q(\xi; N, \gamma, \mu_u, \mu_v)$. We have already seen the expression for $f_q(\xi; N, 1, \mu_u, \mu_v)$ in (28). At the same time, from (23) and (24), there follows

$$f_q(\xi; N-1, 0, 0, 0) = \left(1 - i\xi E_1 + \xi^2 E_2\right)^{-\frac{N-1}{2}}, \quad (34)$$

which is identical to (28). That is,

$$f_q(\xi; N, 1, \mu_u, \mu_v) = f_q(\xi; N-1, 0, 0, 0). \quad (35)$$

Thus the characteristic functions of the two following random variables are identical:

- (1) Sum of N terms with sample mean removal, and the true means arbitrary,
- (2) Sum of $N-1$ terms without sample mean removal, but the true means zero. (36)

The removal of the sample means has eliminated the dependence of the correlator output on the unknown means but has reduced the number of degrees of freedom by 1.

SPECIALIZATION TO THE SIGNAL AND NOISE MODEL

For general scaling factor γ and arbitrary input means μ_u, μ_v , and for the model introduced earlier in (3)-(6), the general characteristic function of the correlator output is still given by (23), but with the parameters in (24) now specialized to the form

$$E_1 = 2\rho_s(S_u S_v)^{1/2}, \quad E_2 = D_u D_v + D_u S_v + D_v S_u + S_u S_v(1-\rho_s^2),$$

$$F_1 = E_1(1-\gamma), \quad F_2 = E_2(1-\gamma)^2,$$

$$G_1 = N(1-\gamma)\mu_u\mu_v, \quad G_2 = \frac{1}{2}N(1-\gamma)^2[(S_u + D_u)\mu_v^2 + (S_v + D_v)\mu_u^2 - 2\rho_s(S_u S_v)^{1/2}\mu_u\mu_v]. \quad (37)$$

The general n-th cumulant is still given by (25); however, the use of (6) allows for determination in terms of the fundamental quantities of the signal and noise model, namely S_u , S_v , D_u , D_v , ρ_s defined in (4)-(5). In particular, the mean and variance of correlator output q are

$$\begin{aligned} \mu_q &= (N-\gamma)\rho_s(S_u S_v)^{1/2} + N(1-\gamma)\mu_u\mu_v, \\ \sigma_q^2 &= (N-2\gamma+\gamma^2)[D_u D_v + D_u S_v + D_v S_u + (1+\rho_s^2)S_u S_v] + \\ &+ N(1-\gamma)^2[(S_u + D_u)\mu_v^2 + (S_v + D_v)\mu_u^2 + 2\rho_s(S_u S_v)^{1/2}\mu_u\mu_v]. \end{aligned} \quad (38)$$

ANALYTIC RESULTS FOR $\gamma=1$, SAMPLE MEAN REMOVAL

In this section and the next, we will confine attention solely to the case of scale factor $\gamma=1$. The characteristic function of the crosscorrelator output q follows from (28) and (24) as

$$f_q(\xi) = [1 - i\xi E_1 + \xi^2 E_2]^{-\frac{N-1}{2}} = [1 - i\xi 2\rho\sigma_U\sigma_V + \xi^2 \sigma_U^2 \sigma_V^2 (1-\rho^2)]^{-\frac{N-1}{2}} =$$

$$= \left\{ [1+i\xi\sigma_U\sigma_V(1-\rho)] [1-i\xi\sigma_U\sigma_V(1+\rho)] \right\}^{-\frac{N-1}{2}} \quad \text{for } \gamma=1, \quad (39)$$

where we must have $N \geq 2$. We observe, for later numerical use in appendix D, that since $|1 \pm i\xi b| = (1 + \xi^2 b^2)^{1/2}$ is monotonically increasing for $\xi \geq 0$, then $|f_q(\xi)|$ is monotonically decreasing for all $\xi \geq 0$ and any $N, \sigma_U, \sigma_V, \rho$.

GENERAL PROBABILITY RESULTS

The cumulants of q have already been listed in (29) and (30). The probability density function corresponding to characteristic function (39) is given by [5, 6.699 12]

$$p_q(u) = \left[\Gamma\left(\frac{N-1}{2}\right) \pi^{1/2} (1-\rho^2)^{1/2} \sigma_U \sigma_V \right]^{-1} \left(\frac{|u|}{2\sigma_U \sigma_V} \right)^{\frac{N}{2} - 1} *$$

$$* K_{\frac{N}{2} - 1} \left(\frac{|u|}{\sigma_U \sigma_V (1-\rho^2)} \right) \exp \left(\frac{\rho u}{\sigma_U \sigma_V (1-\rho^2)} \right) \quad \text{for all } u, \quad \gamma=1, \quad (40)$$

where $K_\nu(z)$ is a modified Bessel function of the second kind [6, section 9.6]. If the number of terms added, N , to yield correlator output q , is odd, simple relations for the probability density function in (40) can be obtained [6, 10.2.15 and 10.1.9, last equation]; letting $n = \frac{N-3}{2}$ for N odd, we find the exact result

$$p_q(u) = \frac{(1-\rho^2)^n}{2\sigma_u\sigma_v 4^n n!} \exp\left(\frac{\rho u - |u|}{\sigma_u\sigma_v(1-\rho^2)}\right) \sum_{m=0}^n \frac{(2n-m)!}{(n-m)! m!} \left(\frac{2|u|}{\sigma_u\sigma_v(1-\rho^2)}\right)^m$$

$$\text{for all } u; n = \frac{N-3}{2}, N = 3, 5, 7, \dots \quad (41)$$

For example, for $N=3$, we have $n=0$, yielding

$$p_q(u) = \frac{1}{2\sigma_u\sigma_v} \exp\left(\frac{\rho u - |u|}{\sigma_u\sigma_v(1-\rho^2)}\right) \text{ for all } u. \quad (42)$$

The corresponding cumulative distribution function for $N=3$ is

$$P_q(u) = \int_{-\infty}^u dt p_q(t) = \frac{1-\rho}{2} \exp\left(\frac{u}{\sigma_u\sigma_v(1-\rho)}\right) \text{ for } u \leq 0, \quad (43A)$$

while the exceedance distribution function is

$$1 - P_q(u) = \int_u^{+\infty} dt p_q(t) = \frac{1+\rho}{2} \exp\left(\frac{-u}{\sigma_u\sigma_v(1+\rho)}\right) \text{ for } u \geq 0. \quad (43B)$$

This dichotomy, of presenting the cumulative distribution function for negative arguments, and the exceedance distribution function for positive arguments, turns out to be notationally convenient and physically meaningful and will be adopted throughout this report.

Although closed form expressions for the exceedance distribution function corresponding to probability density function (40) are not available for general N , the use of [6, 9.7.2] on (40) leads to the dominant term in the asymptotic expansion of the exceedance distribution function:

$$1 - P_q(u) \sim \frac{1+\rho}{2\Gamma\left(\frac{N-1}{2}\right)} \left(\frac{u}{2\sigma_u\sigma_v}\right)^{\frac{N-3}{2}} \exp\left(\frac{-u}{\sigma_u\sigma_v(1+\rho)}\right) \text{ as } u \rightarrow +\infty. \quad (44)$$

For $N=3$, this is precise; see (43B).

POSSIBLE NORMALIZATIONS OF q

If we define a normalized random variable

$$x = \frac{q}{E_2^{1/2}} = \frac{q}{\sigma_u \sigma_v (1-\rho^2)^{1/2}}, \quad (45)$$

then the characteristic function of x is given by (39) as

$$\begin{aligned} f_x(\xi) &= f_q(\xi/E_2^{1/2}) = \left[1 - i\xi E_1/E_2^{1/2} + \xi^2 \right]^{-\frac{N-1}{2}} \\ &= \left[1 - i\xi 2\rho(1-\rho^2)^{-1/2} + \xi^2 \right]^{-\frac{N-1}{2}}, \end{aligned} \quad (46)$$

which has only two fundamental parameters, namely, N and ρ .

A second possibility is the random variable defined by

$$y = \frac{q}{\sigma_u \sigma_v}, \quad (47)$$

for which characteristic function

$$f_y(\xi) = f_q\left(\frac{\xi}{\sigma_u \sigma_v}\right) = \left[1 - i\xi 2\rho + \xi^2(1-\rho^2) \right]^{-\frac{N-1}{2}} \quad (48)$$

also depends only on N and ρ . However, neither of the normalizations, (45) and (47), are of interest to us here; an alternative normalization and reasons for its selection are given below.

SPECIALIZATION TO THE SIGNAL AND NOISE MODEL

For the model presented earlier in (3)-(8), the original E_1 , E_2 parameters in (24) take the form already given in the upper line of (37). Let a normalized random variable, relative to the additive random noise disturbances, be defined according to

$$h = \frac{q}{(D_u D_v)^{1/2}} ; \quad (49)$$

see (5). This normalization for the particular signal model (3) is different from both x and y in the general case above. The reason we employ h is that the normalization depends only on the power of the additive noise disturbances, and not on the signal strengths or correlation coefficients; this is consistent with a system which monitors the noise-only background and sets a threshold for a desired false alarm probability.

The characteristic function of the normalized random variable h in (49) is given by

$$\begin{aligned} f_h(\xi) &= f_q\left(\xi / (D_u D_v)^{1/2}\right) = \left[1 - i\xi \frac{E_1}{(D_u D_v)^{1/2}} + \xi^2 \frac{E_2}{D_u D_v} \right]^{-\frac{N-1}{2}} = \\ &= \left[1 - i\xi 2\alpha + \xi^2 (\beta^2 - \alpha^2) \right]^{-\frac{N-1}{2}}, \end{aligned} \quad (50)$$

where we define auxiliary parameters here as

$$\alpha = \rho_s (R_u R_v)^{1/2}, \quad \beta = [(1+R_u)(1+R_v)]^{1/2}. \quad (51)$$

Here we used (39), (37), and (8). This characteristic function in (50) depends on the four fundamental parameters N , ρ_s , R_u , R_v , where the latter two quantities are the signal-to-noise ratios per sample of the random components of model (3); see (8).

Reference to (40) reveals that the probability density function of h corresponding to characteristic function (50) is given by

$$p_h(u) = \left[\Gamma\left(\frac{N-1}{2}\right) \pi^{1/2} (\beta^2 - \alpha^2)^{1/2} \right]^{-1} \left(\frac{|u|}{2\beta} \right)^{\frac{N}{2} - 1} * \\ * K_{\frac{N}{2} - 1} \left(\frac{\beta |u|}{\beta^2 - \alpha^2} \right) \exp\left(\frac{\alpha u}{\beta^2 - \alpha^2} \right) \quad \text{for all } u. \quad (52)$$

For N odd, alternative forms are available from (41), if desired. The asymptotic behavior of the exceedance distribution function of h follows in a manner similar to that used for (44):

$$1 - P_h(u) \sim \frac{1 + \alpha/\beta}{2\Gamma\left(\frac{N-1}{2}\right)} \left(\frac{u}{2\beta} \right)^{\frac{N-3}{2}} \exp\left(\frac{-u}{\beta + \alpha} \right) \quad \text{as } u \rightarrow +\infty. \quad (53)$$

The cumulants of h follow from (29), (26), and (6)-(8):

$$\chi_h(n) = \frac{1}{2}(n-1)!(N-1)[(\alpha+\beta)^n + (\alpha-\beta)^n], \quad (54)$$

and in particular, the mean and variance of h are

$$\mu_h = (N-1)\alpha = (N-1)\rho_s(R_u R_v)^{1/2}, \\ \sigma_h^2 = (N-1)(\alpha^2 + \beta^2) = (N-1)[1 + R_u + R_v + R_u R_v(1 + \rho_s^2)]. \quad (55)$$

The two parameters, α and β , are given here by (51), in terms of the fundamental quantities R_u , R_v , ρ_s of the signal and noise model.

REDUCTION TO IDENTICAL SIGNAL COMPONENTS

At this point, we will further specialize the results for the signal and noise model in the above subsection. We presume that

$$R_u = R_v = R \quad \text{and} \quad \rho_s = 1, \quad (56A)$$

giving, from (51),

$$\alpha = R, \quad \beta = 1+R; \quad (56B)$$

that is, the signal-to-noise ratios in the two channels are equal, and the two channel signals are fully correlated. This corresponds physically to a case where the random signal components in (3) are identical, $u_s(n) = v_s(n)$, and the independent random noise disturbances have the same power level. This situation will hold for the rest of this section and all of the next section where the graphical results are presented.

Equations (50) and (56B) then yield the characteristic function for normalized random variable h in (49) as

$$\begin{aligned} f_h(\xi) &= [1 - i\xi 2R + \xi^2(1+2R)]^{-\frac{N-1}{2}} = \\ &= [(1 + i\xi)(1 - i\xi(1+2R))]^{-\frac{N-1}{2}}. \end{aligned} \quad (57)$$

The cumulants in (54) reduce to

$$\chi_h(n) = \frac{1}{2}(n-1)!(N-1)[(1+2R)^n + (-1)^n], \quad (58)$$

and in particular, the mean and variance become

$$\mu_h = (N-1)R, \quad \sigma_h^2 = (N-1)(1+2R+2R^2). \quad (59)$$

All the above statistical descriptions depend only on the two parameters R , the per-sample signal-to-noise ratio, and N , the number of terms added to yield the correlator output.

The probability density function for h follows from (52) as

$$p_h(u) = \left[\Gamma\left(\frac{N-1}{2}\right) \pi^{1/2} (1+2R)^{1/2} \right]^{-1} \left(\frac{|u|}{2(1+R)} \right)^{\frac{N}{2}-1} * \\ * K_{\frac{N}{2}-1} \left(\frac{1+R}{1+2R} |u| \right) \exp\left(\frac{Ru}{1+2R}\right) \text{ for all } u, \quad (60)$$

and the asymptotic exceedance distribution function from (53):

$$1 - P_h(u) \sim \frac{1+2R}{2(1+R)\Gamma\left(\frac{N-1}{2}\right)} \left(\frac{u}{2(1+R)} \right)^{\frac{N-3}{2}} \exp\left(\frac{-u}{1+2R}\right) \text{ as } u \rightarrow +\infty. \quad (61)$$

An important word of caution must be mentioned at this point: when N is large, (61) is inadequate for evaluating small false alarm and detection probabilities, since the succeeding terms in the asymptotic expansion contribute significantly. For example, when $R=0$, the maximum value of the dominant term (61) occurs when $u = (N-3)/2$ which, for $N=128$, yields false alarm probability $3.86E-21$, a value far below those of interest. Thus (61) has limited applicability, being best for small N ; in fact, the first correction term to (61) yields the multiplicative factor

$$1 + \frac{1+2R}{1+R} \frac{(N-3)(N+3+4R)}{8u}. \quad (62)$$

It indicates that, for large N , u must be of the order of N^2 in order for the dominant term (61) to be fairly accurate.

Although for N odd, an alternative closed form to the probability density function (60) of h is available from (41), the exceedance distribution function will generate a double sum and be rather cumbersome for large N . On the other hand, the characteristic function in (57) decays rapidly with \mathbb{F} when N is large and yields very nicely to the numerical approach given in [2,3]. The only difficult cases are in fact those for small N ; accordingly, some analytic results for $N = 2, 3, 4, 5$ will now be presented, based on characteristic function (57).

GENERAL DISTRIBUTION INTEGRALS

Suppose a random variable y has characteristic function $f_y(\xi)$. The cumulative distribution function of y can be written as a contour integral [3, (5) & (6)]

$$P_y(u) = -\frac{1}{i2\pi} \int_{C_+} d\xi \frac{f_y(\xi)}{\xi} \exp(-iu\xi) \quad \text{for all } u, \quad (63)$$

where C_+ is a contour along the real axis of the complex ξ -plane, with an upward indentation at the origin $\xi=0$, to avoid the pole of the integrand there.

Similarly, the exceedance distribution function of random variable y can be expressed as

$$1 - P_y(u) = \frac{1}{i2\pi} \int_{C_-} d\xi \frac{f_y(\xi)}{\xi} \exp(-iu\xi) \quad \text{for all } u, \quad (64)$$

where C_- is a contour along the real ξ axis, with a downward indentation at $\xi=0$.

For $u < 0$, both contours can be moved into the upper-half ξ -plane, since the exp term furnishes rapid decay there. Similarly, for $u > 0$, both contours can be moved into the lower-half ξ -plane, to realize exponential decay on the circular arcs tending to infinity.

DISTRIBUTIONS FOR $N=2$

From (57), the characteristic function of normalized correlator output h is

$$f_h(\xi) = [(1+i\xi)(1-i\xi(1+2R))]^{-1/2}, \quad (65)$$

and the probability density function follows from (60) as

$$p_h(u) = \frac{1}{\pi(1+2R)^{1/2}} K_0\left(\frac{1+R}{1+2R}|u|\right) \exp\left(\frac{Ru}{1+2R}\right) \quad \text{for all } u. \quad (66)$$

There is no closed form for the indefinite integral of a K_0 function; see [6, 11.1.8 and 11.1.9]. Instead, we use (65) in (63) and move the contour upwards until it wraps around the branch point at $\xi=i$ and extends vertically upward from there; this is in fact the steepest descent direction for the exponential ^{when $u < 0$} . The contributions of the small and large circular arcs tend to zero as the radii tend to zero and infinity, respectively. Under a change of variable, there follows the cumulative distribution function in the form

$$P_h(u) = \frac{2}{\pi} \int_0^{+\infty} \frac{dt \exp[u(1+t^2)]}{(1+t^2)[1+(1+2R)(1+t^2)]^{1/2}} \quad \text{for } u \leq 0. \quad (67)$$

This is a useful exact result for several reasons: the integrand decays rapidly, has no cusps, and involves only elementary functions which are easily computed; also the integral is a sum of positive quantities and retains significance even for large $|u|$.

In a similar fashion, if characteristic function (65) is substituted in (64) and the contour moved down and wrapped around the branch point at $\xi = -i/(1+2R)$ and along the ^{downward} vertical steepest descent direction for the exponential ^{when $u > 0$} , the exceedance distribution function becomes, upon a change of variable,

$$1 - P_h(u) = \frac{2}{\pi}(1+2R) \exp\left(\frac{-u}{1+2R}\right) \int_0^{+\infty} \frac{dt \exp(-ut^2)}{[1+(1+2R)t^2][1+(1+2R)(1+t^2)]^{1/2}} \quad \text{for } u \geq 0. \quad (68)$$

This is useful for the same reasons given above.

There is one closed form result possible; namely, for $u=0$, direct integration of probability density function (66) yields [5, 6.611 9]

$$P_h(0) = \frac{1}{\pi} \arccos\left(\frac{R}{1+R}\right), \quad 1 - P_h(0) = \frac{1}{\pi} \arccos\left(\frac{-R}{1+R}\right). \quad (69)$$

DISTRIBUTIONS FOR N=3

Use of [6, 10.2.17] on (60) immediately yields probability density function

$$p_h(u) = \left\{ \begin{array}{ll} \frac{1}{2(1+R)} \exp(u) & \text{for } u \leq 0 \\ \frac{1}{2(1+R)} \exp\left(\frac{-u}{1+2R}\right) & \text{for } u \geq 0 \end{array} \right\}. \quad (70)$$

The cumulative and exceedance distribution functions easily follow as

$$\begin{aligned} P_h(u) &= \frac{1}{2(1+R)} \exp(u) && \text{for } u \leq 0, \\ 1 - P_h(u) &= \frac{1+2R}{2(1+R)} \exp\left(\frac{-u}{1+2R}\right) && \text{for } u \geq 0. \end{aligned} \quad (71)$$

This latter result corroborates (61) and (62).

DISTRIBUTIONS FOR N=4

The only closed form result possible is obtained by direct integration of probability density function (60) to get origin value

$$P_h(0) = \frac{1}{\pi} \left[\arccos\left(\frac{R}{1+R}\right) - \frac{R(1+2R)^{1/2}}{(1+R)^2} \right]. \quad (72)$$

This follows by use of the integral

$$\int_0^{+\infty} dx e^{-\alpha x} x K_1(\beta x) = \frac{\beta \arccos(\alpha/\beta)}{(\beta^2 - \alpha^2)^{3/2}} - \frac{\alpha}{\beta(\beta^2 - \alpha^2)} \quad \text{for } \beta > -\alpha, \quad (73)$$

which follows from [5, 6.611 9] by applying α/β to both sides.

DISTRIBUTIONS FOR $N=5$

Use of [6, 10.2.17] on (60) immediately yields probability density function

$$p_h(u) = \left\{ \begin{array}{ll} \frac{1+2R-(1+R)u}{4(1+R)^3} \exp(u) & \text{for } u \leq 0 \\ \frac{1+2R+(1+R)u}{4(1+R)^3} \exp\left(\frac{-u}{1+2R}\right) & \text{for } u \geq 0 \end{array} \right\} . \quad (74)$$

The cumulative and exceedance distribution functions follow as

$$P_h(u) = \frac{2+3R-(1+R)u}{4(1+R)^3} \exp(u) \quad \text{for } u \leq 0,$$

$$1 - P_h(u) = \frac{1+2R}{4(1+R)^3} [(1+2R)(2+R)+(1+R)u] \exp\left(\frac{-u}{1+2R}\right) \quad \text{for } u \geq 0 . \quad (75)$$

This latter result corroborates (61) and (62). Also, this example was used as a check on the numerical procedure [3] applied directly to the characteristic function, which is used in the following section; the agreement was ten decimals for numerous values of R and u .

GRAPHICAL RESULTS FOR $\gamma=1$, SAMPLE MEAN REMOVAL

SUMMARY OF PARTICULAR CASE CONSIDERED

We first summarize here the particular case that will be considered quantitatively in this section. The input samples are

$$\left. \begin{aligned} u_n &= \mu_u + u_s(n) + u_d(n) \\ v_n &= \mu_v + v_s(n) + v_d(n) \end{aligned} \right\} \text{ for } 1 \leq n \leq N, \quad (76)$$

where these Gaussian random variables have statistics

$$\begin{aligned} \overline{u_s(n)} &= \overline{v_s(n)} = \overline{u_d(n)} = \overline{v_d(n)} = 0, \\ \overline{u_s^2(n)} &= S_u, \quad \overline{v_s^2(n)} = S_v, \quad \overline{u_s(n)v_s(n)} = (S_u S_v)^{1/2}, \\ \overline{u_d^2(n)} &= D_u, \quad \overline{v_d^2(n)} = D_v, \quad \overline{u_d(n)v_d(n)} = 0. \end{aligned} \quad (77)$$

We presume that the simultaneous signal components $u_s(n)$, $v_s(n)$ in the two channels are fully correlated, that all other random variables are independent, and that the two channel input signal-to-noise ratios

$$\frac{S_u}{D_u} = \frac{S_v}{D_v} = R \quad (78)$$

have a common value R . More general situations have been considered in earlier sections; however, only this special case will be numerically evaluated here.

The normalized crosscorrelator output, with sample mean removal ($\gamma=1$), is

$$h = \frac{1}{(D_u D_v)^{1/2}} \sum_{n=1}^N \tilde{u}_n \tilde{v}_n, \quad (79)$$

where the sample ac components

$$\tilde{u}_n = u_n - \frac{1}{N} \sum_{m=1}^N u_m, \quad \tilde{v}_n = v_n - \frac{1}{N} \sum_{m=1}^N v_m. \quad (80)$$

The characteristic function of h is given by (57) as

$$f_h(\xi) = [(1+i\xi)(1-i\xi(1+2R))]^{-\frac{N-1}{2}} \quad (81)$$

and depends only on signal-to-noise ratio R and number of terms N . We must have $N \geq 2$.

If $R=0$ and we evaluate the exceedance distribution function corresponding to (81), we then have the false alarm probability. But when $R>0$, the exceedance distribution function corresponding to (81) is the detection probability. In the following, we plot the detection probability vs. the false alarm probability, with signal-to-noise ratio R as a parameter; different values of N are handled in separate plots.

OPERATING CHARACTERISTICS FOR $\gamma=1$

A sample program for evaluation of the cumulative and exceedance distribution functions corresponding to characteristic function (81), and thereby the detection probability vs. false alarm probability operating characteristics of the crosscorrelator with sample mean removal, is given in appendix D. It is heavily based on the technique developed and explained in [3].

In figures* 1-14 are presented the operating characteristics for the crosscorrelator with sample mean removal, for values of

$$N = 2, 3, 4, 6, 8, 12, 16, 24, 32, 48, 64, 96, 128, 256, \quad (82)$$

respectively. The case of $N=2$ was accomplished by use of (67)-(69); results for $N=3$ relied on (71); and the remainder for $N \geq 4$ employed a numerical procedure [3] proceeding directly from characteristic function (81) to the exceedance distribution function. False alarm probabilities P_F in the range $1E-10$ to .5 and detection probabilities P_D covering $1E-10$ to .999 are presented. The abscissa and ordinate on these plots are according to a normal probability transformation, as explained below. Values of signal-to-noise ratio R are taken as $R=2^n$, where n assumes values appropriate for each plot in order to cover the full range of probabilities of interest.

GAUSSIAN APPROXIMATION

Suppose the decision variable of a processor is Gaussian with mean and standard deviation m_0, σ_0 respectively when the input signal is absent, and m_1, σ_1 when signal is present. Then for threshold λ , the false alarm probability and detection probability are

$$P_F = \int_{\lambda}^{+\infty} du \frac{1}{\sigma_0} \phi\left(\frac{u-m_0}{\sigma_0}\right) = \bar{\Phi}\left(\frac{m_0-\lambda}{\sigma_0}\right),$$

$$P_D = \int_{\lambda}^{+\infty} du \frac{1}{\sigma_1} \phi\left(\frac{u-m_1}{\sigma_1}\right) = \bar{\Phi}\left(\frac{m_1-\lambda}{\sigma_1}\right), \quad (83)$$

respectively, where ϕ and $\bar{\Phi}$ are the normalized Gaussian probability density function and cumulative distribution function:

$$\phi(u) = (2\pi)^{-1/2} \exp(-u^2/2), \quad \bar{\Phi}(u) = \int_{-\infty}^u dt \phi(t). \quad (84)$$

If we let $\bar{\Phi}_I$ be the inverse function to $\bar{\Phi}$, and define

$$x = \bar{\Phi}_I(P_F), \quad y = \bar{\Phi}_I(P_D), \quad (85)$$

*See page 51 et seq.

then threshold Λ can be eliminated from (83) to yield

$$y = \frac{m_1 - m_0 + \sigma_0 x}{\sigma_1} . \quad (86)$$

Equation (85) corresponds to the transformation to normal probability coordinates; thus a plot of P_D vs P_F on normal probability paper is the straight line (86) when the decision variable is Gaussian under both hypotheses of signal absent as well as present.

Reference to (59) reveals that, for our application,

$$m_0 = 0, \quad m_1 = (N-1)R, \quad \sigma_0^2 = N-1, \quad \sigma_1^2 = (N-1)(1+2R+2R^2), \quad (87)$$

since setting signal-to-noise ratio $R=0$ corresponds to hypothesis 0, signal absent. Substitution in (86) yields

$$y = \frac{(N-1)^{1/2} R + x}{(1+2R+2R^2)^{1/2}} ; \quad (88)$$

that is, if normalized crosscorrelator output h were Gaussian, the operating characteristics would be straight lines dictated by (88). These straight lines are superposed as dashed lines in figures 12-14 for $N=96, 128, 256$ respectively. Despite the large value of $N=96$ in figure 12, the Gaussian approximation is not that accurate, especially for small false alarm probabilities and large detection probabilities. The exact curve (solid) and the Gaussian approximation (dashed) cross each other, and are labelled at the crossing with the corresponding value of n in signal-to-noise ratio $R=2^n$. For $N=256$ in figure 14, agreement is better and the Gaussian approximation is probably adequate for larger N . If not, an additional term or two in an Edgeworth expansion could be investigated with the aid of the cumulants given in (58).

An obvious shortcoming of the Gaussian approximation (88) may be seen immediately:

$$\lim_{R \rightarrow \infty} y = \left(\frac{N-1}{2}\right)^{1/2} < 1 \text{ for any } x. \quad (89)$$

Reference to (85) then yields the interpretation

$$\lim_{R \rightarrow \infty} P_D = \bar{\Phi}\left(\left(\frac{N-1}{2}\right)^{1/2}\right) < 1 \text{ for any } P_F. \quad (90)$$

That is, as input signal-to-noise ratio R tends to infinity, the approximate detection probability saturates at a value less than 1, regardless of the false alarm probability. Thus the Gaussian approximation must certainly deteriorate for large R ; the exact discrepancy for probabilities of practical interest is displayed in figures 12-14.

ANALYTIC RESULTS FOR $\gamma=0$, SAMPLE MEAN NOT REMOVED

In this section and the next, attention will be confined solely to the case of scale factor $\gamma=0$. The characteristic function of the crosscorrelator output q is then given in (31) and (32), and the mean and variance of q are listed in (33). Due to the complexity of the exponential term in characteristic function (31), there are no general probability density function or cumulative distribution function results for arbitrary N , like those given earlier in (40), (41), and (44) for $\gamma=1$. Here, we can have $N \geq 1$.

SPECIALIZATION TO THE SIGNAL AND NOISE MODEL

For the model presented earlier in (3)-(8), the original parameters in (24) take the form already given in (37), but now with $\gamma=0$. Specifically, characteristic function (31) is

$$f_q(\xi) = \left(1 - i\xi E_1 + \xi^2 E_2\right)^{-N/2} \exp \left[i\xi \frac{G_1^{(0)} + i\xi G_2^{(0)}}{1 - i\xi E_1 + \xi^2 E_2} \right], \quad (91)$$

where

$$E_1 = 2\rho_s (S_u S_v)^{1/2}, \quad E_2 = D_u D_v + D_u S_v + D_v S_u + S_u S_v (1 - \rho_s^2),$$

$$G_1^{(0)} = N\mu_u \mu_v, \quad G_2^{(0)} = \frac{1}{2} N [(S_u + D_u)\mu_v^2 + (S_v + D_v)\mu_u^2 - 2\rho_s (S_u S_v)^{1/2} \mu_u \mu_v]. \quad (92)$$

The mean and variance of crosscorrelator output q follow from (38) according to

$$\mu_q = N[\rho_s (S_u S_v)^{1/2} + \mu_u \mu_v],$$

$$\sigma_q^2 = N[D_u D_v + D_u S_v + D_v S_u + (1 + \rho_s^2) S_u S_v + (S_u + D_u)\mu_v^2 + (S_v + D_v)\mu_u^2 + 2\rho_s (S_u S_v)^{1/2} \mu_u \mu_v]. \quad (93)$$

NORMALIZED CROSSCORRELATOR OUTPUT

As in (49), and for the same reasons, we define a normalized crosscorrelator output, relative to the additive random noise disturbances $u_d(n)$ and $v_d(n)$ in (3) and (5), according to

$$h = \frac{q}{(D_u D_v)^{1/2}} . \quad (94)$$

The characteristic function of h is available from (91) and (92):

$$\begin{aligned} f_h(\xi) &= f_q(\xi / (D_u D_v)^{1/2}) = \\ &= [1 - i\xi 2\alpha + \xi^2 (\beta^2 - \alpha^2)]^{-N/2} \exp \left[i\xi \frac{a + i\xi b}{1 - i\xi 2\alpha + \xi^2 (\beta^2 - \alpha^2)} \right], \end{aligned} \quad (95)$$

where

$$\begin{aligned} \alpha &= \rho_S (R_u R_v)^{1/2}, \quad \beta = [(1+R_u)(1+R_v)]^{1/2}, \\ a &= N r_u r_v, \quad b = \frac{1}{2} N [(1+R_u) r_v^2 + (1+R_v) r_u^2 - 2\rho_S (R_u R_v)^{1/2} r_u r_v], \end{aligned} \quad (96)$$

and where we have defined

$$R_u = \frac{S_u}{D_u}, \quad R_v = \frac{S_v}{D_v}, \quad r_u = \frac{\mu_u}{D_u^{1/2}}, \quad r_v = \frac{\mu_v}{D_v^{1/2}} . \quad (97)$$

The characteristic function in (95) depends on six fundamental parameters, namely N , ρ_S , R_u , R_v , r_u , r_v . The mean and variance of h follow from (94), (93), and (97):

$$\mu_h = N[\rho_s(R_u R_v)^{1/2} + r_u r_v] ,$$

$$\sigma_h^2 = N[(1+R_u)(1+R_v) + \rho_s^2 R_u R_v + (1+R_u)r_v^2 + (1+R_v)r_u^2 + 2\rho_s(R_u R_v)^{1/2} r_u r_v] . \quad (98)$$

r_u and r_v are referred to as normalized means.

REDUCTION TO IDENTICAL SIGNAL COMPONENTS

In order to prepare for numerical evaluation of the operating characteristics of the crosscorrelator with $\gamma=0$, we further specialize the signal and noise model to the case where

$$R_u = R_v = R, \quad \rho_s = 1, \quad r_u = r_v = r ; \quad (99)$$

see (56) et seq. This leads to

$$\alpha = R, \quad \beta = 1+R, \quad a = b = Nr^2 ,$$

via (96). The characteristic function in (95) then reduces to

$$f_h(\xi) = [(1+i\xi)(1-i\xi(1+2R))]^{-N/2} \exp\left[\frac{i\xi Nr^2}{1-i\xi(1+2R)}\right] , \quad (100)$$

and the mean and variance in (98) become

$$\mu_h = N(R+r^2), \quad \sigma_h^2 = N[1+2R+2R^2+2(1+2R)r^2] . \quad (101)$$

The characteristic function in (100) has a branch point at $\xi = i$, and another branch point at $\xi = -i/(1+2R)$ which overlaps an essential singularity; this complicates some of the analytical development to follow.

There are three fundamental parameters in (100), namely N , R , r . Since normalized mean r appears only through its square, we can presume $r \geq 0$ without loss of generality. Furthermore, if $r=0$, characteristic function (100)

reduces to (57) if $N-1$ there is replaced by N . Thus the curves for $r=0$ here can be obtained from the earlier curves for $\gamma=1$ in figures 1-14 by looking at a value for N there which is one greater; accordingly we can confine attention to $r>0$ in this and the next section.

When the random signal components $u_s(n)$, $v_s(n)$ in model (3) are absent, then $R=0$, and the exceedance distribution function corresponding to characteristic function (100) becomes the false alarm probability. However, (100) still depends on r , meaning that the false alarm probability must, likewise. Thus, a non-zero mean in (3), i.e. $r>0$, is not considered a signal attribute here, but rather is a nuisance quantity; it may, in fact, degrade the operating characteristics if not removed.

For notational convenience in the following, we define

$$\omega = 1+2R . \quad (102)$$

The magnitude of the exponential term in characteristic function (100) then can be expressed as

$$\exp\left[\frac{-\xi^2 \omega N r^2}{1+\xi^2 \omega^2}\right], \quad (103)$$

which is monotonically decreasing for $\xi \geq 0$. Coupled with the observation immediately under (39), it is seen that $|f_h(\xi)|$ in (100) is monotonically decreasing for all $\xi \geq 0$ and any N, R, r . This property allows for a convenient termination procedure in the numerical transformation [3] of characteristic function (100). It should however be observed that (103) does not decrease to zero, but saturates at value $\exp(-Nr^2)$, regardless of how ξ increases to infinity; thus the eventual decay of the characteristic function (100) is furnished only by the leading factor.

ASYMPTOTIC BEHAVIOR OF CUMULATIVE AND EXCEEDANCE DISTRIBUTION FUNCTIONS

In appendix E, it is shown that if characteristic function (100) is substituted in (63) and (64), and the contours moved appropriately in the complex s -plane, then the following asymptotic behaviors obtain. The cumulative distribution function

$$P_h(u) \sim \left[\Gamma\left(\frac{N}{2}\right) 2^{N/2} (1+R)^{N/2} \right]^{-1} (-u)^{\frac{N}{2}-1} \exp\left[u - \frac{Nr^2}{2(1+R)}\right] * \\ * \left[1 - \frac{\frac{N}{2}-1}{u} \left(1 + \frac{N(1+2R)}{4(1+R)} + \frac{Nr^2}{4(1+R)^2} \right) \right] \text{ as } u \rightarrow -\infty. \quad (104)$$

We see again, in similar fashion to (61) and (62), that in order for the correction term in the second line of (104) not to be too significant, we must have $u < -N^2$. For reasons elucidated in (61) et seq., (104) is not useful for large N .

As checks on (104), we note that for $r=0$ and $N=2$, (104) reduces precisely to the upper line of (71); this latter result pertains to $\gamma=1$, $N=3$ and is consistent with the observation already made in the paragraph below (101). In addition, if we let $r=0$ and $N=4$ in (104), it reduces to the upper line of (75); this latter result holds for $\gamma=1$, $N=5$ and is likewise consistent.

Also given in appendix E are a variety of asymptotic expansions for the exceedance distribution function; the simplest one is

$$1 - P_h(u) \sim \left[2\pi^{1/2} 2^{N/2} (1+R)^{N/2} (Nr^2)^{\frac{N-1}{4}} \right]^{-1} (1+2R)^{\frac{N+1}{2}} * \\ * u^{\frac{N-3}{4}} \exp\left[-\frac{(u^{1/2} - N^{1/2}r)^2}{1+2R}\right] \text{ as } u \rightarrow +\infty; \quad r > 0. \quad (105)$$

However, the same reservations as above, regarding u large relative to N^2 , are again in order.

DISTRIBUTIONS FOR $N=1$

If characteristic function (100) with $N=1$ is substituted in (63), and if the contour is moved as indicated under (66), there follows the exact result for the cumulative distribution function

$$P_h(u) = \frac{2}{\pi} \int_0^{+\infty} \frac{dt}{(1+t^2)(1+\omega(1+t^2))^{1/2}} \exp \left[u(1+t^2) - \frac{r^2(1+t^2)}{1+\omega(1+t^2)} \right] \text{ for } u \leq 0. \quad (106)$$

(This reduces to (67) for $r=0$, as it must.) This integral form possesses all the desirable attributes listed under (67).

If characteristic function (100) with $N=1$ is substituted in (64) in an attempt to get the exceedance distribution function, the analysis becomes rather difficult, due to the overlapping essential singularity and branch point of the integrand at $\xi = -i/\omega$. This problem is treated in detail in appendix F, with the result that the exceedance distribution function can be found via the characteristic function approach in terms of two integrals; see (F-21)-(F-23). However, a better numerical procedure for the exceedance distribution function is the direct result derived in (F-33); this latter integral is the one actually used here to generate the operating characteristics for $\gamma=0$, $N=1$.

DISTRIBUTIONS FOR $N=2$

The characteristic function is available from (100):

$$f_h(\xi) = (1+i\xi)^{-1} (1-i\xi\omega)^{-1} \exp \left(\frac{i\xi 2r^2}{1-i\xi\omega} \right) \equiv f_1(\xi) * f_2(\xi), \quad (107)$$

where $\omega = 1+2R$. The probability density functions corresponding to these two characteristic functions are [5, 6.631 4]

$$p_1(u) = \exp(u) U(-u) ,$$

$$p_2(u) = \frac{1}{\omega} \exp\left(-\frac{u+2r^2}{\omega}\right) I_0\left(\frac{2r}{\omega}(2u)^{1/2}\right) U(u) , \quad (108)$$

where U is the unit step function

$$U(u) = \begin{cases} 0 & \text{for } u < 0 \\ 1 & \text{for } u > 0 \end{cases} . \quad (109)$$

The probability density function of h is given by convolution

$$p_h(u) = \int_{-\infty}^{+\infty} dt p_1(t) p_2(u-t) \quad \text{for all } u . \quad (110)$$

Substitution of (108) in (110) yields

$$p_h(u) = \begin{cases} \frac{1}{1+\omega} \exp\left(u - \frac{2r^2}{1+\omega}\right) & \text{for } u \leq 0 \\ \frac{1}{1+\omega} \exp\left(u - \frac{2r^2}{1+\omega}\right) Q\left(\frac{2r}{\omega^{1/2}(1+\omega)^{1/2}} , \left(\frac{2(1+\omega)u}{\omega}\right)^{1/2}\right) & \text{for } u \geq 0 \end{cases} \quad (111)$$

where the Q -function is defined in [7] and the two integrals encountered have been evaluated by use of [5, 6.631 4] and [7, (9)], respectively. The cumulative and exceedance distribution functions of h readily follow from (111), the latter by means of [7, (42)]:

$$\begin{aligned}
 P_h(u) &= \frac{1}{1+\omega} \exp\left(u - \frac{2r^2}{1+\omega}\right) \text{ for } u \leq 0, \\
 1 - P_h(u) &= Q\left(\frac{2r}{\omega^{1/2}}, \left(\frac{2u}{\omega}\right)^{1/2}\right) - \\
 &\quad - \frac{1}{1+\omega} \exp\left(u - \frac{2r^2}{1+\omega}\right) Q\left(\frac{2r}{\omega^{1/2}(1+\omega)^{1/2}}, \left(\frac{2(1+\omega)u}{\omega}\right)^{1/2}\right) \text{ for } u \geq 0. \quad (112)
 \end{aligned}$$

(As a check, for $r=0$, then (111) and (112) reduce to (70) and (71) respectively, as they must.)

DISTRIBUTIONS FOR $N=4$

The characteristic function is available from (100):

$$f_h(\xi) = (1+i\xi)^{-2} (1-i\xi\omega)^{-2} \exp\left(\frac{i\xi 4r^2}{1-i\xi\omega}\right) \equiv f_1(\xi) * f_2(\xi), \quad (113)$$

where $\omega = 1+2R$. The probability density functions corresponding to these two characteristic functions are [5, 6.631 4]

$$\begin{aligned}
 p_1(u) &= -u \exp(u) U(-u), \\
 p_2(u) &= \frac{1}{2\omega r} \exp\left(-\frac{u+4r^2}{\omega}\right) u^{1/2} I_1(4ru^{1/2}/\omega) U(u). \quad (114)
 \end{aligned}$$

The probability density function of h is given by convolution (110). In preparation for that result, we use the shorthand notation

$$\begin{aligned}
 q_M(u) &= Q_M\left(2r\left(\frac{2}{\omega(1+\omega)}\right)^{1/2}, \left(\frac{2u(1+\omega)}{\omega}\right)^{1/2}\right), \\
 \tilde{q}_M(u) &= Q_M\left(2r\left(\frac{2}{\omega}\right)^{1/2}, \left(\frac{2u}{\omega}\right)^{1/2}\right), \quad (115)
 \end{aligned}$$

where the Q_M -function is defined in [8]. We also present a new integral result that will be needed in the sequel,

$$\int_c^{+\infty} dx \times Q_M(b, ax) = \frac{1}{2a^2} [b^2 Q_{M+1}(b, ac) + 2M Q_M(b, ac) - a^2 c^2 Q_{M-1}(b, ac)], \quad (116)$$

which can be interpreted as the limit of [8, (31)] as $p \rightarrow 0^+$. Substitution of (114) in (110) yields probability density function

$$p_h(u) = \begin{cases} \frac{1}{(1+\omega)^4} \exp\left(u - \frac{4r^2}{1+\omega}\right) \left[4r^2 + 2\omega(1+\omega) - (1+\omega)^2 u\right] & \text{for } u \leq 0 \\ \frac{1}{(1+\omega)^4} \exp\left(u - \frac{4r^2}{1+\omega}\right) \left[4r^2 q_3(u) + 2\omega(1+\omega) q_2(u) - (1+\omega)^2 u q_1(u)\right] & \text{for } u \geq 0 \end{cases} \quad (117)$$

where (115) has been used; the upper line employed [5, 6.631 4], while the lower line used (116) and an integration by parts procedure to be elaborated below in the exceedance distribution function evaluation.

The cumulative distribution function for $u \leq 0$ follows readily by integration of (117):

$$P_h(u) = \frac{1}{(1+\omega)^4} \exp\left(u - \frac{4r^2}{1+\omega}\right) \left[4r^2 + (1+\omega)(1+3\omega) - (1+\omega)^2 u\right] \quad \text{for } u \leq 0. \quad (118)$$

For $u \geq 0$, a modified approach is required. Integration of (110) yields cumulative distribution function

$$P_h(u) = \int_{-\infty}^{+\infty} dt p_2(t) P_1(u-t). \quad (119)$$

Probability density functions p_1 and p_2 are available in (114), and cumulative distribution function P_1 follows as

$$P_1(u) = \begin{cases} (1-u)\exp(u) & \text{for } u \leq 0 \\ 1 & \text{for } u \geq 0 \end{cases}. \quad (120)$$

Substitution of (114) and (120) in (119) yields, for $u \geq 0$,

$$\begin{aligned} P_h(u) &= \int_0^u dt \frac{1}{2\omega r} \exp\left(-\frac{t+4r^2}{\omega}\right) t^{1/2} I_1\left(4rt^{1/2}/\omega\right) + \\ &+ \int_u^{+\infty} dt \frac{1}{2\omega r} \exp\left(-\frac{t+4r^2}{\omega}\right) t^{1/2} I_1\left(4rt^{1/2}/\omega\right) (1-u+t) \exp(u-t) = \\ &= 1 - \tilde{q}_2(u) + \frac{1}{2\omega r} \exp\left(u - \frac{4r^2}{\omega}\right) \int_u^{+\infty} dt t^{1/2} \exp\left(-t \frac{1+\omega}{\omega}\right) I_1\left(4rt^{1/2}/\omega\right) (1-u+t), \quad (121) \end{aligned}$$

via [8, (22)]. We now integrate by parts, letting $U(t)=1-u+t$, and the remainder $dV(t)$. Then using [8, (22)] again, we find

$$V(t) = -\frac{2\omega r}{(1+\omega)^2} \exp\left(\frac{4r^2}{\omega(1+\omega)}\right) q_2(t). \quad (122)$$

Combining these results, (121) and (116) yield

$$\begin{aligned} 1 - P_h(u) &= \tilde{q}_2(u) - \frac{1}{(1+\omega)^2} \exp\left(u - \frac{4r^2}{1+\omega}\right) q_2(u) - \int_u^{+\infty} dt q_2(t) = \\ &= \tilde{q}_2(u) - \frac{1}{(1+\omega)^4} \exp\left(u - \frac{4r^2}{1+\omega}\right) \left[4r^2 q_3(u) + (1+\omega)(1+3\omega)q_2(u) - (1+\omega)^2 u q_1(u)\right] \\ &\quad \text{for } u \geq 0. \quad (123) \end{aligned}$$

The final results for $N=4$ are given by (115), (118), and (123). This case was used as a numerical check on the computational approach [3] proceeding directly from characteristic function (100) to the exceedance distribution function, with excellent agreement for numerous values of R , r , and u .

GRAPHICAL RESULTS FOR $\gamma=0$, SAMPLE MEAN NOT REMOVED

SUMMARY OF PARTICULAR CASE CONSIDERED

The situation of interest has already been summarized in (76)-(78); in addition, we have a common value for the normalized means,

$$\frac{\mu_u}{D_u^{1/2}} = \frac{\mu_v}{D_v^{1/2}} = r, \quad (124)$$

and the normalized crosscorrelator output is not (79)-(80), but rather is, for $\gamma=0$,

$$h = \frac{1}{(D_u D_v)^{1/2}} \sum_{n=1}^N u_n v_n. \quad (125)$$

The characteristic function is given by (100):

$$f_h(\xi) = [(1+i\xi)(1-i\xi\omega)]^{-N/2} \exp\left(\frac{i\xi Nr^2}{1-i\xi\omega}\right), \quad (126)$$

where $\omega = 1+2R$. When the signal is absent, then $R=0$; however the false alarm probability corresponding to this characteristic function still depends on r . Thus since the sample mean has not been removed, the operating characteristics will also depend on r . Since results for $r=0$ can be found from an earlier section, we only consider $r>0$ here.

OPERATING CHARACTERISTICS FOR $\gamma=0$

A sample program for evaluation of the cumulative and exceedance distribution functions corresponding to characteristic function (126), and thereby the detection probability vs. false alarm probability operating characteristics of the crosscorrelator without sample mean removal, is given in appendix G. In figures* 15-35 are presented the operating characteristics for values of

See page 65 et seq.

$$N = 1, 2, 3, 4, 8, 16, 32, 64, 128, 256, \quad (127)$$

and for various values of r . The case of $N=1$ was accomplished by use of (106) and (F-33); results for $N=2$ employed (112); and the remainder for $N \geq 3$ employed a numerical procedure [3] proceeding directly from characteristic function (126) to the exceedance distribution function. False alarm probabilities P_F in the range $1E-10$ to $.5$ and detection probabilities P_D covering $1E-10$ to $.999$ are presented. The abscissa and ordinate on these plots employ a normal probability transformation, as explained earlier in (84)-(86).

Values of signal-to-noise ratio R are taken as $R=2^n$, where n assumes values appropriate for each plot in order to cover the full range of probabilities of interest. Values of normalized mean r in (124) have been taken as $r=1$ and 2 , with the exception of figure 19 where one example for $r=4$ was added.

Without exception, increasing r from zero degrades the operating characteristics of the crosscorrelator. For example, figures 17, 18, 19 give a succession of operating characteristics for $r = 1, 2, 4$ respectively, and for common values of signal-to-noise ratio R . (In order to determine the operating characteristics for $r=0$ here, we can look at the earlier results in figures 1-14, but for a value of N which is one greater there.) Thus, not removing the sample mean from the crosscorrelator output requires a larger threshold setting for a specified false alarm probability and thereby lowers the detection probability and degrades performance.

GAUSSIAN APPROXIMATION

If the crosscorrelator output is Gaussian, for both signal absent as well as present, the earlier derivations in (83)-(86) pertain. Now reference to (101) yields statistics

$$m_0 = Nr^2, \quad m_1 = N(R+r^2),$$

$$\sigma_0^2 = N(1+2r^2), \quad \sigma_1^2 = N[1+2R+2R^2+2(1+2R)r^2], \quad (128)$$

since setting signal-to-noise ratio $R=0$ corresponds to hypothesis 0, signal absent. Substitution in (86) yields the normal probability approximation

$$y = \frac{N^{1/2} R + (1+2r^2)^{1/2} x}{[1+2R+2R^2+2(1+2R)r^2]^{1/2}} \quad (129)$$

These straight lines are superposed as dashed lines in figures 32-35 for $N=128$ and 256. The Gaussian approximation is moderately good for large N such as 256, and in fact crosses the exact curves (solid) at a point which is labeled with the corresponding value of n in signal-to-noise ratio $R=2^n$.

An obvious shortcoming of the Gaussian approximation (129) is apparent:

$$\lim_{R \rightarrow \infty} y = \left(\frac{N}{2}\right)^{1/2} \quad \text{for any } x, r. \quad (130)$$

Reference to (85) then yields the interpretation

$$\lim_{R \rightarrow \infty} P_D = \Phi\left(\left(\frac{N}{2}\right)^{1/2}\right) < 1 \quad \text{for any } P_F, r. \quad (131)$$

That is, as input signal-to-noise ratio R tends to infinity, the approximate detection probability saturates at a value less than 1, regardless of the false alarm probability and normalized mean r . Thus the Gaussian approximation must certainly be inaccurate for large R ; the exact discrepancy for probabilities of practical interest is displayed in figures 32-35.

SUMMARY

A closed form expression for the characteristic function of the output of a crosscorrelator, with or without sample mean removal, has been derived in (23)-(24) for general values of: the number of terms added to yield the correlator output, the means and variances in each of the two input channels, the degree of correlation between the two channels, and the scale factor employed in the sample mean removal. A program for the evaluation of the cumulative and exceedance distribution functions of this general case has also been presented. These results can furnish the basis of a study of the error probabilities of a correlator required to decide between alternative hypotheses on the input statistics [1]; this problem will in fact be the subject of a future technical report by this author.

The general results were first specialized to a signal and noise model, and then to the two distinct cases of sample mean removal ($\gamma=1$) and no sample mean removal ($\gamma=0$). Plots of the operating characteristics for numerous values of N and signal-to-noise ratio R were then displayed for a wide range of detection probability vs false alarm probability. Some new analytic results for cumulative and exceedance distribution functions, especially for small N , were derived and used as checks on the general numerical procedure. Comparisons with a Gaussian approximation indicated quantitatively when that simplification is valid. Asymptotic results derived were useful for small N , but not for large N except in the region of probabilities too small to be of practical importance.

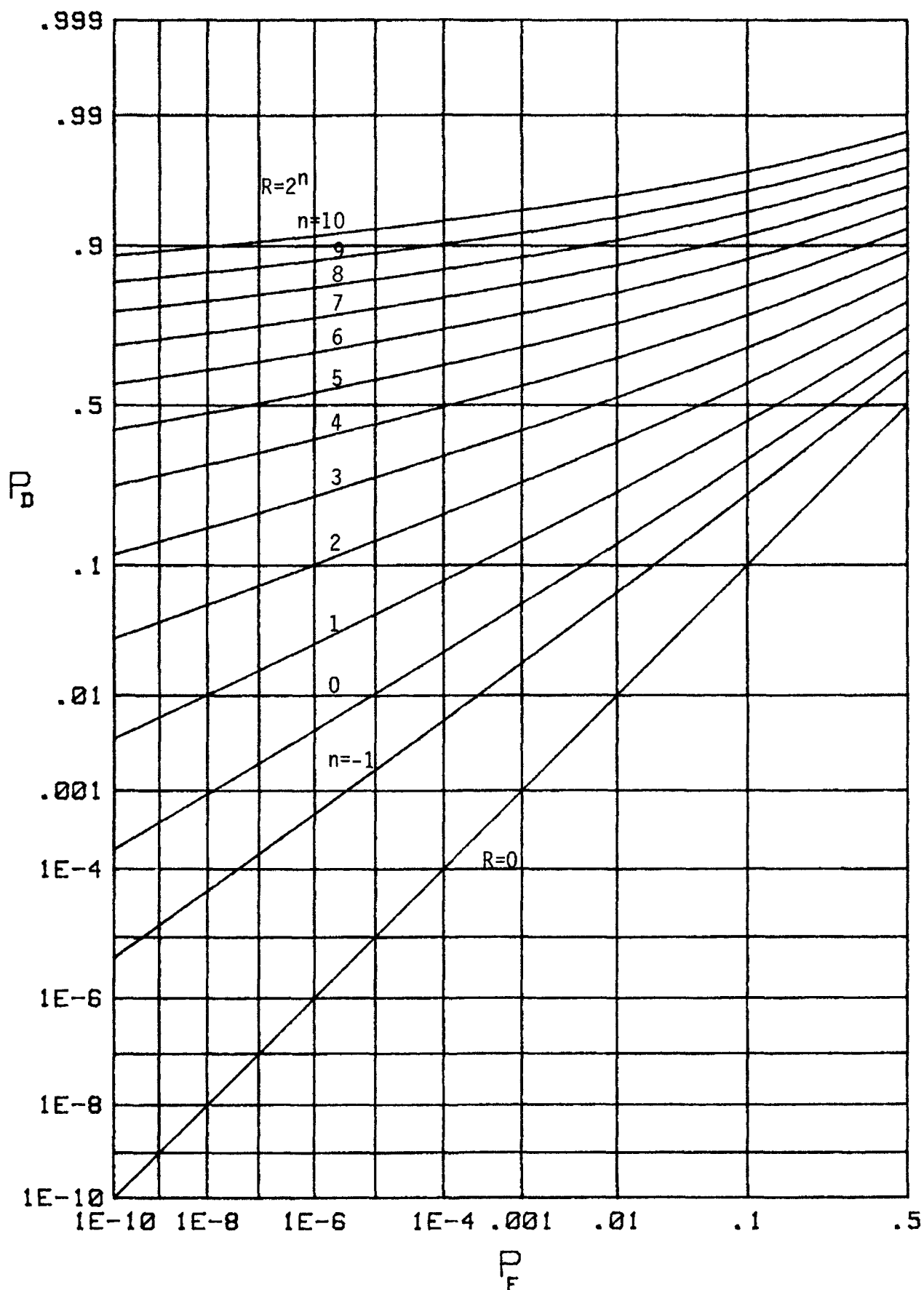


Figure 1. Operating Characteristics for Cross-Correlator with Sample Mean Removal, $N = 2$

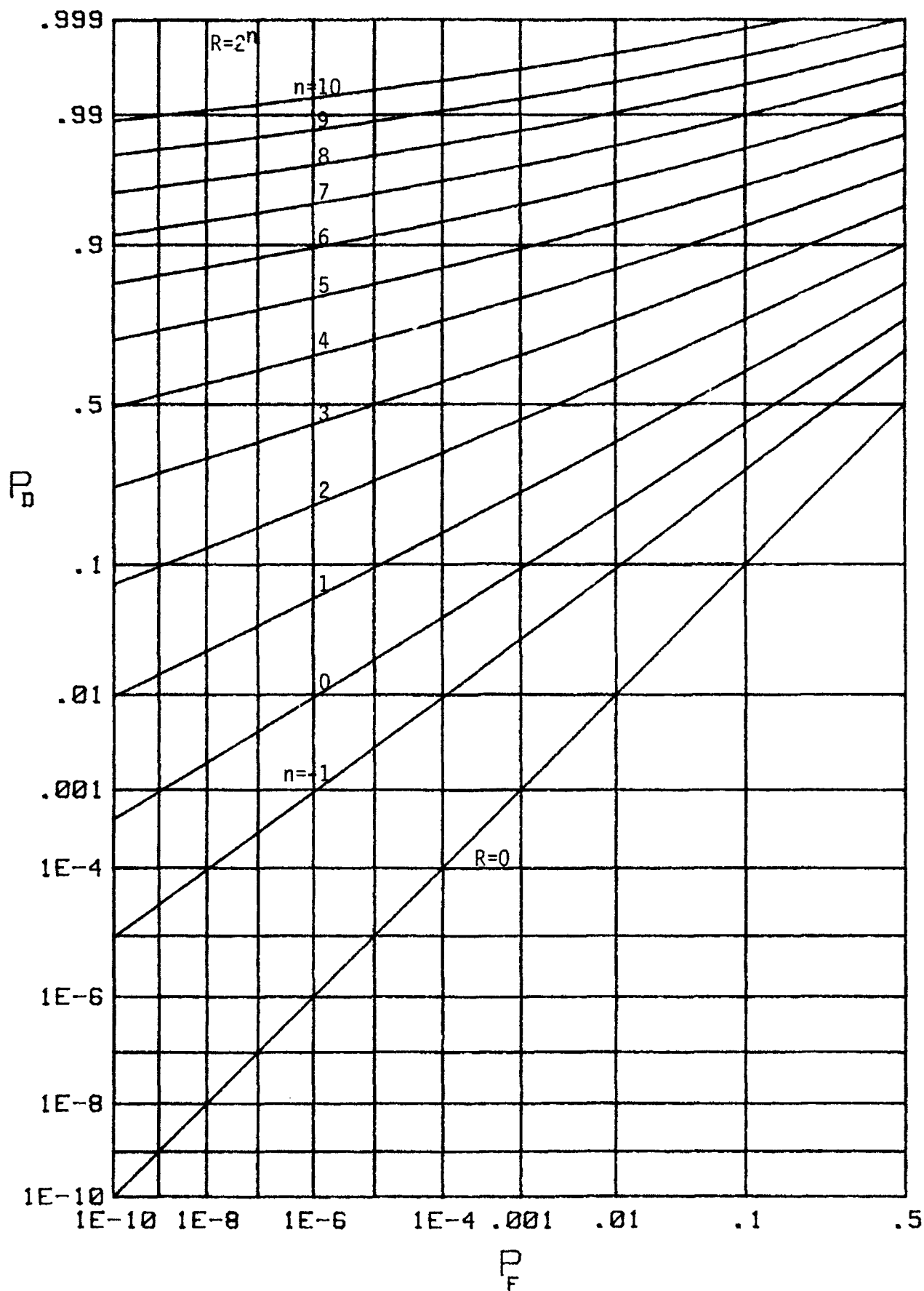


Figure 2. Operating Characteristics for Cross-Correlator with Sample Mean Removal, $N = 3$

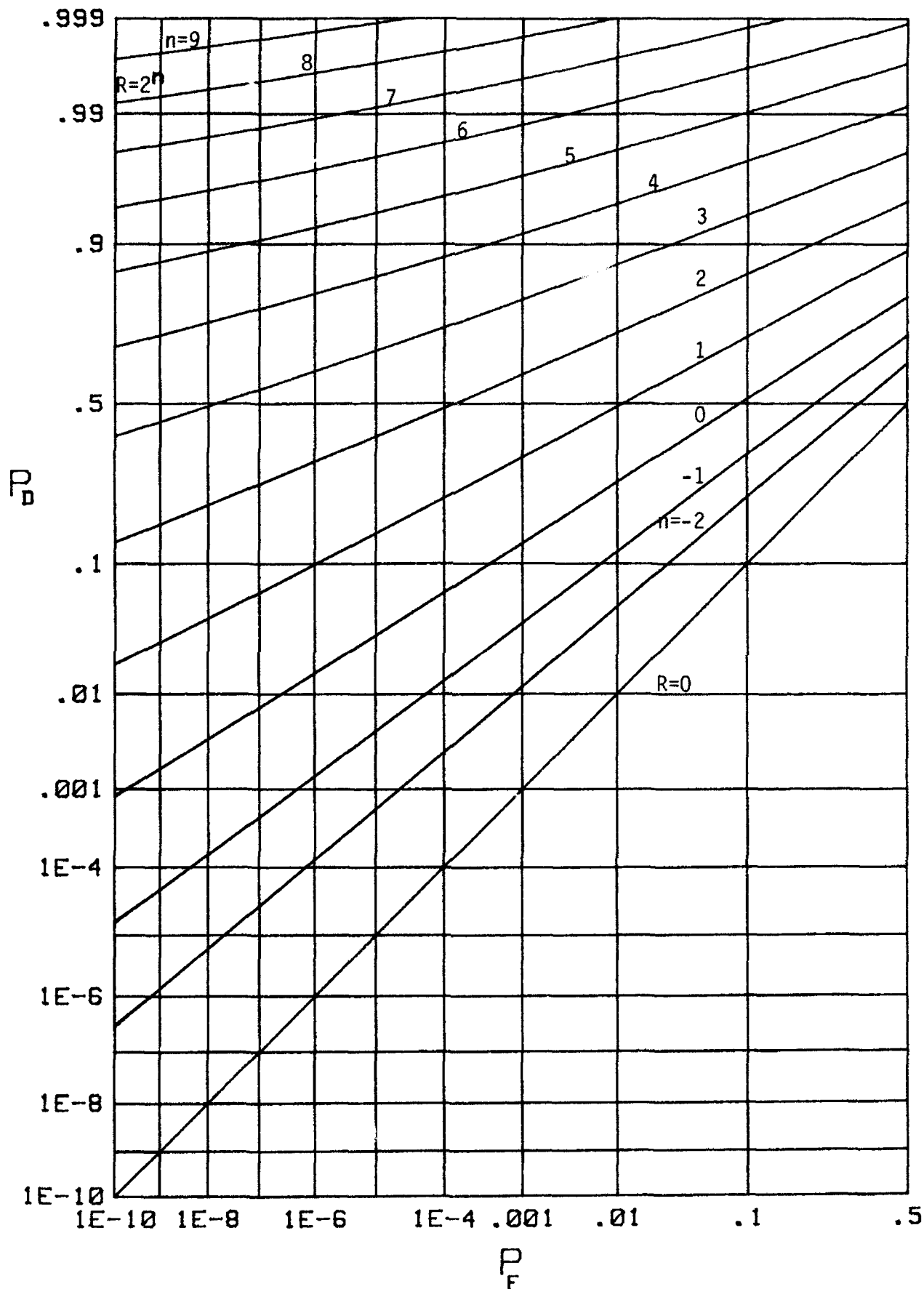


Figure 3. Operating Characteristics for Cross-Correlator with Sample Mean Removal, $N = 4$

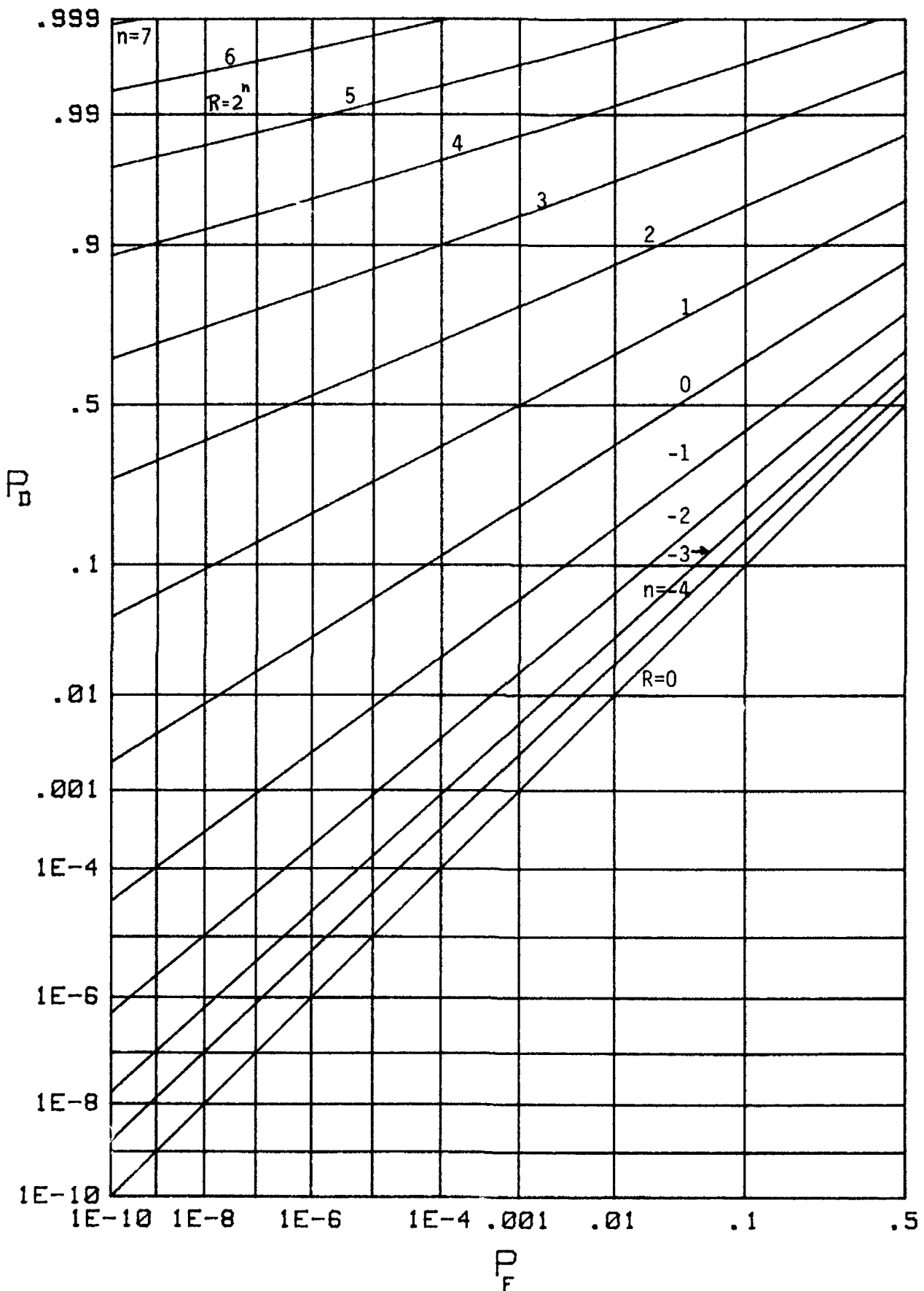


Figure 4. Operating Characteristics for Cross-Correlator with Sample Mean Removal, $N = 6$

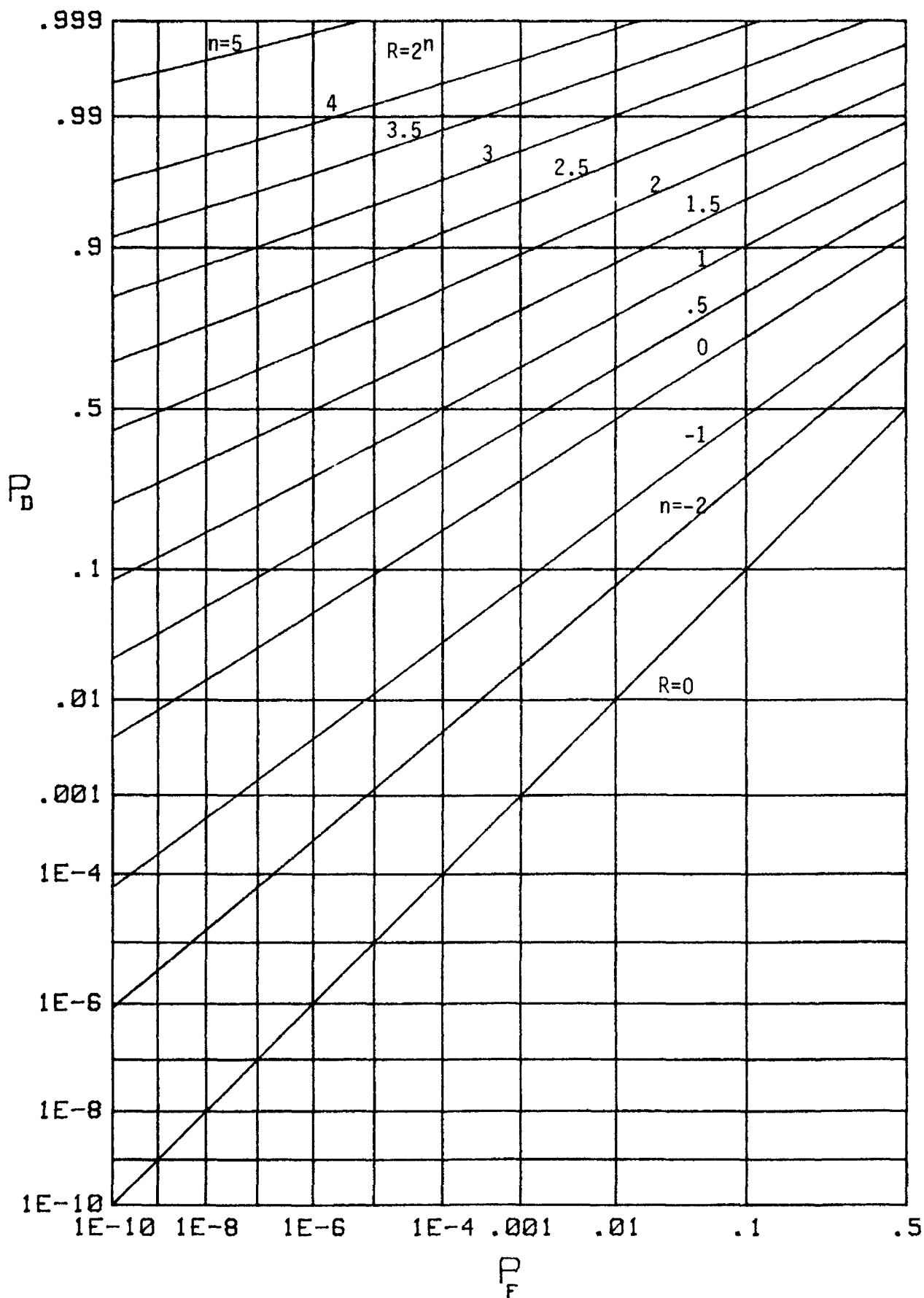


Figure 5. Operating Characteristics for Cross-Correlator with Sample Mean Removal, $N = 8$

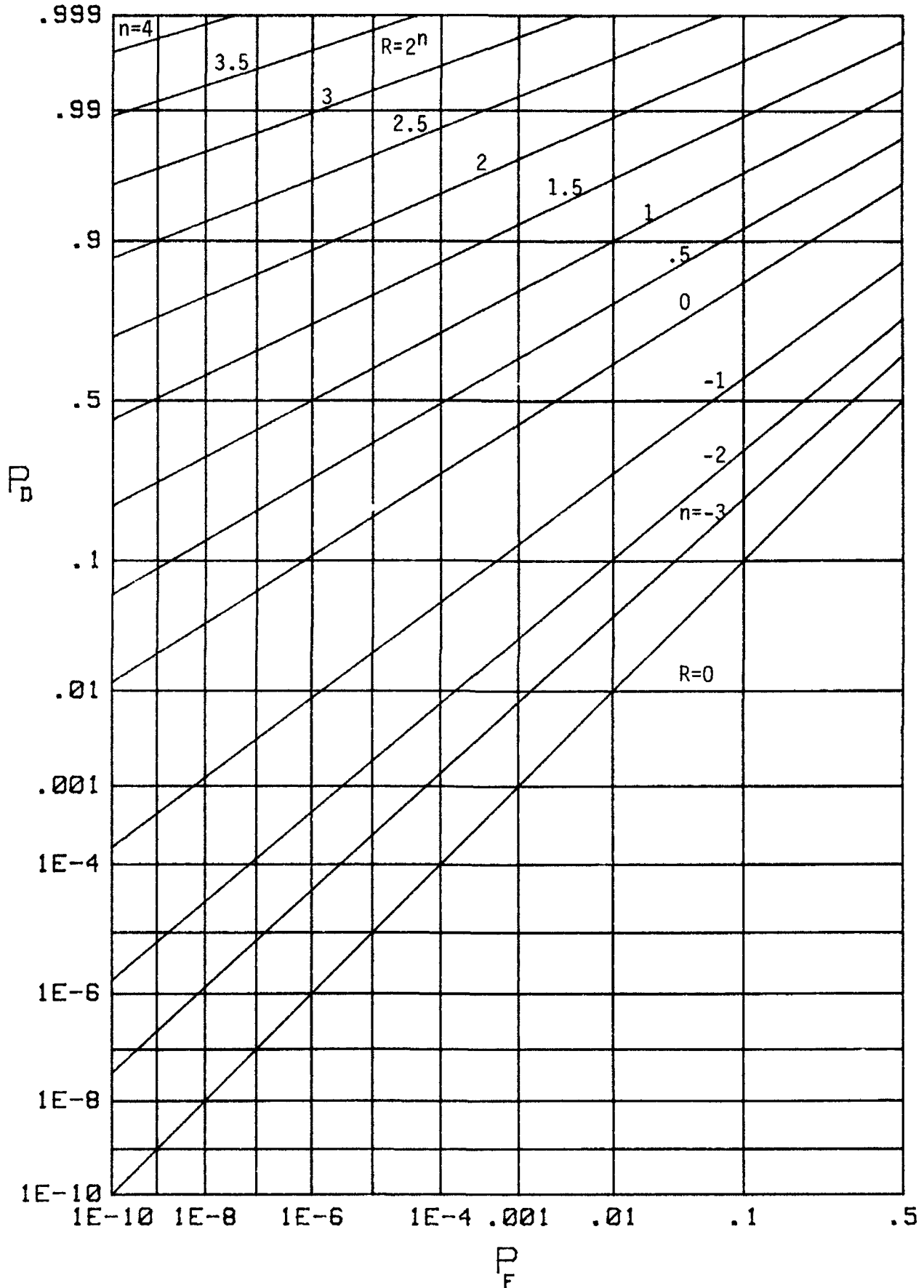


Figure 6. Operating Characteristics for Cross-Correlator with Sample Mean Removal, $N = 12$

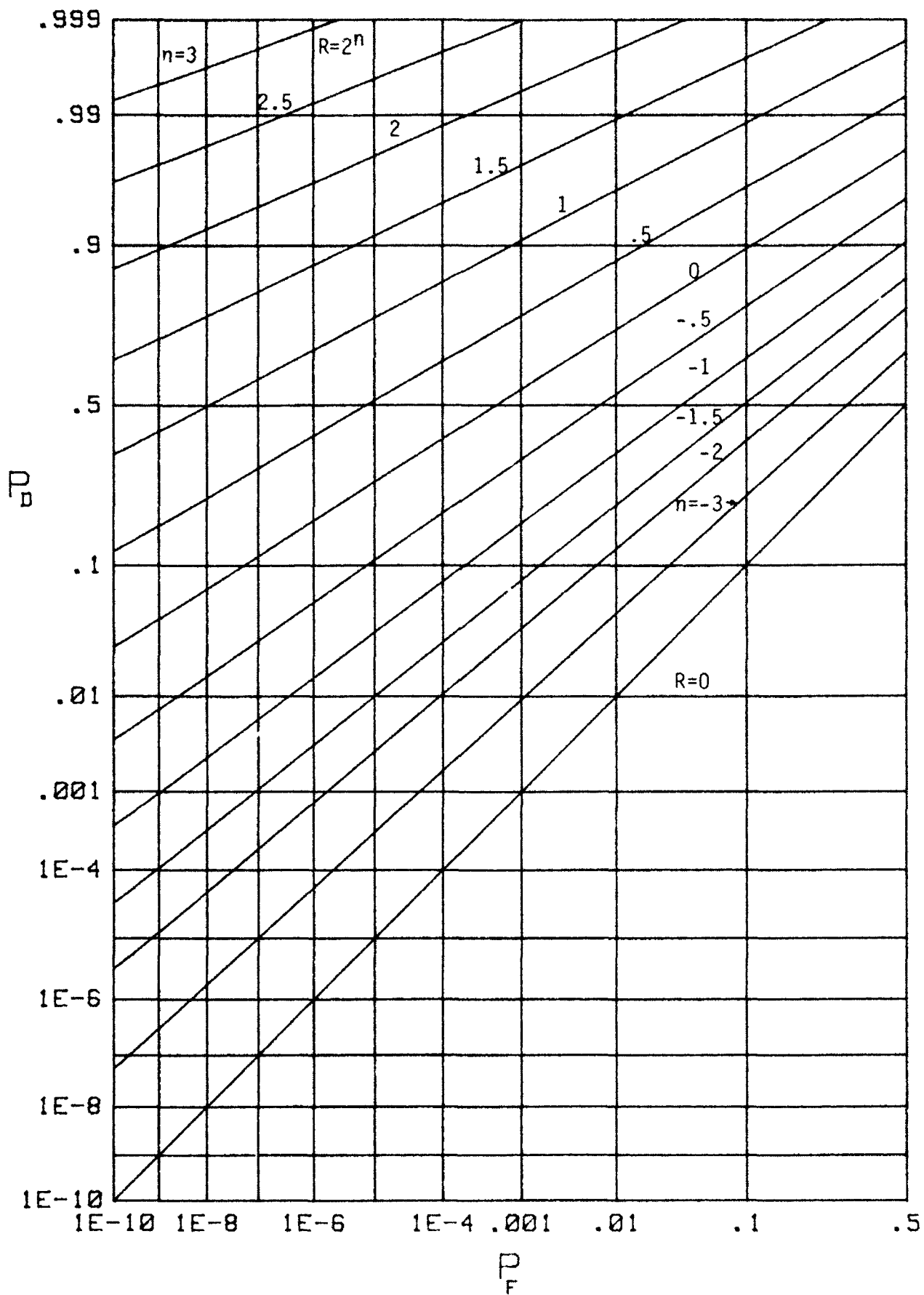


Figure 7. Operating Characteristics for Cross-Correlator with Sample Mean Removal, $N = 16$

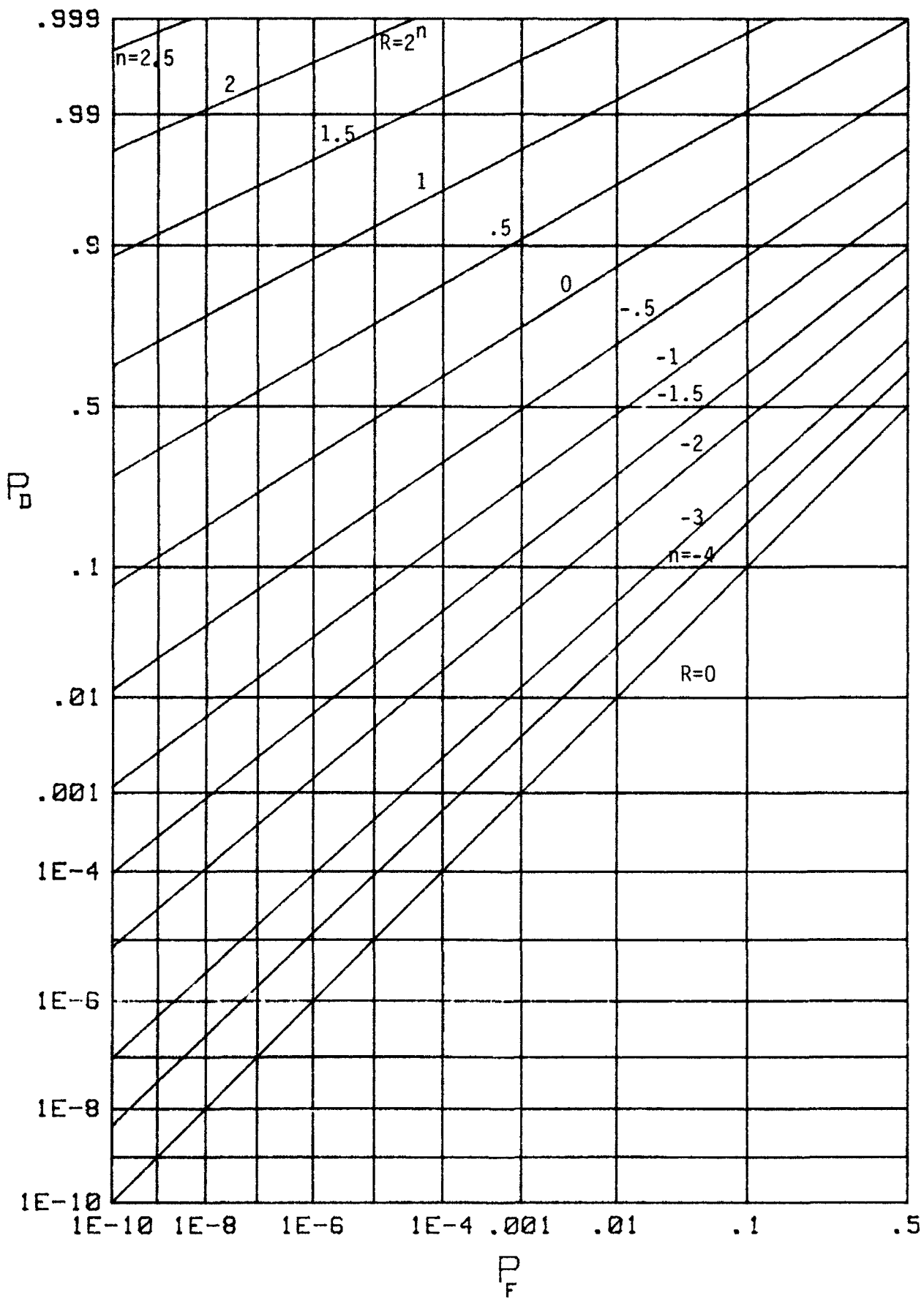


Figure 8. Operating Characteristics for Cross-Correlator with Sample Mean Removal, $N = 24$

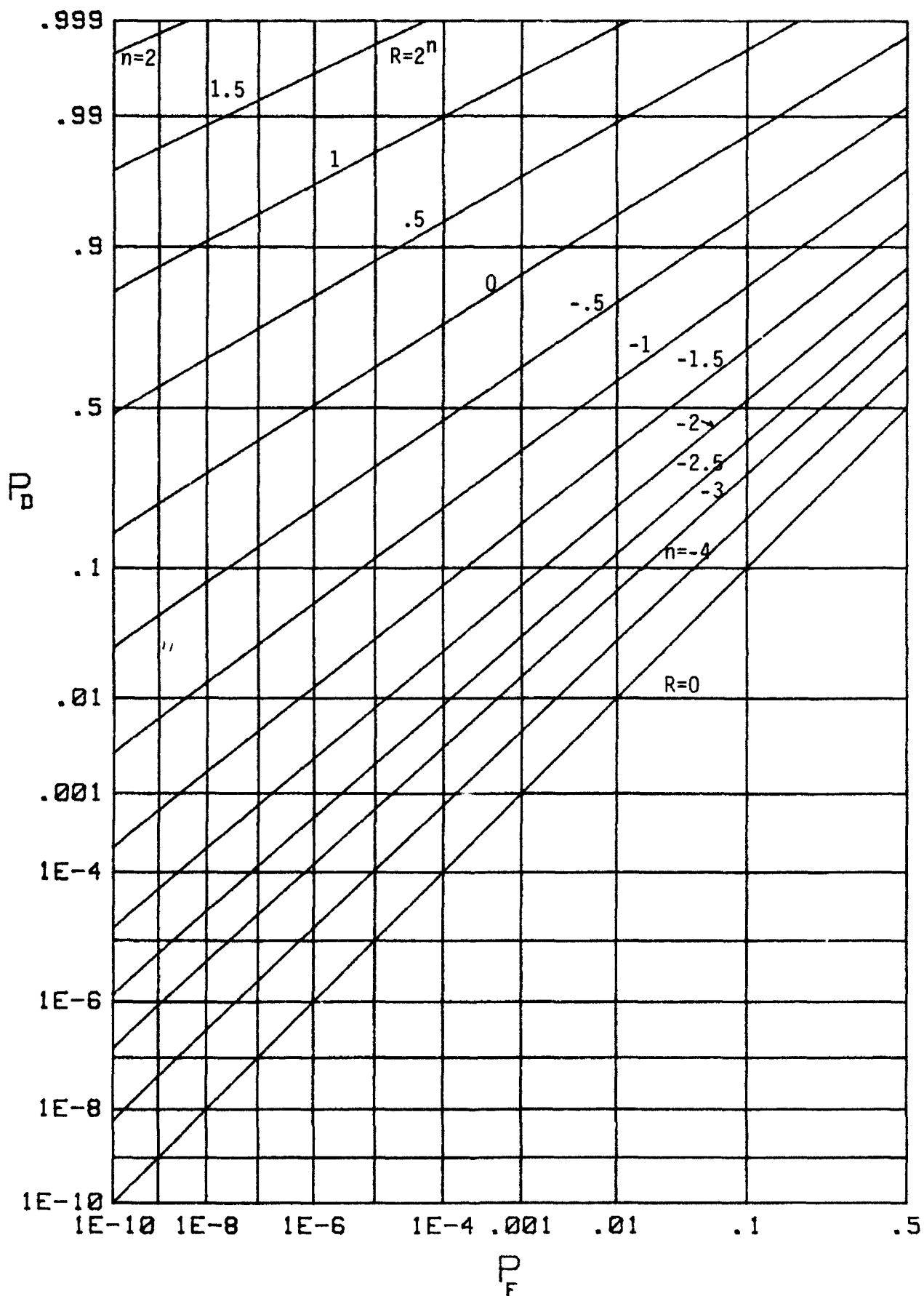


Figure 9. Operating Characteristics for Cross-Correlator with Sample Mean Removal, $N = 32$

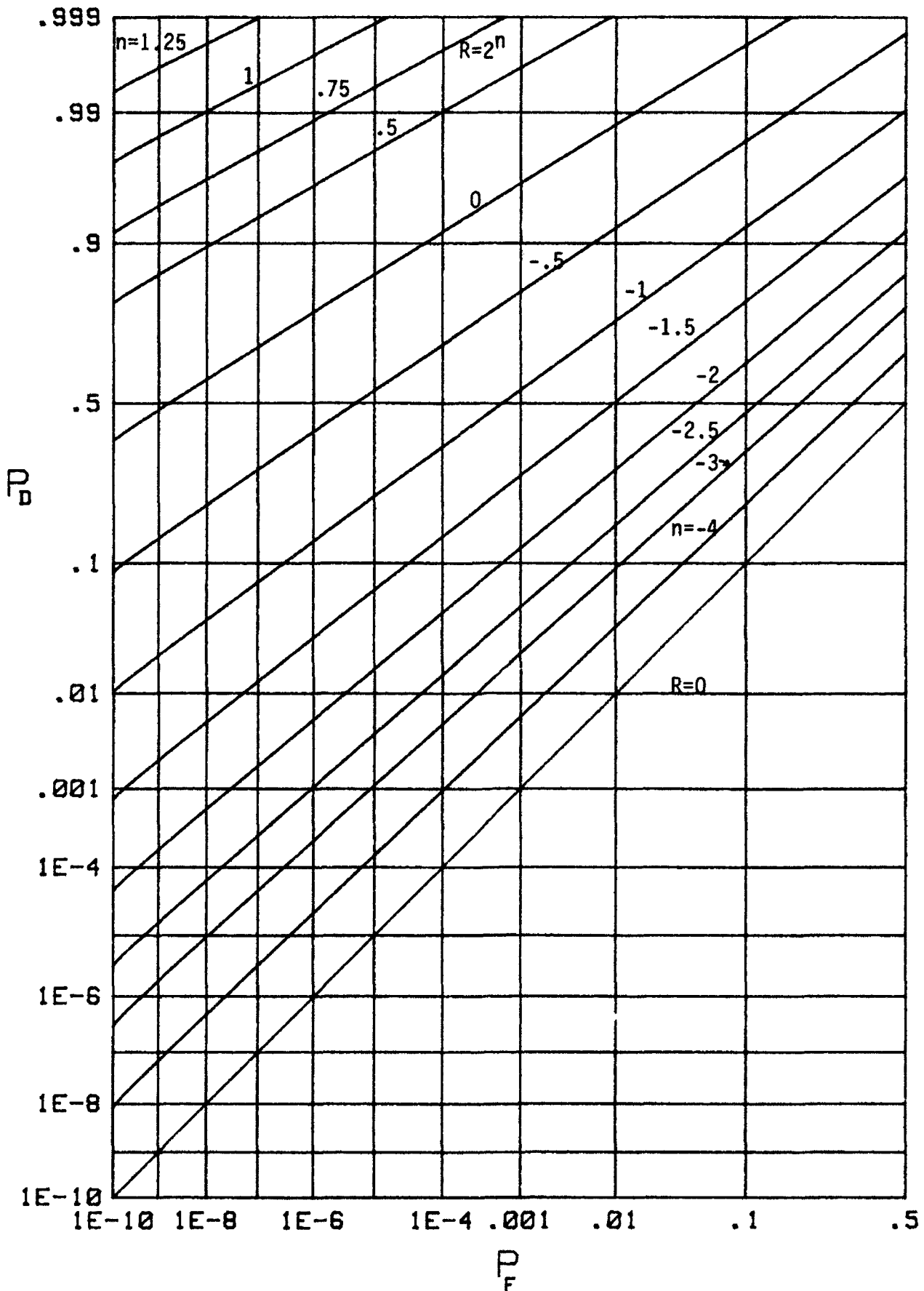


Figure 10. Operating Characteristics for Cross-Correlator with Sample Mean Removal, $N = 48$

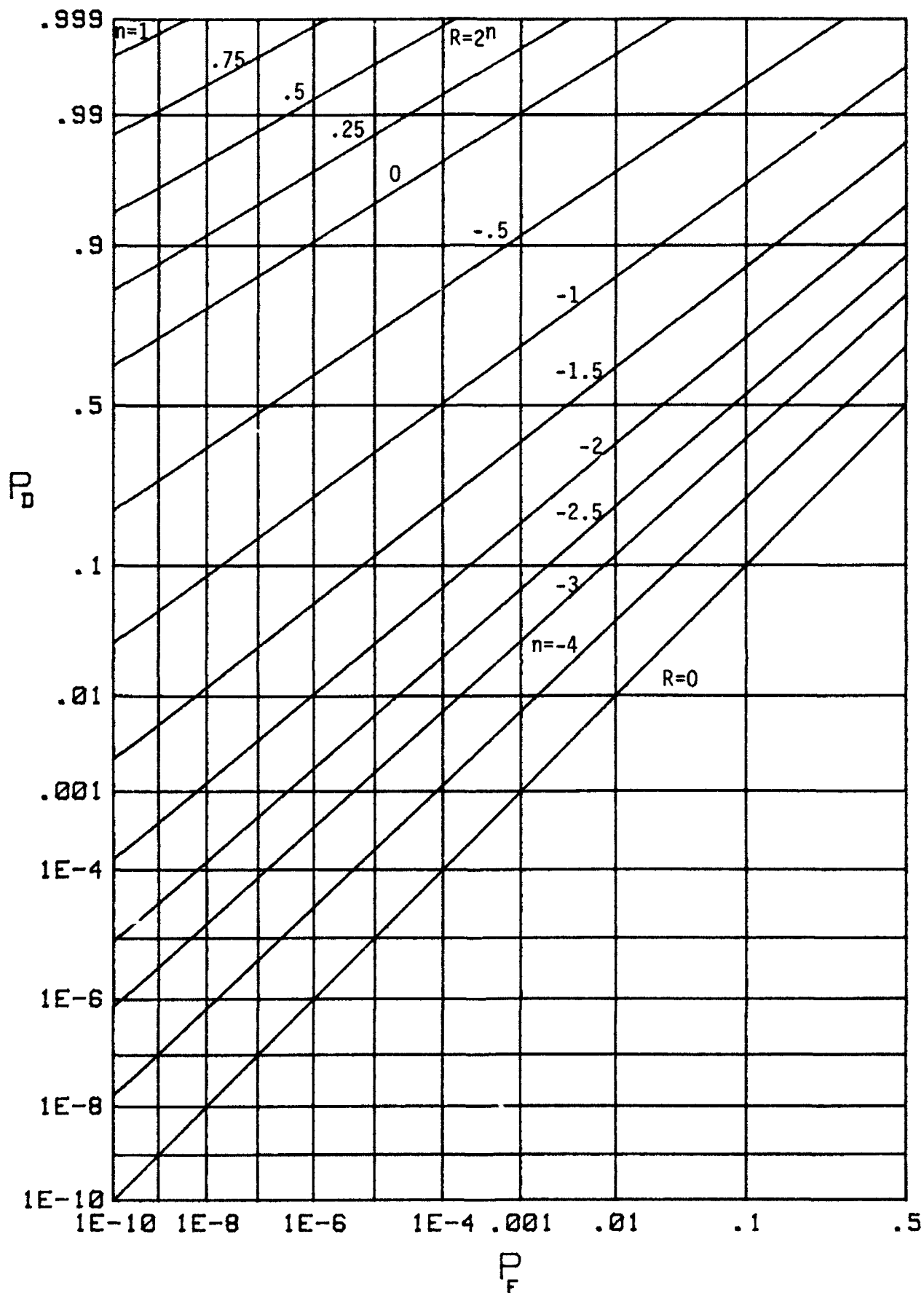


Figure 11. Operating Characteristics for Cross-Correlator with Sample Mean Removal, $N = 64$

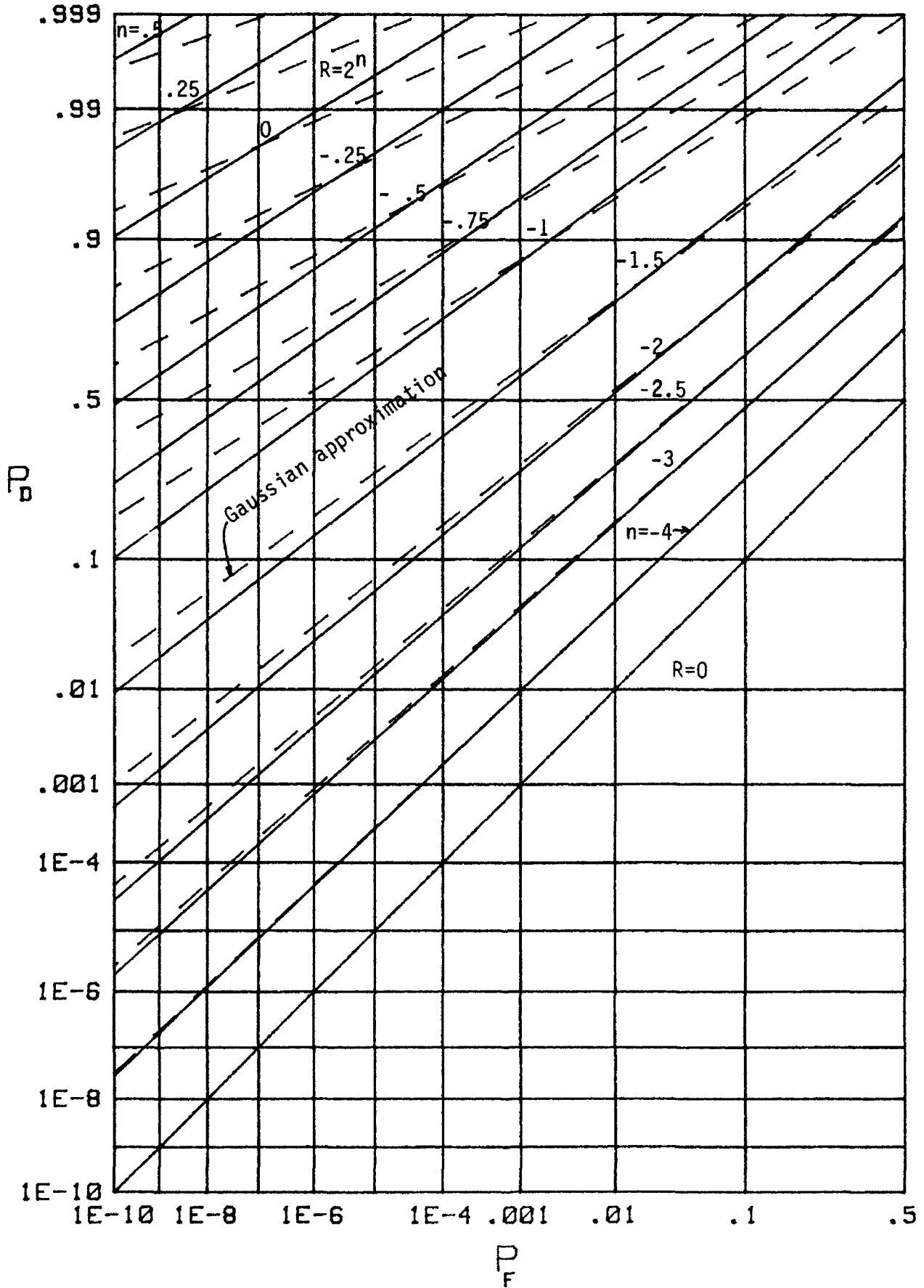


Figure 12. Operating Characteristics for Cross-Correlator with Sample Mean Removal, $N = 96$

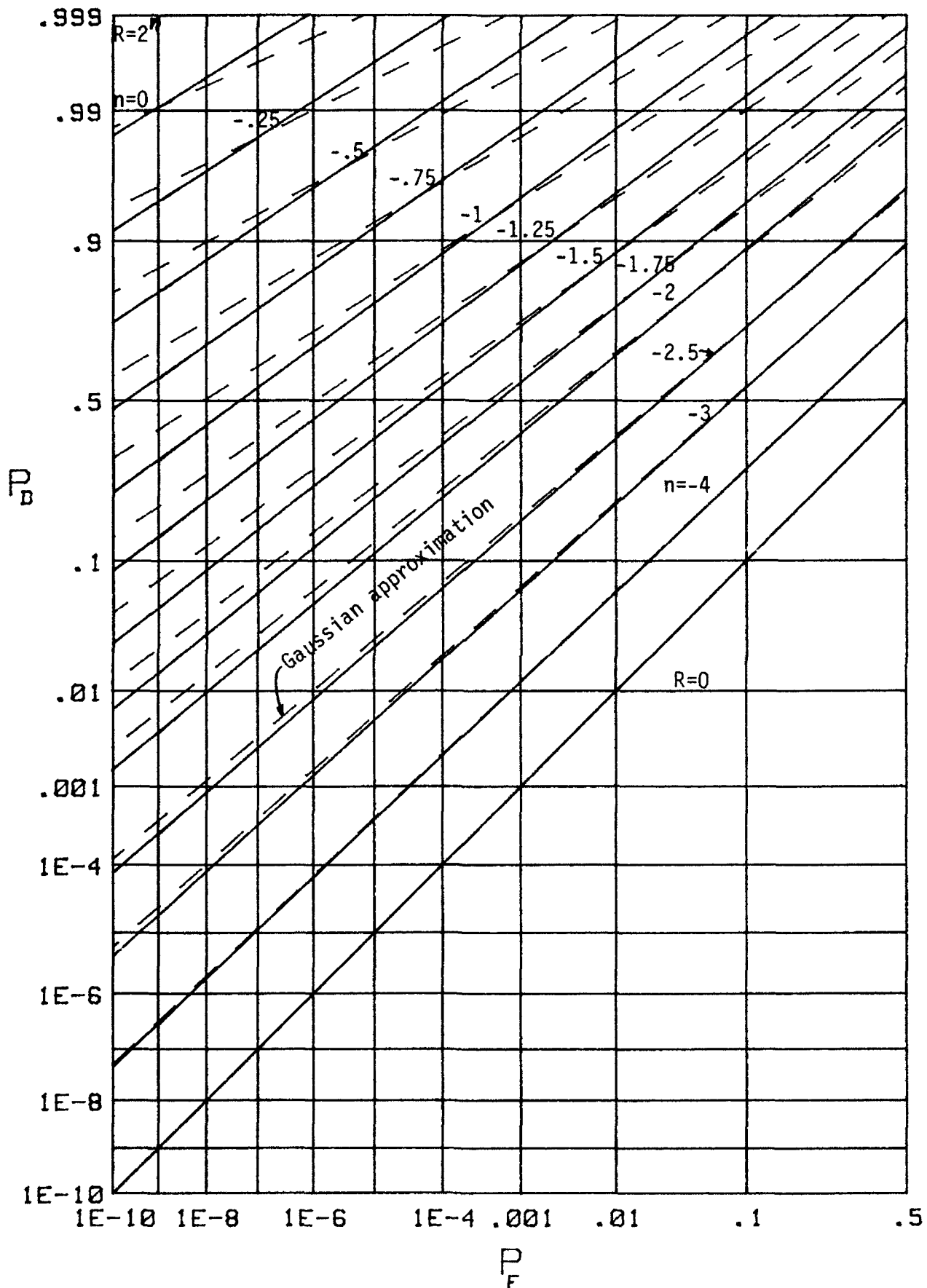


Figure 13. Operating Characteristics for Cross-Correlator with Sample Mean Removal, $N = 128$

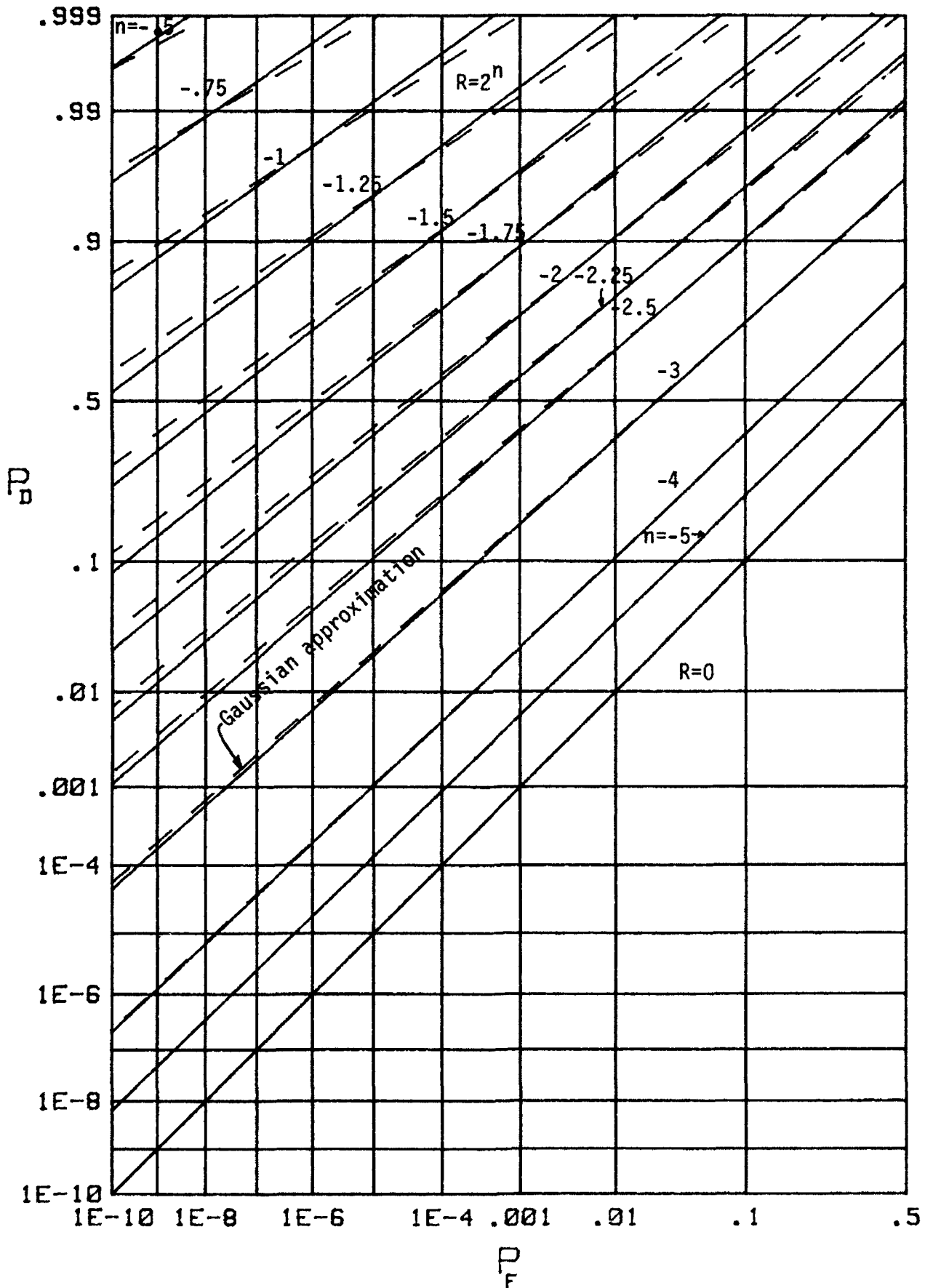


Figure 14. Operating Characteristics for Cross-Correlator with Sample Mean Removal, $N = 256$

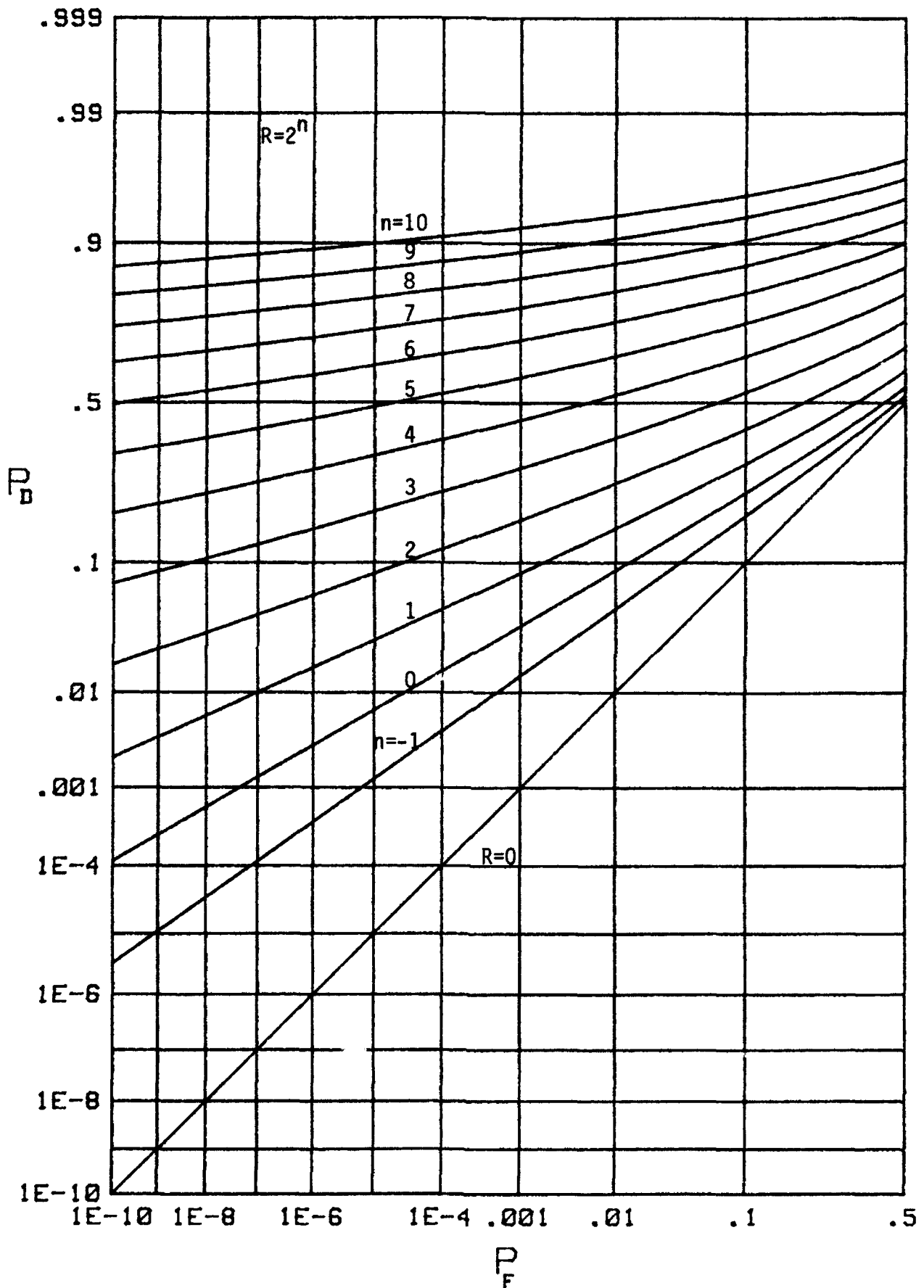


Figure 15. Operating Characteristics for Cross-Correlator without Sample Mean Removal, $N=1$, $r=1$

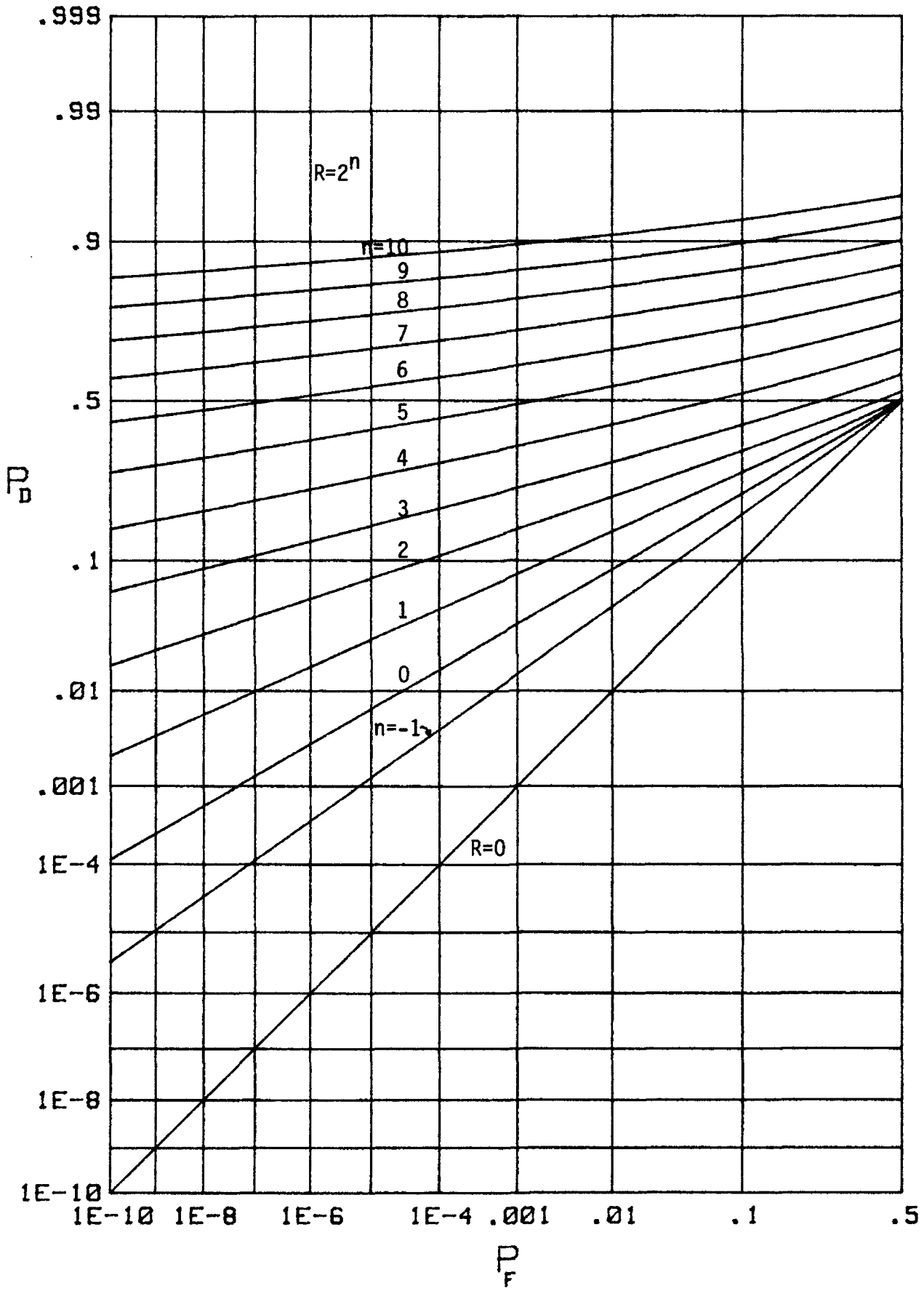


Figure 16. Operating Characteristics for Cross-Correlator without Sample Mean Removal, $N=1$, $r=2$

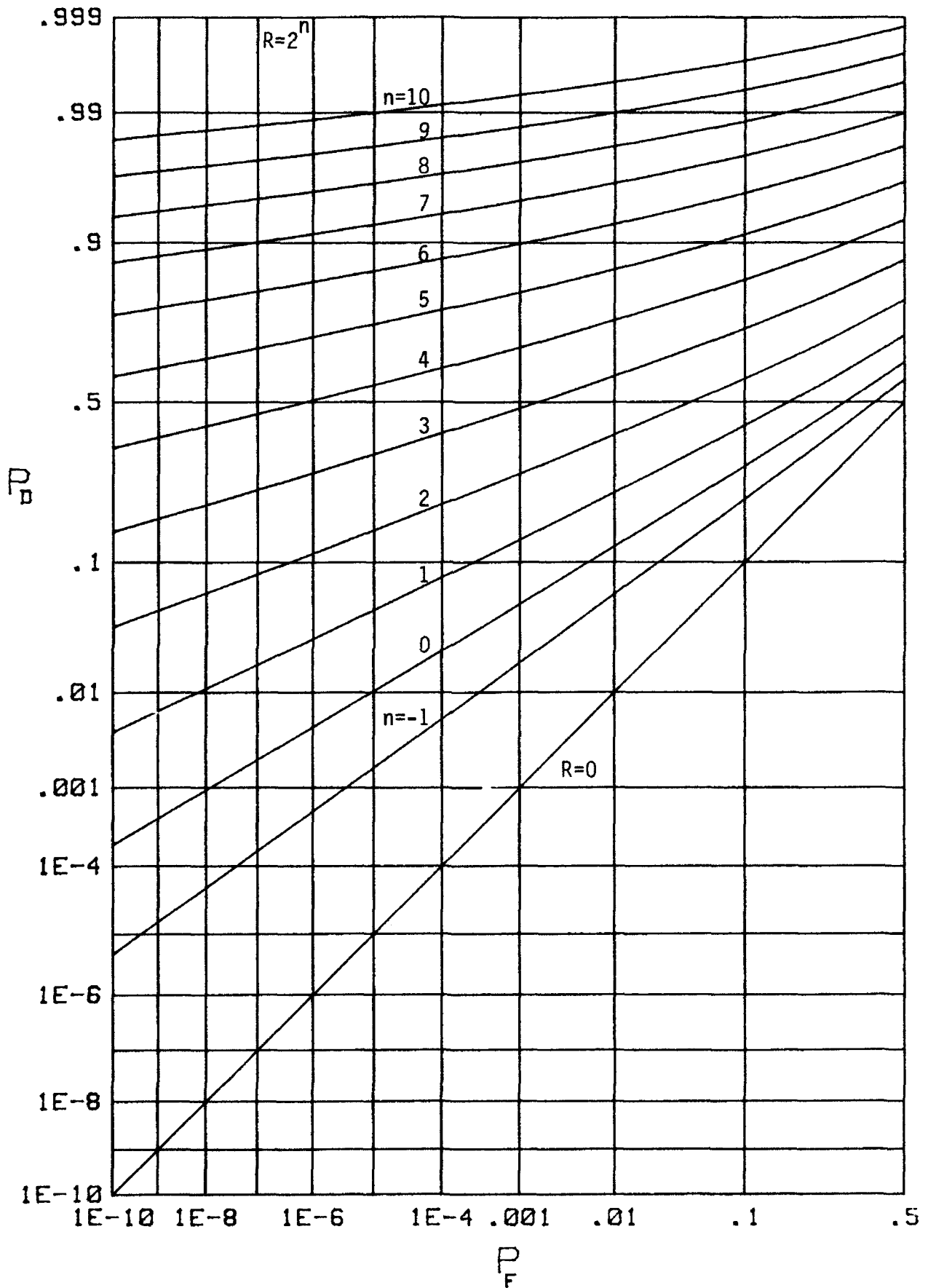


Figure 17. Operating Characteristics for Cross-Correlator without Sample Mean Removal, $N=2$, $r=1$

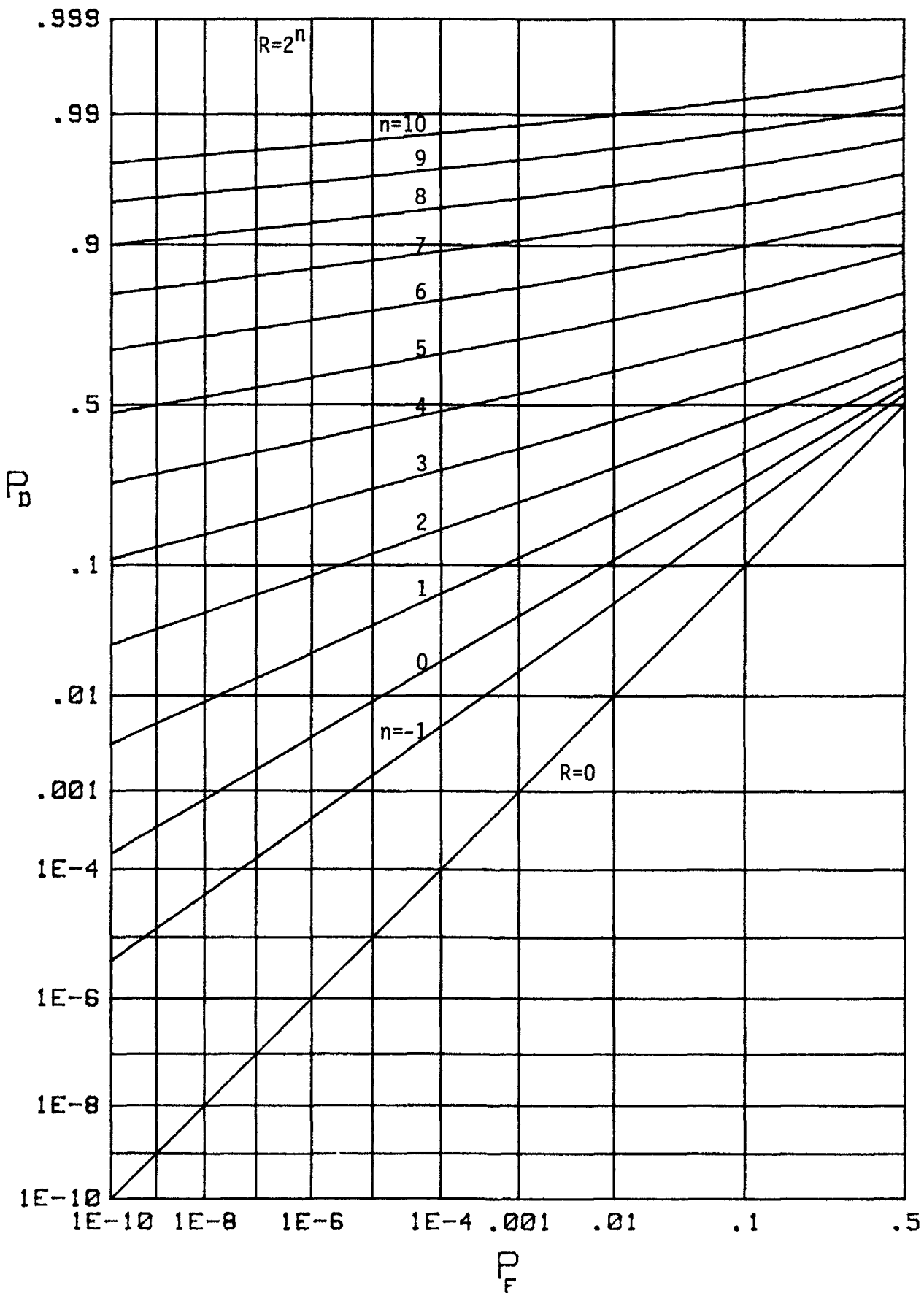


Figure 18. Operating Characteristics for Cross-Correlator without Sample Mean Removal, $N=2, r=2$

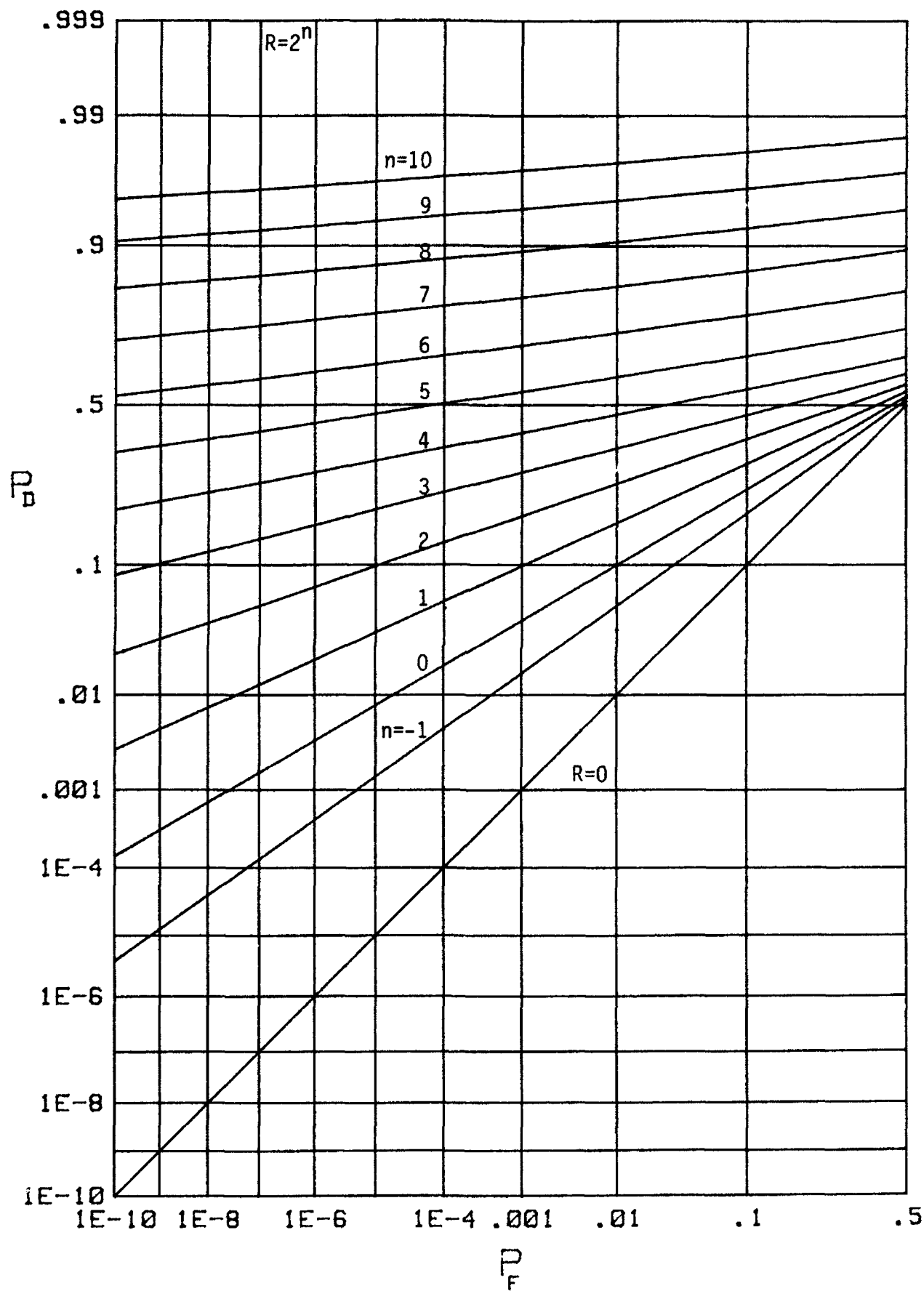


Figure 19. Operating Characteristics for Cross-Correlator without Sample Mean Removal, $N=2$, $r=4$

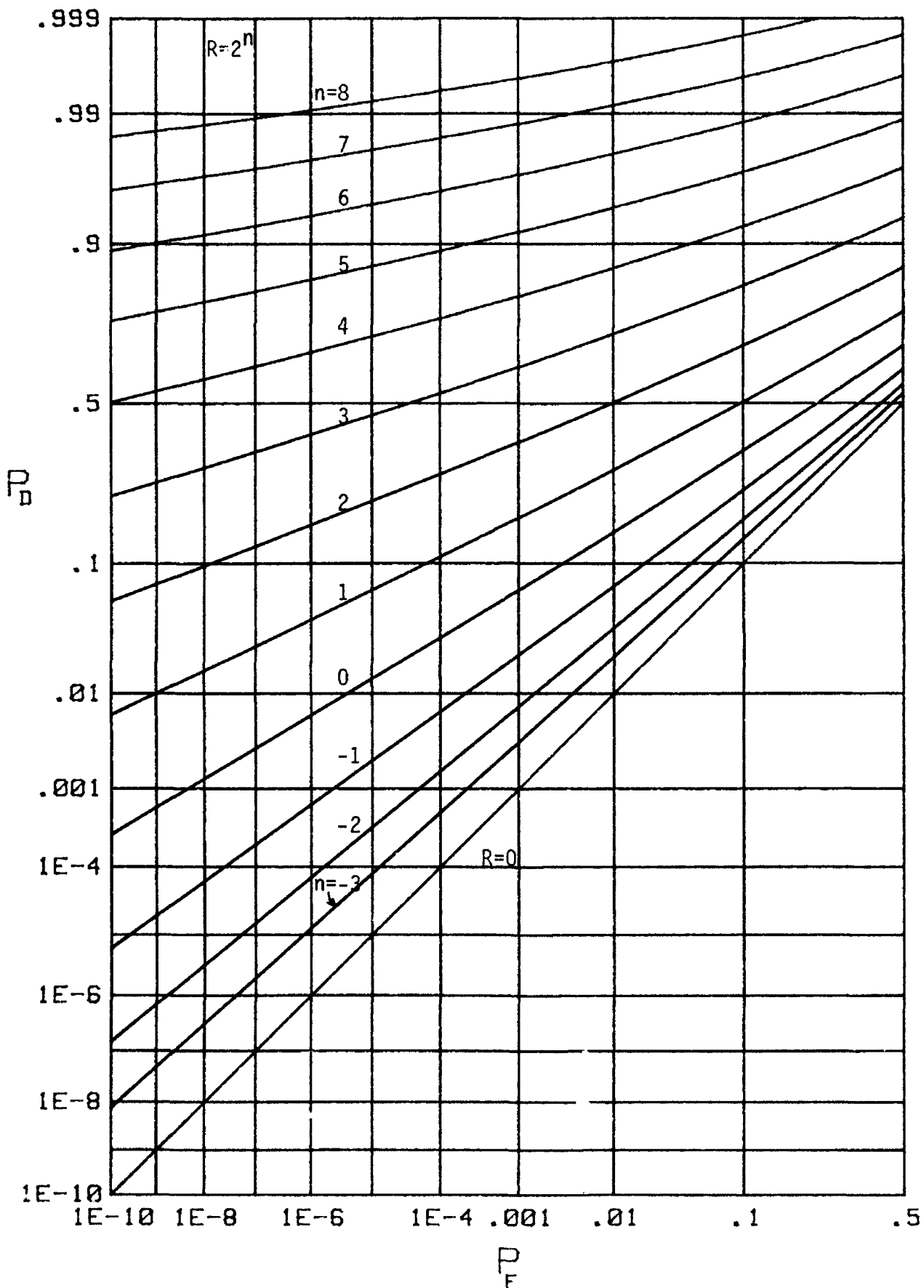


Figure 20. Operating Characteristics for Cross-Correlator without Sample Mean Removal, $N=3$, $r=1$

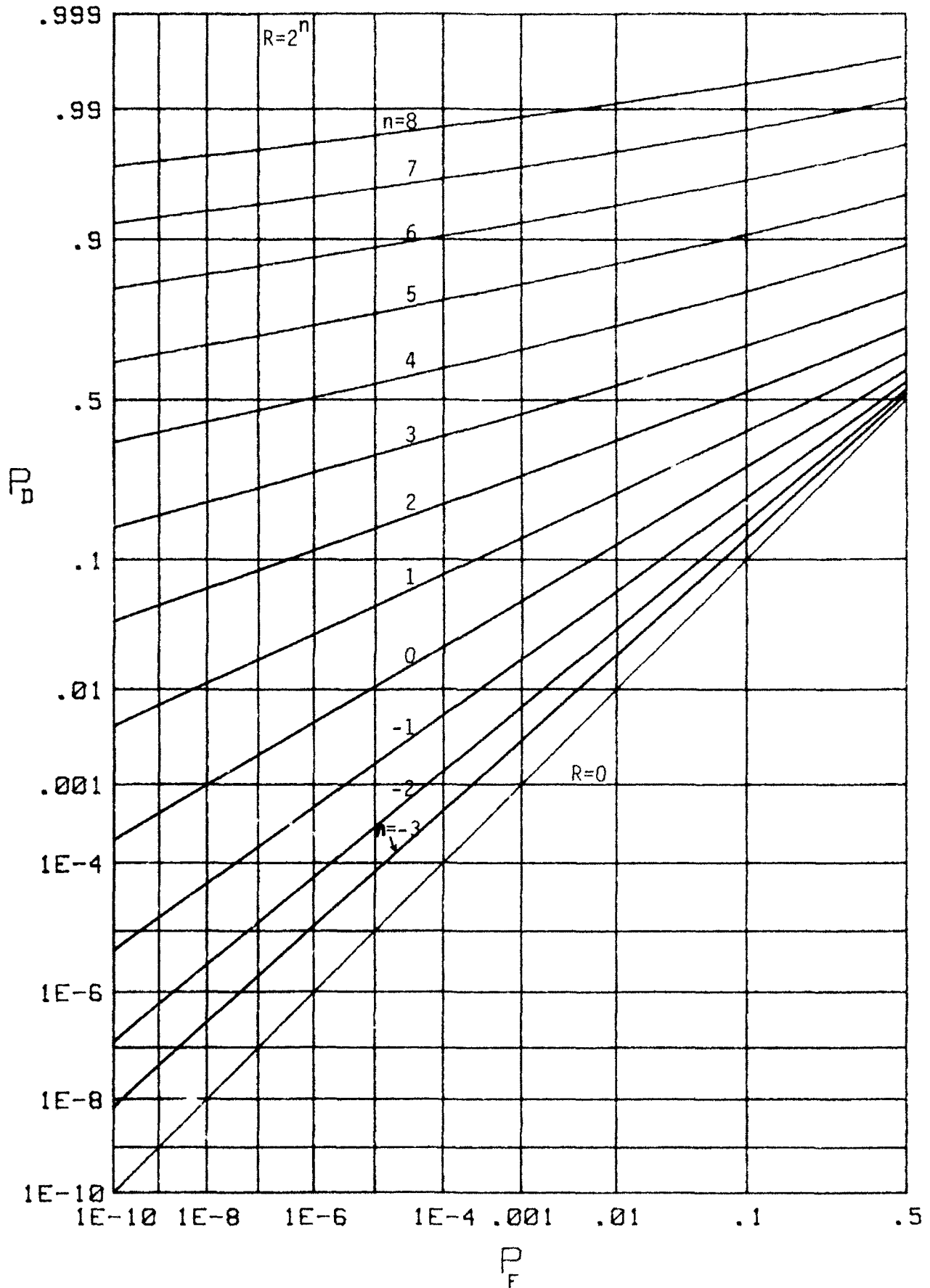


Figure 21. Operating Characteristics for Cross-Correlator without Sample Mean Removal, $N=3$, $r=2$

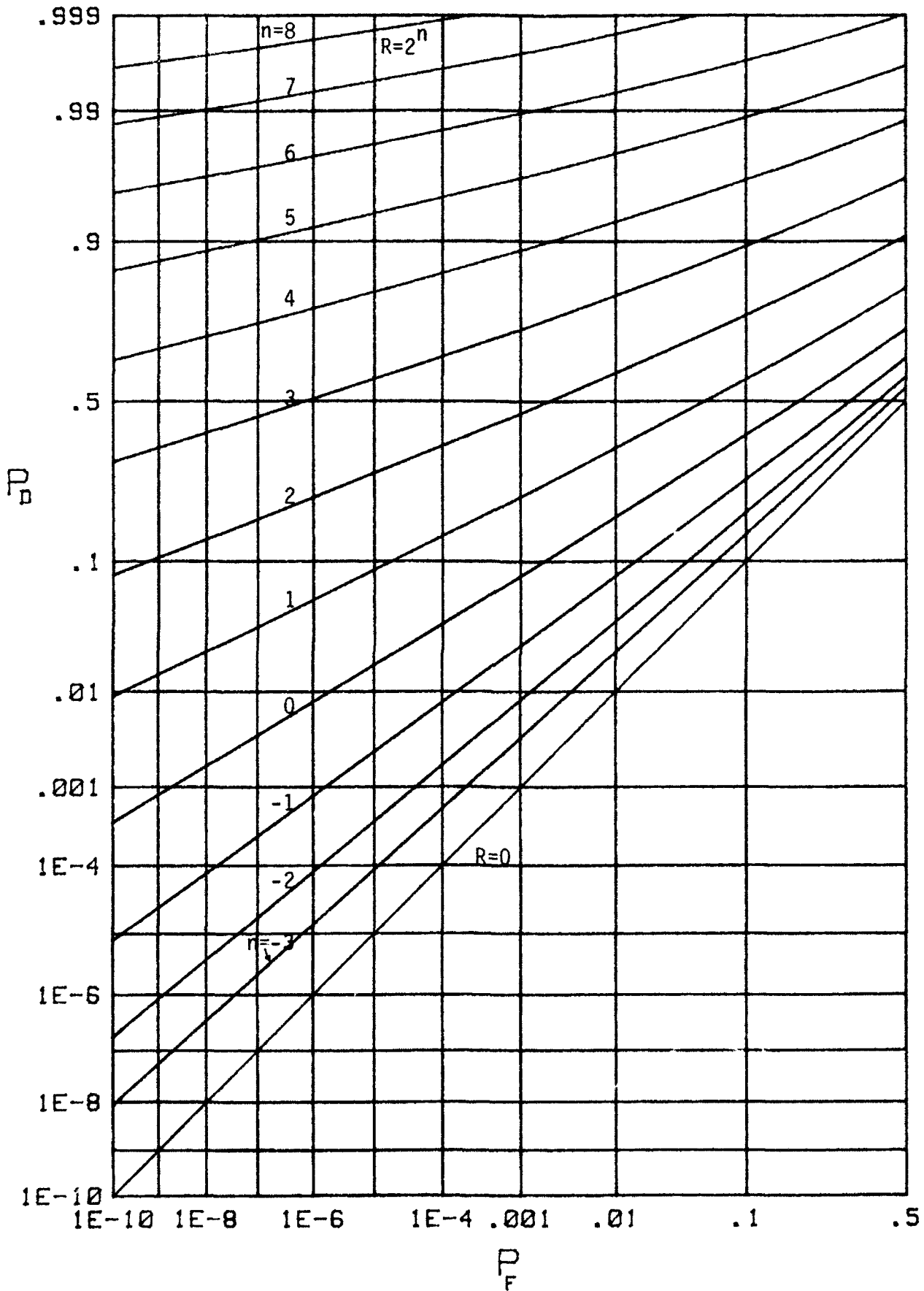


Figure 22. Operating Characteristics for Cross-Correlator without Sample Mean Removal, $N=4$, $r=1$

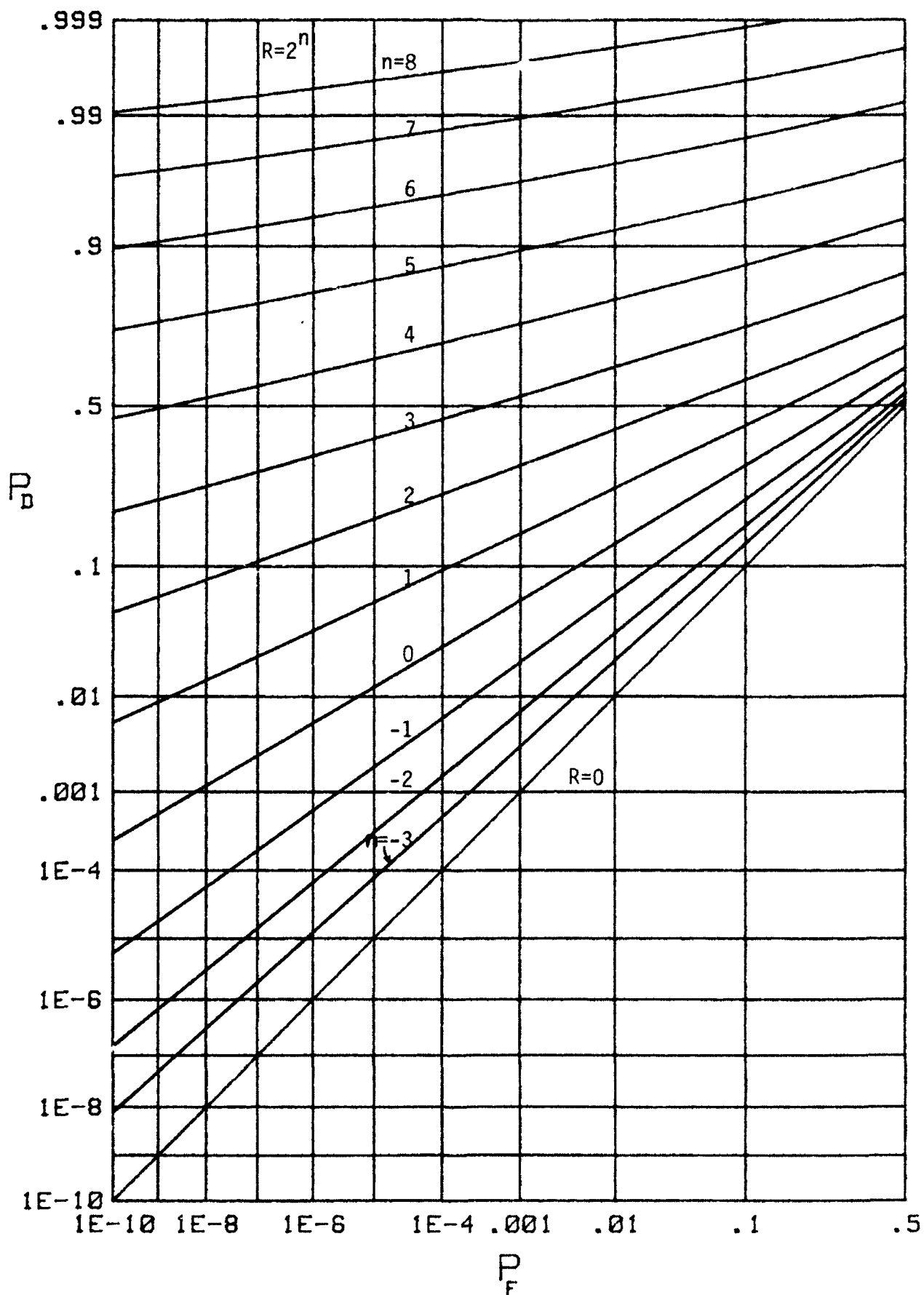


Figure 23. Operating Characteristics for Cross-Correlator without Sample Mean Removal, $N=4$, $r=2$

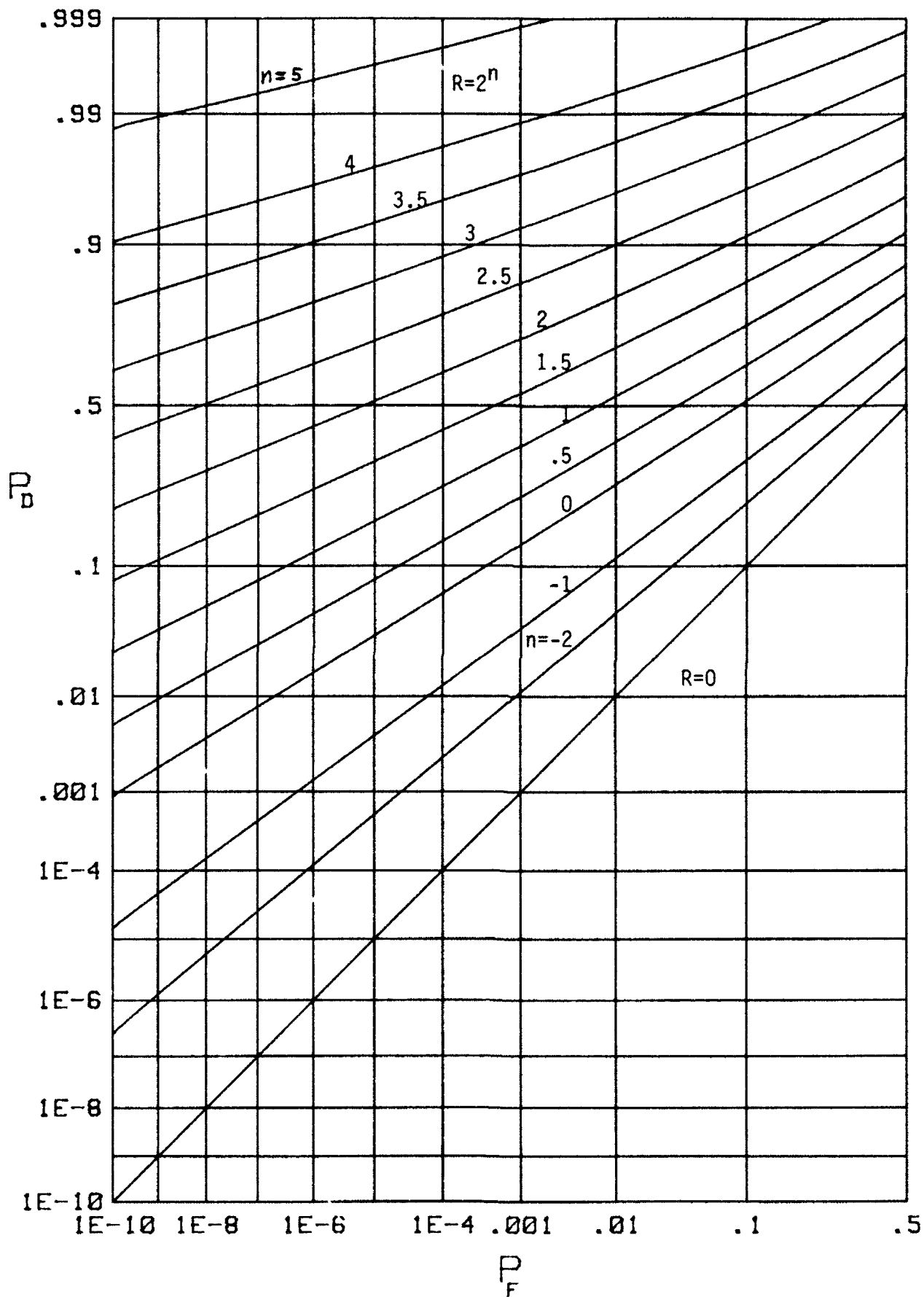


Figure 24. Operating Characteristics for Cross-Correlator without Sample Mean Removal, $N=8$, $r=1$

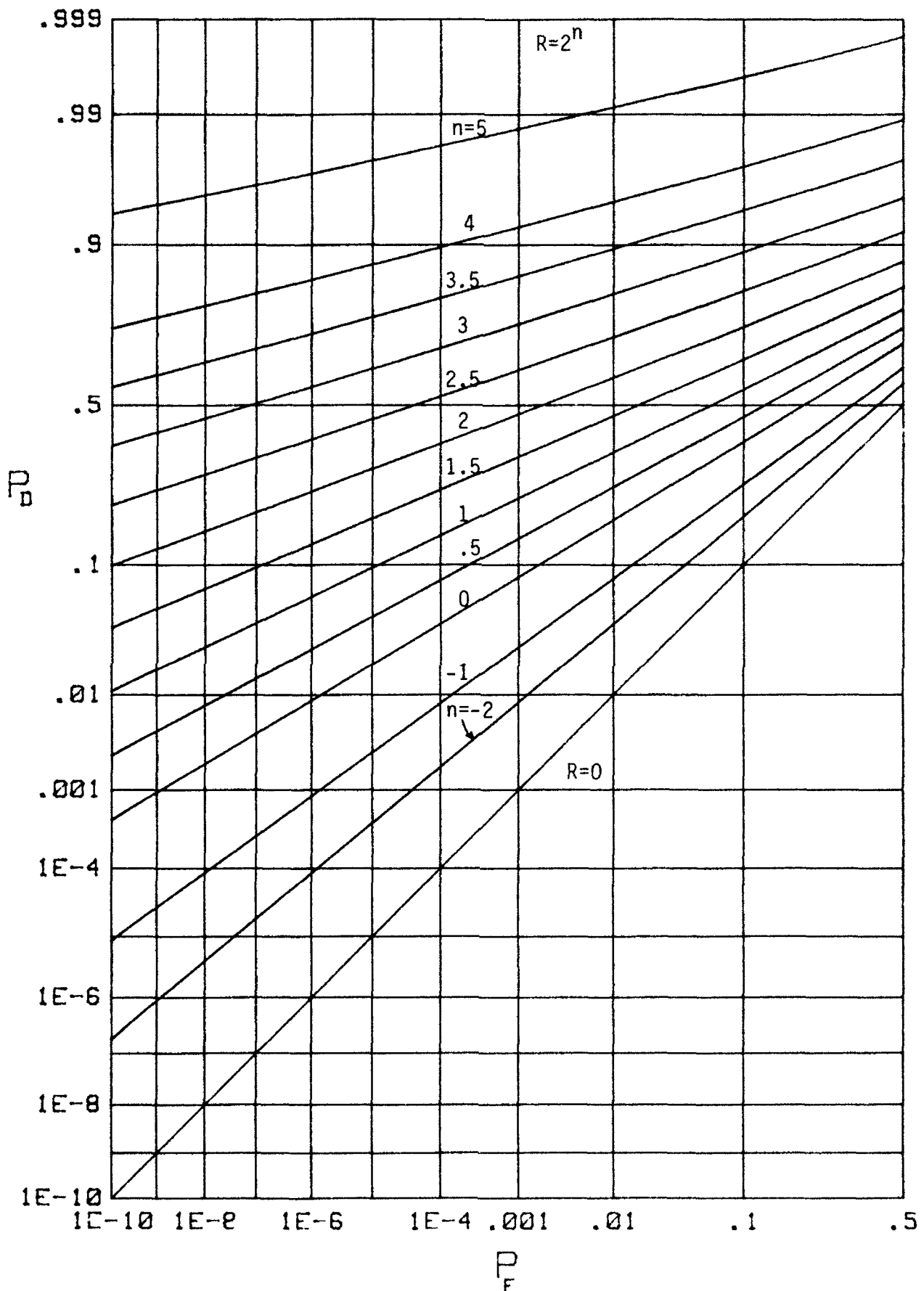


Figure 25. Operating Characteristics for Cross-Correlator without Sample Mean Removal, $N=8$, $r=2$

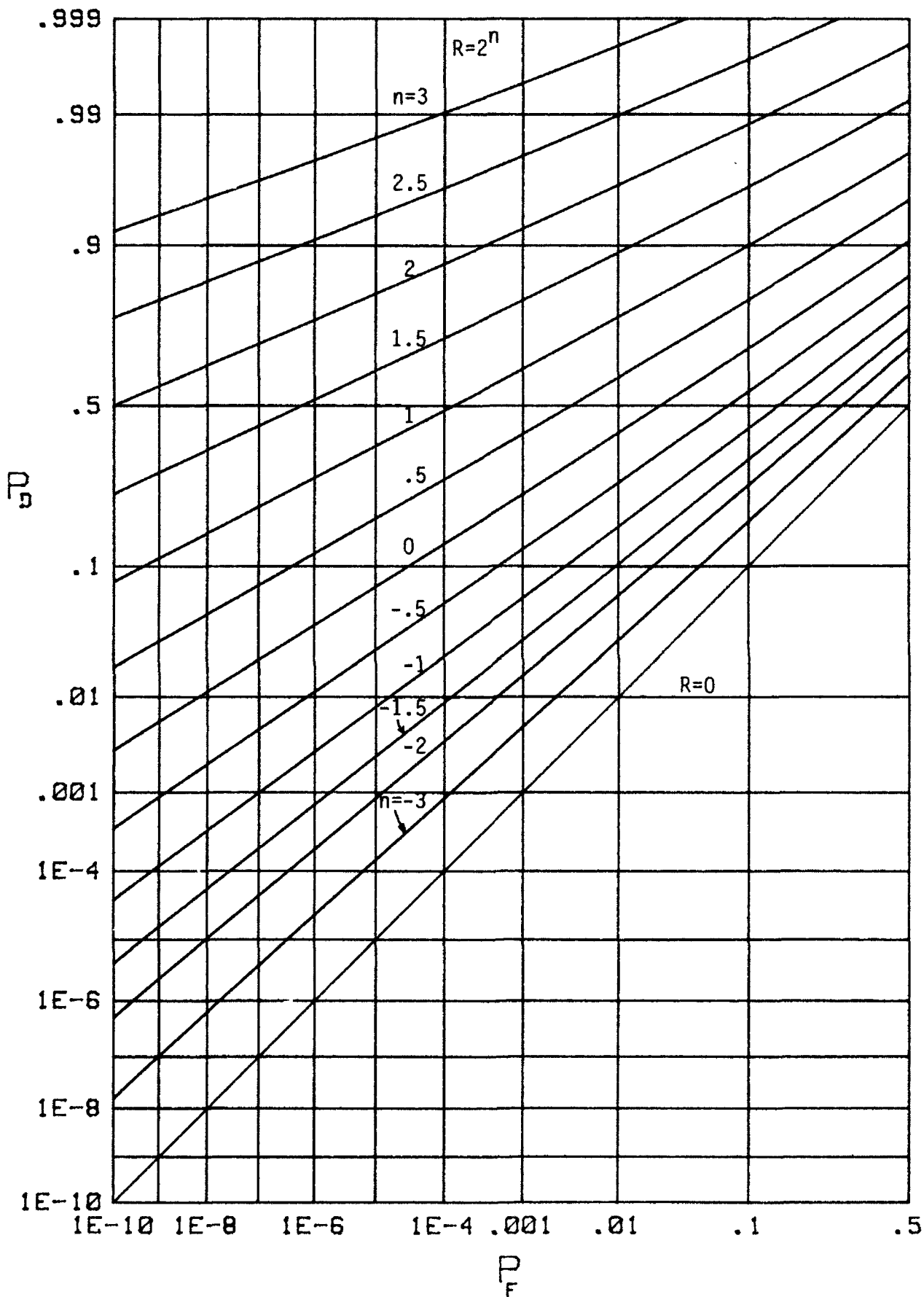


Figure 26. Operating Characteristics for Cross-Correlator without Sample Mean Removal, $N=16$, $r=1$

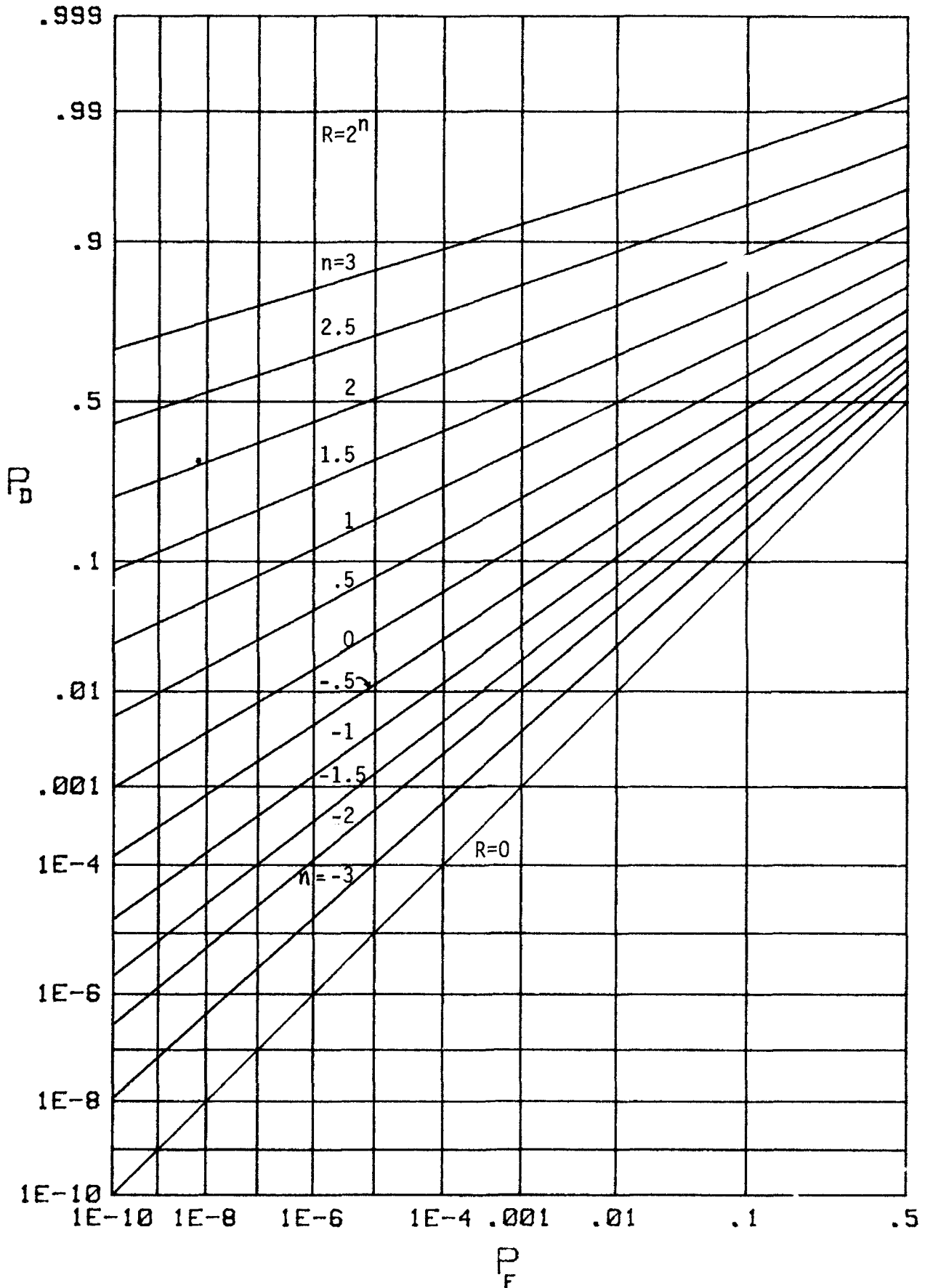


Figure 27. Operating Characteristics for Cross-Correlator without Sample Mean Removal, $N=16$, $r=2$

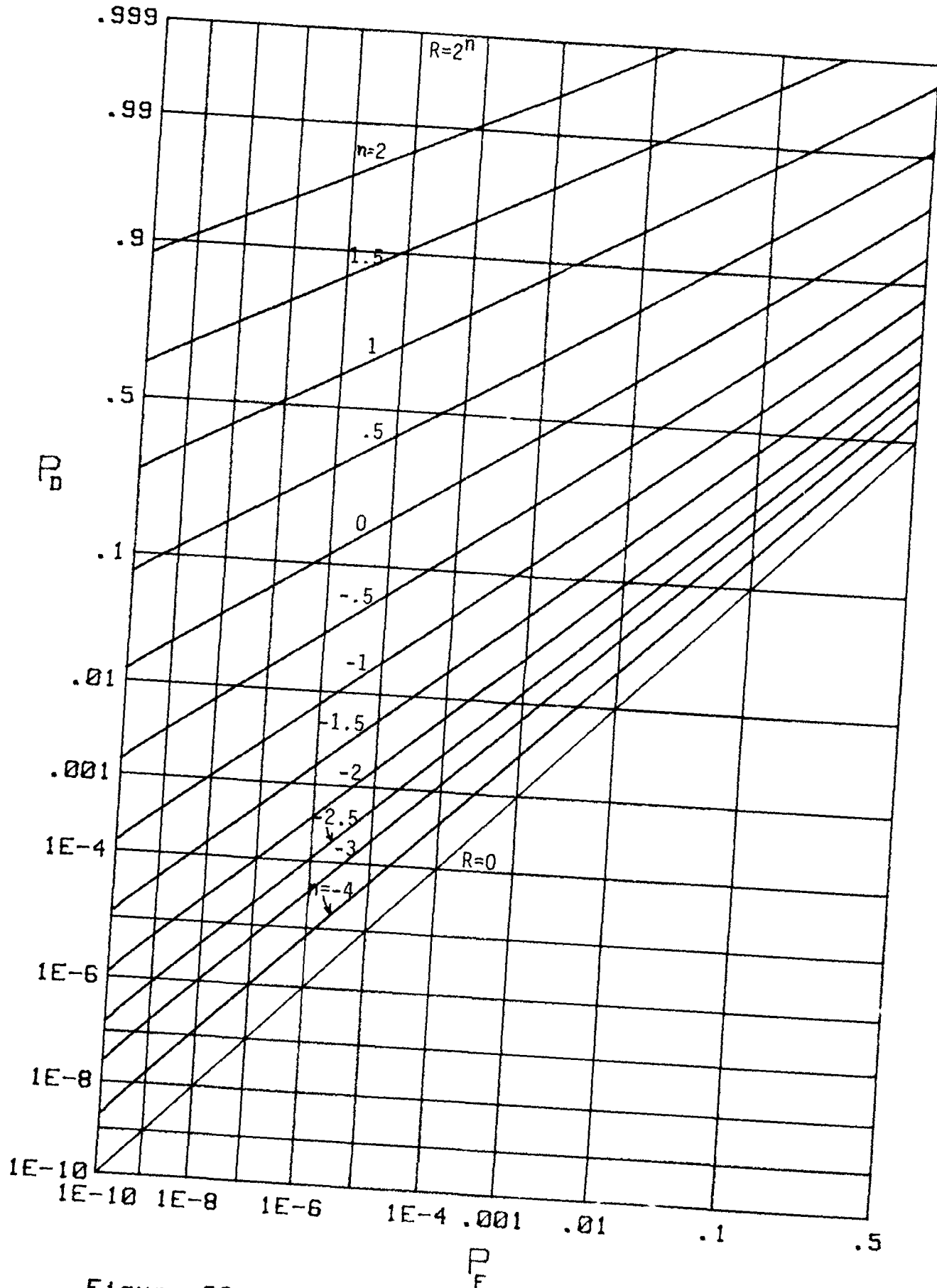


Figure 28. Operating Characteristics for Cross-Correlator without Sample Mean Removal, $N=32$, $r=1$

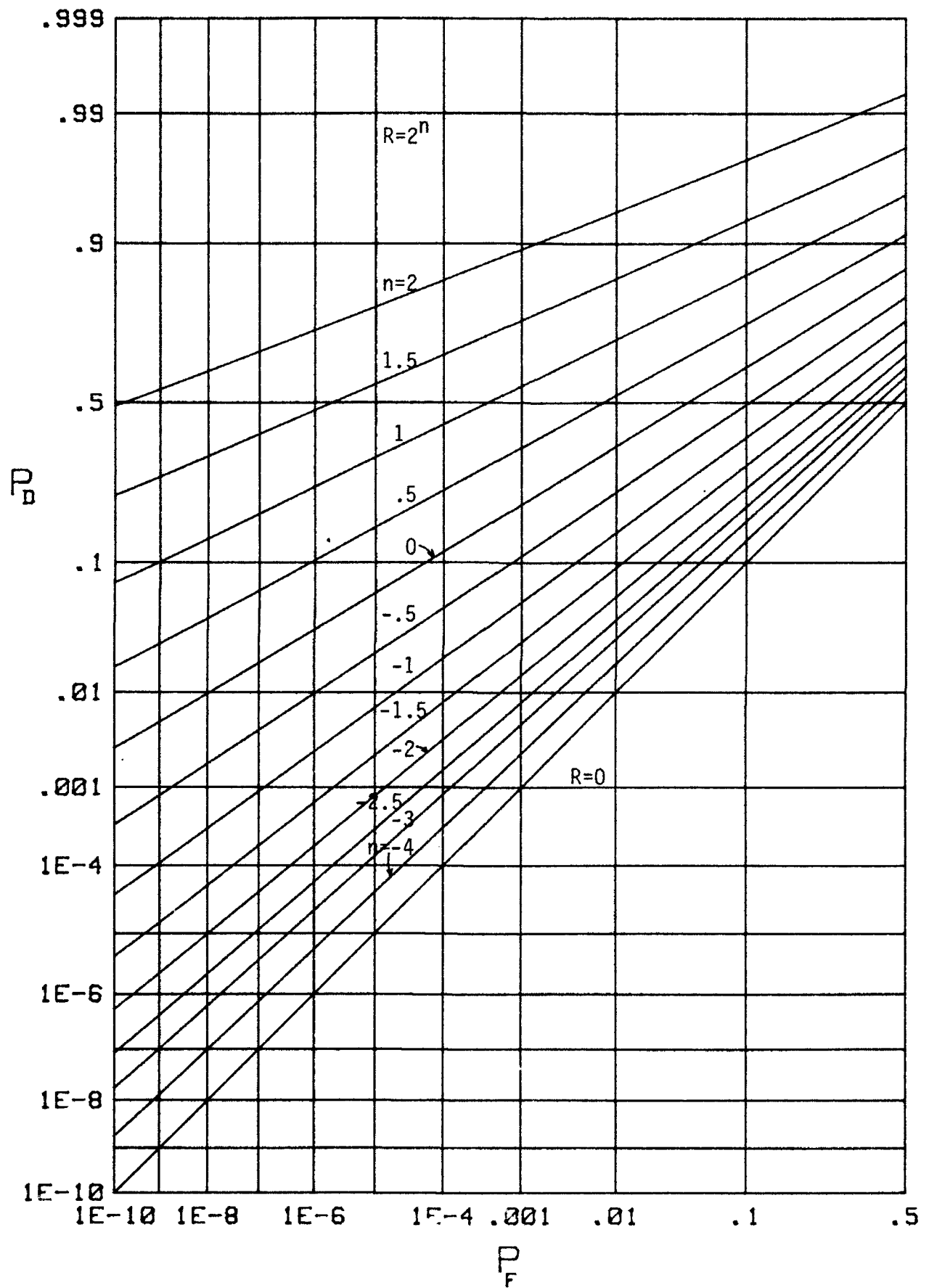


Figure 29. Operating Characteristics for Cross-Correlator without Sample Mean Removal, $N=32$, $r=2$

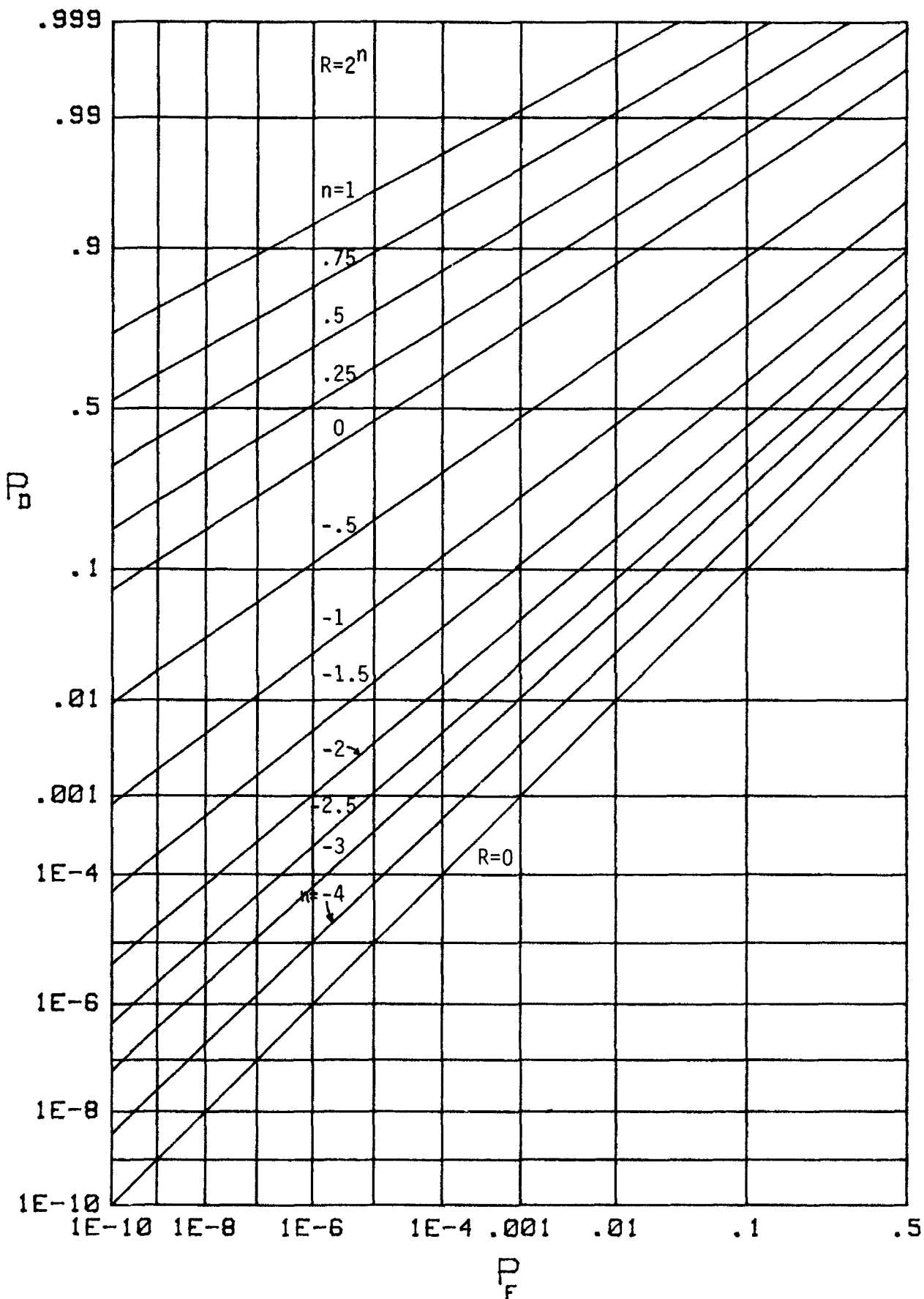


Figure 30. Operating Characteristics for Cross-Correlator without Sample Mean Removal, $N=64$, $r=1$

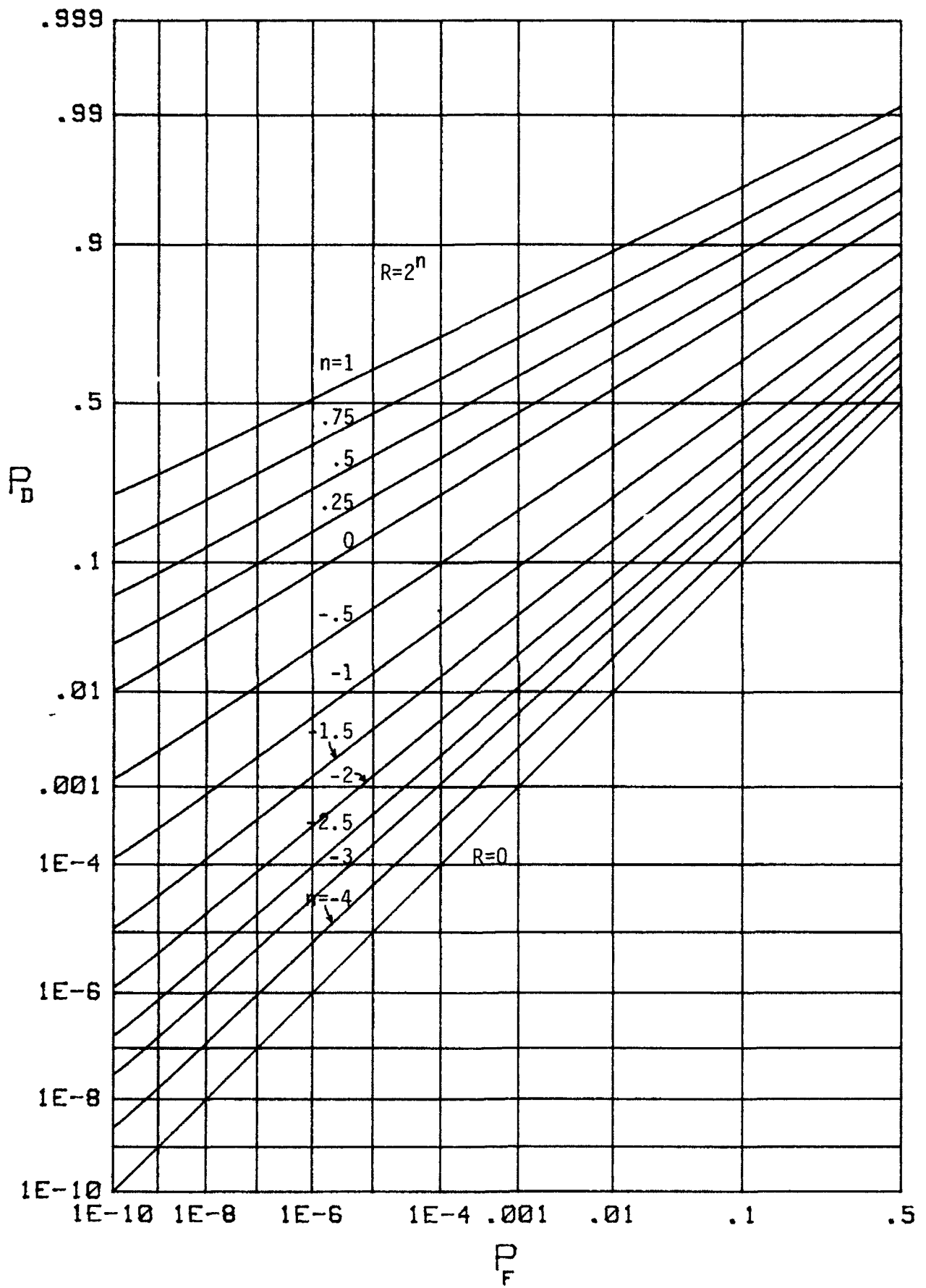


Figure 31. Operating Characteristics for Cross-Correlator without Sample Mean Removal, $N=64$, $r=2$

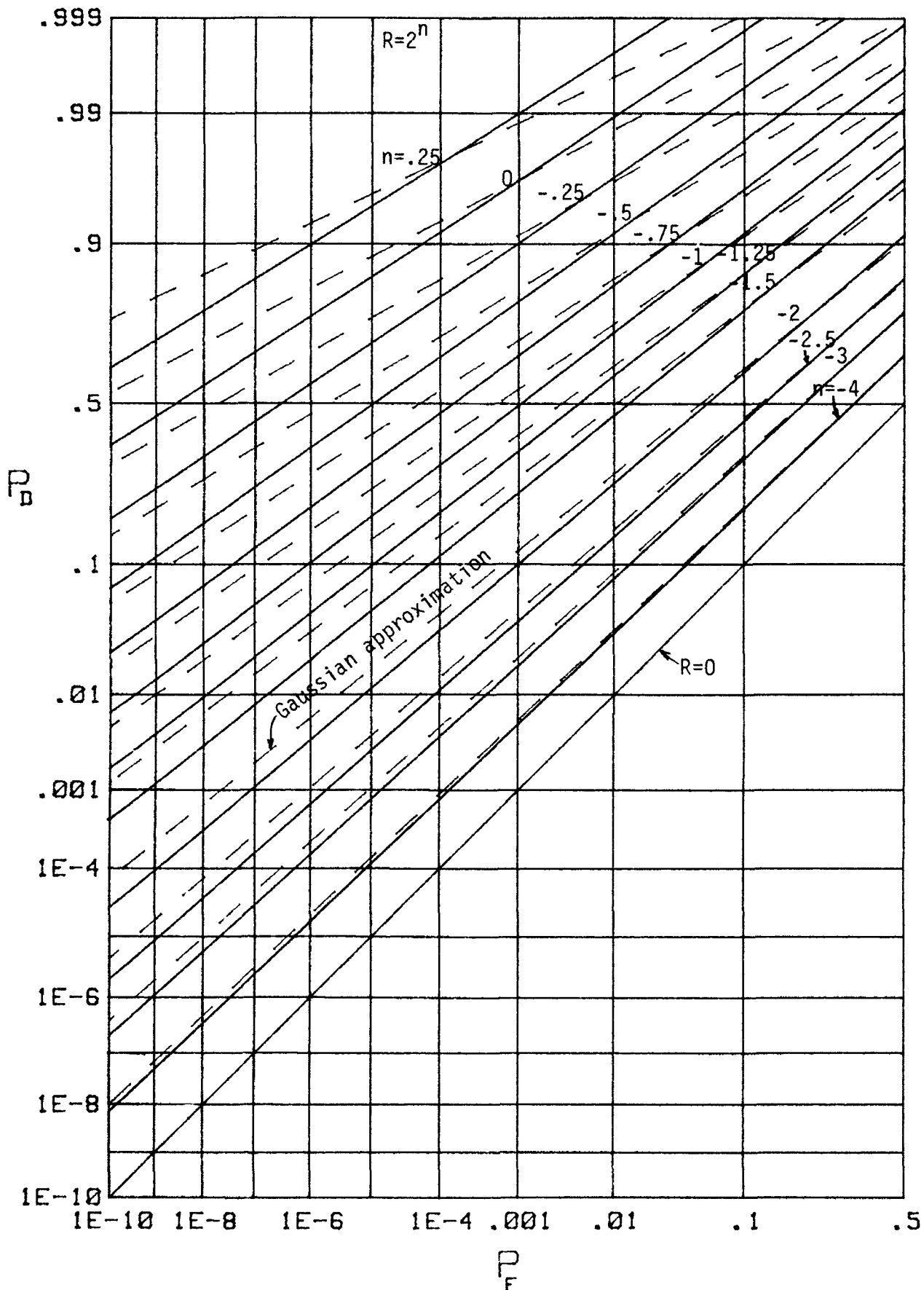


Figure 32. Operating Characteristics for Cross-Correlator without Sample Mean Removal, $N=128$, $r=1$

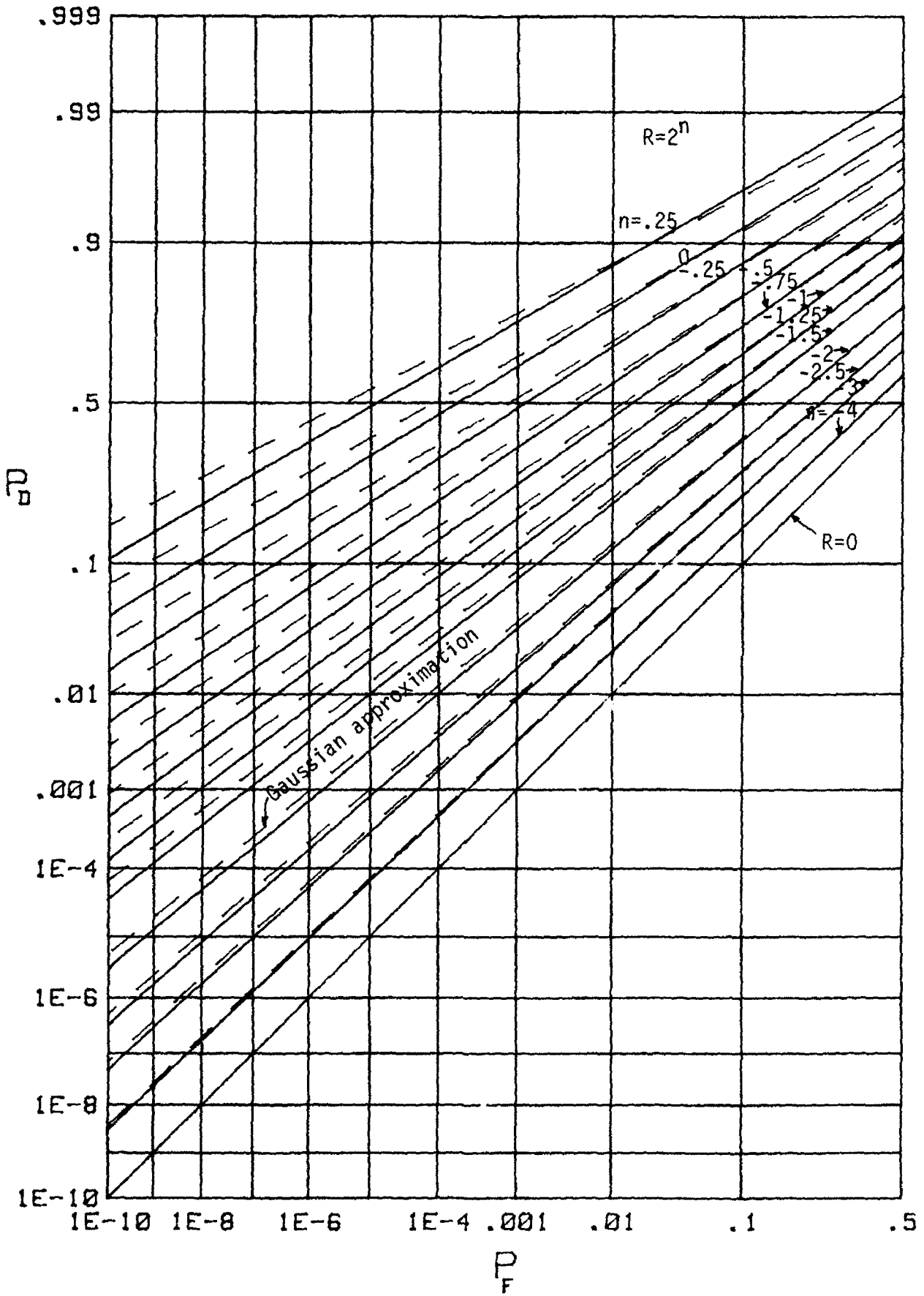


Figure 33. Operating Characteristics for Cross-Correlator without Sample Mean Removal, $N=128$, $r=2$

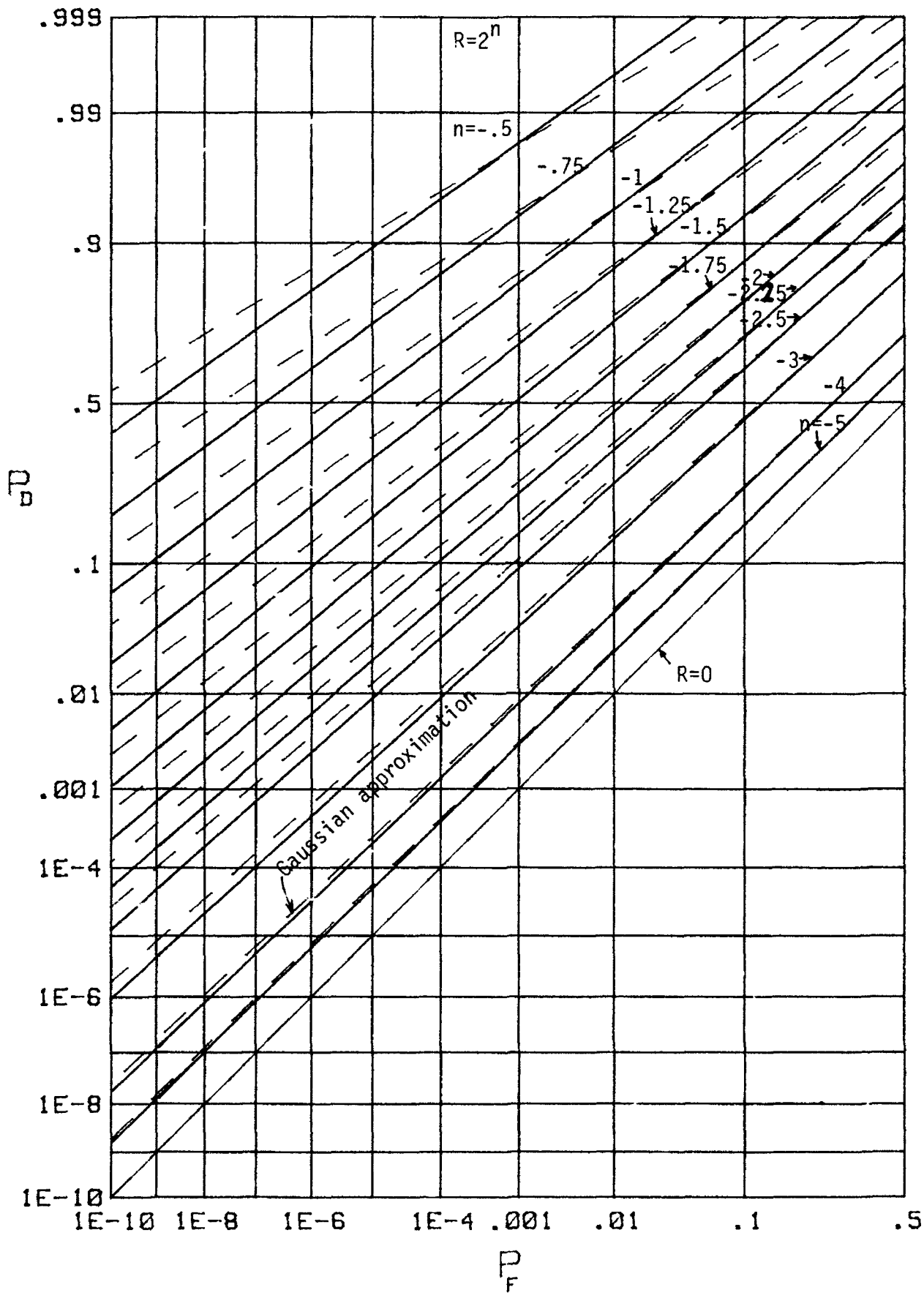


Figure 34. Operating Characteristics for Cross-Correlator without Sample Mean Removal, $N=256$, $r=1$

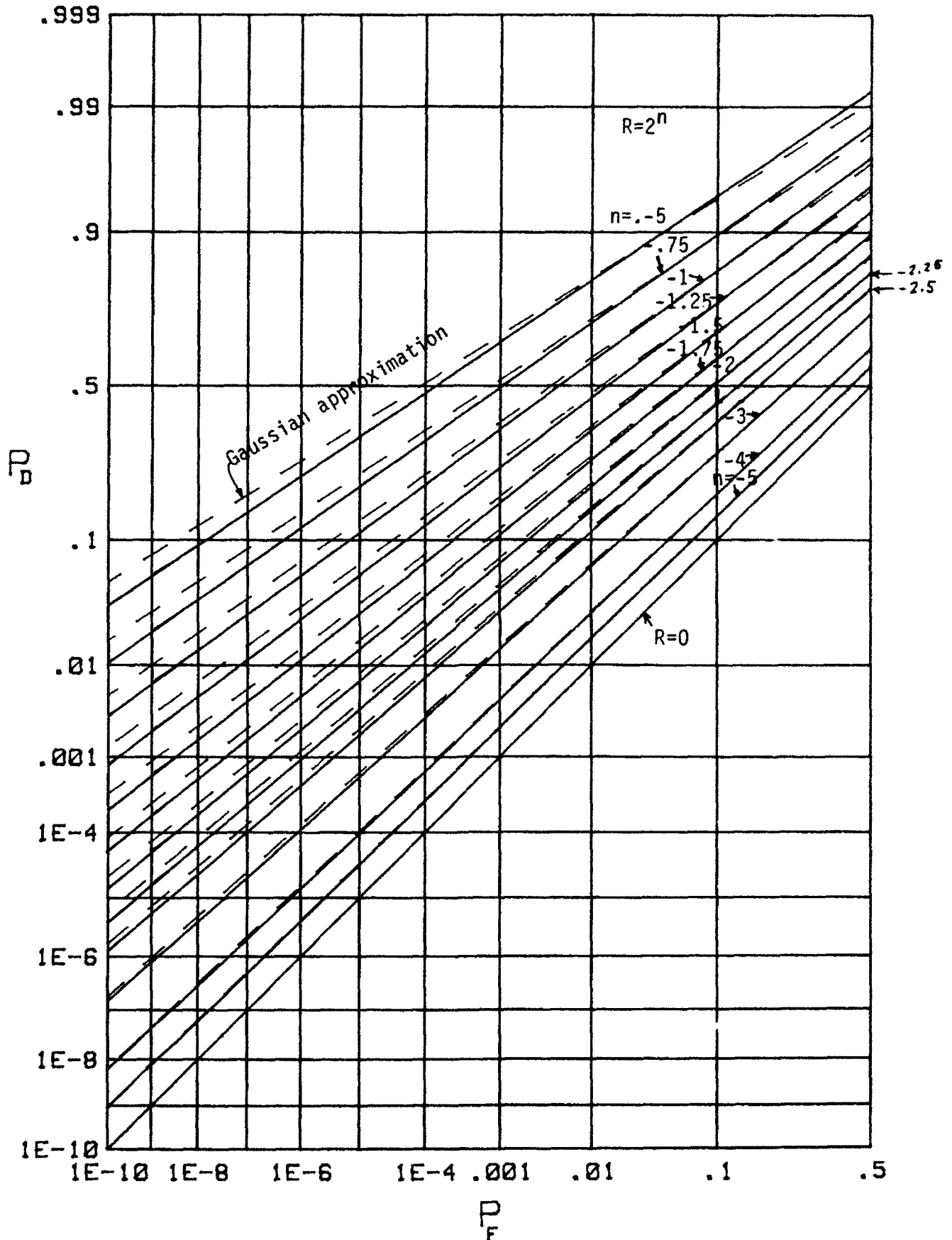


Figure 35. Operating Characteristics for Cross-Correlator without Sample Mean Removal, $N=256$, $r=2$

APPENDIX A. CORRELATOR OUTPUT INDEPENDENCE OF MEANS

If we let scale factors $\alpha=1$ but $\beta \neq 1$ in (11), we still get $\gamma=1$ from (13). This means that correlator output q in (12) is independent of μ_U , μ_V , β . To see this directly, let

$$u_n = \mu_U + y_n, \quad v_n = \mu_V + z_n, \quad (\text{A-1})$$

where means

$$\overline{y_n} = \overline{z_n} = 0. \quad (\text{A-2})$$

Then (11) yields, with $\alpha=1$,

$$\tilde{u}_n = y_n - \frac{1}{N} \sum_{m=1}^N y_m, \quad (\text{A-3})$$

which is obviously independent of the actual value of mean μ_U . Also, (11) yields

$$\tilde{v}_n = z_n - \frac{\beta}{N} \sum_{m=1}^N z_m + \mu_V(1-\beta), \quad (\text{A-4})$$

which still depends on μ_V and β . When (A-4) is substituted in (12), we get correlator output

$$q = \sum_{n=1}^N \tilde{u}_n \left[z_n - \frac{\beta}{N} \sum_{m=1}^N z_m + \mu_V(1-\beta) \right]. \quad (\text{A-5})$$

But since

$$\sum_{n=1}^N \tilde{u}_n = 0 \quad (\text{A-6})$$

from (A-3), (A-5) reduces to

$$\begin{aligned}
 q &= \sum_{n=1}^N \tilde{u}_n z_n = \sum_{n=1}^N \left(y_n - \frac{1}{N} \sum_{m=1}^N y_m \right) z_n = \\
 &= \sum_{n=1}^N y_n z_n - \frac{1}{N} \sum_{m=1}^N y_m \sum_{n=1}^N z_n
 \end{aligned} \tag{A-7}$$

in terms of the ac components defined in (A-1) and (A-2). Correlator output (A-7) is obviously independent of means μ_u , μ_v and scale factor β in (11).

APPENDIX B. A USEFUL INTEGRAL OF EXPONENTIALS OF MATRIX FORMS

For symmetric $K \times K$ matrix M , with $\det M > 0$, the following K -fold integral is well known (see for example, [9, section 8-3]):

$$\int dX \exp\left[-\frac{1}{2}X^T M X + N^T X\right] = \left[\frac{(2\pi)^K}{\det M}\right]^{1/2} \exp\left[\frac{1}{2}N^T M^{-1}N\right]. \quad (B-1)$$

Here X and N are $K \times 1$ column matrices. We wish to extend this result to the case of double integral

$$I = (2\pi)^{-K} \iint dU dV \exp\left[-\frac{1}{2}U^T A U - \frac{1}{2}V^T B V + U^T C V + D^T U + E^T V\right], \quad (B-2)$$

where A and B are symmetric without loss of generality, and the integral converges; here, matrices A , B , C are $K \times K$ while U , V , D , E are $K \times 1$. Notice that if we had the apparently more-general term

$$U^T C_1 V + V^T C_2 U = U^T (C_1 + C_2^T) V, \quad (B-3)$$

we would simply let $C = C_1 + C_2^T$, and thereby immediately have form (B-2).

To accomplish the evaluation of I in (B-2), identify $M = B$, $N^T = U^T C + E^T$, $X = V$ in (B-1), and thereby evaluate the V -integral in (B-2), with result

$$\int dV \dots = \left[\frac{(2\pi)^K}{\det B}\right]^{1/2} \exp\left[\frac{1}{2}(U^T C + E^T) B^{-1} (C^T U + E)\right]. \quad (B-4)$$

Substituting (B-4) in (B-2), regrouping, and using the symmetry of B (and therefore B^{-1}), there follows

$$I = \frac{(2\pi)^{-K/2}}{(\det B)^{1/2}} \int dU \exp\left[-\frac{1}{2}U^T (A - C B^{-1} C^T) U + (D^T + E^T B^{-1} C^T) U + \frac{1}{2}E^T B^{-1} E\right]. \quad (B-5)$$

Now reemploying (B-1) with identifications $M = A - CB^{-1}C^T$, $N = D + CB^{-1}E$, $X = U$, we get a closed form result for (B-5):

$$I = \left[\det(AB - CB^{-1}C^TB) \right]^{-1/2} \exp \left[\frac{1}{2} E^T B^{-1} E + \frac{1}{2} (D + CB^{-1}E)^T (A - CB^{-1}C^T)^{-1} (D + CB^{-1}E) \right]. \quad (B-6)$$

This is the desired general result for integral (B-2).

As an aside, there is probably a more symmetric closed form result than (B-6), since if we represent (B-2) by $I(A, B, C, D, E)$, we quickly see, by interchange of dummy variables U and V , that

$$I(A, B, C, D, E) = I(B, A, C^T, E, D). \quad (B-7)$$

However, we have not discovered the symmetric form of (B-6). The present form follows as a result of the sequential integration of (B-2), first on V , then on U .

APPENDIX C. PROGRAM FOR CUMULATIVE AND EXCEEDANCE DISTRIBUTION
FUNCTIONS VIA CHARACTERISTIC FUNCTION (23)-(24).

The numerical procedure employed in appendices C, D, and G here is heavily based on [3]. The choices of L , Δ , b in lines 90 to 110 to control truncation error and aliasing are also made according to the method of [3]. The parameters in (24) are evaluated once in lines 210-260 so as to minimize computation time. The FFT subroutine used in lines 1030 et seq is listed in [3, pp. B-11 - B-12], and employs a zero-subscripted array. A sample plot of the cumulative and exceedance distribution functions follows the program.

```

10 ! CROSS-CORRELATOR WITH SAMPLE MEAN REMOVAL; NUSC TR 7045
20   N=5                      ! Number of terms summed to yield output
30   Gamma=.5                 ! Scale factor in sample mean removal
40   Mu=-.4                   ! U channel mean
50   Mv=.3                    ! V channel mean
60   Su=.7                    ! U channel standard deviation
70   Sv=.9                    ! V channel standard deviation
80   Rho=.6                   ! Correlation coefficient
90   L=60                     ! Limit on integral of char. function
100  Delta=.12                ! Sampling increment on char. function
110  Bs=.25+(2*PI/Delta)      ! Shift b, as fraction of alias interval
120  Mf=2^8                   ! Size of FFT
130  PRINTER IS 0
140  PRINT "L =";L,"Delta =";Delta,"b =";Bs,"Mf =";Mf
150  REDIM X(0:Mf-1),Y(0:Mf-1)
160  DIM X(0:1023),Y(0:1023)
170  Su2=Su*Su                ! Calculate
180  Sv2=Sv*Sv                ! parameters
190  T1=1-Gamma
200  T2=T1*T1
210  E1=2*Rho*Su*Sv
220  E2=Su2+Sv2*(1-Rho*Rho)
230  F1=E1*T1
240  F2=E2*T2
250  G1=N*Mu+Mv*T1
260  G2=.5*N*(Su2*Mv+Mv+Su2*Mu+Mu-E1*Mu*Mv)*T2
270  N1=.5*(N-1)
280  Muq=G1+(N-Gamma)*Rho*Su*Sv ! Mean of random variable q
290  Muy=Mv+Bs                ! Mean of shifted variable y
300  X(0)=0
310  Y(0)=.5*Delta*Muy
320  FOR Ns=1 TO INT(L/Delta)
330  Xi=Delta*Ns              ! Argument xi of char. function
340  X2=Xi*Xi                 ! Calculation
350  T1=-Xi*F1                ! of
360  T2=1+X2*F2              ! characteristic
370  CALL Dio(-X2*G2,Xi*G1,T2,T1,A,B) ! function
380  CALL Log(1+X2*E2,-Xi*E1,C,D) ! fy(xi)
390  CALL Log(T2,T1,E,F)
400  CALL Exp(A-N1*C-.5*E,B-N1*D-.5*F+Xi*Bs,Fyr,Fyi)

```

```

410 Ms=Ns MOD Mf                                ! Collapsing
420 X(Ns)=X(Ms)+Fyn/Ns
430 Y(Ns)=Y(Ms)+Fyn/Ns
440 NEXT Ns
450 CALL Fft10z(Mf,X(*),Y(*))                  ! 0 subscript FFT
460 PLOTTER IS "GRAPHICS"
470 GRAPHICS
480 SCALE 0,Mf,-14,0
490 LINE TYPE 3
500 GRID Mf/8,1
510 PENUP
520 LINE TYPE 1
530 B=Bs*Mf*Delta/(2*PI)                       ! Origin for random variable q
540 MOVE B,0
550 DRAW B,-14
560 PENUP
570 FOR Ks=0 TO Mf-1
580 T=Y(Ks)/PI-Ks/Mf
590 X(Ks)=.5-T                                  ! Cumulative probability in X(*)
600 Y(Ks)=Pr+.5+T                               ! Exceedance probability in Y(*)
610 IF Pr>=1E-12 THEN Y=LGT(Pr)
620 IF Pr<=-1E-12 THEN Y=-24-LGT(-Pr)
630 IF ABS(Pr)<1E-12 THEN Y=-12
640 PLOT Ks,Y
650 NEXT Ks
660 PENUP
670 PRINT Y(0);Y(1);Y(Mf-2);Y(Mf-1)
680 FOR Ks=0 TO Mf-1
690 Pr=X(Ks)
700 IF Pr>=1E-12 THEN Y=LGT(Pr)
710 IF Pr<=-1E-12 THEN Y=-24-LGT(-Pr)
720 IF ABS(Pr)<1E-12 THEN Y=-12
730 PLOT Ks,Y
740 NEXT Ks
750 PENUP
760 PAUSE
770 DUMP GRAPHICS
780 PRINT LIN(5)
790 PRINTER IS 16
800 END
810 !
820 SUB Div(X1,Y1,X2,Y2,A,B)                   ! 21/22
830 T=X2*X2+Y2*Y2
840 A=(X1*X2+Y1*Y2)/T
850 B=(Y1*X2-X1*Y2)/T
860 SUBEND
870 !
880 SUB Log(X,Y,A,B)                           ! PRINCIPAL LOG(Z)
890 A=.5*LOG(X*X+Y*Y)
900 IF X<>0 THEN 930
910 B=.5*PI*SGN(Y)
920 GOTO 950
930 B=ATN(Y/X)
940 IF X<0 THEN B=B+PI*(1-2*(Y<0))
950 SUBEND
960 !

```

```
970 SUB Exp(X,Y,A,B)           ! EXP(Z)
980 T=EXP(X)
990 A=T*COS(Y)
1000 B=T*SIN(Y)
1010 SUBEND
1020 !
1030 SUB Fft10z(N,X(*),Y(*))    ! N <= 2^10 = 1024, N=2^INTEGER    0 SUBSCRIPT
```

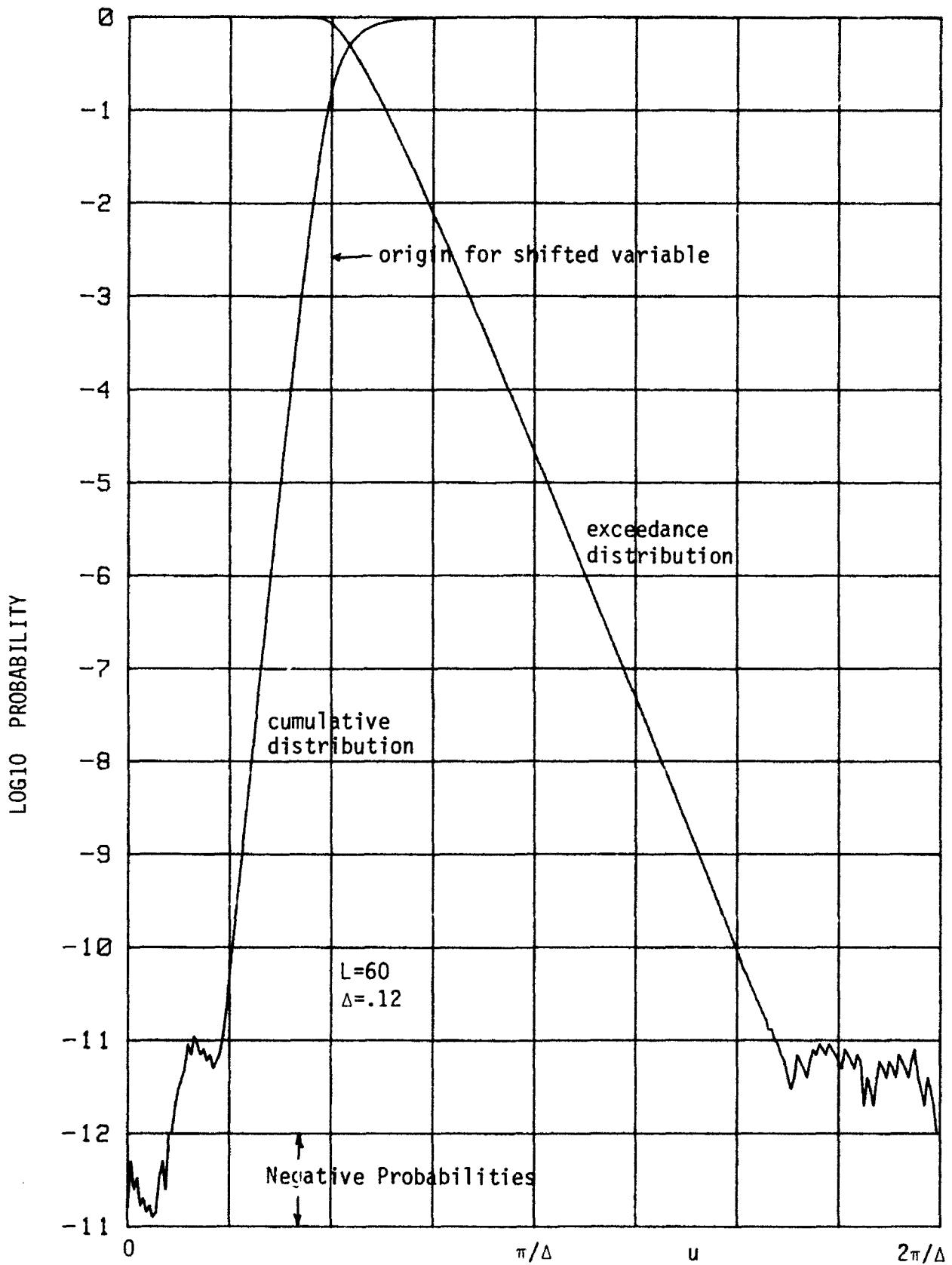



Figure C-1. Cumulative and Exceedance Distribution Functions

APPENDIX D. PROGRAM FOR EVALUATION OF OPERATING
CHARACTERISTICS FOR $\gamma=1$

The comments in appendix C are relevant here also. The characteristic function used as the starting point is given by (81). Sampling increment Δ employed on the characteristic function can be coarse for small signal-to-noise ratio R , but must be finer for larger R . The quantity Δ_0 , in line 30 is that used for $R=0$; all other Δ values are sub-multiples, as indicated by lines 110-130. A table follows.

N	4	6	8	12	16	24	32	48	64	96	128	256
Δ_0	.10	.09	.08	.06	.05	.05	.05	.05	.04	.03	.03	.02

Table D-1. Values of Δ_0 for $\gamma=1$

Let Δ_1 denote the sampling increment employed for a particular value of signal-to-noise ratio $R_1 > 0$. The cumulative and exceedance distribution function values are available at spacing $s = 2\pi/(M_f \Delta)$ in general, where M_f is the FFT size. If, for example, $\Delta_1 = \Delta_0/2$, then $s_1 = 2s_0$, meaning that probability values occur twice as coarsely for R_1 as for $R=0$. Then in order to plot detection probability P_D vs false alarm probability P_F without interpolating points, it is necessary to skip every other P_F point available, and only plot those P_F, P_D pairs corresponding to the same threshold. More generally, if $\Delta_1 = \Delta_0/K$, where K is an integer, then $s_1 = Ks_0$, and we plot only every K -th point of the available P_F values. Here we have chosen K to be a power of 2, for the purpose of ease of plotting.

We choose bias (shift) b in line 50 in order to give a random variable y which is virtually always positive for $R=0$; see [3]. We then keep b fixed as R increases, which makes the probability of $y > 0$ even greater. This feature of choosing the same b for all $R \geq 0$ enables an easy comparison of P_D and P_F , since common threshold values are then conveniently realized.

It was observed under (C) that the characteristic functions (39) or (81) have monotonically decreasing magnitudes for all $\xi > 0$. This makes the choice of L, the truncation value on the characteristic function integral in (63) or (64), rather simple; all we need to do is monitor $|f_h(\xi)|$ of (81) until it decreases below a tolerance, here taken as $1E-12$. There is no trial-and-error procedure required as in [3] to guarantee negligible truncation error.

Subroutines Exp and Log have already been listed in appendix C, and so are not relisted here.

```

10  GAMMA = 1          SAMPLE MEAN REMOVAL
20  Nc=8              ! N, Number of terms summed
30  Delta0=.100      ! Initial delta
40  B=PI/Delta0      ! Bias b
50  M=2*10           ! Size of FFT
60  OUTPUT 0;"GAMMA = 1";"  N =";Nc
70  OUTPUT 0;" "
80  DATA -2,-1,0,.5,1,1.5,2,2.5,3,3.5,4,5
90  READ Ns(*)        ! SHR R=2^n
100 OUTPUT 0;Ns(*);
110 DATA 1,2,2,2,4,4,4,8,8,16,16,32,64
120 READ Idelta(*)
130 MAT Delta=(Delta0)/Idelta
140 OUTPUT 0;Delta+);
150 DATA 1E-10,1E-9,1E-8,1E-7,1E-6,1E-5,1E-4,.001,.01,.1,.5,.9,.99,.999
160 READ Sc(*)
170 DIM Ns(1:12),Idelta(0:12),Delta(0:12),Sc(1:14)
180 DIM X(0:8191),Y(0:8191)
190 FOR I=1 TO 14
200 Sc(I)=FNInophn(Sc(I))
210 NEXT I
220 S=Sc(1)
230 B=Sc(14)
240 Scale=(B-S)/(0-S)
250 X1=30
260 X2=170
270 Y1=35
280 Y2=Y1+(X2-X1)*Scale
290 PLOTTER IS "9872A"
300 LIMIT X1,X2,Y1,Y2
310 OUTPUT 705;"VS3"
320 SCALE S,0,S,B
330 FOR I=1 TO 14
340 MOVE S,Sc(I)
350 DRAW 0,Sc(I)
360 NEXT I
370 FOR I=1 TO 11
380 MOVE Sc(I),S
390 DRAW Sc(I),B
400 NEXT I
410 MOVE S,S
420 DRAW 0,0
430 PENUP

```

```

440 M1=Mf-1
450 M2=Mf/2
460 FOR In=0 TO 12
470 IF In>0 THEN 500
480 Rc=0
490 GOTO 510
500 Rc=2^Ns(In) ! SNR R=2^n
510 OUTPUT 0;"R =" ;Rc," Delta =" ;Delta(In)
520 ASSIGN #1 TO "ABSCIS" ! Temporary storage for
530 Delta=Delta(In) ! false alarm probability
540 R2=Rc+2
550 R21=R2+1
560 N12=(Nc-1)/2
570 Mux=(Nc-1)*Rc ! Mean of random variable h
580 MuY=Mux+Bs ! Mean of shifted variable y
590 REDIM X(0:M1),Y(0:M1)
600 MAT X=ZER
610 MAT Y=ZER
620 X(0)=0
630 Y(0)=.5*Delta+MuY
640 Ls=0
650 Ls=Ls+1
660 Xi=Delta*Ls ! Argument xi of char. fn.
670 CALL Log(1+Xi*Xi*R21,-Xi*R2,Ai,Bi) ! Calculation
680 CALL Exp(-N12*Ai,Xi*Bs-N12*Bi,Fyr,Fyi) ! of
690 Ms=Ls MOD Mf ! characteristic
700 Ar=Fyr/Ls ! function
710 Ai=Fyi/Ls ! fy(xi)
720 X(Ms)=X(Ms)+Ar
730 Y(Ms)=Y(Ms)+Ai
740 Magsq=Ar*Ar+Ai*Ai
750 IF Magsq>1E-24 THEN 650
760 OUTPUT 0;"Xi =" ;Xi;" Mag =" ;SQRT(Magsq)
770 CALL Fft13z(Mf,X(*),Y(*))
780 FOR Ms=0 TO M1
790 T=Y(Ms)/PI-Ms/Mf
800 X(Ms)=.5-T ! Cumulative distribution function
810 Y(Ms)=.5+T ! Exceedance distribution function
820 NEXT Ms
830 OUTPUT 0;Y(0);Y(1);Y(M1-1);Y(M1)
840 PLOTTER IS "GRAPHICS"
850 GRAPHICS
860 SCALE 0,Mf,-14,0
870 LINE TYPE 3
880 GRID Mf/8,1
890 PENUP
900 LINE TYPE 1
910 FOR Ms=0 TO M1
920 Pr=Y(Ms)
930 IF Pr>=1E-12 THEN Y=LGT(Pr)
940 IF Pr<=-1E-12 THEN Y=-24-LGT(-Pr)
950 IF ABS(Pr)<1E-12 THEN Y=-12
960 PLOT Ms,Y
970 NEXT Ms
980 PENUP

```

TR 7045

```

990  FOR M2=0 TO M1
1000  Pr=X(M2)
1010  IF Pr=1E-12 THEN Y=LGT(Pr)
1020  IF Pr=-1E-12 THEN Y=-24-LGT(-Pr)
1030  IF ABS(Pr)<1E-12 THEN Y=-12
1040  PLOT M2,Y
1050  NEXT M2
1060  PENUP
1070  DUMP GRAPHICS
1080  OUTPUT 0;" "
1090  IF In>0 THEN 1200
1100  FOR M2=M2 TO M1
1110  IF Y(M2)<=0 THEN 1130
1120  NEXT M2
1130  M3=M2-1
1140  REDIM X(M2:M3)
1150  FOR M2=M2 TO M3
1160  X(M2)=FNInvphi(Y(M2))
1170  NEXT M2
1180  PRINT #1;X(*)           ! Store false alarm probability
1190  GOTO 1380
1200  REDIM X(M2:M3)
1210  READ #1,X(*)           ! Read in false alarm probability
1220  Id=Idelta(In)
1230  J2=M2/Id
1240  J3=INT(M3/Id)+1
1250  FOR J=J2 TO J3
1260  Y(J)=FNInvphi(Y(J))
1270  NEXT J
1280  PLOTTER IS "9872A"
1290  LIMIT X1,X2,Y1,Y2
1300  OUTPUT 705;"VS3"
1310  SCALE S,0,S,B
1320  FOR J=J2 TO J3
1330  T=J*Id
1340  IF T>M3 THEN 1370
1350  PLOT X(T),Y(J)
1360  NEXT J
1370  PENUP
1380  NEXT In
1390  END
1400  !
1410  SUB Exp(X,Y,A,B)           ! EXP(Z)
1460  !
1470  SUB Log(X,Y,A,B)         ! PRINCIPAL LOG(Z)
1550  !
1560  DEF FNInvphi(X)          ! INVPHI(X) via AMS 55, 26.2.23
1570  IF (X>0) AND (X<1) THEN 1600
1580  P=.9999999999999999E90*(2*X-1)
1590  GOTO 1670
1600  IF X=.5 THEN RETURN 0
1610  P=X
1620  IF X>.5 THEN P=.5-(X-.5)
1630  P=SQR(-2*LOG(P))
1640  T=1+P*(1.432788+P*(.189269+P*.001308))
1650  P=P-(2.515517+P*(.802853+P*.010328))/T
1660  IF X<.5 THEN P=-P
1670  RETURN P
1680  FNEND
1690  !
1700  SUB Fft13z(N,X(*),Y(*))  ! N <= 2^13, N=2^INTEGER, 0 SUBSCRIPT

```

APPENDIX E. ASYMPTOTIC EXPANSIONS FOR DISTRIBUTIONS WHEN $r > 0$

The characteristic function of interest is given by (100) and (102):

$$f_h(\xi) = (1+i\xi)^{-\nu} (1-i\xi\omega)^{-\nu} \exp\left[\frac{i\xi\eta}{1-i\xi\omega}\right], \quad (\text{E-1})$$

where for notational convenience in this appendix, we let

$$\nu = \frac{N}{2}, \quad \eta = Nr^2, \quad \omega = 1+2R. \quad (\text{E-2})$$

The cumulative distribution function is obtained by substitution of (E-1) in (63):

$$P_h(u) = \frac{-1}{i2\pi} \int_{C_+} d\xi \xi^{-1} (1+i\xi)^{-\nu} (1-i\xi\omega)^{-\nu} \exp\left[\frac{i\xi\eta}{1-i\xi\omega} - iu\xi\right]. \quad (\text{E-3})$$

The ν -th powers are principal value, being positive real where C_+ crosses the positive imaginary axis.

Now let $z = 1+i\xi$ in (E-3), yielding

$$P_h(u) = \frac{-1}{i2\pi} \int_{C_1} dz (z-1)^{-1} z^{-\nu} (1+\omega-\omega z)^{-\nu} \exp\left[\frac{(z-1)\eta}{1+\omega-\omega z} - u(z-1)\right]. \quad (\text{E-4})$$

The contours C_+ and C_1 in (E-3) and (E-4) are depicted as dashed lines in figure E-1. The pole at $\xi=0$ is moved to $z=1$; the remaining singularities are branch points (ν non-integer); the ν -th powers are positive real where C_1 crosses the positive real axis. For $u < 0$, an equivalent contour to C_1 is that indicated by C_2 in figure E-1, since the exponential in (E-4) furnishes rapid decay in the left-half z -plane. We write (E-4) in the form

$$P_h(u) = \frac{\exp(u)}{i2\pi} \int_{C_2} dz z^{-\nu} \exp(-uz) g_1(z), \quad (\text{E-5})$$

where

$$g_1(z) = (1-z)^{-1} (1+\omega-\omega z)^{-\nu} \exp\left[\frac{(z-1)\eta}{1+\omega-\omega z}\right]. \quad (\text{E-6})$$

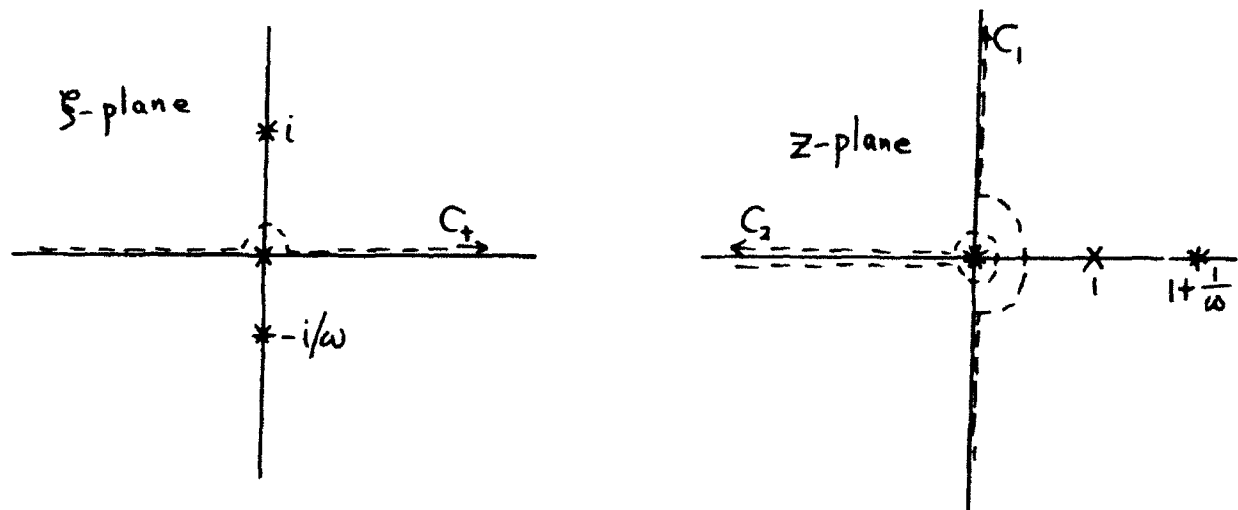


Figure E-1. Contours of Integration for Cumulative Distribution Function

In order to get the asymptotic development of (E-5), we expand $g_1(z)$ in a power series in z ,

$$g_1(z) = g_1(0) + g_1'(0) z + \dots, \quad (\text{E-7})$$

where

$$g_1(0) = (1+\omega)^{-\nu} \exp\left(\frac{-\eta}{1+\omega}\right), \quad \frac{g_1'(0)}{g_1(0)} = 1 + \frac{\nu\omega}{1+\omega} + \frac{\eta}{(1+\omega)^2}. \quad (\text{E-8})$$

Appeal to [10, p. 96, (4)] then yields (for all ν)

$$\begin{aligned} P_h(u) &\sim \exp(u) \left[\frac{(-u)^{\nu-1}}{\Gamma(\nu)} g_1(0) + \frac{(-u)^{\nu-2}}{\Gamma(\nu-1)} g_1'(0) \right] = \\ &= \Gamma(\nu)^{-1} (1+\omega)^{-\nu} (-u)^{\nu-1} \exp\left[u - \frac{\eta}{1+\omega}\right] \left[1 - \frac{\nu-1}{u} \left(1 + \frac{\nu\omega}{1+\omega} + \frac{\eta}{(1+\omega)^2} \right) \right] \\ &\quad \text{as } u \rightarrow -\infty. \quad (\text{E-9}) \end{aligned}$$

Substitution of (E-2) in (E-9) then yields result (104).

When (E-1) is substituted into (64) instead, we obtain the exceedance distribution function in the form

$$1 - P_h(u) = \frac{1}{i2\pi} \int_{C_-} d\xi \xi^{-1} (1+i\xi)^{-\nu} (1-i\xi\omega)^{-\nu} \exp\left[\frac{i\xi\eta}{1-i\xi\omega} - iu\xi\right]. \quad (E-10)$$

Now let $z = \frac{1}{\omega} - i\xi$, to get

$$1 - P_h(u) = \frac{-1}{i2\pi} \int_{C_3} dz \left(z - \frac{1}{\omega}\right)^{-1} \left(1 + \frac{1}{\omega} - z\right)^{-\nu} (\omega z)^{-\nu} * \exp\left[\frac{(1-\omega z)\eta}{\omega^2 z} + u\left(z - \frac{1}{\omega}\right)\right]. \quad (E-11)$$

The contours C_- and C_3 in (E-10) and (E-11) are depicted as dashed lines in figure E-2. The pole at $\xi=0$ is moved to $z = 1/\omega$; the remaining singularities are branch points.

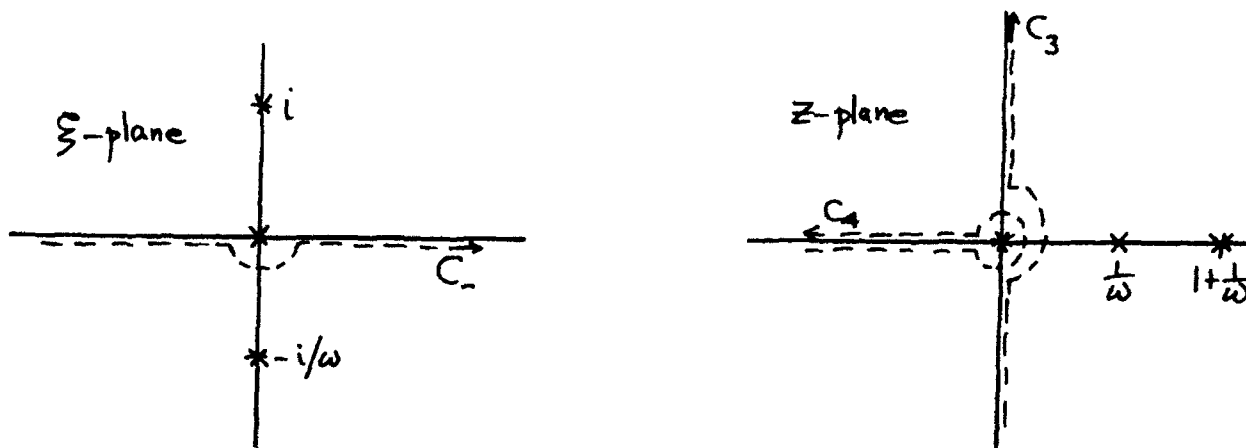


Figure E-2. Contours of Integration for Exceedance Distribution Function

For $u > 0$, an equivalent contour to C_3 is that indicated by C_4 in figure E-2, since the exponential in (E-11) furnishes rapid decay in the left-half z -plane. We write (E-11) in the form

$$1 - P_h(u) = \omega (1+\omega)^{-\nu} \exp\left(-\frac{u+\eta}{\omega}\right) \frac{1}{i2\pi} \int_{C_4} dz z^{-\nu} \exp\left[uz + \frac{\eta}{\omega}z\right] g_2(z), \quad (E-12)$$

where

$$g_2(z) = (1-\omega z)^{-1} \left(1 - \frac{\omega z}{1+\omega}\right)^{-\nu}. \quad (E-13)$$

As above, we expand $g_2(z)$ in a power series in z ,

$$g_2(z) = 1 + \omega \left(1 + \frac{\nu}{1+\omega}\right) z + \dots \quad (E-14)$$

and substitute it in (E-12); employment of [10, p. 105, (2)] now yields (for all ν)

$$1 - P_h(u) \sim \omega (1+\omega)^{-\nu} \exp\left(-\frac{u+\eta}{\omega}\right) * \left[\left(\omega \sqrt{\frac{u}{\eta}}\right)^{\nu-1} I_{\nu-1}\left(\frac{2\sqrt{\eta u}}{\omega}\right) + \omega \left(1 + \frac{\nu}{1+\omega}\right) \left(\omega \sqrt{\frac{u}{\eta}}\right)^{\nu-2} I_{\nu-2}\left(\frac{2\sqrt{\eta u}}{\omega}\right) \right] \quad (E-15)$$

as $u \rightarrow +\infty$,

where $I_\mu(z)$ is the modified Bessel function of the first kind. This is the general result for the exceedance distribution function; the various parameters given in (E-2) relate it back to the problem of interest in the main text.

As a check on this result, we let $r \rightarrow 0$; then $\eta \rightarrow 0$, and (E-15) reduces, via [6, 9.6.7], to

$$1 - P_h(u) \sim \Gamma(\nu)^{-1} \omega (1+\omega)^{-\nu} u^{\nu-1} \exp(-u/\omega) \left[1 + \frac{\nu-1}{u} \omega \left(1 + \frac{\nu}{1+\omega}\right) \right] \quad (E-16)$$

as $u \rightarrow +\infty$; $r=0$.

Employing the identifications in (E-2), there follows from (E-16)

$$1 - P_h(u) \sim \frac{1+2R}{2(1+R)\Gamma(N/2)} \left(\frac{u}{2(1+R)}\right)^{\frac{N-2}{2}} \exp\left(\frac{-u}{1+2R}\right) * \\ * \left[1 + \frac{1+2R}{1+R} \frac{(N-2)(N+4+4R)}{8u}\right] \text{ as } u \rightarrow +\infty; r=0. \quad (E-17)$$

In order to compare this result with that for $\gamma=1$, sample mean removal, we must replace N here by $N-1$; see the paragraph under (101). When this is done, (E-17) reverts precisely to (61) and (62).

Returning to the general result for the exceedance distribution function in (E-15), if we keep $n > 0$ and use [6, 9.7.1] for large arguments of $I_\nu(z)$, there follows the simpler (less accurate) result

$$1 - P_h(u) \sim \left[2\pi^{1/2}(1+\omega)^{\nu} n^{\frac{\nu}{2} - \frac{1}{4}}\right]^{-1} \omega^{\nu + \frac{1}{2}} * \\ * u^{\frac{\nu}{2} - \frac{3}{4}} \exp\left[-\frac{1}{\omega}\left(u^{1/2} - n^{1/2}\right)^2\right] \text{ as } u \rightarrow +\infty. \quad (E-18)$$

When (E-2) is substituted in (E-18), the result quoted in (105) follows.

As a special case of (E-18), if $\nu=1$ (i.e. $N=2$), then

$$1 - P_h(u) \sim \frac{\omega^{3/2}}{2\pi^{1/2}(1+\omega)(\pi u)^{1/4}} \exp\left[-\frac{1}{\omega}\left(u^{1/2} - n^{1/2}\right)^2\right] \text{ as } u \rightarrow +\infty; \nu=1. \quad (E-19)$$

APPENDIX F. EXCEEDANCE DISTRIBUTION FUNCTION FOR $\gamma=0$, $N=1$, $r>0$

CHARACTERISTIC FUNCTION APPROACH

When characteristic function (100) with $N=1$ is substituted in (64), the expression for the exceedance distribution function becomes

$$1 - P_h(u) = \frac{1}{i2\pi} \int_{C_-} d\xi \xi^{-1} (1+i\xi)^{-1/2} (1-i\xi\omega)^{-1/2} \exp\left[\frac{i\xi r^2}{1-i\xi\omega} - iu\xi\right], \quad (F-1)$$

where $\omega = 1+2R$ as in (102). The square roots are taken as $+1$ at $\xi=0$. For $u \geq 0$, the contour C_- can be modified to that indicated in figure F-1, where the contributions of the large circular arcs in the lower-half ξ -plane tend to zero. The small circle of radius ρ centered at branch point $\xi = -i/\omega$ must have $0 < \rho < 1/\omega$, since the latter is the distance to the pole at the origin.

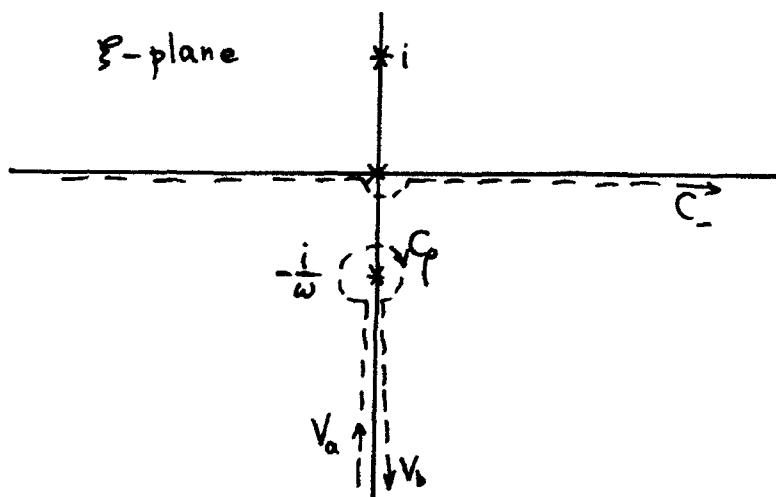


Figure F-1. Equivalent Contours for (F-1)

It is easy to show that the two vertical contributions in figure F-1 are equal. Under the change of variable

$$i\xi = \frac{1+t^2}{\omega}, \quad (F-2)$$

the sum of the two vertical contributions to exceedance distribution function (F-1) becomes

$$V(\rho) = \frac{2\omega^{1/2}}{\pi} \exp\left(-\frac{u+r^2}{\omega}\right) \int_{(\omega\rho)^{1/2}}^{+\infty} dt (1+t^2)^{-1} * \\ * (1+\omega+t^2)^{-1/2} \exp\left(-\frac{u}{\omega}t^2 - \frac{r^2}{\omega t^2}\right). \quad (F-3)$$

This integral remains convergent even as $\rho \rightarrow 0+$. Furthermore, the integrand decays rapidly, has no cusps, and involves only elementary functions; also the integral is a sum of positive quantities and retains significance even for large u .

On the small circular contour C_ρ in figure F-1, let

$$i\zeta = \frac{1}{\omega} - \rho \exp(i\theta), \quad (F-4)$$

to obtain, for the circular contribution to the exceedance distribution function, the quantity

$$C(\rho) = \frac{\omega}{2\pi(1+\omega)^{1/2}} \exp\left(-\frac{u+r^2}{\omega}\right) \rho^{1/2} \int_{-\pi}^{\pi} d\theta (1-\omega\rho E)^{-1} * \\ * \left(1 - \frac{\omega\rho}{1+\omega} E\right)^{-1/2} \exp\left(i\frac{\theta}{2} + \frac{\lambda}{\rho} E^* + \rho u E\right), \quad (F-5)$$

where we define in this appendix

$$\lambda = \frac{r^2}{\omega} = \left(\frac{r}{1+2R}\right)^2, \quad E = \exp(i\theta). \quad (F-6)$$

The exceedance distribution function is given exactly by the sum of (F-3) and (F-5), for any $0 < \rho < 1/\omega$. It would be advantageous numerically to let $\rho \rightarrow 0^+$ in these two equations; however, the limit of (F-5) is not obvious and can easily be done incorrectly.

AN ERRONEOUS APPROACH FOR $C(\rho)$

It is tempting to let $\rho \rightarrow 0^+$ in those locations in (F-5) where it will "do no damage", obtaining for the integral with scale factor $\rho^{1/2}$ the quantity

$$I_\rho \equiv \rho^{1/2} \int_{-\pi}^{\pi} d\theta \exp\left[i \frac{\theta}{2} + \frac{\lambda}{\rho} \exp(-i\theta)\right]. \quad (\text{F-7})$$

(The fallacy of doing this for a residue calculation with an essential singularity is demonstrated in the next subsection.) Furthermore, the limit of (F-7) as $\rho \rightarrow 0^+$ can in fact be determined in closed form, as follows. Observe that the integrand of (F-7) has a saddle point in the complex θ -plane at

$$\theta_s = -iL, \quad L = \ln\left(\frac{2\lambda}{\rho}\right); \quad (\text{F-8})$$

this is in fact the only saddle point in the $(-\pi, \pi)$ strip in the θ -plane. Now let $z = \theta - \theta_s$, getting for (F-7)

$$I_\rho = (2\lambda)^{1/2} \int_{-\pi+iL}^{\pi+iL} dz \exp\left[i \frac{z}{2} + \frac{1}{2} \exp(-iz)\right]. \quad (\text{F-9})$$

The radius ρ now appears only in the limit L of the integral, and the integrand has a saddle point at $z=0$.

The straight line contour for (F-9) can be deformed into contour C, depicted in figure F-2, which goes through the saddle point at $z=0$. Now if

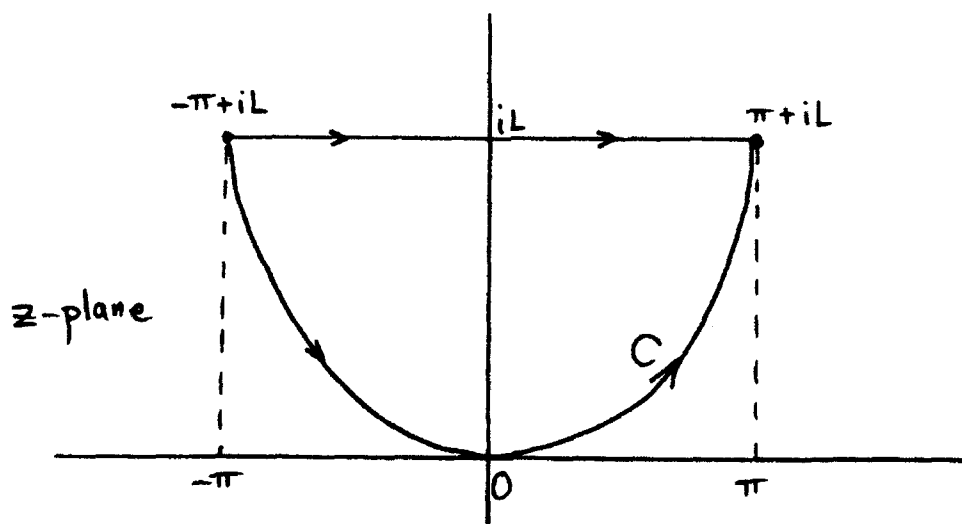


Figure F-2. Equivalent Contours for (F-9)

$\rho \rightarrow 0^+$, then $L \rightarrow +\infty$, and (F-9) yields

$$I_0 = (2\lambda)^{1/2} \int_{-\pi+i\infty}^{\pi+i\infty} dz \exp\left[i \frac{z}{2} + \frac{1}{2} \exp(-iz)\right], \quad (\text{F-10})$$

where the contour is the limit of C in figure F-2 as $L \rightarrow +\infty$; that is, the integral is between the two valleys at $\pm\pi+i\infty$ and is connected by the saddle point at $z=0$.

The steepest descent curves out of the saddle point of the integrand of (F-10) are given explicitly by

$$y = -\ln\left(\frac{\sin x}{x}\right) \quad \text{for } -\pi < x < \pi. \quad (\text{F-11})$$

Thus if we let

$$z = x + iy = x - i \ln\left(\frac{\sin x}{x}\right),$$

$$\frac{dz}{dx} = 1 - i \left(\frac{\cos x}{\sin x} - \frac{1}{x} \right), \quad (\text{F-12})$$

on the steepest descent curves in (F-10), there follows

$$\begin{aligned} I_0 &= (2\lambda)^{1/2} \int_{-\pi}^{\pi} dx \left(1 - i \frac{\cos x}{\sin x} + i \frac{1}{x} \right) \exp \left[i \frac{x}{2} + \frac{1}{2} \ln \left(\frac{\sin x}{x} \right) + \frac{1}{2} \frac{x}{\sin x} \exp(-ix) \right] = \\ &= (2\lambda)^{1/2} \int_{-\pi}^{\pi} dx \left(1 - i \frac{\cos x}{\sin x} + i \frac{1}{x} \right) \left(\frac{\sin x}{x} \right)^{1/2} \exp \left[\frac{x \cos x}{2 \sin x} \right] = \\ &= (2\lambda)^{1/2} 2 \int_0^{\pi} dx \left(\frac{\sin x}{x} \right)^{1/2} \exp \left(\frac{x \cos x}{2 \sin x} \right) = (2\lambda)^{1/2} 2(2\pi)^{1/2} = 4(\lambda\pi)^{1/2}. \quad (\text{F-13}) \end{aligned}$$

(The integral value of $(2\pi)^{1/2}$ in (F-13) was deduced by numerical integration.)

Recalling the definition of I_0 in (F-7), we then have the dubious result for the limit of (F-5):

$$C(0) \stackrel{?}{=} \left(\frac{2}{\pi} \right)^{1/2} \frac{r}{(1+R)^{1/2}} \exp \left(-\frac{u+r^2}{1+2R} \right), \quad (\text{F-14})$$

where we employed (102) and (F-6). Actual numerical evaluation of (F-14), combined with $V(0)$ from (F-3), gives incorrect results for the exceedance distribution function (F-1); thus the replacement of ρ with 0 in (F-5) is invalid. The explanation for this pitfall is the essential singularity of (F-1) at $\xi = -i/\omega$; a simpler illustration follows.

RESIDUE OF ESSENTIAL SINGULARITY

The function

$$\exp\left(\frac{1}{z}\right) = 1 + \frac{1}{z} + \frac{1}{2! z^2} + \dots \quad (\text{F-15})$$

has an essential singularity at $z=0$, with residue 1, as exemplified by this Laurent expansion. Now consider the function

$$f(z) = \exp\left(\frac{1}{z}\right) g(z), \quad (\text{F-16})$$

where $g(z)$ is analytic at $z=0$. Then

$$f(z) = \left(1 + \frac{1}{z} + \frac{1}{2! z^2} + \dots\right) \left(g(0) + g^{(1)}(0) z + \frac{1}{2!} g^{(2)}(0) z^2 + \dots\right). \quad (\text{F-17})$$

The coefficient of $1/z$ in (F-17) is the residue of $f(z)$ at $z=0$; namely

$$\text{Res} = g(0) + \frac{1}{2!} g^{(1)}(0) + \frac{1}{3!} \frac{1}{2!} g^{(2)}(0) + \dots = \sum_{n=0}^{+\infty} \frac{g^{(n)}(0)}{n!(n+1)!}. \quad (\text{F-18})$$

Thus the residue of $f(z)$ at $z=0$ depends on the behavior of $g(z)$ in a neighborhood of $z=0$, and not just the value $g(0)$.

A couple of examples yield the following:

$$g(z) = (1-az)^{-1}, \quad \text{Res} = \frac{\exp(a)-1}{a};$$

$$g(z) = \exp(a^2 z), \quad \text{Res} = \frac{I_1(2a)}{a}. \quad (\text{F-19})$$

CORRECT APPROACH FOR $C(\rho)$

Reconsider the integral in (F-5) plus the scale factor $\rho^{1/2}$; making the substitution $z = \theta + iL$, where L is given in (F-8), there follows for this quantity

$$(2\lambda)^{1/2} \int_{-\pi+iL}^{\pi+iL} dz (1-2\omega\lambda e^{iz})^{-1} \left(1 - \frac{2\omega\lambda}{1+\omega} e^{iz}\right)^{-\frac{1}{2}} * \\ * \exp\left[i \frac{z}{2} + \frac{1}{2} e^{-iz} + 2\lambda u e^{iz}\right]. \quad (F-20)$$

The uppermost singularity of the integrand in the z -plane (within the $-\pi, \pi$ strip) is a pole at $z_p = i \ln(2\omega\lambda)$; however, the straight line contour in (F-20) remains above this pole because $\rho < 1/\omega$; see (F-8). Furthermore, the total integrand of (F-20) has a saddle point on the imaginary axis of the z -plane above the pole location z_p , because the integrand is infinite at the pole and at $z = 0 + i\infty$. Thus the straight line contour in (F-20) can be modified so as to pass through the saddle point, and yet remain above z_p . Finally, letting $\rho \rightarrow 0+$, then $L \rightarrow +\infty$, and (F-20) combined with (F-5) yields the exact result for the circular component

$$C(0) = \frac{r}{\pi 2^{1/2} (1+\omega)^{1/2}} \exp\left(-\frac{u+r^2}{\omega}\right) \int_{-\pi+i\infty}^{\pi+i\infty} dz (1-2\omega\lambda e^{iz})^{-1} * \\ * \left(1 - \frac{2\omega\lambda}{1+\omega} e^{iz}\right)^{-1/2} \exp\left[i \frac{z}{2} + \frac{1}{2} e^{-iz} + 2\lambda u e^{iz}\right], \quad (F-21)$$

where the two valleys of the integrand at $\pm\pi+i\infty$ are joined with a contour through the saddle point lying above the pole at $z_p = i \ln(2\omega\lambda)$. Here $\omega = 1+2R$.

The other component of the exceedance distribution function, corresponding to (F-21), is given by (F-3) at $\rho = 0^+$:

$$V(0) = \frac{2\omega^{1/2}}{\pi} \exp\left(-\frac{u+r^2}{\omega}\right) \int_0^{+\infty} dt (1+t^2)^{-1} * \\ *(1+\omega t^2)^{-1/2} \exp\left(-\frac{u}{\omega} t^2 - \frac{r^2}{\omega t^2}\right). \quad (F-22)$$

Thus for $u \geq 0$, (F-1) and figure F-1 yield exceedance distribution function

$$1 - P_h(u) = C(0) + V(0) = (F-21) + (F-22). \quad (F-23)$$

Computationally, (F-21) is not too attractive, because of the complex integrand and/or the need to determine the steepest descent paths to $\pm\pi+i\infty$ numerically. Accordingly, an alternative direct procedure for determining the exceedance distribution function of random variable h is now presented.

DIRECT EVALUATION OF EXCEEDANCE DISTRIBUTION FUNCTION

For $\gamma=0$, $N=1$, (12) and (3) yield the crosscorrelator output for the signal and noise model as

$$q = u_1 v_1 = [u_u + u_s(1) + u_d(1)] [u_v + v_s(1) + v_d(1)]. \quad (F-24)$$

The normalized crosscorrelator output is then, from (49) and (97),

$$h = \frac{q}{(D_u D_v)^{1/2}} = (r_u + u'_s + u'_d) (r_v + v'_s + v'_d) \equiv xy, \quad (F-25)$$

where x and y are joint Gaussian random variables with statistics

$$\bar{x} = r_u, \quad \bar{y} = r_v,$$

$$\sigma_x^2 = 1 + R_u, \quad \sigma_y^2 = 1 + R_v, \quad \overline{(x-\bar{x})(y-\bar{y})} = \rho_S (R_u R_v)^{1/2}. \quad (\text{F-26})$$

We now make the same assumptions as in (99); see also (56) et seq. Then (F-26) specializes to

$$\bar{x} = \bar{y} = r, \quad \sigma_x^2 = \sigma_y^2 = 1 + R = \sigma^2, \quad \rho_{xy} = \frac{R}{1+R}. \quad (\text{F-27})$$

The joint probability density function of x, y is then given by

$$p_2(x, y) = \left[2\pi\sigma^2 (1 - \rho_{xy}^2)^{1/2} \right]^{-1} \exp \left[- \frac{(x-r)^2 + (y-r)^2 - 2\rho_{xy}(x-r)(y-r)}{2\sigma^2(1 - \rho_{xy}^2)} \right]. \quad (\text{F-28})$$

We now have cumulative distribution function

$$P_h(u) = \iint_{R_2+R_4} dx dy p_2(x, y) \quad \text{for } u \leq 0, \quad (\text{F-29})$$

and exceedance distribution function

$$1 - P_h(u) = \iint_{R_1+R_3} dx dy p_2(x, y) \quad \text{for } u \geq 0, \quad (\text{F-30})$$

where regions R_1, R_2, R_3, R_4 are indicated in figure F-3.

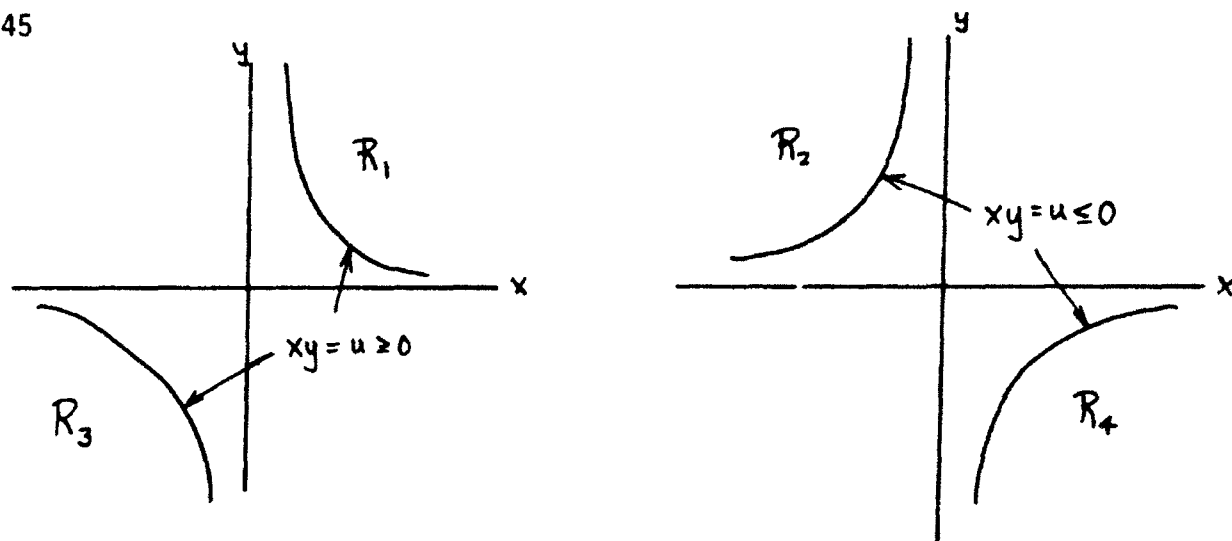


Figure F-3. Regions of Integration

If we now rotate axes according to

$$s = \frac{x+y}{2}, \quad t = \frac{x-y}{2} \quad (\text{F-31})$$

and employ (84) and (F-27), there follows (after scale changes of the variables)

$$P_h(u) = 2 \int_{-\infty}^{+\infty} dv \phi\left(v - r(2/\omega)^{1/2}\right) \Phi\left(-(\omega v^2 - 2u)^{1/2}\right) \quad \text{for } u \leq 0, \quad (\text{F-32})$$

and

$$1 - P_h(u) = 2 \int_0^{+\infty} dv \phi(v) \left[\Phi\left(\frac{r - \sqrt{u+v^2/2}}{\sqrt{\omega/2}}\right) + \Phi\left(\frac{-r - \sqrt{u+v^2/2}}{\sqrt{\omega/2}}\right) \right] \quad \text{for } u \geq 0. \quad (\text{F-33})$$

Here $\omega = 1+2R$. These real integrals are very useful for the evaluation of the distributions of h when $\gamma=0$, $N=1$. In fact, (F-33) is preferred over (F-21)-(F-23); but (106) is preferred over (F-32) since Φ need not be evaluated in (106). This is in fact the procedure utilized here to obtain numerical results for this case of $\gamma=0$, $N=1$.

APPENDIX G. PROGRAM FOR EVALUATION OF OPERATING CHARACTERISTICS FOR $\gamma=0$

The comments in appendices C and D are relevant here also. The characteristic function used as the starting point is given by (100). It was observed under (103) that $|f_h(\xi)|$ for (100) is monotonically decreasing for all $\xi \geq 0$; thus the choice of truncation value L is simplified; see appendix D comments. A table for sampling increment Δ_0 (when $R=0$) follows.

N	Δ_0 for $r=1$	Δ_0 for $r=2$
3	.07	.05
4	.07	.05
8	.05	.03
16	.04	.02
32	.03	.02
64	.025	.015
128	.020	.010
256	.012	.007

Table G-1. Values of Δ_0 for $\gamma=0$

```

10 ! GAMMA = 0          NO SAMPLE MEAN REMOVAL
20 Nc=32                ! N, Number of terms added
30 Rs=1                 ! r, Normalized mean
40 Delta0=.03          ! Initial delta
50 Bs=2*PI/Delta0*.375 ! Bias b (depends on r)
60 Mf=2^10             ! Size of FFT
70 OUTPUT 0;"GAMMA = 0";" N =";Nc;" r =";Rs
80 OUTPUT 0;" "
90 DATA -4,-3,-2.5,-2,-1.5,-1,-.5,0,.5,1,1.5,2
100 READ Ns(*)          ! SNR R=2^n
110 OUTPUT 0;Ns(*);
120 DATA 1,2,2,2,2,2,2,2,2,4,4,4,8
130 READ Idelta(*)
140 MAT Delta=(Delta0)/Idelta
150 OUTPUT 0;Delta(*);
160 DATA 1E-10,1E-9,1E-8,1E-7,1E-6,1E-5,1E-4,.001,.01,.1,.5,.9,.99,.999
170 READ Sc(*)
180 DIM Hs(1:12),Idelta(0:12),Delta(0:12),Sc(1:14)
190 DIM X(0:8191),Y(0:8191)
200 FOR I=1 TO 14
210 Sc(I)=FNIvphi(Sc(I))
220 NEXT I

```

TR 7045

```

230 S=Sc(1)
240 B=Sc(14)
250 Scale=(B-S)/(0-S)
260 X1=30
270 X2=170
280 Y1=35
290 Y2=Y1+(X2-X1)*Scale
300 PLOTTER IS "9873A"
310 LIMIT X1,X2,Y1,Y2
320 OUTPUT 705;"V93"
330 SCALE S,0,S,B
340 FOR I=1 TO 14
350 MOVE S,Sc(I)
360 DRAW 0,Sc(I)
370 NEXT I
380 FOR I=1 TO 11
390 MOVE Sc(I),S
400 DRAW Sc(I),B
410 NEXT I
420 MOVE S,S
430 DRAW 0,0
440 PENUP
450 M1=Mf-1
460 N2=Nc/2
470 Rsn=Nc*Rs*Rs ! N n^2
480 FOR In=0 TO 12
490 IF In>0 THEN 520
500 Rc=0
510 GOTO 530
520 Rc=2^Ns(In) ! SNR R=2^n
530 OUTPUT 0;"R =";Rc," Delta =";Delta(In)
540 ASSIGN #1 TO "ABSCIS" ! Temporary storage
550 Delta=Delta(In) ! for false alarm probability
560 R2=Rc*2
570 R21=R2+1
580 Mux=Nc*Rc+Rsn ! Mean of random variable h
590 Muy=Mux+Bs ! Mean of shifted variable y
600 REDIM X(0:M1),Y(0:M1)
610 MAT X=ZER
620 MAT Y=ZER
630 X(0)=0
640 Y(0)=.5*Delta*Muy
650 Ls=0
660 Ls=Ls+1
670 Xi=Delta*Ls ! Argument xi of char. fn.
680 Ei=Xi*R21 ! Calculation
690 CALL Log(1+Xi*Ei,-Xi*R2,Ai,Bi) ! of
700 CALL Div(0,Xi*Rsn,1,-Ei,Ci,Di) ! characteristic
710 CALL Exp(Ci-N2*Ai,Di+Xi*Bs-N2*Bi,Fyn,Fyi) ! function
720 Ms=Ls MOD Mf ! fy(xi)
730 Ar=Fyn/Ls
740 Ai=Fyi/Ls
750 X(Ms)=X(Ms)+Ar
760 Y(Ms)=Y(Ms)+Ai
770 Magsq=Ar*Ar+Ai*Ai
780 IF Magsq>1E-24 THEN 660
790 OUTPUT 0;"X1 =";Xi;" Mag =";SQR(Magsq)
800 CALL Fft13z(Mf,X(*),Y(*))

```

```

810  FOR Ms=0 TO M1
820  T=Y(Ms)/PI-Ms/Mf
830  X(Ms)=.5-T          ! Cumulative distribution function
840  Y(Ms)=.5+T         ! Exceedance distribution function
850  NEXT Ms
860  OUTPUT 0;Y(0);Y(1);Y(M1-1);Y(M1)
870  PLOTTER IS "GRAPHICS"
880  GRAPHICS
890  SCALE 0,Mf,-14,0
900  LINE TYPE 3
910  GRID Mf/8,1
920  PENUP
930  LINE TYPE 1
940  FOR Ms=0 TO M1
950  Pr=Y(Ms)
960  IF Pr>=1E-12 THEN Y=LGT(Pr)
970  IF Pr<=-1E-12 THEN Y=-24-LGT(-Pr)
980  IF ABS(Pr)<1E-12 THEN Y=-12
990  PLOT Ms,Y
1000 NEXT Ms
1010 PENUP
1020 FOR Ms=0 TO M1
1030 Pr=X(Ms)
1040 IF Pr>=1E-12 THEN Y=LGT(Pr)
1050 IF Pr<=-1E-12 THEN Y=-24-LGT(-Pr)
1060 IF ABS(Pr)<1E-12 THEN Y=-12
1070 PLOT Ms,Y
1080 NEXT Ms
1090 PENUP
1100 DUMP GRAPHICS
1110 OUTPUT 0;""
1120 IF In>0 THEN 1270
1130 FOR Ms=0 TO M1
1140 IF Y(Ms)<.7 THEN 1160
1150 NEXT Ms
1160 M2=Ms-1
1170 FOR Ms=M2 TO M1
1180 IF Y(Ms)<=0 THEN 1200
1190 NEXT Ms
1200 M3=Ms-1
1210 REDIM X(M2:M3)
1220 FOR Ms=M2 TO M3
1230 X(Ms)=FNInuphi(Y(Ms))
1240 NEXT Ms
1250 PRINT #1;X(*)          ! Store false alarm probability
1260 GOTO 1460
1270 REDIM X(M2:M3)
1280 READ #1;X(*)          ! Read in false alarm probability
1290 Id=Idelta(In)
1300 J2=INT(M2/Id)
1310 J3=INT(M3/Id)+1
1320 FOR J=J2 TO J3
1330 Y(J)=FNInuphi(Y(J))
1340 NEXT J

```

TR 7045

```

1350 PLOTTER IS "9872A"
1360 LIMIT X1,X2,Y1,Y2
1370 OUTPUT 705;"VS3"
1380 SCALE S,0,S,B
1390 FOR J=J2 TO J3
1400 T=J*Id
1410 IF T<M2 THEN 1440
1420 IF T>M3 THEN 1450
1430 PLOT X(T),Y(J)
1440 NEXT J
1450 PENUP
1460 NEXT In
1470 END
1480 !
1490 SUB Div(X1,Y1,X2,Y2,A,B) ! DIV(Z)
1540 !
1550 SUB Exp(X,Y,A,B) ! EXP(Z)
1600 !
1610 SUB Log(X,Y,A,B) ! PRINCIPAL LOG(Z)
1690 !
1700 DEF FNInvphi(X) ! INVPHI(X) via AMS 55, 26.2.23
1830 !
1840 SUB Fft13z(N,X(*),Y(*)) ! N <= 2^13, N=2^INTEGER, 0 SUBSCRIPT

```


REFERENCES

1. A. H. Nuttall, "Resolution of Ambiguity for Randomly Moving Line Array," NUSC Technical Memorandum 831150, 3 October 1983.
2. A. H. Nuttall, "Exact Performance of General Second-Order Processors for Gaussian Inputs," NUSC Technical Report 7035, 15 October 1983.
3. A. H. Nuttall, "Accurate Efficient Evaluation of Cumulative or Exceedance Probability Distributions Directly from Characteristic Functions," NUSC Technical Report 7023, 1 October 1983.
4. A. H. Nuttall and B. Dedreux, "Exact Operating Characteristics for Linear Sum of Envelopes of Narrowband Gaussian Process and Sinewave," NUSC Technical Report 7117, 11 January 1984.
5. I. S. Gradshteyn and I. M. Ryzhik, Table of Integrals, Series, and Products, Academic Press, Inc., New York, 1980.
6. Handbook of Mathematical Functions, U. S. Department of Commerce, National Bureau of Standards, Applied Mathematics Series No. 55, U. S. Government Printing Office, June 1964.
7. A. H. Nuttall, "Some Integrals Involving the Q-Function," NUSC Technical Report 4297, 17 April 1972.
8. A. H. Nuttall, "Some Integrals Involving the Q_M -Function," NUSC Technical Report 4755, 15 May 1974.
9. W. B. Davenport and W. L. Root, Random Signals and Noise, McGraw-Hill Book Co., N.Y., 1958.
10. N. W. McLachlan, Complex Variable Theory and Transform Calculus, Cambridge University Press, second edition, N.Y., 1963.

Under-Ice Roughness: Shot Noise Model

A. H. Nuttall

ABSTRACT

The one-dimensional roughness of an under-ice profile of elliptical bosses is modeled in the time domain by a shot-noise process of elliptical pulses of random amplitude, duration, and time of occurrence. A sample realization of 8000 data points is generated and plotted for visual comparison with experimental under-ice data. Also, theoretical and simulation results for the power density spectrum, the auto-correlation function, the characteristic function, the cumulative distribution function, and the probability density function of the shot-noise process are plotted and compared.

INTRODUCTION

The under-ice profile has been observed to appear like a random collection of superposed elliptical bosses, each of random amplitude, length, and location. An analogous model in the time domain is shot noise composed of overlapping pulses of random amplitude, duration, and time of occurrence. Accordingly, we have generated a sample realization of a shot noise process for visual comparison with experimental under-ice data, and for possible corroboration of this model. The particular realization generated has 8000 data points, although the number of effectively-independent samples is far fewer, as will be demonstrated.

A number of analytical results for shot noise have been derived in the past [1]; however, they did not cover the case of random duration modulation. We have extended the analyses to include random durations (as well as random amplitudes and random time occurrences) and evaluated the spectrum of the shot noise process, as well as the autocorrelation function and the first-order characteristic function of the instantaneous amplitude. From the latter, the first-order probability density function and cumulative distribution function of shot noise have been evaluated via a generalized Laguerre expansion employing 32 cumulants or moments. Comparisons of all these theoretical results with the corresponding sample quantities, obtained from the 8000 data point realization above, reveal excellent agreement.

A REALIZATION OF A SHOT-NOISE PROCESS

Shot noise is characterized by a superposition of pulses, each located independently and uniformly on the time scale. A sample pulse is illustrated in figure 1. The time of occurrence t_k (center of symmetrical pulse, for

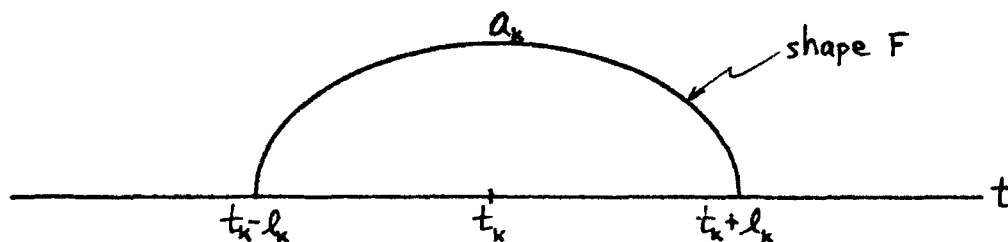


Figure 1. Sample Pulse of Shot Noise

example) is uniformly distributed in time t , with an average number of pulses per second, ν . The amplitude a_k and half-duration l_k of an individual pulse are also all independent and are each identically randomly-distributed with arbitrary probability density functions. Finally the fundamental pulse shape F in figure 1 is arbitrary.

A realization of shot noise is given by

$$I(t) = \sum_k a_k F\left(\frac{t-t_k}{l_k}\right), \quad (1)$$

where the summation extends over all k . The particular data we generate here employs the following example; unscaled pulse shape F is circular:

$$F(x) = \begin{cases} (1-x^2)^{1/2} & \text{for } |x| < 1 \\ 0 & \text{for } |x| > 1 \end{cases}. \quad (2)$$

This pulse is continuous; however, it has cusps (infinite slope) at $x = \pm 1$. The reason for this selection will become apparent when we discuss the spectrum of shot noise process (1).

The amplitude probability density function for random variable a_k is Rayleigh,

$$p(a) = \frac{a}{\sigma_a^2} \exp\left(-\frac{a^2}{2\sigma_a^2}\right) U(a), \quad (3)$$

and the duration probability density function for random variable l_k is also Rayleigh,

$$p(l) = \frac{l}{\sigma_l^2} \exp\left(-\frac{l^2}{2\sigma_l^2}\right) U(l). \quad (4)$$

Here, step function

$$U(x) = \begin{cases} 1 & \text{for } x > 0 \\ 0 & \text{for } x < 0 \end{cases}. \quad (5)$$

The mean values of random variables a_k and l_k are given respectively by

$$\bar{a} = \bar{a}_k = \left(\frac{\pi}{2}\right)^{1/2} \sigma_a, \quad \bar{l} = \bar{l}_k = \left(\frac{\pi}{2}\right)^{1/2} \sigma_l, \quad (6)$$

in terms of the parameters σ_a and σ_l of probability density functions (3) and (4). Alternatively, the mean square values are given by

$$\overline{a^2} = \overline{a_k^2} = 2\sigma_a^2, \quad \overline{l^2} = \overline{l_k^2} = 2\sigma_l^2. \quad (7)$$

Three typical component pulses are depicted in figure 2, and can range from circular through various elongated elliptical shapes. The total length of an individual pulse is $L_k = 2l_k$. An important parameter of this time-

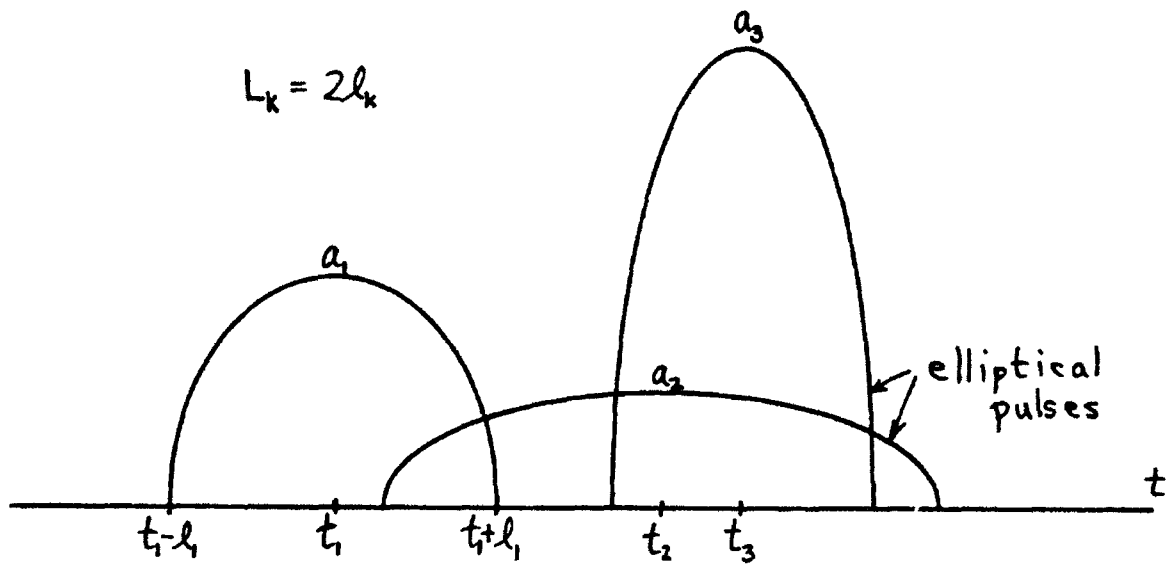


Figure 2. Three Component Pulses

limited pulse shape in figures 1 and 2 is the (dimensionless) overlap factor

$$\bar{L}_k v = 2\bar{L}_k v = 2 \left(\frac{\pi}{2} \right)^{1/2} \sigma_2 v . \quad (8)$$

This is the average number of pulses that are overlapping at any one instant of time, and is a partial measure of the applicability of the central limit theorem. A more meaningful measure are the cumulants; for probability density function (3) and pulse shape (2), the normalized third and fourth cumulants are

$$\frac{1.017}{(\bar{L}_k v)^{1/2}} \quad \text{and} \quad \frac{1.2}{\bar{L}_k v} , \quad (9)$$

respectively. In the sample realization generated here, the overlap factor in (8) was 6.2, leading to normalized cumulant values in (9) of .58 and .39, respectively. Since a Gaussian probability density function would lead to zero cumulants above second-order, the shot noise realization dealt with here is distinctly non-Gaussian.

In the three parts of figure 3, a realization of shot noise model (1) is given for parameter values

$$\sigma_a = 1 \text{ sec}, \quad \sigma_k = 20 \text{ sec}, \quad \nu = .124 \text{ pulses/sec.} \quad (10)$$

The waveform (1) is sampled at unit time increments and connected by straight lines; thus the initial 100 data points illustrated in figure 3A have a jagged appearance for those component pulses with small λ_k , as for example at time instants 67-68. The larger duration pulses, like the one centered at $t = 29$, have a smoother appearance.

In figure 3B, the initial 1000 data points illustrate the very erratic character of shot noise; the waveform consists of some very sharp spiky pulses and other broader smooth components. The appearance of a downward trend in these 1000 data points is erased when the entire 8000 data point sequence is viewed in figure 3C. The possibility of shot noise process (1) reaching a zero value (when no pulses overlap) is confirmed by the waveform values near $t = 6400$.

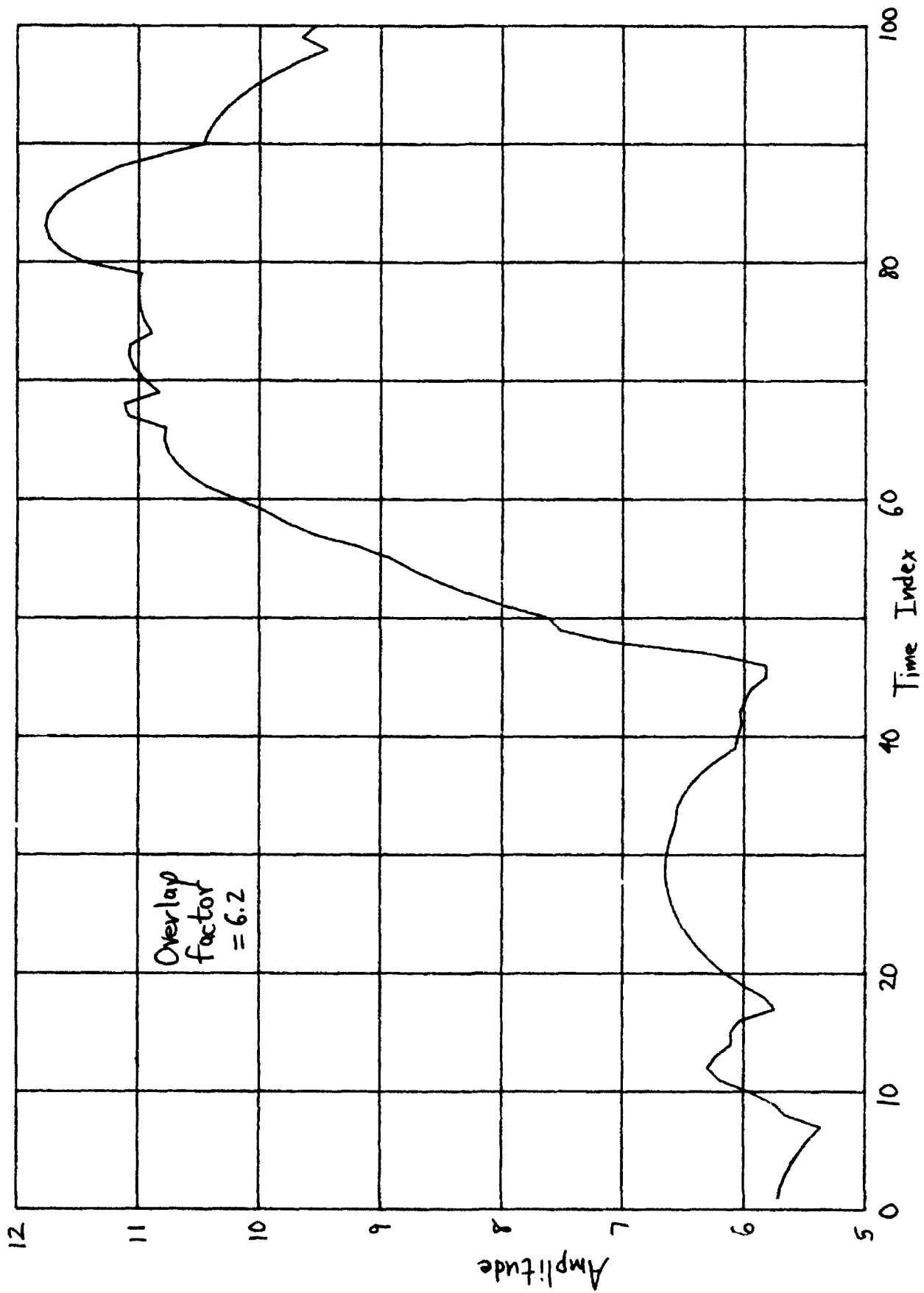


Figure 3A. Initial 100 Data Points

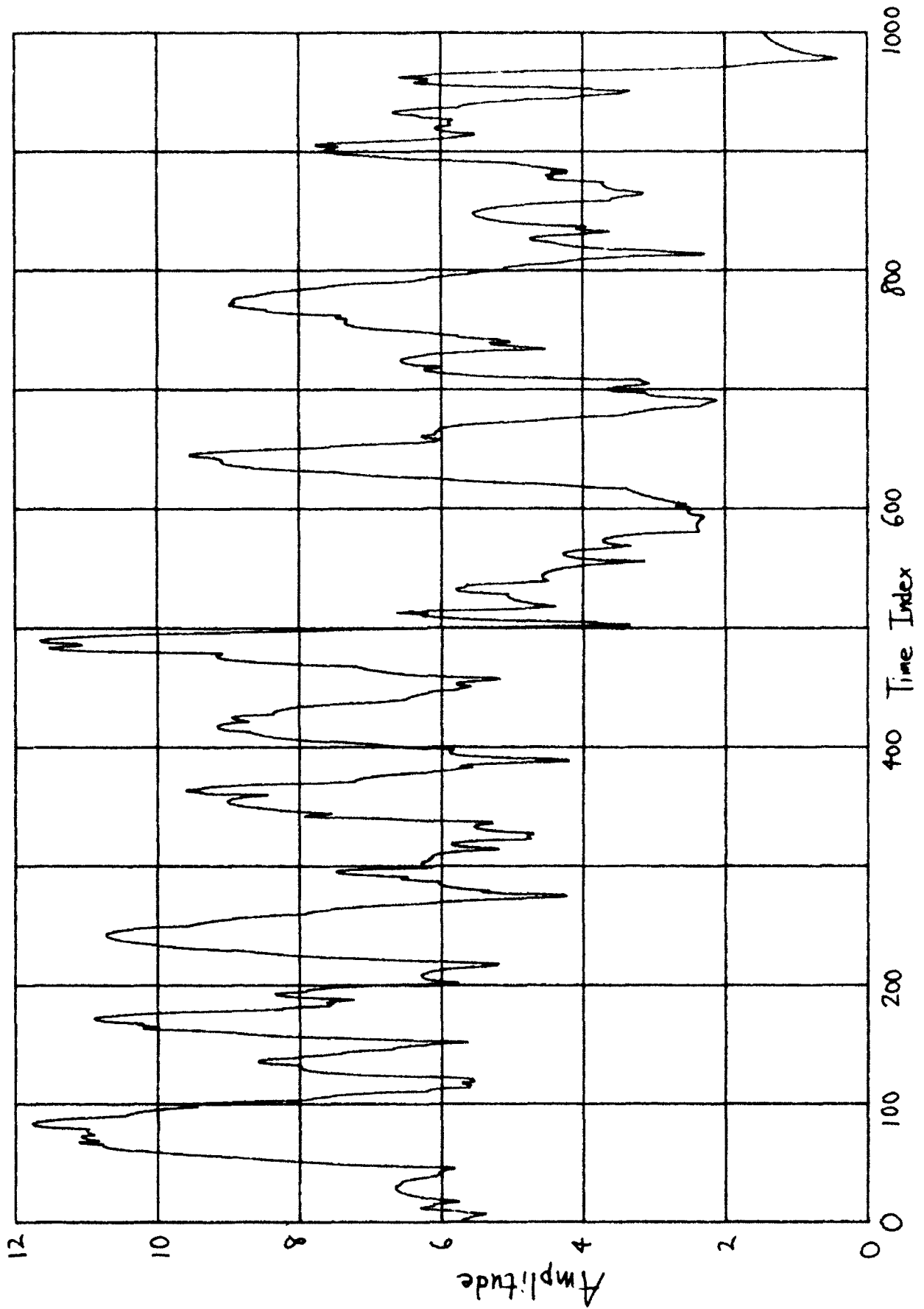


Figure 3B. Initial 1000 Data Points

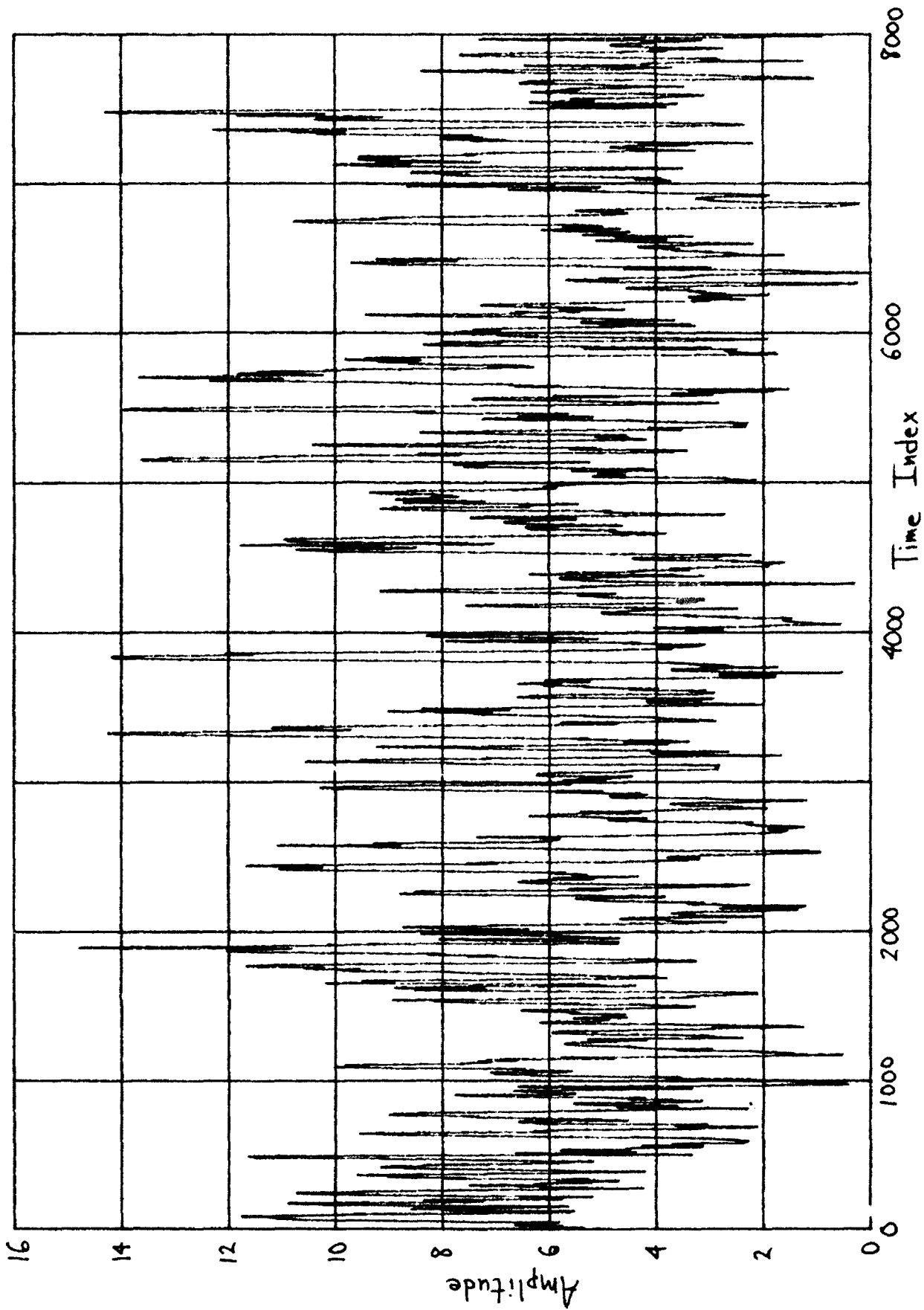


Figure 3C. Total Data Segment

CORRELATION AND SPECTRUM OF SHOT NOISE PROCESS

The derivations of the correlation and spectrum of the shot noise process (1) are given in appendix A; from (A-12), we have, in general, the correlation function at delay τ ,

$$R_I(\tau) = v \bar{a}^2 \int d\ell p(\ell) \ell \phi(\tau/\ell) + I_{dc}^2, \quad (11)$$

where the dc component of $I(t)$ is, from (A-13),

$$I_{dc} = v \bar{a} \bar{\ell} \int dx F(x), \quad (12)$$

and

$$\phi(y) = \int dx F(x) F(x-y) \quad (13)$$

is the (aperiodic) correlation of an individual pulse F . (All integrals are over the range of non-zero integrand.)

Also, from (A-16), the general spectrum of process $I(t)$ is, at frequency f ,

$$G_I(f) = v \bar{a}^2 \int d\ell p(\ell) \ell^2 |S(\ell f)|^2 + I_{dc}^2 \delta(f), \quad (14)$$

where

$$S(f) = \int dx \exp(-i2\pi f x) F(x) \quad (15)$$

is the voltage density spectrum (Fourier transform) of pulse F . Thus $|S(f)|^2$ is the energy density spectrum corresponding to pulse F .

It should be observed that the entire probability density function $p(\ell)$ of half-duration random variable ℓ_k is required in order to evaluate the correlation or spectrum of shot noise. However, only the first two moments, \bar{a} and $\overline{a^2}$, are required known about probability density function $p(a)$ of amplitude random variable a_k . The only way that the dc term I_{dc} can be zero is if random variable a_k has zero mean ($\bar{a} = 0$), or if pulse F has zero area ($S(0) = 0$).

Example

The example of interest here was given earlier in (2) and (4), namely a circular pulse F and a Rayleigh probability density function for random variable ℓ_k . The spectrum $G_I(f)$ in (14) is evaluated in (A-17) through (A-22), with the results

$$S(f) = \frac{J_1(2\pi f)}{2f}, \quad S(0) = \frac{\pi}{2},$$

$$I_{dc} = \left(\frac{\pi}{2}\right)^{3/2} v \bar{a} \sigma_\ell^2,$$

$$G_I(f) = 2\pi^2 v \overline{a^2} \sigma_\ell^2 \frac{2 \exp(-z) I_1(z)}{z} + \left(\frac{\pi}{2}\right)^3 v^2 \bar{a}^2 \sigma_\ell^2 \delta(f)$$

$$\text{with } z = (2\pi\sigma_\ell f)^2. \tag{16}$$

The asymptotic behavior of spectrum (16) is [2, eq. 9.7.1]

$$G_I(f) \sim \frac{v \overline{a^2}}{(2\pi)^{3/2} \sigma_\ell} f^{-3} \quad \text{as } f \rightarrow +\infty. \tag{17}$$

That is, the spectrum decays at a -30 dB/decade rate at large frequencies; this is due to the square root singularities at $x = \pm 1$ of pulse F given in (2). This decay rate has been observed in some spectral analyses of under-ice profiles, and was one of the reasons for choosing the specific circular pulse in (2) for this investigation.

The spectrum in (16) is plotted in figure 4, for the choice of parameters earlier in (10), as a dashed line, normalized to 0 dB at $f = 0$. Superposed is a linear-predictive spectral analysis result with predictive order 10, for the 8000 data points of figure 3C. The two results are in excellent agreement, even at the -50 dB level, with the inevitable 3 dB aliasing effect at the Nyquist frequency, as indicated.

The correlation $R_I(\tau)$ in (11) is evaluated in (A-23) through (A-33), for the example (2) and (4), with the result

$$R_I(\tau) = \frac{8}{3}(2\pi)^{\frac{1}{2}} \sqrt{a^2} \sigma_{\ell} s \exp(-s) [(1+4s) K_1(s) - (3+4s) K_0(s)] + \\ + \left(\frac{\pi}{2}\right)^3 \sqrt{a^2} \frac{2}{\sigma_{\ell}^2}, \quad \text{with } s = \left(\frac{\tau}{4\sigma_{\ell}}\right)^2. \quad (18)$$

This quantity, exclusive of the I_{dc}^2 term, and normalized at the origin, is plotted in figure 5 as a dashed line, for delays (lags) τ up to 100. It is seen to decay monotonically to zero as τ increases, and reach its $1/e$ value at approximately $\tau = 30$.

The remaining solid curve on figure 5 is the normalized sample autocorrelation function of the 8000 data point sequence in figure 3C, where the sample mean was subtracted from the given data. The agreement with theoretical result (18) is excellent. The dotted horizontal lines at $\pm 2\sigma$ in figure 5 are the ± 2 sigma values of the correlation estimate at delays where the true correlation is presumed zero; the details of this analysis are given in appendix B.

This procedure is duplicated in figure 6, where the correlation function estimate out to lag $\tau = 1000$ is plotted. The drifting of the estimate outside the $\pm 2\sigma$ limits (at $\tau = 470$ and 820) is consistent with an occasional excursion of a random variable outside its $\pm 2\sigma$ range. The correlation estimate (used for figures 5 and 6) at time separation k is

$$R_k = \frac{1}{N} \sum_{n=k+1}^N x_n x_{n-k} \quad \text{for } k \geq 0, \quad (19)$$

where $\{x_n\}_1^N$ is the available data in figure 3C, with its sample mean removed.

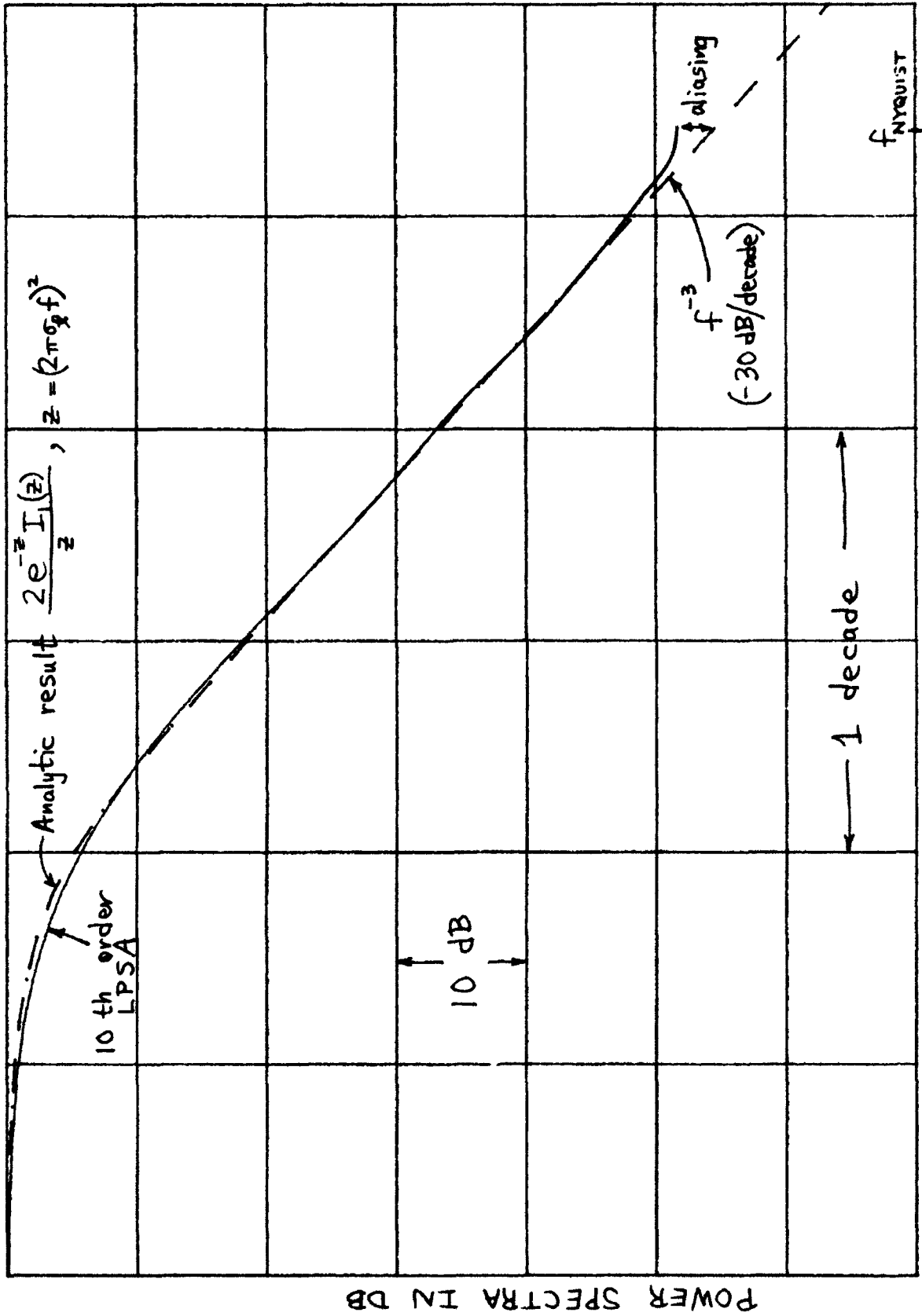


Figure 4. Comparison of Power Spectra

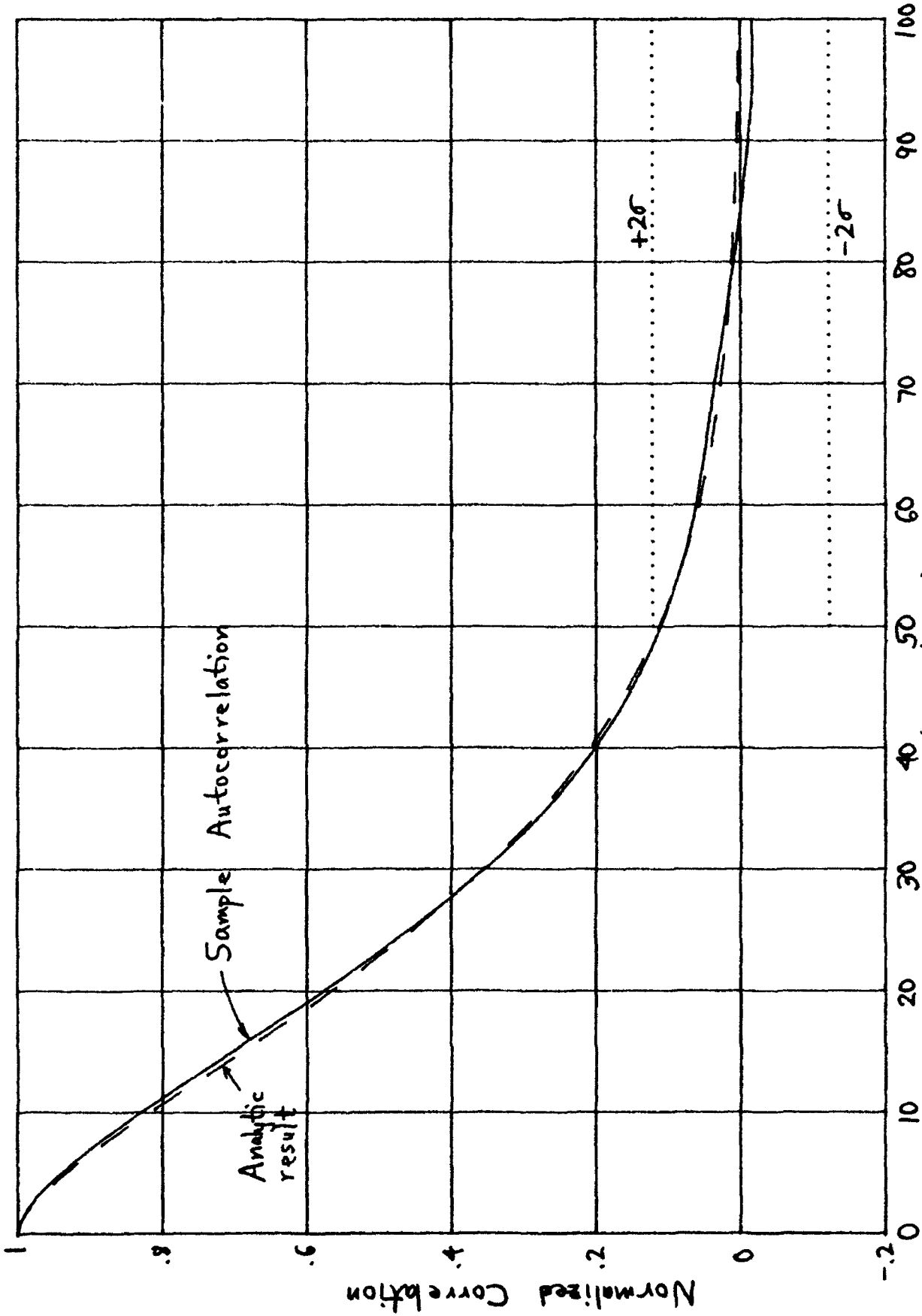


Figure 5. Estimate of Autocorrelation Function near origin

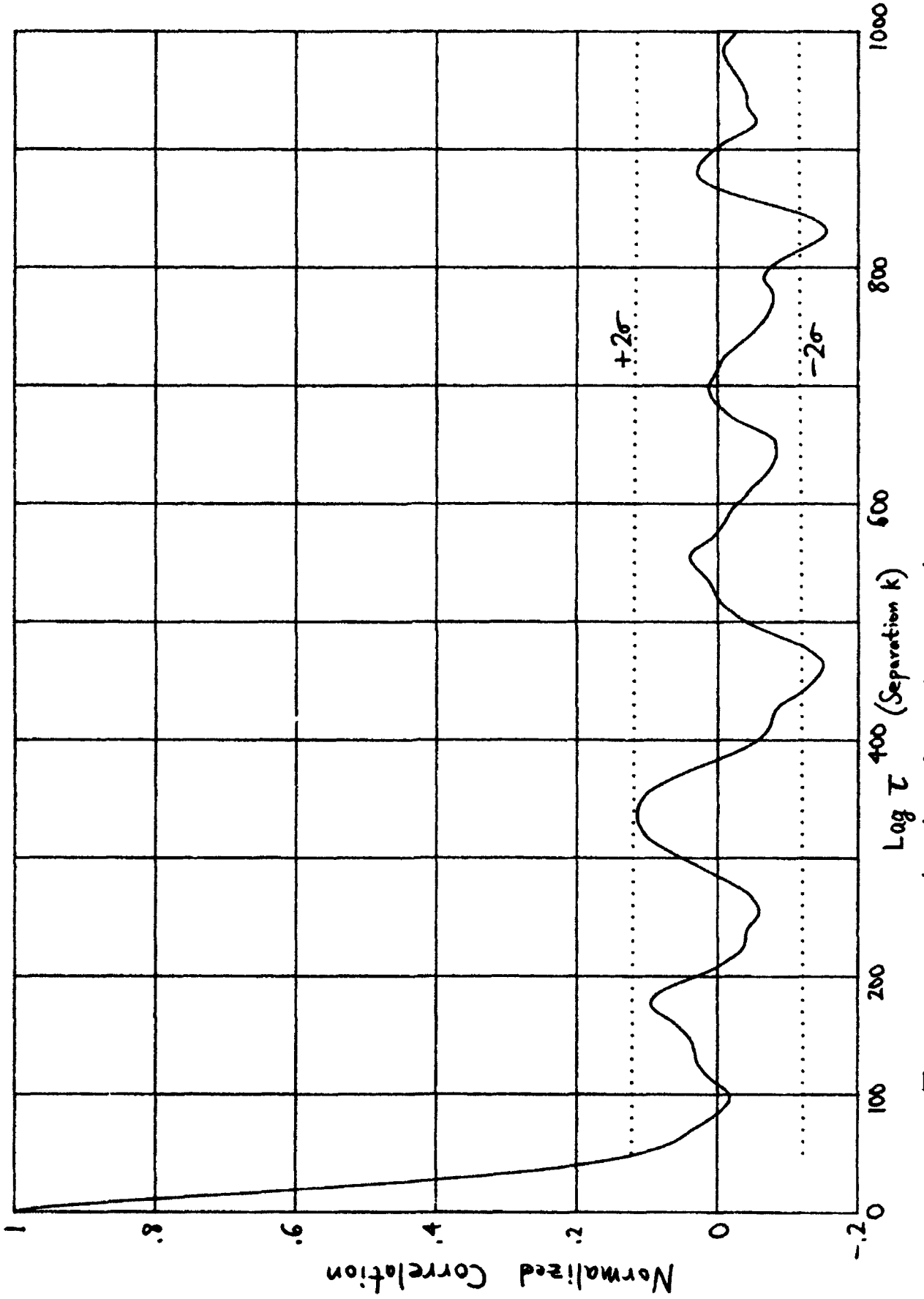


Figure 6. Estimate of Autocorrelation Function

AMPLITUDE STATISTICS OF SHOT NOISE

The first-order characteristic function of shot noise process $I(t)$ is derived in appendix C; it is given by (C-9) as

$$f_I(\xi) = \exp \left[v \bar{\ell} \int dx \left\{ f_a[\xi F(x)] - 1 \right\} \right]. \quad (20)$$

Here f_a is the first-order characteristic function of amplitude random variable a_k . Observe that the probability density function $p(\ell)$ of duration ℓ_k is irrelevant to characteristic function f_I , except for its mean $\bar{\ell}$; this is in contrast to the spectrum and correlation results in (11) and (14), where $p(a)$ was irrelevant except for parameters \bar{a} and $\overline{a^2}$. (For $\ell_k = 1$ for all k , (20) reduces to a simplified version of [1, eq. 4.5-4].)

The characteristic function of the amplitude random variable a_k can be expanded in terms of its moments

$$\mu_a(n) = \overline{a^n} = \int da a^n p(a) \quad \text{for } n \geq 0, \quad (21)$$

according to

$$f_a(\xi) = \sum_{n=0}^{\infty} \mu_a(n) (i\xi)^n / n!. \quad (22)$$

This result is useful if the ℓ_n of (20) is expanded in a series in ξ ; namely

$$\ell_n f_I(\xi) = v \bar{\ell} \sum_{n=1}^{\infty} \mu_a(n) (i\xi)^n \int dx F^n(x) / n!, \quad (23)$$

giving immediately the cumulants of $I(t)$ as

$$\chi_I(n) = v \bar{\ell} \mu_a(n) \int dx F^n(x) \quad \text{for } n \geq 1. \quad (24)$$

That is, the n -th cumulant of $I(t)$ is proportional to the n -th moment of random variable a_k as well as the n -th "moment" of pulse F . (For $l_k = 1$ for all k , (24) reduces to [1, eq. 1.5-2].)

The normalized cumulant of $I(t)$ is

$$\gamma_I(n) = \frac{\chi_I(n)}{[\chi_I(2)]^{n/2}} = \frac{1}{(\nu \bar{l})^{n/2-1}} \frac{\mu_a(n) \int dx F^n(x)}{\left[\mu_a(2) \int dx F^2(x) \right]^{n/2}} . \quad (25)$$

In particular, the coefficients of skewness and excess [3, pp. 184 and 187] are

$$\gamma_I(3) = \frac{1}{(\nu \bar{l})^{3/2}} \frac{\mu_a(3) \int dx F^3(x)}{\left[\mu_a(2) \int dx F^2(x) \right]^{3/2}} \quad (26)$$

and

$$\gamma_I(4) = \frac{1}{\nu \bar{l}} \frac{\mu_a(4) \int dx F^4(x)}{\left[\mu_a(2) \int dx F^2(x) \right]^2} . \quad (27)$$

These quantities are very important measures of the approach of $I(t)$ to a Gaussian process; if $\nu \bar{l}$ is very large, the normalized cumulants $\gamma_I(n)$ are all substantially zero for $n \geq 3$, meaning that $I(t)$ is nearly Gaussian. Thus although probability density function $p(l)$ is not directly relevant to the probability density function or characteristic function (20) of $I(t)$, the exact probability density function of $I(t)$ is critically dependent on the mean \bar{l} through the dimensionless parameter $\nu \bar{l}$. More precisely, (26) and (27) are the critical quantities; see also [1, eq. 1.6-3].

If either the third moment of random variable a_k is zero, or if the third moment of pulse F is zero, then $\gamma_I(3) = 0$. In that case, $\gamma_I(4)$ is the most important statistic measuring the applicability of the central limit theorem; $\gamma_I(4)$ can never be zero for shot noise, since neither the fourth moment of random variable a_k or pulse F can be zero (except in a trivial case).

The first moment of shot noise $I(t)$ is the mean

$$I_{dc} = \overline{I(t)} = \chi_I(1) = v \bar{\lambda} \bar{a} \int dx F(x) \quad (28)$$

and has already been encountered in (12). It can be zero only if the first moment of random variable a_k or of pulse F is zero.

Example

Numerous cases have been considered in appendix C; in the main body here, we limit attention to example (2) and (3) presented earlier. We find

$$\begin{aligned} \mu_a(n) &= 2^{\frac{n}{2}} \Gamma\left(\frac{n}{2} + 1\right) \sigma_a^n \quad \text{for } n \geq 0, \\ \int dx F^n(x) &= \frac{2^{n+1} \Gamma^2\left(\frac{n}{2} + 1\right)}{\Gamma(n+2)} \quad \text{for } n \geq 0. \end{aligned} \quad (29)$$

Then (26) and (27) yield result (9) quoted earlier.

The realization of shot noise process $I(t)$ in figure 3C employed the parameters in (10). The sample cumulative distribution function of these 8000 data points is depicted in figure 7, on a normal probability ordinate; thus a

truly Gaussian random variable would have the straight line character indicated. The significant deviation of the sample cumulative distribution function from the Gaussian line is due to the small value of the overlap factor in (8), namely

$$\Gamma_k \nu = 2 \quad \bar{\Gamma}_k \nu = 6.2 \quad . \quad (30)$$

The moments in (29) are all positive and are easily numerically evaluated via recursion; hence the cumulants in (24) can be accurately evaluated for high-order n . When these cumulants are employed in a generalized Laguerre expansion of the cumulative distribution function of $I(t)$, using 32 moments of (29), the solid curve in figure 8 is obtained. The sample cumulative distribution function of figure 7 is duplicated here, although the abscissa is scaled differently. The agreement between theory and experiment in figure 8 is excellent, considering the fact that we only have about $8000/30 = 270$ effectively independent samples of $I(t)$ in figure 3C; the denominator factor of 30 here is the effective correlation duration, previously identified in figure 5 at the $1/e$ point.

Finally, when the same 32 moments are used in a generalized Laguerre expansion of the probability density function of $I(t)$, the result in figure 9 is obtained. The small bump near the origin is real and accurate; it and the non-symmetric tails of the probability density function confirm the distinctly non-Gaussian character of $I(t)$. The method for the determination of the cumulative distribution function and probability density function in figures 8 and 9 will be presented in a NUSC Technical Report [4] by the author; the programs are listed here in appendix D, along with an example of the sequence of Laguerre coefficients.

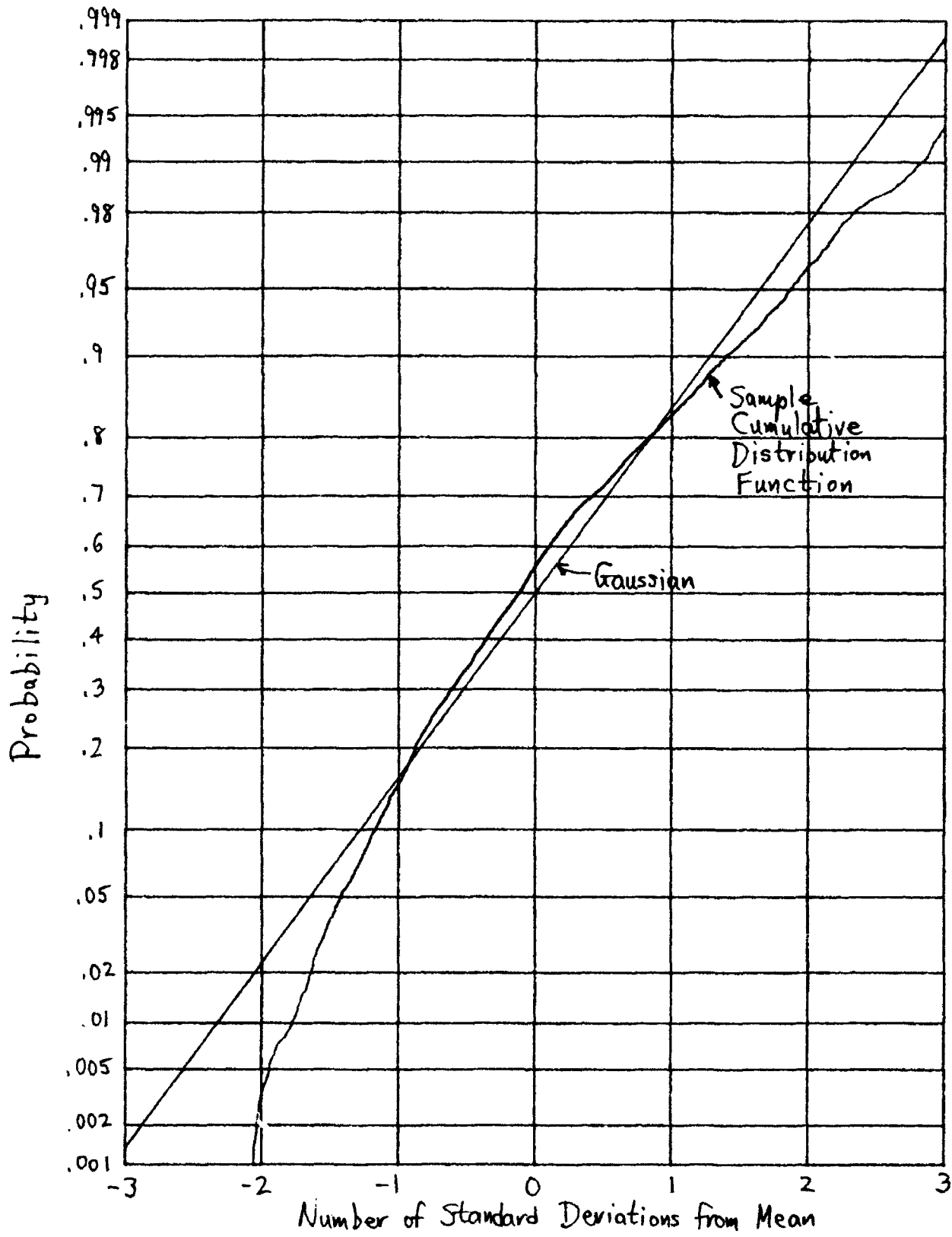


Figure 7. Estimate of Cumulative Distribution Function

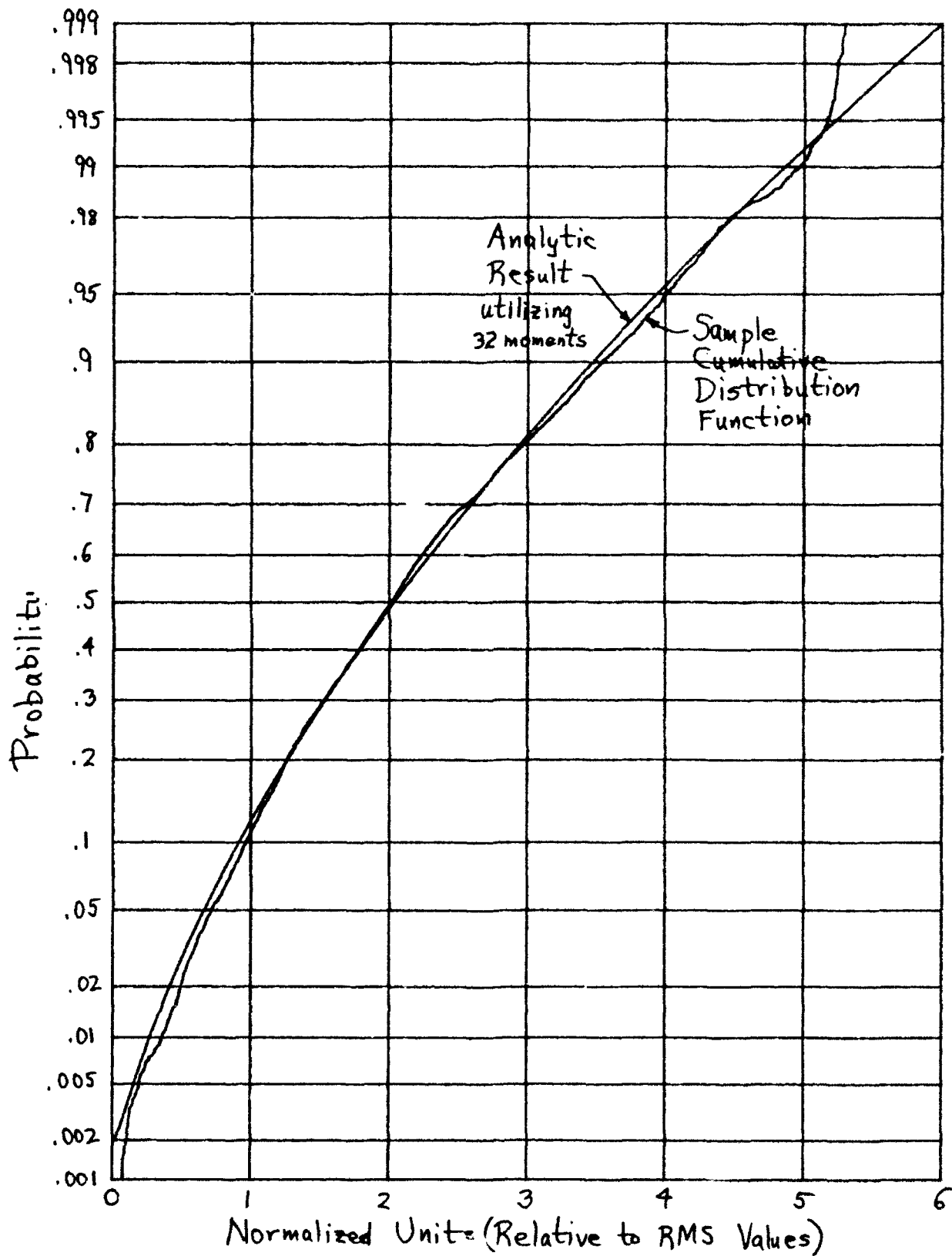


Figure 8. Comparison of Cumulative Distribution Functions

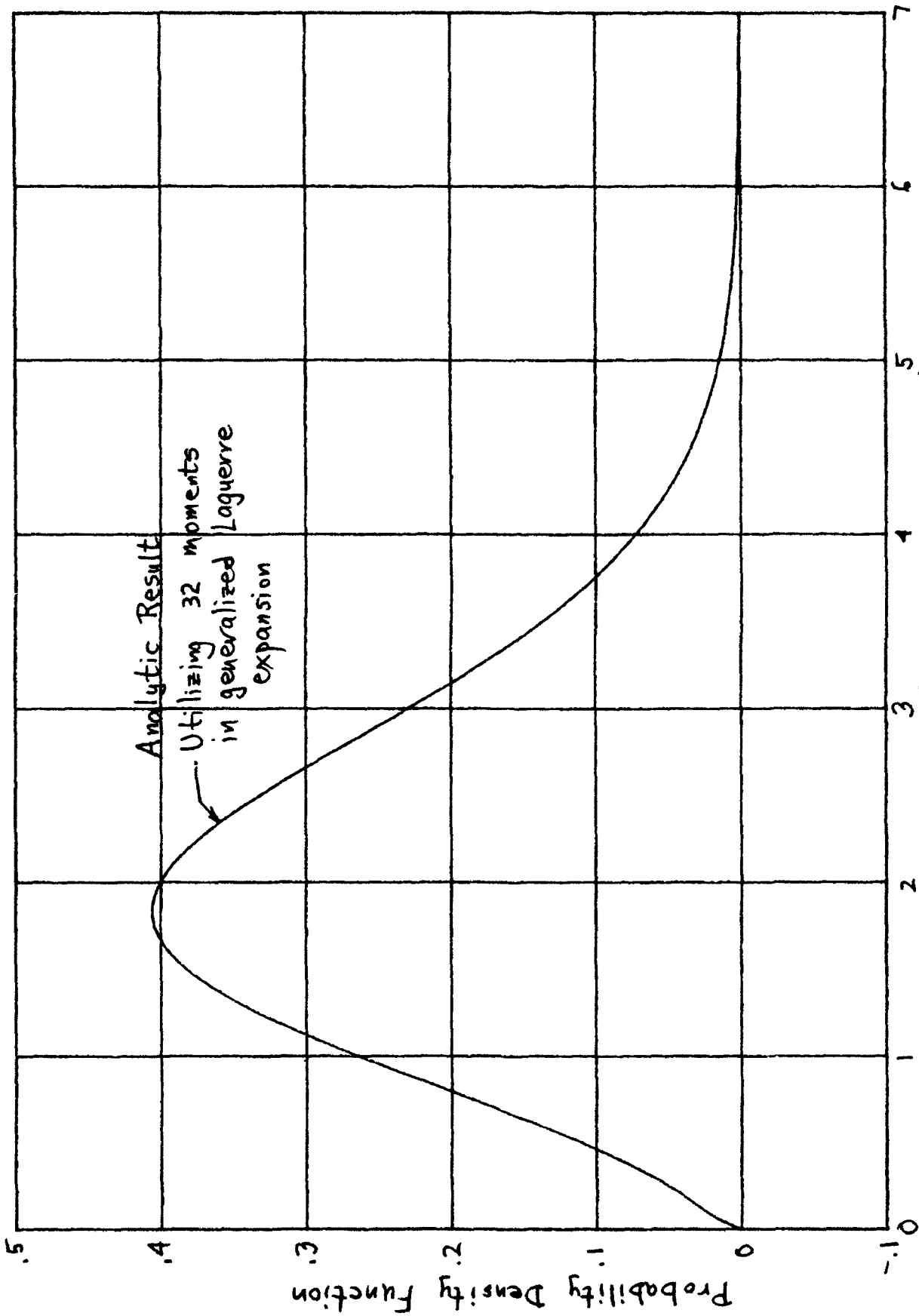


Figure 9. Theoretical Probability Density Function (Continuous Portion)

APPENDIX A. DERIVATION OF SPECTRUM AND CORRELATION

The method employed below follows that given by Rice [1, sections 1.4 and 1.5] rather closely. We generalize [1, eq. 1.3-1] to the current form introduced in (1):

$$I_K(t) = \sum_{k=1}^K a_k F\left(\frac{t-t_k}{\lambda_k}\right), \quad (A-1)$$

where $\{a_k\}$, $\{t_k\}$, $\{\lambda_k\}$ are all independent random variables. K is the presumed number of pulses to occur in a large time interval T , and a_k is a random amplitude as in [1, eq. 1.5-1]; but random duration λ_k is new. Then product

$$\begin{aligned} I_K(t) I_K(t-\tau) &= \sum_{k=1}^K a_k^2 F\left(\frac{t-t_k}{\lambda_k}\right) F\left(\frac{t-\tau-t_k}{\lambda_k}\right) + \\ &+ \sum_{k=1}^K \sum_{\substack{m=1 \\ k \neq m}}^K a_k a_m F\left(\frac{t-t_k}{\lambda_k}\right) F\left(\frac{t-\tau-t_m}{\lambda_m}\right). \end{aligned} \quad (A-2)$$

Holding random variables $\{a_k\}$ and $\{\lambda_k\}$ fixed for now, the statistical average of (A-2) over $\{t_k\}$ is

$$\begin{aligned} &\sum_{k=1}^K a_k^2 \frac{1}{T} \int dt_k F\left(\frac{t-t_k}{\lambda_k}\right) F\left(\frac{t-\tau-t_k}{\lambda_k}\right) + \\ &+ \sum_{k=1}^K \sum_{\substack{m=1 \\ k \neq m}}^K a_k a_m \frac{1}{T} \int dt_k F\left(\frac{t-t_k}{\lambda_k}\right) \frac{1}{T} \int dt_m F\left(\frac{t-\tau-t_m}{\lambda_m}\right) = \\ &\cong \frac{1}{T} \sum_{k=1}^K a_k^2 \lambda_k \phi(\tau/\lambda_k) + \frac{1}{T^2} \sum_{k=1}^K \sum_{\substack{m=1 \\ k \neq m}}^K a_k a_m \lambda_k \lambda_m S^2(0), \end{aligned} \quad (A-3)$$

where T is an arbitrary large (but finite) time interval, and

$$\phi(y) = \int dx F(x) F(x-y) \quad (A-4)$$

is the aperiodic autocorrelation of pulse F, while

$$S(f) = \int dx \exp(-i2\pi fx) F(x) \quad (A-5)$$

is the voltage density spectrum of F.

The remaining averages over independent random variables $\{a_k\}$ and $\{\lambda_k\}$ in (A-3) now yield

$$\frac{1}{T} K \overline{a^2} \int d\lambda p(\lambda) \lambda \phi(\tau/\lambda) + \frac{1}{T^2} (K^2 - K) [\overline{a} \overline{\lambda} S(0)]^2, \quad (A-6)$$

where $p(\lambda)$ is the probability density function of random variable λ_k .

Now K is itself a random variable, with discrete probability

(in an interval T) of [1, eq. 1.1-3]

$$\frac{(vT)^K}{K!} \exp(-vT) \quad \text{for } K = 0, 1, 2, \dots \quad (A-7)$$

There then follows the characteristic function of random variable K as

$$f_K(\xi) = \exp(vT[\exp(i\xi) - 1]), \quad (A-8)$$

with series expansion

$$\ln f_K(\xi) = vT [\exp(i\xi) - 1] = vT \sum_{n=1}^{\infty} (i\xi)^n / n! \quad (A-9)$$

Thus the cumulants of random variable K are all equal,

$$\chi_K(n) = vT \quad \text{for } n \geq 1, \quad (A-10)$$

giving in particular the first two moments

$$\overline{K} = vT, \quad \overline{K^2} = vT(vT + 1) \quad (A-11)$$

The use of (A-11), to perform the remaining average of (A-6) with respect to random variable K , then yields the correlation function of the shot noise process $I(t)$:

$$R_I(\tau) = v \bar{a}^2 \int d\ell p(\ell) \ell \phi(\tau/\ell) + [v \bar{a} \bar{\ell} S(0)]^2. \quad (\text{A-12})$$

The dc component of $I(t)$ is

$$I_{dc} = v \bar{a} \bar{\ell} S(0) = v \bar{a} \bar{\ell} \int dx F(x). \quad (\text{A-13})$$

The spectrum of $I(t)$ is the Fourier transform of (A-12):

$$G_I(f) = v \bar{a}^2 \int d\ell p(\ell) \ell^2 \Phi(\ell f) + I_{dc}^2 \delta(f), \quad (\text{A-14})$$

where

$$\begin{aligned} \Phi(f) &= \int d\tau \exp(-i2\pi f\tau) \phi(\tau) = \\ &= \int d\tau \exp(-i2\pi f\tau) \int dx F(x) F(x-\tau) = |S(f)|^2, \end{aligned} \quad (\text{A-15})$$

by use of (A-4) and (A-5). Thus (A-14) can be expressed as

$$G_I(f) = v \bar{a}^2 \int d\ell p(\ell) \ell^2 |S(\ell f)|^2 + I_{dc}^2 \delta(f). \quad (\text{A-16})$$

$|S(f)|^2$ is the energy density spectrum of pulse F .

Example

The example of interest here is given in (2) and (4):

$$F(x) = \begin{cases} (1-x^2)^{1/2} & \text{for } |x| < 1 \\ 0 & \text{for } |x| > 1 \end{cases},$$

$$p(\ell) = \frac{\ell}{\sigma_\ell} \exp\left(-\frac{\ell^2}{2\sigma_\ell^2}\right) U(\ell). \quad (\text{A-17})$$

Then from (A-5) and [5, eq. 3.752 2],

$$S(f) = \int_{-1}^1 dx \exp(-i2\pi fx) (1-x^2)^{1/2} = \frac{J_1(2\pi f)}{2f}. \quad (\text{A-18})$$

Substitution of (A-17) and (A-18) in the integral in (A-16) yields, by use of [5, eq. 6.633 2],

$$\int d\ell \frac{\ell}{\sigma_\ell^2} \exp\left(-\frac{\ell^2}{2\sigma_\ell^2}\right) \frac{J_1^2(2\pi f)}{4f^2} = 2\pi^2 \sigma_\ell^2 \frac{2 \exp(-z) I_1(z)}{z}, \quad (\text{A-19})$$

where

$$z = (2\pi\sigma_\ell f)^2. \quad (\text{A-20})$$

Then the spectrum (A-16) is given by

$$G_I(f) = 2\pi^2 \nu \bar{a}^2 \sigma_\ell^2 \frac{2 \exp(-z) I_1(z)}{z} + I_{dc}^2 \delta(f), \quad (\text{A-21})$$

where

$$I_{dc} = \nu \bar{a} \bar{\ell} S(0) = \left(\frac{\pi}{2}\right)^{3/2} \nu \bar{a} \sigma_\ell \quad (\text{A-22})$$

by means of (A-13), (A-18), and (6).

To determine the correlation of shot noise process $I(t)$, we consider first the continuous portion of the spectrum in (A-21):

$$G_c(f) = 2\pi^2 \nu \bar{a}^2 \sigma_\ell^2 \frac{2 \exp(-4\pi^2 \sigma_\ell^2 f^2) I_1(4\pi^2 \sigma_\ell^2 f^2)}{4\pi^2 \sigma_\ell^2 f^2}. \quad (\text{A-23})$$

The corresponding correlation is

$$\begin{aligned}
 R_c(\tau) &= \int_{-\infty}^{+\infty} df \exp(i2\pi f\tau) G_c(f) = \\
 &= 4\pi^2 \nu \overline{a^2} \sigma_\lambda^2 \int_0^\infty df 2 \cos(2\pi f\tau) \frac{\exp(-4\pi^2 \sigma_\lambda^2 f^2) I_1(4\pi^2 \sigma_\lambda^2 f^2)}{4\pi^2 \sigma_\lambda^2 f^2} = \\
 &= 2\pi \nu \overline{a^2} \sigma_\lambda \int_0^\infty dz \cos\left(\frac{\tau}{\sigma_\lambda} z^{\frac{1}{2}}\right) \frac{\exp(-z) I_1(z)}{z^{3/2}} = \\
 &= 2^{\frac{3}{2}} \pi \nu \overline{a^2} \sigma_\lambda \exp(-s) W_{-\frac{3}{2}, \frac{1}{2}}(2s), \tag{A-24}
 \end{aligned}$$

where we employed (A-20) and [5, eq. 6.755 2], and defined

$$s = \left(\frac{\tau}{4\sigma_\lambda}\right)^2. \tag{A-25}$$

The W-function in (A-24) is the Whittaker function [2, p. 505].

Now by [5, eqs. 9.232 1 and 9.222 1], we have

$$\begin{aligned}
 W_{-\frac{3}{2}, \frac{1}{2}}(2s) &= W_{-\frac{3}{2}, -\frac{1}{2}}(2s) = \frac{\exp(-s)}{\Gamma(3/2)} \int_0^\infty dt \exp(-2st) t^{\frac{1}{2}} (1+t)^{-s/2} = \\
 &= \frac{2}{\pi^{1/2}} \exp(-s) \int_0^\infty dt \exp(-2st) \left[\frac{1}{t^{\frac{1}{2}} (1+t)^{3/2}} - \frac{1}{t^{\frac{1}{2}} (1+t)^{5/2}} \right]. \tag{A-26}
 \end{aligned}$$

But according to [5, eq. 3.364 3],

$$\int_0^\infty dt \frac{\exp(-2st)}{t^{\frac{1}{2}} (a+t)^{\frac{1}{2}}} = \exp(as) K_0(as). \tag{A-27}$$

Partial differentiation with respect to a then yields

$$-\frac{1}{2} \int_0^{\infty} dt \frac{\exp(-2st)}{t^{1/2} (a+t)^{3/2}} = s \exp(as) [K_0(as) - K_1(as)] \quad (A-28)$$

and (repeated)

$$\frac{3}{4} \int_0^{\infty} dt \frac{\exp(-2st)}{t^{1/2} (a+t)^{5/2}} = s^2 \exp(as) \left[2K_0(as) - 2K_1(as) + \frac{K_1(as)}{as} \right]. \quad (A-29)$$

Here we used [2, eq. 9.6.28] in the forms

$$K_0'(z) = -K_1(z), \quad K_1'(z) = -K_0(z) - \frac{K_1(z)}{z}. \quad (A-30)$$

If we now set $a = 1$ in (A-28) and (A-29), and then employ these results in (A-26), we obtain

$$W_{-\frac{3}{2}, \frac{1}{2}}(2s) = \frac{2}{\pi^{1/2}} \frac{2}{3s} [(1+4s)K_1(s) - (3+4s)K_0(s)]. \quad (A-31)$$

Finally, the use of (A-31) in (A-24) yields

$$R_C(\tau) = \frac{8}{3}(2\pi)^{1/2} \nu \overline{a^2} \frac{1}{2} s \exp(-s) [(1+4s)K_1(s) - (3+4s)K_0(s)]. \quad (A-32)$$

The Fourier transform of the impulsive part of the spectrum in (A-21) is simply the constant

$$I_{dc}^2 = \left(\frac{\pi}{2}\right)^3 \nu^2 \overline{a^2} \frac{1}{2}, \quad (A-33)$$

which must be added to $R_C(\tau)$ in (A-32) to obtain $R_I(\tau)$. Here s is given by (A-25).

As $\tau \rightarrow 0^+$, there follows from (A-32),

$$\lim_{\tau \rightarrow 0^+} R_C(\tau) = \frac{8}{3}(2\pi)^{1/2} \nu \overline{a^2} \frac{1}{2}. \quad (A-34)$$

APPENDIX B. VARIANCE OF CORRELATION ESTIMATE

Let the available data be $\{x_n\}_1^N$, with zero mean and variance σ^2 :

$$\bar{x}_n = 0, \quad \overline{x_n^2} = \sigma^2 \quad \text{for } 1 \leq n \leq N. \quad (\text{B-1})$$

The autocorrelation estimate at delay k is defined here as

$$R_k = \frac{1}{N} \sum_{n=k+1}^N x_n x_{n-k} \quad \text{for } k \geq 0. \quad (\text{B-2})$$

At delay 0, the mean value of estimate R_0 is

$$\bar{R}_0 = \frac{1}{N} \sum_{n=1}^N \overline{x_n^2} = \sigma^2. \quad (\text{B-3})$$

We now want to evaluate the standard deviation of estimate R_k at delays k large enough that x_n and x_{n-k} are statistically independent. We have mean value

$$\bar{R}_k = \frac{1}{N} \sum_{n=k+1}^N \bar{x}_n \bar{x}_{n-k} = 0, \quad (\text{B-4})$$

using the independence at separation k . The mean square value of estimate R_k is

$$\overline{R_k^2} = \frac{1}{N^2} \sum_{m, n=k+1}^N \overline{x_m x_n x_{m-k} x_{n-k}}. \quad (\text{B-5})$$

For the large separation values k of interest here, the only statistical dependence that contributes non-trivially to the double sum is the following:

$$\begin{aligned} \overline{R_k^2} &= \frac{1}{N^2} \sum_{m,n=k+1}^N \overline{x_m x_n x_{m-k} x_{n-k}} = \frac{\sigma^4}{N^2} \sum_{m,n=k+1}^N \rho^2(m-n) = \\ &= \frac{\sigma^4}{N^2} \sum_{|n| < N-k} (N-k-|n|) \rho^2(n) \cong \frac{\sigma^4}{N^2} (N-k) \sum_n \rho^2(n). \quad (B-6) \end{aligned}$$

Here ρ is the correlation coefficient of data $\{x_n\}$, and we have assumed that N is moderately larger than the effective correlation length of ρ . The ratio of the standard deviation of estimate R_k to the mean value at $k=0$ is then the normalized standard deviation at separation k :

$$\sigma'_k \cong \frac{1}{N} \left[(N-k) \sum_n \rho^2(n) \right]^{1/2}. \quad (B-7)$$

Notice that no Gaussian assumptions on data $\{x_n\}_1^N$ have been employed in this analysis; however, $\rho(k)$ is essentially zero at the k values of interest.

As an example, for an exponential correlation of effective length K_e , there follows

$$\sum_n \rho^2(n) = \sum_n \exp\left(-2\frac{|n|}{K_e}\right) \cong \int dx \exp\left(-2\frac{|x|}{K_e}\right) = K_e, \quad (B-8)$$

where we assume that K_e is moderately larger than unity. Then (B-7) yields

$$\sigma'_k \cong \frac{1}{N} [(N-k)K_e]^{1/2}. \quad (B-9)$$

These results hold only for those values of k where $\rho(k)$ has substantially gone to zero. Larger values of K_e lead to larger relative standard deviations; this is consistent with the fact that there are then a lesser number of effectively-independent samples in the limited data set of length N .

For the 8000 data point example of interest here, inspection of figure 5 reveals that $K_e \cong 30$. Thus

$$\pm 2\sigma'_k = \pm \frac{(8000-k)^{K_e}}{730}. \quad (8-10)$$

These confidence limits are superposed as dotted lines on figures 5 and 6.

APPENDIX C. PROPERTIES OF CHARACTERISTIC FUNCTION OF SHOT NOISE

Derivation of Characteristic Function

The method of derivation of the characteristic function of $I(t)$ presented here parallels that of Rice [1, sections 1.4 and 1.5] very closely. We generalize [1, eq. 1.3-1] to

$$I_K(t) = \sum_{k=1}^K a_k F\left(\frac{t-t_k}{\lambda_k}\right) \quad (C-1)$$

where $\{a_k\}$, $\{t_k\}$, $\{\lambda_k\}$ are all independent random variables; see (A-1) and the ensuing discussion. The characteristic function of an individual component in (C-1) is

$$f_1(\xi) = \overline{\exp\left[i\xi a_k F\left(\frac{t-t_k}{\lambda_k}\right)\right]}, \quad (C-2)$$

where the statistical average is over a_k , t_k , λ_k . The average over t_k (for fixed a_k , λ_k) is, for T a large but finite time interval [1, p. 152],

$$\begin{aligned} & \frac{1}{T} \int_0^T dt_k \exp\left[i\xi a_k F\left(\frac{t-t_k}{\lambda_k}\right)\right] = \\ & = \frac{1}{T} \int_0^T dt_k \left\{ \exp\left[i\xi a_k F\left(\frac{t-t_k}{\lambda_k}\right)\right] - 1 \right\} + 1 = \\ & \cong \frac{1}{T} \int d\tau \left\{ \exp\left[i\xi a_k F\left(\frac{t-\tau}{\lambda_k}\right)\right] - 1 \right\} + 1, \end{aligned} \quad (C-3)$$

for large T, where we have used the fact that

$$F(x) \rightarrow 0 \text{ as } x \rightarrow \pm\infty. \quad (\text{C-4})$$

Let $x = (t - \tau_k) / \lambda_k$ in (C-3) to get

$$\frac{1}{T} \lambda_k \int dx \{ \exp[i \xi a_k F(x)] - 1 \} + 1. \quad (\text{C-5})$$

Now performing the averages on random variables λ_k and a_k , we have, for the characteristic function of an individual component of (C-1),

$$f_1(\xi) = \frac{1}{T} \bar{\lambda} \int da p(a) \int dx \{ \exp[i \xi a F(x)] - 1 \} + 1, \quad (\text{C-6})$$

where $p(a)$ is the probability density function of random variable a_k .

Interchanging integrals, (C-6) becomes

$$f_1(\xi) = \frac{1}{T} \bar{\lambda} \int dx \{ f_a[\xi F(x)] - 1 \} + 1, \quad (\text{C-7})$$

where f_a is the characteristic function of amplitude a_k . Then from (C-1), since all the individual random variables are independent, the characteristic function of $I_k(t)$ is

$$f_{I_k}(\xi) = [f_1(\xi)]^k. \quad (\text{C-8})$$

Finally, the characteristic function of total shot noise process (1) is, by use of discrete probability distribution (A-7) for random variable K, given by the average

$$\begin{aligned}
 f_I(\xi) &= \sum_{K=0}^{\infty} \frac{(vT)^K}{K!} \exp(-vT) f_{I_K}(\xi) = \\
 &= \exp[-vT + vT f_1(\xi)] = \\
 &= \exp[v\bar{\lambda} \int dx \{f_a[\xi F(x)] - 1\}] . \quad (C-9)
 \end{aligned}$$

The (imprecise) large time interval T has dropped out of the general result (C-9). Also, the only parameter required about the duration random variable λ_k is its mean. The exact characteristic function f_a of amplitude a_k and the exact pulse shape F directly affect the characteristic function of $I(t)$. For $\lambda_k = 1$ for all k , (C-9) reduces to a simplified version of [1, eq. 1.5-4].

Cumulants of $I(t)$

The characteristic function of random amplitude a_k can be expanded in a power series

$$f_a(\xi) = \sum_{n=0}^{\infty} \mu_a(n) \frac{(i\xi)^n}{n!}, \quad (C-10)$$

where $\mu_a(n)$ is the n -th moment of a_k :

$$\mu_a(n) = \overline{a^n} = \int da a^n p(a). \quad (C-11)$$

Then from (C-9), we develop

$$\begin{aligned} \ln f_I(\xi) &= \nu \bar{\ell} \int dx \{f_a[\xi F(x)] - 1\} = \\ &= \nu \bar{\ell} \sum_{n=1}^{\infty} \mu_a(n) \frac{(i\xi)^n}{n!} \int dx F^n(x), \end{aligned} \quad (C-12)$$

allowing for immediate identification of the cumulants of $I(t)$ as

$$\chi_I(n) = \nu \bar{\ell} \mu_a(n) \int dx F^n(x) \quad \text{for } n \geq 1; \chi_I(0) = 0. \quad (C-13)$$

For $\ell_k = 1$ for all k , this reduces to [1, eq. 1.5-2].

The normalized cumulants of $I(t)$ are

$$\gamma_I(n) = \frac{\chi_I(n)}{[\chi_I(2)]^{n/2}} = \frac{1}{(\nu \bar{\ell})^{n/2 - 1}} \frac{\mu_a(n) \int dx F^n(x)}{\left[\mu_a(2) \int dx F^2(x) \right]^{n/2}}. \quad (C-14)$$

These quantities tend to zero rapidly for $\nu \bar{\ell} \gg 1$; see also [1, eq. 1.6-3].

Thus $\nu \bar{\ell}$ has a pronounced effect on how Gaussian $I(t)$ is.

Behavior of characteristic function $f_I(\xi)$ at $\xi = \pm\infty$

If pulse $F(x)$ is non-zero only over (x_1, x_2) , we have

$$\int dx \{f_a[\xi F(x)] - 1\} = \int_{x_1}^{x_2} dx \{f_a[\xi F(x)] - 1\}. \quad (C-15)$$

Now if random variable a_k has a characteristic function f_a with the property that

$$f_a(\pm\infty) = 0, \quad (C-16)$$

then

$$(C-15) \rightarrow \int_{x_1}^{x_2} dx \{0-1\} = -(x_2 - x_1) \text{ as } \xi \rightarrow \pm\infty, \quad (C-17)$$

in which case (C-9) yields

$$f_I(\pm\infty) = \exp[-v\bar{\lambda}(x_2 - x_1)] . \quad (C-18)$$

If pulse extent $x_2 - x_1$ is infinite, as for the Gaussian or exponential pulses,

$$F(x) = \exp(-x^2) \text{ or } \exp(-x)U(x) , \quad (C-19)$$

then (C-18) is zero. On the other hand, if $x_2 - x_1$ is finite, as for circular pulse

$$F(x) = \left\{ \begin{array}{ll} (1-x^2)^{1/2} & \text{for } |x| < 1 \\ 0 & \text{for } |x| > 1 \end{array} \right\} , \quad (C-20)$$

then

$$f_I(\pm\infty) = \exp[-v\bar{\lambda}2] > 0 \text{ for circular pulse.} \quad (C-21)$$

This non-zero characteristic function value corresponds to an impulse at the origin of probability density function p_I , with area (C-21). Physically, this means that there are occasionally regions of the t -scale where no pulses overlap, and there $I(t) = 0$. The probability of this happening is, generally,

$$P_0 = \text{Prob} \{I(t) = 0\} = f_I(\pm\infty) = \exp[-v\bar{\lambda}(x_2 - x_1)] . \quad (C-22)$$

On the other hand, for the Gaussian or exponential pulses cited in (C-19), $x_2 - x_1 = +\infty$, and $f_I(\pm\infty) = 0$, meaning that there is no impulse at the origin of probability density function p_I . Physically, the infinite tails (even if single-sided, as for the exponential pulse) disallow $I(t)$ ever from becoming zero.

Cumulants of Continuous Portion of p_I .

The impulse at the origin means that probability density function p_I and cumulative distribution function P_I can be expressed respectively as

$$p_I(u) = P_0 \delta(u) + p_C(u) ,$$

$$P_I(u) = P_0 + \int_0^u dt p_C(t) \quad \text{for } u > 0, \quad (C-23)$$

where $p_C(u)$ is a continuous function of u , with area $1-P_0$. The characteristic function relation corresponding to (C-23) is

$$f_I(\xi) = P_0 + f_C(\xi) , \quad (C-24)$$

and the moments are related according to

$$\mu_C(n) = \begin{cases} \mu_I(0) - P_0 & \text{for } n=0 \\ \mu_I(n) & \text{for } n \geq 1 \end{cases} . \quad (C-25)$$

The cumulants of f_C or p_C can then be found from these moments (C-25), by recursive relations; see [4] or [6]. This procedure is necessary to get accurate series expansions for the probability density function p_C and its cumulative distribution function, without having to approximate a delta function.

Overlap Factor

In the case where pulse extent $x_2 - x_1$ is finite, it is possible to find the average number of overlapping pulses at any one time instant; this statistic, denoted by \bar{K}_1 , is called the overlap factor. In order to determine it in a simple fashion, we concoct a very special shot noise process: let

$$a_k = 1 \text{ for all } k ,$$

$$F(x) = 1 \text{ for } x_1 < x < x_2 . \quad (\text{C-26})$$

Then $I(t)$ is a step function with amplitudes limited to the values 0, 1, 2, Then obviously, the average number of overlapping pulses at one time instant is just

$$\bar{K}_1 = \bar{I(t)} = v \bar{\lambda} \mu_a(1) \int dx F(x) = v \bar{\lambda} (x_2 - x_1) , \quad (\text{C-27})$$

upon use of (C-13) with $n=1$ and (C-26). If we let

$$\bar{L} = \bar{\lambda} (x_2 - x_1) \quad (\text{C-28})$$

denote the average pulse duration, we have the overlap factor in the form

$$\bar{K}_1 = v \bar{L} . \quad (\text{C-29})$$

For the Gaussian or exponential pulses in (C-19), we have $x_2 - x_1 = +\infty$, giving $\bar{L} = +\infty$, $\bar{K}_1 = +\infty$. This is in fact true, since all the infinite tails overlap; however, it is not then an informative statistic.

Closed Form Characteristic Function Examples

There are a couple of examples of the circular pulse shape F and amplitude characteristic function f_a , where (C-9) can be evaluated in closed form. This furnishes an alternative to the moment approach [4] used here.

Consider the circular pulse in (C-20); then the integral in (C-9) is (using (C-15))

$$\int_{-1}^1 dx \left\{ f_a \left[\xi (1-x^2)^{1/2} \right] \right\} = 2 \int_0^{\pi/2} d\theta \cos\theta f_a \left[\xi \cos\theta \right] \quad (C-30)$$

which holds for any characteristic function f_a . Now first let the probability density function of a_k be exponential:

$$p(a) = \frac{1}{\mu_a} \exp\left(-\frac{a}{\mu_a}\right) U(a), \quad f_a(\xi) = (1 - i\xi\mu_a)^{-1} \quad (C-31)$$

Substitution in (C-30) yields

$$2 \int_0^{\pi/2} \frac{d\theta \cos\theta}{1 - i\xi\mu_a \cos\theta} \quad (C-32)$$

But we know that

$$\begin{aligned} 2 \int_0^{\pi/2} \frac{d\theta \cos\theta}{1 - z \cos\theta} &= -\frac{\pi}{z} + \frac{4}{z(1-z^2)^{1/2}} \arctan \left[\left(\frac{1+z}{1-z} \right)^{1/2} \right] = \\ &= -\frac{\pi}{z} + \frac{2}{z(1-z^2)^{1/2}} \arccos(-z), \end{aligned} \quad (C-33)$$

via [5, eqs. 2.554 2 and 2.553 3]. Then letting $z = i\xi\mu_a$ and using [2, eqs. 4.4.2 with 4.4.26], (C-32) becomes

$$\frac{-2 \ln(s - \mu_a \xi) + i\pi(s-1)}{\mu_a \xi s} - 2, \quad \text{with } s = \left(1 + \mu_a^2 \xi^2\right)^{1/2}. \quad (\text{C-34})$$

Combining these results in (C-9), the closed form characteristic function is

$$f_I(\xi) = \exp \left[-\frac{2\sqrt{2}}{\mu_a \xi} \left\{ \mu_a \xi s + \ln(s - \mu_a \xi) - i \frac{\pi}{2}(s-1) \right\} \right], \quad (\text{C-35})$$

which holds for a circular pulse F and an exponential probability density function $p(a)$.

The second example is the one considered in detail here, namely the Rayleigh probability density function $p(a)$ given in (3). First substituting (C-30) in (C-9), we have characteristic function

$$f_I(\xi) = \exp[2\sqrt{2}(J(\xi)-1)], \quad (\text{C-36})$$

where integral $J(\xi)$ is defined as

$$J(\xi) = \int_0^{\pi/2} d\theta \cos\theta f_a[\xi \cos\theta]. \quad (\text{C-37})$$

For Rayleigh probability density function (3), (C-37) can be expressed as follows:

$$J(\xi) = \int_0^{\pi/2} d\theta \cos\theta \int_0^{\infty} da \exp(ia\xi \cos\theta) \frac{a}{\sigma_a^2} \exp\left(\frac{-a^2}{2\sigma_a^2}\right). \quad (\text{C-38})$$

Transform to rectangular coordinates according to $a \cos \theta = \sigma_a x$,
 $a \sin \theta = \sigma_a y$, and obtain

$$J(\xi) = \int_0^{\infty} \int_0^{\infty} dx dy \frac{x}{(x^2+y^2)^{1/2}} \exp\left(i\xi \sigma_a x - \frac{x^2+y^2}{2}\right). \quad (\text{C-39})$$

But the integral on y here is, via $y = x u^{1/2}$, equal to

$$\frac{1}{2} \int_0^{\infty} \frac{du}{u^{1/2}(1+u)^{1/2}} \exp\left(-\frac{1}{2} x^2 u\right) = \frac{1}{2} \exp\left(\frac{x^2}{4}\right) K_0\left(\frac{x^2}{4}\right), \quad (C-40)$$

the latter by means of [5, eq. 3.364 3]. Thus (C-39) becomes

$$\begin{aligned} J(\xi) &= \int_0^{\infty} dx \, x \exp\left(i \xi \sigma_a x - \frac{x^2}{2}\right) \frac{1}{2} \exp\left(\frac{x^2}{4}\right) K_0\left(\frac{x^2}{4}\right) = \\ &= \int_0^{\infty} du \exp\left(i 2^{1/2} \sigma_a \xi u\right) u \exp\left(-\frac{u^2}{2}\right) K_0\left(\frac{u^2}{2}\right). \end{aligned} \quad (C-41)$$

At this point, we have two alternatives. First, (C-41) could be efficiently evaluated for all ξ via an FFT; the decay of the integrand is according to $\exp(-u^2)$ for large u . Secondly, $J(\xi)$ can be expressed in a closed form in terms of a hypergeometric function; specifically

$$\begin{aligned} J(\xi) &= {}_2F_2\left(1, 1; \frac{1}{2}, \frac{3}{2}; -2b^2\right) + \\ &+ i\left(\frac{\pi}{2}\right)^{1/2} b \exp(-b^2) [I_0(b^2) - I_1(b^2)], \end{aligned} \quad (C-42)$$

where $b = \sigma_a \xi / 2$. The upper line follows from [5, eq. 6.755 6], while the lower line used [5, eq. 6.755 9] with an application of partial derivative $\partial/\partial a$ to both sides. The characteristic function f_I is finally obtained by employing (C-42) in (C-36).

Still another alternative is afforded by use of the closed form for the characteristic function of the Rayleigh probability density function, as given in [7, eq. 6].

Moments for Some Particular Pulse Shapes F

The moments of pulse shape F were encountered in evaluating the cumulants $\chi_1(n)$ of shot noise $I(t)$, according to (24) or (C-13) as

$$\mu_F(n) = \int dx F^n(x) \quad \text{for } n \geq 1. \quad (\text{C-43})$$

For circular pulse (C-20), [5, eq. 3.621 1] yields moments

$$\mu_F(n) = \int_{-1}^1 dx (1-x^2)^{n/2} = 2 \int_0^{\pi/2} d\theta (\cos\theta)^{n+1} = \frac{2^{n+1} \Gamma^2\left(\frac{n+1}{2}\right)}{\Gamma(n+2)}, \quad (\text{C-44})$$

a result already quoted in (29).

More generally, for

$$F(x) = \begin{cases} (1-x^2)^\alpha & \text{for } |x| < 1 \\ 0 & \text{for } |x| > 1 \end{cases}, \quad (\text{C-45})$$

[5, eq. 3.621 1] yields, with a trigonometric substitution,

$$\mu_F(n) = 2^{2n\alpha+1} \frac{\Gamma^2(n\alpha+1)}{\Gamma(2n\alpha+2)}. \quad (\text{C-46})$$

For

$$F(x) = \begin{cases} (\cos x)^\alpha & \text{for } |x| < \frac{\pi}{2} \\ 0 & \text{for } |x| > \frac{\pi}{2} \end{cases}, \quad (\text{C-47})$$

[5, eq. 3.621 1] yields directly

$$\mu_F(n) = 2^{n\alpha} \frac{\Gamma^2\left(\frac{n\alpha+1}{2}\right)}{\Gamma(n\alpha+1)}. \quad (\text{C-48})$$

For

$$F(x) = x^\alpha \exp(-x) U(x) ,$$

$$\mu_F(n) = \frac{\Gamma(n\alpha+1)}{n^{\alpha+1}} , \quad (C-49)$$

while for

$$F(x) = x^\alpha \exp(-x^2/2) U(x) ,$$

$$\mu_F(n) = \frac{2^{\frac{n\alpha-1}{2}} \Gamma\left(\frac{n\alpha+1}{2}\right)}{n^{\frac{\alpha+1}{2}}} . \quad (C-50)$$

Both relations follow directly from the definition of the Γ function.

Some Probability Density Functions for Amplitude a_k

For probability density function

$$p(a) = \frac{(a/\alpha)^\gamma \exp(-a/\alpha)}{\alpha \Gamma(\gamma+1)} U(a) , \quad (C-51)$$

we have characteristic function

$$f_a(\xi) = (1-i\xi\alpha)^{-\gamma-1} \quad (C-52)$$

with moments

$$\mu_a(n) = (\gamma+1)_n \alpha^n \quad \text{for } n \geq 0 \quad (C-53)$$

and cumulants

$$\chi_a(n) = (n-1)! (\gamma+1) \alpha^n \quad \text{for } n \geq 1 . \quad (C-54)$$

This example subsumes the exponential probability density function, upon setting $\gamma = 0$.

For probability density function

$$p(a) = \frac{2(a/\alpha)^\gamma \exp(-a^2/\alpha^2)}{\alpha \Gamma\left(\frac{\gamma+1}{2}\right)} U(a), \quad (C-55)$$

we have moments

$$\mu_a(n) = \frac{\Gamma\left(\frac{n+\gamma+1}{2}\right)}{\Gamma\left(\frac{\gamma+1}{2}\right)} \alpha^n \quad \text{for } n \geq 0. \quad (C-56)$$

This example subsumes respectively the one-sided Gaussian for $\gamma=0$, the Rayleigh for $\gamma=1$, and the Maxwell probability density functions for $\gamma=2$. The result in (29) follows immediately by setting $\gamma=1$, $\alpha = 2^{1/2} \sigma_a$.

Convergence of Series for $\ln f_I(\xi)$

A power series expansion for $\ln f_I(\xi)$ was developed in (C-12), namely,

$$\ln f_I(\xi) = \sqrt{\lambda} \sum_{n=1}^{\infty} \mu_a(n) \mu_F(n) \frac{(i\xi)^n}{n!}; \quad (C-57)$$

here we employed (C-43). Since the moments in (C-57) can be easily evaluated via recursion, according to results in the above two subsections, it might be thought that (C-57) could be employed to evaluate the characteristic function of $I(t)$ directly, without recourse to the more difficult approaches required in (C-9) or (C-35) or (C-36)-(C-42).

To see the drawbacks of this approach, consider first a circular pulse F and a generalized exponential probability density function $p(a)$ as in (C-51); then a combination of (C-44) and (C-53) yields, for the n -th term of the sum in (C-57),

$$T_n = \frac{2(\gamma+1)_n \Gamma^2\left(\frac{n+1}{2}\right)}{n!(n+1)!} (i\xi\alpha 2)^n. \quad (C-58)$$

Then ratio

$$\frac{T_n}{T_{n-2}} = -\frac{(n+\gamma)(n+\gamma-1)}{n^2-1} \xi^2 \alpha^2 \sim -\xi^2 \alpha^2 \quad \text{as } n \rightarrow +\infty, \quad (C-59)$$

regardless of the value of γ . Therefore

$$\left| \frac{T_n}{T_{n-1}} \right| \sim |\xi| \alpha \quad \text{as } n \rightarrow +\infty, \quad (C-60)$$

meaning that series (C-57) only converges for $|\xi| < 1/\alpha$. So (C-57) is not a viable approach for the calculation of the characteristic function in this case.

As a second example, we consider the circular pulse F with the generalized Rayleigh probability density function in (C-55). Combination of (C-44) with (C-56) yields for the n-th term of series (C-57),

$$T_n = \frac{2\Gamma^2\left(\frac{n+1}{2}\right) \Gamma\left(\frac{n+\gamma+1}{2}\right)}{n!(n+1)! \Gamma\left(\frac{\gamma+1}{2}\right)} (i\xi\alpha 2)^n. \quad (C-61)$$

Then ratio

$$\frac{T_n}{T_{n-2}} = -\frac{n+\gamma-1}{n^2-1} \frac{\xi^2 \alpha^2}{2} \sim -\frac{\xi^2 \alpha^2}{2n} \quad \text{as } n \rightarrow +\infty, \quad (C-62)$$

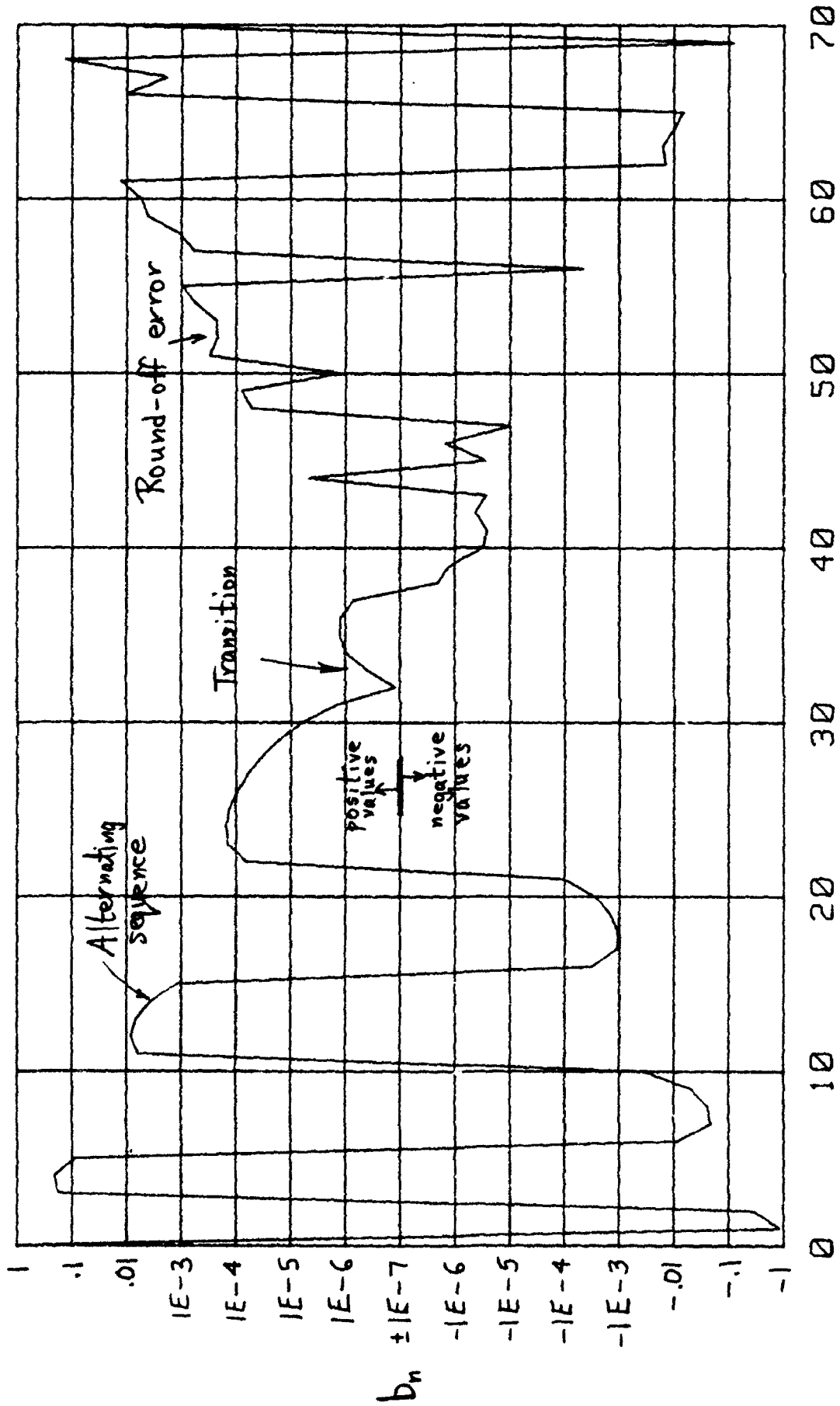
regardless of γ . Therefore

$$\left| \frac{T_n}{T_{n-1}} \right| \sim \frac{|\xi| \alpha}{(2n)^{1/2}} \quad \text{as } n \rightarrow +\infty, \quad (C-63)$$

meaning that series (C-57) converges for all ξ . However, direct numerical evaluation of (C-57) via (C-61) and (C-62) loses all its significant digits for large ξ , long before $\ln f_I(\xi)$ reaches its final value of $-2\bar{Q}_v + i0$, due to the alternating character of the series. So (C-57) is not a useful approach for evaluation of the characteristic function, except for small ξ . By contrast, the series expansion technique employed in [4] uses the moments to directly estimate the desired probability density function and cumulative distribution function of interest, for large arguments as well as small.

APPENDIX D. PROGRAMS FOR CUMULATIVE DISTRIBUTION FUNCTION
AND PROBABILITY DENSITY FUNCTION

The programs used here to evaluate the cumulative distribution function and probability density function of shot noise are listed below. The n -th coefficient in a generalized Laguerre expansion of orthonormal polynomials is denoted by b_n and is plotted in figure D-1 for $n = 0(1)70$. It is seen to oscillate and decay with n until $n = 32$, at which point round-off error becomes important; however, by this time, $|b_n|$ has decayed below the $1E-5$ level. The round-off error is so dominant beyond $n = 35$, that no useful results for b_n can be obtained then. The particular parameter values (α, β) used for the Laguerre weighting are indicated in the listings.



n, NUMBER OF TERM
 Figure D-1. Coefficient b_n in Laguerre Expansion

```

10 ! STEP PLUS CONTINUOUS PART OF SHOT NOISE CDF, Po(u),
20 ! VIA GENERALIZED LAGUERRE EXPANSION AND MOMENTS
30 N=70 ! MAXIMUM ORDER OF APPROXIMATION; NUMBER OF MOMENTS REQUIRED
40 DOUBLE N,I,N,K ! INTEGERS 1 2 31 = 2,147,483,648
50 REDIM Mom(0:M),R(0:M),L(0:M)
60 REAL Mom(0:100),R(0:100),L(0:100),Y(1:21)
70 CALL Moments(M,P0,Mom(*) ! P0 IS STEP AT ORIGIN
80 Center=Mom(1)/Mom(0) ! CENTER OF po(u)
90 R2=Mom(2)/Mom(0)-Center*Center ! MEAN SQUARE SPREAD OF po(u)
100 Rms=SQR(R2) ! RMS SPREAD OF po(u)
110 Alpha0=Center*Center/R2-1. ! THE CHOICES Alpha=Alpha0 AND
120 Beta0=R2/Center ! Beta=Beta0 WOULD MAKE R(1)=R(2)=0
130 Alpha=.74
140 Beta=2.1
150 CALL Coeff1d_via_mom(M,Alpha,Beta,Mom(+),R(+)) ! DIRECT MOMENTS
160 ! CALL Coeff1r_via_mom(M,Alpha,Beta,Mom(+),R(+)) ! RECURSIVE MOMENTS
170 PRINT "Center = ";Center
180 PRINT "Rms = ";Rms
190 A1=Alpha+1.
200 O1=1./A1
210 F1=1./FNGamma(A1)
220 DATA .001,.002,.005,.01,.02,.05,.1,.2,.3,.4,.5
230 DATA .6,.7,.8,.9,.95,.98,.99,.995,.998,.999
240 READ Y(*)
250 FOR I=1 TO 21
260 Y(I)=FNIInvphi(Y(I))
270 NEXT I
280 Y1=Y(1)
290 Y2=Y(21)
300 INPUT "ORDER AND LIMITS: ",N,U1,U2
310 PRINT "ORDER AND LIMITS: ",N;U1;U2
320 Du=(U2-U1)/100.
330 PLOTTER IS "GRAPHICS"
340 GRAPHICS ON
350 WINDOW U1,U2,Y1,Y2
360 FOR U=U1 TO U2 STEP (U2-U1)*.1
370 MOVE U,Y1
380 DRAW U,Y2
390 NEXT U
400 FOR I=1 TO 21
410 MOVE U1,Y(I)
420 DRAW U2,Y(I)
430 NEXT I
440 PENUP
450 FOR I=1 TO 100
460 U=U1+Du*I
470 T=U/Beta
480 CALL Laguerre(N-1,A1,T,L(*)
490 Sum=R(0)*FNF11(A1,T)*O1
500 FOR K=1 TO N
510 Sum=Sum+R(K)*L(K-1)/K
520 NEXT K
530 P=P0+F1*EXP(-T+A1*LOG(T))*Sum ! PROBABILITY THAT RV < U
540 IF P>0. AND P<1. THEN 570
550 PENUP
560 GOTO 580
570 PLOT U,FNIInvphi(P)
580 NEXT I
590 PENUP
600 GOTO 300
610 END
620 !

```

```

630 DEF FNInuphi(X) ! INVPHI(X) via 26.2.23 with modification
640 D=X-.5
650 IF ABS(D)>.01 THEN 680
660 P=2.50662827463*D*(1.+D*D*1.04719755120)
670 RETURN P
680 P=X
690 IF X>.5 THEN P=1.-X
700 P=SQR(-2.*LOG(P))
710 T=1.+P*(1.432788+P*(.189269+P*.001308))
720 P=P-(2.515517+P*(.802853+P*.010328))/T
730 IF X<.5 THEN P=-P
740 RETURN P
750 FNEND
760 !
770 DEF FNGamma(X) ! Gamma(X) via HART, page 282, #5243
780 DOUBLE N,K
790 N=INT(X)
800 R=X-N
810 IF N>0 OR R<>0. THEN 840
820 PRINT "FNGamma(X) IS NOT DEFINED FOR X = ";X
830 STOP
840 IF R>0. THEN 870
850 Gamma2=1.
860 GOTO 940
870 P=439.330444060025676+R*(50.1086937529709530+R*6.74495072459252899)
880 P=8762.71029785214896+R*(2008.52740130727912+R*P)
890 P=42353.6895097440896+R*(20886.8617892698874+R*P)
900 Q=499.028526621439048-R*(189.498234157028016-R*(23.081551524580125-R))
910 Q=9940.30741508277090-R*(1528.60727377952202+R*Q)
920 Q=42353.6895097440900+R*(2980.38533092566499-R*Q)
930 Gamma2=P/Q ! Gamma(2+R) for 0 < R < 1
940 IF N>2 THEN 980
950 IF N<2 THEN 1030
960 Gamma=Gamma2
970 RETURN Gamma
980 Gamma=Gamma2
990 FOR K=1 TO N-2
1000 Gamma=Gamma*(X-K)
1010 NEXT K
1020 RETURN Gamma
1030 R=1.
1040 FOR K=0 TO 1-N
1050 R=R*(X+K)
1060 NEXT K
1070 Gamma=Gamma2/R
1080 RETURN Gamma
1090 FNEND
1100 !

```

```

1110 DEF FNF11(A1,X) ! 1F1(1;A1+1;X)
1120 DOUBLE K
1130 T=S=1.
1140 FOR K=1 TO 200
1150 T=T*X/(A1+K)
1160 S=S+T
1170 IF T<=1.E-17*S THEN RETURN S
1180 NEXT K
1190 PRINT "200 TERMS IN FNF11 AT";A1;X
1200 RETURN S
1210 FNEND
1220 !
1230 SUB Laguerre(DOUBLE N,REAL Alpha,X,L(*) ! Ln\alpha(X)
1240 DOUBLE K
1250 A1=Alpha-1.
1260 L(0)=1.
1270 L(1)=Alpha+1.-X
1280 FOR K=2 TO N
1290 L(K)=((K+K+A1-X)*L(K-1)-(K+A1)*L(K-2))/K
1300 NEXT K
1310 SUBEND
1320 !
1330 SUB Momnt_via_cumnt(DOUBLE M,REAL Cum(*),Mom(*))
1340 DOUBLE K,J
1350 REAL Mom0
1360 Mom(0)=Mom0=EXP(Cum(0))
1370 FOR K=1 TO M
1380 T=1.
1390 S=Cum(K)*Mom0
1400 FOR J=1 TO K-1
1410 T=T*(K-J)/J
1420 S=S+T*Cum(K-J)*Mom(J)
1430 NEXT J
1440 Mom(K)=S
1450 NEXT K
1460 SUBEND
1470 !

```

```

1480 SUB Coeff1d_via_mom(DOUBLE I,REAL Alpha,Beta,Mom(*),R(*))
1490 ALLOCATE B(0:M)
1500 DOUBLE K,K1,J,Mx
1510 T=1.
1520 FOR K=1 TO M
1530 T=T*(Alpha+K)*Beta
1540 Mom(K)=Mom(K)/T ! NORMALIZED MOMENTS, RELATIVE TO Alpha AND Beta
1550 NEXT K
1560 Q=1.
1570 R(0)=B(0)=Mom(0)
1580 FOR K=1 TO M
1590 K1=K+1
1600 T=1.
1610 S=Mom(2)
1620 FOR J=1 TO K
1630 T=T*(J-K1)/J
1640 S=S+T*Mom(J)
1650 NEXT J
1660 Q=Q*(Alpha+K)/K
1670 R(K)=S
1680 B(K)=S*SQR(Q)
1690 NEXT K
1700 Mx=Mx+10
1710 IF Mx<M THEN 1700
1720 Threshold=-7.
1730 T2=Threshold*2.
1740 V=10.^Threshold
1750 GINIT
1760 PLOTTER IS "GRAPHICS"
1770 GRAPHICS ON
1780 WINDOW 0.,FLT(Mx),T2,0.
1790 LINE TYPE 3
1800 FOR J=0 TO Mx STEP 10
1810 MOVE J,T2
1820 DRAW J,0.
1830 NEXT J
1840 FOR J=T2 TO 0
1850 MOVE 0.,J
1860 DRAW Mx,J
1870 NEXT J
1880 PENUP
1890 LINE TYPE 1
1900 IMAGE 4D,2(4X,M.17DE)
1910 PRINT " K B(K) Sum"
1920 Sum=0.
1930 FOR K=0 TO M
1940 B=B(K)
1950 Sum=Sum+B*B
1960 PRINT USING 1900;K,B,Sum
1970 IF B<V THEN 2000
1980 Y=LGT(B)
1990 GOTO 2040
2000 IF B>-V THEN 2030
2010 Y=T2-LGT(-B)
2020 GOTO 2040
2030 Y=Threshold
2040 PLOT K,Y
2050 NEXT K
2060 PENUP
2070 SUBEND
2080 !

```

```

2090 SUB Coeffln_via_mom(DOUBLE M,REAL Alpha,Beta,Mom(*),A(*))
2100 ALLOCATE B(0:M)
2110 DOUBLE K,K1,J,Mx
2120 T=1.
2130 FOR K=1 TO M
2140 T=T*(Alpha+K)*Beta
2150 Mom(K)=Mom(K)/T ! NORMALIZED MOMENTS, RELATIVE TO Alpha AND Beta
2160 NEXT K
2170 Q=1.
2180 A0=A(0)=B(0)=Mom(0)
2190 FOR K=1 TO M
2200 K1=K+1
2210 T=1.
2220 S=Mom(K)-A0
2230 FOR J=1 TO K-1
2240 T=T*(J-K1)/J
2250 S=S-T*A(J)
2260 NEXT J
2270 IF K MOD 2=1 LN S=-S
2280 Q=Q*(Alpha+K)/K
2290 A(K)=S
2300 B(K)=S*SQR(Q)
2310 NEXT K
2320 Mx=Mx+10
2330 IF Mx<M THEN 2320
2340 Threshold=-7.
2350 T2=Threshold*2.
2360 V=10.^Threshold
2370 GINIT
2380 PLOTTER IS "GRAPHICS"
2390 GRAPHICS ON
2400 WINDOW 0.,FLT(Mx),T2,0.
2410 LINE TYPE 3
2420 FOR J=0 TO Mx STEP 10
2430 MOVE J,T2
2440 DRAW J,0.
2450 NEXT J
2460 FOR J=T2 TO 0
2470 MOVE 0.,J
2480 DRAW Mx,J
2490 NEXT J
2500 PENUP
2510 LINE TYPE 1
2520 IMAGE 4D,2(4X,M.17DE)
2530 PRINT " K B(K) Sum"
2540 Sum=0.
2550 FOR K=0 TO M
2560 B=B(K)
2570 Sum=Sum+B*B
2580 PRINT USING 2520;K,B,Sum
2590 IF B<V THEN 2620
2600 Y=LGT(B)
2610 GOTO 2660
2620 IF B>-V THEN 2650
2630 Y=T2-LGT(-B)
2640 GOTO 2660
2650 Y=Threshold
2660 PLOT K,Y
2670 NEXT K
2680 PENUP
2690 SUBEND
2700 !

```

```

2710 SUB Moments(DOUBLE M,REAL P0,Mom(*)) ! SHOT NOISE
2720 Overlap=6.2 ! AV. NO. PULSES/SEC * AVERAGE PULSE DURATI
2730 Sigmaa=1. ! PARAMETER OF RAYLEIGH AMPLITUDE PDF
2740 P0=EXP(-Overlap) ! PROBABILITY OF ZERO AMPLITUDE OF SHOT NOISE
2750 ALLOCATE Cum(0:M) ! ARRAY FOR CUMULANTS
2760 DOUBLE K
2770 S=Sigmaa*Sigmaa
2780 Cum(0)=0.
2790 Cum(1)=Overlap*Sigmaa*.25*PI*SQR(.5*PI)
2800 Cum(2)=Overlap*S*4./3.
2810 FOR K=3 TO M
2820 Cum(K)=Cum(K-2)*S*K*K/(K+1)
2830 NEXT K
2840 CALL Momnt_via_cumnt(M,Cum(*),Mom(*))
2850 Mom(0)=Mom(0)-P0
2860 SUBEND

10 ! CONTINUOUS PART OF SHOT NOISE PDF, pc(u), VIA
20 ! GENERALIZED LAGUERRE EXPANSION AND MOMENTS
30 M=90 ! MAXIMUM ORDER OF APPROXIMATION; NUMBER OF MOMENTS REQUIRED
40 DOUBLE M,I,N,K ! INTEGERS < 2^31 = 2,147,483,648
50 REDIM Mom(0:M),A(0:M),L(0:M)
60 REAL Mom(0:100),A(0:100),L(0:100)
70 CALL Moments(M,P0,Mom(*)) ! P0 IS STEP AT ORIGIN
80 Center=Mom(1)/Mom(0) ! CENTER OF pc(u)
90 R2=Mom(2)/Mom(0)-Center*Center ! MEAN SQUARE SPREAD OF pc(u)
100 Rms=SQR(R2) ! RMS SPREAD OF pc(u)
110 Alpha0=Center*Center/R2-1. ! THE CHOICES Alpha=Alpha0 AND
120 Beta0=R2/Center ! Beta=Beta0 WOULD MAKE A(1)=A(2)=0
130 Alpha=.74
140 Beta=2.1
150 CALL Coeffld_via_mom(M,Alpha,Beta,Mom(*),A(*)) ! DIRECT MOMENTS
160 ! CALL Coefflr_via_mom(M,Alpha,Beta,Mom(*),A(*)) ! RECURSIVE MOMENTS
170 PRINT "Center = ";Center
180 PRINT "Rms = ";Rms
190 F1=1./(Beta*FNGamma(Alpha+1.))
200 INPUT "ORDER AND LIMITS:",N,U1,U2
210 PRINT "ORDER AND LIMITS:",N;U1;U2
220 Du=(U2-U1)/100.
230 H=4./(U2-U1)
240 PLOTTER IS "GRAPHICS"
250 GRAPHICS ON
260 WINDOW U1,U2,-H*.1,H
270 GRID (U2-U1)*.1,H*.1
280 PLOT 0.,0.
290 FOR I=1 TO 100
300 U=U1+Du*I
310 T=U/Beta
320 CALL Laguerre(N,Alpha,T,L(*))
330 Sum=A(0)
340 FOR K=1 TO N
350 Sum=Sum+A(K)*L(K)
360 NEXT K
370 P=F1*EXP(-T+Alpha*LOG(T))*Sum ! PDF OF RV AT U
380 PLOT U,P
390 NEXT I
400 PENUP
410 GOTO 200
420 END
430 !

```


REFERENCES

1. S. O. Rice, "Mathematical Analysis of Random Noise," Bell System Technical Journal, vols. 23 and 24, 1945. Also in Noise and Stochastic Processes, edited by N. Wax, Dover Publications, N.Y., 1954.
2. Handbook of Mathematical Functions, National Bureau of Standards, Applied Math Series, No. 55, U.S. Dept. of Comm., U.S. Govt. Printing Office, Wash. D.C., June 1964.
3. H. Cramer, Mathematical Methods of Statistics, Princeton University Press, 1961.
4. A. H. Nuttall, "Determination of Densities and Distributions via Hermite and Generalized Laguerre Expansions, Employing High-Order Recursive Cumulants or Moments," NUSC Technical Report, to be published.
5. I. S. Gradshteyn and I. M. Ryzhik, Table of Integrals, Series, and Products, Academic Press Inc., N.Y., 1980.
6. A. H. Nuttall, "Recursive Inter-Relationships Between Moments, Central Moments, and Cumulants," NUSC Technical Memorandum TC-201-71, 12 October 1971.
7. A. H. Nuttall and B. Dedreux, "Exact Operating Characteristics for Linear Sum of Envelopes of Narrowband Gaussian Process and Sinewave," NUSC Technical Report 7117, 11 January 1984.

Evaluation of Densities and Distributions via Hermite and Generalized Laguerre Series Employing High-Order Expansion Coefficients Determined Recursively via Moments or Cumulants

A. H. Nuttall

ABSTRACT

High-order series expansions of probability density functions and cumulative distribution functions, in Hermite as well as generalized Laguerre orthogonal polynomials, have been obtained, where the weighting functions in both cases can have arbitrary (mismatched) parameter values.

The high-order expansion coefficients for both the Hermite and generalized Laguerre series can each be obtained by any one of three fast recursive procedures (all of which have been programmed, and for which program listings are presented). The forms of these three recursive procedures differ in the Hermite versus Laguerre cases; however, they are basically either convolutions or finite alternating series with binomial coefficients. Accuracy of the three procedures is compared. Numerous examples of series expansions of probability density functions and cumulative distribution functions are given.

ABSTRACT

High-order series expansions of probability density functions and cumulative distribution functions, in Hermite as well as generalized Laguerre orthogonal polynomials, have been obtained, where the weighting functions in both cases can have arbitrary (mismatched) parameter values; that is, the two free parameters α and β in the weightings

$$w(u) = \frac{1}{\sqrt{2\pi}\beta} \exp\left(-\frac{(u-\alpha)^2}{2\beta^2}\right) \text{ for all } u, \quad \text{Hermite}$$

$$w(u) = \frac{u^\alpha \exp(-u/\beta)}{\beta^{\alpha+1} \Gamma(\alpha+1)} \text{ for } u > 0, \quad \text{generalized Laguerre}$$

need not be chosen so that the first two expansion coefficients b_1 and b_2 in the orthonormal series are zero. (The zero-th order expansion coefficient b_0 is never zero.) Nonetheless, all the available N lowest-order moments of the approximating probability density function are maintained identical to those of the given probability density function, regardless of the weighting employed and any of its free parameter values.

It has been discovered that deliberate mismatch of α and β results in faster-decaying coefficient sequences $\{b_n\}_0^N$ than when α and β are chosen to make $b_1 = b_2 = 0$, which is a common choice. For example, the central limit theorem is just such a case, where α and β in the Hermite expansion are taken as the mean and standard deviation, respectively, and the number of moments employed is limited to just order $N = 2$.

A fast trial-and-error procedure is used in general to determine good values of weighting parameters α and β . The only statistics needed about the given probability density function or cumulative distribution function are either its moments or cumulants, through order N . Furthermore, all the results presented actually apply to functions which have arbitrary area (not necessarily equal to unity) and to functions which can become negative. In fact, one of the applications considered is to a shot noise process where the continuous part of the probability density function has area less than 1, and which is well approximated by a generalized Laguerre series expansion.

The high-order expansion coefficients for both the Hermite and generalized Laguerre series can each be obtained by any one of three fast recursive procedures (all of which have been programmed, and for which program listings are presented):

- (a) recursively via cumulants,
- (b) directly via moments,
- (c) recursively via moments.

The forms of these three recursive procedures differ in the Hermite versus Laguerre cases; however, they are basically either convolutions or finite alternating series with binomial coefficients. The occurrence and quantitative value of round-off error for large N is easily discerned in a plot of the expansion coefficient sequence for each choice of α and β , and for each of the three procedures, as well as for both types of series expansions.

Comparisons of the accuracy of the three alternative recursive procedures reveals that expansion coefficients determined recursively via cumulants are generally most accurate and least susceptible to round-off error. Numerous examples of series expansions of probability density functions and cumulative distribution functions are given, including one with $N = 150$ terms, where the last expansion coefficient is of size $1E-10$ relative to the leading coefficient b_0 . Estimates of the error associated with the approximations obtained by the Hermite and generalized Laguerre series are derived and compared with results of several examples.

TABLE OF CONTENTS

	PAGE
LIST OF ILLUSTRATIONS	v
LIST OF SYMBOLS	vii
INTRODUCTION	1
FUNDAMENTAL EQUATIONS	5
Definition of Statistics	5
Weighting Function Properties	7
Approximation Procedure	8
Equality of Probability Density Function Moments	10
Parameters of Given Probability Density Function p	11
General Results for Three Lowest-Order Polynomials Q_n	12
Special Choices of Weighting Parameters	13
Example of Divergent Error Integral for $b_1 = 0, b_2 = 0$	15
HERMITE EXPANSION	18
Properties of Polynomials and Expansions	18
Expansion of Characteristic Function f	21
Coefficients Recursively via Cumulants	23
Coefficients Directly via Moments	26
Coefficients Recursively via Moments	28
Summary	29
GENERALIZED LAGUERRE EXPANSION	30
Properties of Polynomials and Expansions	31
Expansion of Characteristic Function f	35

TABLE OF CONTENTS (Cont'd)

	PAGE
Coefficients Recursively via Cumulants	37
Coefficients Directly via Moments	40
Coefficients Recursively via Moments	42
Summary	43
EXAMPLES OF HERMITE EXPANSION	44
Example A	44
Example B	49
Example C	51
Example D	55
EXAMPLES OF GENERALIZED LAGUERRE EXPANSION	61
Example E	61
Example F	65
Example G	67
Example H	69
Example I	71
Example J	76
ESTIMATED ERRORS OF APPROXIMATIONS	80
Hermite Expansion	80
Generalized Laguerre Expansion	84
DISCUSSION	90

TABLE OF CONTENTS (Cont'd)

	PAGE
APPENDICES	
A. COEFFICIENT RECURSION FOR EXPONENTIAL OF POWER SERIES	93
B. EXPANSION OF $He_n(x+y)$	95
C. EVALUATION OF $I_n(y)$ IN (94)	97
D. FOURIER TRANSFORM OF GENERALIZED LAGUERRE POLYNOMIAL	99
E. RECURRENCE FOR EXAMPLE C	101
F. PROGRAM LISTINGS	103
REFERENCES	127

LIST OF ILLUSTRATIONS

FIGURE	PAGE
1. Hermite Coefficients for Example A	48
2. Distributions for Example A	48
3. Hermite Coefficients for Example B	50
4. Distributions for Example B	50
5. Hermite Coefficients for Example C	54
6. Distributions for Example C	54
7. Hermite Coefficients for Example D	58
8. Distributions for Example D	58
9. Linear Density for Example D	60
10. Log Density for Example D	60
11. Generalized Laguerre; Example E	64
12. Distributions for Example E	64
13. Generalized Laguerre; Example F	68
14. Distributions for Example F	68
15. Generalized Laguerre; Example G	70
16. Distributions for Example G	70
17. Generalized Laguerre; Example H	72
18. Distributions for Example H	72
19. Generalized Laguerre; Example I	73
20. Distributions for Example I	73
21. Linear Density for Example I	75
22. Log Density for Example I	75

LIST OF ILLUSTRATIONS (Cont'd)

FIGURE	PAGE
23. Generalized Laguerre; Example J	77
24. Distributions for Example J	77
25. Linear Density for Example J	79
26. Log Density for Example J	79
27. Estimated Error of Figure 8	83
28. Estimated Error of Figure 10	83
29. Estimated Error of Figure 20	86
30. Estimated Error of Figure 22	86
31. Estimated Error of Figure 24	87
32. Estimated Error of Figure 26	87
33. Estimated Error of Figure 16	89

LIST OF SYMBOLS

$w(u)$	Weighting function at argument u
α, β	Parameters of weighting w ; (1),(2)
b_n	n -th expansion coefficient in orthonormal polynomial series
N	Number of terms employed in series expansion
p	Probability density function
P	Cumulative distribution function; integral of p
$1-P$	Exceedance distribution function
f	Characteristic function corresponding to p
μ_n	n -th moment of p or f ; (3)
χ_n	n -th cumulant of p or f ; (7)
ν_n	n -th moment of weighting w ; (11)
Q_n	n -th order orthonormal polynomial
P_N, P_N	N -th order approximations to p, P
E_N	Weighted squared error
A	Area of p ; (24)
M	Mean location of p ; (24)
R	Rms width of p ; (24)
γ, ω	Parameters of probability density function p
ϕ	Normalized Gaussian function; (41)
Φ	Integral of ϕ ; (41)
He_n	n -th Hermite polynomial; (50)
a_n, c_n	Auxiliary expansion coefficients; (44)-(47) or (90)-(92)
w, z	Auxiliary variables

LIST OF SYMBOLS (Cont'd)

$\hat{\chi}_n$	Normalized cumulants; (62)
\hat{u}_n	Normalized moments; (69)
\tilde{u}_n	Alternative normalized moments; (118)
\hat{H}_{e_n}	n-th normalized Hermite polynomial; (68)
H_i	n-th modified Hermite polynomial; (74)
\hat{H}_i	n-th normalized modified Hermite polynomial; (80)
$L_n^{(\alpha)}$	n-th generalized Laguerre polynomial; (96)
${}_1F_1$	Confluent hypergeometric function
d_m	Auxiliary variables in (112)
RC	Recursively via Cumulants
DM	Directly via Moments
RM	Recursively via Moments
J, θ	Parameters of p in (141)
Q_v	Generalized Q-function; (165)
P_0	Area of impulse at origin of p, for shot noise
F	Hypergeometric function ${}_2F_1$
Env	Envelope function
$E_n(u;p)$	Estimated error of p_n ; (178) or (183)
$E_n(u;P)$	Estimated error of P_n ; (180) or (185)

EVALUATION OF DENSITIES AND DISTRIBUTIONS VIA HERMITE AND GENERALIZED
LAGUERRE SERIES EMPLOYING HIGH-ORDER EXPANSION COEFFICIENTS
DETERMINED RECURSIVELY VIA MOMENTS OR CUMULANTS

INTRODUCTION

In the theoretical analysis of performance of some systems with nonlinearities and/or memory, it often happens that the only statistics about the decision (or output) random variable of interest that can be easily found are the moments, or in other cases, the cumulants. Explicit relations for the low-order expansion coefficients in Edgeworth or Gram-Charlier series are available in terms of the available moments or cumulants [1, pp. 172 and 191], [2, pp. 223 and 226], [3, pp. 157 and 159]. However, for higher-order moments and cumulants, these explicit nonrecursive relations are very tedious to derive, become extremely lengthy, and are not practical to use.

We will address the problem of obtaining accurate high-order series expansion approximations of the probability density function and cumulative distribution function of a random variable of interest, in terms of the available moments or cumulants of that random variable. The necessity of being able to approximate probability density functions and cumulative distribution functions from knowledge of either the moments or the cumulants, is that some physical problems have these particular statistics as natural and convenient starting points. For example, if a physical processor sums together a number of independent Gaussian random variates, the characteristic function and cumulants of the individual random variables or their sum are not available in any useful analytic form; however, the high-order moments of an

individual Rician variate can be easily and accurately evaluated by recurrence, and thereby the moments of the sum can be obtained. Conversely, for shot noise with random amplitude and duration modulation, the probability density function is not readily available, whereas the characteristic function is, and the cumulants are simple to evaluate [4, appendix C].

The particular series expansions we employ are based on the two special classes of weighting functions

$$w(u) = \frac{1}{(2\pi)^{1/2} \beta} \exp\left(-\frac{(u-\alpha)^2}{2\beta^2}\right) \quad \text{for all } u \quad \text{Hermite} \quad (1)$$

and

$$w(u) = \frac{u^\alpha \exp(-u/\beta)}{\beta^{\alpha+1} \Gamma(\alpha+1)} \quad \text{for } u > 0 \quad \text{generalized Laguerre.} \quad (2)$$

The orthonormal polynomials associated with these weightings are directly related to the Hermite and generalized Laguerre polynomials, respectively [5, 22.2.15 and 22.2.13]. The weightings each have two free parameters, α and β , which can be manipulated to advantage in obtaining finite (high-order) series expansions which well approximate a given (unknown) probability density function and cumulative distribution function.

The question of when a set of moments uniquely determines the probability density function is a difficult one; see, for example, [3, pp. 109-112 and 179]. Also, the convergence of the series is very involved [2, pp. 223 and 258], [3, pp. 161-163]. But, even if the series is divergent, use of a limited number of expansion coefficients often gives a satisfactory approximation to the desired probability density function [3, p. 167]. We

presume here that the moments do uniquely determine the probability density function and are buoyed in that respect by the comment [3, p. 87] that most distributions in statistical practice do possess this property.

The main idea in the series expansion approach here is not necessarily to get as many terms as possible, but rather to get as rapid convergence as possible of the series. If a particular choice of weighting parameters α and β results in sufficiently small expansion coefficients, say, at order 10, this is better than another choice of α and β where 20 or 30 terms are required for the same size coefficients. In fact, if α and β could be chosen such that the series terminated (zero coefficients) after a few terms, that would be ideal; however, this is not the case, and in fact, the choice of α and β requires some trial-and-error to achieve rapidly decreasing coefficients.

The expansion coefficients of a given probability density function, in an orthonormal set of Hermite or generalized Laguerre polynomials, are denoted by $\{b_n\}_0^N$, where N is the number of available or known moments or cumulants. Very often, the choice of α and β in (1) or (2) has been made such that $b_1 = 0$ and $b_2 = 0$, for purposes of analytic simplicity and for hopeful early termination of the series; see for example [1, pp. 171 and 191], [2, p. 223], [3, p. 159]. However, it will be demonstrated that this is generally not the best choice, and that more rapidly decaying coefficients can be achieved by other (mismatched) values of α and β , which must be searched for numerically; this possibility is also mentioned in [3, p. 164]. In fact, an example will be given which illustrates that the choice of parameters α and β to make expansion coefficients b_1 and b_2 zero, can in fact, lead to a divergent Hermite series.

Depending on the available information about the probability density function, i.e., moments or cumulants, a variety of methods will be given for determining the expansion coefficients $\{b_n\}$. In particular, for both the Hermite and generalized Laguerre series, we can get the coefficients by three different procedures:

- (a) recursively via cumulants,
- (b) directly via moments,
- (c) recursively via moments.

The reason for having these alternatives is that the calculation of expansion coefficients $\{b_n\}$ for high-order n invariably runs into large round-off error. In order to reduce this round-off error, the amount of number-crunching on the computer should be minimized, and any spurious transformations between moments and cumulants should be avoided if possible. Thus it is desirable to have techniques which can accomplish the desired goal of evaluating expansion coefficients $\{b_n\}$ as directly as possible from the available information. The use of different alternatives also enables comparisons of the computed expansion coefficients and thereby furnishes quantitative assessment of the amount of round-off error. Recursive inter-relationships between moments, central moments, and cumulants are given in [6], including cases of two dependent random variables.

FUNDAMENTAL EQUATIONS

DEFINITION OF STATISTICS

Suppose a function p has known moments*

$$\mu_n = \int du u^n p(u) \quad \text{for } 0 \leq n \leq N. \quad (3)$$

The function p need not have unit area, i.e., $\mu_0 \neq 1$ is allowed, and p can become negative at some arguments u . Nevertheless, for convenience, and since most of our applications are to random variables, we shall refer to p as a probability density function, and to its running integral

$$P(u) = \int_{-\infty}^u dt p(t) \quad (4)$$

as a cumulative distribution function. We shall presume that $\mu_0 > 0$ in all cases.

The characteristic function corresponding to probability density function p is the Fourier transform

$$f(i\xi) = \int du \exp(i\xi u) p(u). \quad (5)$$

When f is expanded in a power series, the result is

$$f(i\xi) = \sum_{n=0}^{\infty} \mu_n (i\xi)^n / n! \quad (6)$$

* Integrals without limits are over the range of nonzero integrand.

in terms of the moments in (3). Alternatively, if $\ln f$ is expanded in a power series,

$$\ln f(i\xi) = \sum_{n=0}^{\infty} \chi_n (i\xi)^n / n! , \quad (7)$$

where the quantities $\{\chi_n\}$ are the cumulants of p or f . Observe that generally, to the lowest three orders,

$$\begin{aligned} \chi_0 &= \ln f(0) = \ln \mu_0 \neq 0 , \\ \chi_1 &= \frac{\mu_1}{\mu_0} , \\ \chi_2 &= \frac{\mu_2}{\mu_0} - \left(\frac{\mu_1}{\mu_0} \right)^2 . \end{aligned} \quad (8)$$

The available information on probability density function p will be either

$$\text{moments } \{\mu_n\}_0^N \quad \text{or cumulants } \{\chi_n\}_0^N . \quad (9)$$

Whichever is available, we wish to get high-order accurate approximations to p and cumulative distribution function P in (4); that is, values of N in the order of 10 to 100 are of interest.

WEIGHTING FUNCTION PROPERTIES

We select a nonnegative weighting function w such that

$$w(u) > 0 \text{ at least where } p(u) \neq 0 . \quad (10)$$

We also disallow any impulses in w . The moments of weighting w are defined analogously to (3) as

$$v_n = \int du u^n w(u) \quad \text{for } n \geq 0 ; \quad (11)$$

it is presumed that these quantities can be evaluated for as large n as required.

Suppose weighting w has r free parameters (plus a scaling parameter). It might then seem beneficial to choose them such that the moments of w and p are approximately equal,

$$v_n \cong \mu_n \quad \text{for } 1 \leq n \leq r \quad (\text{plus } v_0 \cong \mu_0) , \quad (12)$$

for then the abscissa scales of w and p would tend to match. However, (12) will turn out to be not so desirable, and the choice of the r weighting parameter values should be based on another criterion. The ordinate scale of w is actually immaterial, since the expansion coefficients $\{b_n\}$ will absorb this scaling; so henceforth we presume that $v_0 = 1$ with no loss of generality.

APPROXIMATION PROCEDURE

Let Q_n be any n -th order polynomial, and approximate probability density function p by function

$$p_N(u) \equiv w(u) \sum_{n=0}^N b_n Q_n(u) \quad \text{where } w(u) > 0, \quad (13)$$

where $\{b_n\}_0^N$ are the expansion coefficients. Define weighted squared error

$$\begin{aligned} E_N &= \int du \gamma(u) [p(u) - p_N(u)]^2 = \\ &= \int du \gamma(u) [p(u) - w(u) \sum_{n=0}^N b_n Q_n(u)]^2, \end{aligned} \quad (14)$$

where error-weighting γ is nonnegative. If we minimize E_N by choice of expansion coefficients $\{b_n\}_0^N$, there follows the set of linear equations

$$\sum_{n=0}^N b_n \int du \gamma(u) w^2(u) Q_k(u) Q_n(u) = \int du \gamma(u) w(u) p(u) Q_k(u) \quad \text{for } 0 \leq k \leq N. \quad (15)$$

In order to use only the available information in (9) about p , the right-hand side of (15) must simplify according to the selection

$$\gamma(u) = \frac{K}{w(u)} \quad \text{where } w(u) > 0 \text{ (and arbitrary elsewhere)}. \quad (16)$$

Furthermore, since constant K merely scales error E_N , and appears on both sides of (15), we can set $K = 1$ without loss of generality. Then (14) becomes

$$E_N = \int du w(u) \left[\frac{p(u)}{w(u)} - \sum_{n=0}^N b_n Q_n(u) \right]^2 \quad \text{where } w(u) > 0, \quad (17)$$

and (15) reduces to

$$\sum_{n=0}^N b_n \int du w(u) Q_k(u) Q_n(u) = \int du p(u) Q_k(u) \quad \text{for } 0 \leq k \leq N. \quad (18)$$

In general, this is $N+1$ simultaneous linear equations in the $N+1$ unknowns $\{b_n\}_0^N$. The choice $Q_k(u) = u^k$ would lead to an apparently simple set of equations, when (11) and (3) are used. However, a few numerical examples quickly reveals that they are very ill-conditioned, due to the character of the nondiagonal matrix with elements

$$\int du w(u) Q_k(u) Q_n(u) \quad \text{for } 0 \leq k, n \leq N \quad (19)$$

that appears on the left-hand side of (18). In order to avoid the significant round-off error associated with solving such a system for large N , we choose $\{Q_n\}_0^N$ to be a set of orthonormal polynomials with respect to weighting w ; i.e., (19) is 1 for $k = n$, and 0 otherwise. Also recall that $v_0 = \int du w(u) = 1$ without loss of generality.

Equation (18) then reduces to an explicit relation for the expansion coefficients:

$$b_k = \int du p(u) Q_k(u) \quad \text{for } 0 \leq k \leq N, \quad (20)$$

and (17) for the error becomes merely

$$E_N = \int du \frac{p^2(u)}{w(u)} - \sum_{n=0}^N b_n^2. \quad (21)$$

It will be presumed that the integral in (21) is finite; otherwise, the error would be infinite, which is a meaningless problem. This will put some restrictions on the parameter choices of weighting w , since this error integral depends on these parameters as well as on the given probability density function p . The sum of squares in (21) must then be bounded, and in fact affords a measure of the adequacy of approximation (13), by saturating (at an a priori unknown value) for large N .

As N increases, the values of the lower-order expansion coefficients $\{b_k\}$ in (20) do not change. Therefore they only have to be computed once and do not have to be revised as more terms are added in series approximation (13), i.e., larger N .

EQUALITY OF PROBABILITY DENSITY FUNCTION MOMENTS

A very important property of expansion (13) is obtained as follows:

$$\begin{aligned} \int du Q_k(u) p_N(u) &= \int du Q_k(u) w(u) \sum_{n=0}^N b_n Q_n(u) = \\ &= b_k = \int du Q_k(u) p(u) \quad \text{for } 0 \leq k \leq N, \end{aligned} \quad (22)$$

where we used, in order, (13), the orthonormality of (19), and (20). But since Q_k is a k -th order polynomial, relation (22) states that approximation p_N has exactly the same moments as given probability density function p , from order 0 through order N . This matching of moments between probability density functions p_N and p has been achieved regardless of the weighting w and its particular parameter values. Furthermore, (22) holds independently of whether the weighting-moment equalities in (12) are satisfied or not.

The cumulative distribution function corresponding to approximation p_N is defined as

$$P_N(u) \equiv \int_{-\infty}^u dt p_N(t) = \sum_{n=0}^N b_n \int_{-\infty}^u dt w(t) Q_n(t). \quad (23)$$

Its utility depends on getting closed forms and simple recursions for the general integral on the right-hand side.

PARAMETERS OF GIVEN PROBABILITY DENSITY FUNCTION p

The moments of p were defined in (3). It is useful to define three important parameters of p :

$$\text{Area } A = \int du p(u) = \mu_0 \quad (\mu_0 > 0, \text{ but need not be } 1);$$

$$\text{Mean Location } M = \frac{\int du u p(u)}{\int du p(u)} = \frac{\mu_1}{\mu_0};$$

$$\text{RMS Width } R = \left[\frac{\int du (u-M)^2 p(u)}{\int du p(u)} \right]^{1/2} = \left[\frac{\mu_2}{\mu_0} - \left(\frac{\mu_1}{\mu_0} \right)^2 \right]^{1/2}. \quad (24)$$

(Conversely, $\mu_0 = A$, $\mu_1 = AM$, $\mu_2 = A(M^2 + R^2)$.) These parameters depend on the probability density function p that we are trying to approximate and can be computed from the available information (9). They are useful for determining where the major concentration of $p(u)$ lies on the u -scale, and have obvious physical interpretations.

In terms of the cumulants of p defined in (5)-(8), we have the alternative expressions

$$A = \exp(\chi_0), \quad M = \chi_1, \quad R = \chi_2^{1/2}, \quad (25)$$

or conversely

$$\chi_0 = \ln \mu_0 = \ln A, \quad \chi_1 = \frac{\mu_1}{\mu_0} = M, \quad \chi_2 = \frac{\mu_2}{\mu_0} - \left(\frac{\mu_1}{\mu_0}\right)^2 = R^2. \quad (26)$$

GENERAL RESULTS FOR THREE LOWEST-ORDER POLYNOMIALS Q_n

The weighting function w and associated orthonormal polynomials satisfy the following equation:

$$\int du w(u) Q_k(u) Q_n(u) = \delta_{kn}. \quad (27)$$

Also we have weighting moments

$$v_n = \int du u^n w(u), \quad \text{with } v_0 = 1. \quad (28)$$

It is then a straightforward matter to evaluate the three lowest-order orthonormal polynomials:

$$\begin{aligned} Q_0(u) &= 1, \\ Q_1(u) &= \frac{1}{D_1}(u - v_1), \\ Q_2(u) &= \frac{1}{D_2} \left[u^2(v_2 - v_1^2) - u(v_3 - v_2 v_1) + (v_3 v_1 - v_2^2) \right], \end{aligned} \quad (29)$$

where

$$D_1 = (v_2 - v_1^2)^{1/2},$$

$$D_2 = (v_2 - v_1^2)^{1/2} \left[(v_4 - v_2^2)(v_2 - v_1^2) - (v_3 - v_2 v_1)^2 \right]^{1/2}. \quad (30)$$

The general expansion coefficients in (20) then become

$$b_0 = \mu_0,$$

$$b_1 = \frac{1}{D_1} (\mu_1 - v_1 \mu_0),$$

$$b_2 = \frac{1}{D_2} \left[\mu_2 (v_2 - v_1^2) - \mu_1 (v_3 - v_2 v_1) + \mu_0 (v_3 v_1 - v_2^2) \right]. \quad (31)$$

All these results above are general and make no presumption about weighting moment equalities such as (12).

SPECIAL CHOICES OF WEIGHTING PARAMETERS

Suppose that weighting w has free parameters that can be varied so as to make the mean locations of w and p coincide (see (24)); that is,

$$\text{let } v_1 = \frac{\mu_1}{\mu_0}. \quad (32A)$$

(The reason for the discrepancy with (12) is that we have set $v_0 = 1$ but have allowed $\mu_0 \neq 1$.) Inspection of (31) gives the following:

$$\text{then } b_1 = 0 \quad \text{and} \quad b_2 = -\frac{\mu_0}{D_2} \left(v_2 - \frac{\mu_2}{\mu_0} \right) \left(v_2 - \frac{\mu_1^2}{\mu_0^2} \right). \quad (32B)$$

Conversely, (31) shows that requiring $b_1 = 0$ forces the choice in (32A) for v_1 . Thus equality of the first weighting moment v_1 of w with the first (normalized) moment of probability density function p implies (and is implied by) the vanishing of the first expansion coefficient b_1 . This may or may not be a useful choice, but, whether adopted or not, has no bearing on the equality of probability density function moments already demonstrated in (22).

As a second special choice, suppose that weighting w has enough free parameters that we can vary, so as to make the mean locations and rms widths of w and p coincide (see (24)); that is

$$\text{let } v_1 = \frac{\mu_1}{\mu_0} \quad \text{and} \quad v_2 = \frac{\mu_2}{\mu_0} . \quad (33A)$$

(Again we have used $v_0 = 1$.) Manipulation of (31) yields the following conclusion:

$$\text{then } b_1 = 0 \quad \text{and} \quad b_2 = 0 . \quad (33B)$$

Conversely, imposition of (33B) implies the results in (33A), as may be seen by reference to (31). (The apparent additional solution $v_2 = \mu_1^2/\mu_0^2 = v_1^2$ would yield an impulse for w and is disallowed.) Thus equality of the first two weighting moments of w with the first two (normalized) moments of probability density function p implies (and is implied by) the vanishing of the first two expansion coefficients b_1 and b_2 . This common choice of weighting parameter values can be made if desired, but is not necessary (or recommended) for series approximations by orthonormal polynomials. The equality of probability density function moments in (22) will hold whether (33) is true or not.

EXAMPLE OF DIVERGENT ERROR INTEGRAL FOR $b_1 = 0$, $b_2 = 0$

As a demonstration of what forcing expansion coefficients b_1 and b_2 equal to zero can do, consider probability density function

$$p(u) = \frac{2 u^\gamma \exp(-u^2/\omega^2)}{\omega^{\gamma+1} \Gamma\left(\frac{\gamma+1}{2}\right)} \quad \text{for } u > 0 \quad (\gamma > -1, \omega > 0) \quad (34)$$

with moments

$$\mu_n = \omega^n \frac{\Gamma\left(\frac{\gamma+1+n}{2}\right)}{\Gamma\left(\frac{\gamma+1}{2}\right)}. \quad (35)$$

This class of probability density functions includes the one-sided Gaussian, Rayleigh, and Maxwell as special cases, for $\gamma = 0, 1, 2$, respectively.

Consider also the Hermite weighting given in (1), which has moments (11) equal to

$$v_0 = 1, \quad v_1 = \alpha, \quad v_2 = \alpha^2 + \beta^2. \quad (36)$$

If we now insist on property (33B), then (33A) yields

$$\alpha = \omega \frac{\Gamma\left(\frac{\gamma+1}{2}\right)}{\Gamma\left(\frac{\gamma+1}{2}\right)}, \quad \beta^2 = \omega^2 \left[\frac{\gamma+1}{2} - \frac{\Gamma^2\left(\frac{\gamma+1}{2}\right)}{\Gamma^2\left(\frac{\gamma+1}{2}\right)} \right]. \quad (37)$$

But the leading integral in minimum error E_N in (21) is convergent only if $p^2(u)/w(u)$ decays sufficiently rapid for large u . We have from (34) and (1), the dominant behavior

$$p^2(u)/w(u) \propto \exp\left(-\frac{2u^2}{\omega^2} + \frac{u^2}{2\beta^2}\right) \quad \text{for large positive } u, \quad (38)$$

where \propto denotes proportionality, but disregards the exact scale factor and subdominant behavior. Thus the integral in (21) is convergent only if

$$1 < \frac{4\beta^2}{\omega^2} = 2(\gamma+1) - 4 \frac{\Gamma^2(\frac{\gamma+1}{2})}{\Gamma^2(\frac{\gamma+1}{2})}. \quad (39)$$

However, calculation of (39) reveals that this inequality is never satisfied for any value of $\gamma > -1$; the function on the right-hand side starts at 0 when $\gamma = -1$, and increases monotonically towards 1 as $\gamma \rightarrow +\infty$, behaving like $1 - 1/(4\gamma)$ in this limit.

Thus expansion of probability density function (34) according to a Hermite weighting has an infinite error integral (21) (and perhaps a divergent series expansion) regardless of the values of γ and ω in the true probability density function, if we insist on expansion coefficients $b_1 = b_2 = 0$. Yet if we relax requirement (33B), and choose β according to (39) such that $\beta > \omega/2$, the error integral in (21) is certainly finite, regardless of α .

However, making the error integral in (21) finite is not the whole story, in so far as realizing useful approximations to the probability density function or cumulative distribution function. An example of probability density function (34) was taken with $\gamma = 3$, $\omega = 1$. When α and β were chosen according to (33) and (37) (giving $\beta = .48 < .5 = \omega/2$), the expansion coefficients $\{b_n\}$ initially decreased to approximately $1E-3$ at $n = 40$ terms, and then diverged; yet a plot of the approximate exceedance distribution function obtained by a Hermite expansion overlaid the exact answer down to the $1E-16$ level. On the other hand, when the weighting parameters in the Hermite expansion were chosen as* $\alpha = 0$, $\beta = .7 > .5 = \omega/2$, giving $b_1 \neq 0$ and

*This is example B in a later section

$b_2 \neq 0$, the expansion coefficients $\{b_n\}$ decreased to the $1E-4$ level at $n = 70$ before round-off error became dominant; despite this apparent improvement in coefficient level, the approximate exceedance distribution function overlaid a plot of the exact result down to the $1E-10$ probability level, which is several orders of magnitude worse than the above result. Thus emphasis on getting a convergent error integral in (21) may not always be desired.

For Hermite weighting (1) and the class of probability density functions which decay as $\exp(-u^q)$ as $u \rightarrow +\infty$, the error integral is always convergent if $q > 2$, and always divergent if $q < 2$. So an exponential probability density function, like $u^\gamma \exp(-u/\omega)$ for $u > 0$, always yields a divergent error integral when expanded in a Hermite series.

For generalized Laguerre weighting (2), it is necessary to consider $u = 0^+$ and $u = +\infty$ separately. If probability density function p behaves like u^γ as $u \rightarrow 0^+$, then a finite error integral requires that we choose $\alpha < 1 + 2\gamma$. Coupled with the finite area restriction on weighting w , a range of values of α is allowed, namely, $-1 < \alpha < 1 + 2\gamma$; this range always exists since $\gamma > -1$ is necessary for the probability density function itself to have finite area.

If also the probability density function behaves as $\exp(-u/\omega)$ as $u \rightarrow +\infty$, then a finite error integral with generalized Laguerre weighting requires that we choose $\beta > \omega/2$. So the range of choice of β is open on the large side, whereas that for α is a limited one, for this particular class of probability density functions.

HERMITE EXPANSION

In this section, we will deal exclusively with weighting (1),

$$w(u) = \frac{1}{\beta} \phi\left(\frac{u-\alpha}{\beta}\right) \text{ for all } u \quad (\beta > 0), \quad (40)$$

where

$$\phi(x) = (2\pi)^{-1/2} \exp(-x^2/2), \quad \bar{\Phi}(x) = \int_{-\infty}^x dt \phi(t). \quad (41)$$

This weighting has two free parameters, α and β , and moments

$$v_0 = 1, \quad v_1 = \alpha, \quad v_2 = \alpha^2 + \beta^2. \quad (42)$$

If v_1 and v_2 are specified, the parameters must then satisfy $\alpha = v_1$, $\beta = (v_2 - v_1^2)^{1/2}$. However, we shall keep α and β general and unspecified.

PROPERTIES OF POLYNOMIALS AND EXPANSIONS

The orthonormal polynomials associated with weighting (40) are the Hermite polynomials [5, 22.1.2 and 22.2.15]

$$Q_n(u) = He_n\left(\frac{u-\alpha}{\beta}\right) (n!)^{-1/2} \text{ for } n \geq 0. \quad (43)$$

The expansion coefficients are given by (20) as

$$b_n = \int du p(u) Q_n(u) = (n!)^{-1/2} c_n \text{ for } n \geq 0, \quad (44)$$

where we define

$$c_n = \int du p(u) \text{He}_n\left(\frac{u-\alpha}{\beta}\right) \quad \text{for } n \geq 0. \quad (45)$$

The approximate probability density function then follows from (13) in the form

$$p_N(u) = w(u) \sum_{n=0}^N b_n Q_n(u) = \frac{1}{\beta} \phi\left(\frac{u-\alpha}{\beta}\right) \sum_{n=0}^N a_n \text{He}_n\left(\frac{u-\alpha}{\beta}\right), \quad (46)$$

where we used (40), (43), (44), and defined

$$(n!)^{1/2} a_n = b_n = (n!)^{-1/2} c_n \quad \text{for } n \geq 0. \quad (47)$$

These three different coefficients in (44)-(47) are introduced for convenience in further equation manipulations. Expansion coefficient b_n is the geometric mean of auxiliary coefficients a_n and c_n (with polarity). Expansion (46) is also called a Gram-Charlier series of type A [2, p. 222], [3, p. 156].

The approximate cumulative distribution function corresponding to (46) is

$$\begin{aligned} P_N(u) &= \int_{-\infty}^u dt p_N(t) = \sum_{n=0}^N a_n \int_{-\infty}^u \frac{dt}{\beta} \phi\left(\frac{t-\alpha}{\beta}\right) \text{He}_n\left(\frac{t-\alpha}{\beta}\right) = \\ &= \sum_{n=0}^N a_n \int_{-\infty}^T dx \phi(x) \text{He}_n(x) = a_0 \Phi(T) - \phi(T) \sum_{n=1}^N a_n \text{He}_{n-1}(T), \quad (48) \end{aligned}$$

where

$$T = \frac{u-\alpha}{\beta} \quad (49)$$

and we used (41) and [5, 22.11.8].

The Hermite polynomials $\{He_n\}$ satisfy the recurrence [5, 22.7.14]

$$He_n(x) = x He_{n-1}(x) - (n-1) He_{n-2}(x) \quad \text{for } n \geq 2, \quad (50)$$

with starting values $He_0(x) = 1$, $He_1(x) = x$ [5, 22.3.11]. The highest-order term in $He_n(x)$ is x^n , with coefficient 1 [5, 22.1.2 and 22.3.11].

The magnitude of the term multiplying b_n in (46) has an envelope that decays approximately as $n^{-1/4}$ with n , regardless of argument u . This may be seen by using (47) and (49) to get

$$a_n He_n(T) = b_n (n!)^{-1/2} He_n(T) \propto b_n \left(n^{n+1/2} e^{-n} \right)^{-1/2} (n/e)^{n/2} = b_n n^{-1/4}$$

as $n \rightarrow +\infty$, for all T , (50A)

where we also used [5, 6.1.39 and 22.5.18] and [7, 8.22.8]. Here, \propto denotes proportionality and we have taken the magnitude of the terms; the exact scale factor of proportionality will be presented in a later section where the errors of the approximations are estimated. So if b_n were to decay faster than $n^{-3/4}$, the probability density function series in (46) would converge absolutely.

Conditions are better for the cumulative distribution function series in (48); namely, based on the above result, there follows (for the envelope)

$$a_n He_{n-1}(T) = b_n (n!)^{-1/2} He_{n-1}(T) = b_n n^{-1/2} [(n-1)!]^{-1/2} He_{n-1}(T) =$$

$$\propto b_n n^{-1/2} n^{-1/4} = b_n n^{-3/4} \quad \text{as } n \rightarrow +\infty, \text{ for all } T. \quad (50B)$$

Thus if b_n decays faster than $n^{-1/4}$, the cumulative distribution function series converges absolutely. Furthermore, if the leading error integral in

(21) is finite, the sum of b_n^2 must be finite, meaning that b_n must decay faster than $n^{-1/2}$. So we can conclude that if the error integral is finite, the Hermite series for the cumulative distribution function in (48) converges. (Notice that this particular decay $n^{-1/2}$ of b_n is not sufficiently fast to make the same conclusion about the Hermite series for the probability density function in (46).) The above are sufficient conditions on expansion coefficients $\{b_n\}$, and are not necessary.

EXPANSION OF CHARACTERISTIC FUNCTION f

The coefficients a_n and c_n were defined in (45) and (47). Then the sum

$$\begin{aligned} \sum_{n=0}^{\infty} a_n w^n &= \sum_{n=0}^{\infty} \frac{1}{n!} c_n w^n = \sum_{n=0}^{\infty} \frac{w^n}{n!} \int du p(u) \text{He}_n\left(\frac{u-\alpha}{\beta}\right) = \\ &= \int du p(u) \sum_{n=0}^{\infty} \frac{w^n}{n!} \text{He}_n\left(\frac{u-\alpha}{\beta}\right) = \int du p(u) \exp\left(\frac{u-\alpha}{\beta} w - \frac{1}{2} w^2\right) = \\ &= \exp\left(-\frac{1}{2} w^2 - \frac{\alpha}{\beta} w\right) f\left(\frac{w}{\beta}\right), \end{aligned} \quad (51)$$

where f is the characteristic function, and where we used (45), [5, 22.5.19 and 22.9.17], and (5). Letting $w = \beta z$, we have

$$f(z) \exp\left(-\alpha z - \frac{1}{2} \beta^2 z^2\right) = \sum_{n=0}^{\infty} a_n (\beta z)^n = \sum_{n=0}^{\infty} \frac{1}{n!} c_n (\beta z)^n. \quad (52)$$

Thus $\{a_n\}$ and $\{c_n\}$ are the coefficients in these power series expansions of the function $f(z) \exp(-\alpha z - \beta^2 z^2/2)$, where f is the characteristic function corresponding to probability density function p , and α and β are arbitrary. A special case of (52) is given in [2, 17.6.10].

Collecting (46) and (52) together for comparison, and assuming that $p_n \rightarrow p$ as $N \rightarrow +\infty$, we have

$$p(u) = \frac{1}{\beta} \phi\left(\frac{u-\alpha}{\beta}\right) \sum_{n=0}^{\infty} a_n \text{He}_n\left(\frac{u-\alpha}{\beta}\right),$$

$$f(i\xi) = \exp\left(i\alpha\xi - \frac{1}{2}\beta^2\xi^2\right) \sum_{n=0}^{\infty} a_n (i\beta\xi)^n. \quad (53)$$

Thus expansion of probability density function p in an infinite Hermite series is equivalent to an expansion of a modified form of the characteristic function in a power series, according to (53). Equations (51)-(53) will serve as very convenient starting points for the derivation of several alternative recurrences for the expansion coefficients $\{a_n\}$. Notice that weighting parameters α and β are completely unrestricted in (52) and (53), except that $\beta > 0$.

An analogous result holds for N finite, but must be derived in a different fashion, because we no longer can use infinite sum [5, 22.9.17]. Define the Fourier transform of (46) as the N -th order approximation to the characteristic function:

$$f_N(i\xi) = \int du \exp(i\xi u) p_N(u) =$$

$$= \sum_{n=0}^N a_n \int du \exp(i\xi u) \frac{1}{\beta} \phi\left(\frac{u-\alpha}{\beta}\right) \text{He}_n\left(\frac{u-\alpha}{\beta}\right) =$$

$$= \sum_{n=0}^N a_n \int dt \exp(i\xi\alpha + i\xi\beta t) \phi(t) \text{He}_n(t) =$$

$$= \exp(i\alpha\xi) \sum_{n=0}^N a_n \int dt \exp(i\xi\beta t) \left(-\frac{d}{dt}\right)^n \phi(t) =$$

$$\begin{aligned}
&= \exp(i\alpha\xi) \sum_{n=0}^N a_n (i\beta\xi)^n \int dt \exp(i\beta\xi t) \phi(t) = \\
&= \exp\left(i\alpha\xi + \frac{1}{2} \beta^2 (i\xi)^2\right) \sum_{n=0}^N a_n (i\beta\xi)^n, \tag{54}
\end{aligned}$$

where we used [5, 22.11.8] in line 4, and repeated integration by parts in line 5. This result is the leading N terms of (53). As a by-product of this derivation, we have

$$\int dt \exp(zt) \phi(t) \text{He}_n(t) = \exp\left(\frac{1}{2} z^2\right) z^n. \tag{55}$$

COEFFICIENTS RECURSIVELY VIA CUMULANTS

We are now in a position to obtain some useful recursive relations for the expansion coefficients $\{a_n\}$ in (51)-(54). The first one is obtained by taking the \ln of (51):

$$\ln f\left(\frac{w}{\beta}\right) - \frac{\alpha}{\beta} w - \frac{1}{2} w^2 = \ln \left\{ \sum_{n=0}^{\infty} a_n w^n \right\}. \tag{56}$$

Then using (7) and identifying the right-hand side of (56) as a new power series, we have

$$\sum_{n=0}^{\infty} \frac{1}{n!} \chi_n \left(\frac{w}{\beta}\right)^n - \frac{\alpha}{\beta} w - \frac{1}{2} w^2 = \sum_{n=0}^{\infty} \chi'_n w^n. \tag{57}$$

There follows immediately

$$h_n = \left. \begin{array}{ll} \frac{\chi_n}{n! \beta^n} & \text{for } n \neq 1, 2 \\ \frac{\chi_1 - \alpha}{\beta} & \text{for } n = 1 \\ \frac{1}{2} \left(\frac{\chi_2}{\beta^2} - 1 \right) & \text{for } n = 2 \end{array} \right\}. \quad (58)$$

But equality of the right-hand sides of (56) and (57) also requires that

$$\sum_{n=0}^{\infty} a_n w^n = \exp \left\{ \sum_{n=0}^{\infty} h_n w^n \right\}. \quad (59)$$

It is shown in appendix A that a recursive solution to (59) for the $\{a_n\}$ is given by

$$a_n = \frac{1}{n} \sum_{m=1}^n m h_m a_{n-m} \quad \text{for } n \geq 1, \quad a_0 = \exp(h_0). \quad (60)$$

Then eliminating $\{h_m\}$ by means of (58),

$$a_n = \frac{1}{n} \left[\left(\frac{\chi_1}{\beta} - \frac{\alpha}{\beta} \right) a_{n-1} + \left(\frac{\chi_2}{\beta^2} - 1 \right) a_{n-2} + \sum_{m=3}^n \frac{\chi_m}{(m-1)! \beta^m} a_{n-m} \right] \quad \text{for } n \geq 1, \\ a_0 = \exp(\chi_0), \quad (61)$$

where $a_n \equiv 0$ for $n < 0$, and the sum is zero for $n < 3$.

Now define normalized cumulants (excluding $n=0$) according to

$$\hat{\chi}_n = \frac{\chi_n}{(n-1)! \beta^n} \quad \text{for } n \geq 1. \quad (62)$$

Then (61) becomes

$$a_n = \frac{1}{n} \left[\left(\hat{\chi}_1 - \frac{\alpha}{\beta} \right) a_{n-1} + \left(\hat{\chi}_2 - 1 \right) a_{n-2} + \sum_{m=3}^n \hat{\chi}_m a_{n-m} \right] \text{ for } n \geq 1, \\ a_0 = \exp(\chi_0). \quad (63)$$

This convolution is the desired recursion for expansion coefficients $\{a_n\}$ via cumulants.

As particular cases, we have

$$a_1 = \frac{\chi_1 - \alpha}{\beta} a_0, \quad a_2 = \frac{1}{2} \left[\left(\frac{\chi_1 - \alpha}{\beta} \right)^2 + \frac{\chi_2}{\beta^2} - 1 \right] a_0. \quad (64A)$$

Parameters α and β (>0) are completely arbitrary in the above three equations, and $\{\chi_n\}_0^N$ are the available cumulants of the probability density function under consideration.

Observe that if we choose $\alpha = \chi_1 = M$ and $\beta = \chi_2^{1/2} = R$ (see (24)-(25)), which is a very common choice, we have $a_1 = 0$ and $a_2 = 0$; this is a special case of the general property (33) stated earlier. This special choice of α and β corresponds to choosing the mean location and rms width of Hermite weighting (40) identical to those same parameters of the given probability density function. There then also follows, in this special case,

$$a_3 = \frac{1}{3} \hat{\chi}_3 a_0, \quad a_4 = \frac{1}{4} \hat{\chi}_4 a_0, \quad a_5 = \frac{1}{5} \hat{\chi}_5 a_0, \\ a_n = \frac{1}{n} \left[\hat{\chi}_n a_0 + \sum_{m=3}^{n-3} \hat{\chi}_m a_{n-m} \right] \text{ for } n \geq 6 \text{ when } \alpha = \chi_1, \beta = \chi_2^{1/2}. \quad (64B)$$

COEFFICIENTS DIRECTLY VIA MOMENTS

Before we begin this derivation, we present the following useful expansion [5, 22.9.17 and 22.5.19]:

$$\exp\left(-\frac{1}{2}y^2 + xy\right) = \sum_{n=0}^{\infty} \frac{1}{n!} \text{He}_n(x) y^n. \quad (65)$$

We now again refer to (51) and expand the terms as follows:

$$\begin{aligned} \sum_{n=0}^{\infty} a_n w^n &= \exp\left(-\frac{1}{2}w^2 - \frac{\alpha}{\beta}w\right) f\left(\frac{w}{\beta}\right) = \\ &= \sum_{k=0}^{\infty} \frac{1}{k!} \text{He}_k\left(-\frac{\alpha}{\beta}\right) w^k \sum_{m=0}^{\infty} \frac{1}{m!} \mu_m \left(\frac{w}{\beta}\right)^m, \end{aligned} \quad (66)$$

where we utilized (65) and (6). Equating coefficients of w^n on both sides of this equation, we have

$$a_n = \sum_{k=0}^n \frac{1}{k!} \text{He}_k\left(-\frac{\alpha}{\beta}\right) \frac{\mu_{n-k}}{(n-k)! \beta^{n-k}} \quad \text{for } n \geq 0. \quad (67)$$

We now define, for convenience, the normalized Hermite polynomials

$$\hat{\text{He}}_n(x) = \frac{1}{n!} \text{He}_n(x) \quad \text{for } n \geq 0, \quad (68)$$

and the normalized moments

$$\hat{\mu}_n = \frac{\mu_n}{n! \beta^n} \quad \text{for } n \geq 0. \quad (69)$$

(Notice the difference with the definition of the normalized cumulants (62).)

Then (67) becomes

$$a_n = \sum_{k=0}^n \hat{H}e_k \left(-\frac{\alpha}{\beta} \right) \hat{\mu}_{n-k} \quad \text{for } n \geq 0, \quad (70)$$

which gives expansion coefficients $\{a_n\}$ directly in terms of the (normalized) moments of the given probability density function. The recurrence in (50) can be used to generate the Hermite factors needed in convolution (70). Parameters α and β (>0) of weighting (40) are arbitrary.

$$\hat{H}e_0(x) = 1, \quad \hat{H}e_1(x) = x, \quad \hat{H}e_n(x) = \frac{1}{n} [x \hat{H}e_{n-1}(x) - \hat{H}e_{n-2}(x)] \quad \text{for } n \geq 2.$$

As particular cases, we have

$$a_0 = \mu_0, \quad a_1 = \frac{\mu_1 - \alpha\mu_0}{\beta}, \quad a_2 = \frac{\mu_2 - 2\alpha\mu_1 + (\alpha^2 - \beta^2)\mu_0}{2\beta^2}. \quad (71)$$

These agree with (64) which utilized cumulants. If we make the special choice of $\alpha = \mu_1/\mu_0$ and $\beta^2 = \mu_2/\mu_0 - (\mu_1/\mu_0)^2$, then $a_1 = 0$ and $a_2 = 0$.

An alternative more direct derivation of (67) is possible: from (47), (45), (B-3) in appendix B, and (3),

$$\begin{aligned} a_n &= \frac{1}{n!} c_n = \frac{1}{n!} \int du p(u) \hat{H}e_n \left(\frac{u-\alpha}{\beta} \right) = \\ &= \frac{1}{n!} \int du p(u) \sum_{k=0}^n \binom{n}{k} \hat{H}e_k \left(-\frac{\alpha}{\beta} \right) \left(\frac{u}{\beta} \right)^{n-k} = \\ &= \sum_{k=0}^n \frac{1}{k!} \hat{H}e_k \left(-\frac{\alpha}{\beta} \right) \frac{\mu_{n-k}}{(n-k)! \beta^{n-k}} \quad \text{for } n \geq 0. \end{aligned} \quad (72)$$

COEFFICIENTS RECURSIVELY VIA MOMENTS

Before we begin this derivation, we replace $x \rightarrow -ix$, $y \rightarrow iy$ in (65) to get

$$\exp\left(\frac{1}{2} y^2 + xy\right) = \sum_{n=0}^{\infty} \frac{1}{n!} \text{He}_n(-ix) (iy)^n = \sum_{n=0}^{\infty} \frac{1}{n!} \text{Hi}_n(x) y^n, \quad (73)$$

where $\text{Hi}_n(x)$ is a real n -th order modified Hermite polynomial in x defined by

$$\text{Hi}_n(x) = i^n \text{He}_n(-ix) \quad \text{for } n \geq 0. \quad (74)$$

The recursion for these polynomials follows immediately from (50) as

$$\text{Hi}_n(x) = x \text{Hi}_{n-1}(x) + (n-1) \text{Hi}_{n-2}(x) \quad \text{for } n \geq 2, \quad (75)$$

with starting values $\text{Hi}_0(x) = 1$, $\text{Hi}_1(x) = x$. The difference with (50) is the polarity of the last term; thus for example, $\text{Hi}_2(x) = x^2 + 1$, $\text{Hi}_3(x) = x^3 + 3x$, versus $\text{He}_2(x) = x^2 - 1$, $\text{He}_3(x) = x^3 - 3x$.

We now rewrite (51) in the following form:

$$f\left(\frac{w}{\beta}\right) = \exp\left(\frac{1}{2} w^2 + \frac{\alpha}{\beta} w\right) \sum_{m=0}^{\infty} a_m w^m. \quad (76)$$

Expanding in power series by means of (6) and (73),

$$\sum_{n=0}^{\infty} \frac{1}{n!} \mu_n \left(\frac{w}{\beta}\right)^n = \sum_{k=0}^{\infty} \frac{1}{k!} \text{Hi}_k\left(\frac{\alpha}{\beta}\right) w^k \sum_{m=0}^{\infty} a_m w^m. \quad (77)$$

Equating coefficients of w^n , there follows

$$\frac{\mu_n}{n! \beta^n} = \sum_{k=0}^n \frac{1}{k!} \text{Hi}_k\left(\frac{\alpha}{\beta}\right) a_{n-k} \quad \text{for } n \geq 0, \quad (78)$$

or

$$\hat{\mu}_n = \sum_{k=0}^n \hat{H}i_k\left(\frac{\alpha}{\beta}\right) a_{n-k} = a_n + \sum_{k=1}^n \hat{H}i_k\left(\frac{\alpha}{\beta}\right) a_{n-k} \quad \text{for } n \geq 0, \quad (79)$$

where we have used normalized moments (69), and defined the normalized modified Hermite polynomials

$$\hat{H}i_n(x) = \frac{1}{n!} H_i_n(x) \quad \text{for } n \geq 0. \quad (80)$$

Finally, the desired recursion for expansion coefficients $\{a_n\}$ in terms of the moments follows as

$$a_n = \hat{\mu}_n - \sum_{k=1}^n \hat{H}i_k\left(\frac{\alpha}{\beta}\right) a_{n-k} \quad \text{for } n \geq 0. \quad (81)$$

Parameters α and β (>0) are arbitrary in (81) and (69).

SUMMARY

The approximations to the probability density function and cumulative distribution function are given by (46) and (48), respectively, where α and β are arbitrary constants, except that $\beta > 0$. The functions ϕ and Φ are defined in (41), while the Hermite polynomials $\{H_e_n\}$ are available via (50). The expansion coefficients $\{a_n\}$ are given by the three alternatives (63), (70), (81), in terms of normalized cumulants (62), normalized moments (69), normalized Hermite polynomials (68), and normalized modified Hermite polynomials (80) and (74). Programs for all three alternative procedures for determining expansion coefficients $\{a_n\}$ are listed in an appendix. The basis for these relations is the characteristics function expansion in (51)-(53).

GENERALIZED LAGUERRE EXPANSION

This section will treat weighting (2), namely,

$$w(u) = \frac{u^\alpha \exp(-u/\beta)}{\beta^{\alpha+1} \Gamma(\alpha+1)} \quad \text{for } u > 0 \quad (\alpha > -1, \beta > 0). \quad (82)$$

This weighting is a special case of the three-parameter weighting

$$\frac{(u-\gamma)^\alpha \exp\left(-\frac{u-\gamma}{\beta}\right)}{\beta^{\alpha+1} \Gamma(\alpha+1)} \quad \text{for } u > \gamma, \quad (83)$$

which is the most general scaled linear shift of the generalized Laguerre weighting [5, 22.2.12]

$$x^\alpha \exp(-x) \quad \text{for } x > 0. \quad (84)$$

We will consider only $\gamma = 0$ here. For a probability density function $p_0(u)$ which is known to be nonzero only for $u > u_0$, we would consider the modified probability density function $p(u) = p_0(u+u_0)$, because then $p(u) \neq 0$ only for $u > 0$, and the simpler weighting (82) would be directly applicable. This procedure is equivalent to choosing $\gamma = u_0$ in the three-parameter weighting (83) above, and requires knowledge of u_0 . We presume that $p(u) \neq 0$ only for $u > 0$ henceforth in this section, and that any necessary shifting has already taken place.

Weighting (82) has two free parameters, α and β , and moments

$$v_n = (\alpha+1)_n \beta^n \quad \text{for } n \geq 0. \quad (85)$$

In particular,

$$v_0 = 1, \quad v_1 = (\alpha+1)\beta, \quad v_2 = (\alpha+2)(\alpha+1)\beta^2. \quad (86)$$

If v_1 and v_2 are specified, then the parameters must satisfy

$$\alpha = \frac{v_1^2}{v_2 - v_1^2} - 1, \quad \beta = \frac{v_2 - v_1^2}{v_1}. \quad (87)$$

However, we shall keep α and β general and unspecified except for the conditions in (82).

PROPERTIES OF POLYNOMIALS AND EXPANSIONS

The orthonormal polynomials associated with weighting (82) are the generalized Laguerre polynomials [5, 22.1.2 and 22.2.12]

$$Q_n(u) = L_n^{(\alpha)}\left(\frac{u}{\beta}\right) \left(\frac{n!}{(\alpha+1)_n}\right)^{1/2} \quad \text{for } n \geq 0, \quad u > 0. \quad (88)$$

The expansion coefficients are given by (20) as

$$b_n = \int_0^\infty du p(u) Q_n(u) = \left(\frac{n!}{(\alpha+1)_n}\right)^{1/2} c_n \quad \text{for } n \geq 0, \quad (89)$$

where we define

$$c_n = \int_0^\infty du p(u) L_n^{(\alpha)}\left(\frac{u}{\beta}\right) \quad \text{for } n \geq 0. \quad (90)$$

The approximate probability density function follows from (13) according to

$$\begin{aligned}
 p_N(u) &= w(u) \sum_{n=0}^N b_n Q_n(u) = \\
 &= \frac{u^\alpha \exp(-u/\beta)}{\beta^{\alpha+1} \Gamma(\alpha+1)} \sum_{n=0}^N a_n L_n^{(\alpha)}\left(\frac{u}{\beta}\right) \quad \text{for } u > 0, \quad (91)
 \end{aligned}$$

where we used (82), (88), (89), and defined

$$\left(\frac{(\alpha+1)_n}{n!}\right)^{1/2} a_n = b_n = \left(\frac{n!}{(\alpha+1)_n}\right)^{1/2} c_n \quad \text{for } n \geq 0. \quad (92)$$

These three different coefficients in (89)-(92) are introduced for convenience in further equation manipulations. Expansion coefficient b_n is the geometric mean of auxiliary coefficients a_n and c_n (with polarity).

The approximate cumulative distribution function corresponding to (91) is

$$\begin{aligned}
 P_N(u) &= \int_0^u dt p_N(t) = \sum_{n=0}^N a_n \int_0^u dt \frac{t^\alpha \exp(-t/\beta)}{\beta^{\alpha+1} \Gamma(\alpha+1)} L_n^{(\alpha)}\left(\frac{t}{\beta}\right) = \\
 &= \frac{1}{\Gamma(\alpha+1)} \sum_{n=0}^N a_n I_n\left(\frac{u}{\beta}\right) \quad \text{for } u > 0, \quad (93)
 \end{aligned}$$

where we define

$$I_n(y) = \int_0^y dx x^\alpha e^{-x} L_n^{(\alpha)}(x) \quad \text{for } n \geq 0, y > 0. \quad (94)$$

These quantities are evaluated in appendix C; when substituted in (93), they yield

$$P_N(u) = \frac{(u/\beta)^{\alpha+1} \exp(-u/\beta)}{\Gamma(\alpha+1)} \left[\frac{a_0}{\alpha+1} {}_1F_1\left(1; \alpha+2; \frac{u}{\beta}\right) + \sum_{n=1}^N \frac{a_n}{n} L_{n-1}^{(\alpha+1)}\left(\frac{u}{\beta}\right) \right] \quad \text{for } u > 0,$$

where ${}_1F_1$ is the confluent hypergeometric function.

The generalized Laguerre polynomials $\{L_n^{(\alpha)}\}$ satisfy the recurrence [5, 22.7.12]

$$L_n^{(\alpha)}(x) = \frac{1}{n} \left[(\alpha - 1 + 2n - x) L_{n-1}^{(\alpha)}(x) - (\alpha - 1 + n) L_{n-2}^{(\alpha)}(x) \right] \quad \text{for } n \geq 2, \quad (96)$$

with starting values $L_0^{(\alpha)}(x) = 1$, $L_1^{(\alpha)}(x) = \alpha + 1 - x$ [5, 22.4.7]. The highest order term in $L_n^{(\alpha)}(x)$ is $(-x)^n/n!$ [5, 22.1.2 and 22.3.9]; this is distinctly different from the coefficient 1 for the Hermite polynomials. Yet the envelope decay with n of the generalized Laguerre series for the probability density function and cumulative distribution function are identical to those of the Hermite series, for $u > 0$. To prove this, use (91) and (92) to get

$$a_n L_n^{(\alpha)}\left(\frac{u}{\beta}\right) = b_n \left(\frac{n!}{(\alpha+1)_n}\right)^{1/2} L_n^{(\alpha)}\left(\frac{u}{\beta}\right) \propto b_n (n^{-\alpha})^{1/2} n^{\frac{\alpha}{2} - \frac{1}{4}} = b_n n^{-\frac{1}{4}}$$

as $n \rightarrow +\infty$, for $u > 0$, (97)

where we also used [5, 6.1.39] and [7, 8.22.1]. Again, \propto denotes proportionality with n only; the exact scale factor will be presented in a later section where the errors of the approximations are estimated. So if b_n decays faster than $n^{-3/4}$, the probability density function series in (91) converges absolutely.

For the generalized Laguerre series of the cumulative distribution function in (95), we have, for the envelope of the general term,

$$\frac{1}{n} a_n L_{n-1}^{(\alpha+1)}\left(\frac{u}{\beta}\right) = b_n \frac{1}{n} \left(\frac{n!}{(\alpha+1)_n}\right)^{1/2} L_{n-1}^{(\alpha+1)}\left(\frac{u}{\beta}\right) =$$

$$\propto b_n \frac{1}{n} (n^{-\alpha})^{1/2} (n-1)^{\frac{\alpha+1}{2} - \frac{1}{4}} \sim b_n n^{-3/4} \text{ as } n \rightarrow +\infty, \text{ for } u > 0. \quad (98)$$

Thus if b_n decays faster than $n^{-1/4}$, (95) converges absolutely. And if the error integral (21) is finite, this property of the $\{b_n\}$ is true. So if error integral (21) is finite, the generalized Laguerre series for the cumulative distribution function converges absolutely for $u > 0$; this is a sufficient, but not necessary, condition.

For zero argument, the generalized Laguerre polynomials behave differently for large n . From [5, 22.4.7 and 6.1.39],

$$L_n^{(\alpha)}(0) = \binom{n+\alpha}{n} = \frac{(\alpha+1)_n}{n!} \sim \frac{n^\alpha}{\Gamma(\alpha+1)} \text{ as } n \rightarrow +\infty. \quad (99)$$

Then (97) and (98) are both replaced by $b_n n^{\alpha/2}$ as $n \rightarrow +\infty$. However, for $\alpha > 0$, the probability density function in (91) is zero at $u = 0$ due to the u^α term, so there is no need to perform the sum then. And the cumulative distribution function is always zero at $u = 0$, again eliminating the need to evaluate the sum in (95). So the difference in behavior at $u = 0$ is of no consequence.

EXPANSION OF CHARACTERISTIC FUNCTION f

The coefficients a_n and c_n for the generalized Laguerre series were defined in (90) and (92). Then the sum

$$\begin{aligned} \sum_{n=0}^{\infty} c_n w^n &= \sum_{n=0}^{\infty} w^n \int_0^{\infty} du p(u) L_n^{(\alpha)}(u/\beta) = \\ &= \int_0^{\infty} du p(u) \sum_{n=0}^{\infty} w^n L_n^{(\alpha)}(u/\beta) = \int_0^{\infty} du p(u) (1-w)^{-\alpha-1} \exp\left(-\frac{uw/\beta}{1-w}\right) = \\ &= (1-w)^{-\alpha-1} f\left(\frac{-w/\beta}{1-w}\right), \end{aligned} \quad (100)$$

where f is the characteristic function, and where we used (90), [5, 22.9.15], and (5). Thus $\{c_n\}$ are the expansion coefficients of the right-hand side of (100) in powers of w . If we let $w = \frac{-\beta z}{1-\beta z}$, we have the expansion for the characteristic function

$$f(z) = (1-\beta z)^{-\alpha-1} \sum_{n=0}^{\infty} c_n \left(\frac{-\beta z}{1-\beta z}\right)^n, \quad (101)$$

corresponding to given probability density function p . Weighting parameters α and β are arbitrary in (100) and (101).

Collecting (91) and (101) together for comparison, and assuming that $p_N \rightarrow p$ as $N \rightarrow +\infty$, we have, upon use of (92),

$$\begin{aligned} p(u) &= \frac{u^\alpha \exp(-u/\beta)}{\beta^{\alpha+1} \Gamma(\alpha+1)} \sum_{n=0}^{\infty} a_n L_n^{(\alpha)}\left(\frac{u}{\beta}\right) \quad \text{for } u > 0, \\ f(i\xi) &= (1-i\beta\xi)^{-\alpha-1} \sum_{n=0}^{\infty} a_n \frac{(\alpha+1)_n}{n!} \left(\frac{-i\beta\xi}{1-i\beta\xi}\right)^n. \end{aligned} \quad (102)$$

Thus, expansion of probability density function p in an infinite generalized Laguerre series is equivalent to an expansion of the corresponding characteristic function in the series of the particular form in (102).

Equations (100)-(102) will serve as very convenient starting points for the derivation of several alternative recurrences for expansion coefficients $\{a_n\}$. We reiterate that α and β are arbitrary in the above, except that $\alpha > -1$, $\beta > 0$.

An analogous result holds for N finite, but must be derived differently since we can no longer use infinite sum [5, 22.9.15]. Define the Fourier transform of (91) as the N -th order approximation to the characteristic function:

$$\begin{aligned} f_N(i\xi) &= \int du \exp(i\xi u) p_N(u) = \\ &= \int_0^\infty du \exp(i\xi u) \frac{u^\alpha \exp(-u/\beta)}{\beta^{\alpha+1} \Gamma(\alpha+1)} \sum_{n=0}^N a_n L_n^{(\alpha)}\left(\frac{u}{\beta}\right) = \\ &= \frac{1}{\Gamma(\alpha+1)} \sum_{n=0}^N a_n \int_0^\infty dt \exp(i\beta\xi t) t^\alpha e^{-t} L_n^{(\alpha)}(t). \end{aligned} \quad (103)$$

In appendix D, it is shown that

$$\int_0^\infty dt e^{i\omega t} t^\alpha e^{-t} L_n^{(\alpha)}(t) = \frac{\Gamma(\alpha+1+n)}{n!} \frac{(-i\omega)^n}{(1-i\omega)^{\alpha+1+n}}. \quad (104)$$

Substitution in (103) then yields

$$f_N(i\xi) = \sum_{n=0}^N a_n \frac{(\alpha+1)_n}{n!} \frac{(-i\beta\xi)^n}{(1-i\beta\xi)^{\alpha+1+n}} = \sum_{n=0}^N c_n \frac{(-i\beta\xi)^n}{(1-i\beta\xi)^{\alpha+1+n}}, \quad (105)$$

where the last relation follows by use of (92). This result is the leading N terms of (102).

COEFFICIENTS RECURSIVELY VIA CUMULANTS

We can now obtain some useful recursive relations for expansion coefficients $\{a_n\}$ and/or $\{c_n\}$ in (100)-(105). We start by taking the \ln of (100):

$$\ln \left\{ \sum_{n=0}^{\infty} c_n w^n \right\} = -(\alpha+1) \ln(1-w) + \ln f\left(\frac{-w/\beta}{1-w}\right). \quad (106)$$

Identify the left-hand side as a new power series, and use (7) and [5, 15.1.8] to yield

$$\begin{aligned} \sum_{n=0}^{\infty} h_n w^n &= (\alpha+1) \sum_{n=1}^{\infty} \frac{1}{n} w^n + \sum_{k=0}^{\infty} \frac{1}{k!} \chi_k \left(\frac{-w/\beta}{1-w}\right)^k = \\ &= (\alpha+1) \sum_{n=1}^{\infty} \frac{1}{n} w^n + \sum_{k=0}^{\infty} \frac{(-1)^k \chi_k}{k! \beta^k} w^k \sum_{m=0}^{\infty} \frac{(k)_m}{m!} w^m. \end{aligned} \quad (107)$$

Equating coefficients of w^n , there follows $h_0 = \chi_0$, while for $n \geq 1$,

$$\begin{aligned} h_n &= \frac{1}{n}(\alpha+1) + \sum_{k=0}^n \frac{(-1)^k \chi_k}{k! \beta^k} \frac{(k)_{n-k}}{(n-k)!} = \\ &= \frac{1}{n} \left[\alpha+1 + \sum_{k=1}^n (-1)^k \binom{n}{k} \hat{\chi}_k \right], \end{aligned} \quad (108)$$

where we used the normalized cumulants defined in (62).

But since the left-hand sides of (106) and (107) are equal, we have

$$\sum_{n=0}^{\infty} c_n w^n = \exp \left\{ \sum_{n=0}^{\infty} h_n w^n \right\}, \quad (109)$$

or via appendix A, the recurrence

$$c_n = \frac{1}{n} \sum_{m=1}^n m h_m c_{n-m} \quad \text{for } n \geq 1, \quad c_0 = \exp(h_0). \quad (110)$$

Finally, define

$$d_m = m h_m \quad \text{for } m \geq 1 \quad (111)$$

for notational convenience and thereby obtain

$$d_m = \alpha + 1 + \sum_{k=1}^m (-1)^k \binom{m}{k} \hat{\chi}_k \quad \text{for } m \geq 1,$$

$$c_n = \frac{1}{n} \sum_{m=1}^n d_m c_{n-m} \quad \text{for } n \geq 1, \quad c_0 = \exp(\chi_0), \quad (112)$$

by means of (108) and (110), respectively. Equation (112) is a recursive relation for expansion coefficients $\{c_n\}$ in terms of cumulants $\{\chi_n\}$ and auxiliary variables $\{d_m\}$. The $\{\alpha_n\}$ are immediately available via (92).

As particular cases, we have, employing (62),

$$c_1 = \left(\alpha + 1 - \frac{\chi_1}{\beta} \right) c_0,$$

$$c_2 = \frac{1}{2} \left[(\alpha + 2)(\alpha + 1) - 2(\alpha + 2) \frac{\chi_1}{\beta} + \frac{\chi_2 + \chi_1^2}{\beta^2} \right] c_0. \quad (113)$$

Parameters α and β are completely arbitrary in all the above equations, except that $\alpha > -1$ and $\beta > 0$, and $\{\chi_n\}_0^N$ are the available cumulants.

Observe that if we

$$\text{let } \alpha + 1 = \frac{\chi_1^2}{\chi_2} = \frac{\mu_1^2}{\mu_2 \mu_0 - \mu_1^2} = \frac{M^2}{R^2}$$

$$\text{and } \beta = \frac{\chi_2}{\chi_1} = \frac{\mu_2 \mu_0 - \mu_1^2}{\mu_1 \mu_0} = \frac{R^2}{M}, \quad (114)$$

then $c_1 = 0$ and $c_2 = 0$ (here we also used (8) and (25)); this is a special case of general property (33) stated earlier. Since the probability density function $p(u)$ is nonzero only for $u > 0$, then $\chi_1 > 0$ and $\chi_2 > 0$, giving allowable solutions to (114) in all cases. There then also follows, along with $d_1 = d_2 = 0$ in this special case, the explicit results

$$c_0 = \exp(\chi_0), \quad c_1 = 0, \quad c_2 = 0,$$

$$c_3 = \frac{\chi_1^2}{3! \chi_2^3} (2\chi_2^2 - \chi_3 \chi_1) c_0,$$

$$c_4 = \frac{\chi_1^2}{4! \chi_2^4} (18\chi_2^3 - 12\chi_3 \chi_2 \chi_1 + \chi_4 \chi_1^2) c_0,$$

$$c_5 = \frac{\chi_1^2}{5! \chi_2^5} (144\chi_2^4 - 120\chi_3 \chi_2^2 \chi_1 + 20\chi_4 \chi_2 \chi_1^2 - \chi_5 \chi_1^3) c_0,$$

$$c_6 = \frac{\chi_1^2}{6! \chi_2^6} \left(40(30\chi_2 + \chi_1^2)(\chi_2^2 - \chi_3 \chi_1)\chi_2^2 + 10\chi_3^2 \chi_1^4 + \right. \\ \left. + 300\chi_4 \chi_2^2 \chi_1^2 - 30\chi_5 \chi_2 \chi_1^3 + \chi_6 \chi_1^4 \right) c_0,$$

$$c_7 = \frac{\chi_1^2}{7! \chi_2^7} \left(10800\chi_2^6 + 1260\chi_2^5 \chi_1^2 - 12600\chi_3 \chi_2^4 \chi_1 - 1470\chi_3 \chi_2^3 \chi_1^3 + \right.$$

$$+ 420\chi_3^2 \chi_2 \chi_1^4 + 4200\chi_4 \chi_2^3 \chi_1^2 + 70\chi_4 \chi_2^2 \chi_1^4 - 35\chi_4 \chi_3 \chi_1^5 - \\ \left. - 630\chi_5 \chi_2^2 \chi_1^3 + 42\chi_6 \chi_2 \chi_1^4 - \chi_7 \chi_1^5 \right) c_0. \quad (115)$$

These relations have been confirmed by numerical comparison with (112).

These results greatly extend those of [1, (129)-(131)], where the equivalent of our c_3 is given (in terms of moments instead of cumulants, and with $\chi_0 = 0$), along with the comment that "the higher-order coefficients are so complicated that the whole value of this type of series seems to depend on the fact that the first term alone (c_0) is often a good approximation." We find, on the other hand, that not only can we avoid the special choice in (114) and the corresponding complicated special results in (115), but we can handle any α, β pair and get very high-order coefficients c_n , simply by using the recurrence in (112), which is easily programmed. The only thing we lose are explicit results of the type given in (115); however, the latter are so complicated that they are of limited utility anyway.

COEFFICIENTS DIRECTLY VIA MOMENTS

We will need the following expression [5, 22.3.9]:

$$\frac{n!}{(\alpha+1)_n} L_n^{(\alpha)}(x) = \frac{n!}{(\alpha+1)_n} \sum_{k=0}^n \binom{n+\alpha}{n-k} \frac{(-x)^k}{k!} = \sum_{k=0}^n \binom{n}{k} \frac{(-x)^k}{(\alpha+1)_k}. \quad (116)$$

Then (92), (90), and (3) yield, for $n \geq 0$,

$$\begin{aligned} a_n &= \frac{n!}{(\alpha+1)_n} c_n = \frac{n!}{(\alpha+1)_n} \int_0^\infty du p(u) L_n^{(\alpha)}\left(\frac{u}{\beta}\right) = \\ &= \sum_{k=0}^n \binom{n}{k} \frac{1}{(\alpha+1)_k} \int_0^\infty du p(u) (-u/\beta)^k = \sum_{k=0}^n (-1)^k \binom{n}{k} \frac{\mu_k}{(\alpha+1)_k \beta^k}. \end{aligned} \quad (117)$$

It is useful, in this generalized Laguerre series case, to define an alternative set of normalized moments

$$\tilde{\mu}_n = \frac{\mu_n}{(\alpha+1)_n \beta^n} \quad \text{for } n \geq 0. \quad (118)$$

(Although this seems to be very different from the earlier normalization in (69), (118) actually reduces to (69) for the α here equal to zero.) When (118) is utilized in (117), we have the desired expression for expansion coefficients $\{a_n\}$, directly in terms of (normalized) moments, in the surprisingly simple form

$$a_n = \sum_{k=0}^n (-1)^k \binom{n}{k} \tilde{\mu}_k \quad \text{for } n \geq 0. \quad (119)$$

Parameters α and β in (118) are arbitrary, except that $\alpha > -1$, $\beta > 0$.

As particular cases, (117)-(119) yield

$$a_0 = \mu_0, \quad a_1 = \mu_0 - \frac{\mu_1}{(\alpha+1)\beta}, \quad a_2 = \mu_0 - \frac{2\mu_1}{(\alpha+1)\beta} + \frac{\mu_2}{(\alpha+1)(\alpha+2)\beta^2}. \quad (120)$$

These agree with (113) which utilized cumulants. If we make the special choices of $\alpha+1 = \mu_1^2/(\mu_2\mu_0 - \mu_1^2)$ and $\beta = (\mu_2\mu_0 - \mu_1^2)/(\mu_1\mu_0)$, then $a_1 = 0$ and $a_2 = 0$; this is a common approach to the approximation problem, but totally unnecessary.

An alternative derivation of the direct moment relation (117) is possible: from (100), (6), and [5, 15.1.8],

$$\begin{aligned} \sum_{n=0}^{\infty} c_n w^n &= (1-w)^{-\alpha-1} \sum_{k=0}^{\infty} \frac{1}{k!} \mu_k \left(\frac{-w/\beta}{1-w}\right)^k = \\ &= \sum_{k=0}^{\infty} \frac{1}{k!} \mu_k \left(-\frac{w}{\beta}\right)^k (1-w)^{-\alpha-1-k} = \sum_{k=0}^{\infty} \frac{1}{k!} \mu_k \left(-\frac{w}{\beta}\right)^k \sum_{m=0}^{\infty} \frac{(\alpha+1+k)_m}{m!} w^m. \end{aligned} \quad (121)$$

Equating coefficients of w^n , we have, for $n \geq 0$,

$$c_n = \sum_{k=0}^n \frac{1}{k!} \mu_k \left(-\frac{1}{\beta}\right)^k \frac{(\alpha+1+k)_{n-k}}{(n-k)!} = \frac{(\alpha+1)_n}{n!} \sum_{k=0}^n (-1)^k \binom{n}{k} \frac{\mu_k}{(\alpha+1)_k \beta^k}, \quad (122)$$

which is equivalent to (117).

COEFFICIENTS RECURSIVELY VIA MOMENTS

The starting point for this case is the characteristic function expansion in (101):

$$f(z) = \sum_{m=0}^{\infty} c_m (-\beta z)^m (1-\beta z)^{-\alpha-1-m} = \sum_{m=0}^{\infty} c_m (-\beta z)^m \sum_{k=0}^{\infty} \frac{(\alpha+1+m)_k}{k!} (\beta z)^k \quad (123)$$

by use of [5, 15.1.8]. Now expand the left-hand side of (123) in powers of z , according to (6), and equate the coefficients of z^n to get, for $n \geq 0$,

$$\frac{1}{n!} \mu_n = \sum_{m=0}^n c_m (-\beta)^m \frac{(\alpha+1+m)_{n-m}}{(n-m)!} \beta^{n-m} = \beta^n \sum_{m=0}^n \frac{c_m (-1)^m (\alpha+1)_n}{(n-m)! (\alpha+1)_m}. \quad (124)$$

Therefore

$$\frac{\mu_n}{(\alpha+1)_n \beta^n} = \sum_{m=0}^n (-1)^m \frac{n!}{(n-m)!} \frac{c_m}{(\alpha+1)_m} = \sum_{m=0}^n (-1)^m \binom{n}{m} a_m \quad \text{for } n \geq 0, \quad (125)$$

by use of (92). Then using normalized moment definition (118), (125) can be expressed as

$$a_n = (-1)^n \left[\tilde{\mu}_n - \sum_{m=0}^{n-1} (-1)^m \binom{n}{m} a_m \right] \quad \text{for } n \geq 0. \quad (126)$$

This is a recursive relation for expansion coefficients $\{a_n\}$ in terms of (normalized) moments. The parameters α and β in (118) are arbitrary, except that $\alpha > -1$, $\beta > 0$.

SUMMARY

The approximations to the probability density function and cumulative distribution function are given by (91) and (95), respectively, where α and β are arbitrary constants, except that $\alpha > -1$, $\beta > 0$. The generalized Laguerre polynomials are available via (96). The expansion coefficients $\{a_n\}$ are given by the three alternatives (112), (119), (126), in terms of normalized cumulants (62) and normalized moments (118); in the case of (112), the interrelationship between expansion coefficients $\{a_n\}$ and $\{c_n\}$ is given in (92). Programs for all three alternative procedures for determining the expansion coefficients $\{a_n\}$ are listed in an appendix. The basis for these relations is the characteristic function expansion in (100)-(102).

EXAMPLES OF HERMITE EXPANSION

EXAMPLE A

The first example is one which can be handled analytically, and thereby furnishes checks on numerical procedures and results. Consider the Gaussian probability density function

$$p(u) = \frac{1}{\omega} \phi\left(\frac{u-\gamma}{\omega}\right) \quad (\omega > 0) \quad (12.7A)$$

with cumulative distribution function and characteristic function

$$P(u) = \Phi\left(\frac{u-\gamma}{\omega}\right), \quad f(i\xi) = \exp\left(i\xi\gamma - \frac{1}{2}\xi^2\omega^2\right). \quad (12.7B)$$

The cumulants are

$$\chi_0 = 0, \quad \chi_1 = \gamma, \quad \chi_2 = \omega^2, \quad \chi_n = 0 \quad \text{for } n \geq 3, \quad (12.8A)$$

while the moments are most easily evaluated by the recurrence

$$\mu_n = \gamma \mu_{n-1} + (n-1) \omega^2 \mu_{n-2} \quad \text{for } n \geq 2, \quad \mu_0 = 1, \quad \mu_1 = \gamma. \quad (12.8B)$$

It is obvious in this Hermite expansion case that the best choice of weighting parameters would be $\alpha = \gamma$, $\beta = \omega$, for then weighting w would match p perfectly and there would follow $b_n = 0$ for $n \geq 1$. We consider a mismatched choice of α and β to illustrate rapid decay of the expansion coefficients and some conditions on convergence.

Expansion coefficient c_n follows from (45) and (12.7A) according to

$$\begin{aligned}
 c_n &= \int du p(u) \text{He}_n\left(\frac{u-\alpha}{\beta}\right) = \beta \int dx p(\alpha+\beta x) \text{He}_n(x) = \\
 &= \beta \int dx \frac{1}{\omega} \phi\left(\frac{\alpha-\gamma+\beta x}{\omega}\right) \text{He}_n(x) = \left(\frac{\sqrt{\beta^2-\omega^2}}{\beta}\right)^n \text{He}_n\left(\frac{\gamma-\alpha}{\sqrt{\beta^2-\omega^2}}\right), \quad (129)
 \end{aligned}$$

the last step via use of [5, 22.5.18] and [8, 7.374 10]. Then from (47),

$$b_n = (n!)^{-1/2} \left(\frac{\sqrt{\beta^2-\omega^2}}{\beta}\right)^n \text{He}_n\left(\frac{\gamma-\alpha}{\sqrt{\beta^2-\omega^2}}\right) \quad \text{for } n \geq 0. \quad (130)$$

This equation is correct for all positive values of β and ω . However, for $\beta < \omega$, a more convenient form can be obtained by use of (74), if desired:

$$b_n = (n!)^{-1/2} \left(\frac{\sqrt{\omega^2-\beta^2}}{\beta}\right)^n \text{Hi}_n\left(\frac{\gamma-\alpha}{\sqrt{\omega^2-\beta^2}}\right), \quad (131)$$

where Hi_n is the modified Hermite polynomial. For $\beta = \omega$, a limit of (130) yields $b_n = (n!)^{-1/2} ((\gamma-\alpha)/\beta)^n$.

If $\beta > \omega$, we can use the result in (50A) on (130) and obtain

$$b_n \propto \left(\frac{\sqrt{\beta^2-\omega^2}}{\beta}\right)^n n^{-1/4} \quad \text{as } n \rightarrow +\infty. \quad (132)$$

Since the quantity in parentheses is always less than 1 in this case of $\beta > \omega$, we have $b_n \rightarrow 0$ as $n \rightarrow +\infty$.

For $\beta < \omega$, we use [7, theorem 8.22.7] and find now that

$$b_n \propto \exp(\sqrt{2n} A) \left(\frac{\sqrt{\omega^2-\beta^2}}{\beta}\right)^n n^{-1/4} \quad \text{as } n \rightarrow +\infty, \quad (133)$$

where A is the absolute value of the argument of He_n in (130). This quantity (133) tends to zero with n , regardless of A , when $\beta > \omega/\sqrt{2}$.

Combining with the result above, we can conclude that

$$b_n > 0 \text{ as } n \rightarrow +\infty \quad \text{for } \frac{\omega}{\sqrt{2}} < \beta < +\infty. \quad (134)$$

Furthermore, b_n behaves as an n -th power, which is faster than $n^{-1/4}$, thereby guaranteeing convergence of the probability density function and cumulative distribution function series, according to the discussion in (50A) et seq. On the other hand, $\{b_n\}$ diverges when $0 < \beta < \omega/\sqrt{2}$, as may be seen from (133).

The error integral in (21) is, for Hermite weighting (40) and probability density function (127),

$$\int du \frac{p^2(u)}{w(u)} = \frac{\beta^2}{\omega \sqrt{2\beta^2 - \omega^2}} \exp\left(\frac{(\gamma - \alpha)^2}{2\beta^2 - \omega^2}\right) \quad \text{if } \frac{\omega}{\sqrt{2}} < \beta, \quad (135)$$

by use of [8, 3.323 2]; this integral is divergent if $\beta < \omega/\sqrt{2}$. Thus, for this particular example, the error integral and expansion coefficient sequence $\{b_n\}$ converge or diverge together, depending on the condition $\beta \gtrless \omega/\sqrt{2}$. The choice of α is irrelevant in this case.

A numerical example of sequence $\{b_n\}$ for

$$\gamma = 1.1, \quad \omega = 2.3 \quad \alpha = 1.14, \quad \beta = 2.34 \quad (136)$$

is plotted in figure 1 on a logarithmic ordinate. Values of b_n less than $1E-7$ in absolute value are all plotted at the $\pm 1E-7$ line. The critical ratio $\sqrt{2-\omega^2}/\beta$ in (130) is .184 for this example, leading to rapid decay of expansion coefficients $\{b_n\}$. The three sets of expansion coefficients in figure 1 are labelled according to the shorthand notation

- RC: Recursively via Cumulants,
 DM: Directly via Moments,
 RM: Recursively via Moments. (137)

It is seen that the expansion coefficients determined recursively via cumulants, namely, the RC plot, decay rapidly and never encounter round-off error, whereas the DM and RM procedures both are subject to large round-off error for $n > 70$, as indicated by the large increasing oscillations. This example can be rather misleading, however, since all the cumulants (128A) of Gaussian probability density function (127A) are zero, except for $\chi_1 = \gamma$, $\chi_2 = \omega^2$; this leads to a very special form of the RC procedure unique to the Gaussian case.

In figure 2, the cumulative distribution function and exceedance distribution function, $1-P(u)$, as determined by Hermite expansion (48) using $N = 50$ terms, are plotted. The exact result, (127B), overlapped these curves over the full range plotted. The three procedures, RC, DM, and RM, all yielded identical distributions in figure 2, as inspection of figure 1 confirms, since the three sets of expansion coefficients are virtually the same for $n < 50$. Even though the three sets of expansion coefficients differ significantly for $n > 60$, the corresponding approximate probability density

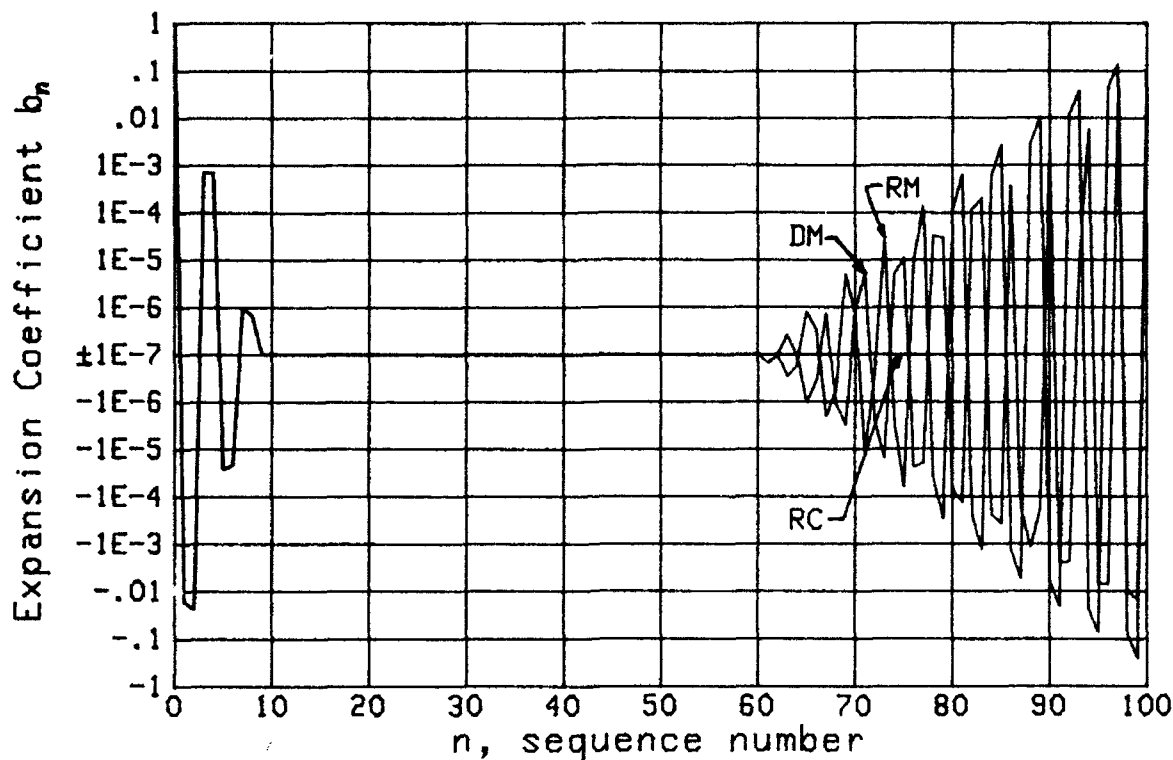


Figure 1. Hermite Coefficients for Example A

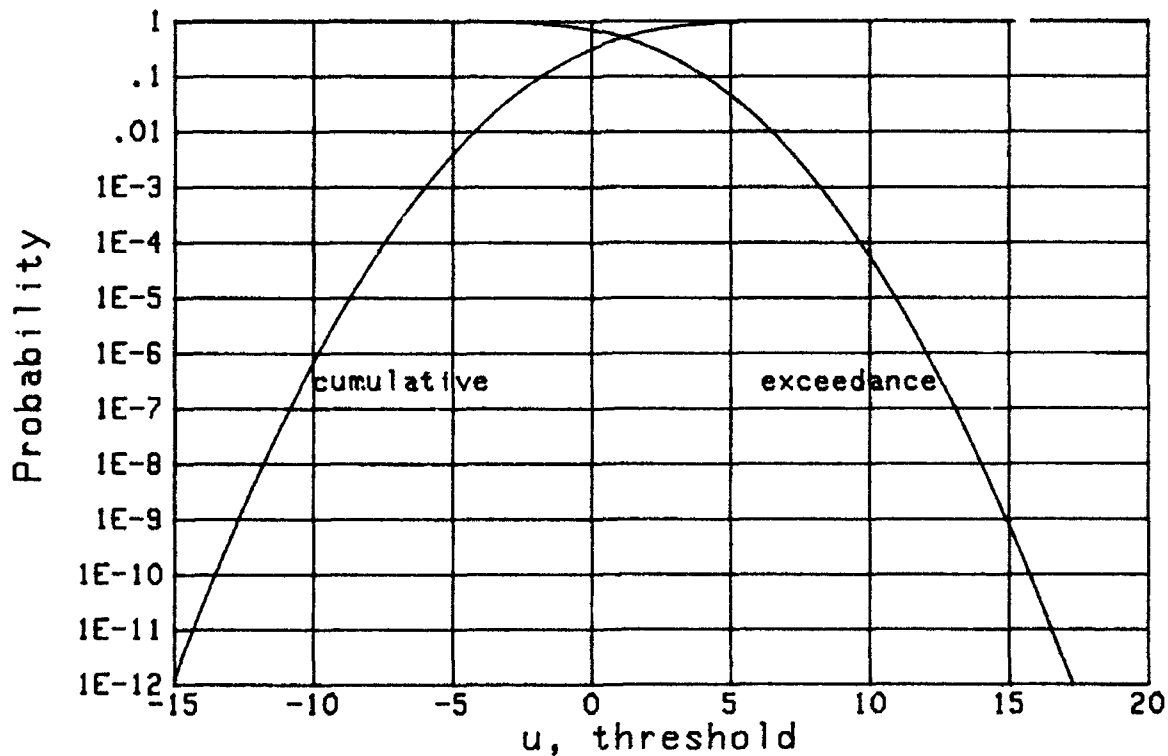


Figure 2. Distributions for Example A

functions and cumulative distribution functions for $N = 70$, say, would not be very different, because the relative differences in p and P are very small, somewhere in the $1E-5$ range; see figure 1 for $n = 70$, and recall that $b_0 = 1$ for this example.

EXAMPLE B

The probability density function of interest here is the one previously considered in (34) et seq.:

$$p(u) = \frac{2 u^\gamma \exp(-u^2/\omega^2)}{\omega^{\gamma+1} \Gamma\left(\frac{\gamma+1}{2}\right)} \quad \text{for } u > 0 \quad (\gamma > -1, \omega > 0). \quad (138)$$

This class of probability density functions includes, for $\gamma = 0, 1, 2$, respectively, the one-sided Gaussian, Rayleigh, and Maxwell as special cases. The characteristic function and cumulants are not easily determined directly for this function. However, the moments, as given already in (35), are readily evaluated via the simple recursion

$$\mu_n = \mu_{n-2} \frac{\omega^2}{2} (\gamma-1+n) \quad \text{for } n \geq 2, \quad \mu_0 = 1, \quad \mu_1 = \omega \frac{\Gamma\left(\frac{\gamma+1}{2}\right)}{\Gamma\left(\frac{\gamma+1}{2}\right)}. \quad (139)$$

An example of the expansion coefficients for

$$\gamma = 3, \omega = 1 \quad \alpha = 0, \beta = .7 \quad (140)$$

is depicted in figure 3. The values of b_n for $n = 0, 1, 2, 3$ are 1, 1.90, 2.18, 1.63, respectively, and lie above the top of the plotted region. The

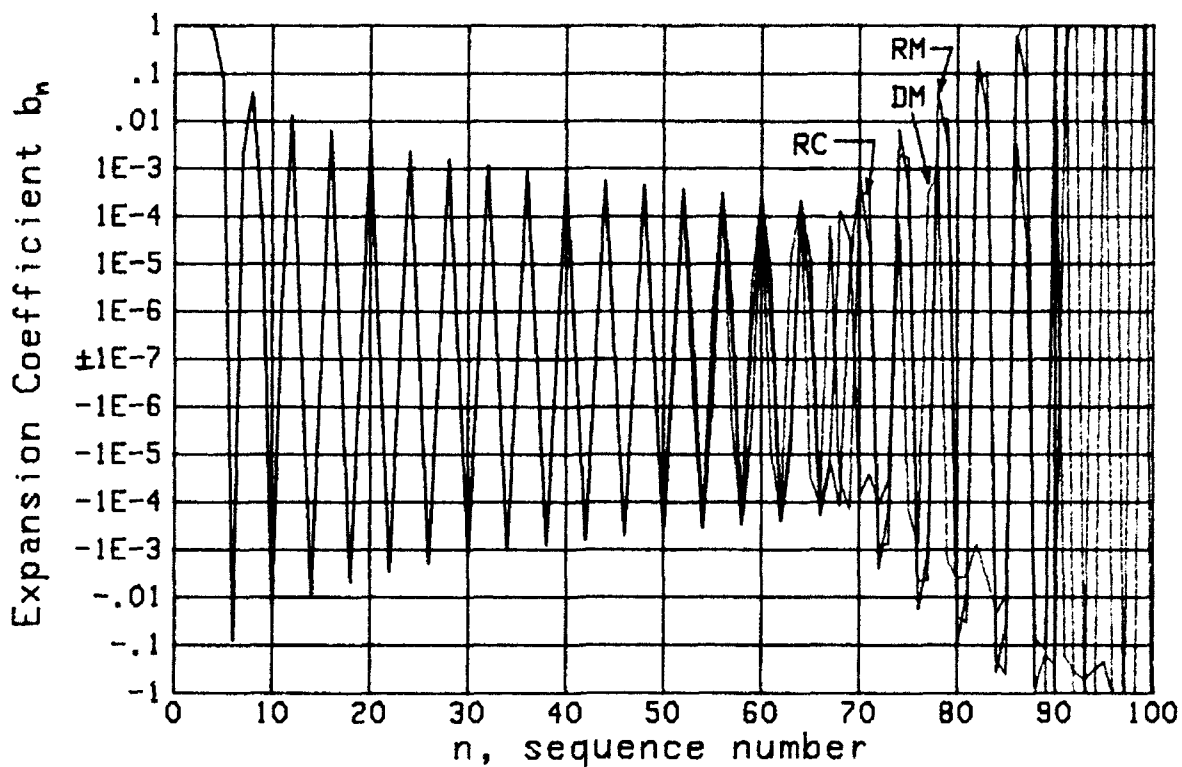


Figure 3. Hermite Coefficients for Example B

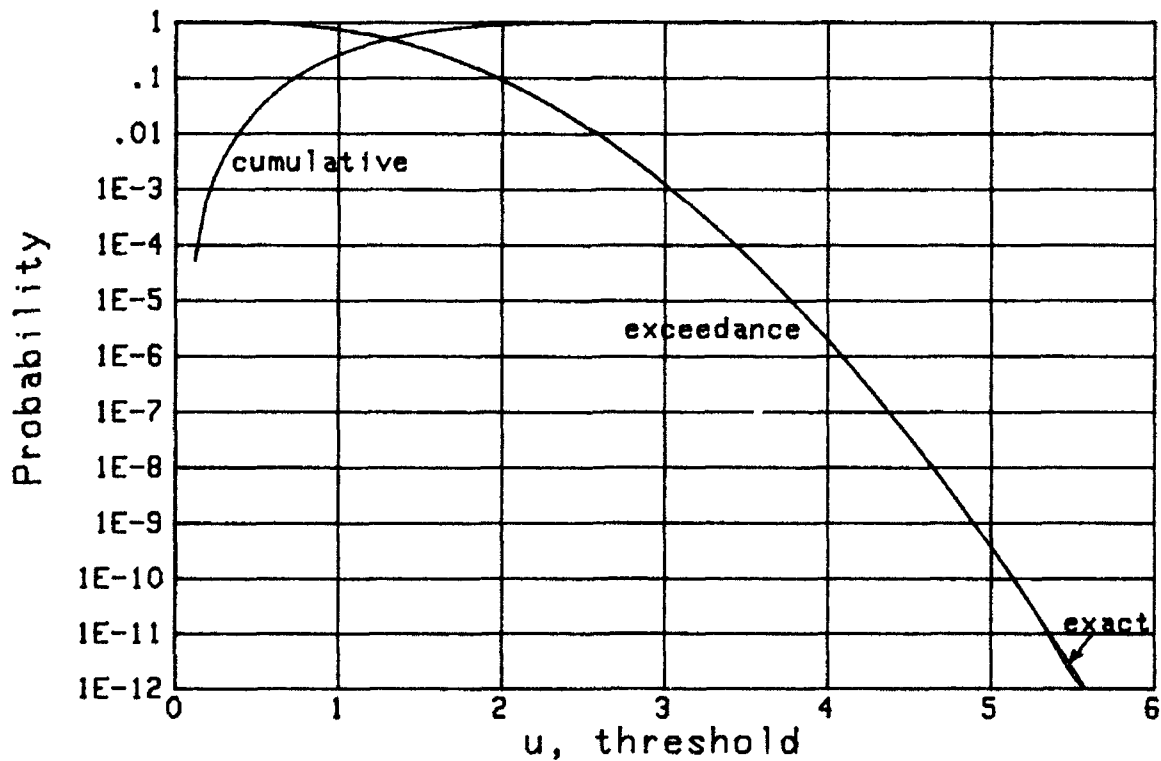


Figure 4. Distributions for Example B

coefficients obtained directly via moments, DM, decay to approximately $1E-4$ near $n = 70$ and then encounter round-off error. The expansion coefficients corresponding to RC and RM are more noisy. The procedure used for RC was to determine the moments via (139), transform directly to cumulants according to (A-7), and then use (63).

A plot of the distributions using $N = 65$ terms is given in figure 4; the results are the same for all three sets of expansion coefficients, as may be seen by reference to figure 3. Furthermore, the exact cumulative distribution function, $P(u) = 1 - (1+u^2) \exp(-u^2)$ for $u > 0$, overlays these results except for the bow in the exceedance distribution function below $1E-11$ near $u = 5.5$. Values of the cumulative distribution function for $u < 0$ as determined by series (48) are not zero, although they should be for this example; the generalized Laguerre series would fit this example better, since it is nonzero only for positive arguments.

EXAMPLE C

Consider the class of Bessel-function probability density functions

$$p(u) = \mathcal{L} u^\gamma \exp(-u^2/\omega^2) I_\gamma(\theta u) \quad \text{for } u > 0, \quad (141)$$

which includes the Rice and generalized Q_M distributions, for example. The n -th moment is [8, 6.631 1]

$$\mu_n = \mathcal{L} \frac{\theta^\gamma \Gamma\left(\frac{n}{2} + h\right) \omega^{n+2h}}{2^{\gamma+1} \Gamma(\gamma+1)} {}_1F_1\left(\frac{n}{2} + h; \gamma+1; \frac{1}{4} \omega^2 \theta^2\right) \quad \text{for } n \geq 0, \quad (142)$$

with $h = (\gamma + \mathcal{J} + 1)/2$; in order for μ_0 to be finite, we must have $h > 0$. The ${}_1F_1$ function in (142) can be evaluated via recursion; this leads to a recursion for the moments (see appendix E).

We consider here only the special case of the Rice probability density function, namely,

$$\mathcal{L} = \frac{2}{\omega} \exp\left(-\frac{1}{4} \omega^2 \theta^2\right), \quad \gamma = 1, \quad \mathcal{J} = 0, \quad (143)$$

for which

$$p(u) = \frac{2u}{\omega^2} \exp\left(-\frac{u^2}{\omega^2} - \frac{\omega^2 \theta^2}{4}\right) I_0(\theta u) \quad \text{for } u > 0. \quad (144)$$

The moments in (142) then reduce to

$$\mu_n = \Gamma\left(\frac{n+1}{2}\right) \omega^n {}_1F_1\left(-\frac{n}{2}; 1; -\frac{1}{4} \omega^2 \theta^2\right), \quad (145)$$

and can be easily determined by the recurrence presented in (E-5). The cumulative distribution function corresponding to (144) is the Q function [1]

$$P(u) = 1 - Q\left(\frac{\omega \theta}{\sqrt{2}}, \frac{\sqrt{2} u}{\omega}\right) \quad \text{for } u > 0; \quad (146)$$

the characteristic function is given in [9, appendix A] as an infinite series, meaning that the cumulants cannot be determined directly, except via the moments.

The particular example we consider here for the Hermite expansion is a sum of 8 independent random variables, each with Rice probability density function (144). For direct comparison with the exact results in [9], we also consider the normalized form of (144), namely $\omega^2 = 2$. Furthermore, we limit

numerical consideration in this particular example to evaluation of the cumulative and exceedance distribution functions for $\theta = 0$, which corresponds physically to the false alarm probability for the sum of eight normalized envelopes of narrowband Gaussian noise (i.e., a Rayleigh probability density function for the individual random variables).

For $\alpha = 4$, $\beta = 2.15$, the expansion coefficients $\{b_n\}$ are displayed in figure 5 for the RC, DM, and RM approaches. All the $\{b_n\}$ for $1 \leq n \leq 20$ are bigger than 1; the biggest is $b_6 = 12.25$. The $\{b_n\}$, for both moment approaches, have not been plotted for $n > 60$ because they continue to oscillate well beyond the ± 1 limits, while the RC coefficients decay exponentially with n . Despite the fact that the moments were the initially determined quantities for this example, the RC method far outperforms the DM and RM methods, as seen in figure 5. The reason for this is as follows: for the RC method, the procedure was to obtain moments via (145), cumulants via (A-7), cumulants of the sum of 8 independent random variables by simple scaling by a factor of 8, and then expansion coefficients via (63). For the DM and RM methods, the moments of the sum of 8 random variables were determined via [6, (14)] which progressively determined the moments of a sum of 2 random variables, then 3, 4, ..., 8 in order, and then employed (70). This iterated procedure for moments requires more number-crunching and leads to considerably larger round-off error than the simple scaling required for the RC procedure. Thus it appears that when the random variable of interest is obtained as a sum of several independent random variables, the RC approach will be the prime candidate for expansion coefficient evaluation; this applies also if the individual random variables have different statistics, but remain independent.

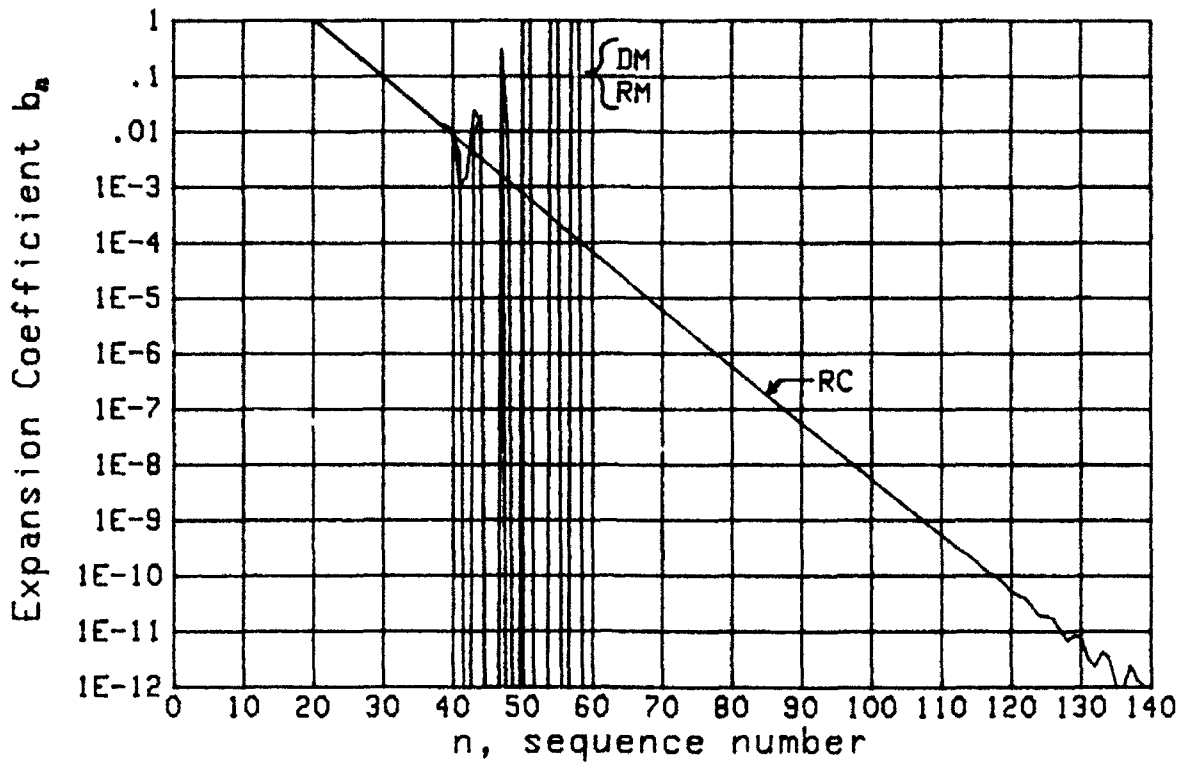


Figure 5. Hermite Coefficients for Example C

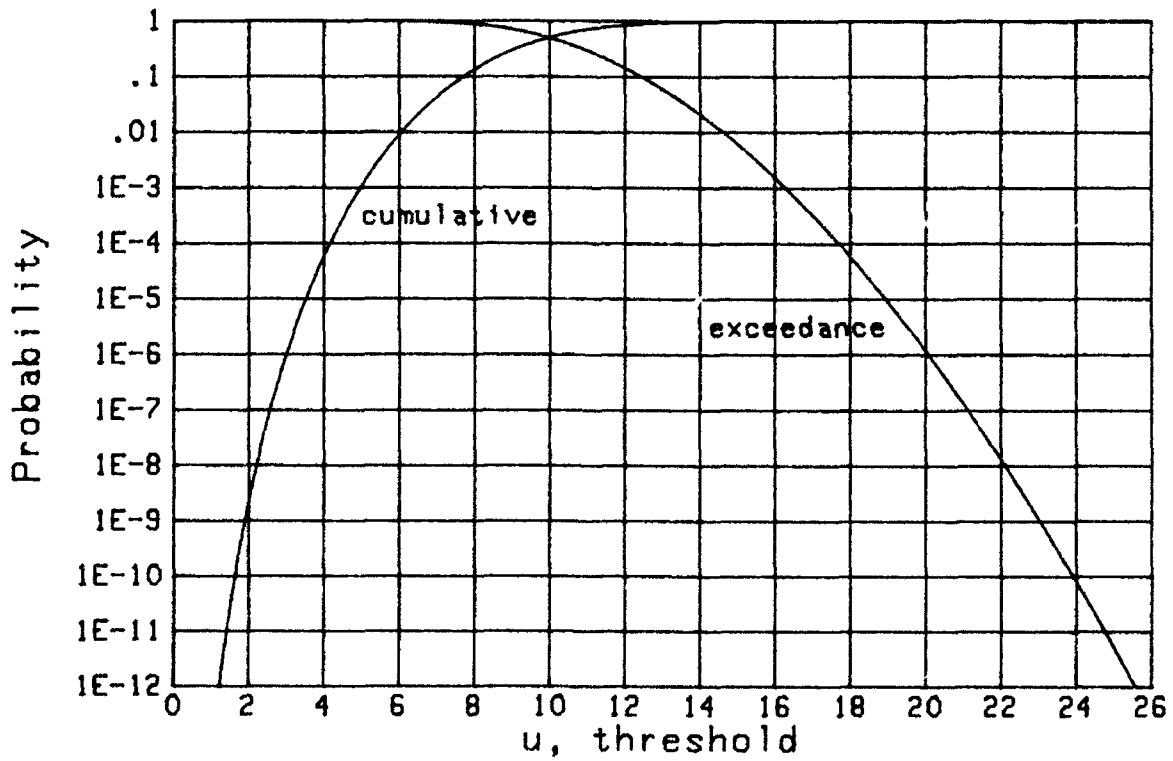


Figure 6. Distributions for Example C

The cumulative and exceedance distribution functions for this sum of 8 normalized Rayleigh variates are plotted in figure 6, for the $N = 140$ expansion coefficients of the RC procedure in figure 5. In order to make a precise determination of the accuracy of this Hermite series approach, the false alarm probabilities were computed at the eight thresholds listed under $M = 8$ in [9, table 1]. To the precision given in that table, the computed probabilities were exactly the specified values $1E-m$ for $m = 1(1)8$. Thus, as anticipated by figure 5, very accurate evaluation of false alarm probabilities are possible by this series approach.

A short search of values of the best weighting parameters α and β , to use with the DM approach, led to $\alpha = 5.84$, $\beta = 2.28$ and expansion coefficients b_n near $1E-4$ at $n = 28$, before round-off error became dominant. This is better than the result of DM in figure 5 for $\alpha = 4$, $\beta = 2.15$. Evaluation of the false alarm probabilities at the thresholds in [9, table 1] gave 7 decimal accuracy at .1, and 4 decimal accuracy at $1E-8$. This is adequate for most purposes, but is not as good as the RC approach.

EXAMPLE D

In [4, appendix C], the characteristic function for shot noise with random amplitude and duration modulation, and arbitrary individual pulse shape, is derived. (This result is then specialized to elliptical pulses and Rayleigh amplitude modulation [4, (C-36)-(C-42)].) Also, the cumulants are extracted, with general result [4, (24)], where ν is the average number of pulses/second, $\bar{\lambda}$ is the average length of the duration modulation, $\mu_a(n)$ is

the n -th moment of the amplitude modulation, and $F(x)$ is the individual pulse shape of the shot noise. Thus shot noise is a case where the cumulants are directly capable of evaluation, whereas the moments must be found indirectly.

For the special case of elliptical pulses and Rayleigh amplitude modulation, there follows for the cumulants [4, (29)]:

$$\chi_n = \sqrt{\bar{l}} \sigma_a^n 2^{\frac{3}{2}n+1} \Gamma^3\left(\frac{n+1}{2}\right) / \Gamma(n+2) \quad \text{for } n \geq 1, \quad \chi_0 = 0. \quad (147)$$

These quantities are easily evaluated via recurrence

$$\chi_n = \chi_{n-2} \sigma_a^2 n^2 / (n+1) \quad \text{for } n \geq 3, \quad \chi_1 = \left(\frac{\pi}{2}\right)^{3/2} \sqrt{\bar{l}} \sigma_a, \quad \chi_2 = \frac{8}{3} \sqrt{\bar{l}} \sigma_a^2. \quad (148)$$

This procedure was used in [4, appendix D] to obtain the probability density function and cumulative distribution function results given there.

There is a nuance that arises in shot noise for pulse shapes of finite duration; see [4, pp. 40-42]. Namely, there is an impulse in the probability density function, at $u = 0$, of area

$$P_0 = \exp[-\sqrt{\bar{l}}(x_2 - x_1)], \quad (149)$$

where (x_1, x_2) is the non-zero extent of an unmodulated individual pulse. Since an impulse is very difficult to approximate by a finite series of continuous functions, the effect of this quantity should be subtracted from the statistics (moments or cumulants), and the continuous portion of the probability density function should be approximated. Similarly, the

corresponding step in the cumulative distribution function at the origin should be eliminated from the approximation procedure.

This feature is easily incorporated if P_0 is subtracted from the zero-th order moment [4, p. 42]. The only undesirable side-effect of this manipulation is that the initially computed cumulants must be transformed to moments, then μ_0 corrected, and then all the new cumulants evaluated. This double transformation is necessary because the correction (subtraction) procedure can only be accomplished in the moment domain. Of course, when the DM or RM procedures are employed instead of RC, the last transformation to cumulants is unnecessary; this was, in fact, the procedure used in [4, p. 60].

When the individual pulse $F(x)$ has infinite duration, as for an exponential or Gaussian waveform, then $x_2 - x_1$ is infinite and P_0 in (149) is zero. In that case, the considerations in the last two paragraphs can be disregarded, and the cumulants generated via (148) used as is. It is then very likely that even better accuracy in the expansion coefficients will be achieved than for this current example.

For overlap factor [4, p. 43]

$$\bar{K}_1 = \sqrt{L}(x_2 - x_1) = 6.2, \quad P_0 = \exp(-6.2) = .00203, \quad \sigma_a = 1, \quad (150)$$

and for weighting parameters $\alpha = 6.1$, $\beta = 4.3$, the expansion coefficients $\{b_n\}$ are displayed in figure 7 for the three recursive procedures. The RM results are considerably poorer than the RC and DM coefficients, which are

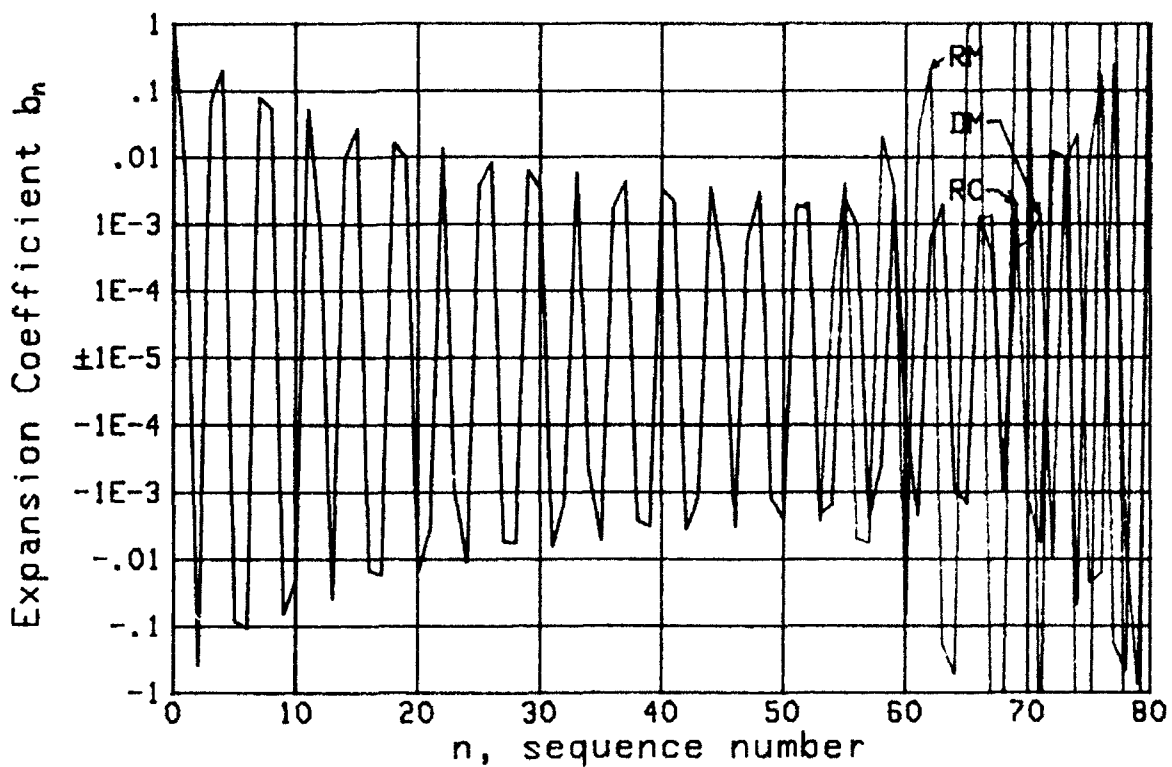


Figure 7. Hermite Coefficients for Example D

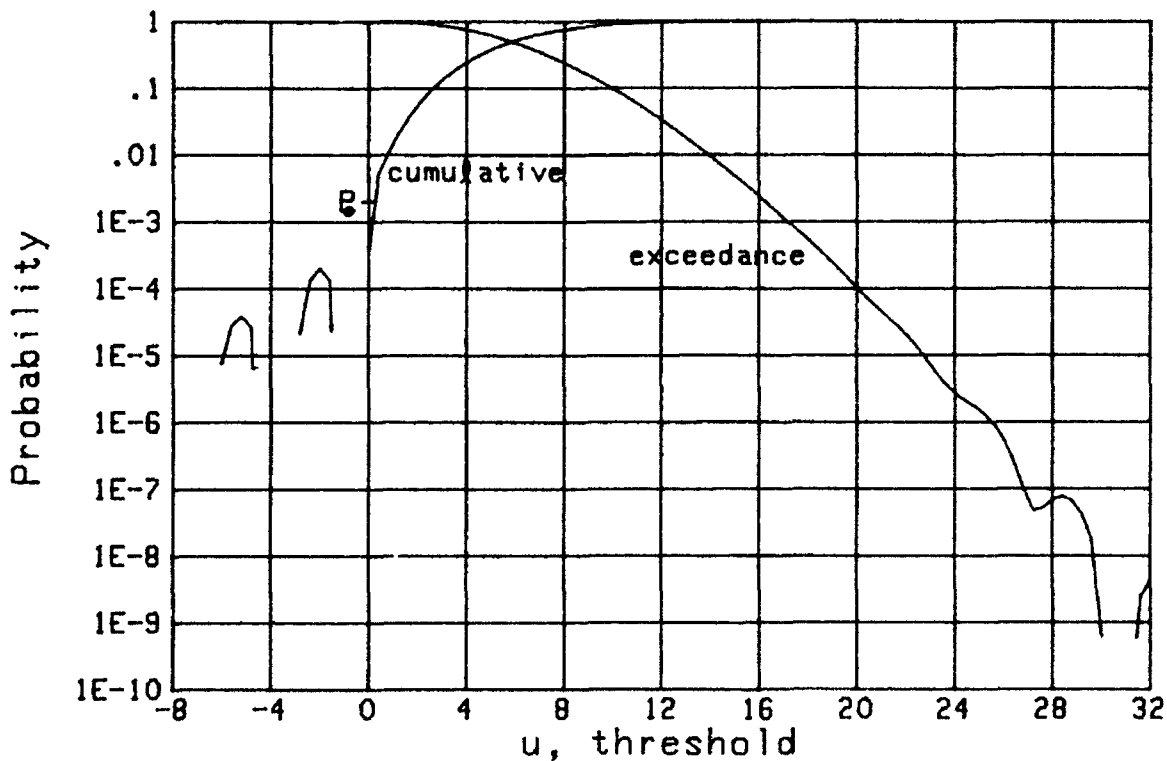


Figure 8. Distributions for Example D

comparable for $n < 65$. However, even here, the coefficients have only decayed to the $1E-3$ level, which may not be sufficiently small for accurate results.

The distributions using $N = 65$ terms and the RC expansion coefficients are given in figure 8. Although the actual cumulative distribution function is zero for $u < 0$, the approximation oscillated around zero, reaching a positive peak of value $.22E-3$ at $u = -2$. Similarly, significant wiggles develop in the exceedance distribution function below the $1E-4$ level. The reason for the inadequacy of these Hermite expansions near $u = 0$ is the abrupt zero behavior of the true probability density function for negative arguments, a feature inherently difficult to approximate by means of smooth continuous functions. The error of the approximations in figure 8 is estimated in a later section and superposed on the plot, for ease of ascertaining the reliability of the curves. The corresponding approximations for the generalized Laguerre series are better for this type of probability density function, as will be demonstrated in the next section.

The approximate probability density function for this example, again with $N = 65$ terms, is given in figure 9 on a linear ordinate. It reaches a negative peak of $-8E-4$, and crosses the $u = 0$ axis with value $.004$; both of these values should be zero, and will be for the generalized Laguerre series. To see how the approximate probability density function behaves for larger arguments, the logarithmic plot in figure 10 is used. Wiggles develop near the $1E-4$ level and become large enough that negative values of the density are yielded near $u = 28$ and 31 . It will be worthwhile to compare this Hermite series with the generalized Laguerre series to be presented in the next section. The estimated error associated with figure 10 is developed in a later section.

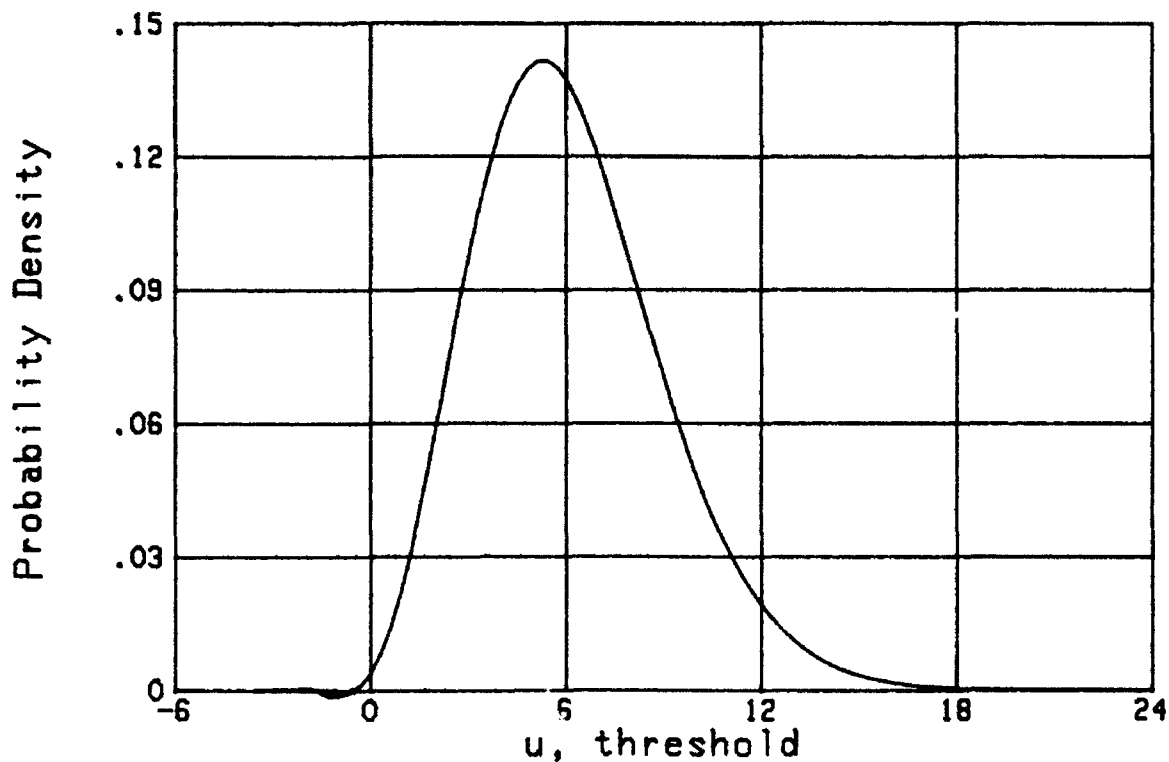


Figure 9. Linear Density for Example D

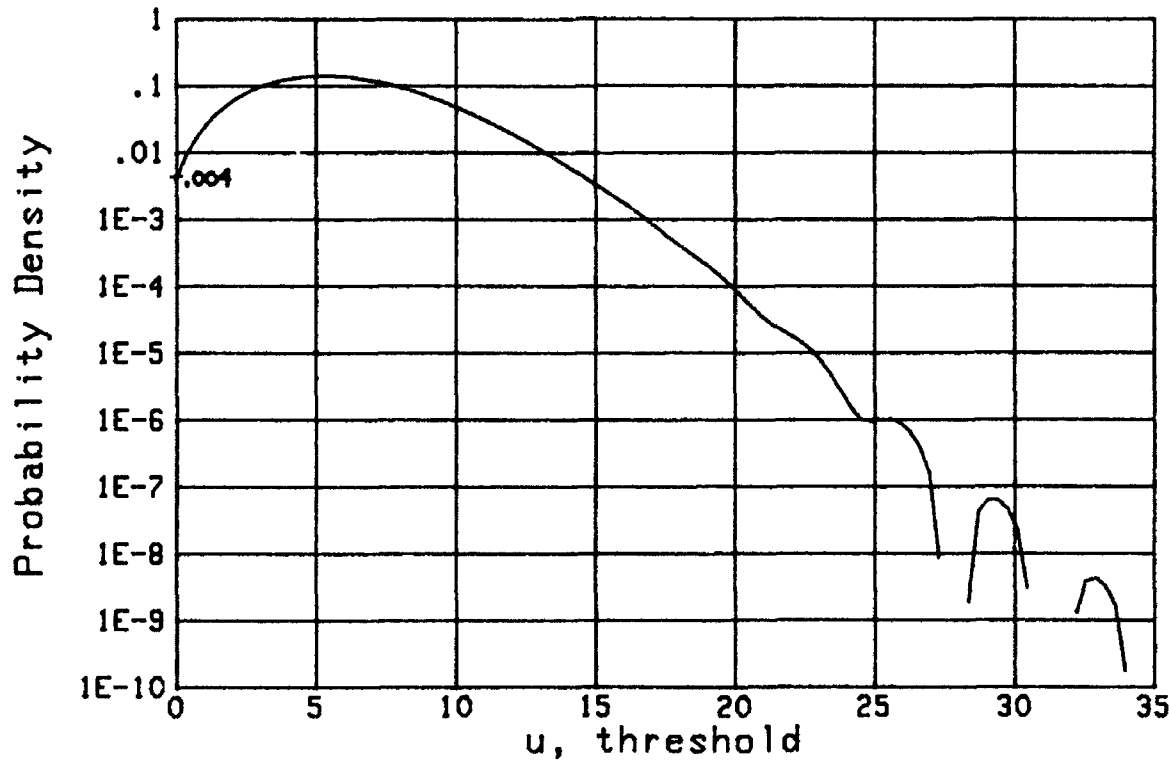


Figure 10. Log Density for Example D

EXAMPLES OF GENERALIZED LAGUERRE EXPANSION

EXAMPLE E

As with the earlier Hermite expansions, the first generalized Laguerre example here is one that can be evaluated analytically, for purposes of checking numerical procedures and results. Namely consider the Chi-square probability density function of $2(\gamma+1)$ degrees of freedom (which need not be integer):

$$p(u) = \frac{u^\gamma \exp(-u/\omega)}{\omega^{\gamma+1} \Gamma(\gamma+1)} \quad (\gamma > -1, \omega > 0) . \quad (151)$$

All probability density functions and approximations are limited to $u > 0$ in this section, since they are zero for $u < 0$; this restriction will be presumed in the remainder of the presentation.

The exceedance distribution function is related to the incomplete Gamma function [5, 6.5.3]:

$$1 - P(u) = \int_u^\infty dt p(t) = \Gamma(\gamma+1, u/\omega) / \Gamma(\gamma+1) . \quad (152)$$

The characteristic function follows from (151) as

$$f(i\xi) = (1 - i\xi\omega)^{-\gamma-1} , \quad (153)$$

with cumulants

$$\chi_k = (k-1)! (\gamma+1) \omega^k \quad \text{for } k \geq 1, \quad \chi_0 = 0 , \quad (154)$$

and moments

$$\mu_k = (\gamma+1)_k \omega^k \quad \text{for } k \geq 0 . \quad (155)$$

Thus either set of statistics can be used as a starting position. The error integral in (21) is finite if

$$-1 < \alpha < 2\gamma + 1 \quad \text{and} \quad \beta > \omega/2 . \quad (156)$$

We will find the expansion coefficients by means of the characteristic function expansion (100), developed earlier for the generalized Laguerre series. Specifically, we utilize the power series expansion

$$\begin{aligned} (1-w)^{-\alpha-1} f\left(\frac{-w/\beta}{1-w}\right) &= (1-w)^{\gamma-\alpha} \left(1-w\frac{\beta-\omega}{\beta}\right)^{-\gamma-1} = \\ &= \sum_{m=0}^{\infty} \frac{(\alpha-\gamma)_m}{m!} w^m \sum_{k=0}^{\infty} \frac{(\gamma+1)_k}{k!} \left(\frac{\beta-\omega}{\beta}\right)^k w^k , \end{aligned} \quad (157)$$

where we used (153) and [5, 15.1.8] twice. The coefficient of a general term w^n is then immediately given by the closed form

$$c_n = \sum_{m=0}^n \frac{(\alpha-\gamma)_m}{m!} \frac{(\gamma+1)_{n-m}}{(n-m)!} \left(\frac{\beta-\omega}{\beta}\right)^{n-m} \quad \text{for } n \geq 0 . \quad (158)$$

Alternative expressions for the expansion coefficients are

$$\begin{aligned} c_n &= \frac{(\gamma+1)_n}{n!} \left(\frac{\beta-\omega}{\beta}\right)^n F\left(\alpha-\gamma, -n; -n-\gamma; \frac{\beta}{\beta-\omega}\right) = \\ &= \frac{(\gamma+1)_n}{n!} \left(\frac{-\omega}{\beta}\right)^n F\left(-n, -n-\alpha; -n-\gamma; \frac{\beta}{\omega}\right) = \\ &= \frac{(\alpha+1)_n}{n!} F\left(-n, \gamma+1; \alpha+1; \frac{\omega}{\beta}\right) \quad \text{for } n \geq 0 , \end{aligned} \quad (159)$$

obtained by means of [5, 15.1.1, 15.3.5, 15.3.7] respectively. In fact, the last result can be obtained directly by using [8, 7.414 7] on (90) and (151):

$$c_n = \int_0^{\infty} du \frac{u^\gamma \exp(-u/\omega)}{\omega^{\gamma+1} \Gamma(\gamma+1)} L_n^{(\alpha)} \left(\frac{u}{\beta} \right). \quad (160)$$

However, the latter two results in (159) are not numerically stable, whereas (158) and the first line of (159) are stable for large n , without encountering round-off error.

Some special cases of (158) are as follows:

$$\text{if } \alpha = \gamma, \text{ then } c_n = \frac{(\gamma+1)_n}{n!} \left(\frac{\beta-\omega}{\beta} \right)^n ;$$

$$\text{if } \beta = \omega, \text{ then } c_n = \frac{(\alpha-\gamma)_n}{n!} ;$$

$$\text{if } \alpha = \gamma \text{ and } \beta = \omega, \text{ then } c_n = \delta_{n0} . \quad (161)$$

The last case is to be expected, since the weighting exactly matches the probability density function (151) then.

A numerical example of sequence $\{b_n\}$ for

$$\gamma = 1.1, \quad \omega = 2.3 \quad \alpha = 1.105, \quad \beta = 2.1 \quad (162)$$

is shown in figure 11, using the three recursive procedures developed earlier for the generalized Laguerre series in (112), (119), (126). In addition, exact result (158) is plotted for comparison. The expansion coefficients have a rapidly decaying transient for $n < 10$, and then a decay approximately proportional to $n^{-3/2}$ for large n . The abrupt change of character at $n = 5$ does not signify the onset of round-off error; rather, the latter is indicated

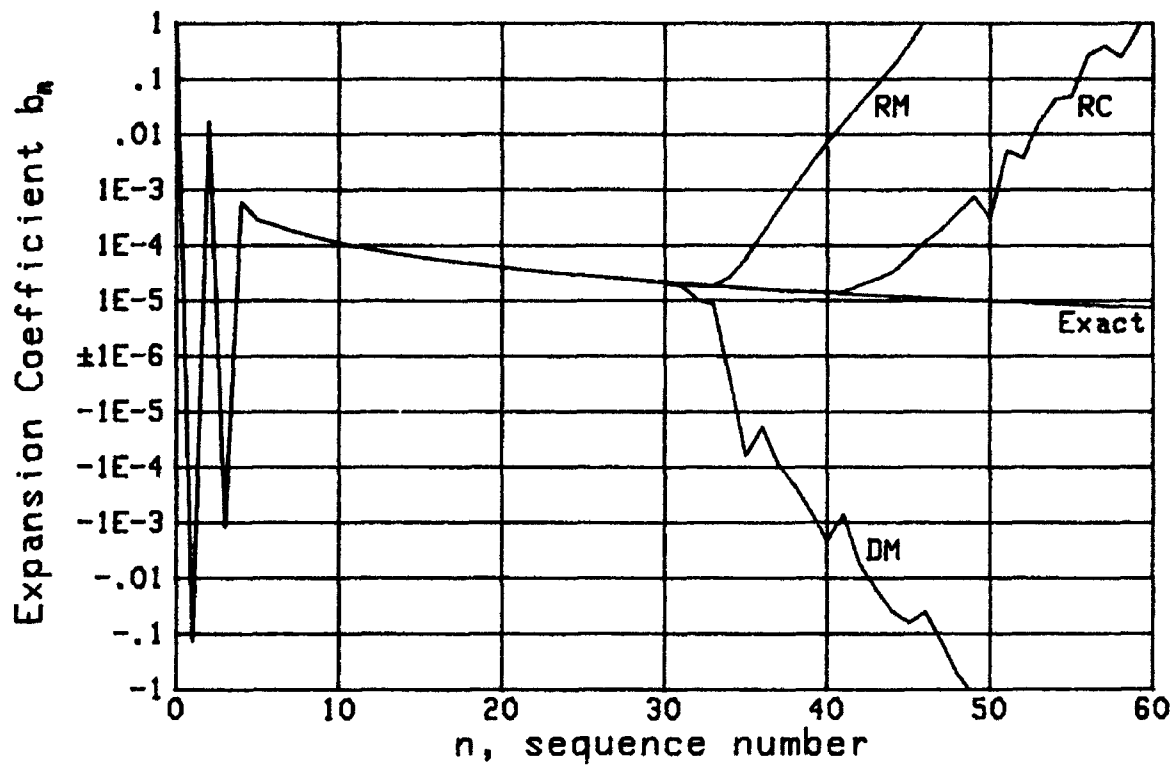


Figure 11. Generalized Laguerre; Example E

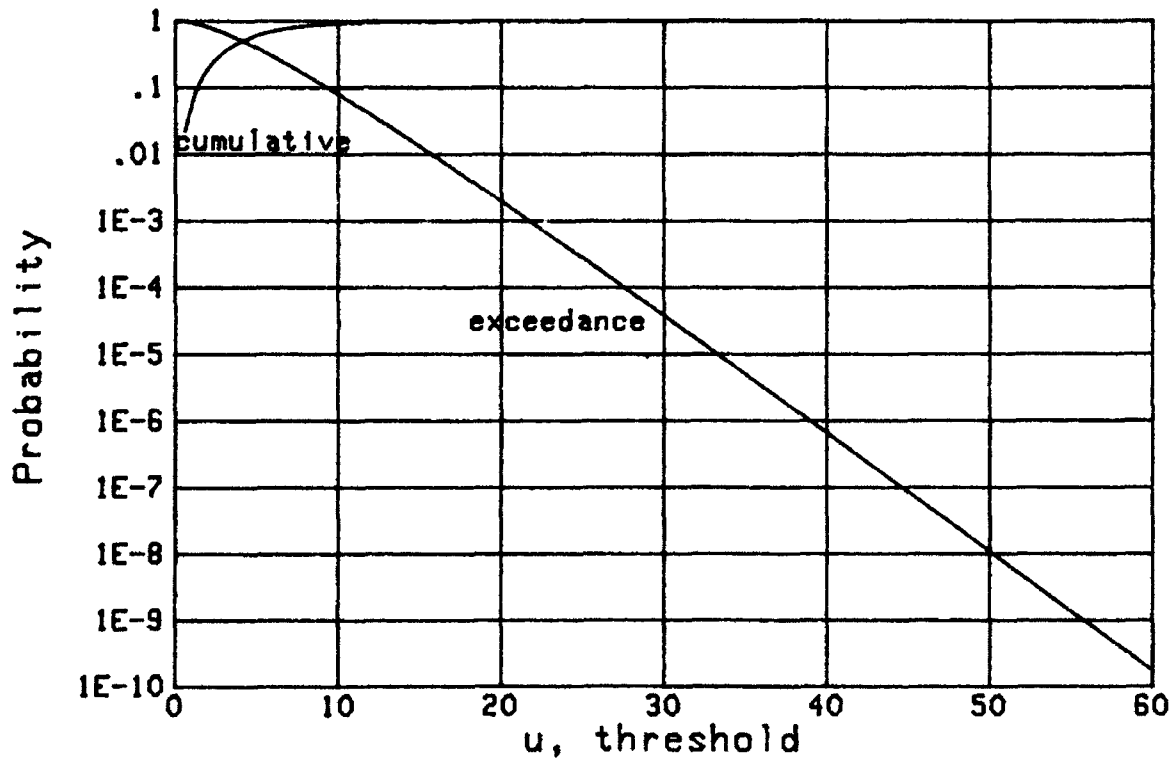


Figure 12. Distributions for Example E

by an erratic behavior, typically increasing exponentially with n (linear growth on a logarithmic ordinate).

A different plotting strategy will be adopted henceforth for the expansion coefficients $\{b_n\}$, in order not to clutter the diagrams with large oscillations as in figures 1, 3, 5, 7. Specifically, when the expansion coefficient b_n first exceeds the ± 1 limits, the remainder of sequence $\{b_n\}$ will not be plotted, since this is a region of large round-off error. Thus, although the RM curve in figure 11 returns to the ± 1 limits briefly at $n = 52, 53$, these values are not displayed.

Round-off error for the RC procedure does not become as significant as for the two moment approaches until n has increased by almost 10, for this example in figure 11. In fact, the expansion coefficients for the RC procedure overlap the exact values until $n = 40$. The corresponding approximate distributions, using $N = 40$ terms in expansion (95) as determined by RC, are plotted in figure 12. The exact result (152) overlays these results over the entire range plotted.

EXAMPLE F

The following probability density function corresponds to a noncentral Chi-square variate of 2ν degrees of freedom:

$$p(u) = \frac{1}{2} \exp\left(-\frac{d^2+u}{2}\right) \left(\frac{\sqrt{u}}{d}\right)^{\nu-1} I_{\nu-1}(d\sqrt{u}) \quad (\nu > 0); \quad (163)$$

d is the noncentrality parameter, and 2ν need not be integer. The characteristic function is [8, 6.631 4]

$$f(i\xi) = (1-i2\xi)^{-\nu} \exp\left(\frac{id^2\xi}{1-i2\xi}\right), \quad (164)$$

and is the same as the one considered in [10, (50) et seq.]. The exceedance distribution function is the generalized Q-function:

$$\begin{aligned} 1 - P(u) &= \int_u^\infty dt \frac{1}{2} \exp\left(-\frac{d^2+t}{2}\right) \left(\frac{\sqrt{t}}{d}\right)^{\nu-1} I_{\nu-1}(d\sqrt{t}) = \\ &= \int_{\sqrt{u}}^\infty dx x \exp\left(-\frac{d^2+x^2}{2}\right) \left(\frac{x}{d}\right)^{\nu-1} I_{\nu-1}(dx) = Q_\nu(d, \sqrt{u}). \end{aligned} \quad (165)$$

By expanding the \ln of (164) in a power series in $i\xi$, the cumulants follow as

$$\chi_n = 2^{n(n-1)!} \left(\nu + \frac{1}{2} d^2 n\right) \quad \text{for } n \geq 1, \quad \chi_0 = 0. \quad (166)$$

And the moments are obtained from (163) as

$$\begin{aligned} \mu_n &= 2^n (\nu)_n {}_1F_1(-n; \nu; -d^2/2) = \\ &= 2^n n! L_n^{(\nu-1)}(-d^2/2) \quad \text{for } n \geq 0, \end{aligned} \quad (167)$$

by use of [8, 6.631 1] and [5, 13.6.9]. Both (166) and (167) lend themselves to simple recurrences which involve only positive quantities; thus the starting statistics can be quickly and accurately evaluated.

The numerical example we consider here will be compared with the exact results in [10, figure 11], namely,

$$\nu = 2.7, \quad d = 3 \quad \alpha = 1.7, \quad \beta = 5.5 . \quad (168)$$

Since the probability density function in (163) behaves as $u^{\nu-1}$ as $u \rightarrow 0^+$, it is reasonable to choose weighting parameter α in (82) as $\nu-1$, as indicated in (168). And since (163) behaves as $\exp(-u/2)$ as $u \rightarrow +\infty$, we must choose $\beta > 1$ in order that the error integral in (21) is finite. The particular values in (168) approximately minimize the sum of $\{b_n^2\}_0^N$ in (21).

The expansion coefficients $\{b_n\}$ as determined by the three available recursive procedures are displayed in figure 13. The RC coefficients decrease to values less than $1E-10$ near $n = 50$, before round-off error becomes significant. The two moment approaches deteriorate near $n = 30$, which is markedly poorer than the cumulant approach. The distributions, as determined by $N = 50$ terms of the RC approach, are given in figure 14, and agree with the $d = 3$ curve of [10, figure 11]. When the approximate probability density function for $N = 50$ was compared with exact result (163), 10 decimals of agreement were obtained; this is due to the ability to get very small $\{b_n\}$ in figure 13 via the RC method.

EXAMPLE G

This example is the Rice probability density function given in (144), with moments (145) and cumulative distribution function (146). The starting statistics are the moments as determined by recurrence (E-5)-(E-6).

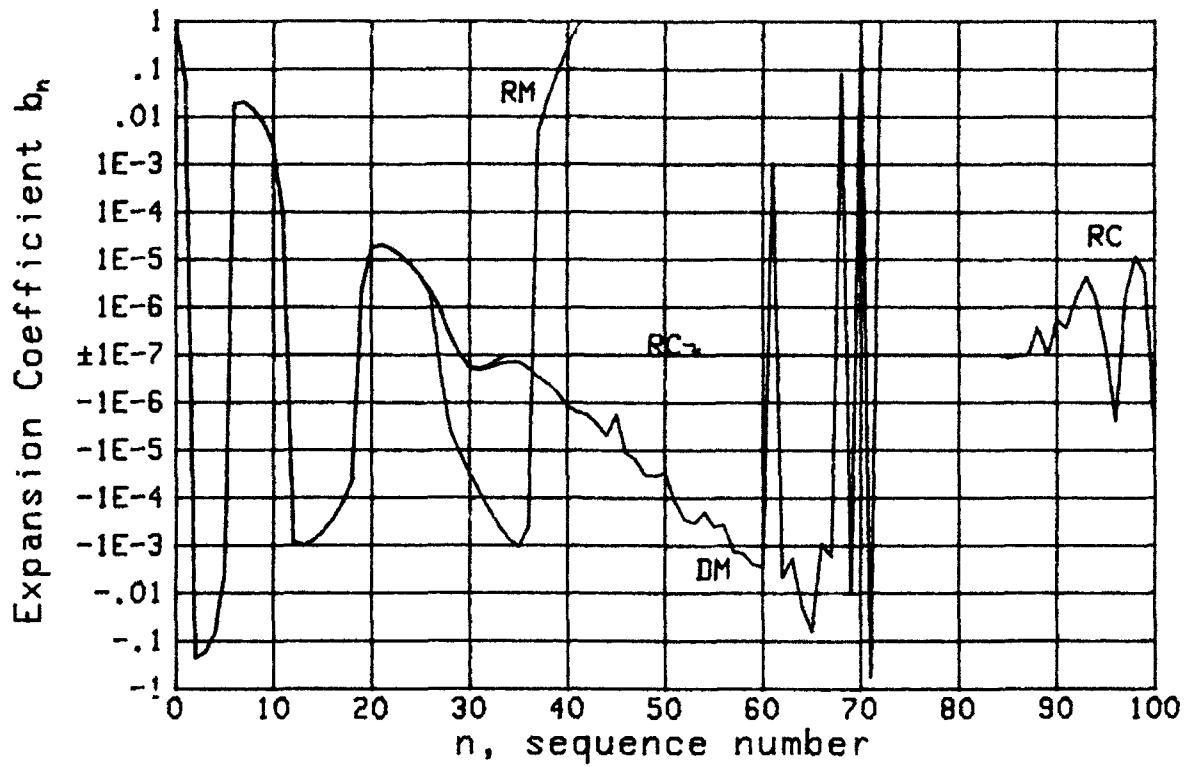


Figure 13. Generalized Laguerre; Example F

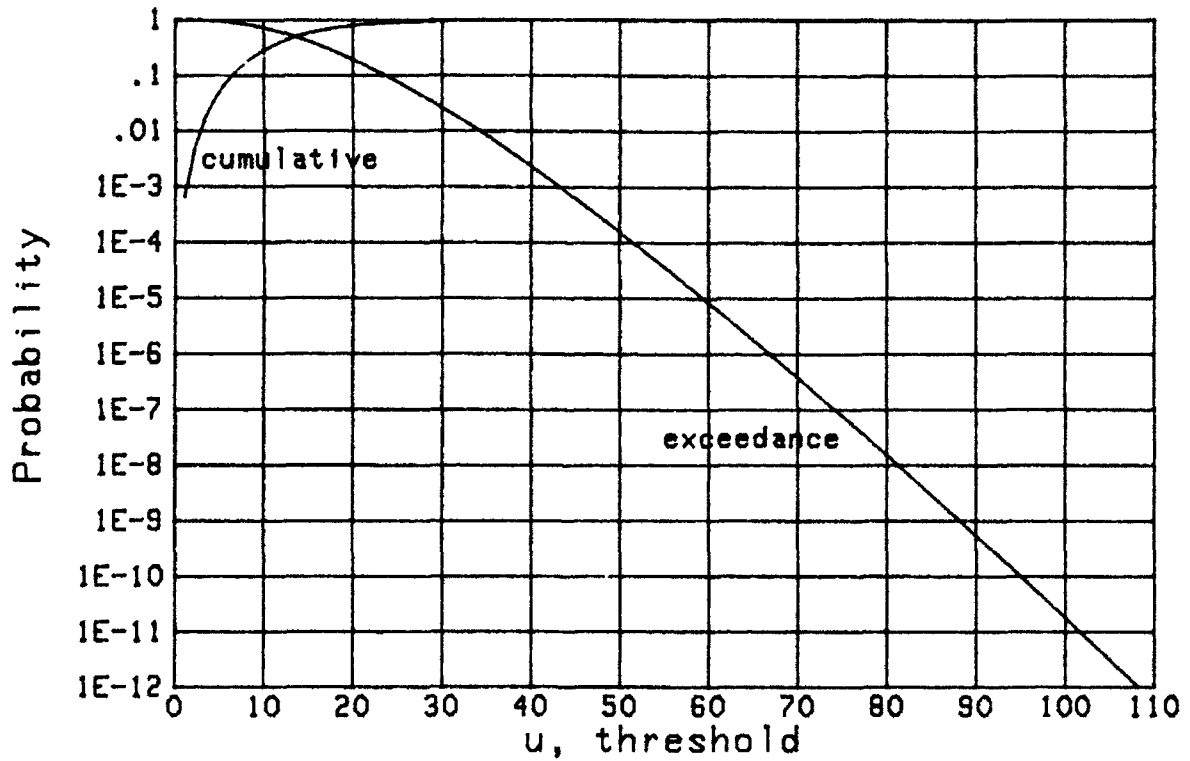


Figure 14. Distributions for Example F

The particular numerical case of interest is

$$\theta = 3, \quad \omega^2 = 2 \quad \alpha = 1, \quad \beta = 1. \quad (169)$$

The values of α and β were found by the usual trial and error search procedure of observing plots of expansion coefficients $\{b_n\}$, looking for rapid decay and small round-off error; results for this example are displayed in figure 15. The RM procedure deteriorates rapidly at $n = 30$, whereas DM and RC are useable up to $n = 55$ and 65 approximately.

The cumulative and exceedance distribution functions for $N = 65$ terms of the RC procedure are plotted in figure 16, along with exact result (146). The approximate exceedance distribution function overlaps the exact one until slightly below the probability level $1E-4$, which corresponds to the level of reliability of b_n in figure 15 at $n = 65$. Then the exceedance distribution function makes a positive (upward) turn below $1E-6$, which is impossible for a physical density function which must remain positive; thus the approximation deteriorates rapidly for $u > 7$.

EXAMPLE H

This is a follow-on to the previous example, in that we consider a sum of 8 Rice variates, each with the statistics in (169). The expansion coefficients for

$$\theta = 3, \quad \omega^2 = 2 \quad \alpha = 26, \quad \beta = 1 \quad (170)$$

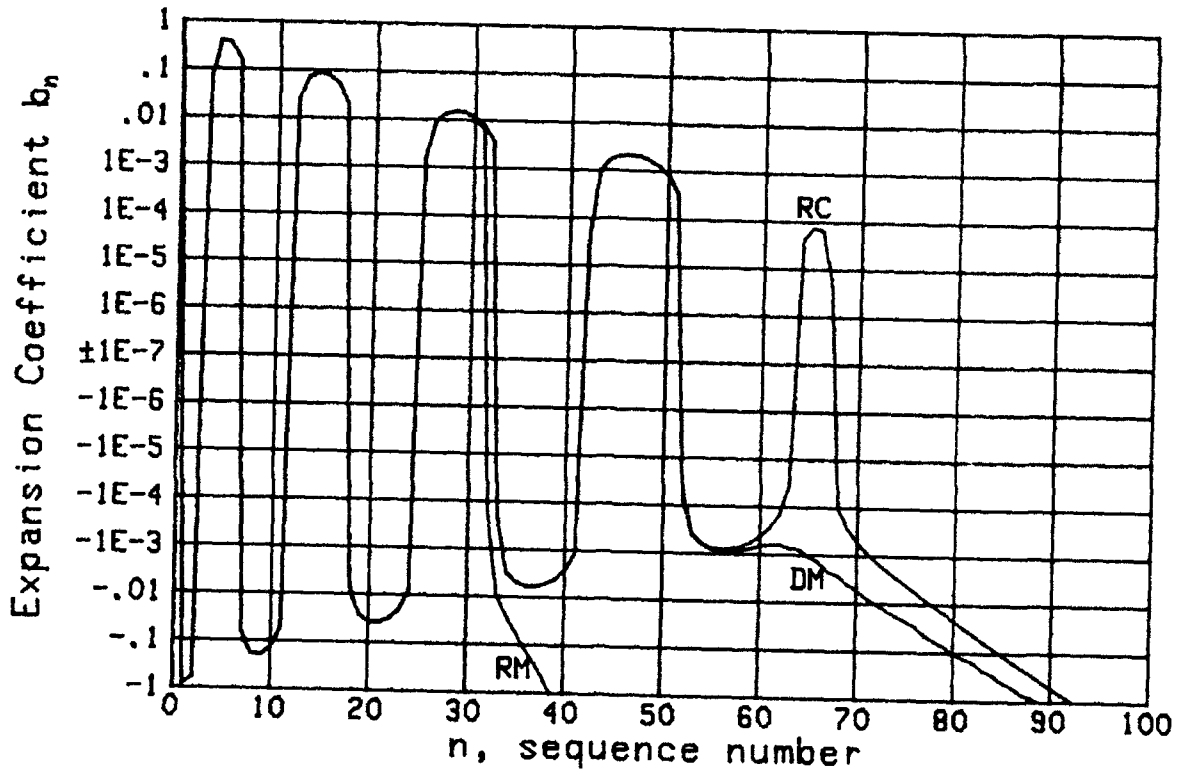


Figure 15. Generalized Laguerre; Example G

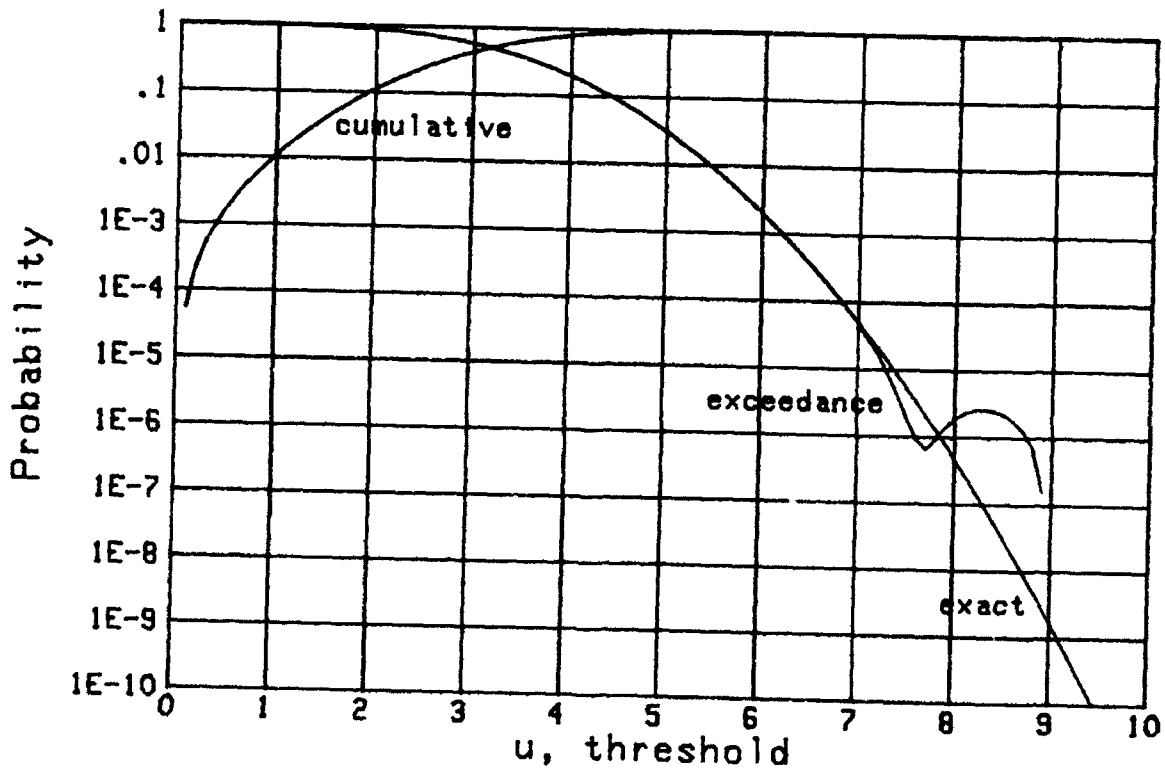


Figure 16. Distributions for Example G

are displayed in figure 17. Whereas both DM and RM are useless beyond $n = 25$, the expansion coefficients determined by RC decay down to the $1E-10$ level at $n \approx 150$ before round-off error becomes significant. The corresponding distributions in figure 18, using $N = 143$ terms of the expansion via RC, reveal accurate results down to the $1E-12$ level of probability, except for a slight flare in the exceedance distribution function below $1E-11$.

We also checked the example of the sum of 8 normalized Rayleigh variates considered earlier via a Hermite series in example C. For $\alpha = 10$, $\beta = .9$, the expansion coefficients $\{b_n\}$ decayed to the $1E-11$ level at $n = 100$ for the RC approach and agreed with the false alarm probabilities calculated exactly in [9, table 1] for $M = 8$. By contrast, the DM expansion coefficients were subject to significant round-off error by the time n reached 30, and were useless for small probability calculations.

EXAMPLE I

We return to the shot noise process previously considered via a Hermite series in example D. The equations and discussions there should be reviewed, since they are directly relevant to the generalized Laguerre expansion here. For the choice of parameters in (150), the selection of generalized Laguerre weighting parameters

$$\alpha = .74, \quad \beta = 2.1 \quad (171)$$

leads to the expansion coefficients plotted in figure 19. The DM and RC results agree to $n = 32$, and then begin to diverge from each other. By way of

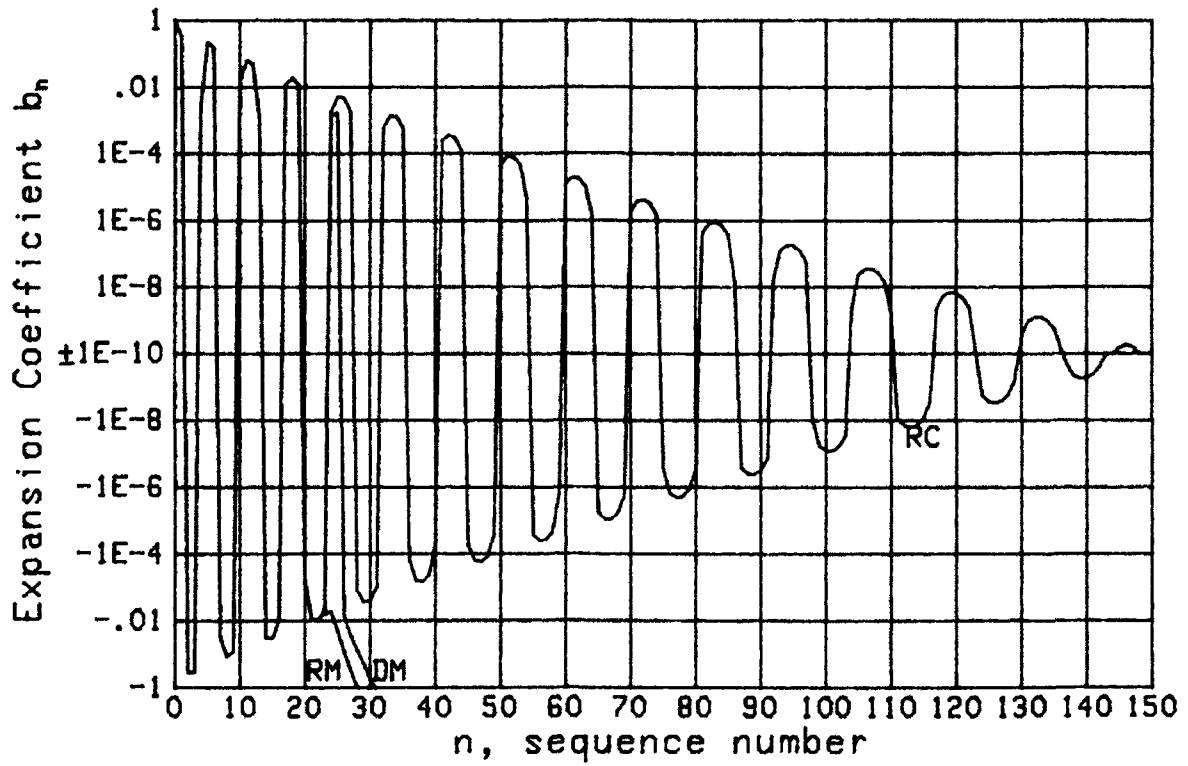


Figure 17. Generalized Laguerre; Example H

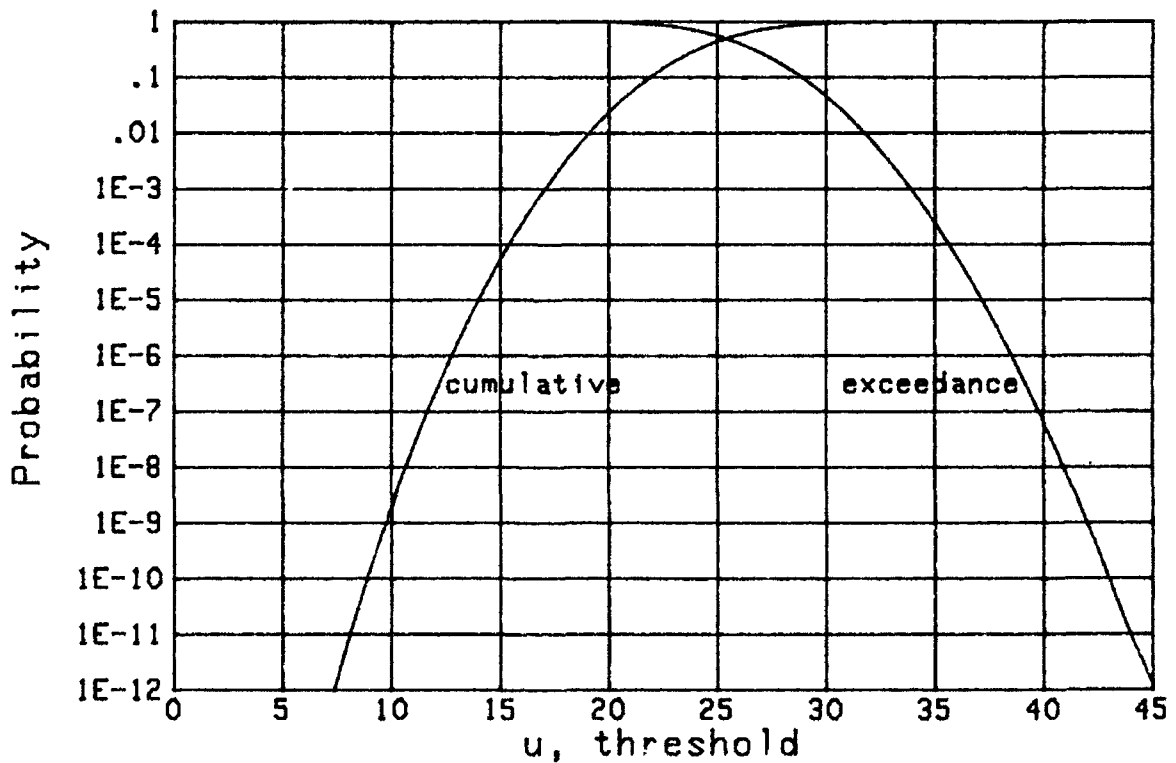


Figure 18. Distributions for Example H

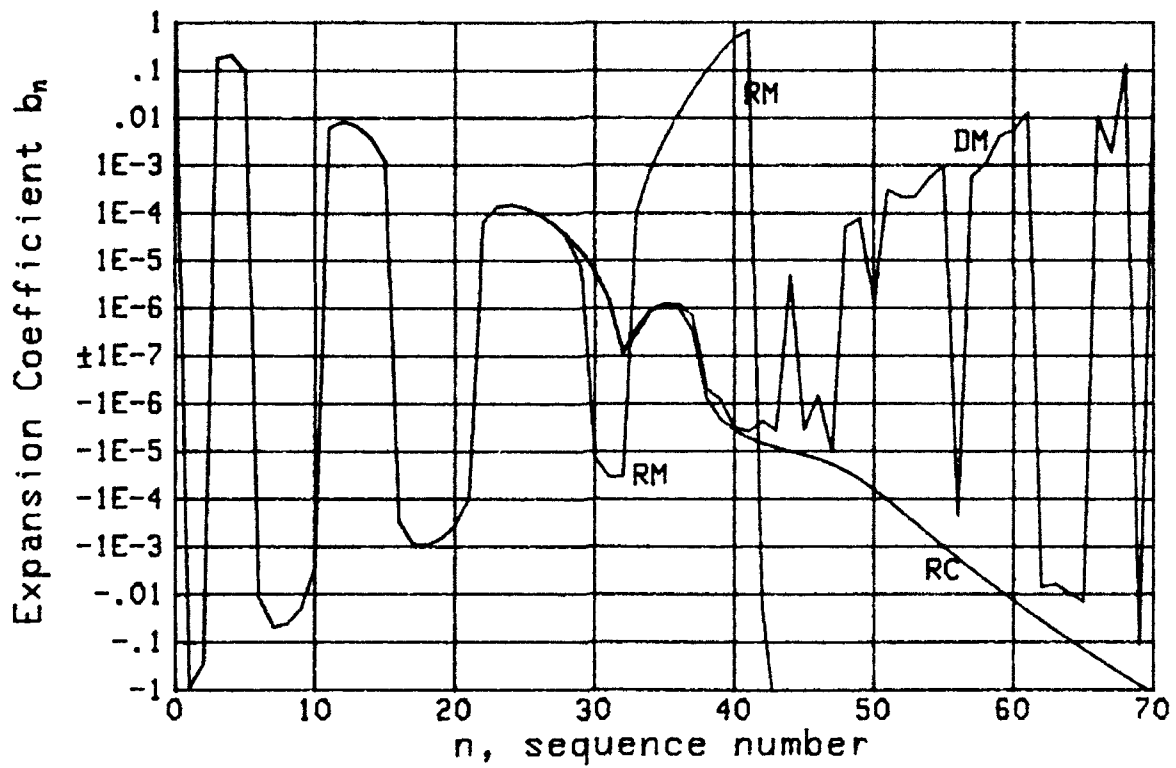


Figure 19. Generalized Laguerre; Example I

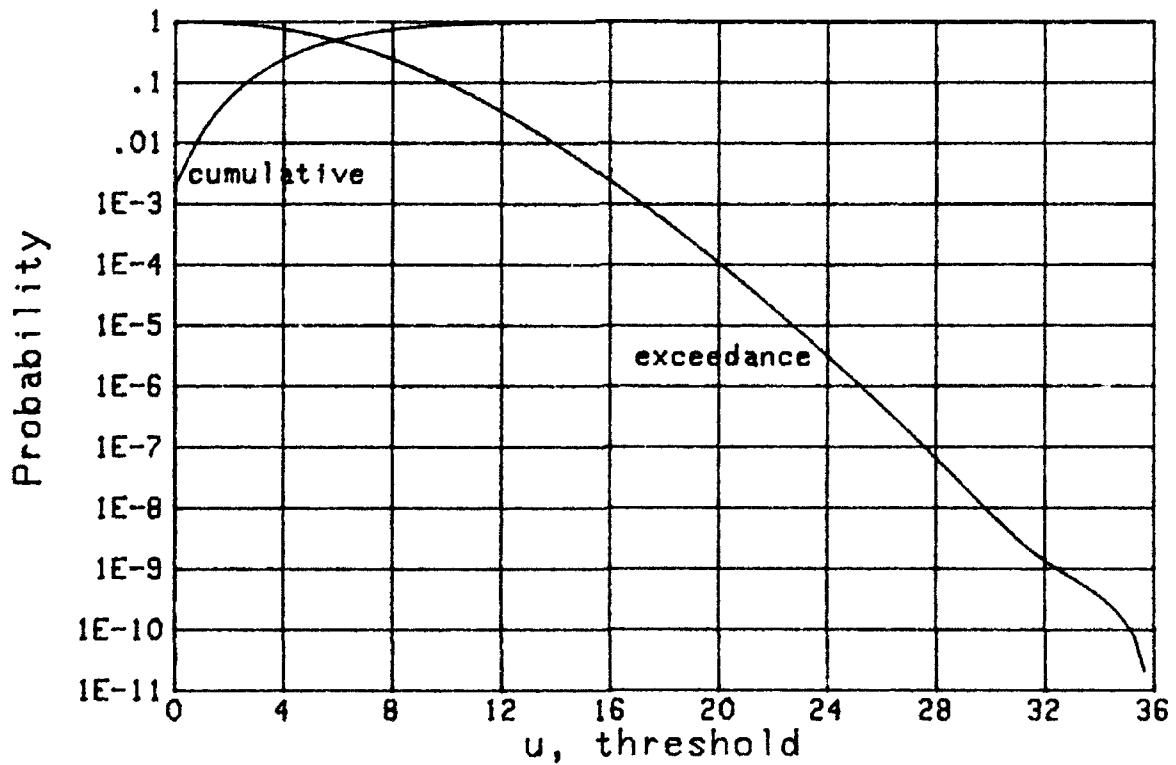


Figure 20. Distributions for Example I

contrast with the Hermite expansion coefficients in figure 7, where values in the $1E-3$ range were achieved, values in the $1E-6$ range can be obtained here for the generalized Laguerre expansion, for n in the mid-30s. The DM result was previously given in [4, figure D-1].

The distributions for $N = 32$ terms of the RC procedure are plotted in figure 20. This result is considerably better than the Hermite expansion in figure 8; instead of the wiggles which developed at $1E-4$ in figure 8, the curve in figure 20 is smooth down to the $1E-8$ probability level, and then develops a bump. Also, the cumulative distribution function is accurate at $u = 0$, where it takes on the value $P_0 = .002$ given in (150), and is zero for $u < 0$. This cumulative distribution function was previously given in [4, figure 8].

The probability density function for $N = 32$ terms of the RC procedure is given in figure 21; this result was previously given in [4, figure 9]. It is significantly better near the origin than the Hermite approximation given earlier in figure 9, which developed negative values for $u < 0$. In order to see what the probability density function does for larger u values, the same probability density function is plotted on a logarithmic ordinate in figure 22. It is accurate to the $1E-9$ level but then develops a hook that is incorrect; however, this approximation remains positive even at this very low value of the density, whereas the corresponding result via a Hermite expansion in figure 10 developed negative values. The estimated errors in figures 20 and 22 are evaluated in a later section.

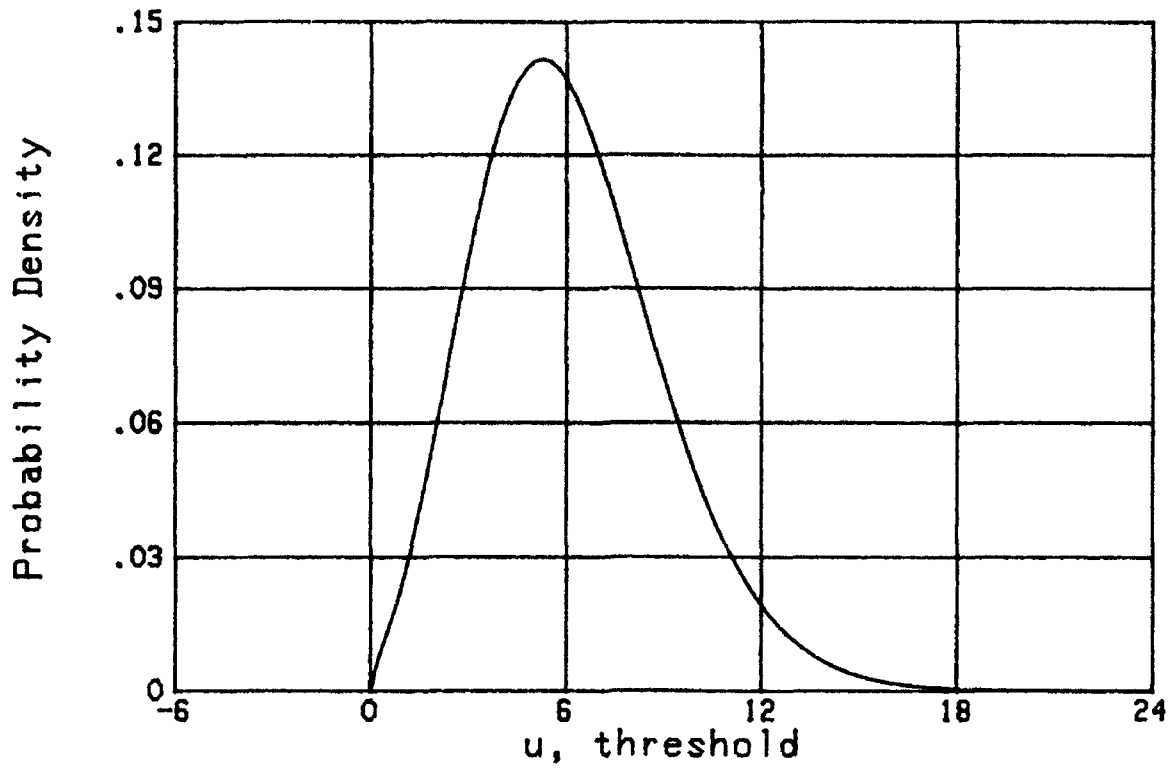


Figure 21. Linear Density for Example I

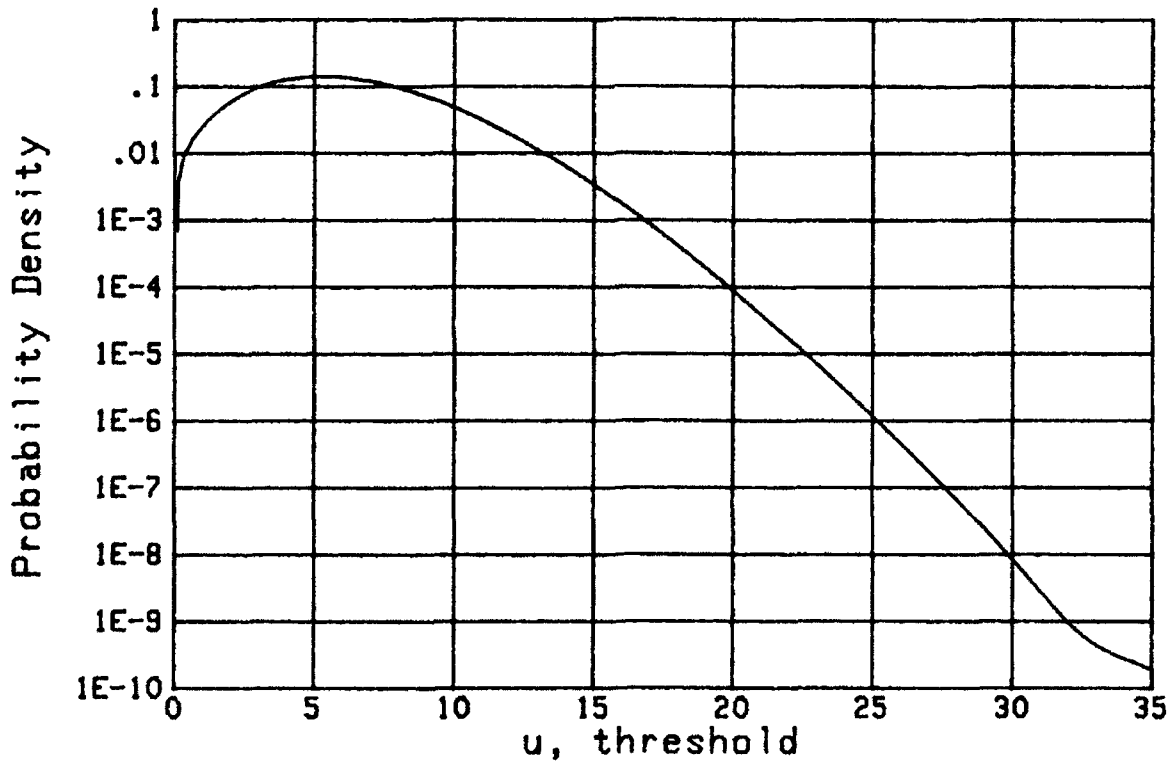


Figure 22. Log Density for Example I

EXAMPLE J

This last example is for probability density function

$$p(u) = \frac{1}{2} \exp(-u^{1/2}) \quad \text{for } u > 0, \quad (172)$$

for which the moments are

$$\mu_n = (2n+1)! \quad (173)$$

The characteristic function and cumulants are not available in any convenient analytic form.

This is a particularly difficult example, since the characteristic function expansion in (6) has a zero radius of convergence; thus the moments do not uniquely determine the probability density function or cumulative distribution function. Also, the error integral in (21) is always infinite; in fact, regardless of the choice of weighting parameters α and β used in the generalized Laguerre series, the expansion coefficients $\{b_n\}$ always diverged. Nevertheless, a search of parameter values led to a pair of selections, namely,

$$\alpha = -.35, \quad \beta = 30, \quad (174)$$

for which the expansion coefficients had an initial decay to the $1E-2$ level before divergence took over; see figure 23. In fact, the identical same results were obtained for all three methods, RC, DM, RM; this is probably due to the fact that divergence of $\{b_n\}$ dominated before round-off error became significant.

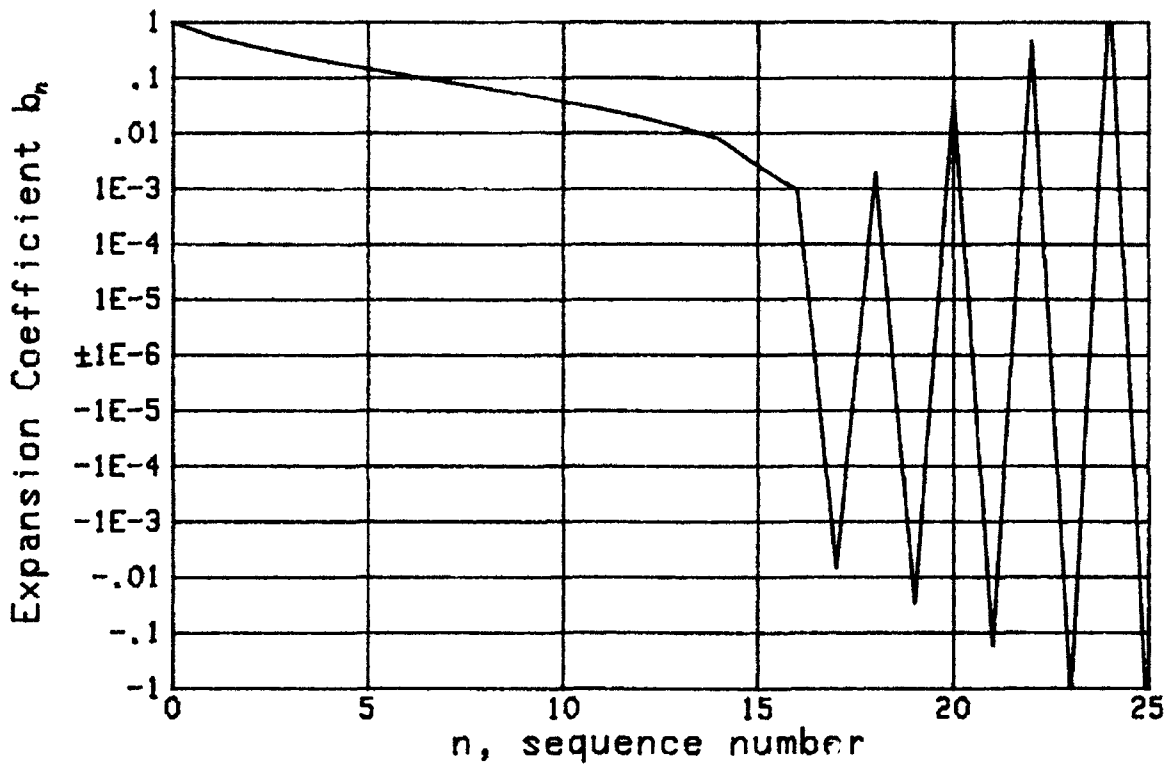


Figure 23. Generalized Laguerre; Example J

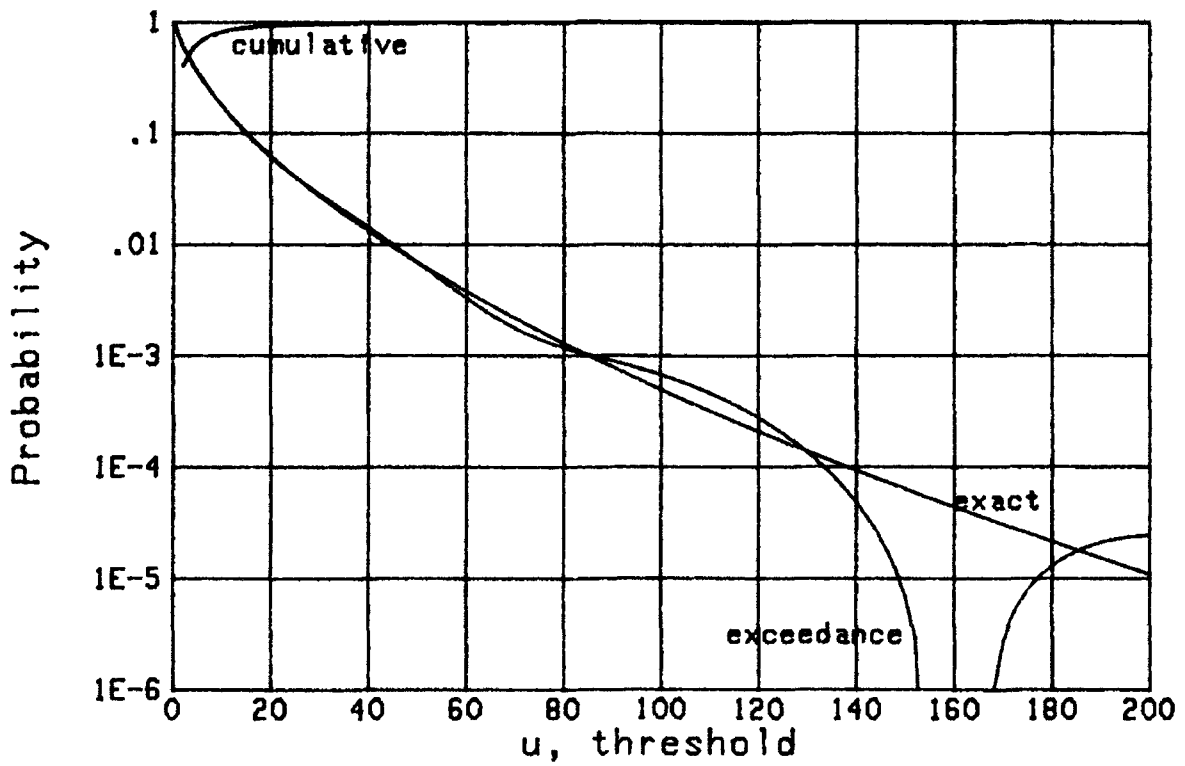


Figure 24. Distributions for Example J

The distributions are plotted in figure 24 for $N = 15$ terms of the generalized Laguerre series. Comparison with the exact exceedance distribution function

$$1 - P(u) = (1 + u^{1/2}) \exp(-u^{1/2}) \quad \text{for } u > 0 \quad (175)$$

reveals that the approximation is decent down to the .01 probability level, but then oscillates more and more violently as u increases. Thus even in this non-unique example, a limited-quality approximation is achieved by the generalized Laguerre series; this example confirms the comment in [3, p. 167] that, even for a divergent series, a limited number of expansion coefficients often gives a satisfactory approximation.

The exact and approximate probability density functions are plotted on a linear ordinate in figure 25, and on a logarithmic ordinate in figure 26, using $N = 15$ terms of the generalized Laguerre series, when the expansion coefficients were determined by the DM method. The approximate probability density function is negative for $150 < u < 190$, around the $1E-6$ level. The estimated errors of the approximations in figures 24 and 26 will be developed in the next section.

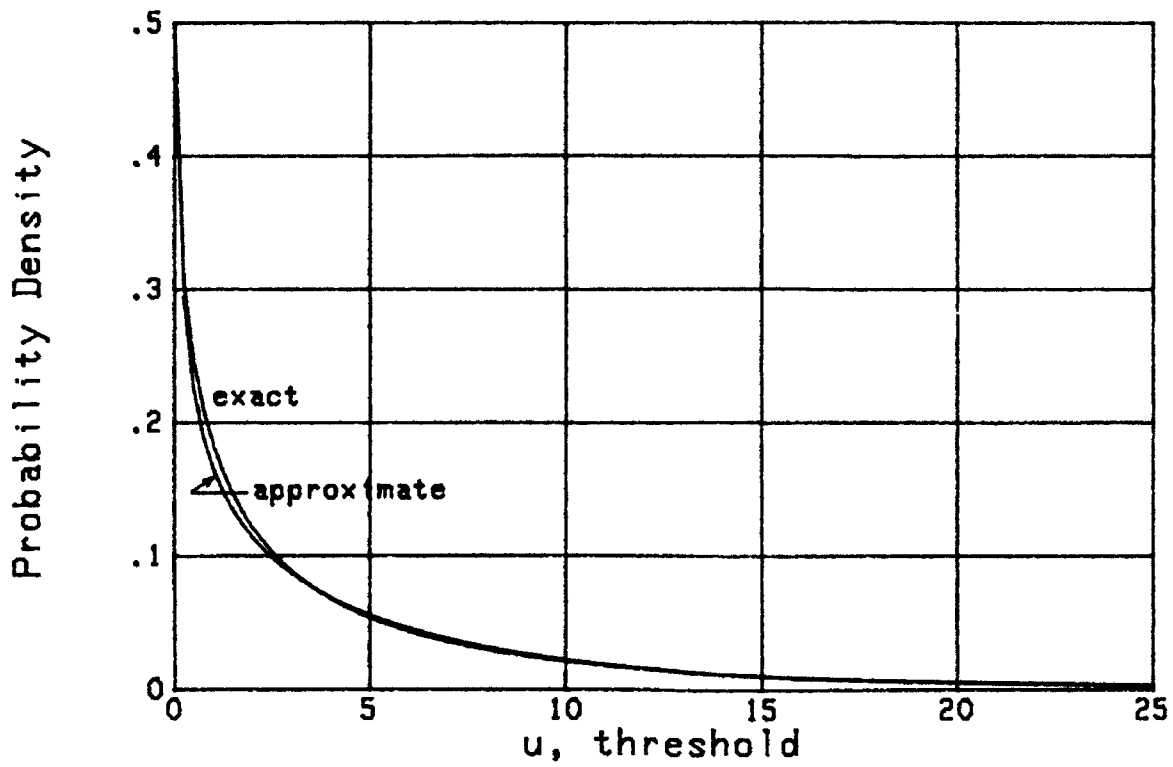


Figure 25. Linear Density for Example J

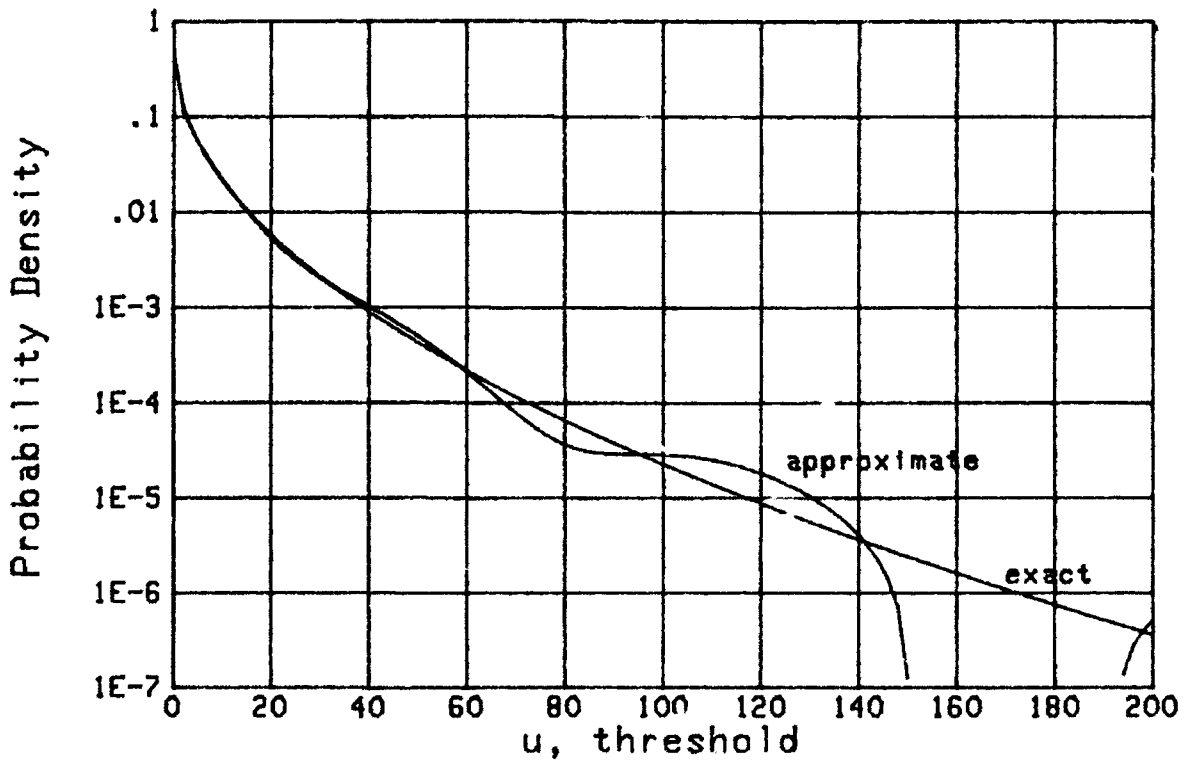


Figure 26. Log Density for Example J

ESTIMATED ERRORS OF APPROXIMATIONS

When the calculations of the approximate cumulative or exceedance distribution functions or the corresponding probability density function are made, it would be very useful to have a rough estimate of their reliability. One way, as discussed in the previous sections, is to look for nonsmooth or anomalous behavior on the tails of the functions. Here, we will develop a more quantitative estimate of the error and superpose it on some of the previous examples, for confirmation.

Both the Hermite and generalized Laguerre orthonormal polynomials oscillate with n and decay slowly. The same general behavior is true of expansion coefficients $\{b_n\}$. This leads to summations for the various functions with terms that also oscillate and decay. A rough estimate of the error is afforded by the envelope of these oscillations, evaluated at the first neglected term of the summation. This procedure will be pursued for both types of expansions; how useful it is will be indicated by numerical examples.

HERMITE EXPANSION

The following result for the envelope of the Hermite polynomial is obtained from [5, 6.1.39 and 22.5.18] and [7, 8.22.8]:

$$\text{Env} \left\{ (n!)^{-1/2} \text{He}_n(x) \right\} \sim \exp(x^2/4) \left(\frac{2}{\pi n} \right)^{1/4} \text{ as } n \rightarrow +\infty. \quad (176)$$

Also, from (46) and (47), the n -th term of the approximate probability density function is

$$\frac{1}{\beta} \phi\left(\frac{u-\alpha}{\beta}\right) b_n (n!)^{-1/2} \text{He}_n\left(\frac{u-\alpha}{\beta}\right). \quad (177)$$

Then the magnitude of the error of the probability density function approximation, if the n -th term is the first one neglected, is roughly

$$E_n(u; p) \equiv \frac{1}{\beta} \phi\left(\frac{u-\alpha}{\beta}\right) \text{Env}\{b_n\} \text{Env}\left\{(n!)^{-1/2} \text{He}_n\left(\frac{u-\alpha}{\beta}\right)\right\} = \\ \sim \left[2^{1/4} \pi^{3/4} \beta\right]^{-1} \exp\left(-\frac{(u-\alpha)^2}{4\beta^2}\right) n^{-1/4} \text{Env}\{b_n\} \text{ as } n \rightarrow +\infty. \quad (178)$$

Here we used (176).

As for the cumulative distribution function, we have from (47)-(49), the n -th term of the approximation as

$$-\phi\left(\frac{u-\alpha}{\beta}\right) b_n (n!)^{-1/2} \text{He}_{n-1}\left(\frac{u-\alpha}{\beta}\right). \quad (179)$$

The magnitude of the error for the cumulative and exceedance distribution functions, if the n -th term is the first one neglected, is then defined as

$$E_n(u; P) \equiv \phi\left(\frac{u-\alpha}{\beta}\right) \text{Env}\{b_n\} \text{Env}\left\{(n!)^{-1/2} \text{He}_{n-1}\left(\frac{u-\alpha}{\beta}\right)\right\} = \\ \sim \left[2^{1/4} \pi^{3/4}\right]^{-1} \exp\left(-\frac{(u-\alpha)^2}{4\beta^2}\right) n^{-3/4} \text{Env}\{b_n\} \text{ as } n \rightarrow +\infty. \quad (180)$$

Again, (176) was of crucial importance in getting this result.

Since the above estimates are asymptotic in n , they will be most reliable for n large; their use for small n could be very misleading. The way to use these error estimates for the density and distribution approximations is as follows. First, a search on α and β , to find the fastest decaying expansion coefficients $\{b_n\}$, is conducted. The weighting parameter values, α and β , and the corresponding envelope value of the expansion coefficients $\{b_n\}$ at the point, n , where round-off error becomes dominant, are then noted. (For example, for figure 7, we observe that $\text{Env}\{b_n\} \approx 2E-3$ at $n = 65$, when $\alpha = 6.1$, $\beta = 4.3$; see example D.) Then (178) and (180) can be computed and plotted in the ranges of u of interest.

An example of this procedure for the shot noise process in example D is given in figures 27 and 28. In particular, the approximate results are repeated from figures 8 and 10, and error measures (180) and (178), respectively, are superposed as dashed lines, each on the appropriate figure. Just where the approximations develop large wiggles, the errors are of comparable magnitude, indicating unreliable estimates there.

It should be observed from these figures (or from (178) and (180)) that the absolute error is maximum at $u = \alpha$, but that the relative error is a minimum in that neighborhood. Also, although the absolute error decays with u , the correct answer decays faster, leading to an increasing relative error, which eventually becomes so excessive in the tails of the various functions that the approximations are useless.

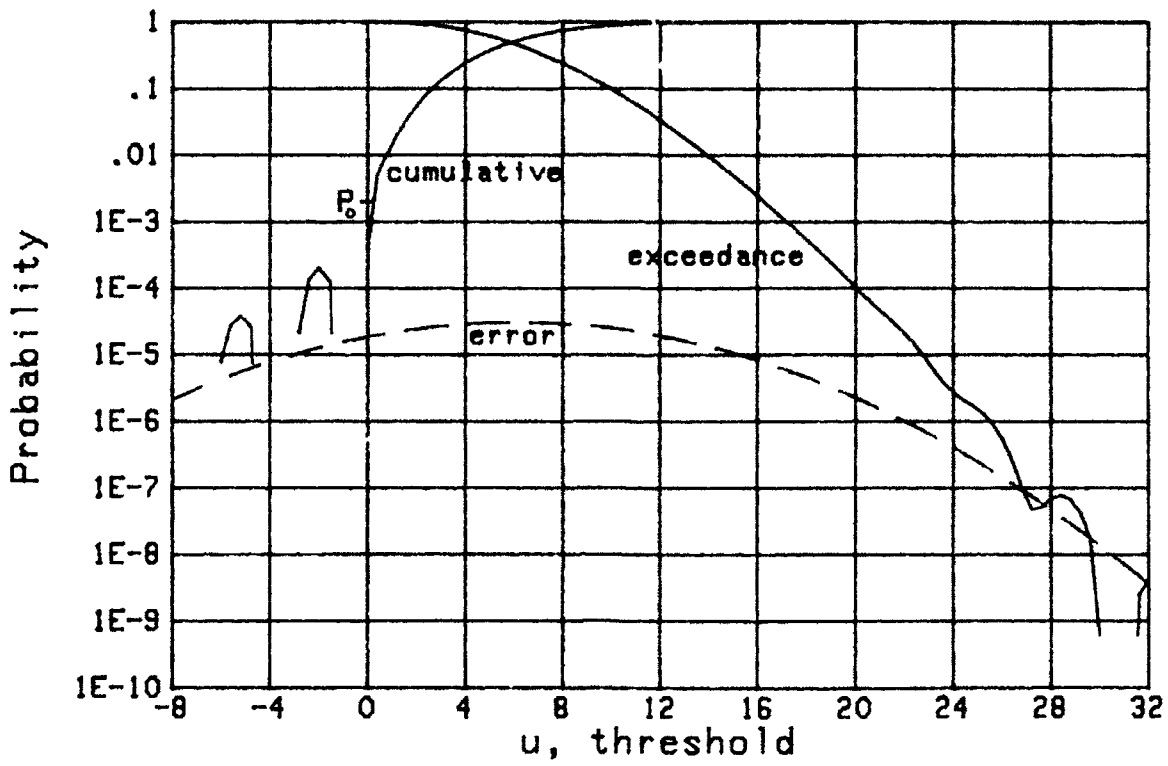


Figure 27. Estimated Error of Figure 8

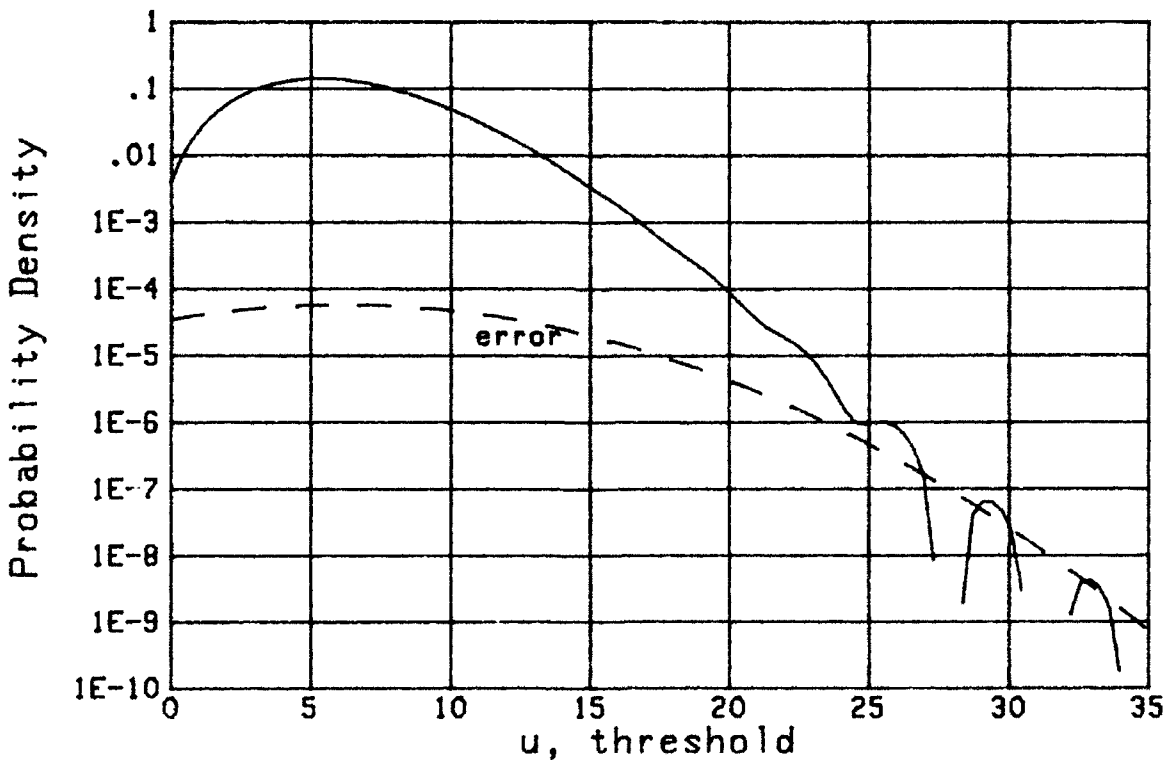


Figure 28. Estimated Error of Figure 10

GENERALIZED LAGUERRE EXPANSION

The details for the generalized Laguerre series are very similar to those above and so will be abbreviated. The envelope of the generalized Laguerre polynomial is [7, 8.22.1]

$$\text{Env} \left\{ L_n^{(\alpha)}(x) \right\} \sim \pi^{-\frac{1}{2}} e^{\frac{x}{2}} x^{-\frac{\alpha}{2} - \frac{1}{4}} n^{\frac{\alpha}{2} - \frac{1}{4}} \quad \text{as } n \rightarrow +\infty, \quad \text{for } x > 0. \quad (181)$$

From (91) and (92), the n -th term of the approximate probability density function is

$$\frac{u^\alpha \exp(-u/\beta)}{\beta^{\alpha+1} \Gamma(\alpha+1)} b_n \left(\frac{n!}{(\alpha+1)_n} \right)^{1/2} L_n^{(\alpha)} \left(\frac{u}{\beta} \right). \quad (182)$$

Then the magnitude of the error of the probability density function approximation is, for $u > 0$,

$$\begin{aligned} E_n(u;p) &\equiv \frac{u^\alpha \exp(-u/\beta)}{\beta^{\alpha+1} \Gamma(\alpha+1)} \text{Env} \{ b_n \} \text{Env} \left\{ \left(\frac{n!}{(\alpha+1)_n} \right)^{1/2} L_n^{(\alpha)} \left(\frac{u}{\beta} \right) \right\} = \\ &\sim \left[\pi \Gamma(\alpha+1) \beta^2 \right]^{-1/2} \left(\frac{u}{\beta} \right)^{\frac{\alpha}{2} - \frac{1}{4}} \exp \left(-\frac{u}{2\beta} \right) n^{-1/4} \text{Env} \{ b_n \} \text{as } n \rightarrow +\infty, \end{aligned} \quad (183)$$

where we used [5, 6.1.47] and (181). This quantity peaks at $u = \beta(\alpha - \frac{1}{2})$.

With regards to the cumulative distribution function, the n -th term of the approximation is, from (95) and (92),

$$\frac{u^{\alpha+1} \exp(-u/\beta)}{\beta^{\alpha+1} \Gamma(\alpha+1)} b_n \frac{1}{n} \left(\frac{n!}{(\alpha+1)_n} \right)^{1/2} L_{n-1}^{(\alpha+1)} \left(\frac{u}{\beta} \right). \quad (184)$$

Then the magnitude of the distribution error, for both the cumulative and the exceedance distribution functions, is roughly

$$E_n(u;P) \cong \frac{u^{\alpha+1} \exp(-u/\beta)}{\beta^{\alpha+1} \Gamma(\alpha+1)} \text{Env} \{b_n\} \text{Env} \left\{ \frac{1}{n} \left(\frac{n!}{(\alpha+1)_n} \right)^{1/2} L_{n-1}^{(\alpha+1)} \left(\frac{u}{\beta} \right) \right\} =$$

$$\sim \left[\pi \Gamma(\alpha+1) \right]^{-1/2} \left(\frac{u}{\beta} \right)^{\frac{\alpha}{2} + \frac{1}{4}} \exp \left(-\frac{u}{2\beta} \right) n^{-3/4} \text{Env} \{b_n\} \quad \text{as } n \rightarrow +\infty, \text{ for } u > 0, \quad (185)$$

upon use of (181). This quantity reaches its peak at $u = \beta(\alpha + \frac{1}{2})$.

An application of these results to the shot noise process, which was re-investigated in example I via the generalized Laguerre series, is given in figures 29 and 30. Specifically, the approximate results from figures 20 and 22 have been repeated, and error measures (185) and (183), respectively, superposed as dashed lines. They confirm the earlier observations that the distribution and density approximations are reliable until the anomalous behavior on the tails manifests itself.

The difficult example J is considered in figures 31 and 32. Since the expansion coefficient sequence $\{b_n\}$ in figure 23 diverged for large n , the selection of $n = 15$, as used in figures 24-26, is not the large value needed to justify the use of (183) and (185). Thus, the dashed curves on figures 31 and 32 must be considered only as ball-park estimates; in general, the approximate error appears to be too conservative in these two figures.

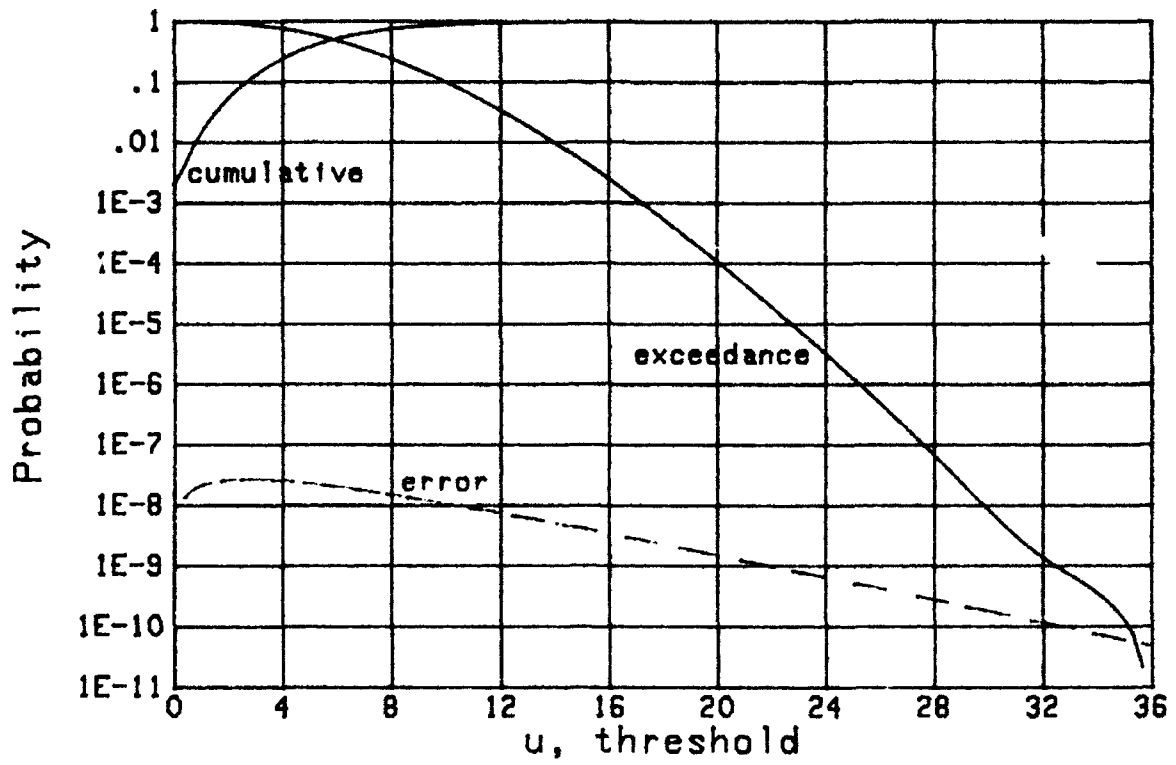


Figure 29. Estimated Error of Figure 20

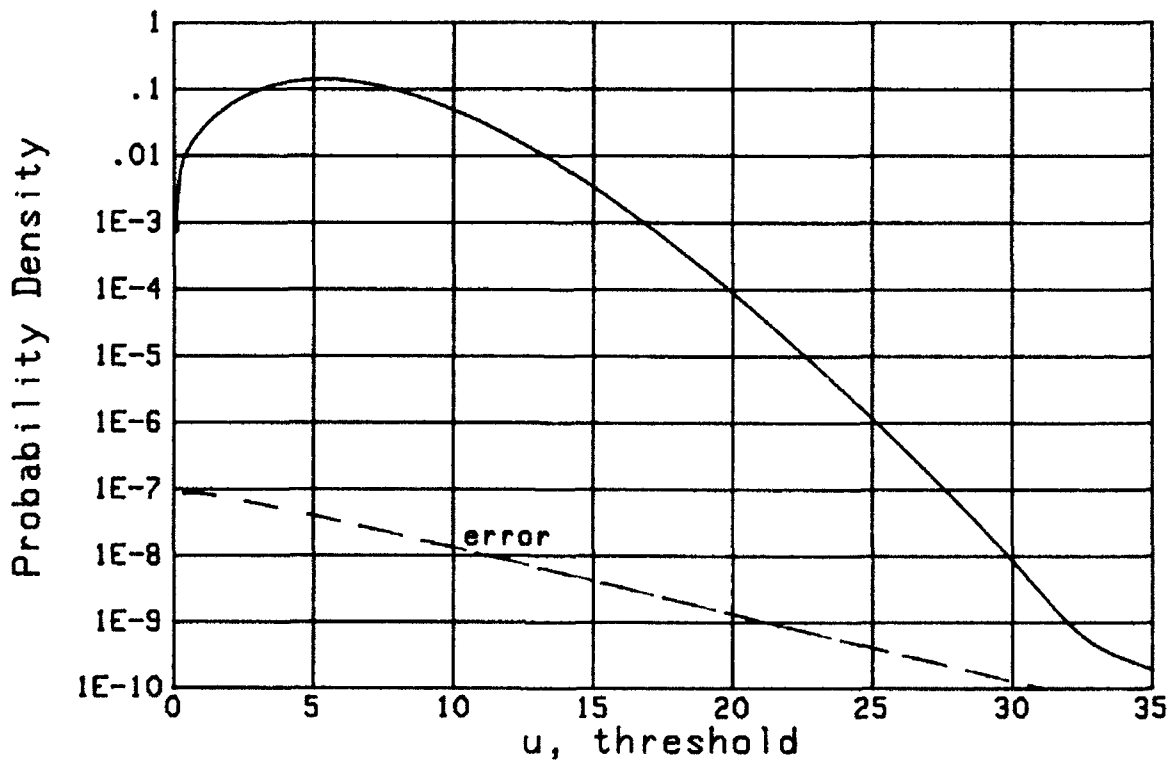


Figure 30. Estimated Error of Figure 22

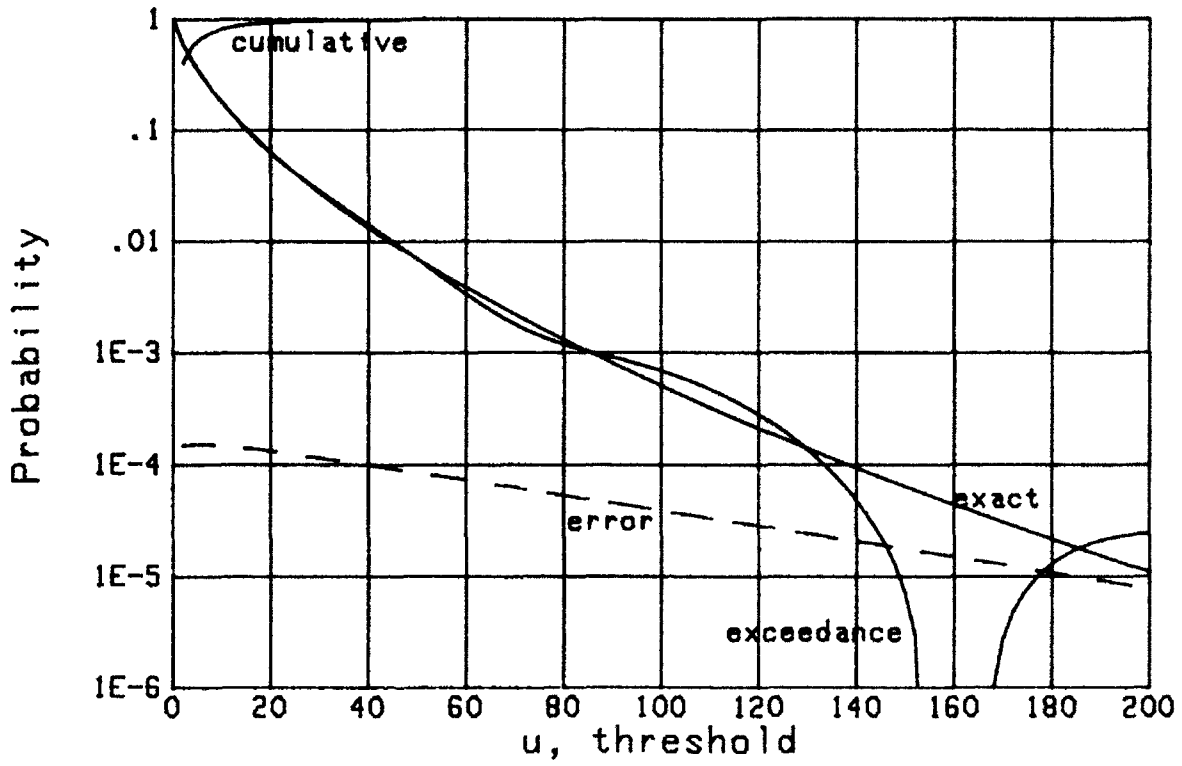


Figure 31. Estimated Error of Figure 24

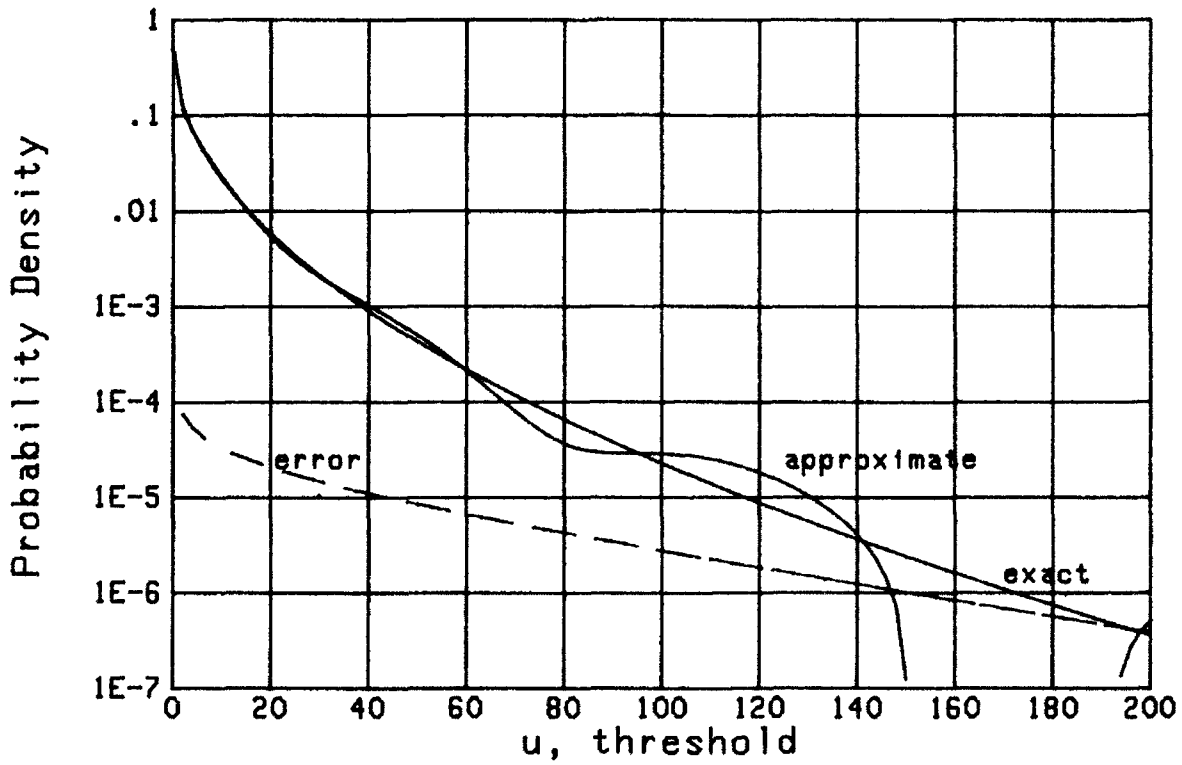


Figure 32. Estimated Error of Figure 26

Finally, the Rice variate of example G is re-considered in figure 33. We took $\text{Env}\{b_n\} \approx 3E-4$ at $n = 65$, by extrapolating in figure 15 from smaller n , since round-off error is becoming significant by this value. It verifies the unreliability of the approximation in figure 33 for $u > 7$.

Although all the examples in this report have the capability of evaluating either the moments or the cumulants via recursion, this is by no means necessary. Any method whatsoever of accurately calculating the starting statistics, be they moments or cumulants, is acceptable. For example, if a random variable with known probability density function q is passed through a complicated nonlinearity g , the moments of the output are given by

$$\mu_n = \int du g^n(u) q(u) . \quad (186)$$

These quantities could be evaluated for $0 \leq n \leq N$ by brute-force numerical procedures if necessary. The limit value N will depend on the accuracy with which g and q can be evaluated; if $g(u) \geq 0$ for all u , these integrals can be accomplished to a high degree of accuracy, thereby allowing large values of N to be employed.

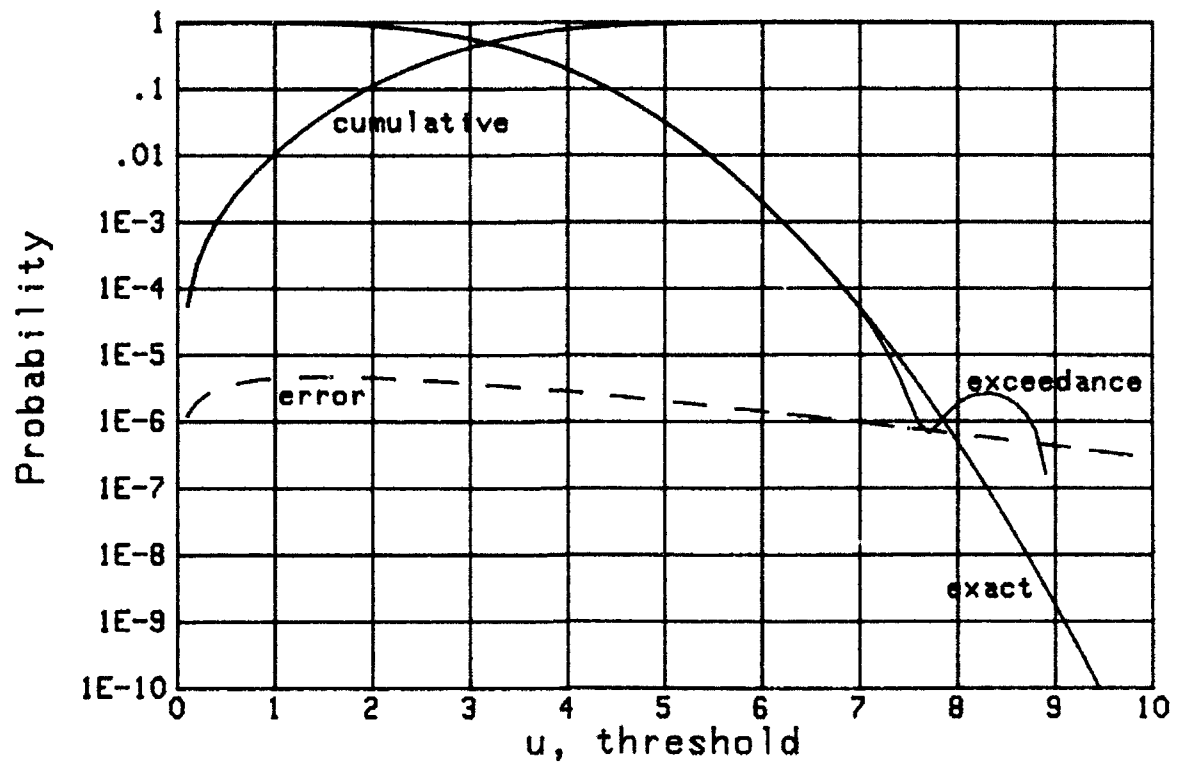


Figure 33. Estimated Error of Figure 16

DISCUSSION

Several alternative methods have been presented for obtaining either Hermite or generalized Laguerre series expansions of probability density functions or cumulative and exceedance distribution functions, by means of recursive relations involving either moments or cumulants. Furthermore, estimates of the errors of the approximations are furnished so that the reliability can be assessed. Comparisons between approximations obtained by either the Hermite or the generalized Laguerre series afford an assessment of the accuracy of each; also, the availability of three alternative recursive procedures for the expansion coefficients allows for selection of the best method and results, and determination of the amount of round-off error.

The key feature to this approach is the rapid calculation and observation of the orthonormal expansion coefficients $\{b_n\}$ for each particular guess of weighting parameters α and β . A trial and error procedure is suggested for determining α and β values that yield the set of fastest-decaying expansion coefficients. From observation of the expansion coefficients, the number of terms to retain in the series expansions is ascertained, being sure to avoid the effects of round-off error which dominates the calculated expansion coefficients $\{b_n\}$ for large n . Since the amount and location of round-off error on the plot of expansion coefficients also depends on α and β , a judicious search may be required to find acceptable weighting parameter values. Of course, a computer with a larger number of significant digits would greatly alleviate this drawback; the particular computer used for all the calculations reported here is the Hewlett-Packard 9000 Model 520 which

devotes 52 bits (15.65 decimal digits) to the mantissa and 11 bits to the exponent. Failure of the technique is indicated by divergence of the expansion coefficient sequence $\{b_n\}$.

Programs for the shot noise process considered in examples D and I are presented in appendix F. Times of execution are as follows. For the Hermite series, the 80 cumulants or 80 moments required as input for figure 7 took .7 or .35 seconds, respectively. The calculation, plotting, and display of the 80 expansion coefficients in figure 7 took 1.6 seconds via the RC approach and 1.75 seconds via the two moment approaches. The computation and display of the 100-point plots of the cumulative distribution function in figure 8 and the probability density function in figure 9, each using 65 terms in the series expansion, took 1.1 and .95 seconds, respectively.

For the generalized Laguerre series, the 70 cumulants or 70 moments required as input for figure 19 took .54 seconds or .28 seconds, respectively. The calculation and display of the 70 expansion coefficients in figure 19 took 1.8 seconds via the RC approach and 1.5 seconds via the two moment approaches. The computation and display of the 100-point plots of the cumulative distribution function in figure 20 and the probability density function in figure 21 took 1.1 and .7 seconds, respectively. These execution times are short enough to allow a human observer to conduct a rapid trial-and-error search of α, β space, determine adequate parameter values, and assess their accuracy.

Alternative exact procedures for determination of cumulative and exceedance distribution functions via characteristic functions have been presented in [9, 10, 11]. Those methods generally have the potential for

greater accuracy, are less subject to round-off-error, and would be preferred if possible. However, analysis of systems with nonlinearities and memory sometimes precludes or greatly hinders their application; in such cases, the current approach is a very good candidate for consideration.

The two weightings in (1) and (2), namely the Hermite and generalized Laguerre, have been investigated rather intensively here, because so many properties and recursions are available for the corresponding (orthonormal) polynomials. These properties have been utilized to derive simple recursive relations for the expansion coefficients and density and distribution functions, thereby realizing quick efficient procedures for numerical evaluation and observation.

It would be extremely useful to be able to extend these results to the weighting

$$u^\alpha \exp(-u^2/\beta^2) \text{ for } u > 0, \quad (187)$$

since this class of probability density functions is often encountered in nonlinear systems with Gaussian inputs. However, there are several pivotal recursive relations for the corresponding orthonormal polynomials that would be needed, and it is questionable if a fast procedure could be devised without them. Also, it is unknown if recursive procedures for the expansion coefficients in terms of moments or cumulants could be derived, as was done here for the Hermite and generalized Laguerre weightings. This is a topic worthy of further investigation.

APPENDIX A. COEFFICIENT RECURSION FOR EXPONENTIAL OF POWER SERIES

Suppose power series $\sum_{n=0}^{\infty} h_n z^n$ converges for some $|z| > 0$, and we exponentiate it, getting a new power series

$$\sum_{n=0}^{\infty} g_n z^n = \exp \left\{ \sum_{n=0}^{\infty} h_n z^n \right\}. \quad (\text{A-1})$$

Then the lowest order coefficient is

$$g_0 = \exp(h_0), \quad (\text{A-2})$$

while for $k \geq 1$, we have

$$\begin{aligned} g_k &= \frac{1}{k!} \left(\frac{d}{dz} \right)^k \left[\exp \left\{ \sum_{n=0}^{\infty} h_n z^n \right\} \right]_{z=0} = \\ &= \frac{1}{k!} \left(\frac{d}{dz} \right)^{k-1} \left[\sum_{n=1}^{\infty} n h_n z^{n-1} \exp \left\{ \sum_{n=0}^{\infty} h_n z^n \right\} \right]_{z=0} = \\ &= \frac{1}{k!} \sum_{p=0}^{k-1} \binom{k-1}{p} \left(\frac{d}{dz} \right)^p \left[\sum_{n=1}^{\infty} n h_n z^{n-1} \right]_{z=0} \left(\frac{d}{dz} \right)^{k-1-p} \left[\exp \left\{ \sum_{n=0}^{\infty} h_n z^n \right\} \right]_{z=0} = \\ &= \frac{1}{k!} \sum_{p=0}^{k-1} \binom{k-1}{p} (p+1)! h_{p+1} (k-1-p)! g_{k-1-p} = \\ &= \frac{1}{k} \sum_{p=0}^{k-1} (p+1) h_{p+1} g_{k-1-p} = \frac{1}{k} \sum_{m=1}^k m h_m g_{k-m}. \end{aligned} \quad (\text{A-3})$$

Thus we have the recursion for coefficients $\{g_k\}$ in terms of the $\{h_m\}$:

$$g_k = \frac{1}{k} \sum_{m=1}^k m h_m g_{k-m} \quad \text{for } k \geq 1, \quad g_0 = \exp(h_0). \quad (\text{A-4})$$

If we now refer to (6) and (7) and identify

$$g_n = \mu_n/n! , \quad h_n = \chi_n/n! , \quad (A-5)$$

there follows the moments in terms of the cumulants according to

$$\mu_k = \sum_{m=0}^{k-1} \binom{k-1}{m} \chi_{k-m} \mu_m \quad \text{for } k \geq 1, \quad \mu_0 = \exp(\chi_0) . \quad (A-6)$$

This is a slight generalization of [6, (10)]. This equation is immediately inverted, to yield the cumulants in terms of moments:

$$\chi_k = \frac{1}{\mu_0} \left[\mu_k - \sum_{m=1}^{k-1} \binom{k-1}{m} \chi_{k-m} \mu_m \right] \quad \text{for } k \geq 1, \quad \chi_0 = \ln \mu_0 , \quad (A-7)$$

which generalizes [6, (11)].

In terms of the normalized cumulants and moments defined in (62) and (69) respectively, we have

$$\hat{\mu}_k = \frac{1}{k} \sum_{m=0}^{k-1} \hat{\chi}_{k-m} \hat{\mu}_m \quad \text{for } k \geq 1, \quad \hat{\mu}_0 = \exp(\chi_0) , \quad (A-8)$$

and

$$\hat{\chi}_k = \frac{1}{\hat{\mu}_0} \left[k \hat{\mu}_k - \sum_{m=1}^{k-1} \hat{\chi}_{k-m} \hat{\mu}_m \right] \quad \text{for } k \geq 1, \quad (\chi_0 = \ln \mu_0) . \quad (A-9)$$

APPENDIX B. EXPANSION OF $He_n(x+y)$

The quantity $He_n(x+y)$ is a polynomial of degree n in y . Therefore we can expand

$$He_n(x+y) = \sum_{m=0}^n \gamma_m \frac{y^m}{m!}, \quad (B-1)$$

where γ_m will also depend on n and x . In fact,

$$\begin{aligned} \gamma_m &= \left(\frac{\partial}{\partial y}\right)^m \left[He_n(x+y) \right]_{y=0} = \left(\frac{\partial}{\partial t}\right)^m \left[He_n(t) \right]_{t=x} = \\ &= \left(\frac{\partial}{\partial t}\right)^{m-1} \left[n He_{n-1}(t) \right]_{t=x} = n(n-1) \dots (n-m+1) He_{n-m}(x) = \\ &= \frac{n!}{(n-m)!} He_{n-m}(x), \end{aligned} \quad (B-2)$$

where we used [5, 22.8.8] repeatedly. Using (B-2) in (B-1), we have the alternative forms for the expansion,

$$\begin{aligned} He_n(x+y) &= \sum_{m=0}^n \binom{n}{m} He_{n-m}(x) y^m = \\ &= \sum_{m=0}^n \binom{n}{m} He_{n-m}(y) x^m = \\ &= \sum_{k=0}^n \binom{n}{k} He_k(y) x^{n-k} \quad \text{for } n \geq 0. \end{aligned} \quad (B-3)$$

APPENDIX C. EVALUATION OF $I_n(y)$ IN (94)

We have, from (94),

$$I_n(y) = \int_0^y dx x^\alpha e^{-x} L_n^{(\alpha)}(x) \quad \text{for } n \geq 0. \quad (\text{C-1})$$

Then

$$I_0(y) = \int_0^y dx x^\alpha e^{-x} 1 = \gamma(\alpha+1, y) = \frac{y^{\alpha+1} e^{-y}}{\alpha+1} {}_1F_1(1; \alpha+2; y), \quad (\text{C-2})$$

using [5, 22.4.7, 6.5.2, and 6.5.12]. Also, we have from [5, 22.11.6],

$$x^\alpha e^{-x} L_n^{(\alpha)}(x) = \frac{1}{n!} \left(\frac{d}{dx} \right)^n \{ e^{-x} x^{\alpha+n} \}. \quad (\text{C-3})$$

Then for $n \geq 1$, (C-1) can be developed as

$$\begin{aligned} I_n(y) &= \int_0^y dx \frac{1}{n!} \left(\frac{d}{dx} \right)^n \{ e^{-x} x^{\alpha+n} \} = \\ &= \frac{1}{n!} \int_0^y d \left(\frac{d}{dx} \right)^{n-1} \{ e^{-x} x^{\alpha+n} \} = \frac{1}{n!} \left(\frac{d}{dy} \right)^{n-1} \{ e^{-y} y^{\alpha+n} \} = \\ &= \frac{1}{n} y^{\alpha+1} e^{-y} L_{n-1}^{(\alpha+1)}(y), \end{aligned} \quad (\text{C-4})$$

where we set the lower limit of the evaluated integral to zero since $\alpha+n \geq \alpha+1 > 0$.

APPENDIX D. FOURIER TRANSFORM OF GENERALIZED LAGUERRE POLYNOMIAL

We wish to evaluate transform

$$A(\omega) = \int_0^{\infty} dt e^{i\omega t} t^{\alpha} e^{-t} L_n^{(\alpha)}(t) . \quad (D-1)$$

Now

$$n! t^{\alpha} e^{-t} L_n^{(\alpha)}(t) = \left(\frac{d}{dt}\right)^n \{e^{-t} t^{\alpha+n}\} \quad \text{for } n \geq 0 , \quad (D-2)$$

according to [5, 22.11.6]. Therefore for $n \geq 1$,

$$\begin{aligned} n! A(\omega) &= \int_0^{\infty} dt e^{i\omega t} \left(\frac{d}{dt}\right)^n \{e^{-t} t^{\alpha+n}\} = \\ &= \int_0^{\infty} e^{i\omega t} d\left(\frac{d}{dt}\right)^{n-1} \{e^{-t} t^{\alpha+n}\} = \\ &= -i\omega \int_0^{\infty} dt e^{i\omega t} \left(\frac{d}{dt}\right)^{n-1} \{e^{-t} t^{\alpha+n}\} , \end{aligned} \quad (D-3)$$

where we used integration by parts with the fact that the integrated part is zero at $t = 0$ and ∞ , since $\alpha+n \geq \alpha+1 > 0$. Repeated integration by parts then yields

$$n! A(\omega) = (-i\omega)^n \int_0^{\infty} dt e^{i\omega t} e^{-t} t^{\alpha+n} = \Gamma(\alpha+1+n) \frac{(-i\omega)^n}{(1-i\omega)^{\alpha+1+n}} . \quad (D-4)$$

This is the result quoted in (104).

APPENDIX E. RECURRENCE FOR EXAMPLE C

The starting point is the moment expression in (142):

$$\mu_n = \omega \frac{e^{\gamma} \Gamma\left(\frac{n}{2}+h\right) \omega^{n+2h}}{2^{\gamma+1} \Gamma(\gamma+1)} {}_1F_1\left(\frac{n}{2}+h; \gamma+1; z\right), \quad (E-1)$$

where $h = (\gamma + \gamma + 1)/2$, $z = \omega^2 \theta^2/4$. Denote the ${}_1F_1$ term in (E-1) by F_n , and the leading factor by G_n ; thus $\mu_n = G_n F_n$. There follows immediately

$$G_n = G_{n-2} \omega^2 \left(\frac{n}{2}+h-1\right) \quad \text{for } n \geq 2. \quad (E-2)$$

For the ${}_1F_1$ function, we refer to [5, 13.4.1] to get

$$F_n = \frac{1}{\frac{n}{2}+h-1} \left[(n+2h-3-\gamma+z) F_{n-2} + \left(\gamma+2-\frac{n}{2}-h\right) F_{n-4} \right]. \quad (E-3)$$

If we substitute (E-2) and (E-3) into $\mu_n = G_n F_n$, and then re-apply (E-2) in the second term, we obtain

$$\mu_n = \omega^2 (n+\gamma-2+z) \mu_{n-2} - \frac{1}{4} \omega^4 \left[(n+\gamma-3)^2 - \gamma^2 \right] \mu_{n-4}; \quad (E-4)$$

we also eliminated h . Starting values for μ_n can be obtained from (E-1).

For the special case (143) and (144), (E-4) reduces to

$$\mu_n = \omega^2 (n-1+z) \mu_{n-2} - \frac{1}{4} \omega^4 (n-2)^2 \mu_{n-4}, \quad (E-5)$$

with starting values

$$\begin{aligned} \mu_0 &= 1, \quad \mu_1 = \frac{1}{2} \pi^{1/2} \omega e^{-z} {}_1F_1\left(\frac{3}{2}; 1; z\right), \\ \mu_2 &= \omega^2(1+z), \quad \mu_3 = \frac{3}{4} \pi^{1/2} \omega^3 e^{-z} {}_1F_1\left(\frac{5}{2}; 1; z\right). \end{aligned} \quad (\text{E-6})$$

Kummer's transformation [5, 13.1.27] was employed in this last equation; these forms afford accurate starting values for recursion (E-5).

APPENDIX F. PROGRAM LISTINGS

Eight programs are listed in this appendix. They are given in BASIC for the Hewlett Packard 9000 Model 520 computer. For ease of reference, a shorthand notation is adopted:

P	denotes	cumulative or exceedance distribution function
p	denotes	probability density function
H	denotes	Hermite expansion
L	denotes	generalized Laguerre expansion
RC	denotes	recursively via cumulants
DM	denotes	directly via moments
RM	denotes	recursively via moments

Table F-1. Shorthand Notation

Then, for example, the combination PHRC means that this program yields the cumulative or exceedance distribution function in terms of a Hermite expansion, by means of expansion coefficients determined recursively via cumulants. The eight programs listed here are, in order,

PHRC	Figures 7 and 8
pHRC	Figures 7, 9, and 10
PHDMandRM	Figures 7 (and 8)
pHDMandRM	Figures 7 (and 9, 10)
PLRC	Figures 19 and 20
pLRC	Figures 19, 21, and 22
PLDMandRM	Figures 19 (and 20)
pLDMandRM	Figures 19 (and 21, 22)

Table F-2. Program Abbreviations

The combination DMandRM means that this program gives the expansion coefficients directly via moments as well as recursively via moments; the user must select the procedure of interest.

The only input statistics we have given a listing for here is the shot noise process used in examples D and I; in particular, the cumulant and moment routines are listed at the very end of PHRC and PHDMandRM, respectively. The figure references given in table F-2 indicate where each particular program was used in this report; the parenthetical references are alternative ways of generating those figures. The remaining figures in this report require that the cumulant and moment subroutines be replaced by the appropriate statistics of interest.

To save space, no subroutines are listed more than once; instead, comments are made indicating where the needed routines are located, according to the coding in table F-2. For example, in program PHDMandRM, function subprogram FNPhi, line 570, the comment is made that this routine has already been listed in PHRC.

We now explain some of the details of the PHRC program, as an example, so that a user can apply these techniques and routines to his particular problem. The user must specify M in line 30, which is the maximum order of approximation desired, or the number of cumulants or moments that can be calculated. The notation DOUBLE in line 40 denotes INTEGER variables. The user must select α and β in lines 130,140; if they are chosen equal to α_0, β_0 which have been computed in lines 110,120, then expansion coefficients $a_1 = a_2 = 0$, or equivalently $b_1 = b_2 = 0$. However, this choice is recommended only as a starter on the search in α, β space.

The CALL in line 150 is to the subroutine which calculates the expansion coefficients for a Hermite series, recursively via cumulants, as can be deciphered from the abbreviated subroutine title. The expansion coefficients $\{b_n\}$ are calculated and the running sum of b_n^2 is calculated, both of which are printed on the CRT vs n . Also, a plot of the expansion coefficients $\{b_n\}$ is made in this subroutine, from which the user must decide on the order, N , to employ in the approximate cumulative and exceedance distribution function; alternatively, he can reject the sequence of $\{b_n\}$ so obtained, and re-run the program with different α, β values.

When a satisfactory α, β pair is obtained, the limits u_1, u_2 on the range of arguments of the distribution must also be specified; this selection is aided by the print-out of the center and rms width of the density under investigation. A plot of 100 values of the cumulative and exceedance distribution functions is then made on a logarithmic ordinate. The various subroutines are self-explanatory and are keyed to the equation numbers in this report.

PROGRAM PHRC

```

10 ! STEP PLUS CONTINUOUS PART OF SHOT NOISE CDF, P<U> TR 7377, FIGURE 8
20 ! COEFFICIENTS OF HERMITE EXPANSION FOUND RECURSIVELY VIA CUMULANTS
30 N=80 ! MAXIMUM ORDER OF APPROXIMATION; NUMBER OF CUMULANTS REQUIRED
40 DOUBLE M,I,N,K ! INTEGERS < 2^31 = 2,147,483,648
50 REDIM Cum(0:M),A(0:M),He(0:M)
60 REAL Cum(0:100),A(0:100),He(0:100),P(0:100)
70 CALL Cumulants(M,P0,Cum(*)) ! P0 IS STEP AT ORIGIN
80 Center=Cum(1) ! CENTER OF PDF p<u>
90 R2=Cum(2) ! MEAN SQUARE SPREAD OF p<u>
100 Rms=SQR(R2) ! RMS SPREAD OF p<u>
110 Alpha0=Center ! THE CHOICES Alpha=Alpha0 AND
120 Beta0=Rms ! Beta=Beta0 WOULD MAKE A(1)=A(2)=0
130 Alpha=Center
140 Beta=Rms*1.5
150 CALL Coeffhr_via_cum(M,Alpha,Beta,Cum(*),A(*)) ! RC
160 PRINT "Center = ";Center
170 PRINT "Rms = ";Rms
180 F1=1./SQR(2.*PI)
190 INPUT "ORDER AND LIMITS:",N,U1,U2
200 PRINT "ORDER AND LIMITS:",N;U1;U2
210 Du=(U2-U1)/100.
220 PLOTTER IS "GRAPHICS"
230 GRAPHICS ON
240 WINDOW U1,U2,-10.,0.
250 GRID Du*10.,1.
260 FOR I=0 TO 100
270 U=U1+Du*I
280 T=(U-Alpha)/Beta
290 CALL Pte(N,T,He(*))
300 Sum=0.
310 FOR K=1 TO N
320 Sum=Sum+A(K)*He(K-1)
330 NEXT K
340 P=A(0)*FNPhi(T)-F1*EXP(-.5*T*T)*Sum ! PROBABILITY THAT RV < U
350 IF U>=0. THEN P=P+P0 ! ADDITION OF STEP AT ORIGIN
360 P(I)=P
370 IF P>0. THEN 400
380 PENUP
390 GOTO 410
400 PLOT U,LGT(P)
410 NEXT I
420 PENUP
430 FOR I=0 TO 100
440 U=U1+Du*I
450 P1=1.-P(I)
460 IF P1>0. THEN 490
470 PENUP
480 GOTO 500
490 PLOT U,LGT(P1)
500 NEXT I
510 PENUP
520 GOTO 190
530 END
540 !

```

PROGRAM PHRC (cont'd)

```

550   DEF FNPhi(X)           ! HART, page 140, #5708 & #5725           eq. 41
560   Y=ABS(SQR(.5)*X)
570   SELECT Y
580   CASE <8.
590   P=1631.76026875371470+Y*(456.261458706092631+Y*(86.0827622119485951+Y*
(10.0648589749095425+Y*.564189586761813614)))
600   P=3723.50798155480672+Y*(7113.66324695404987+Y*(6758.21696411048589+Y*
(4032.26701083004974+Y*P)))
610   Q=7542.47951019347576+Y*(2968.00490148230872+Y*(817.622386304544077+Y*
(153.077710750362216+Y*(17.8394984391395565+Y))))
620   Q=3723.50798155480654+Y*(11315.1920818544055+Y*(15802.5359994020425+Y*
(13349.3465612844574+Y*Q)))
630   Phi=.5*EXP(-Y*Y)*P/Q
640   CASE <26.6
650   P=2.97886562639399289+Y*(7.40974060596474179+Y*(6.16020985310963054+Y*
(5.01904972678426746+Y*(1.27536664472996595+Y*.564189583547755074))))
660   Q=3.36907520698275277+Y*(9.60896532719278787+Y*(17.0814407474660043+Y*
(12.0489519278551290+Y*(9.39603401623505415+Y*(2.26052852076732697+Y))))))
670   Phi=.5*EXP(-Y*Y)*P/Q
680   CASE ELSE
690   Phi=0.
700   END SELECT
710   IF X>0. THEN Phi=1.-Phi
720   RETURN Phi
730   FNEND
740   !
750   SUB Hermite(DOUBLE N,REAL X,He(*))           ! He/n(X)           eq. 50
760   DOUBLE K
770   He(0)=1.
780   He(1)=X
790   FOR K=2 TO N
800   He(K)=X*He(K-1)-(K-1)*He(K-2)
810   NEXT K
820   SUBEND
830   !
840   SUB Momnt_via_cumnt(DOUBLE M,REAL Cum(*),Mom(*))           ! eq. A-6
850   DOUBLE K,J
860   REAL Mom0
870   Mom(0)=Mom0=EXP(Cum(0))
880   FOR K=1 TO M
890   T=1.
900   S=Cum(K)*Mom0
910   FOR J=1 TO K-1
920   T=T*(K-J)/J
930   S=S+T*Cum(K-J)*Mom(J)
940   NEXT J
950   Mom(K)=S
960   NEXT K
970   SUBEND
980   !

```

PROGRAM PHRC (cont'd)

```

990   SUB Cumnt_via_momnt(DOUBLE M,REAL Mom(*),Cum(*))           !   eq. A-7
1000  DOUBLE K,J
1010  REAL Mom0
1020  Mom0=Mom(0)
1030  Cum(0)=LOG(Mom0)
1040  FOR K=1 TO M
1050  T=1.
1060  S=Mom(K)
1070  FOR J=1 TO K-1
1080  T=T*(K-J)/J
1090  S=S-T*Mom(J)*Cum(K-J)
1100  NEXT J
1110  Cum(K)=S/Mom0
1120  NEXT K
1130  SUBEND
1140  !
1150  SUB Coeffhr_via_cum(DOUBLE M,REAL Alpha,Beta,Cum(*),A(*))
1160  ALLOCATE B(0:M)
1170  DOUBLE K,J,Mx
1180  F=Beta*Beta
1190  Cum(1)=(Cum(1)-Alpha)/Beta           !   MODIFIED NORMALIZED
1200  Cum(2)=Cum(2)/F-1.                 !   CUMULANTS FOR K=1 & 2; eq. 63
1210  FOR K=3 TO M
1220  F=F*Beta*(K-1)
1230  Cum(K)=Cum(K)/F                   !   NORMALIZED CUMULANTS; eq. 62
1240  NEXT K
1250  A(0)=B(0)=EXP(Cum(0))
1260  F=1.
1270  FOR K=1 TO M
1280  S=0.
1290  FOR J=1 TO K
1300  S=S+Cum(J)*A(K-J)
1310  NEXT J
1320  A(K)=S/K
1330  F=F*K
1340  B(K)=A(K)*SQRT(F)
1350  NEXT K
1360  Mx=Mx+10
1370  IF Mx<M THEN 1360
1380  Threshold=-7.
1390  T2=Threshold*2.
1400  V=10.^Threshold
1410  GINIT
1420  PLOTTER IS "GRAPHICS"
1430  GRAPHICS ON
1440  WINDOW 0.,FLT(Mx),T2,0.
1450  LINE TYPE 3

```

PROGRAM PHRC (cont'd)

```

1460   FOR J=0 TO Mx STEP 10
1470   MOVE J,T2
1480   DRAW J,0.
1490   NEXT J
1500   FOR J=T2 TO 0
1510   MOVE 0.,J
1520   DRAW Mx,J
1530   NEXT J
1540   PENUP
1550   LINE TYPE 1
1560   IMAGE 4D,2(4X,M.17DE)
1570   PRINT "   K           B(K)           Sum"
1580   Sum=0.
1590   FOR K=0 TO M
1600   B=B(K)
1610   Sum=Sum+B*B
1620   PRINT USING 1560;K,B,Sum
1630   IF B<V THEN 1660
1640   Y=LGT(B)
1650   GOTO 1700
1660   IF B>-V THEN 1690
1670   Y=T2-LGT(-B)
1680   GOTO 1700
1690   Y=Threshold
1700   PLOT K,Y
1710   NEXT K
1720   PENUP
1730   SUBEND
1740   !
1750   SUB Cumulants(DOUBLE M,REAL P0,Cum(*)) ! SHOT NOISE eqs. 147-150
1760   Overlap=6.2 ! AV. NO. PULSES/SEC * AVERAGE PULSE DURATION
1770   Sigmaa=1. ! PARAMETER OF RAYLEIGH AMPLITUDE PDF
1780   P0=EXP(-Overlap) ! PROBABILITY OF ZERO AMPLITUDE OF SHOT NOISE
1790   ALLOCATE Mom(0:M) ! ARRAY FOR MOMENTS
1800   DOUBLE K
1810   S=Sigmaa*Sigmaa
1820   Cum(0)=0.
1830   Cum(1)=Overlap*Sigmaa*.25*PI*SQR(.5*PI)
1840   Cum(2)=Overlap*S*4./3.
1850   FOR K=3 TO M
1860   Cum(K)=Cum(K-2)*S*K*K/(K+1)
1870   NEXT K
1880   CALL Momnt_via_cumnt(M,Cum(*),Mom(*))
1890   Mom(0)=Mom(0)-P0 ! MOMENT CORRECTION FOR IMPULSE AT ORIGIN
1900   CALL Cumnt_via_momnt(M,Mom(*),Cum(*))
1910   SUBEND

```

PROGRAM PHRC

```

10 ! CONTINUOUS PART OF SHOT NOISE PDF, pc(u)          TR 7377, FIGURE 9
20 ! COEFFICIENTS OF HERMITE EXPANSION FOUND RECURSIVELY VIA CUMULANTS
30 M=80 ! MAXIMUM ORDER OF APPROXIMATION; NUMBER OF CUMULANTS REQUIRED
40 DOUBLE M,I,N,K ! INTEGERS < 2^31 = 2,147,483,648
50 REDIM Cum(0:M),A(0:M),He(0:M)
60 REAL Cum(0:100),A(0:100),He(0:100)
70 CALL Cumulants(M,P0,Cum(*)) ! P0 IS STEP AT ORIGIN
80 Center=Cum(1) ! CENTER OF PDF pc(u)
90 R2=Cum(2) ! MEAN SQUARE SPREAD OF pc(u)
100 Rms=SQR(R2) ! RMS SPREAD OF pc(u)
110 Alpha0=Center ! THE CHOICES Alpha=Alpha0 AND
120 Beta0=Rms ! Beta=Beta0 WOULD MAKE A(1)=A(2)=0
130 Alpha=Center
140 Beta=Rms*1.5
150 CALL Coeffhr_via_cum(M,Alpha,Beta,Cum(*),A(*)) ! RC
160 PRINT "Center = ";Center
170 PRINT "Rms = ";Rms
180 F1=1./((Beta*SQR(2.*PI)))
190 INPUT "ORDER AND LIMITS: ",N,U1,U2
200 PRINT "ORDER AND LIMITS: ",N;U1;U2
210 Du=(U2-U1)/100.
220 PLOTTER IS "GRAPHICS"
230 GRAPHICS ON
240 WINDOW U1,U2,0.,.15
250 GRID 6.,.03
260 FOR I=0 TO 100
270 U=U1+Du*I
280 T=(U-Alpha)/Beta
290 CALL Hermite(N,T,He(*))
300 Sum=A(0)
310 FOR K=1 TO N
320 Sum=Sum+A(K)*He(K)
330 NEXT K
340 P=F1*EXP(-.5*T*T)*Sum ! PDF OF RV AT U
350 PLOT U,P
360 NEXT I
370 PENUP
380 GOTO 190
390 END
400 ! USE ROUTINES IN PHRC

```

PROGRAM PHDMandRM

```

10 ! STEP PLUS CONTINUOUS PART OF SHOT NOISE CDF, Pc(u); COEFFICIENTS OF
20 ! HERMITE EXPANSION FOUND DIRECTLY VIA MOMENTS OR RECURSIVELY VIA MOMENTS
30 M=80 ! MAXIMUM ORDER OF APPROXIMATION; NUMBER OF MOMENTS REQUIRED
40 DOUBLE M,I,N,K ! INTEGERS < 2^31 = 2,147,483,648
50 REDIM Mom(0:M),A(0:M),He(0:M)
60 REAL Mom(0:100),A(0:100),He(0:100),P(0:100)
70 CALL Moments(M,P0,Mom(*)) ! P0 IS STEP AT ORIGIN
80 Center=Mom(1)/Mom(0) ! CENTER OF PDF pc(u)
90 R2=Mom(2)/Mom(0)-Center*Center ! MEAN SQUARE SPREAD OF pc(u)
100 Rms=SQR(R2) ! RMS SPREAD OF pc(u)
110 Alpha0=Center ! THE CHOICES Alpha=Alpha0 AND
120 Beta0=Rms ! Beta=Beta0 WOULD MAKE A(1)=A(2)=0
130 Alpha=Center
140 Beta=Rms*1.5
150 CALL Coeffhd_via_mom(M,Alpha,Beta,Mom(*),A(*)) ! DM
160 ! CALL Coeffhr_via_mom(M,Alpha,Beta,Mom(*),A(*)) ! RM
170 PRINT "Center = ";Center
180 PRINT "Rms = ";Rms
190 F1=1./SQR(2.*PI)
200 INPUT "ORDER AND LIMITS: ",N,U1,U2
210 PRINT "ORDER AND LIMITS: ",N;U1;U2
220 Du=(U2-U1)/100.
230 PLOTTER IS "GRAPHICS"
240 GRAPHICS ON
250 WINDOW U1,U2,-10.,0.
260 GRID Du*10.,1.
270 FOR I=0 TO 100
280 U=U1+Du*I
290 T=(U-Alpha)/Beta
300 CALL Hermite(N,T,He(*))
310 Sum=0.
320 FOR K=1 TO N
330 Sum=Sum+A(K)*He(K-1)
340 NEXT K
350 P=A(0)*FNPhi(T)-F1*EXP(-.5*T*T)*Sum ! PROBABILITY THAT RV < U
360 IF U>=0. THEN P=P+P0 ! ADDITION OF STEP AT ORIGIN
370 P(I)=P
380 IF P>0. THEN 410
390 PENUP
400 GOTO 420
410 PLOT U,LGT(P)
420 NEXT I
430 PENUP
440 FOR I=0 TO 100
450 U=U1+Du*I
460 P1=1.-P(I)
470 IF P1>0. THEN 500
480 PENUP
490 GOTO 510
500 PLOT U,LGT(P1)
510 NEXT I
520 PENUP
530 GOTO 200
540 END
550 !

```


PROGRAM PHDMandRM (cont'd)

```

560   DEF FNPhi(X)           ! HART, page 140, #5708 & #5725
570   ! LISTED IN PHRC
740   FNEND
750   !
760   SUB Hermite(DOUBLE N,REAL X,He(*)) ! He/n(X)
770   ! LISTED IN PHRC
830   SUBEND
840   !
850   SUB Hermite_i(DOUBLE N,REAL X,Hi(*)) ! Hi/n(X)=(-i)^n He/n(iX) eq.74-5
860   DOUBLE K           ! MODIFIED HERMITE POLYNOMIALS
870   Hi(0)=1.
880   Hi(1)=X
890   FOR K=2 TO N
900   Hi(K)=X*Hi(K-1)+(K-1)*Hi(K-2)
910   NEXT K
920   SUBEND
930   !
940   SUB Momnt_via_cumnt(DOUBLE M,REAL Cum(*),Mom(*))
950   ! LISTED IN PHRC
1070  SUBEND
1080  !
1090  SUB Coeffhd_via_mom(DOUBLE M,REAL Alpha,Beta,Mom(*),A(*))
1100  ALLOCATE He(0:M),F(0:M),B(0:M)
1110  DOUBLE K,J,Mx
1120  CALL Hermite(M,-Alpha/Beta,He(*))
1130  T=F(0)=1.
1140  FOR K=1 TO M
1150  F=F(K)=F(K-1)*K
1160  T=T*Beta
1170  He(K)=He(K)/F           ! NORMALIZED HERMITE POLYNOMIALS; eq. 68
1180  Mom(K)=Mom(K)/(F*T)    ! NORMALIZED MOMENTS re Beta; eq. 69
1190  NEXT K
1200  FOR K=0 TO M
1210  S=0.
1220  FOR J=0 TO K
1230  S=S+He(J)*Mom(K-J)
1240  NEXT J
1250  A(K)=S
1260  NEXT K
1270  MAT F=SQR(F)
1280  MAT B=A.F
1290  Mx=Mx+10
1300  IF Mx<M THEN 1290
1310  Threshold=-7.
1320  T2=Threshold*2.
1330  V=10.^Threshold
1340  GINIT
1350  PLOTTER IS "GRAPHICS"
1360  GRAPHICS ON
1370  WINDOW 0.,FLT(Mx),T2,0.
1380  LINE TYPE 3

```

PROGRAM PHDMandRM (cont'd)

```

1390   FOR J=0 TO Mx STEP 10
1400   MOVE J,T2
1410   DRAW J,0.
1420   NEXT J
1430   FOR J=T2 TO 0
1440   MOVE 0.,J
1450   DRAW Mx,J
1460   NEXT J
1470   PENUP
1480   LINE TYPE 1
1490   IMAGE 4D,2(4X,M.17DE)
1500   PRINT "    K           B(K)           Sum"
1510   Sum=0.
1520   FOR K=0 TO M
1530   B=B(K)
1540   Sum=Sum+B*B
1550   PRINT USING 1490;K,B,Sum
1560   IF B<Y THEN 1590
1570   Y=LGT(B)
1580   GOTO 1630
1590   IF B>-Y THEN 1620
1600   Y=T2-LGT(-B)
1610   GOTO 1630
1620   Y=Threshold
1630   PLOT K,Y
1640   NEXT K
1650   PENUP
1660   SUBEND
1670   !
1680   SUB Coeffhr_via_mom(DOUBLE M,REAL Alpha,Beta,Mom(*),A(*))
1690   ALLOCATE Hi(0:M),F(0:M),B(0:M)
1700   DOUBLE K,J,Mx
1710   CALL Hermite_i(M,Alpha/Beta,Hi(*))
1720   T=F(0)=1.
1730   FOR K=1 TO M
1740   F=F(K)=F(K-1)*K
1750   T=T*Beta
1760   Hi(K)=Hi(K)/F ! NORMALIZED MODIFIED HERMITE POLYNOMIALS; eqs. 80 & 74
1770   Mom(K)=Mom(K)/(F*T) ! NORMALIZED MOMENTS re Beta; eq. 69
1780   NEXT K
1790   FOR K=0 TO M
1800   S=Mom(K)
1810   FOR J=1 TO K
1820   S=S-Hi(J)*A(K-J)
1830   NEXT J
1840   A(K)=S
1850   NEXT K
1860   MAT F=SQR(F)
1870   MAT B=A.F

```

PROGRAM PHDMandRM (cont'd)

```

1880   Mx=Mx+10
1890   IF Mx<M THEN 1880
1900   Threshold=-7.
1910   T2=Threshold*2.
1920   V=10.^Threshold
1930   GINIT
1940   PLOTTER IS "GRAPHICS"
1950   GRAPHICS ON
1960   WINDOW 0.,FLT(Mx),T2,0.
1970   LINE TYPE 3
1980   FOR J=0 TO Mx STEP 10
1990   MOVE J,T2
2000   DRAW J,0.
2010   NEXT J
2020   FOR J=T2 TO 0
2030   MOVE 0.,J
2040   DRAW Mx,J
2050   NEXT J
2060   PENUP
2070   LINE TYPE 1
2080   IMAGE 4D,2(4X,M.17DE)
2090   PRINT "      K          B(K)          Sum"
2100   Sum=0.
2110   FOR K=0 TO M
2120   B=B(K)
2130   Sum=Sum+B*B
2140   PRINT USING 2080;K,B,Sum
2150   IF B<V THEN 2180
2160   Y=LGT(B)
2170   GOTO 2220
2180   IF B>-V THEN 2210
2190   Y=T2-LGT(-B)
2200   GOTO 2220
2210   Y=Threshold
2220   PLOT K,Y
2230   NEXT K
2240   PENUP
2250   SUBEND
2260   !
2270   SUB Moments(DOUBLE M,REAL P0,Cum(*) ) ! SHOT NOISE eqs. 147-150
2280   Overlap=6.2 ! AV. NO. PULSES/SEC * AVERAGE PULSE DURATION
2290   Sigmaa=1. ! PARAMETER OF RAYLEIGH AMPLITUDE PDF
2300   P0=EXP(-Overlap) ! PROBABILITY OF ZERO AMPLITUDE OF SHOT NOISE
2310   ALLOCATE Cum(0:M) ! ARRAY FOR CUMULANTS
2320   DOUBLE K
2330   S=Sigmaa*Sigmaa
2340   Cum(0)=0.
2350   Cum(1)=Overlap*Sigmaa*.25*PI*SQR(.5*PI)
2360   Cum(2)=Overlap*S*4./3.
2370   FOR K=3 TO M
2380   Cum(K)=Cum(K-2)*S*K*K/(K+1)
2390   NEXT K
2400   CALL Momnt_via_cumnt(M,Cum(*),Mom(*))
2410   Mom(0)=Mom(0)-P0 ! MOMENT CORRECTION FOR IMPULSE AT ORIGIN
2420   SUBEND

```

PROGRAM pHDMandRM

```

10 ! CONTINUOUS PART OF SHOT NOISE PDF, pc(u); COEFFICIENTS OF HERMITE
20 ! EXPANSION FOUND DIRECTLY VIA MOMENTS OR RECURSIVELY VIA MOMENTS
30 M=80 ! MAXIMUM ORDER OF APPROXIMATION; NUMBER OF MOMENTS REQUIRED
40 DOUBLE M,I,N,K ! INTEGERS < 2^31 = 2,147,483,648
50 REDIM Mom(0:M),A(0:M),He(0:M)
60 REAL Mom(0:100),A(0:100),He(0:100)
70 CALL Moments(M,P0,Mom(*)) ! P0 IS STEP AT ORIGIN
80 Center=Mom(1)/Mom(0) ! CENTER OF PDF pc(u)
90 R2=Mom(2)/Mom(0)-Center*Center ! MEAN SQUARE SPREAD OF pc(u)
100 Rms=SQR(R2) ! RMS SPREAD OF pc(u)
110 Alpha0=Center ! THE CHOICES Alpha=Alpha0 AND
120 Beta0=Rms ! Beta=Beta0 WOULD MAKE A(1)=A(2)=0
130 Alpha=Center
140 Beta=Rms*1.5
150 CALL Coeffhd_via_mom(M,Alpha,Beta,Mom(*),A(*)) ! DM
160 ! CALL Coeffhr_via_mom(M,Alpha,Beta,Mom(*),A(*)) ! RM
170 PRINT "Center = ";Center
180 PRINT "Rms = ";Rms
190 F1=1./(Beta*SQR(2.*PI))
200 INPUT "ORDER AND LIMITS: ",N,U1,U2
210 PRINT "ORDER AND LIMITS: ",N;U1;U2
220 Du=(U2-U1)/100.
230 PLOTTER IS "GRAPHICS"
240 GRAPHICS ON
250 WINDOW U1,U2,0.,.15
260 GRID 6.,.03
270 FOR I=0 TO 100
280 U=U1+Du*I
290 T=(U-Alpha)/Beta
300 CALL Hermite(N,T,He)
310 Sum=A(0)
320 FOR K=1 TO N
330 Sum=Sum+A(K)*He(K)
340 NEXT K
350 P=F1*EXP(-.5*T*T)*Sum ! PDF OF RV AT U
360 PLOT U,P
370 NEXT I
380 PENUP
390 GOTO 200
400 END
410 ! USE ROUTINES IN PHDM&RM

```

PROGRAM PLRC

```

10 ! STEP PLUS CONTINUOUS PART OF SHOT NOISE CDF, Pc(u); TR 7377, FIGURE 20
20 ! COEFFICIENTS OF GEN. LAGUERRE EXPANSION FOUND RECURSIVELY VIA CUMULANTS
30 M=70 ! MAXIMUM ORDER OF APPROXIMATION; NUMBER OF CUMULANTS REQUIRED
40 DOUBLE M,I,N,K ! INTEGERS < 2^31 = 2,147,483,648
50 REDIM Cum(0:M),A(0:M),L(0:M)
60 REAL Cum(0:100),A(0:100),L(0:100),P(0:100)
70 CALL Cumulants(M,P0,Cum(*)) ! P0 IS STEP AT ORIGIN
80 Center=Cum(1) ! CENTER OF PDF pc(u)
90 R2=Cum(2) ! MEAN SQUARE SPREAD OF pc(u)
100 Rms=SQR(R2) ! RMS SPREAD OF pc(u)
110 Alpha0=Center*Center/R2-1. ! THE CHOICES Alpha=Alpha0 AND
120 Beta0=R2/Center ! Beta=Beta0 WOULD MAKE A(1)=A(2)=0
130 Alpha=.74
140 Beta=2.1
150 CALL Coeffln_via_cum(M,Alpha,Beta,Cum(*),A(*)) ! RC
160 PRINT "Center = ";Center
170 PRINT "Rms = ";Rms
180 A1=Alpha+1.
190 O1=1./A1
200 F1=1./FNGamma(A1)
210 INPUT "ORDER AND LIMITS: ",N,U1,U2
220 PRINT "ORDER AND LIMITS: ",N;U1;U2
230 Du=(U2-U1)/100.
240 PLOTTER IS "GRAPHICS"
250 GRAPHICS ON
260 WINDOW U1,U2,-11.,0.
270 GRID 4.,1.
280 P(0)=P0
290 PLOT 0.,LGT(P0)
300 FOR I=1 TO 100
310 U=U1+Du*I
320 T=U/Beta
330 CALL Laguerre(N-1,A1,T,L(*))
340 Sum=A(0)*FNF1(A1,T)*O1
350 FOR K=1 TO N
360 Sum=Sum+A(K)*L(K-1)/K
370 NEXT K
380 P(I)=P=F0+F1*EXP(-T+A1*LOG(T))*Sum ! PROBABILITY THAT RV < U
390 IF P>0. THEN 420
400 PENUP
410 GOTO 430
420 PLOT U,LGT(P)
430 NEXT I
440 PENUP
450 FOR I=0 TO 100
460 U=U1+Du*I
470 P1=1.-P(I)
480 IF P1>0. THEN 510
490 PENUP
500 GOTO 520
510 PLOT U,LGT(P1)
520 NEXT I
530 PENUP
540 GOTO 210
550 END
560 !

```

PROGRAM PLRC (cont'd)

```

570 DEF FNGamma(X) ! Gamma(X) via HART, page 282, #5243 eq. 2
580 DOUBLE N,K
590 N=INT(X)
600 R=X-N
610 IF N>0 OR R<>0. THEN 640
620 PRINT "FNGamma(X) IS NOT DEFINED FOR X = ";X
630 STOP
640 IF R>0. THEN 670
650 Gamma2=1.
660 GOTO 740
670 P=439.330444060025676+R*(50.1086937529709530+R*6.74495072459252899)
680 P=8762.71029785214896+R*(2008.52740130727912+R*P)
690 P=42353.6895097440896+R*(20886.8617892698874+R*P)
700 Q=499.028526621439048-R*(189.498234157028016-R*(23.081551524580125-R))
710 Q=9940.30741508277090-R*(1528.60727377952202+R*Q)
720 Q=42353.6895097440900+R*(2980.38533092566499-R*Q)
730 Gamma2=F/Q ! Gamma(2+R) for R < 1
740 IF N>2 THEN 780
750 IF N<2 THEN 830
760 Gamma=Gamma2
770 RETURN Gamma
780 Gamma=Gamma2
790 FOR K=1 TO N-2
800 Gamma=Gamma*(X-K)
810 NEXT K
820 RETURN Gamma
830 R=1.
840 FOR K=0 TO 1-N
850 R=R*(X+K)
860 NEXT K
870 Gamma=Gamma2/R
880 RETURN Gamma
890 FNEND
900 !
910 DEF FNF1(A1,X) ! 1F1(1;A1+1;X) eq. C-2
920 DOUBLE K
930 T=S=1.
940 FOR K=1 TO 200
950 T=T*X/(A1+K)
960 S=S+T
970 IF T<=1.E-17*S THEN RETURN S
980 NEXT K
990 PRINT "200 TERMS IN FNF1 AT";A1;X
1000 RETURN S
1010 FNEND
1020 !

```

PROGRAM PLRC (cont'd)

```

1030 SUB Laguerre(DOUBLE N,REAL Alpha,X,L(*)> ! eq. 96
1040 DOUBLE K
1050 A1=Alpha-1.
1060 L(0)=1.
1070 L(1)=Alpha+1.-X
1080 FOR K=2 TO N
1090 L(K)=((K+K+A1-X)*L(K-1)-(K+A1)*L(K-2))/K
1100 NEXT K
1110 SUBEND
1120 !
1130 SUB Momnt_via_cumnt(DOUBLE M,REAL Cum(*),Mom(*))
1140 ! LISTED IN PHRC
1260 SUBEND
1270 !
1280 SUB Cumnt_via_momnt(DOUBLE M,REAL Mom(*),Cum(*))
1290 ! LISTED IN PHRC
1420 SUBEND
1430 !
1440 SUB Coefflr_via_cum(DOUBLE M,REAL Alpha,Beta,Cum(*),A(*))
1450 ALLOCATE B(0:M),C(0:M),D(1:M)
1460 DOUBLE K,J,J1,Mx
1470 T=Beta
1480 Cum(1)=Cum(1)/T
1490 FOR K=2 TO M
1500 T=T*Beta*(K-1)
1510 Cum(K)=Cum(K)/T ! NORMALIZED CUMULANTS; eq. 62
1520 NEXT K
1530 A1=Alpha+1.
1540 FOR J=1 TO M
1550 J1=J+1
1560 T=1.
1570 S=A1
1580 FOR K=1 TO J
1590 T=T*(K-J1)/K
1600 S=S+T*Cum(K)
1610 NEXT K
1620 D(J)=S
1630 NEXT J
1640 A(0)=B(0)=C(0)=EXP(Cum(0))
1650 Q=1.
1660 FOR K=1 TO M
1670 S=0.
1680 FOR J=1 TO K
1690 S=S+D(J)*C(K-J)
1700 NEXT J
1710 C(K)=C=S/K
1720 Q=Q*K/(Alpha+K)
1730 A(K)=C*Q
1740 B(K)=C*SQR(Q)
1750 NEXT K

```

PROGRAM PLRC (cont'd)

```

1760   Mx=Mx+10
1770   IF Mx<M THEN 1760
1780   Threshold=-7.
1790   T2=Threshold*2.
1800   V=10.^Threshold
1810   GINIT
1820   PLOTTER IS "GRAPHICS"
1830   GRAPHICS ON
1840   WINDOW 0.,FLT(Mx),T2,0.
1850   LINE TYPE 3
1860   FOR J=0 TO Mx STEP 10
1870     MOVE J,T2
1880     DRAW J,0.
1890   NEXT J
1900   FOR J=T2 TO 0
1910     MOVE 0.,J
1920     DRAW Mx,J
1930   NEXT J
1940   PENUP
1950   LINE TYPE 1
1960   IMAGE 4D,2(4X,M.17DE)
1970   PRINT "   K           B(K)           Sum"
1980   Sum=0.
1990   FOR K=0 TO M
2000     B=B(K)
2010     Sum=Sum+B*B
2020     PRINT USING 1960;K,B,Sum
2030     IF B<V THEN 2060
2040     Y=LGT(B)
2050     GOTO 2100
2060     IF B>-V THEN 2090
2070     Y=T2-LGT(-B)
2080     GOTO 2100
2090     Y=Threshold
2100     PLOT K,Y
2110   NEXT K
2120   PENUP
2130   SUBEND
2140   !
2150   SUB Cumulants(DOUBLE M,REAL P0,Cum(*))           ! SHOT NOISE
2160   ! LISTED IN PHRC
2310   SUBEND

```


PROGRAM pLRC

```

10 ! CONTINUOUS PART OF SHOT NOISE PDF, pc(u)          TR 7377, FIGURE 21
20 ! COEFFS. OF GENERAL. LAGUERRE EXPANSION FOUND RECURSIVELY VIA CUMULANTS
30 M=70 ! MAXIMUM ORDER OF APPROXIMATION; NUMBER OF CUMULANTS REQUIRED
40 DOUBLE M,I,N,K ! INTEGERS < 2^31 = 2,147,483,648
50 REDIM Cum(0:M),A(0:M),L(0:M)
60 REAL Cum(0:100),A(0:100),L(0:100)
70 CALL Cumulants(M,P0,Cum(*)) ! P0 IS STEP AT ORIGIN
80 Center=Cum(1) ! CENTER OF PDF pc(u)
90 R2=Cum(2) ! MEAN SQUARE SPREAD OF pc(u)
100 Rms=SQR(R2) ! RMS SPREAD OF pc(u)
110 Alpha0=Center*Center/R2-1. ! THE CHOICES Alpha=Alpha0 AND
120 Beta0=R2/Center ! Beta=Beta0 WOULD MAKE A(1)=A(2)=0
130 Alpha=.74
140 Beta=2.1
150 CALL Coeffln_via_cum(M,Alpha,Beta,Cum(*),A(*)) ! RC
160 PRINT "Center = ";Center
170 PRINT "Rms = ";Rms
180 F1=1./(Beta*FNGamma(Alpha+1.))
190 INPUT "ORDER AND LIMITS:",N,U1. :
200 PRINT "ORDER AND LIMITS:",N;U1;U2
210 Du=(U2-U1)/100.
220 PLOTTER IS "GRAPHICS"
230 GRAPHICS ON
240 WINDOW U1,U2,0.,.15
250 GRID 6.,.03
260 FOR I=0 TO 100
270 U=U1+Du*I
280 IF U<0. THEN 400
290 IF U>0. THEN 320
300 PLOT 0.,0.
310 GOTO 400
320 T=U/Beta
330 CALL Laguerre(N,Alpha,T,L(*))
340 Sum=A(0)
350 FOR K=1 TO N
360 Sum=Sum+A(K)*L(K)
370 NEXT K
380 P=F1*EXP(-T+Alpha*LOG(T))*Sum ! PDF OF RV AT U
390 PLOT U,P
400 NEXT I
410 PENUP
420 GOTO 190
430 END
440 ! USE ROUTINES IN PLRC

```

PROGRAM PLDMandRM

```

10 ! STEP PLUS CONTINUOUS PART OF SHOT NOISE CDF, Pc(u); COEFFICIENTS OF
20 ! GENERALIZED LAGUERRE EXPAN. FOUND DIRECTLY AND RECURSIVELY VIA MOMENTS
30 N=70 ! MAXIMUM ORDER OF APPROXIMATION; NUMBER OF MOMENTS REQUIRED
40 DOUBLE M,I,N,K ! INTEGERS < 2^31 = 2,147,483,648
50 REDIM Mom(0:M),A(0:M),L(0:M)
60 REAL Mom(0:100),A(0:100),L(0:100),P(0:100)
70 CALL Moments(M,P0,Mom(*)) ! P0 IS STEP AT ORIGIN
80 Center=Mom(1)/Mom(0) ! CENTER OF PDF pc(u)
90 R2=Mom(2)/Mom(0)-Center*Center ! MEAN SQUARE SPREAD OF pc(u)
100 Rms=SQR(R2) ! RMS SPREAD OF pc(u)
110 Alpha0=Center*Center/R2-1. ! THE CHOICES Alpha=Alpha0 AND
120 Beta0=R2/Center ! Beta=Beta0 WOULD MAKE A(1)=A(2)=0
130 Alpha=.74
140 Beta=2.1
150 CALL Coeffld_via_mom(M,Alpha,Beta,Mom(*),A(*)) ! DM
160 ! CALL Coefflr_via_mom(M,Alpha,Beta,Mom(*),A(*)) ! RM
170 PRINT "Center = ";Center
180 PRINT "Rms = ";Rms
190 A1=Alpha+1.
200 O1=1./A1
210 F1=1./FNGamma(A1)
220 INPUT "ORDER AND LIMITS: ",N,U1,U2
230 PRINT "ORDER AND LIMITS: ",N;U1;U2
240 Du=(U2-U1)/100.
250 PLOTTER IS "GRAPHICS"
260 GRAPHICS ON
270 WINDOW U1,U2,-11.,0
280 GRID 4.,1.
290 P(0)=P0
300 PLOT 0.,LGT(P0)
310 FOR I=1 TO 100
320 U=U1+Du*I
330 T=U/Beta
340 CALL Laguerre(N-1,A1,T,L(*))
350 Sum=A(0)*FNF1(A1,T)*O1
360 FOR K=1 TO N
370 Sum=Sum+A(K)*L(K-1)/K
380 NEXT K
390 P(I)=P=P0+F1*EXP(-T+P1*LOG(T))*Sum ! PROBABILITY THAT RV < U
400 IF P>0. THEN 430
410 PENUP
420 GOTO 440
430 PLOT U,LGT(P)
440 NEXT I
450 PENUP
460 FOR I=0 TO 100
470 U=U1+Du*I
480 P1=1.-P(I)
490 IF P1>0. THEN 520
500 PENUP
510 GOTO 530
520 PLOT U,LGT(P1)
530 NEXT I
540 PENUP
550 GOTO 220
560 END
570 !

```

PROGRAM PLDMandRC (cont'd)

```

580   DEF FNGamma(X) ! Gamma(X) via HART, page 282, #5243
590   ! LISTED IN PLRC
900   FNEND
910   !
920   DEF FNF1(A1,X) ! 1F1(1;A1+1;X)
930   ! LISTED IN PLRC
1020  FNEND
1030  !
1040  SUB Laguerre(DOUBLE N,REAL Alpha,X,L(*) ! Ln\alpha(X)
1050  ! LISTED IN PLRC
1120  SUBEND
1130  !
1140  SUB Momnt_via_cumnt(DOUBLE M,REAL Cum(*),Mom(*))
1150  ! LISTED IN PHRC
1270  SUBEND
1280  !
1290  SUB Coeffld_via_mom(DOUBLE M,REAL Alpha,Beta,Mom(*),A(*)
1300  ALLOCATE B(0:M)
1310  DOUBLE K,K1,J,Mx
1320  T=1.
1330  FOR K=1 TO M
1340  T=T*(Alpha+K)*Beta ! NORMALIZED MOMENTS re
1350  Mom(K)=Mom(K)/T ! Alpha and Beta; eq. 118
1360  NEXT K
1370  Q=1.
1380  A(0)=B(0)=Mom(0)
1390  FOR K=1 TO M
1400  K1=K+1
1410  T=1.
1420  S=Mom(0)
1430  FOR J=1 TO K
1440  T=T*(J-K1)/J
1450  S=S+T*Mom(J)
1460  NEXT J
1470  Q=Q*(Alpha+K)/K
1480  A(K)=S
1490  B(K)=S*SQR(Q)
1500  NEXT K
1510  Mx=Mx+10
1520  IF Mx<M THEN 1510
1530  Threshold=-7.
1540  T2=Threshold*2.
1550  V=10.^Threshold
1560  GINIT
1570  PLOTTER IS "GRAPHICS"
1580  GRAPHICS ON
1590  WINDOW 0.,FLT(Mx),T2,0.
1600  LINE TYPE 3

```

PROGRAM PLDMandRM (cont'd)

```

1610   FOR J=0 TO Mx STEP 10
1620   MOVE J,T2
1630   DRAW J,0.
1640   NEXT J
1650   FOR J=T2 TO 0
1660   MOVE 0.,J
1670   DRAW Mx,J
1680   NEXT J
1690   PENUP
1700   LINE TYPE 1
1710   IMAGE 4D,2(4X,M.17DE)
1720   PRINT "   K           B(K)           Sum"
1730   Sum=0.
1740   FOR K=0 TO M
1750   B=B(K)
1760   Sum=Sum+B*B
1770   PRINT USING 1710;K,B,Sum
1780   IF B<Y THEN 1810
1790   Y=LGT(B)
1800   GOTO 1850
1810   IF B>-Y THEN 1840
1820   Y=T2-LGT(-B)
1830   GOTO 1850
1840   Y=Threshold
1850   PLOT K,Y
1860   NEXT K
1870   PENUP
1880   SUBEND
1890   !
1900   SUB Coefflr_via_mom(DOUBLE M,REAL Alpha,Beta,Mom(*),A(*))
1910   ALLOCATE B(0:M)
1920   DOUBLE K,K1,J,Mx
1930   T=1.
1940   FOR K=1 TO M
1950   T=T*(Alpha+K)*Beta           ! NORMALIZED MOMENTS re
1960   Mom(K)=Mom(K)/T           ! Alpha and Beta; eq. 118
1970   NEXT K
1980   Q=1.
1990   A(0)=B(0)=Mom(0)
2000   FOR K=1 TO M
2010   K1=K+1
2020   T=1.
2030   S=Mom(K)-A(0)
2040   FOR J=1 TO K-1
2050   T=T*(J-K1)/J
2060   S=S-T*A(J)
2070   NEXT J
2080   IF K MOD 2=1 THEN S=-S
2090   A(K)=S
2100   Q=Q*(Alpha+K)/K
2110   B(K)=S*SQR(Q)
2120   NEXT K

```

PROGRAM PLDMandRM (cont'd)

```

2130 Mx=Mx+10
2140 IF Mx<M THEN 2130
2150 Threshold=-7.
2160 T2=Threshold*2.
2170 V=10.^Threshold
2180 GINIT
2190 PLOTTER IS "GRAPHICS"
2200 GRAPHICS ON
2210 WINDOW 0.,FLT(Mx),T2,0.
2220 LINE TYPE 3
2230 FOR J=0 TO Mx STEP 10
2240 MOVE J,T2
2250 DRAW J,0.
2260 NEXT J
2270 FOR J=T2 TO 0
2280 MOVE 0.,J
2290 DRAW Mx,J
2300 NEXT J
2310 PENUP
2320 LINE TYPE 1
2330 IMAGE 4D,2(4X,M.17DE)
2340 PRINT " K B(K) Sum"
2350 Sum=0.
2360 FOR K=0 TO M
2370 B=B(K)
2380 Sum=Sum+B*B
2390 PRINT USING 2330;K,B,Sum
2400 IF B<V THEN 2430
2410 Y=LGT(B)
2420 GOTO 2470
2430 IF B>-V THEN 2460
2440 Y=T2-LGT(-B)
2450 GOTO 2470
2460 Y=Threshold
2470 PLOT K,Y
2480 NEXT K
2490 PENUP
2500 SUBEND
2510 !
2520 SUB Momentsz(DDOUBLE M,REAL P0,Mom(*)) ! SHOT NOISE
2530 ! LISTED IN PHDM&RM
2670 SUBEND

```

PROGRAM pLDMandRM

```

10 ! CONTINUOUS PART OF SHOT NOISE PDF, pc(u); COEFFICIENTS OF GENERALIZED
20 ! LAGUERRE EXPANSION FOUND DIRECTLY AND RECURSIVELY VIA MOMENTS
30 M=70 ! MAXIMUM ORDER OF APPROXIMATION; NUMBER OF MOMENTS REQUIRED
40 DOUBLE M,I,N,K ! INTEGERS < 2^31 = 2,147,483,648
50 REDIM Mom(0:M),A(0:M),L(0:M)
60 REAL Mom(0:100),A(0:100),L(3:100)
70 CALL Moments(M,P0,Mom(*)) ! P0 IS STEP AT ORIGIN
80 Center=Mom(1)/Mom(0) ! CENTER OF PDF pc(u)
90 R2=Mom(2)/Mom(0)-Center*Center ! MEAN SQUARE SPREAD OF pc(u)
100 Rms=SQR(R2) ! RMS SPREAD OF pc(u)
110 Alpha0=Center*Center/R2-1. ! THE CHOICES Alpha=Alpha0 AND
120 Beta0=R2/Center ! Beta=Beta0 WOULD MAKE A(1)=A(2)=0
130 Alpha=.74
140 Beta=2.1
150 CALL Coeffld_via_mom(M,Alpha,Beta,Mom(*),A(*)) ! DM
160 ! CALL Coefflr_via_mom(M,Alpha,Beta,Mom(*),A(*)) ! RM
170 PRINT "Center = ";Center
180 PRINT "Rms = ";Rms
190 F1=1./(Beta*FNGamma(Alpha+1.))
200 INPUT "ORDER AND LIMITS:",N,U1,U2
210 PRINT "ORDER AND LIMITS:",N;U1;U2
220 Du=(U2-U1)/100.
230 PLOTTER IS "GRAPHICS"
240 GRAPHICS ON
250 WINDOW U1,U2,0.,.15
260 GRID 6.,.03
270 PLOT 0.,0.
280 FOR I=1 TO 100
290 U=U1+Du*I
300 T=U/Beta
310 CALL Laguerre(N,Alpha,T,L(*))
320 Sum=A(0)
330 FOR K=1 TO N
340 Sum=Sum+A(K)*L(K)
350 NEXT K
360 P=F1*EXP(-T+Alpha*LOG(T))*Sum ! PDF OF RV AT U
370 PLOT U,P
380 NEXT I
390 PENUP
400 GOTO 200
410 END
420 ! USE ROUTINES IN PLDM&RM

```

REFERENCES

1. J. I. Marcum, "A Statistical Theory of Target Detection by Pulsed Radar: Mathematical Appendix, "Research Memorandum RM-753, RAND Corp., Santa Monica, Calif., 1 July 1948. Also in IRE Trans. on Information Theory, Vol. IT-6, No. 2, April 1960.
2. H. Cramér, Mathematical Methods Of Statistics, Princeton University Press, Princeton, N. J., 1961.
3. M. G. Kendall and A. Stuart, The Advanced Theory of Statistics; Vol. 1, Distribution Theory, Hafner Publishing Co., N. Y., 3rd edition, 1969.
4. A. H. Nuttall, "Under-Ice Roughness: Shot Noise Model," NUSC Technical Memorandum 841208, 31 December 1984.
5. Handbook of Mathematical Functions, U. S. Department of Commerce, National Bureau of Standards, Applied Mathematics Series No. 55, U. S. Government Printing Office, June 1964.
6. A. H. Nuttall, "Recursive Inter-Relationships Between Moments, Central Moments, and Cumulants," NUSC Technical Memorandum No. TC-201-71, 12 October 1971.
7. G. Szegő, Orthogonal Polynomials, American Mathematical Society, Vol. 23, Providence, R. I., 3rd edition, 1967.

8. I. S. Gradshteyn and I. M. Ryzhik, Table of Integrals, Series, and Products, Academic Press, Inc., New York, 1980.
9. A. H. Nuttall and B. Dedreux, "Exact Operating Characteristics for Linear Sum Of Envelopes of Narrowband Gaussian Process and Sinewave," NUSC Technical Report 7117, 11 January 1984.
10. A. H. Nuttall, "Accurate Efficient Evaluation of Cumulative or Exceedance Probability Distributions Directly from Characteristic Functions," NUSC Technical Report 7023, 1 October 1983.
11. A. H. Nuttall, "Exact Performance of General Second-Order Processors for Gaussian Inputs," NUSC Technical Report 7035, 15 October 1983.

Error of Zero-Crossing Location for Straight-Line Interpolation of Sampled Sinewave in Noise

A. H. Nuttall

ABSTRACT

The maximum error, rms error, and the average-magnitude error are evaluated for the approximate zero-crossing location obtained by using linearly-interpolated values of a sampled sinewave. If the sampling rate is greater than four times the sinewave frequency, all three errors are less than 1.1 percent of the period of the sinewave. In the presence of additive noise, the rms error is derived and plotted for different signal-to-noise ratios and noise-bandwidth to signal-frequency ratios. Limitations on the approximate analytic result are pointed out and compared with simulation results.

INTRODUCTION

Sampling of a bandlimited waveform, at a frequency greater than twice the highest frequency contained in the waveform, loses no information according to the sampling theorem. However, perfect reconstruction of the original waveform from the samples requires that two conditions be met: all the samples over $(-\infty, +\infty)$ must be available, and $\sin(x)/x$ interpolation must be used. The first condition can never be met exactly and the second is often too time-consuming to be practical. Furthermore, determination of the zero crossings requires solution of a transcendental equation, which is very time-consuming. Accordingly, simpler schemes for waveform reconstruction, such as sample-and-hold or linear interpolation, are often employed.

Here we investigate the error incurred by using linear interpolation of the samples, in order to determine the zero-crossing locations of the original waveform. In particular, we first consider a pure sinewave and sample it at a rate greater than twice the sinewave frequency. The error in zero-crossing locations, afforded by linear interpolation between adjacent samples, is evaluated as a function of the ratio of sampling period to sinewave period. When noise is added, the error depends additionally on the signal-to-noise ratio and the noise correlation. Plots of the maximum, rms, and mean-magnitude errors are given in the noise-free case, whereas the rms error is presented for the noise-present cases.

NOISE-FREE ZERO-CROSSING ESTIMATION

A sinewave of amplitude A and frequency F is sampled at intervals T seconds apart. The sampling is not synchronous with the sinewave frequency; thus a random phase is associated with the occurrence of sampling relative to the sinewave. The situation is depicted in figure 1, where we are trying to estimate the actual zero-crossing of $y(t)$ at $t=(2F)^{-1}$; we must have $y(b) \leq 0 \leq y(a)$ for this plot to be relevant.

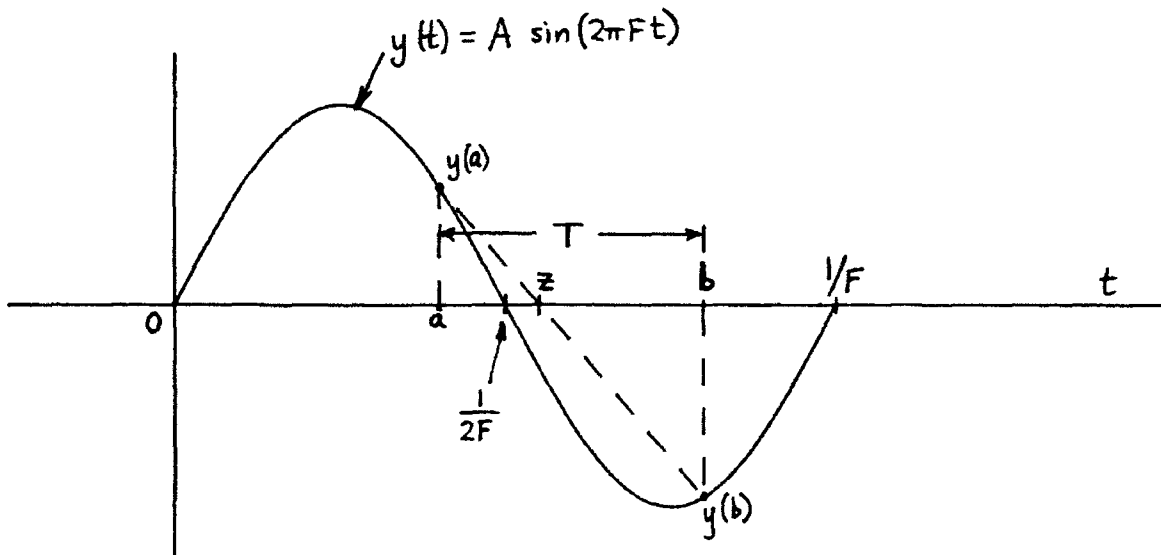


Figure 1. Estimated Zero-Crossing Location z

The interval between the samples at $t=a$ and $t=b$ is

$$T = b - a. \quad (1)$$

Since the sampling is not synchronized with the sinewave, the sampling instant, a , is uniformly distributed in an interval such that

$$a \leq \frac{1}{2F} \leq b = T + a, \quad \text{i.e.,} \quad \frac{1}{2F} - T \leq a \leq \frac{1}{2F}. \quad (2)$$

The zero-crossing location, z , obtained by linearly-interpolating between the sample values at a and b , is

$$z = \frac{b y(a) - a y(b)}{y(a) - y(b)} = \frac{b \sin(2\pi Fa) - a \sin(2\pi Fb)}{\sin(2\pi Fa) - \sin(2\pi Fb)}, \quad (3)$$

where the sinewave amplitude cancels out. If we eliminate b via use of (1), (3) becomes

$$z = a + T \frac{\sin(2\pi Fa)}{\sin(2\pi Fa) - \sin(2\pi F(a+T))} \quad , \quad (4)$$

in terms of sampling interval T .

Instead of using the non-symmetric interval for a as given by (2), we let

$$a = \frac{1}{2F} - \frac{T}{2} + c \quad , \quad (5)$$

where now c is uniformly distributed in the interval

$$-\frac{T}{2} \leq c \leq \frac{T}{2} \quad . \quad (6)$$

Physically, c is the displacement of the midpoint of interval (a,b) from the true zero-crossing at $(2F)^{-1}$. Under the substitution (5), (4) simplifies to

$$z = \frac{1}{2F} + c - \frac{T}{2} \frac{\tan(2\pi Fc)}{\tan(\pi FT)} \quad . \quad (7)$$

The error in estimation of the true zero-crossing location is then

$$e = z - \frac{1}{2F} = c - \frac{T}{2} \frac{\tan(2\pi Fc)}{\tan(\pi FT)} \quad . \quad (8)$$

It is seen from (8) that the error e is odd in c . Furthermore, e is zero for $c=0$ and $c = \pm T/2$. A plot of error e in (8), normalized relative to the sinewave period, is given in figure 2 for different values of FT . It will be observed that the error increases significantly, for all c , as FT approaches .5-. Also, the maximum error, $e = .25/F$, occurs for $FT = .5-$, which corresponds to two samples per period. For small FT , the error is given from (8) by

$$e \approx \frac{(\pi FT)^2}{3} c \left(1 - \frac{4c^2}{T^2} \right) \quad \text{for} \quad FT \ll 1 \quad . \quad (9)$$

The maximum error in (9) occurs at $c \cong T/\sqrt{12}$ with value

$$\frac{e(\max)}{1/F} \cong \frac{\pi^2}{9\sqrt{3}} (FT)^3 = .633 (FT)^3 \quad \text{for } FT \ll 1 \quad (10)$$

Thus the maximum error behaves as the cube of FT for small FT; FT is the ratio of sampling period T to sinewave period 1/F.

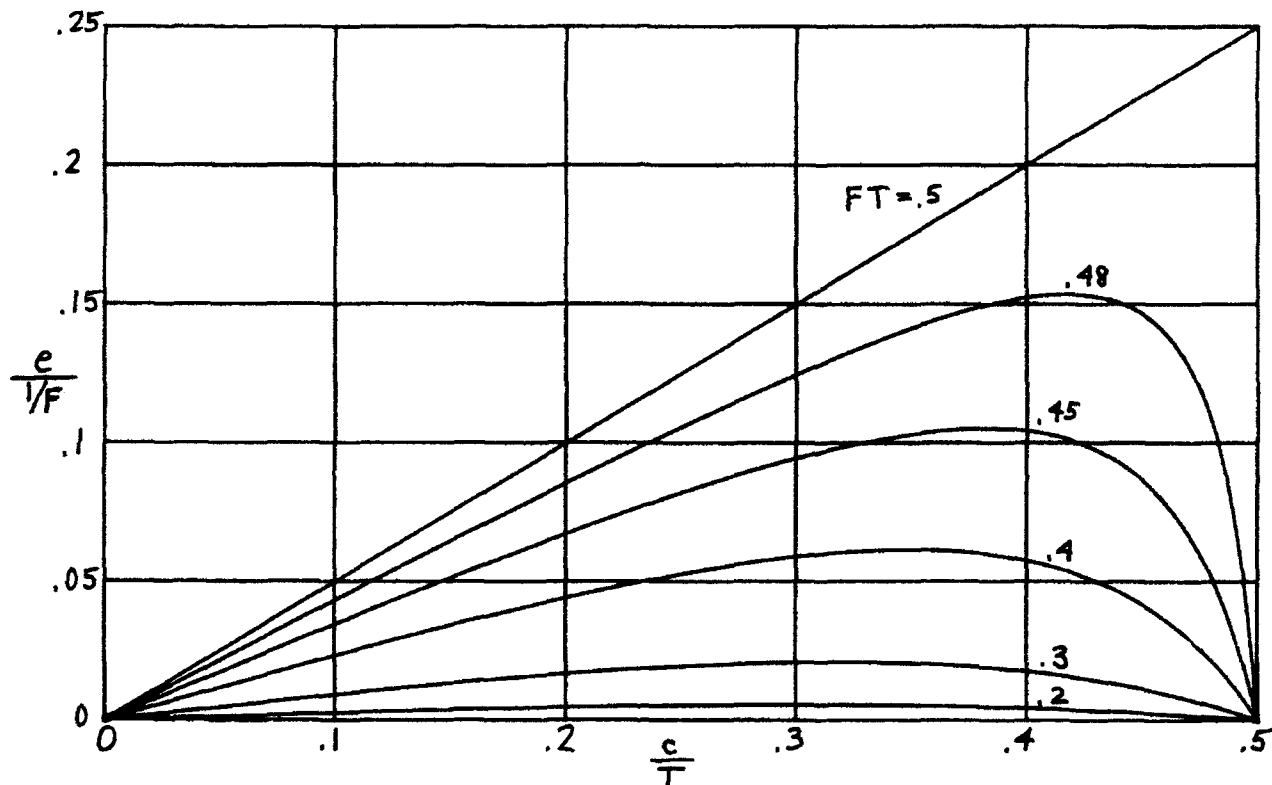


Figure 2. Error e, Relative to Sinewave Period 1/F

Since c is a random variable and uniformly distributed over $\pm T/2$ according to (6), we can compute rms or mean-magnitude errors. But first observe from (8) that the average error, \bar{e} , is zero, since (8) is odd in c, which is itself symmetrically distributed about $c=0$.

We are interested in the following three error measures:

$$\begin{aligned}
 e(\max) &= \max_{|c| < T/2} |e| , \\
 e(\text{rms}) &= \left[\int_{-T/2}^{T/2} dc e^2 p(c) \right]^{1/2} , \\
 e(\text{mag}) &= \int_{-T/2}^{T/2} dc |e| p(c) , \tag{11}
 \end{aligned}$$

where $p(c)$ is the uniform probability density function of random variable c . These are respectively the maximum error, root-mean-square error, and mean-magnitude error. We always have

$$e(\text{mag}) \leq e(\text{rms}) \leq e(\max); \tag{12}$$

the first inequality follows from use of Schwartz's inequality on (11).

Maximum Error

To determine the location of the maximum of the error e in (8), we differentiate with respect to c and set the derivative equal to zero, getting location c_0 where

$$\cos^2(2\pi Fc_0) = \frac{\alpha}{\tan(\alpha)} , \tag{13}$$

and where

$$\alpha \equiv \pi FT . \tag{14}$$

Then the location is explicitly

$$c_0 = \frac{1}{2\pi F} \arctan(\sqrt{r-1}) , \tag{15}$$

where

$$r \equiv \frac{\tan(\alpha)}{\alpha} = \frac{\tan(\pi FT)}{\pi FT} . \tag{16}$$

Substitution of (15) in (8) now yields

$$\frac{e(\max)}{1/F} = \frac{1}{2\pi} \left[\arctan(\sqrt{r-1}) - \frac{\sqrt{r-1}}{r} \right]. \quad (17)$$

As $FT \rightarrow 0$, $r \rightarrow 1+$, and the bracket of (17) approaches

$$\frac{2}{3}(r-1)^{3/2} \approx \frac{2}{3} \left(\frac{\alpha^2}{3} \right)^{3/2}, \quad (18)$$

the last step via use of (16). Then (17) yields

$$\frac{e(\max)}{1/F} \approx \frac{\pi^2}{9\sqrt{3}} (FT)^3 = .633 (FT)^3 \text{ as } FT \rightarrow 0, \quad (19)$$

in agreement with (10).

As $FT \rightarrow .5-$, $r \rightarrow +\infty$, and (17) yields

$$\frac{e(\max)}{1/F} \rightarrow \frac{1}{4} \text{ as } FT \rightarrow .5- \quad (20)$$

in agreement with figure 2.

RMS Error

We have already shown that $\bar{e}=0$ by use of (8) and (6). The mean-square value of e is

$$\bar{e}^2 = \frac{2}{T} \int_0^{T/2} dc \left[c - \frac{T}{2} \frac{\tan(2\pi Fc)}{\tan(\alpha)} \right]^2. \quad (21)$$

Alternatively, using (14),

$$\frac{e(\text{rms})}{1/F} = \frac{\alpha}{2\pi} \left[\int_0^1 dx \left(x - \frac{\tan(\alpha x)}{\tan(\alpha)} \right)^2 \right]^{1/2}. \quad (22)$$

This integral cannot be evaluated in closed form, due to the cross-product term in the integrand; see ref. 1, eq. 2.646 1.

For small FT, we have $\alpha \ll 1$, and then

$$x - \frac{\tan(\alpha x)}{\tan(\alpha)} \sim \frac{1}{3} \alpha^2 x(1-x^2) \quad , \quad (23)$$

leading to

$$\frac{e(\text{rms})}{1/F} \sim \frac{\pi^2}{3} \sqrt{\frac{2}{105}} (FT)^3 = .454 (FT)^3 \text{ as } FT \rightarrow 0. \quad (24)$$

Just as for $e(\text{max})$ in (19), this is cubic in FT; however, the scale factor is smaller here, as anticipated in (12).

As $FT \rightarrow .5^-$, $\alpha \rightarrow \pi/2^-$, and $\tan(\alpha) \rightarrow +\infty$ in (22); then

$$\frac{e(\text{rms})}{1/F} \rightarrow \frac{1}{4\sqrt{3}} = .144 \text{ as } FT \rightarrow .5^- \quad . \quad (25)$$

Mean-Magnitude Error

The mean-magnitude error is, from (8) and (6),

$$\overline{|e|} = \frac{2}{T} \int_0^{T/2} dc \left| c - \frac{T}{2} \frac{\tan(2\pi Fc)}{\tan(\alpha)} \right| \quad (26)$$

Alternatively, using (14) and ref. 1, eq. 2.526 17,

$$\frac{e(\text{mag})}{1/F} = \frac{\alpha}{2\pi} \int_0^1 dx \left| x - \frac{\tan(\alpha x)}{\tan(\alpha)} \right| = \frac{1}{2\pi} \left[\frac{\alpha}{2} + \frac{\ln(\cos(\alpha))}{\tan(\alpha)} \right] \quad (27)$$

We are able to eliminate the absolute value, by reference to figure 2.

For small FT, $\alpha \ll 1$, and we use (23) again to find

$$\frac{e(\text{mag})}{1/F} \sim \frac{\pi^2}{24} (FT)^3 = .411 (FT)^3 \text{ as } FT \rightarrow 0 \quad . \quad (28)$$

The scale factor is smaller than in (24), in keeping with (12).

And as $FT \rightarrow .5^-$, $\alpha \rightarrow \pi/2^-$, $\tan(\alpha) \rightarrow +\infty$, giving rise to

$$\frac{e(\text{mag})}{1/F} \rightarrow \frac{1}{8} \quad \text{as } FT \rightarrow .5^- \quad . \quad (29)$$

Plot of Three Error Measures

A plot of the three errors (normalized by the sinewave period) as given by (17), (22), and (27), is given in figure 3. The errors are monotonically increasing in FT, the ratio of sampling period to sinewave period. They are all cubic in FT for small FT, and increase rapidly as $FT \rightarrow .5^-$. For $FT = .25$, the errors are 1.13%, .81%, and .73% of the sinewave period; thus increasing the sampling frequency to double the minimum required for the sampling theorem allows for linear interpolation with an error in zero-crossing location only about 1% of the sinewave period.

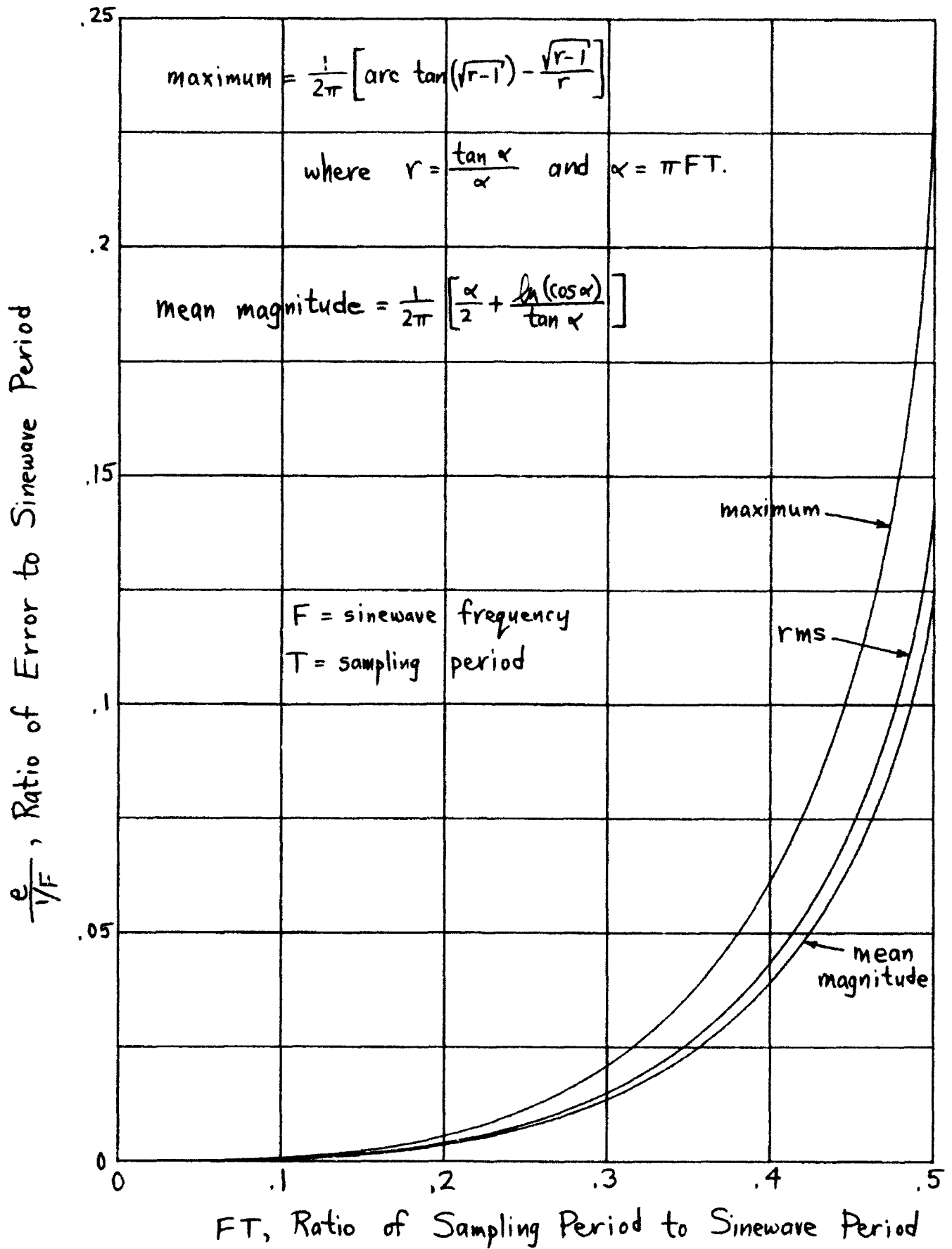


Figure 3. Three Error Measures for Noise-Free Case

ZERO-CROSSING ESTIMATION IN ADDITIVE NOISE

The observed waveform in this case is

$$y(t) = s(t) + n(t) = A \sin(2\pi Ft) + n(t), \quad (30)$$

where the additive independent noise $n(t)$ is stationary and zero-mean. The noise need not be Gaussian; in fact, the only statistics required of the noise are the noise power and correlation coefficient respectively:

$$\sigma^2 = \overline{n^2(t)}, \quad \rho(\tau) = \frac{1}{\sigma^2} \overline{n(t)n(t+\tau)}. \quad (31)$$

(Actually, these are sufficient only for the high signal-to-noise ratio case considered below.)

The estimated zero-crossing is still given by the first equation in (3). When (30) is substituted, there follows, for the zero-crossing, the nonlinear functional

$$z = \frac{[b s(a) - a s(b)] + [b n(a) - a n(b)]}{[s(a) - s(b)] + [n(a) - n(b)]} \cong \frac{u_1 + v_1}{u_2 + v_2}. \quad (32)$$

The signal terms are u_1, u_2 , while the noise terms are v_1, v_2 . Since random variables v_1 and v_2 can take on any value, there is no limit on the maximum error, as there was in the noise-free case. And since the rms error is intermediate to the three errors considered above and easier to evaluate than the mean-magnitude error, we will concentrate solely on the rms error in the noise case.

We begin by making a high signal-to-noise ratio assumption; that is, we assume

$$\frac{\text{signal power}}{\text{noise power}} = \frac{A^2/2}{\sigma^2} \cong R \gg 1. \quad (33)$$

Then (32) becomes approximately

$$\begin{aligned}
 z &= \frac{u_1}{u_2} \frac{1 + v_1/u_1}{1 + v_2/u_2} \approx \frac{u_1}{u_2} \left(1 + \frac{v_1}{u_1}\right) \left(1 - \frac{v_2}{u_2}\right) \\
 &\approx \frac{u_1}{u_2} \left(1 + \frac{v_1}{u_1} - \frac{v_2}{u_2}\right) = \frac{u_1}{u_2} + \frac{v_1}{u_2} - \frac{u_1 v_2}{u_2^2} .
 \end{aligned} \tag{34}$$

The u_1/u_2 term in (34) is exactly the last term in (3) et seq.; the additional two terms in (34) are noise terms that are linearly dependent on the noise samples $n(a)$ and $n(b)$, under the high signal-to-noise ratio assumption. If we did not make this assumption, we would need the joint probability density function of the noise at the two sample instants a and b .

To evaluate the mean and variance of z in (34), we will temporarily hold sample times a and b fixed, and average over the noise statistics, getting conditional properties. Then we will employ (1), (5), and (6) and average over random variable c which reflects the random nature of the sampling mechanism. The preliminary average over the noise will be denoted by a wavy overline; thus from (34), the conditional mean

$$\tilde{z} = \frac{u_1}{u_2} + \frac{1}{u_2} \tilde{v}_1 - \frac{u_1}{u_2^2} \tilde{v}_2 = \frac{u_1}{u_2} , \tag{35}$$

since noise $n(t)$ has zero-mean for all t . Then appeal to (3)-(7) gives

$$\bar{z} = \frac{1}{2F} , \tag{36}$$

just as in the noise-free case; this conclusion is heavily based on the high signal-to-noise ratio assumption.

We now consider the zero-mean random variable

$$\begin{aligned}
 w \equiv z - \bar{z} &= c - \frac{T}{2} \frac{\tan(2\pi Fc)}{\tan(\alpha)} + \frac{v_1}{u_2} - \frac{u_1 v_2}{u_2^2} \\
 &= e + \frac{v_1}{u_2} - \frac{u_1 v_2}{u_2^2} \quad , \quad (37)
 \end{aligned}$$

which is the perturbation of the estimated zero-crossing location from the true value $(2F)^{-1}$; here we used (34), (36), (7), (8), and (14). The conditional mean-square value of w is

$$\overline{w^2} = e^2 + \frac{1}{u_2^2} \overline{v_1^2} - \frac{2u_1}{u_2^3} \overline{v_1 v_2} + \frac{u_1^2}{u_2^4} \overline{v_2^2} \quad (38)$$

since v_1 and v_2 have zero-mean. Now from (32),

$$v_1 = b n(a) - a n(b), \quad v_2 = n(a) - n(b) \quad . \quad (39)$$

Therefore

$$\begin{aligned}
 \overline{v_1^2} &= \sigma^2(b^2 + a^2 - 2ab\rho) = 2\sigma^2 \left[(1-\rho) \left(c + \frac{1}{2F} \right)^2 + (1+\rho) \frac{T^2}{4} \right] \quad , \\
 \overline{v_1 v_2} &= \sigma^2(b - b\rho - a\rho + a) = \sigma^2(1-\rho)(a+b) = 2\sigma^2(1-\rho) \left(c + \frac{1}{2F} \right) \quad , \quad (40) \\
 \overline{v_2^2} &= \sigma^2(1 + 1 - 2\rho) = 2\sigma^2(1 - \rho) \quad ,
 \end{aligned}$$

where we used (31), (1), (5), and defined

$$\rho = \frac{1}{\sigma^2} \overline{n(a)n(b)} = \frac{1}{\sigma^2} \overline{n(a)n(a+T)} = \rho(T) \quad . \quad (41)$$

Before substituting (40) in (38), we derive simpler expressions for u_1 and u_2 . From (32), (1), (5), and (30), we find

$$u_1 = 2A \left(c + \frac{1}{2F} \right) \sin(\alpha) \cos(2\pi Fc) - AT \cos(\alpha) \sin(2\pi Fc),$$

$$u_2 = 2A \sin(\alpha) \cos(2\pi Fc) \quad . \quad (42)$$

Then expressing (38) as the sum of four terms,

$$\tilde{w}^2 = T_1 + T_2 + T_3 + T_4 \quad , \quad (43)$$

and defining

$$\beta = 2\pi Fc \quad , \quad (44)$$

we have, upon use of (33),

$$T_1 = \left[c - \frac{T \tan(\beta)}{2 \tan(\alpha)} \right]^2 \quad ,$$

$$T_2 = \frac{1}{4R} \frac{(1-\rho) \left(c + \frac{1}{2F} \right)^2 + (1+\rho) \cdot \frac{T^2}{4}}{\sin^2(\alpha) \cos^2(\beta)} \quad ,$$

$$T_3 = \frac{-1+\rho}{4R} \frac{\left(c + \frac{1}{2F} \right) \left[2 \left(c + \frac{1}{2F} \right) \sin(\alpha) \cos(\beta) - T \cos(\alpha) \sin(\beta) \right]}{\sin^3(\alpha) \cos^3(\beta)} \quad ,$$

$$T_4 = \frac{1-\rho}{16R} \frac{\left[2 \left(c + \frac{1}{2F} \right) \sin(\alpha) \cos(\beta) - T \cos(\alpha) \sin(\beta) \right]^2}{\sin^4(\alpha) \cos^4(\beta)} \quad . \quad (45)$$

We now have to average the sum of the four terms in (45) over the symmetric distribution for c given in (6). However, each of the terms T_2 , T_3 , T_4 have even and odd components in c , and the odd components will average to zero. When we retain only the even functions of c in (45) and then add them together, a number of terms cancel, after considerable manipulation, leading to the significantly simpler expression

$$\text{even } \{T_2 + T_3 + T_4\} = \frac{T^2}{16R} \frac{(1-\rho) \cos^2(\alpha) \sin^2(\beta) + (1+\rho) \sin^2(\alpha) \cos^2(\beta)}{\sin^4(\alpha) \cos^4(\beta)} \quad . \quad (46)$$

When we employ (44) in (46) and average over c , we find, upon use of ref. 1, eqs. 2.526 30 and 2.526 10, the mean-square error of the zero-crossing location (due to the additive noise) as the surprisingly brief expression

$$\frac{e^2(\text{noise})}{1/F^2} = \frac{1}{4\pi^2} \frac{1}{R} \frac{2+\rho(T)}{3} \frac{\alpha}{\sin(2\alpha)} \quad , \quad (47)$$

upon simplification and use of (41). To this term must be added the averaged T_1 term in (45), which is simply the square of (22). The total normalized rms error is then

$$\frac{e(\text{rms})}{1/F} = \frac{1}{2\pi} \left[\alpha^2 \int_0^1 dx \left(x - \frac{\tan(\alpha x)}{\tan(\alpha)} \right)^2 + \frac{1}{R} \frac{2+\rho(T)}{3} \frac{\alpha}{\sin(2\alpha)} \right]^{1/2} \quad . \quad (48)$$

Here signal-to-noise ratio R and parameter α are given by

$$R = \frac{A^2/2}{\sigma^2} \quad , \quad \alpha = \pi FT \quad . \quad (49)$$

We must emphasize that (48) is only valid for large signal-to-noise ratio, $R \gg 1$, so that approximation (34) is valid.

As $FT \rightarrow .5^-$, $2\alpha \rightarrow \pi$, and the $\sin(2\alpha)$ term in the denominator of (48) approaches zero. This appears to cause the rms error to tend to $+\infty$ at $FT = .5^-$. However, this obvious shortcoming of (48) is due to a breakdown of the approximation in (34). Specifically, (34) presumes that u_2 is not zero and that it is large compared to v_2 ; but (32) and (42) show that this quantity, given exactly by

$$u_2 = s(a) - s(b) = 2A \sin(\alpha) \cos(2\pi Fc) = 2A \sin(\pi FT) \cos(2\pi Fc) \quad , \quad (50)$$

can be small for some values of c . In particular, the minimum of u_2 is

$$\min_c u_2 = 2A \sin(\pi FT) \cos(\pi FT) = A \sin(2\pi FT) \quad , \quad (51)$$

which tends to zero as $FT \rightarrow .5$. Thus the occasional values of c near $\pm T/2$ cause u_2 to be small if FT is near $.5$, and the approximation in (34) to be invalid. Thus (48) is invalid as $FT \rightarrow .5$, regardless of the signal-to-noise ratio.

At the same time, we observe that the $\sin(\pi FT)$ term in (50) reaches a maximum of 1 at $FT = .5$, but becomes small for FT near zero. Thus approximation (34) is not expected to be valid, nor (48) too accurate, for small FT . In fact, the maximum value of the minimum in (51) is A , at $FT = .25$. Thus (48) is expected to be most accurate in the neighborhood of $FT = .25$. Simulation results bear this conclusion out. Furthermore, FT values in the region about $.25$, like $(.15, .35)$, encompass the range of most practical interest anyway; we cannot get away with two samples per cycle and we don't want to oversample if we don't have to.

As $T \rightarrow 0$, the first term in the bracket of (48) tends to zero; see (24). However, the second term does not, and we get

$$\frac{e(\text{rms})}{1/F} \sim \frac{1}{2\pi} \frac{1}{\sqrt{2R}} \text{ as } T \rightarrow 0 \quad . \quad (52)$$

This term constitutes a lower bound on the zero-crossing error, even as sampling period T tends to zero. (Notice that the error decays inversely with the square root of the signal-to-noise ratio R .) However, the precautionary note in the above paragraph makes (52) suspect, since $u_2 \rightarrow 0$ then.

Plot of RMS Error

In order to plot (48) versus FT , we must have a functional form for the noise correlation coefficient $\rho(\tau)$. We take here the example of a Gaussian correlation:

$$\rho(\tau) = \exp(-\pi^2 W^2 \tau^2) \quad . \quad (53)$$

The spectrum corresponding to (53) is proportional to

$$\exp(-f^2/W^2) \quad . \quad (54)$$

Thus at $f = \pm W$, this low-pass spectrum has dropped to $1/e$ of its peak value at $f=0$. Other correlations and spectra are possible, including bandpass cases if desired.

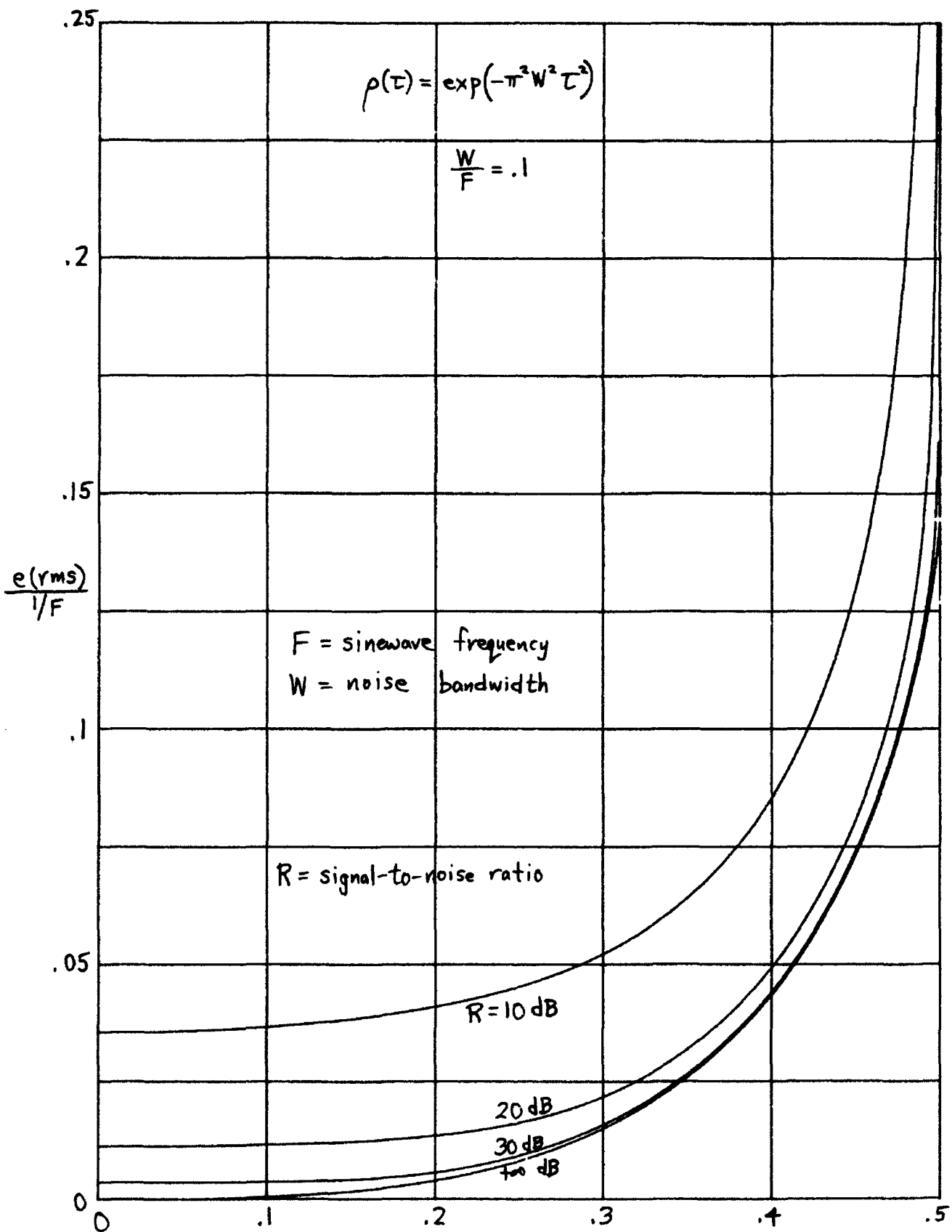
Equation (48) requires the quantity

$$\rho(T) = \exp(-\pi^2 W^2 T^2) = \exp(-\alpha^2 W^2 / F^2) \quad , \quad (55)$$

where α is given by (49) as usual. The parameter W/F measures the ratio of the noise bandwidth (at the $1/e$ point) to the signal frequency and must be specified in order to plot (48) vs FT . In figures 4-6 are plotted the normalized rms error (48) for $W/F = .1, 1, \text{ and } 10$ respectively, for various signal-to-noise ratios.

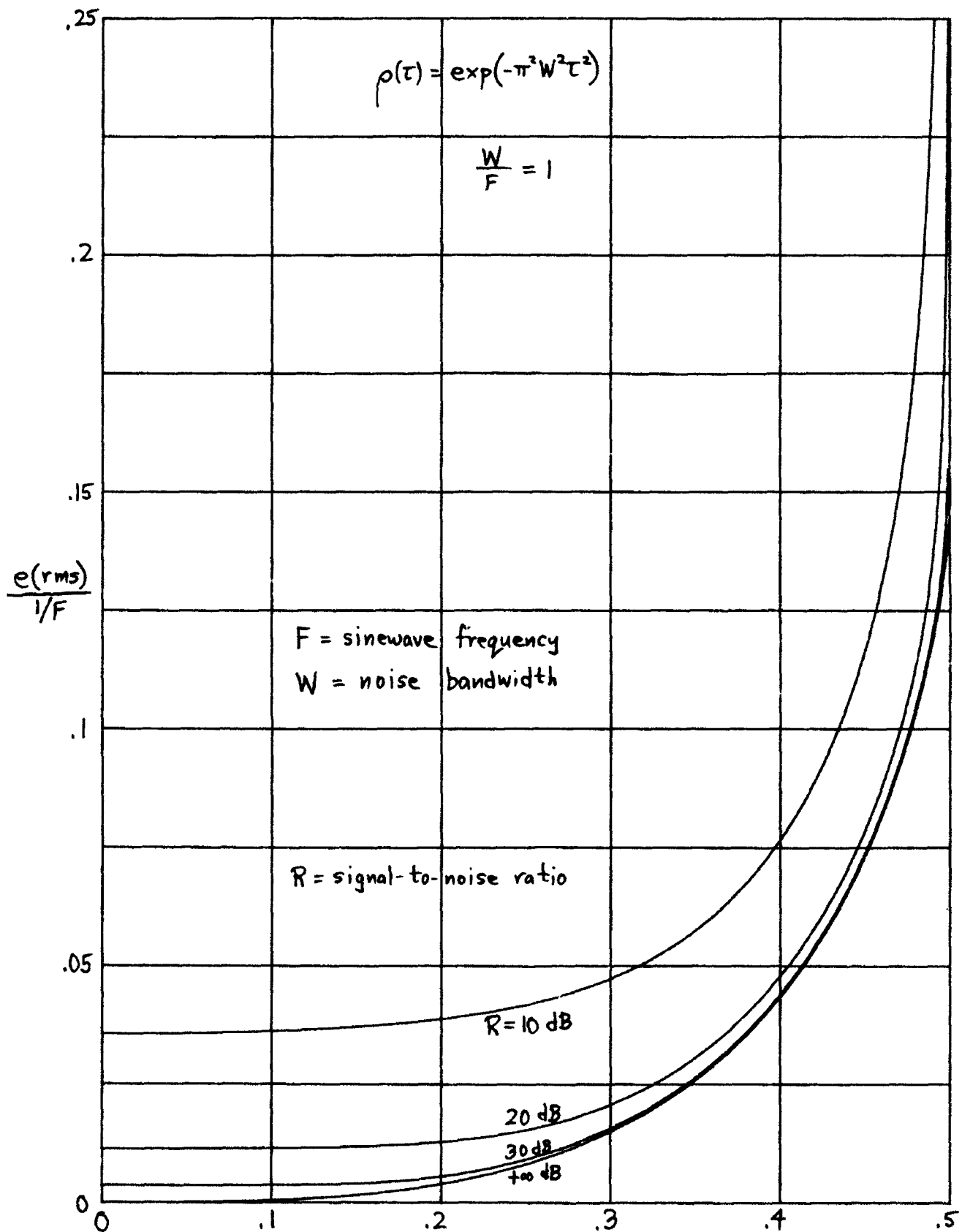
The accuracy of the analytic results in figures 4-6 for the relatively low signal-to-noise ratio of $R = 10 = 10 \text{ dB}$ is not too good, because (34) is a marginal approximation in this situation. Simulation results in the next section verify that (48) is a good approximation for $R=20 \text{ dB}$ and an excellent approximation for $R=30 \text{ dB}$, provided that FT is not near 0 or .5.

The reason for the dip near the origin in figure 6 is that $\rho(T)$ in (48) decreases rapidly when the signal bandwidth is large. The eventual rise of the $\alpha/\sin(2\alpha)$ term has not taken effect before $\rho(T)$ has essentially decayed to zero. Physically, noise samples that are highly correlated cause more of a zero-crossing perturbation than uncorrelated noise samples. However, the region near $FT=0$ in figures 4-6 is not expected to be reliable because the approximation in (34) is invalid.

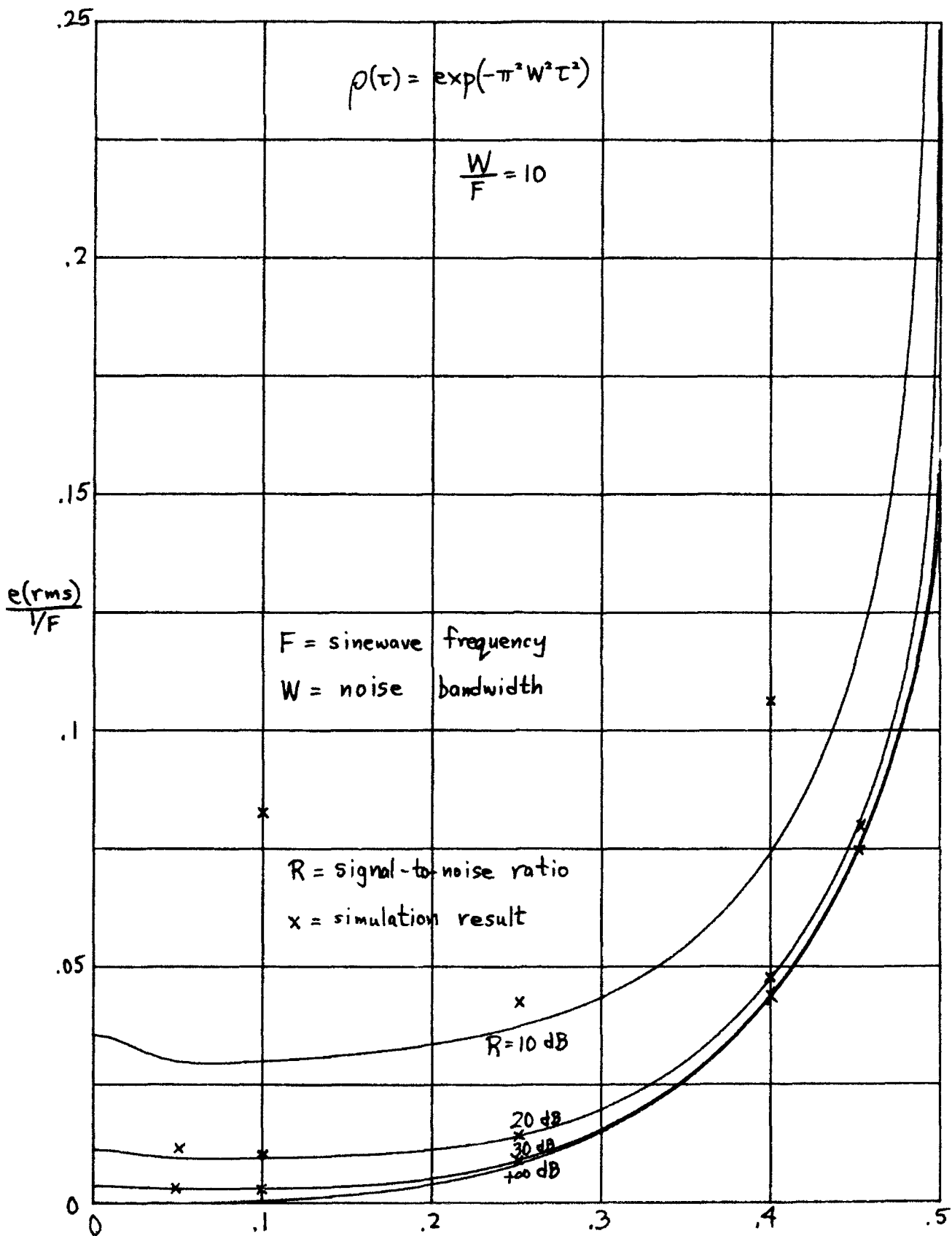


FT, Ratio of Sampling Period to Sinewave Period

Figure 4. Normalized RMS Error for $W/F = .1$



FT, Ratio of Sampling Period to Sinewave Period
 Figure 5. Normalized RMS Error for $W/F = 1$



FT, Ratio of Sampling Period to Sinewave Period
Figure 6. Normalized RMS Error for W/F = 10

SIMULATION RESULTS

A program for simulation of exact relation (32) is given in the appendix. A result for the noise-free case for $F=1$, $T=.3$, and 100,000 trials is given in table 1, and compared with the analytical results in (17), (22), and (27) respectively. The agreement is excellent for all three error measures.

Error	Analytical	Simulation
Maximum	.020936	.020936
RMS	.014978	.014995
Mean-Magnitude	.013553	.013572

Table 1. Noise-Free Comparison for $F=1$, $T=.3$, 100,000 trials

When noise is added, a simulation result for $F=1$, $T=.3$, $\rho=.4$, $R=1000=30$ dB, and 100,000 trials is given by (see appendix)

$$\frac{e(\text{rms})}{1/F} = .015621 \quad . \quad (56)$$

The corresponding analytic result from (48) is .015634.

A check on (52) is afforded by a simulation with $F=1$, $T=.001$, $\rho=1$, $R=30$ dB. The contribution of the first term in (48) is $.454 (.001)^3 = .454E-9$, as given by (24), and is negligible compared with the second term. Whereas (52) yields .0035588, the simulation yielded .0035660, which is excellent agreement, considering that $FT \ll 1$ for this example. The saving feature here is the very large signal-to-noise ratio of $R=1000$.

Several simulation results, at 100,000 trials each, are displayed as Xs in figure 6. They were run at signal-to-noise ratio R equal to 10 dB, 20 dB, and 30 dB, for values of FT equal to .05, .1, .25, .4, and .45. The agreement between analysis and simulation is: excellent for all $R=30$ dB results; very good for $R=20$ dB except when FT is very small or near .5; and poor for $R=10$ dB except when FT is near .25. In fact, the $R=10$ dB results for $FT=.05$ and .45 were off the graph, and those for $FT=.1$ and .4 are rather inaccurate. These

results are consistent with the expectations given above for the approximate analytical result.

Finally, a simulation result for $F=1$, $T=.5$, $W/F=.5$, $R=30$ dB, and 100,000 trials gave 1.9488, which is much larger than any of the ordinates in figures 4-6. There is no check on this result since (48) is not valid at $FT=.5$. The value of ρ in this case is, from (55), $\exp(-(\pi/2)^2(1/2)^2) = \exp(-\pi^2/16) = .54$.

SUMMARY

In the noise-free case, the maximum error, rms error, and mean-magnitude error have been derived, and the normalized error has been plotted (in figure 3) as a function of FT , the ratio of sampling period T to sinewave period $1/F$. The normalization is with respect to the sinewave period.

For the additive noise case, the rms error has been evaluated and plotted (in figures 4-6) for a variety of signal-to-noise ratios and ratios of noise bandwidth to signal frequency. The result is not correct for small signal-to-noise ratio or as $FT \rightarrow 0$ or $.5-$, due to approximations adopted in the analysis, in order to obtain a tractable result. Simulation results corroborate the analysis for FT values not near 0 or $.5$, and for large signal-to-noise ratio.

REFERENCE

1. I. S. Gradshteyn and I. M. Ryzhik, Table of Integrals, Series, and Products, Academic Press Inc., NY, 1980.

APPENDIX. PROGRAM FOR SIMULATION

```

10      T=.3           ! SAMPLING PERIOD; TAKE F=1
20      Rho=.4        ! CORRELATION COEFFICIENT
30      R=1000        ! SIGNAL-TO-NOISE RATIO
40      Tt=100000     ! NUMBER OF TRIALS
50      Th=.5*ACS(Rho)
60      Ct=COS(Th)
70      St=SIN(Th)
80      Fac=SQR(6/R)
90      Tm=.5-T/2
100     Tp=.5+T/2
110     T2=2*PI
120     M1=M2=M3=M4=0
130     FOR It=1 TO Tt
140     C=(RND-.5)*T
150     A=Tm+C         ! SAMPLING
160     B=Tp+C         ! TIMES
170     ! GO TO 240     INSERT THIS LINE FOR NOISE-FREE CASE
180     X=(RND-.5)*Fac
190     Y=(RND-.5)*Fac
200     Tc=Ct*X
210     Ts=St*Y
220     G=Tc+Ts       ! ADDITIVE NOISE WITH DESIRED
230     H=Tc-Ts       ! LEVEL AND CORRELATION
240     Ya=SIN(T2*A)+G
250     Yb=SIN(T2*B)+H
260     Z=(B*Ya-A*Yb)/(Ya-Yb) ! ZERO-CROSSING ESTIMATION
270     E=Z-.5        ! ERROR
280     M1=M1+E       ! AVERAGE ERROR
290     M2=M2+E*E     ! SQUARED ERROR
300     M3=M3+ABS(E)  ! MAGNITUDE ERROR
310     M4=MAX(M4,ABS(E)) ! MAXIMUM ERROR
320     NEXT It
330     PRINT T;M1/Tt;SQR(M2/Tt);M3/Tt;M4
340     END

```

```
.3 -1.11951611792E-05  1.56208250187E-02  1.38355727005E-02  .0302450328
```


Mean and Variance of Product Array Response: Application to a Cross-Line Array

A. H. Nuttall

ABSTRACT

The mean and variance of the product of the narrowband responses of two arrays steered to the same look direction is evaluated and shown to depend on the complex coherence between the two array outputs. For a cross-line array of perpendicular equi-spaced elements, the stability is much poorer than for a sum array processor, due to the largely uncommon volume of intersection of the two cones of response of each line. When each array is extended to be planar, the degradation in stability is lessened, tending towards the sum array performance as the number of common elements increases.

ADMINISTRATIVE INFORMATION

This memorandum was prepared under NUSC Project No. N70021, "ACSAS Exploratory Development", Principal Investigator Dr. C. H. Sherman, Code 3292. The sponsoring activity is DARPA and ONR, Program Manager James Webster, ONR 280. Also this memorandum was prepared under NUSC Project No. A75205, Subproject No. ZR0000101, "Applications of Statistical Communication Theory to Acoustic Signal Processing", Principal Investigator Dr. A. H. Nuttall, Code 33, Program Manager Capt. Z. L. Newcomb, Naval Material Command, MAT 05B.

The author of this technical memorandum is located at the Naval Underwater Systems Center, New London, CT 06320.

INTRODUCTION

A planar array with a grid structure of $M_1 \times M_2$ elements requires a large number of receivers and considerable signal processing when all the elements are employed and actively utilized. In an effort to conserve on the number of elements and amount of signal processing, the possibility of using a sparse array seems to have merit. In particular, it has been found that an equi-weighted planar array has the same auto spectral density response as the cross spectrum of a pair of perpendicular lines of double the length and with triangular weighting on each line. However, without investigating the variances of these sum and cross-line arrays, respectively, it is impossible to decide on their relative merits.

Here we will consider two arbitrary planar arrays (which may have some common elements and may even be linear arrays), both of which are steered to the same look direction and employ weightings for sidelobe control. The sample cross-spectral density of the two array outputs is the output variable of interest. Thus the combination of arrays is resolving in both spatial angles (wavenumber) as well as in temporal frequency. We will evaluate the mean and variance of the cross-spectral density estimate at the system output in terms of the statistical properties of the impinging noise field and the array parameters, such as look direction and weighting.

As a special case, by choosing the two planar arrays identical in element usage and weighting, we will reduce to the sum array since the cross-spectrum then becomes the auto-spectrum. Thus we can compare the performances of product arrays and sum arrays in terms of the mean and variance of their responses.

CROSS-SPECTRAL DENSITY ESTIMATE

Let $x(t)$ and $y(t)$ be any two array outputs which are stationary in time, zero-mean, and have auto-spectra and cross-spectrum $G_x(f)$, $G_y(f)$, $G_{xy}(f)$, respectively. f is temporal frequency in Hz. Sections of each waveform are gated out by multiplying by temporal weightings and then subjected to Fourier analysis according to*

$$\begin{aligned} X_m(f) &= \int dt \exp(-i2\pi ft) w_m(t) x(t) \quad \text{for } 1 \leq m \leq N, \\ Y_n(f) &= \int dt \exp(-i2\pi ft) w_n(t) y(t) \quad \text{for } 1 \leq n \leq N. \end{aligned} \quad (1)$$

These temporal weightings are generally taken as delayed versions of a basic weighting $w(t)$ according to

$$w_n(t) = w(t-nS), \quad (2)$$

where S is a shift or time delay; however, we keep the more general case in (1) for the time being.

The cross-spectral density estimate at frequency f is obtained by multiplying outputs (1) and averaging in time according to

$$v \equiv \sum_{n=1}^N X_n(f) Y_n^*(f). \quad (3)$$

This is the product array output; it has resolution capability in the spatial angles by virtue of each array output being steered to the same desired look direction, and it has frequency resolution governed by the lengths of the weightings in (1) or (2).

The mean of a general product term of components of (1) is

*An integral without limits is over the entire range of its non-zero integrand.

$$\begin{aligned}
\overline{X_m(f)Y_n^*(f)} &= \iint dt du \exp[-i2\pi f(t-u)] w_m(t) w_n(u) R_{xy}(t-u) = \\
&= \int d\tau \exp(-i2\pi f\tau) R_{xy}(\tau) \phi_{mn}(\tau) = G_{xy}(f) \bullet \Phi_{mn}(f) = \\
&= \int du G_{xy}(u) \Phi_{mn}(f-u), \tag{4}
\end{aligned}$$

where

$$R_{xy}(\tau) = \overline{x(t) y(t-\tau)} \tag{5}$$

is the cross-correlation of array outputs,

$$\phi_{mn}(\tau) = \int dt w_m(t) w_n(t-\tau) \tag{6}$$

is the aperiodic correlation of w_m and w_n , \bullet denotes convolution, and

$$\Phi_{mn}(f) = \int d\tau \exp(-i2\pi f\tau) \phi_{mn}(\tau) = W_m(f) W_n^*(f) \tag{7}$$

is the product of windows of the individual temporal weightings.

If cross-spectrum G_{xy} does not vary significantly in the width of window Φ_{mn} , (4) yields approximation

$$\overline{X_m(f)Y_n^*(f)} \cong G_{xy}(f) \int du \Phi_{mn}(f-u) = G_{xy}(f) \phi_{mn}(0). \tag{8}$$

Now we apply these results to find the mean of the system output cross-spectral density estimate in (3):

$$\mu_v = \bar{v} = G_{xy}(f) \sum_{n=1}^N \phi_{nn}(0) = G_{xy}(f) \sum_{n=1}^N \int dt w_n^2(t), \tag{9}$$

which is proportional to the true cross-spectral density G_{xy} between the two array outputs.

In order to evaluate the variance of system output v in (3), we need magnitude-square value (suppressing f)

$$\overline{|v|^2} = \sum_{m,n=1}^N \overline{X_m Y_m^* X_n^* Y_n} \quad (10)$$

We assume that the filtered outputs X_m and Y_n in (1) are complex Gaussian (as, for example, if $x(t)$ and $y(t)$ were Gaussian). We then observe that

$$\begin{aligned} \overline{X_m Y_n} &= \iint dt du \exp[-i2\pi f(t+u)] w_m(t) w_n(u) R_{xy}(t-u) = \\ &= \int dv G_{xy}(v) W_m(f-v) W_n(f+v). \end{aligned} \quad (11)$$

Now for f removed from zero by at least the reciprocal of the segment length, the two windows in (11) do not overlap, and we get

$$\overline{X_m Y_n} \cong 0 \text{ for } f \neq 0. \quad (12)$$

Then using the factoring property of zero-mean Gaussian random variables, (10) becomes

$$\overline{|v|^2} = \sum_{m,n=1}^N \left[\overline{X_m Y_m^* X_n^* Y_n} + \overline{X_m X_n^* Y_m^* Y_n} \right], \quad (13)$$

where we used (12). The variance of random variable v is

$$\begin{aligned} \sigma_v^2 &= \overline{|v-\bar{v}|^2} = \overline{|v|^2} - |\bar{v}|^2 = \sum_{m,n=1}^N \overline{X_m X_n^* Y_m^* Y_n} = \\ &= \sum_{m,n=1}^N [G_x(f) \otimes \Phi_{mn}(f)] [G_y(f) \otimes \Phi_{mn}^*(f)] = \\ &\cong G_x(f) G_y(f) \sum_{m,n=1}^N \phi_{mn}^2(0), \end{aligned} \quad (14)$$

where we used (9), (4), and (8).

We now specialize the general weightings in (1) to the particular case in (2), obtaining from (6)

$$\phi_{mn}(0) = \int dt w(t-mS) w(t-nS) = \phi_w((n-m)S), \quad (15)$$

where

$$\phi_w(\tau) = \int dt w(t) w(t-\tau) \quad (16)$$

is the aperiodic correlation of basic temporal weighting w . Then variance σ_v^2 in (14) becomes

$$\sigma_v^2 = G_x(f) G_y(f) \sum_{m,n=1}^N \phi_w^2((n-m)S) = G_x(f) G_y(f) \sum_{p=1-N}^{N-1} (N-|p|) \phi_w^2(pS). \quad (17)$$

We are now in position to formulate a quality ratio for the output of the product array. Namely we define the complex (voltage) quality ratio

$$\frac{H_v}{\sigma_v} = \sqrt{N} \gamma_{xy}(f) \left[\sum_{p=1-N}^{N-1} \left(1 - \frac{|p|}{N}\right) \frac{\phi_w^2(pS)}{\phi_w^2(0)} \right]^{-1/2}, \quad (18)$$

where we define the complex coherence between the array outputs as

$$\gamma_{xy}(f) = \frac{G_{xy}(f)}{[G_x(f) G_y(f)]^{1/2}}, \quad (19)$$

and have employed (9), (17), and (15). The quantity in (18) is desired large; it has leading factor \sqrt{N} , which however is partially compensated by the last factor of (18) if shift S is less than the segment length of temporal weighting w . A detailed investigation of the temporal processing factors in (18) is given in [1]; for present purposes, the factor is nearly maximized if shift S is taken about 50% of the segment length.

However, the most important quantity in quality ratio (18) is the complex coherence at frequency f , $\gamma_{xy}(f)$. It is always bounded in magnitude by 1, and can be significantly less than 1 if the two array outputs $x(t)$ and $y(t)$ are incoherent at frequency f of interest.

On the other hand, for identical arrays and array weightings, we have $y(t) = x(t)$, and the quality ratio is again given by (18), where $\gamma_{xy}(f)$ is replaced by

$$\gamma_{xx}(f) = 1. \quad (20)$$

That is, the sum array and product array differ in their complex quality ratios simply by the factor $\gamma_{xy}(f)$, which is the complex coherence of the two arrays in the product formulation. Thus the relative performance of a product array can be investigated by determining the coherence of its component array outputs.

With this information, we can now give a qualitative measure of performance of the cross-line array. Consider two line arrays lying along the horizontal and vertical axes, respectively. Suppose both lines are steered to the same look direction in three-dimensional space. Since a line array must inherently have maximum response everywhere in a cone of symmetry centered on the line, the two cones will intersect at the desired look direction, but will have largely non-overlapping cones at other angles. Thus only a small fraction of the output of each array is in common; in fact, most of each array output comes from uncommon arrival angles.

Thus the two line array outputs will be largely independent of each other, meaning low coherence. Furthermore, the longer the line arrays, the finer becomes the angular resolution, and the common intersection volume of the cones decreases. Thus the performance of the product array relative to the sum array becomes poorer as the line arrays become longer. In the next section, these conclusions will be verified by a detailed quantitative analysis of the coherence between two general array outputs.

CROSS-SPECTRUM OF INDIVIDUAL ARRAY OUTPUTS

Let the pressure field at time t and general location x,y in a planar array be denoted by $p(t,x,y)$. Let the field be stationary and homogeneous, with temporal-spatial correlation

$$\overline{p(t_1, x_1, y_1) p(t_2, x_2, y_2)} = R_p(t_1 - t_2, x_1 - x_2, y_1 - y_2) . \quad (21)$$

The frequency-wavenumber spectrum corresponding to R_p is $\Phi_p(f, u, v)$, where

$$R_p(\tau, u, v) = \iiint df \, d\mu \, dv \exp(i2\pi f\tau + iu\mu + ivv) \Phi_p(f, u, v) . \quad (22)$$

We also define a partial transform of (22) as

$$G_p(f, u, v) = \iint d\mu \, dv \exp(iu\mu + ivv) \Phi_p(f, u, v) . \quad (23)$$

This mixed function of temporal frequency and spatial separations will be of prime importance later, especially if it can be evaluated in closed form.

The grid structure of the planar array is such that the elements are equi-spaced, being located at positions md, nd in the x, y plane, for m, n integer. If a particular element is absent or is not used in an array output, the weighting of that element output is simply set equal to zero. For polar angle ϕ as measured from the z -axis, and azimuthal angle θ as measured from the x -axis, the time delay τ_{mn} employed at location md, nd , in order to steer in desired look direction ϕ_l, θ_l , is [2, Appendix A]

$$\tau_{mn} = -\frac{d}{c}(\alpha m + \beta n) , \quad (24)$$

where d is the element spacing, c is the speed of propagation, and

$$\alpha = \sin\phi_l \cos\theta_l , \quad \beta = \sin\phi_l \sin\theta_l . \quad (25)$$

Broadside to the planar array corresponds to $\phi_l = 0$.

Array output $x(t)$ is synthesized by choosing a particular subset of elements in the planar grid structure, weighting their outputs, and time-delay steering to the desired look direction ϕ_ℓ, θ_ℓ . Thus*

$$x(t) = \sum_{k\ell} w_x(k, \ell) p(t - \tau_{k\ell}, kd, \ell d). \quad (26)$$

By simply setting some weights to zero, a line array or a cross-line, or any desired array configuration, can be realized. Similarly, a second array output, which may employ some or all of the same elements, is

$$y(t) = \sum_{mn} w_y(m, n) p(t - \tau_{mn}, md, nd). \quad (27)$$

The cross-correlation of array outputs (26) and (27) is, upon use of (21),

$$R_{xy}(\tau) = \overline{x(t)y(t-\tau)} = \sum_{k\ell mn} w_x(k, \ell) w_y(m, n) R_p(\tau + \tau_{mn} - \tau_{k\ell}, (k-m)d, (\ell-n)d). \quad (28)$$

Using (23) and (24), the cross-spectrum of x and y is

$$\begin{aligned} G_{xy}(f) &= \sum_{k\ell mn} w_x(k, \ell) w_y(m, n) \exp[i2\pi f(\tau_{mn} - \tau_{k\ell})] \mathcal{J}_p(f, (k-m)d, (\ell-n)d) = \\ &= \sum_{k\ell mn} w_x(k, \ell) w_y(m, n) \exp[i2\pi f \frac{d}{c} (\alpha k + \beta \ell - \alpha m - \beta n)] \mathcal{J}_p(f, (k-m)d, (\ell-n)d) = \\ &= \sum_{qr} \phi_{xy}(q, r) \exp[i2\pi f \frac{d}{c} (\alpha q + \beta r)] \mathcal{J}_p(f, qd, rd), \end{aligned} \quad (29)$$

where we let $q=k-m$, $r=\ell-n$, and defined

$$\phi_{xy}(q, r) = \sum_{k\ell} w_x(k, \ell) w_y(k-q, \ell-r) \quad (30)$$

*A summation without limits is over the entire range of its non-zero summand.

as the two-dimensional cross-correlation of the weight structure employed to yield array outputs $x(t)$ and $y(t)$.

As the first special case of the above, a pair of perpendicular cross-lines can be realized by setting

$$\begin{aligned} w_x(k, \ell) &= 0 \text{ except for } \ell = 0, \\ w_y(m, n) &= 0 \text{ except for } m = 0; \end{aligned} \quad (31)$$

in this case, (30) yields

$$\phi_{xy}(q, r) = w_x(q, 0) w_y(0, -r), \quad (32)$$

and (29) becomes the cross-spectrum of the cross-line array,

$$G_{xy}^{(c)}(f) = \sum_{qr} w_x(q, 0) w_y(0, -r) \exp[i2\pi f \frac{d}{c}(\alpha q + \beta r)] \mathcal{A}_p(f, qd, rd). \quad (33)$$

A second special case is obtained by considering the sum array, which corresponds to setting

$$w_x(k, \ell) = w_y(k, \ell) = w(k, \ell), \quad (34)$$

thereby getting from (30)

$$\phi_{xy}(q, r) = \sum_{k\ell} w(k, \ell) w(k-q, \ell-r) \equiv \phi_s(q, r), \quad (35)$$

and from (29), the auto-spectrum of the sum array,

$$G_{xy}^{(s)}(f) = \sum_{qr} \phi_s(q, r) \exp[i2\pi f \frac{d}{c}(\alpha q + \beta r)] \mathcal{A}_p(f, qd, rd). \quad (36)$$

Comparison of special cases (33) and (36) reveals that the mean responses of the cross-line and sum arrays can be made equal by setting

$$w_x(q,0) w_y(0,-r) = \phi_s(q,r) = \sum_{kl} w(k,l) w(k-q,l-r) \text{ for all } q, r. \quad (37)$$

So, for example, if the sum weighting $w(k,l)$ is flat over a rectangle, $\phi_s(q,r)$ is triangular in q as well as r , over a rectangle twice the size. Thus, if line weightings $w_x(q,0)$ and $w_y(0,-r)$ are each triangular over this double-length, (37) is satisfied, and $G_{xy}^{(c)}(f) = G_{xy}^{(s)}(f)$. This conclusion holds irrespective of the pressure field statistics $\Phi_p(f,qd,rd)$.

Returning now to the general case of (29) and (30), the auto-spectrum $G_x(f)$ of array output $x(t)$ in (26) is easily obtained by replacing w_y by w_x in (30) and using that result for ϕ_{xy} in (29). A similar procedure, but now replacing w_x by w_y , yields the auto-spectrum $G_y(f)$ of array output $y(t)$ in (27). Combined with (29) itself, we now have the capability of calculating coherence $\gamma_{xy}(f)$ as given earlier by (19).

An alternative illuminating form for cross-spectrum $G_{xy}(f)$ is obtained by substituting, for Φ_p in the second line of (29), the expression (23) and interchanging summation and integration:

$$G_{xy}(f) = \iint d\mu d\nu \Phi_p(f,\mu,\nu)^* *W_x(2\pi f \frac{d}{c} \alpha + d\mu, 2\pi f \frac{d}{c} \beta + d\nu) W_y^*(2\pi f \frac{d}{c} \alpha + d\mu, 2\pi f \frac{d}{c} \beta + d\nu), \quad (38)$$

where

$$W_x(a,b) = \sum_{kl} w_x(k,l) \exp(ika+ilb),$$

$$W_y(a,b) = \sum_{mn} w_y(m,n) \exp(ima+inb), \quad (39)$$

are the response patterns of the x and y arrays. Since the patterns in (39) peak at $a = b = 0$, the integral in (38) is dominated by the contribution at spatial frequencies

$$\mu = -2\pi \frac{f}{c} \alpha = - \frac{2\pi}{\lambda} \sin \theta_l \cos \theta_l ,$$

$$\nu = -2\pi \frac{f}{c} \beta = - \frac{2\pi}{\lambda} \sin \theta_l \sin \theta_l . \quad (40)$$

That is, the cross-spectrum in (38) is influenced mainly by frequency-wavenumber spectrum value $\bar{\Phi}_p(f, \mu, \nu)$ at the values given by (40). $\lambda=c/f$ is the wavelength at the frequency f of interest.

EXAMPLES OF FREQUENCY-WAVENUMBER SPECTRA

Square Support

Suppose that at some frequency $f=f_0$, the frequency-wavenumber spectrum is flat over a square:

$$\Phi_p(f_0, u, v) = \left\{ \begin{array}{l} \bar{\Phi}_1(f_0) \frac{1}{4k_L^2} \text{ for } |u| < k_L, |v| < k_L \\ 0 \text{ otherwise} \end{array} \right\}, \quad (41)$$

where k_L is the common limit of wavenumbers in u and v . Then from (23),

$$\mathcal{G}_p(f_0, u, v) = \bar{\Phi}_1(f_0) \frac{\sin(k_L u)}{k_L u} \frac{\sin(k_L v)}{k_L v}. \quad (42)$$

This closed-form expression is separable in u and v and will lead to worthwhile simplifications when employed in (29), and especially cross-line result (33).

Circular Support

Suppose instead that

$$\Phi_p(f_0, u, v) = \left\{ \begin{array}{l} \bar{\Phi}_1(f_0) \frac{1}{\pi k_L^2} \text{ for } u^2 + v^2 < k_L^2 \\ 0 \text{ otherwise} \end{array} \right\}. \quad (43)$$

Then (23) yields

$$\mathcal{G}_p(f_0, u, v) = \bar{\Phi}_1(f_0) \frac{2J_1(k_L \sqrt{u^2 + v^2})}{k_L \sqrt{u^2 + v^2}}, \quad (44)$$

which has circular symmetry in separation space u,v . Although in closed form, it is not separable in u and v , and is more time-consuming to evaluate than (42).

CROSS-LINE ARRAY WITH SQUARE-SUPPORT SPECTRUM

In this section, we specialize to a cross-line array as depicted in figure 1 and couple it with the square-support frequency-wavenumber spectrum

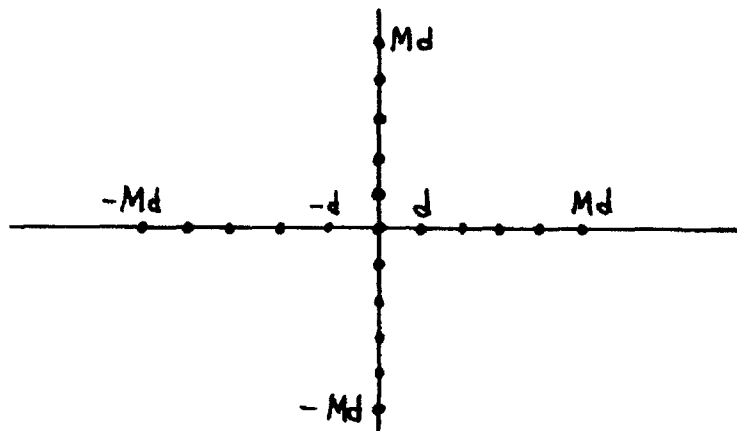


Figure 1. Cross-Line Array of 4M+1 Elements

of (41). The cross-line array has one element at the origin and M elements in each of the four perpendicular legs protruding from the origin, for a total of 4M+1 elements. All elements are spaced by d in both directions, consistent with (24)-(27).

The cross-spectrum at frequency f_0 , between the two perpendicular lines, is given by (33) with (42):

$$G_{xy}^{(c)}(f_0) = \Phi_1(f_0) \sum_{qr} w_x(q,0) w_y(0,-r) \exp[ik_0 d(\alpha q + \beta r)] \frac{\sin(k_L dq)}{k_L dq} \frac{\sin(k_L dr)}{k_L dr} =$$

$$= 4\Phi_1(f_0) \sum_{q=0}^M \epsilon_q w_x(q,0) \cos(k_0 d\alpha q) \frac{\sin(k_L dq)}{k_L dq} \sum_{r=0}^M \epsilon_r w_y(0,r) \cos(k_0 d\beta r) \frac{\sin(k_L dr)}{k_L dr}, \quad (45)$$

where

$$k_0 \equiv \frac{2\pi}{\lambda_0} = 2\pi f_0 / c, \quad \epsilon_q \equiv \begin{cases} 1/2 & \text{for } q = 0 \\ 1 & \text{for } q \geq 1 \end{cases}, \quad (46)$$

and the weight structure on each line has been assumed real and symmetric about the origin. The quantities in (45) are all real and require only two single-summations of size M at each value of the three dimensionless parameters $k_0 d\alpha$, $k_0 d\beta$, $k_L d$. Here, k_L is the common limit on allowed wavenumbers in square-support spectrum (41), and k_0 is the wavenumber corresponding to frequency f_0 of interest. Quantities α and β are given in terms of the look direction according to (25).

To find the auto-spectrum of line-array output $x(t)$, we replace w_y by w_x in (30) and use the upper line of (31):

$$\phi_{xx}(q,r) = \sum_k w_x(k,0) w_x(k-q,-r) = \psi_{xx}(q) \delta_{r0}, \quad (47)$$

where

$$\psi_{xx}(q) \equiv \sum_k w_x(k,0) w_x(k-q,0) \quad (48)$$

is the auto-correlation of the x-array weights. Substitution of (47) in (29) yields

$$\begin{aligned} G_x^{(c)}(f_0) &= \sum_q \psi_{xx}(q) \exp(ik_0 d\alpha q) \phi_p(f_0, qd, 0) = \\ &= 2 \Phi_1(f_0) \sum_{q=0}^{2M} \epsilon_q \psi_{xx}(q) \cos(k_0 d\alpha q) \frac{\sin(k_L dq)}{k_L dq}, \end{aligned} \quad (49)$$

where we used (42) and (46). In a similar fashion, the auto-spectrum of line-array output $y(t)$ is given by

$$G_y^{(c)}(f_0) = 2 \Phi_1(f_0) \sum_{r=0}^{2M} \epsilon_r \psi_{yy}(r) \cos(k_0 d\beta r) \frac{\sin(k_L dr)}{k_L dr}, \quad (50)$$

where

$$\Psi_{yy}(r) \equiv \sum_{\ell} w_y(0, \ell) w_y(0, \ell - r), \quad (51)$$

in keeping with (31). The auto-spectral results in (49) and (50) each require real single-sums of size $2M$. No double summations are required in the cross-spectral result of (45) or in the auto-spectral results of (49) and (50), although in the latter cases, the auto-correlations Ψ_{xx} and Ψ_{yy} must be pre-computed. The complex coherence at frequency f_0 , $\gamma_{xy}^{(c)}(f_0)$, between individual array outputs $x(t)$ and $y(t)$ of the cross-line, is given by ratio (19) as usual; the factor $\Phi_1(f_0)$, as well as the absolute scales of the weight structures $\{w_x(k, 0)\}$, $\{w_y(0, \ell)\}$, will cancel out in the ratio. The fundamental parameters are $k_0 d\alpha$, $k_0 d\beta$, $k_L d$.

For broadside steering of the cross-line array, we have $\phi_2 = 0$ and (25) yields $\alpha = \beta = 0$. Then (45), (49), (50) are independent of k_0 , and the coherence depends only on $k_L d$.

CROSS-LINE ARRAY WITH CIRCULAR-SUPPORT SPECTRUM

By combining (33) with the circular-support frequency-wavenumber spectrum of (44), and using assumed symmetry of the line-array weights, we obtain cross spectrum

$$G_{xy}^{(c)}(f_0) = 4\bar{\Phi}_1(f_0) \sum_{q=0}^M \epsilon_q w_x(q,0) \cos(k_0 d \alpha q) \sum_{r=0}^M \epsilon_r w_y(0,r) \cos(k_0 d \beta r) \frac{2J_1(k_L d \sqrt{q^2+r^2})}{k_L d \sqrt{q^2+r^2}}. \quad (52)$$

This double sum can no longer be separated into the product of two single sums, as (45) was, due to the coupling caused by the Bessel function. However, the Bessel function need only be computed in a 45° sector of the q,r plane and then reflected about the 45° line; i.e., the same value is attained for q,r = m,n as for q,r = n,m.

The auto-spectrum of the x-array output is obtained by utilizing (44) in the top line of (49):

$$G_x^{(c)}(f_0) = 2\bar{\Phi}_1(f_0) \sum_{q=0}^{2M} \epsilon_q \psi_{xx}(q) \cos(k_0 d \alpha q) \frac{2J_1(k_L d q)}{k_L d q}, \quad (53)$$

where ψ_{xx} is again given by (48). In a similar fashion, there follows

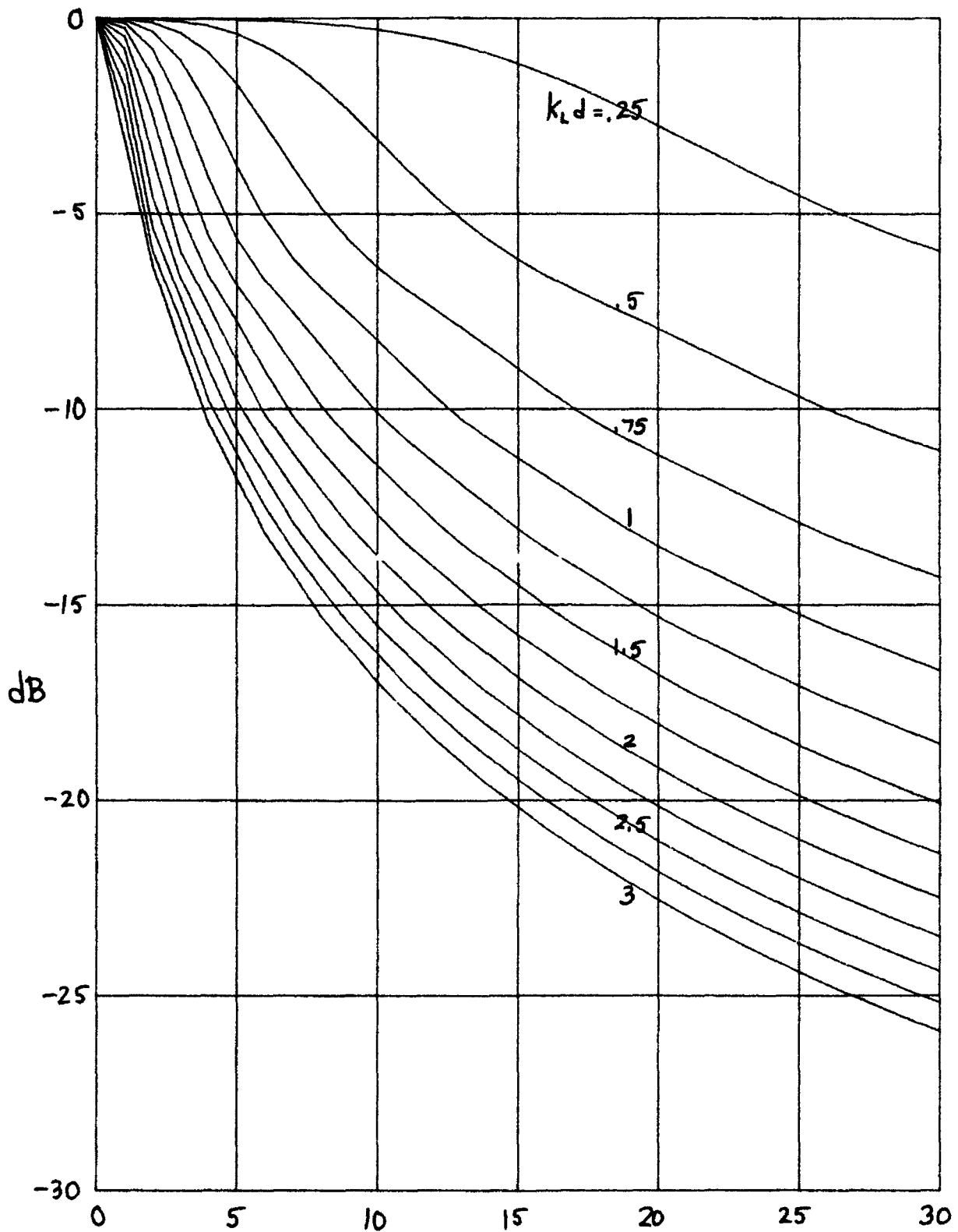
$$G_y^{(c)}(f_0) = 2\bar{\Phi}_1(f_0) \sum_{r=0}^{2M} \epsilon_r \psi_{yy}(r) \cos(k_0 d \beta r) \frac{2J_1(k_L d r)}{k_L d r}. \quad (54)$$

The coherence is now available from (52)-(54). This example was not pursued numerically.

RESULTS

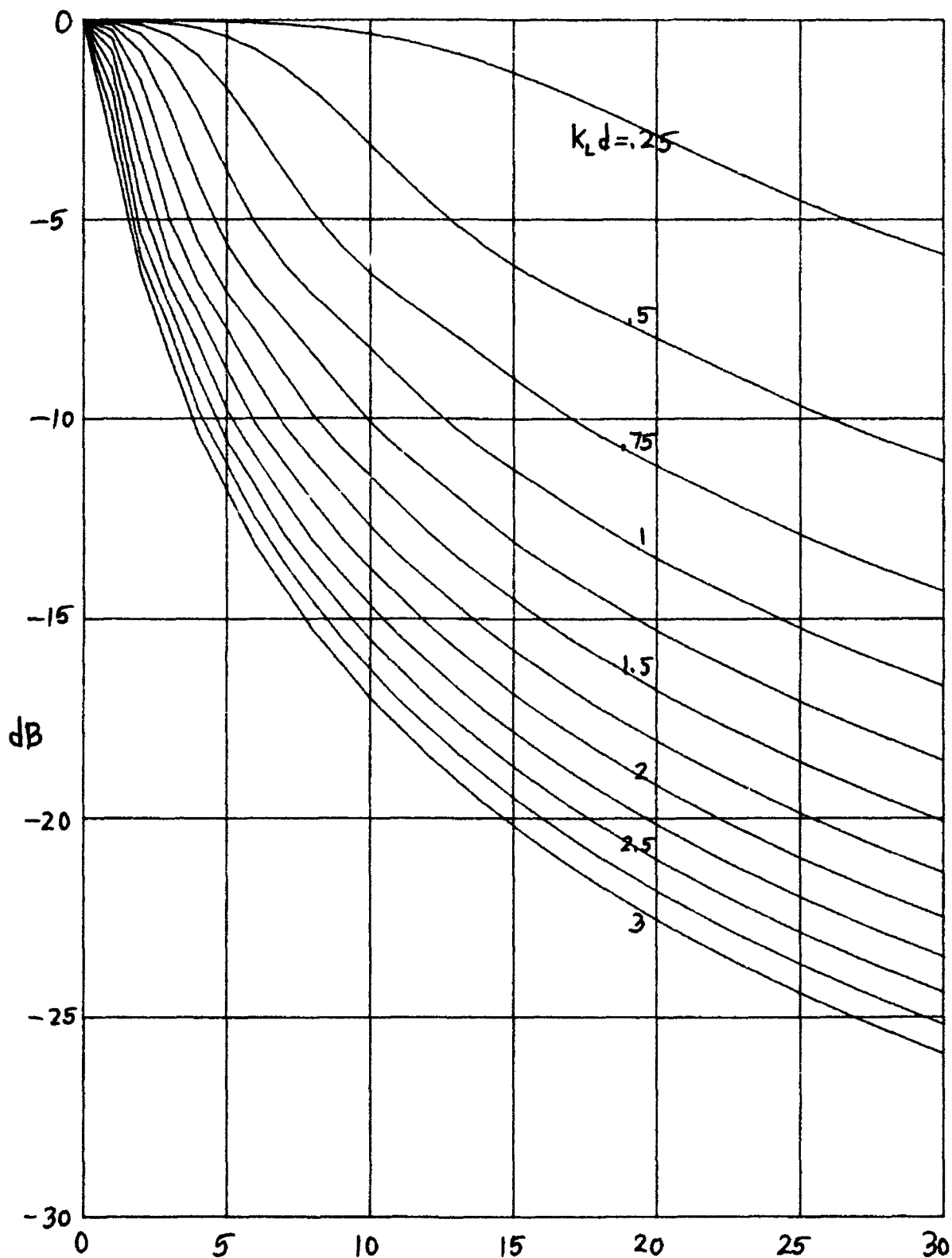
A program for the calculation of the coherence of a cross-line array, via (45)-(51), is given in appendix A. It was exercised to give the following results in figures 2-6. Although these plots look virtually identical, closer inspection of the numerical values (not included) reveals that there are small (insignificant) differences, even for the widely different values of $k_0 d$, ϕ_0 , θ_0 considered here. The degradation of the cross-line array relative to the sum array is virtually independent of the particular look angle ϕ_0 , θ_0 . This can be partially explained by virtue of the fact that at broadside steering, a line array has a narrow beam but covers a full 360° angular sweep, whereas at endfire, the beam is broad but exists at only one angle. Thus the total angular coverage is essentially constant.

The overriding impression of figures 2-6 is that the degradation of the cross-line array is significant, relative to a sum array, in terms of the stability of the cross-spectral estimate. This is particularly so as the size of the array ($4M+1$ total elements) grows, or as $k_L d$ increases above .5. Further examples of interest may be obtained from the program in appendix A.



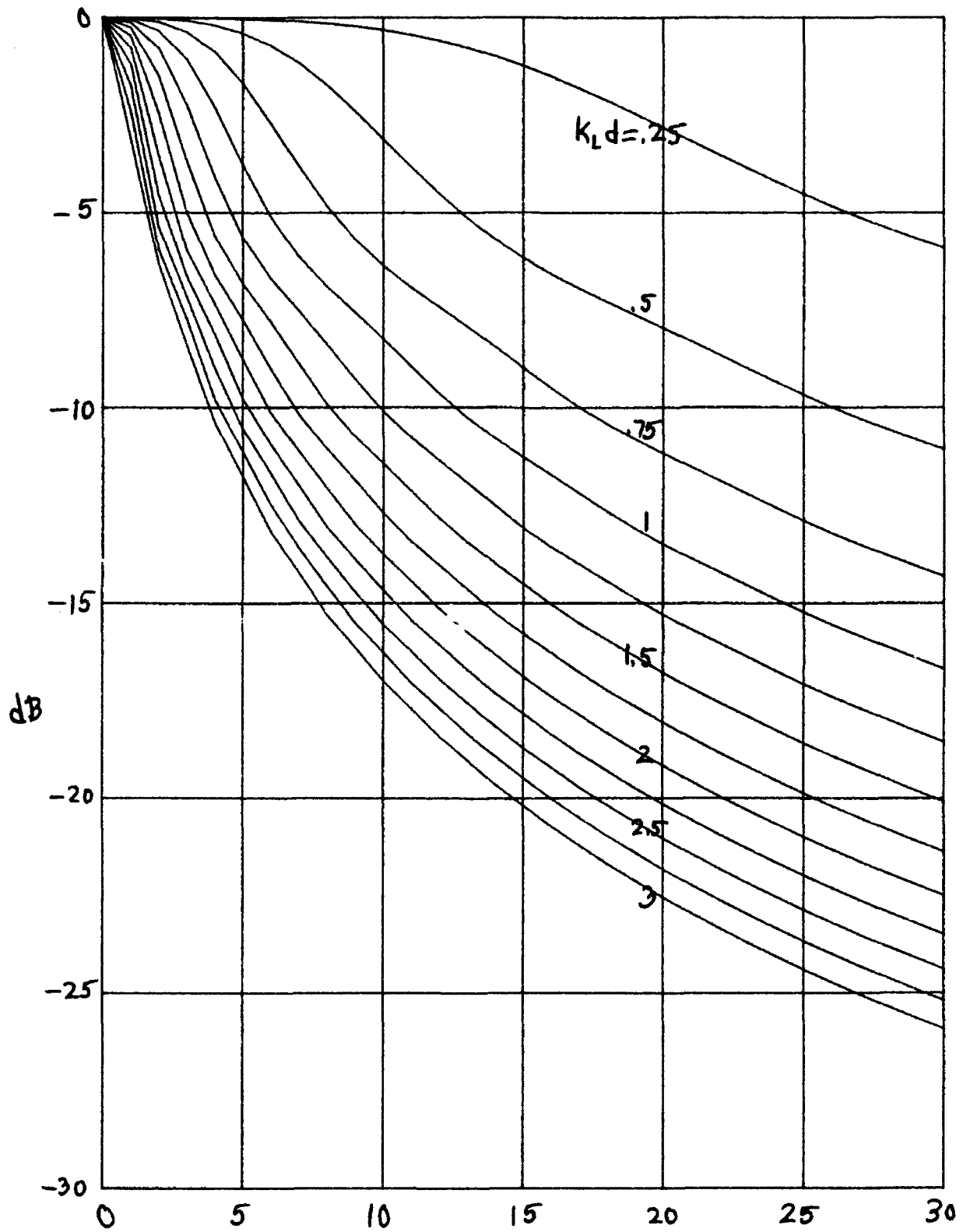
M , Number of Elements per Leg

Figure 2. Degradation for $k_{\perp}d = \frac{\pi}{60}$, $\phi_{\perp} = 0$, $\theta_{\perp} = 0$



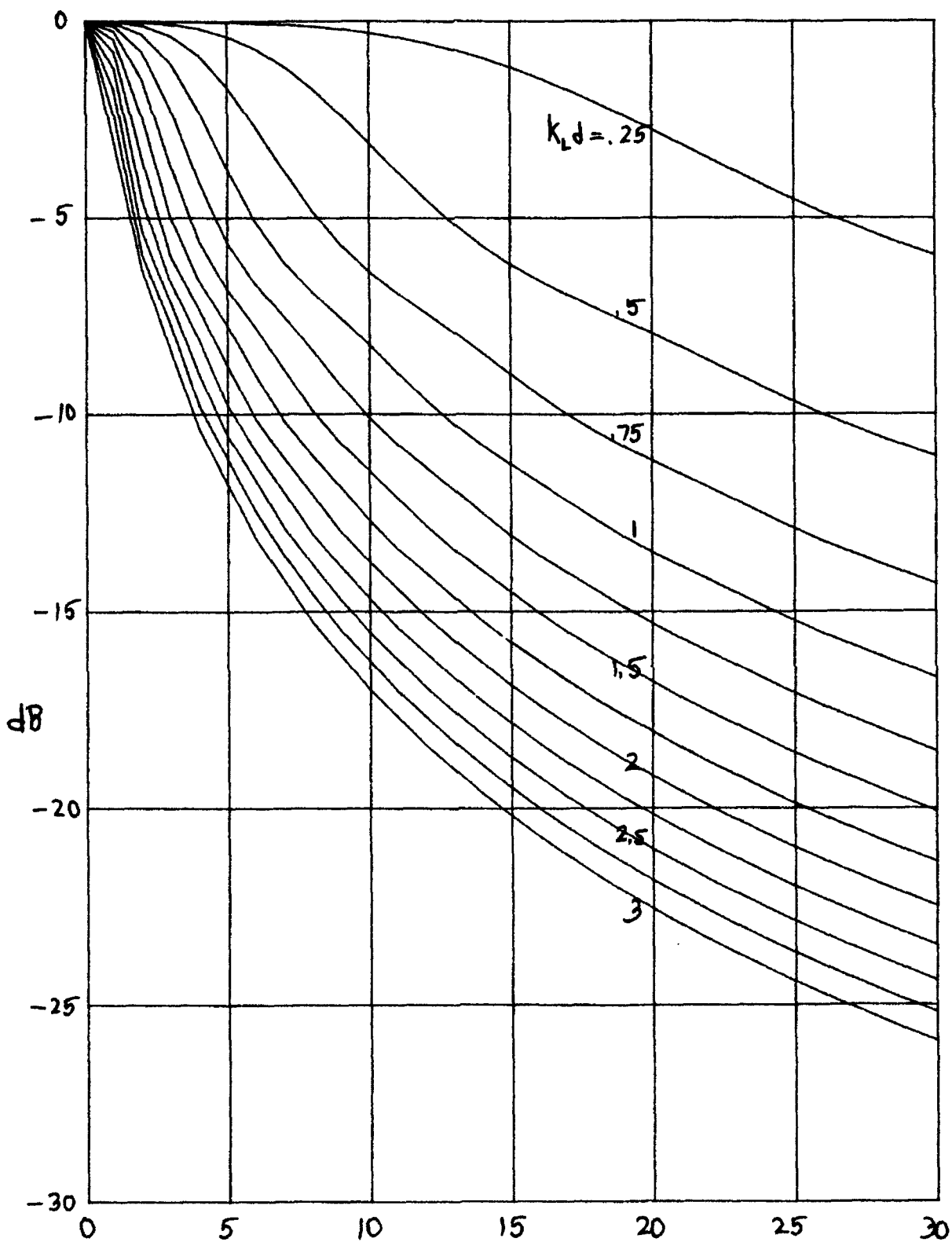
M, Number of Elements per Leg

Figure 3. Degradation for $k_0d = \frac{\pi}{60}$, $\phi_2 = \frac{\pi}{2}$, $\theta_2 = 0$



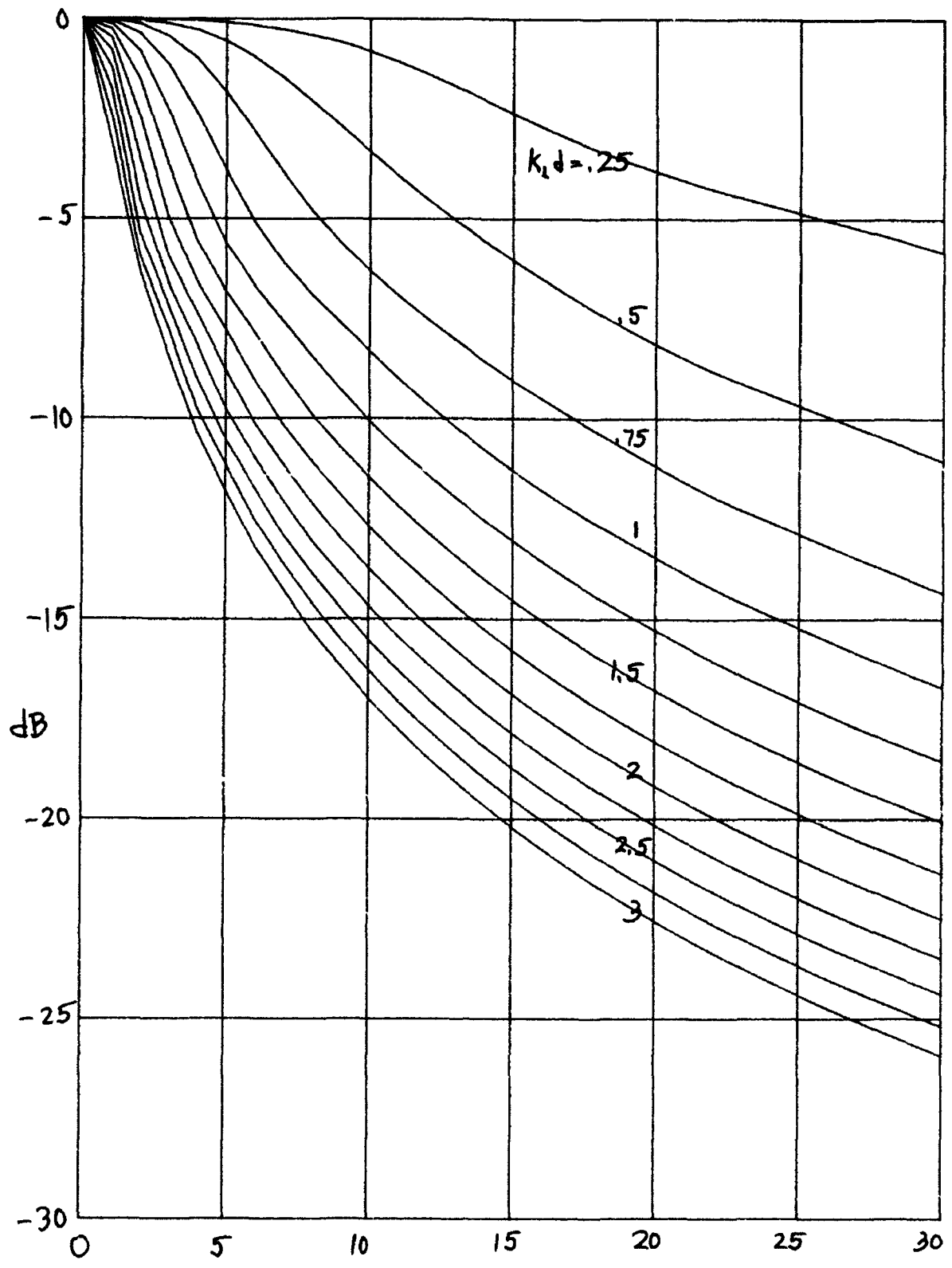
M, Number of Elements per Leg

Figure 4. Degradation for $K_0 d = \frac{\pi}{60}$, $\phi_0 = \frac{\pi}{4}$, $\theta_0 = \frac{\pi}{4}$



M, Number of Elements per Leg

Figure 5. Degradation for $k_0 d = \frac{\pi}{150}$, $\phi_2 = \frac{\pi}{4}$, $\theta_2 = \frac{\pi}{4}$



M, Number of Elements per Leg

Figure 6. Degradation for $k_0 d = \frac{\pi}{15}$, $\phi_2 = \frac{\pi}{4}$, $\theta_2 = \frac{\pi}{4}$

SUMMARY

When the horizontal line array in figure 1 is time-delay steered to look in some desired direction ϕ_r, θ_r , it must also respond in a cone of symmetry centered on the axis of the line. Similarly, although the vertical line is steered to look in the same direction ϕ_r, θ_r , it too has a cone of equal response, but now centered on the vertical axis. These two cones will intersect at ϕ_r, θ_r and thereby lead to some common power at frequency f at their respective array outputs, prior to multiplication and averaging according to (3). However, both arrays also respond to uncommon (i.e. uncorrelated) power contributions from other directions, each within its own cone of response. The sharper the beams of each line array, the less common power will be intercepted, leading to less coherence between the two line outputs. Thus the stability of the cross-line array, relative to the sum array, degrades as the size of each line array increases.

If each of the product arrays were made of a parallel pair of lines (separated by some integer multiple of d), the responses of each would be rather complicated. However, there would again be some common overlap at ϕ_r, θ_r , but a great deal of uncommon response at other sidelobe regions, still causing a decreased coherence and unstable estimates. As more parallel lines are added to each product array, the performance should monotonically approach that of the sum array, being actually realized when all of the available parallel lines are employed, since the outputs of the horizontal and vertical arrays are then identical.

APPENDIX A. PROGRAM FOR CROSS-LINE ARRAY

The following program calculates the coherence of a cross-line array by means of (45)-(51). M is the number of elements in each of the four perpendicular legs protruding from the origin. The weighting in line 60 is assumed the same for both lines and is triangular. The autocorrelation of the weight structure is computed and stored in line 130. Inputs of $k_0 d$, ϕ_x , θ_x are required in lines 160-180 respectively. When these latter inputs are desired changed, the program can be continued at line 160 instead of 10, provided that the array weights have not also been changed. The input of $k_L d$ occurs in line 320. The dB output in line 520 is according to

$$dB = 10 \log_{10} \left| \gamma_{xy}(f_0) \right|^2 ,$$

since γ_{xy} is proportional to the voltage quality ratio.

```

10 DIM W(0:100), S(0:100), P(0:100), Q(0:100)
20 DIM CO(0:100), C(0:100), S(0:100), S(0:100), P(0:100), Q(0:100)
30 FOR NA=0 TO 99
40 NI=NA+1
50 FOR NB=0 TO NI
60 W(NI+NB)=1.0-ABS(NI-NB)/NI
70 NE=NI+NB
80 FOR DB=0 TO NE-NI
90 S=0
100 FOR LB=0 TO NI-DB
110 S=S+W(LB)*W(LB+DB)
120 NE=NI+NB
130 P(NE+DB)=S
140 NE=NI+NB
150 NE=NI

```

```

160 K0d=PI/15          ! INPUT
170 Polan=PI/4        ! INPUT
180 Azimuth=PI/4     ! INPUT
190 S=K0d*SIN(Polan)
200 Ta=3+COS(Azimuth)
210 Tb=3+SIN(Azimuth)
220 FOR Qs=0 TO 60
230 Cosa(Qs)=COS(Ta+Qs)
240 Cosb(Qs)=COS(Tb+Qs)
250 NEXT Qs
260 PLOTTER IS "S872R"
270 LIMIT 30,170,10,205
280 OUTPUT 755;"V32"
290 SCALE 0,30,-30,0
300 GRID 5,5
310 PENUF
320 FOR K1d=.25 TO 3 STEP .25
330 Sinc(w)=1
340 FOR Qs=1 TO 60
350 S=K1d+Qs
360 Sinc(Qs)=SIN(S)/S
370 NEXT Qs
380 FOR M=0 TO 30
390 S1a=S1b=.5+WN(M,0)
400 FOR Qs=1 TO M
410 S=WN(M,Qs)*Sinc(Qs)
420 S1a=S1a+S*Cosa(Qs)
430 S1b=S1b+S*Cosb(Qs)
440 NEXT Qs
450 S2a=S2b=.5+Ps1(M,0)
460 FOR Qs=1 TO M+M
470 S=Ps1(M,Qs)*Sinc(Qs)
480 S2a=S2a+S*Cosa(Qs)
490 S2b=S2b+S*Cosb(Qs)
500 NEXT Qs
510 Coherence=2+S1a+S1b/SQR(S2a+S2b)
520 Db(M)=10*LGT(Coherence+2)
530 NEXT M
540 FOR M=0 TO 30
550 PLOT M,Db(M)
560 NEXT M
570 PENUF
580 NEXT K1d
590 END

```

REFERENCES

1. Nuttall, A. H., "Spectral Estimation by Means of Overlapped FFT Processing of Windowed Data", NUSC Report No. 4169, 13 October 1971.
2. Nuttall, A. H., "A Two-Parameter Class of Bessel Weightings with Controllable Sidelobe Behavior for Linear, Planar-Circular, and Volumetric-Spherical Arrays; The Ideal Weighting-Pattern Pairs", NUSC Technical Report 6761, 1 July 1982.

Subject Matter Index

- Aliasing, 7023, 7117
- Ambiguity of line array, 831150, 841013
- Asymptotic performance, 7117, 7045
- Autocorrelation, 841208
- Characteristic function, 7023, 7035, 7117, 7045, 7377
- Closed form characteristic function, 7035, 7045, 841208
- Collapsing, 7023
- Complex coherence, 841013
- Crosscorrelator, 831150, 7045
- Cross line array, 841013
- Cumulants, 7045, 841208, 7377
- Cumulative distribution, 7023, 7035, 7117, 7045, 841208, 7377
- Detection probability, 7117, 7045, 7377
- Equality of moments, 7377
- Error of approximation, 7377
- Error of interpolation, 831078
- Estimation of arrival angle, 831150
- Exceedance distribution, 7023, 7035, 7117, 841208, 7377
- Fading, 7035
- False alarm probability, 7117, 7045, 7377
- Fast Fourier transform, 7023, 7035
- Free parameters, 7377
- Gaussian approximation, 7045
- Generalized Laguerre expansion, 841208, 7377
- Generalized likelihood ratio, 831150
- Hermite expansion, 7377
- Hermitian form, 7035
- High-order expansion coefficients, 7377
- Linear interpolation, 831078
- Linear sum of envelopes, 7117
- Minimum squared error, 7377
- Mismatched parameters, 7377
- Moments, 841208, 7377
- Narrowband crosscorrelator, 7035, 841013
- Narrowband Gaussian process, 7117
- Nonstationary process, 7035
- Operating characteristics, 7045
- Orthogonal polynomials, 7377
- Power density spectrum, 841208, 841013
- Probability density, 7023, 841208, 7377
- Probability distribution, 7023, 7035, 7117, 7377
- Product array, 841013
- Randomly moving array, 831150
- Receiver operating characteristics, 7117, 7045
- Recursions for expansion coefficients, 7377
- Recursions for moments or cumulants, 7377
- Resolution of ambiguity, 831150
- Rice characteristic function, 7117, 7377
- Right-left ambiguity, 831150
- Round-off error, 7023, 7377
- Sample ac components, 831150, 7045
- Sample mean removal, 831150, 7045
- Sampling, 831078
- Second-order processors, 7035
- Shot noise model, 841208, 7377
- Smirnov example, 7023
- Straight-line interpolation, 831078
- Truncation error, 7023
- Under-ice roughness, 841208
- Weighted energy detector, 7035
- Weighting functions, 7377, 841013
- Zero-crossing estimation, 831078